

## THESE TERMS GOVERN YOUR USE OF THIS DOCUMENT

**Your use of this Ontario Geological Survey document (the “Content”) is governed by the terms set out on this page (“Terms of Use”). By downloading this Content, you (the “User”) have accepted, and have agreed to be bound by, the Terms of Use.**

**Content:** This Content is offered by the Province of Ontario’s *Ministry of Northern Development and Mines* (MNDM) as a public service, on an “as-is” basis. Recommendations and statements of opinion expressed in the Content are those of the author or authors and are not to be construed as statement of government policy. You are solely responsible for your use of the Content. You should not rely on the Content for legal advice nor as authoritative in your particular circumstances. Users should verify the accuracy and applicability of any Content before acting on it. MNDM does not guarantee, or make any warranty express or implied, that the Content is current, accurate, complete or reliable. MNDM is not responsible for any damage however caused, which results, directly or indirectly, from your use of the Content. MNDM assumes no legal liability or responsibility for the Content whatsoever.

**Links to Other Web Sites:** This Content may contain links, to Web sites that are not operated by MNDM. Linked Web sites may not be available in French. MNDM neither endorses nor assumes any responsibility for the safety, accuracy or availability of linked Web sites or the information contained on them. The linked Web sites, their operation and content are the responsibility of the person or entity for which they were created or maintained (the “Owner”). Both your use of a linked Web site, and your right to use or reproduce information or materials from a linked Web site, are subject to the terms of use governing that particular Web site. Any comments or inquiries regarding a linked Web site must be directed to its Owner.

**Copyright:** Canadian and international intellectual property laws protect the Content. Unless otherwise indicated, copyright is held by the Queen’s Printer for Ontario.

It is recommended that reference to the Content be made in the following form: <Author’s last name>, <Initials> <year of publication>. <Content title>; Ontario Geological Survey, <Content publication series and number>, <total number of pages>p.

**Use and Reproduction of Content:** The Content may be used and reproduced only in accordance with applicable intellectual property laws. *Non-commercial* use of unsubstantial excerpts of the Content is permitted provided that appropriate credit is given and Crown copyright is acknowledged. Any substantial reproduction of the Content or any *commercial* use of all or part of the Content is prohibited without the prior written permission of MNDM. Substantial reproduction includes the reproduction of any illustration or figure, such as, but not limited to graphs, charts and maps. Commercial use includes commercial distribution of the Content, the reproduction of multiple copies of the Content for any purpose whether or not commercial, use of the Content in commercial publications, and the creation of value-added products using the Content.

### Contact:

FOR FURTHER INFORMATION ON	PLEASE CONTACT:	BY TELEPHONE:	BY E-MAIL:
The Reproduction of Content	MNDM Publication Services	Local: (705) 670-5691 Toll Free: 1-888-415-9845, ext. 5691 (inside Canada, United States)	<a href="mailto:Pubsales@ndm.gov.on.ca">Pubsales@ndm.gov.on.ca</a>
The Purchase of MNDM Publications	MNDM Publication Sales	Local: (705) 670-5691 Toll Free: 1-888-415-9845, ext. 5691 (inside Canada, United States)	<a href="mailto:Pubsales@ndm.gov.on.ca">Pubsales@ndm.gov.on.ca</a>
Crown Copyright	Queen’s Printer	Local: (416) 326-2678 Toll Free: 1-800-668-9938 (inside Canada, United States)	<a href="mailto:Copyright@gov.on.ca">Copyright@gov.on.ca</a>

**LES CONDITIONS CI-DESSOUS RÉGISSENT L'UTILISATION DU PRÉSENT DOCUMENT.**

***Votre utilisation de ce document de la Commission géologique de l'Ontario (le « contenu ») est régie par les conditions décrites sur cette page (« conditions d'utilisation »). En téléchargeant ce contenu, vous (l'« utilisateur ») signifiez que vous avez accepté d'être lié par les présentes conditions d'utilisation.***

**Contenu :** Ce contenu est offert en l'état comme service public par le *ministère du Développement du Nord et des Mines* (MDNM) de la province de l'Ontario. Les recommandations et les opinions exprimées dans le contenu sont celles de l'auteur ou des auteurs et ne doivent pas être interprétées comme des énoncés officiels de politique gouvernementale. Vous êtes entièrement responsable de l'utilisation que vous en faites. Le contenu ne constitue pas une source fiable de conseils juridiques et ne peut en aucun cas faire autorité dans votre situation particulière. Les utilisateurs sont tenus de vérifier l'exactitude et l'applicabilité de tout contenu avant de l'utiliser. Le MDNM n'offre aucune garantie expresse ou implicite relativement à la mise à jour, à l'exactitude, à l'intégralité ou à la fiabilité du contenu. Le MDNM ne peut être tenu responsable de tout dommage, quelle qu'en soit la cause, résultant directement ou indirectement de l'utilisation du contenu. Le MDNM n'assume aucune responsabilité légale de quelque nature que ce soit en ce qui a trait au contenu.

**Liens vers d'autres sites Web :** Ce contenu peut comporter des liens vers des sites Web qui ne sont pas exploités par le MDNM. Certains de ces sites pourraient ne pas être offerts en français. Le MDNM se dégage de toute responsabilité quant à la sûreté, à l'exactitude ou à la disponibilité des sites Web ainsi reliés ou à l'information qu'ils contiennent. La responsabilité des sites Web ainsi reliés, de leur exploitation et de leur contenu incombe à la personne ou à l'entité pour lesquelles ils ont été créés ou sont entretenus (le « propriétaire »). Votre utilisation de ces sites Web ainsi que votre droit d'utiliser ou de reproduire leur contenu sont assujettis aux conditions d'utilisation propres à chacun de ces sites. Tout commentaire ou toute question concernant l'un de ces sites doivent être adressés au propriétaire du site.

**Droits d'auteur :** Le contenu est protégé par les lois canadiennes et internationales sur la propriété intellectuelle. Sauf indication contraire, les droits d'auteurs appartiennent à l'Imprimeur de la Reine pour l'Ontario.

Nous recommandons de faire paraître ainsi toute référence au contenu : nom de famille de l'auteur, initiales, année de publication, titre du document, Commission géologique de l'Ontario, série et numéro de publication, nombre de pages.

**Utilisation et reproduction du contenu :** Le contenu ne peut être utilisé et reproduit qu'en conformité avec les lois sur la propriété intellectuelle applicables. L'utilisation de courts extraits du contenu à des fins *non commerciales* est autorisée, à condition de faire une mention de source appropriée reconnaissant les droits d'auteurs de la Couronne. Toute reproduction importante du contenu ou toute utilisation, en tout ou en partie, du contenu à des fins *commerciales* est interdite sans l'autorisation écrite préalable du MDNM. Une reproduction jugée importante comprend la reproduction de toute illustration ou figure comme les graphiques, les diagrammes, les cartes, etc. L'utilisation commerciale comprend la distribution du contenu à des fins commerciales, la reproduction de copies multiples du contenu à des fins commerciales ou non, l'utilisation du contenu dans des publications commerciales et la création de produits à valeur ajoutée à l'aide du contenu.

**Renseignements :**

<b>POUR PLUS DE RENSEIGNEMENTS SUR</b>	<b>VEUILLEZ VOUS ADRESSER À :</b>	<b>PAR TÉLÉPHONE :</b>	<b>PAR COURRIEL :</b>
<b>la reproduction du contenu</b>	Services de publication du MDNM	Local : (705) 670-5691 Numéro sans frais : 1 888 415-9845, poste 5691 (au Canada et aux États-Unis)	<a href="mailto:Pubsales@ndm.gov.on.ca">Pubsales@ndm.gov.on.ca</a>
<b>l'achat des publications du MDNM</b>	Vente de publications du MDNM	Local : (705) 670-5691 Numéro sans frais : 1 888 415-9845, poste 5691 (au Canada et aux États-Unis)	<a href="mailto:Pubsales@ndm.gov.on.ca">Pubsales@ndm.gov.on.ca</a>
<b>les droits d'auteurs de la Couronne</b>	Imprimeur de la Reine	Local : 416 326-2678 Numéro sans frais : 1 800 668-9938 (au Canada et aux États-Unis)	<a href="mailto:Copyright@gov.on.ca">Copyright@gov.on.ca</a>



Ministry of  
Northern Development  
and Mines

Ontario

ONTARIO GEOLOGICAL SURVEY  
Open File Report 5831

Ontario Geoscience Research Grant Program  
Grant No. 364

Archean Au-Ag-(W) Quartz Vein/Disseminated Mineralisation within the Larder Lake -  
Cadillac Break, Kerr Addison - Chesterville System, North East Ontario, Canada

By

J.P. Smith, E.T.C. Spooner, D.W. Broughton and F.R. Ploeger

1993

Parts of this publication may be quoted if credit is given. It is recommended that  
reference to this publication be made in the following form:

Smith, J.P., Spooner, E.T.C., Broughton, D.W. and Ploeger, F.R. 1993. Archean  
Au-Ag-(W) Quartz Vein/Disseminated mineralisation within the Larder Lake -  
Cadillac Break, Kerr Addison - Chesterville System, North East Ontario, Canada,  
Ontario Geoscience Research Grant Program, Grant No. 364; Ontario Geological  
Survey, Open File Report 5831, 310p.

PSS LIBRARY





Ontario Geological Survey

OPEN FILE REPORT

Open File Reports are made available to the public subject to the following conditions:

This report is unedited. Discrepancies may occur for which the Ontario Geological Survey does not assume liability. Recommendations and statements of opinions expressed are those of the author or authors and are not to be construed as statements of government policy.

This Open File Report is available for viewing at the following locations:

Mines Library  
Level A3, 933 Ramsey Lake Road  
Sudbury, Ontario P3E 6B5

Mines and Minerals Information Centre (MMIC)  
Rm. M2-17, Macdonald Block  
900 Bay St.  
Toronto, Ontario M7A 1C3

The office of the Resident Geologist whose district includes the area covered by this report.

Copies of this report may be obtained at the user's expense from:

OGS On-Demand Publications  
Level B4, 933 Ramsey Lake Road  
Sudbury, Ontario P3E 6B5  
Tel. (705) 670-5691 Collect calls accepted.

Handwritten notes and sketches may be made from this report. Check with MMIC, the Mines Library or the Resident Geologist's office whether there is a copy of this report that may be borrowed. A copy of this report is available for Inter-Library loan.

This report is available for viewing at the following Resident Geologists' offices:

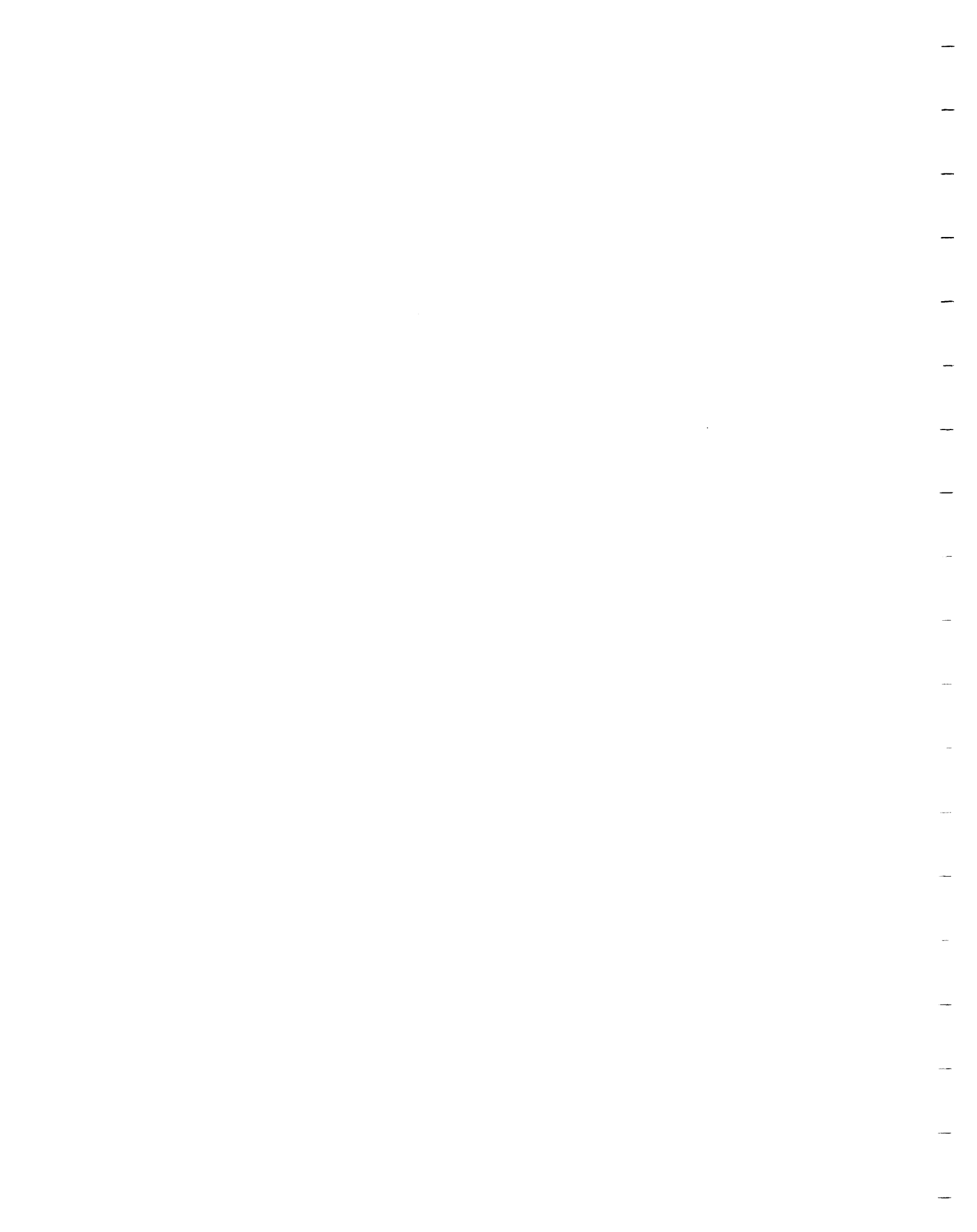
Cobalt, Box 230, Presley St., Cobalt P0J 1C0

Kirkland Lake, 4 Government Rd. E., Kirkland Lake P2N 1A2

Porcupine, 60 Wilson Ave., Timmins P4N 2S7

Sudbury, WGMC, 933 Ramsey Lake Rd., Level B3, P3E 6B5

The right to reproduce this report is reserved by the Ontario Ministry of Northern Development and Mines. Permission for other reproductions must be obtained in writing from the Director, Ontario Geological Survey - Geoscience Branch.

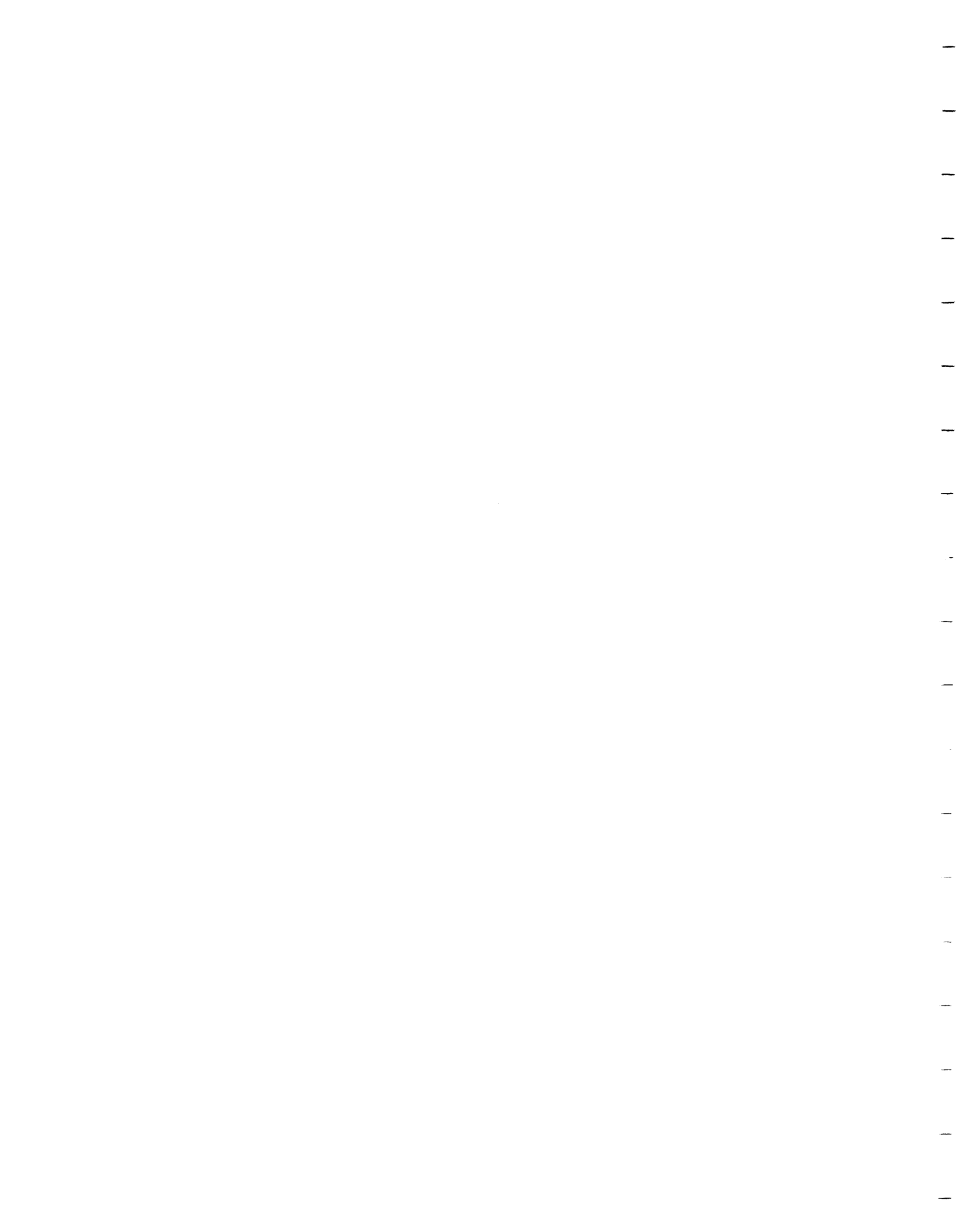


## TABLE OF CONTENTS

ABSTRACT.....	LXI
INTRODUCTION.....	1
Discovery and Production History.....	4
The Structural Nature of the Larder Lake-Cadillac Break.....	8
Structural and Kinematic observations; Kirkland Lake - Val d'Or.....	9
Lithologies associated with the Larder Lake-Cadillac Break....	14
North of the Larder Lake-Cadillac Break.....	14
South of the Larder Lake-Cadillac Break; West of Kearns...	19
South of the Larder Lake-Cadillac Break; East of Kearns...	20
Distribution of Ore Host Lithologies in the Kerr Addison- Chesterville Area.....	21
Ultramafic Horizon (Base of Larder Lake Group).....	21
South of the Ultramafic Horizon (Larder Lake Group).....	22
North of the Ultramafic Horizon (Timiskaming and Kinojevis Groups.....	23
Structural Development in the Virginiatown Area.....	25
The Nature of the Larder Lake-Cadillac Break.....	25
Sequence of Deformation (after Hamilton, 1986).....	26
Strain of host lithologies in the Kerr Addison-Chesterville Au system.....	29
Geological Characteristics and Distribution of the Principal Ore Types.....	32
Green Carbonate/Siliceous Break Ore.....	33
Flow Ore.....	35
"Albitite" Dyke Ore.....	38
Graphitic Ore.....	39
Ore Distribution Relative to Level Plan Geology.....	40
Ore Distribution Relative to Longitudinal Sections.....	41
Ore Distribution Relative to True Scale Vertical Cross Sections.....	43
Mineralised Zones outside the main Ore Zone.....	44
Time Sequence of Deformation, Hydrothermal Alteration, Mineralization and Igneous Intrusive Events.....	48
Kerr Addison Green Carbonate Ore Vein Stages.....	49
Kerr Addison Flow Ore Vein Stages.....	55
Kerr Addison Graphitic Ore Timing Relations.....	57
Kerr Addison "Albitite" Ore Timing Relations.....	58
Discussion of Timing Relationships; Correlation of Ore Types.....	58
Mafic "Albitite" Dyke Swarm/Intrusive Plug Igneous System....	60
Intrusive Time Sequence Relative To Deformation, Veining and Au introduction.....	62
Discussion of mafic "Albitite" Dyke Relationships.....	67
Characteristics, Distribution and Timing of Hydrothermal Alteration.....	69



Stages of Alteration; Ultramafic host rock.....	70
Type of Carbonate Alteration and their relevance to Au exploration.....	72
Longitudinal Contour Diagrams (Green Carbonate Ore).....	73
Methodology.....	73
Green Carbonate Alteration (Minus contained intrusion widths).....	74
Quartz veins (>0.3 m width).....	75
Percent quartz veins (>0.3 m width) in green carbonate Alteration.....	76
Total and percent mafic "Albitite" Dyke/Plug thickness....	77
General points from the longitudinal contour diagrams....	78
Vertical Trends in Green Carbonate Alteration and Quartz Vein/Dyke Area per Level.....	80
Methodology.....	80
Green carbonate Alteration.....	80
Quartz vein area.....	82
"Albitite" intrusion (Dyke/Plug) area.....	83
General points: Green carbonate/quartz vein/"Albitite" Dyke areal expansions.....	84
Vertical Trends in Ore Tonnage/Grade/Total Au and Au:Ag Ratio per Level.....	85
Ore Tonnage Vertical Trends.....	85
Ore grade vertical trends.....	87
Total Au vertical trends.....	89
Au:Ag ratio vertical trends.....	91
The Nature of the Bottom and Top of the Kerr Addison- Chesterville Ore System.....	93
The bottom.....	93
Genetic aspects of deep level studies.....	99
The top.....	100
Discussion; Exploration, Ore Controls and Genetic Aspects....	103
Principal geological/geochemical exploration guides.....	103
The Kerr Fault: A late post-ore, Not a major hydrothermal feeder structure.....	107
Principal macroscopic ore controls.....	108
Evidence for Au precipitation mechanisms.....	116
Discussion of the "Fault Valve" model.....	119
Discussion: Relevance of "Young" U-Pb ages.....	122
Comparison with Archean Au-quartz vein systems in the Timmins-Val d'Or area.....	124
Overall genetic aspects and significance of the Kerr Addison "Albitites".....	127
Principal Conclusions.....	130
Dedication to J.W. Baker.....	138
Acknowledgements.....	139
References.....	140
Appendix: Deep Quartz Vein/Dyke Intersections(4800/5600 ft levels and below.....	168



## List of Figure Captions

- |          |   |                                  |
|----------|---|----------------------------------|
| Figure 1 | Location map showing the Larder Lake - Cadillac Break, the distribution of stratigraphic units and the location of 71 major Au mines along the Break structural corridor in Ontario and Quebec. The key to mine numbers and sizes, and the stratigraphic legend (after MERQ-OGS, 1983) are shown in map insets.   |                                  |
| Figure 2 | Yearly Au and Ag production, 1938-1989; Kerr Addison mine.  | <b>Back pocket</b><br><b>168</b> |
| Figure 3 | Compiled $D_1/D_2$ kinematics of the Larder Lake - Cadillac Break based on work by previous structural geologists. Most published results are compatible with $D_1$ NNE-SSW compression event followed by $D_2$ NW-SE compression. The precise kinematics observed depend on the relative orientation of the Break segment to each of these deformation events.   | <b>169</b>                       |
| Figure 4 | S. Abitibi regional geochronological and structural time sequence compilation diagram based on published data by Frarey and Krogh (1986), Mortensen (1987a,b), Corfu et al. (1989), Wyman and Kerrich (1989) and Corfu et al. (1991). Based on this study, the shaded interval represents the most likely period of Au mineralisation at Kerr Addison (syn-kinematic to late $D_2$ deformation) from ~2675-2670 Ma i.e. syn-"albitite" intrusion in age.  | <b>170</b>                       |
| Figure 5 | Distribution of ultramafic lithologies along the Larder Lake - Cadillac Break (after Tihor and Crocket, 1977). Ultramafic rocks showing various stages of alteration occur semi-continuously all the way along the Break from Kerr Addison to west of Kirkland Lake, supporting the hypothesis that these were laterally extensive and important in localising the fundamental Break thrust contact.  | <b>171</b>                       |
| Figure 6 | Geological map of McVittie and McGarry Townships (modified from Downes, 1980) showing the distribution of lithologies, and the opposing plunges of macroscopic folds on either side of the Break structure. Hamilton's (1986) structural domains and the structural breaks between them are indicated. The location of the Kerr Addison mine area in Figure 7 is also indicated. From west to east, the mine sites shown along the Break are: Omega (O), Fernland (FL), Cheminis (C), Barber-Larder (BL) and Armistice (A). | <b>172</b>                       |

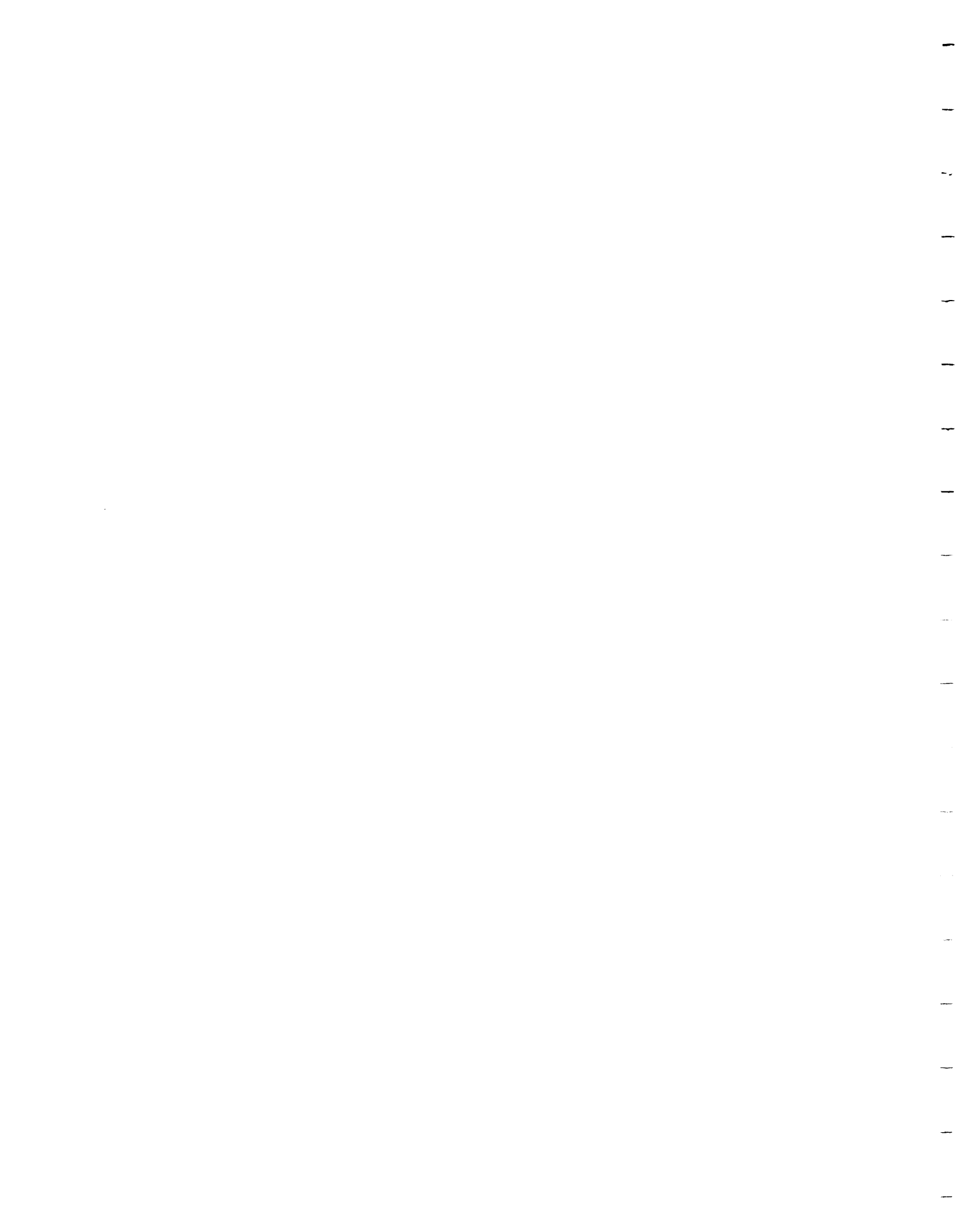




Figure 7 Surface geological map (1 inch : 400 ft) of the Kerr Addison - Chesterville mine area, showing the trace of the Larder Lake - Cadillac Break, and the Town/ Chesterville "G" Zone, Mill Zone and Lake Zone outside the main ore system (redrawn from a 1940s Kerr Addison mine surface geological plan, with additions from mapping and surface observations by Ruth Jones, B.Sc. student, Oxford University, J.P.S. and E.T.C.S., 1989, and a surface map of McGarry Township in Hamilton, 1986). The location of mine shafts, adits, original surface outcrops of quartz-carbonate veining, and the location of the 175 ft level plan (Figure 27) are indicated; adits are from Thomson, J.E. (1941).

**Back pocket**

Figure 8 Schematic section across the Barber-Larder open pit, looking ENE along the strike of the Break. The most important features to note are the fundamental Break thrust contact between Larder Lake ultramafic komatiites and Timiskaming sediments (north), and the south-facing nature of the stratigraphic successions either side of this contact as inferred from way-up determinations (trough cross-bedding in Timiskaming fluvial sandstones, normal grading and load structures in Larder Lake distal turbidites). Ore in the Barber Pit was of a pyritic replacement type. Late carbonate extension veins also occur, which are similar to those at Kerr Addison. Dip of the sediments and mafic/graphite contact is  $\sim 60^\circ\text{S}$ ; dip of mafic/ultramafic contact is sub-vertical (D.W.B.).

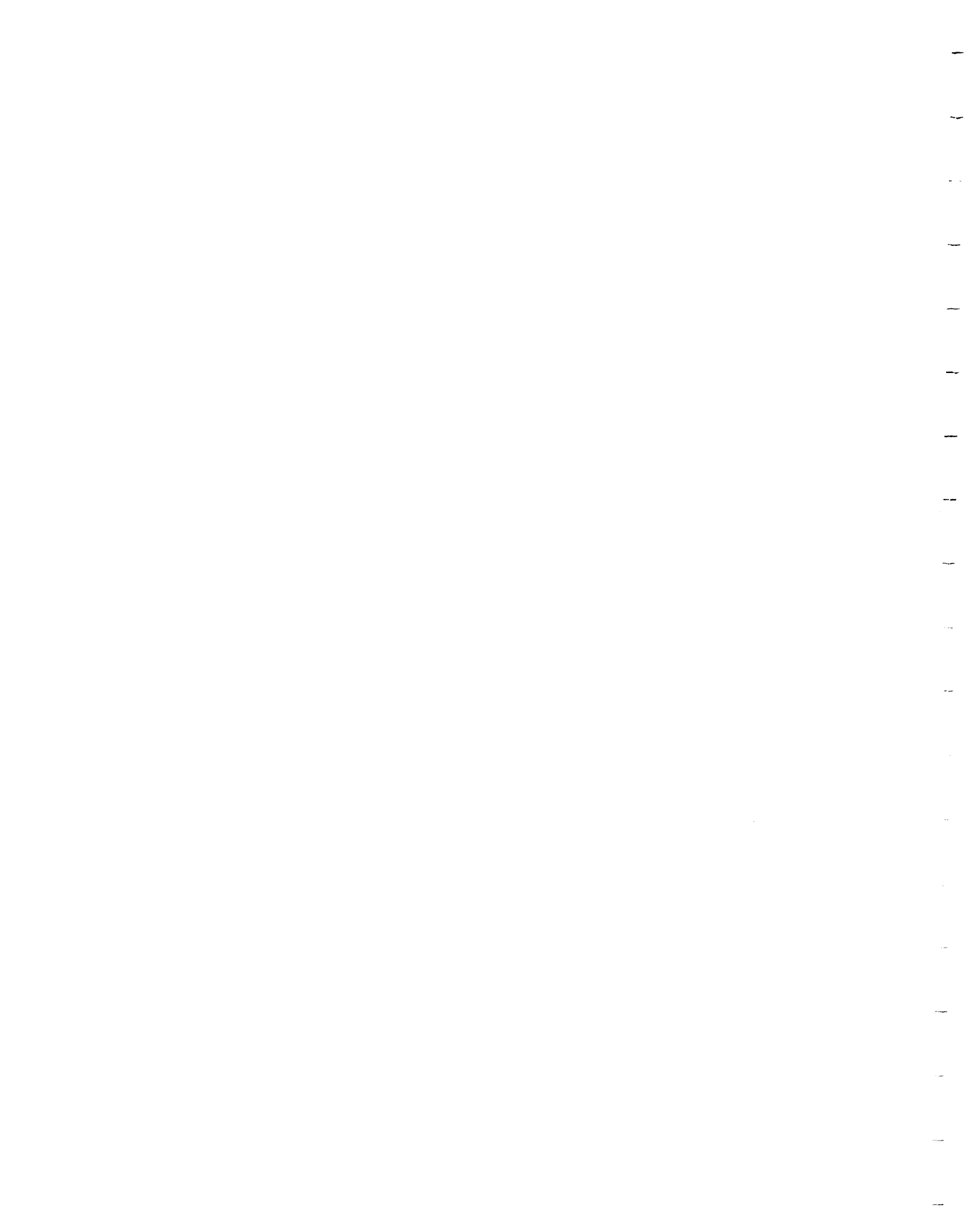
173

Figure 9a Stereographic projection of poles to  $S_0$  (bedding) fabric, McGarry Township (redrawn from Hamilton, 1986). These show  $\pi$ -girdles with opposite senses on either side of the Break (i. and ii.) due to the superimposed effects of both  $D_1$  (N-S compression) and  $D_2$  (NW-SE compression).

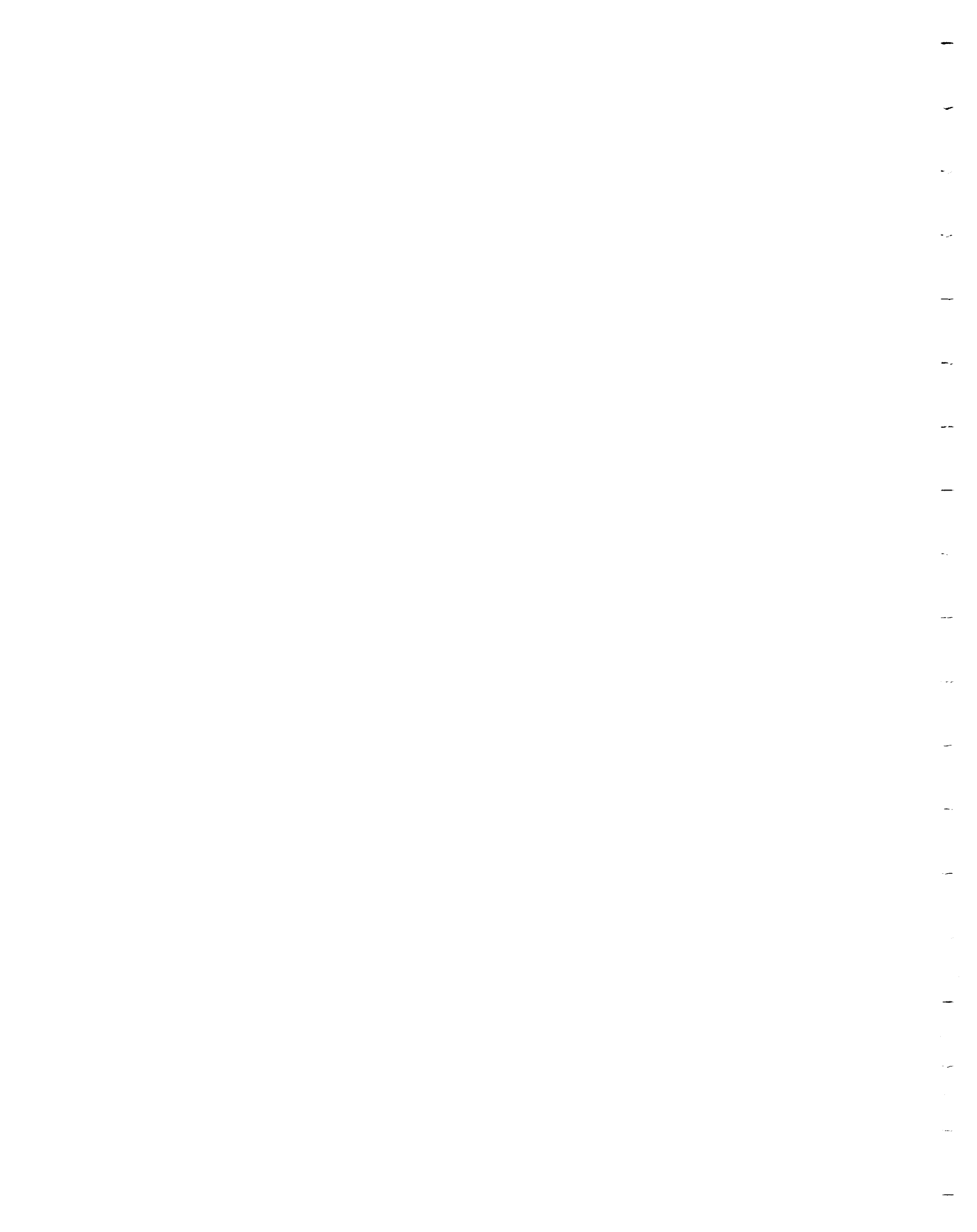
Figures 9b Stereographic projection of poles to  $S_1$  fabric, and  $L_1$  intersection lineation, McGarry Township (after Hamilton, 1986). Hamilton (1986) found that near the Break the  $S_1$  fabric was almost replaced by the stronger  $S_2$  fabric.

Figures 9c Stereographic projection of poles to  $S_2/S_3$  fabrics, and  $L_2$  stretching lineation, McGarry Township (after Hamilton, 1986). Sub-vertical lineations suggest a significant vertical component of displacement on Break-related shear zone structures. The regional  $S_2$  cleavage has identical strike ( $\sim 055^\circ$ ) and dip (mostly steep NW-dip) to the predominant fabric in the Kerr Addison mine (see Figure 34). Locally south-dipping fabrics suggest that fabrics may anastomose in three dimensions within zones of deformation.  $S_3$  is a sub-vertical crenulation cleavage noted by Hamilton (1986) to offset  $S_2$  with sinistral sense.

174



- Figures 10a/b Stereographic projection of poles to foliation in: (a) green carbonate ore and (b) flow ore (based on mapping data of J.P.S. and D.W.B.). The predominant foliation in both ore types is that of the Break in this locality i.e. steep NW dip, mean strike direction 055°. There are, however, a few cases of steep SE dipping fabrics. 175 176
- Figure 11a Foliation intensification in talcose ultramafic rocks typical of a ~12 m wide, very highly strained zone south of the fundamental structural contact between Timiskaming sediments to the north and spinifex-textured ultramafic rocks (Figure 15a) at the base of the Larder Lake group to the south; 3850 ft level. The exact location of the photograph (P2) is given on the 3850 ft level plan (Figure 23). The visible part of the scale is 9 cm long. 177
- Figure 11b Foliation intensification in fine-grained sediments typical of a ~26 m wide very highly strained zone north of the fundamental structural contact between Timiskaming sediments and spinifex-textured ultramafic rocks (Figure 15a) at the base of the Larder Lake group to the south; 3850 ft level. The exact location of the photograph (P1) is given on the 3850 ft level plan (Figure 23). The visible part of the scale is 12 cm long.
- Figure 12 Steep east-plunging lineation defined by stretched varioles in pillowed Fe-tholeiite host rocks to the flow ore; 1021-58 drift, 1000 ft level, scale in cm. 178
- Figure 13 Typical "siliceous break" feeder quartz vein ~1.1 m wide; note included wallrock fragments which are typical and in many cases more abundant (see Figures 33d, 40a and 62). The lower right hand side of this "siliceous break" vein contained significant fine-grained visible Au. Location: 1014-52 stope, central western part of the system; 1000 ft level. Scale in cm and inches. 179
- Figure 14. Typical well-defined "albitite" dyke ~1 m wide; 3850 ft level. In relative timing it is an A<sub>1</sub> dyke (see relative timing summary diagram; Figure 32). The exact location of the photograph (P1) is given on the map of the 3815-79 stope (Figure 46b). Scale = 1 m. 180
- Figure 15a Pseudomorphed spinifex texture in green (fuchsitic) carbonate-altered ultramafic rocks cross-cut by a network of quartz-carbonate veins and veinlets; sub-ore grade; 3850 ft level. The olivine pseudomorphs are up to ~15 cm long.



The exact location of the photograph (P5) in the 3803 East Drift is given on the 3850 ft level plan (Figure 23). Scale in cm and inches.

Figure 15b Typical example of an  $A_1$  "albitite" dyke ~1.5 m wide; 3850 ft level. The dyke cross-cuts stage #2 carbonate veining and is cross-cut by late, shallow-dipping stage #8 quartz-carbonate veins (see Figure 32). The exact location of the photograph (P3) in the 3803-57 North Crosscut is given on the 3850 ft level plan (Figure 23). Scale = 1 m.

Figure 15c Typical green carbonate ore showing a network of milky quartz-carbonate veins many with "open" intersections cross-cutting green carbonate altered ultramafic material; 3850 ft level. Note the higher density of occurrence of thicker quartz veins in this ore grade material compared with the sub-ore grade material in Figure 15a. The quartz veins are typically ~0.5-10 cm wide. Scale in cm and inches.

Figure 15d Hydrothermal brecciation in the hanging wall of a thick quartz vein in a green carbonate ore stope; 3850 ft level. The entire vein system which defines this small stope (3815-73 stope) originates from this major guide quartz vein. The exact location of the photograph (P6) is given on the 3850 ft level plan (Figure 23). The scale is ~0.7 m long.

181

Figure 16 Geological map of the Chesterville 9D1 green carbonate orebody at the extreme east end of the ore system; ~1150 ft level (after Buffam and Allen, 1948). Note the extremely irregular, branching quartz veins which constitute the ore in this stope; these die out into less altered talcose ultramafic rocks to the east.

182

Figure 17a Typical strained (flattened) Fe-tholeiite pillow showing a variolitic rim; note the moderately developed foliation. This lithology is typical of the host for flow ore; 1117-66 stope (back), 1000 ft level. The deformed pillow is ~30-40 cm wide.

Figure 17b Typical flow ore showing four, sub-parallel, weakly deformed and relatively thin quartz-carbonate veins cutting moderately foliated Fe-tholeiite volcanic material. Note (i) the approximately symmetrically developed selvages of

183



disseminated pyrite with thicknesses (~3-6 cm) greater than the quartz-carbonate veins (~1-2 cm), and (ii) the preferential location of pyrite grains along the foliation. Au is present as small blebs in the pyrite grains. 2616-53 stope, 2500 ft level.

Figure 18 Underground geological map of the 1117-63 flow ore stope, showing primary lithological variations and their controls on the location of Au mineralisation; 1000 ft level, Kerr Addison (by D.W.B.). Note the deformed pillow outlines shown schematically in the Fe-tholeiite volcanics (see Figure 17a).

184

Figure 19 Underground geological map of the 814-61 Au-quartz vein/disseminated pyritic ore sill, showing the control on Au mineralisation of two bounding vein/fault structures; all veins inside the stope either branch off one of the major structures, or else connect between the two; disseminated pyrite occurs as selvages to the larger veins; 1000 ft level (by D.W.B.). P1 = Figure 36b.

185

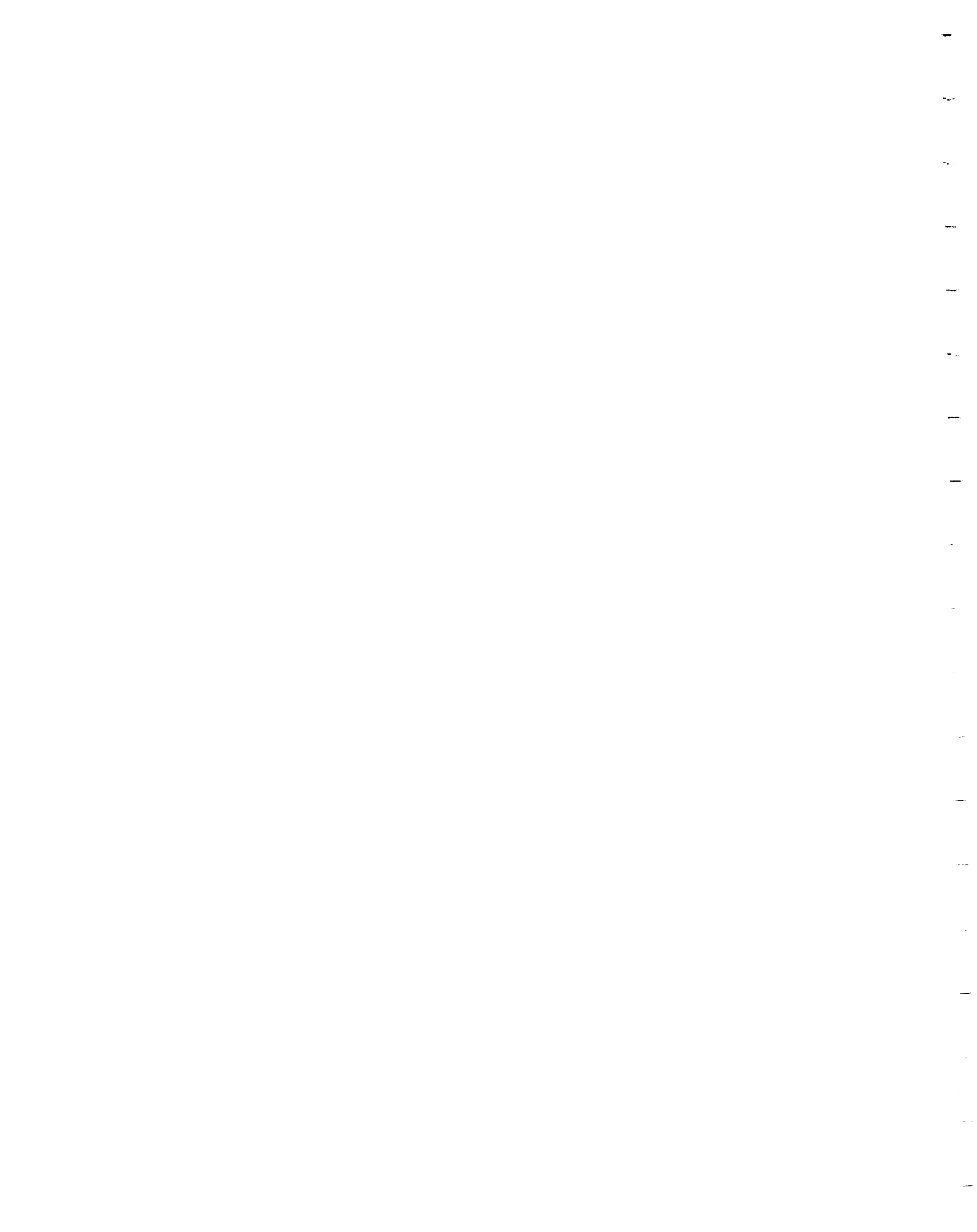
Figure 20 Reconstructed geological level plan, Kerr Addison mine; 5600 ft level. The entire hydrothermal envelope of the ore system has condensed down to a single small root zone of dimensions ~300 m (strike length) x 20-50 m (width). The total volume of hydrothermal fluid and magma which produced Au-quartz vein mineralisation and the "albitite" dyke swarm at higher levels must have passed up through this small root zone. Also of interest on this level is a discontinuous ~250 m strike length weakly mineralised zone ("Diorite Zone") within and localised along an elongate porphyritic intrusion (identification based on drill core examination). This zone may connect to the Town Zone or other Au exploration targets at higher levels (e.g. 3700 ft; 1000 ft levels).

**Back pocket**

Figure 21 Reconstructed geological level plan, Kerr Addison mine; 4800 ft level. This plan shows the small, limited area occupied by the green carbonate alteration envelope, centred around the deep Chesterville intrusive plug.

**Back pocket**

Figure 22. Kerr Addison 4400 and 4200 ft level reconstructed geological plans. Large (up to ~8-10 m wide) central vein feeder structures can be seen to branch upwards supplying hydrothermal ore fluids to higher levels of the mine and causing the green carbonate alteration envelope to widen upwards. *However, these veins do not carry significant Au values at these levels and have not been stoped.* The





- bottom of the #21 flow orebody lies in the SW corner of the ore system at these levels (e.g. 4421-54 1/2 stope, 4200 ft level). 186
- 187
- Figure 23 Reconstructed geological level plan for the 3850 ft level of the Kerr Addison mine (see Figures 28 and 29). The exact area of the detailed geological map for the 3815-79 stope and north crosscut (Figures 46a and b) is shown at the east end of the plan. The exact locations of the following photographs are also shown: P1, Figure 11b; P2, Figure 11a; P3, Figure 15b; P4, Figure 33b; P5, Figure 15a; P6, Figure 15d; and P7, Figure 36a. **Back pocket**
- Figure 24 Reconstructed geological level plan, Kerr Addison - Chesterville mines; 2650 ft level. This plan shows the separate Chesterville East Zone to the east along the Break. **Back pocket**
- Figure 25 Reconstructed geological level plan, Kerr Addison - Chesterville mines; 1750 ft level. This plan shows the Chesterville intrusive plug branching laterally to the west into the "albitite" dyke swarm. **Back pocket**
- Figure 26 Reconstructed geological level plan, Kerr Addison - Chesterville mines; 700 ft level. **Back pocket**
- Figure 27 Reconstructed geological level plan, Kerr Addison mine; 175 ft level. This plan shows the extremely patchy development of economic Au mineralisation, quartz veins and "albitite" dykes near the surface. The #26 orebody (83 ft level) was the site of some early (1907) exploration drifts by the Reddick party from the Reddick shaft. The #10 orebody is the location of the original discovery intersection hole, and presently the site of a large 300 ft deep glory hole due to a surface cave-in. **Back pocket**
- Figure 28 Vertical longitudinal section of the green carbonate ore; looking NW perpendicular to the strike of the Larder Lake - Cadillac Break which contains the ore system. The diagram shows a number of green carbonate orebodies which originate at three root zones within an overall green carbonate alteration envelope plunging at ~70°E to a deep (≥4 km) focal fluid source. The root zones, on the ~4000 ft level, are related to two minor and one major mafic "albitite" intrusive plug (outlined in bold). The major plug in the east part of the system is known as the Chesterville plug, and was stoped in places for ore, as was the western plug (15W orebody). The alteration envelope contracts with depth around the down-



dip extension of the Chesterville plug (see 4800 ft level, Figure 21; deep drill section, Figure 63) and deep drill holes (marked) intersected economic Au mineralisation within this plug at ~2000 m depth. The smaller, blind Chesterville East orebody plunges sub-parallel to the main Kerr Addison - Chesterville ore system and remains a good exploration target, open at depth and to the east. It contained "albitite" dykes and green carbonate alteration at the 2650 ft level (see Figure 24).

188

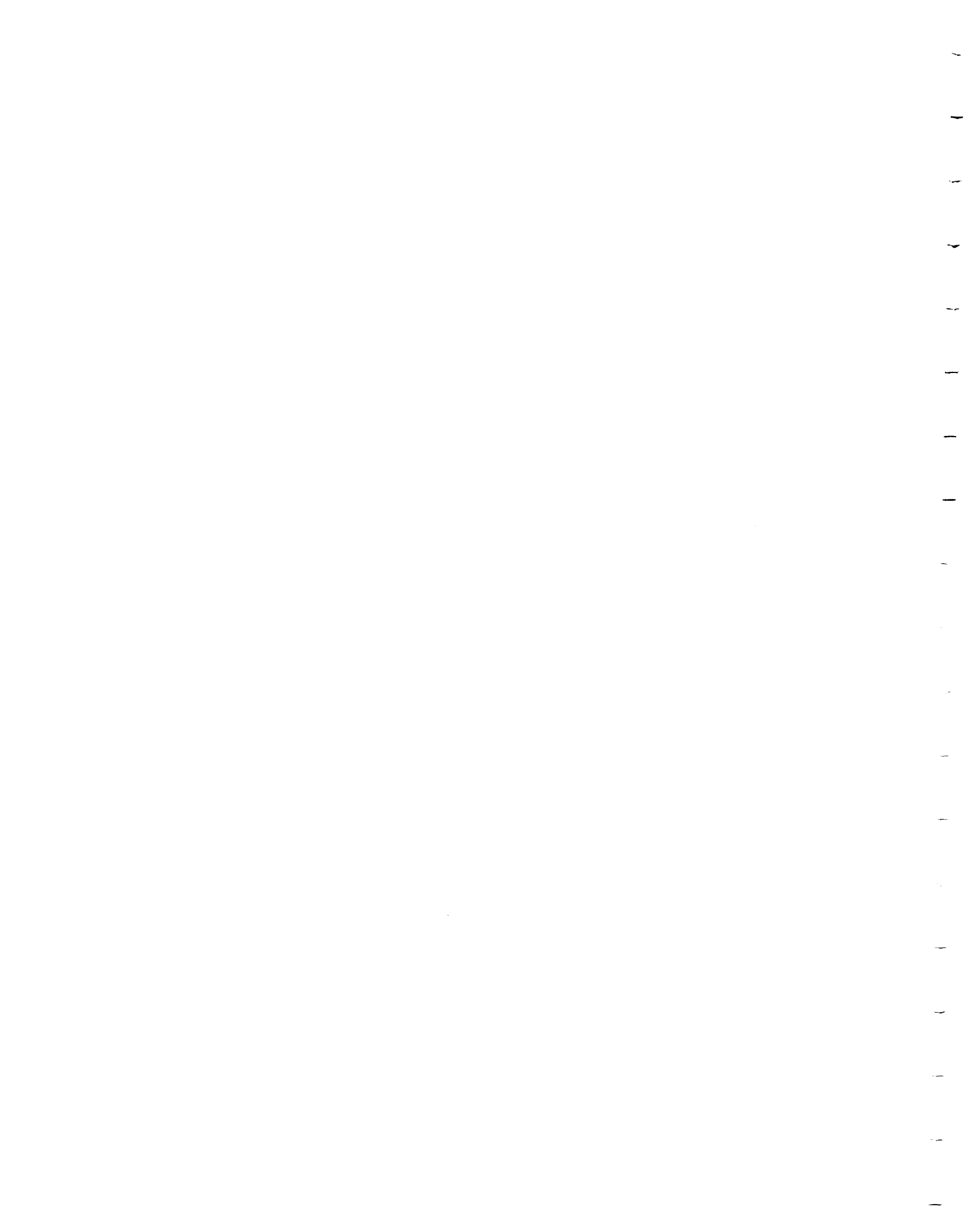
Figure 29 Vertical longitudinal section of the flow ore, Kerr Addison - Chesterville Au system; looking NW perpendicular to the strike of the Larder Lake - Cadillac Break which contains the ore system. The outline of the green carbonate alteration envelope in the adjacent ultramafic host rock has been shown for reference. The flow ore is spatially related to the adjacent green carbonate (i.e. they share a common source of hydrothermal ore fluids from depth) but occurs slightly asymmetrically to the west of the alteration envelope. A number of flow orebodies were developed at the upper east part of the ore system, where there has been some stacking due to post-ore faulting (e.g. branches of the Kerr Fault). Flow ore pinches out stratigraphically in a root zone at the 4600 ft level of Kerr Addison and the favourable Fe-tholeiite horizon susceptible to Au mineralisation is not found again at depth adjacent to the path of fluid ascent north of the Kerr Fault. The #16 and #21 flow ore bodies die out upwards before reaching surface due to a combination of stratigraphic and fault termination.

189

Figure 30 True-scale vertical cross-section normal to the strike of the Kerr Addison orebody; mine section 56E; looking ENE along the Break. This section demonstrates the extreme down-dip continuity of the orebody (~1340 m) compared to its average width (~120 m max.). Green carbonate alteration in the ultramafic host rock and stoped ore can be shown to be exactly spatially related to "siliceous break" major Au-quartz vein feeder structures (in black). Sheet-like barren "horses" of relict talc-chlorite-carbonate ultramafic host rock, essentially unaltered by Au-related hydrothermal ore fluids, occur especially in the upper part of the mine (e.g. 300 ft to 1900 ft level). The bulk of the ore is developed either side of the footwall contact of the ultramafic host rock with Fe-tholeiites (e.g. #21 orebody).

**Back pocket**

Figure 31 True-scale cross-section of the upper levels of the Chesterville mine; looking ENE along the strike of Break; redrawn from Buffam and Allen (1948). This diagram shows the close correspondence of green carbonate ore (D, F and J orebodies) in



the ultramafic host rock with intrusive dykes and plugs of "albitite" (termed "syenite" by the authors). Some of the orebodies were developed within the syenite plugs themselves. The fundamental Break contact with Timiskaming sediments to the north is also shown.

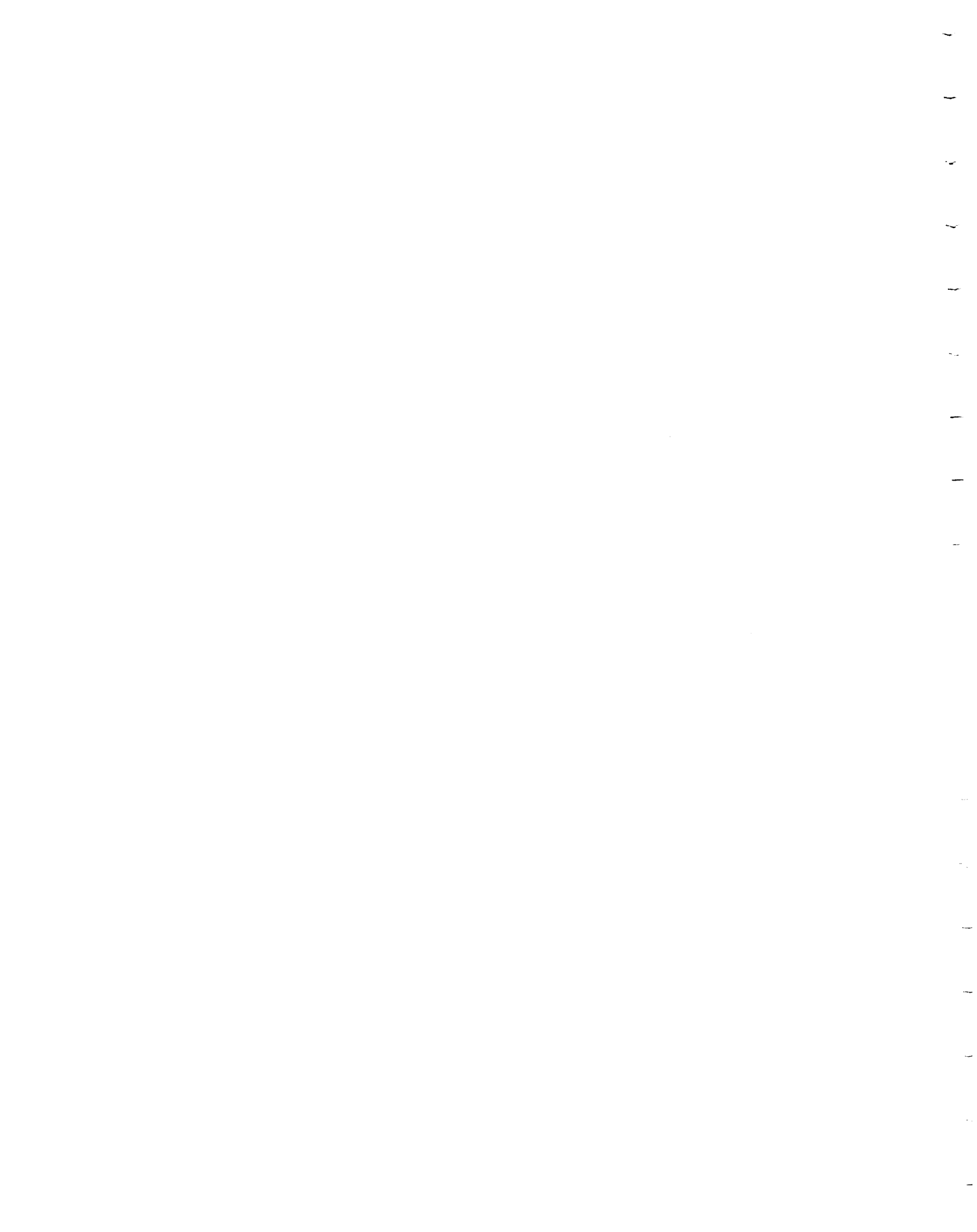
190

**Figure 32** Relative time sequence diagram of quartz-carbonate veining, ductile deformation, hydrothermal alteration, Au mineralisation and igneous intrusive events in the two major ore types of the Kerr Addison - Chesterville Au system. Correlation between the flow and green carbonate ores is based on mapping and tracing vein structures across their mutual boundary (e.g. 850 ft level, 821-66 rib), their identical average ore Au:Ag ratios of ~18:1, and similar vein geometries and orientations (see Figure 34a,b). Au mineralisation in both ore types is contained within the interval of ductile deformation in the Break (based on mapping and underground observations). Green carbonate ore shows five Au-related vein stages, whereas the flow ore, being a more competent unit, shows only two. Green carbonate ore is also intruded by three stages of mafic "albitite" dykes and plugs which are syn-Au mineralisation - this observation being constrained by rigorous underground mapping and documentation of cross-cutting and relative timing relationships (see text and photographs). Both ore types are affected by a number of post-ore faults, slips and barren quartz-carbonate veins, indicating that fluids were still active post-Au mineralisation.

191

**Figure 33a** Early, unstrained in this case, stage #1 (Figure 32) polygonal carbonate veins cutting talc-chlorite altered ultramafic material; 1014-52 stope, 1000 ft level. The polygonal carbonate veins in this example are thicker than normal and contain coarse "lumpy" carbonate grains; the geometry, however, is typical. As can be seen, the polygons are ~1-10 cm across; scale in cm and inches.

**Figure 33b** Strained, approximately fabric-parallel, early (stage #1, Figure 32) polygonal carbonate veins in foliated talc-chlorite altered ultramafic material; 3850 ft level. Note (i) some long sections of carbonate veins sub-parallel to the foliation indicating that an early fabric was present at the time of vein formation (Figure 32) in order to provide controlling anisotropy, and (ii) several examples of folded vein "bridges" defining the flattened polygons where carbonate veins are at a high angle to fabric. The carbonate veins are a typical ~0.25-1 cm wide. The exact location of the photograph (P4) is given on the 3850 ft level plan (Figure 23). Scale in cm.



- Figure 33c Typical stage #3 (Figure 32) grey-green, fine-grained "cherty siliceous break" vein ~8 cm wide (tip of ruler). The "cherty sil. break" is pale grey in the photograph and guides a younger (stage #4) main stage milky white quartz vein on its left margin. 814-61 sill, 850 ft level; scale in inches.
- Figure 33d Main stage (stage #4; Figure 32) "siliceous break" vein ~40 cm wide containing numerous  $A_1$  "albitite" dyke fragments and cross-cut by post-ductile deformation late, shallow dipping stage #8 quartz-carbonate "flat" veins (see Figure 32). This photograph shows clearly that main stage Au veins cut earlier  $A_1$  "albitite" dykes (Figure 32). 1014-52 stope, 1000 ft level; scale in cm and inches. 192
- Figures 34a/b Stereographic projections of poles to main stage (#4) Au-quartz veins in (a) green carbonate ore and (b) flow ore; from mapping in green carbonate ore stopes (D.W.B., J.P.S.). The two ore types show a great deal of similarity in their vein orientations (e.g. similar clusters of steep NW- and SE-dipping veins, possibly a conjugate set related to the strike of pervasive Break foliation). However, the green carbonate ore appears to have an extra steep SW- and NE-dipping vein set not found in the flow ore. Both ore types show a relatively low frequency of flat or shallow veins. 193
- Figure 34c Stereographic projections of poles to late  $020^\circ$  trending Au-quartz-galena-sphalerite (#5) veins and late (#6) mylonitic faults; from mapping in green carbonate ore stopes (J.P.S., D.W.B.). The majority of these veins are steep NW-dipping, but their strike orientations can be quite variable. 194
- Figure 34d Stereographic projections of poles to "albitite" dyke contacts; from mapping in green carbonate ore stopes (J.P.S., D.W.B.). The majority of dykes are north-dipping and sub-parallel to the predominant foliation. However, a few are south-dipping or locally have south-dipping contacts, cross-cutting foliation. Very few dykes have shallow or flat orientations. Thus dykes are broadly co-structural with major "siliceous break" quartz veins (see open circles in Figure 34a) in the green carbonate ore but do not exhibit the wide range (e.g. flat veins) shown by the thinner Au-quartz veins and stringers. 195
- 196

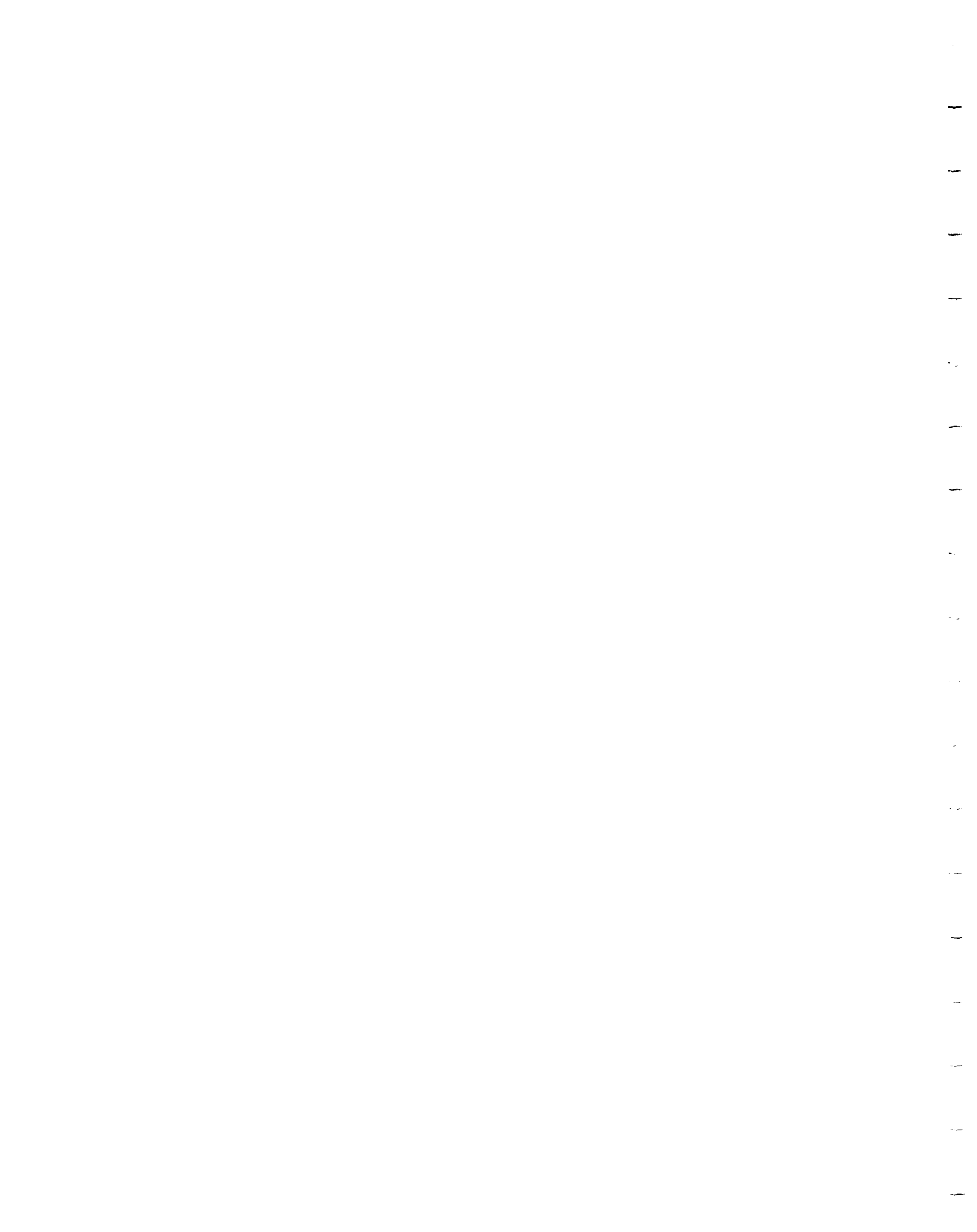




Figure 35 Geological map of the deepest green carbonate ore stope (4014-63 1/2) and area in the root zone of the green carbonate ore, Kerr Addison mine, showing the control on deep Au mineralisation by a single, branching and anastomosing "siliceous break" vein structure (by J.P.S.). This ~2 m wide feeder quartz vein was photographed at point P1 in the diagram (see Figure 62).

197

Figure 36a Clear example of folded main stage #4 milky quartz veins in a ductile high strain zone in green carbonate altered ultramafic material; 3815-73 stope, 3850 ft level. The fact that the main stage veins are deformed indicates that they formed before the end of ductile deformation (see Figure 32). The exact location of the photograph (P7) is given on the 3850 ft level plan (Figure 23). For scale, the rock bolt plate is 10.5 cm square.

Figure 36b Tightly folded main stage (FL#2; Figure 32) quartz vein in flow ore developed in strained transitional mafic-ultramafic host rocks; 814-61 sill, 850 ft level. The exact location of the photograph (P1) is shown on the map of the 814-61 sill in Figure 19. The end of the ruler is 20 cm long.

Figure 36c Partially rounded main stage (#4) vein fragments in a post-Au mineralisation, post-ductile deformation stage #6 fault breccia (see Figure 32 for relative timing). The fault breccia is ~2 m wide in this location and partly follows an earlier "siliceous break" structure. 2015-62 East Drift, 2050 ft level. Scale in cm and inches.

Figure 36d Relatively undeformed, thin quartz vein stringers with marginal pyrite alteration contrasting with an earlier deformed (folded) thicker main stage (FL#2; Figure 32) vein, all developed in flow ore; 1117-66 stope, 1000 ft level. The thicker quartz veins can be dark and smoky. For scale, the rock bolt plates are 10.5 cm square.

198

Figure 37 Width histogram of Au-quartz veins, Kerr Addison - Chesterville Au system, based on measurement of 10,459 individual random drillhole intersections normal to quartz vein average strike direction. The distribution is logarithmic with a mean width of 0.62 m. Au-quartz veins measured ranged from <0.3 m (data truncated at this cut-off) to ~11 m in width. Veins <0.3 m wide were observed during mapping to be twice as numerous as those >0.3 m.

199

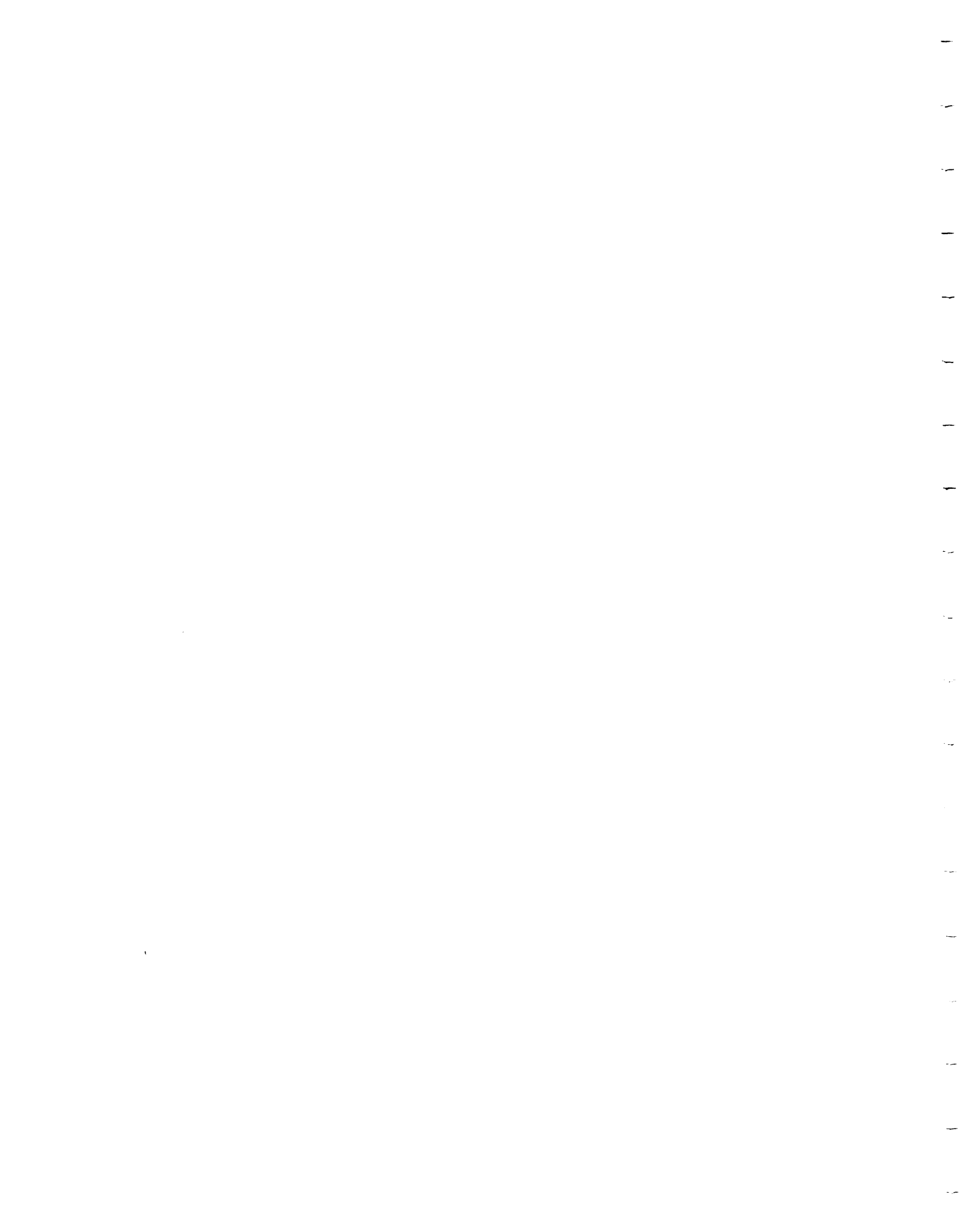


Figure 38 Looking up into the back; late (stage #5, Figure 32) Au-quartz-galena-sphalerite vein cross-cutting mottled main stage (#4) "siliceous break" vein material; 1610-251/2 sill, 1600 ft level. Stage #5 is the last stage of primary Au mineralisation and the last vein stage to have formed within the period of Break related ductile deformation (see Figure 32). This vein shows a well developed ribbon texture formed by crack-seal. For scale, the rock bolt plate is 10.5 cm square.

200

Figure 39 Vertical longitudinal projection of the Kerr Addison - Chesterville Au system showing the effect of the Kerr Fault displacing the flow ore bodies; looking NNW perpendicular to the strike of the Break. Fault vectors A-A', B-B' and C-C' match up the eastern edge of the present #16 orebody with the intersection trace of the Kerr Fault and the present western edge of the #21 orebody. The north-dipping Kerr Fault apparently displaced the south side, including a block of flow ore formerly connecting the #21 and #6 orebodies, downwards (~300 m) and to the east (~340 m) i.e. reverse north side up sinistral motion. These data are in agreement with mapped small-scale kinematic indicators and matching of Au grade-depth peaks (see text).

201

Figure 40a Typical "siliceous break" main stage vein ~1 m wide showing well developed sub-parallel elongate wall rock inclusions formed by a coarse crack-seal process. This "siliceous break" vein is part of the main stage (#4) event in green carbonate ore (see Figure 32). At this locality (866 South Crosscut; 850 ft level) this main stage "siliceous break" vein is developed in transitional material only ~3.5 m north of the contact with the Fe-tholeiite volcanic material which is the host to flow ore. In fact, this photograph and Figures 40b-d are of locations in a crosscut within a rib separating two major stopes in the upper part of the largest flow orebody (#21; see Table 3) - the 1021-65 and 1021-68 stopes. This crosscut contains a mapped transition from green carbonate ore into flow ore; marginal veins from the main stage "siliceous break" vein in this photograph pass laterally into flow ore host rock where their margins become rich in disseminated pyrite thus demonstrating a direct correlation between green carbonate main stage (#4) and flow ore main stage (FL#2). The visible part of the scale is ~8 cm long.

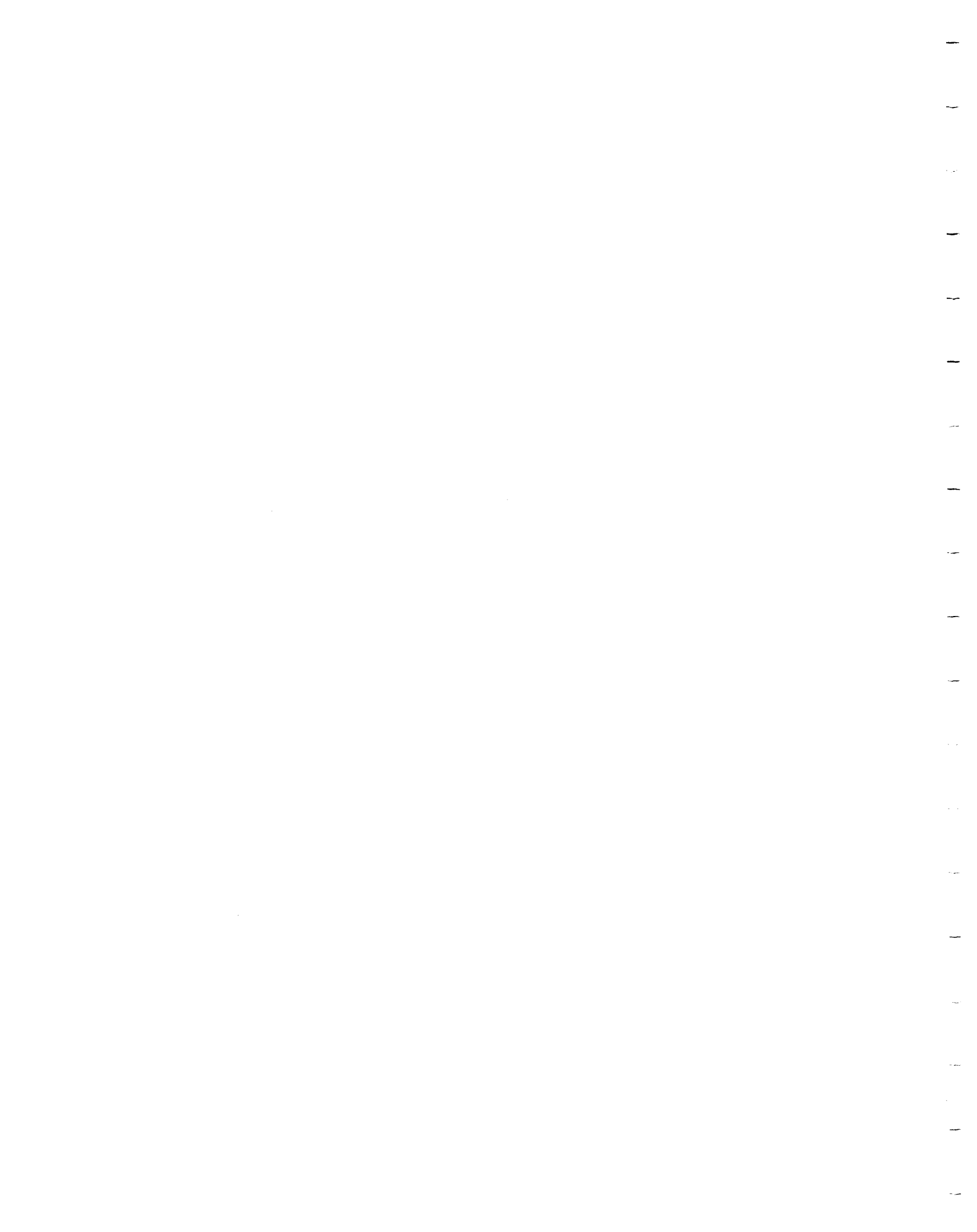


Figure 40b Looking up into the back; "siliceous break" related quartz veining (main stage #4) cross-cutting the contact between transitional material (lower part of the photograph) and flow ore host material (Fe-tholeiite volcanics; upper part of the photograph). Visible part of the scale is ~7 cm long. 866 South Crosscut, 850 ft level.

Figure 40c Curved and branching "Hollinger-McIntyre" style sub-parallel quartz-carbonate veins with sharp terminations within flow ore host material; 866 South Crosscut, 850 ft level. The veins, especially the terminations, show well-developed pyritic selvages. For scale, the end of the ruler is 20 cm long.

Figure 40d Strong development of wall rock disseminated pyrite around the angular termination of a quartz-carbonate vein in flow ore host material; #21 orebody, 866 South Crosscut, 850 ft level. Similar features have been observed in the Hollinger-McIntyre ore system, Timmins (e.g. see Figure 6 of Wood et al., 1986). Scale in cm.

Figure 41 Comparison of the distribution of "albitite" intrusions on Kerr Addison - Chesterville level plans for the 1150, 1000, 850 and 500ft levels which clearly shows a drop in size and frequency of intrusions per level as the Chesterville plug branches and feathers out upwards into a swarm of thinner "albitite" dykes. These dykes also die out upwards as the system closes off towards surface, particularly at its east end. Dykes become extremely sparse above the 500 ft level.

Figure 42 Width histogram of "albitite" dykes, Kerr Addison - Chesterville Au system, based on measurement of 6,483 individual random drillhole intersections normal to dyke average strike direction. The distribution is logarithmic with a mean width of 1.97 m. "Albitite" intrusions measured ranged from <0.3 m (data truncated at this cut-off) to ~35 m (Chesterville plug) in width. Dykes <0.3 m in width were observed in mapping to be as numerous as those >0.3 m in width.

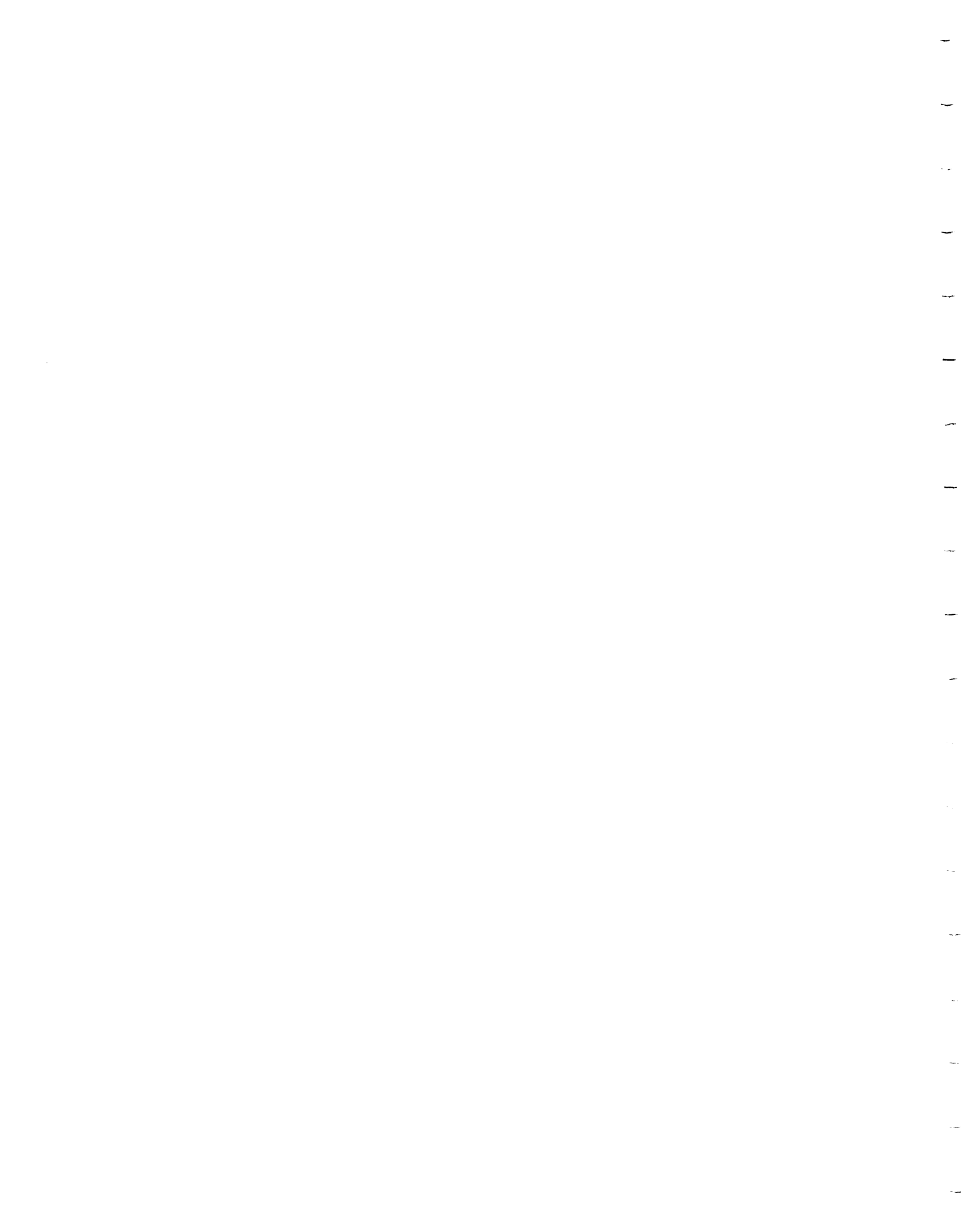
Figure 43 Graph of total number of "albitite" dyke drillhole intersections per level (counted in this study) against depth, Kerr Addison - Chesterville Au system. This diagram shows that an increasing number of dykes were intersected in the upper levels of the system as it expanded (especially in length) and because the intrusive bodies branched upwards. A peak is reached at the 1000 ft level followed by a decline near surface. Drilling was carried out at an ~11 m spacing perpendicular to the strike of the deposit.

202

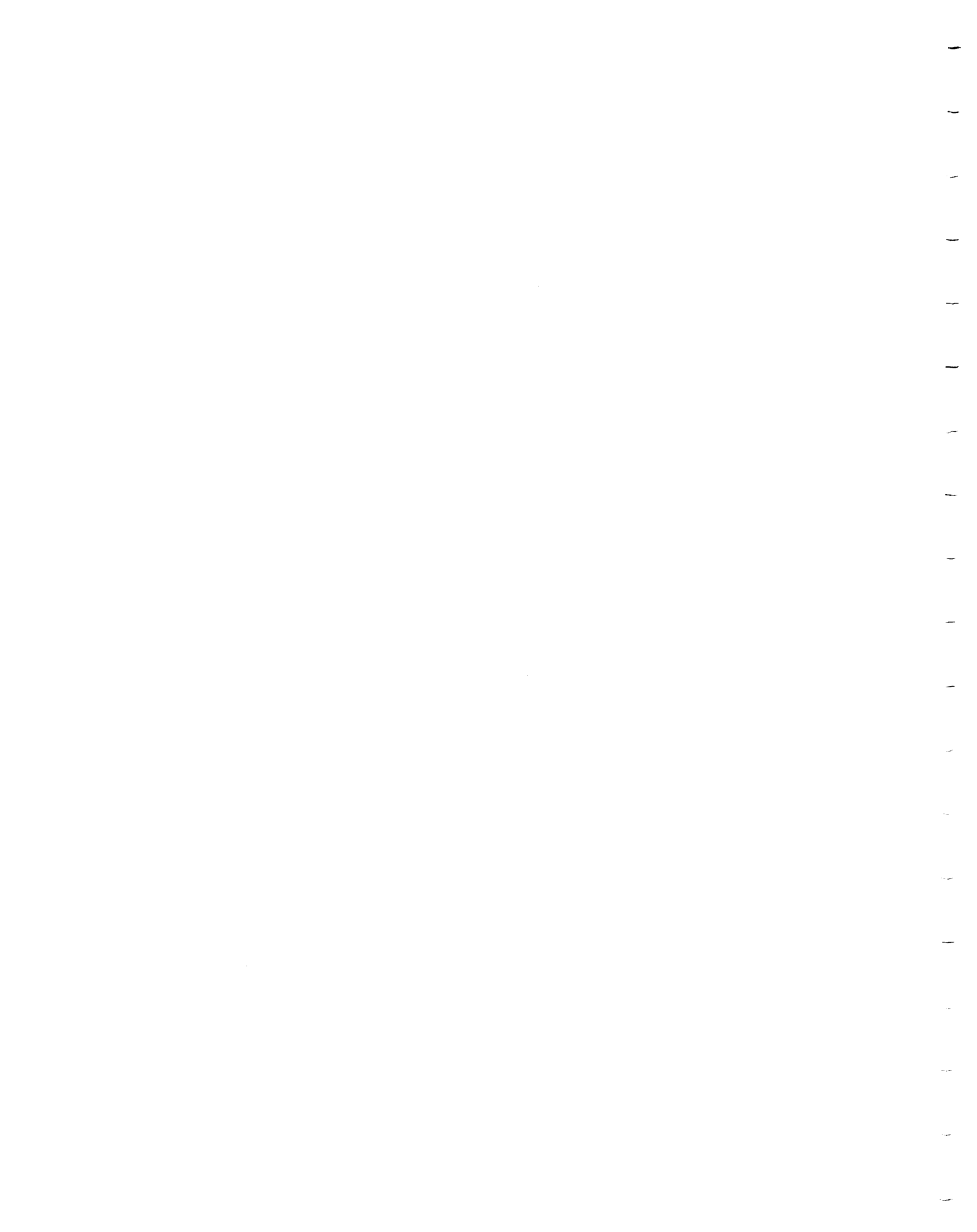
203

204

205

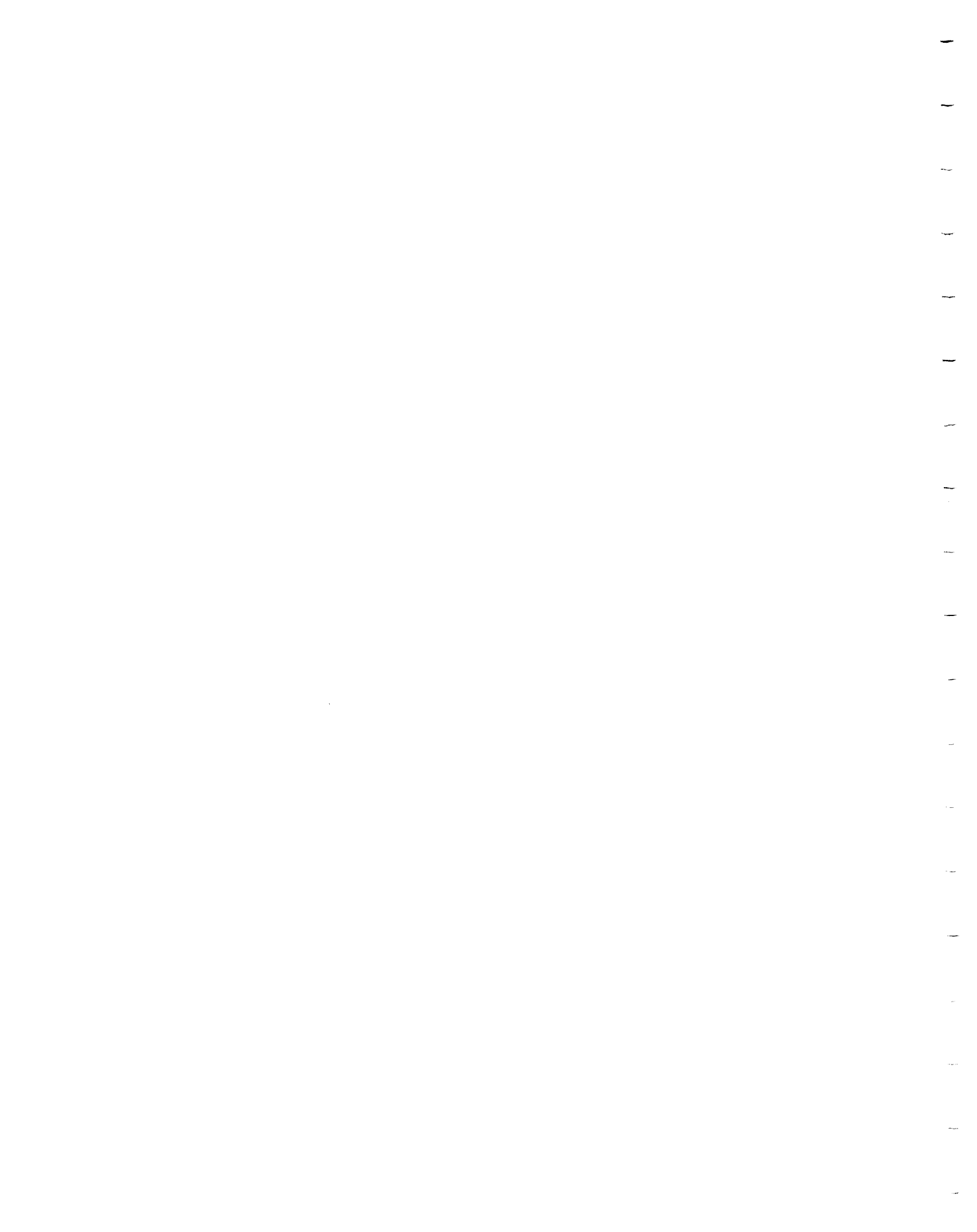


- Figure 44 Graph of average "albitite" dyke width per level against depth, Kerr Addison - Chesterville Au system. This diagram shows a peak of ~3.5 m at the ~3550 ft level (due to the development of fewer, but larger dykes and plugs at depth) followed by fairly constant to moderately increasing average dyke widths of ~1.5-2.5 m upwards to a subsidiary peak on the 850 ft level (~3 m). Average dyke width then declines near surface to ~1 m. 206
- Figure 45 Graph of "albitite" intrusion area per level (as a % of ultramafic host rock area within the green carbonate envelope east and west limits) against depth, Kerr Addison - Chesterville Au system. This diagram shows two peaks (~15%) in dyke area, at the 3700 ft level and 1150 ft levels respectively, separated by a minimum at the ~2350 ft level. % values decrease at the bottom and top of the Au system. 207
- Figure 46a Detailed geological map of the 3815-79 stope and north crosscut at the east end of the 3803-69 East Drift (for exact location see Figure 23). This map records the locations and relationships of the three principal generations of "albitite" dyke: A<sub>1</sub>, A<sub>2</sub> and A<sub>3</sub> (see Figure 32 for inferred relative timing relationships). A<sub>1</sub> predates main stage (#4) Au mineralisation and, as shown on the map, is host to anastomosing quartz veinlet systems together with the green carbonate altered ultramafic host rock. A<sub>2</sub> and A<sub>3</sub> are both weakly hydrothermally altered, weakly Au mineralised and cross-cut by minor quartz veining. As the photographs (Figures 48 and 49) show, however, A<sub>2</sub> and A<sub>3</sub> cut and are therefore younger than the bulk of main stage Au-quartz vein mineralisation. Hence, a significant proportion of main stage Au mineralisation is intra-"albitite" dyke in relative age (see Figure 32) and, in fact, all dyke generations are also intra-Au-quartz vein mineralisation (see Figure 32). *The location of this stope (section ~78E relative to baseline) is important because it is near the bottom of the Chesterville plug which runs up the eastern edge of the orebody (see Figures 28 and 29), and around which the entire ore and vein/feeder system contracts at depth (see text).* 208
- Figure 46b This map shows the locations of the following 11 photographs referred to in the text from the 3815-79 stope and north crosscut: P1, Figure 14; P2, Figure 49b; P3, Figure 49c; P4, Figure 49a; P5, Figure 47c; P6, Figure 48a; P7, Figure 48b; P8, Figure 47a; P9, Figure 47b; P10, Figure 47d; and P11, Figure 49d. 209





- Figure 47a Intense quartz veining and silicification superimposed on an  $A_1$  "albitite" dyke (left hand side) - green carbonate altered ultramafic (right hand side) contact; 3850 ft level. The photograph shows the similar degrees of main stage (#4, Figure 32) quartz veining and silicification which have affected both lithologies. The exact location of the photograph (P8) is given on the map of the 3815-79 stope (Figure 46b). The visible part of the scale is ~45 cm long.
- Figure 47b Well defined apophysis of an  $A_2$  "albitite" dyke cutting foliation fabric in green carbonate altered ultramafic material showing that intrusion of  $A_2$  dykes post-dated development of some fabric (see relative timing in Figure 32); 3850 ft level. The exact location of the photograph (P9) is given on the map of the 3815-79 stope (Figure 46b). Scale in cm and inches.
- Figure 47c Well developed fabric and elongation in thin (0.5-4 cm)  $A_2$  "albitite" dyke segments in a localised high ductile strain zone; 3850 ft level. The fact that "albitite" dykes,  $A_2$  in this case, both cut weak fabric (Figure 47b) and are strongly affected by well developed fabric (this photograph) shows that they intruded during ductile deformation, mainly flattening, in the Break zone (see Figure 32). The exact location of the photograph (P5) is given on the map of the 3815-79 stope (Figure 46b). The visible part of the scale is ~23 cm long.
- Figure 47d Well defined relatively thin (~15-20 cm)  $A_2$  "albitite" dyke cross-cut by main stage (#4) Au-quartz veins; 3850 ft level.  $A_2$  "albitite" dykes also cross-cut a large part of main stage #4 Au-quartz veining (see Figures 48 a-d and 49a and c below); hence  $A_2$  "albitite" dykes are intra-main stage Au-quartz veining in relative timing (see Figure 32). The exact location of the photograph (P10) is given on the map of the 3815-79 stope (Figure 46b). The visible part of the scale is ~19 cm long.
- Figure 48a Well developed  $A_2$  "albitite" dyke ~50-65 cm wide which intruded both foliated green carbonate altered ultramafic material (left hand side) and strongly quartz-veined and silicified  $A_1$  "albitite" dyke material (right hand side); 3850 ft level. The exact location of the photograph (P6) is given on the map of the 3815-79 stope (Figure 46b). The visible part of the scale is ~18 cm long.
- Figure 48b Detail of area in Figure 48a; this photograph clearly shows an  $A_2$  "albitite" dyke cutting and truncating main stage (#4) Au-quartz veins and silicification which



have affected an  $A_1$  "albitite" dyke. Hence, (i) a significant amount of main stage (#4) Au-quartz vein mineralisation is intra-"albitite" dyke intrusion in relative age, and (ii) since  $A_2$  "albitite" dykes are also hydrothermally altered and weakly Au mineralised, then  $A_2$  "albitite" dyke intrusion was intra-main stage Au mineralisation in relative timing (see Figure 32). The exact location of the photograph (P7) is given on the map of the 3815-79 stope (Figure 46b). The visible part of the scale is ~40 cm long.

Figure 48c Looking along the strike of a ~1.2 m wide  $A_2$  "albitite" dyke internally cutting a heavily silicified and quartz veined  $A_1$  "albitite" dyke; 1915-69 exploration drift, 1900 ft level. The contacts of the  $A_2$  "albitite" dyke are between the person's (J.P.S.) finger on the left hand side and the arrow on the right hand side. Scale 1 m.

Figure 48d Detail of area in Figure 48c; this photograph clearly shows an  $A_2$  "albitite" dyke (left hand side) cross-cutting and truncating quartz veins cutting an  $A_1$  "albitite" dyke (right hand side). The two dykes also show a very marked contrast in the degree of silicification, with the younger  $A_2$  dyke showing very much less. Further east along the 1915-69 exploration drift (1900 ft level) it can be seen that the quartz veining and silicification which has been superimposed on the  $A_1$  "albitite" dyke is related directly to a typical main stage (#4) "siliceous break" vein. *Since the large "siliceous break" veins were the principal feeders for main stage Au mineralisation and since the latter mineralisation both cuts an  $A_1$  "albitite" dyke but is clearly cross-cut by an  $A_2$  "albitite" dyke, this photograph clearly documents that in this location the bulk of main stage Au mineralisation is intra-"albitite" dyke intrusion in relative age (see Figure 32).* The  $A_2$  "albitite" dyke is also weakly altered and mineralised, as is the  $A_2$  dyke in Figures 48a and 48b; hence, the  $A_2$  "albitite" dyke is also intra-main stage Au-quartz vein mineralisation in relative timing. The visible part of the scale is ~20 cm.

Figure 49a  $A_2$  "albitite" dyke with a mixed xenolithic suite including a pale, angular xenolith above the left hand end of the scale; this xenolith is a fragment of main stage mineralisation, strongly silicified, with dispersed pyrite and low grade Au (see text; 3850 ft level). The presence of this xenolith confirms that  $A_2$  "albitite" dykes intruded after at least some main stage Au mineralisation (see Figure 32). The exact location of this photograph (P4) is given on the map of the 3815-79 stope (Figure 46b). Scale in cm and inches.

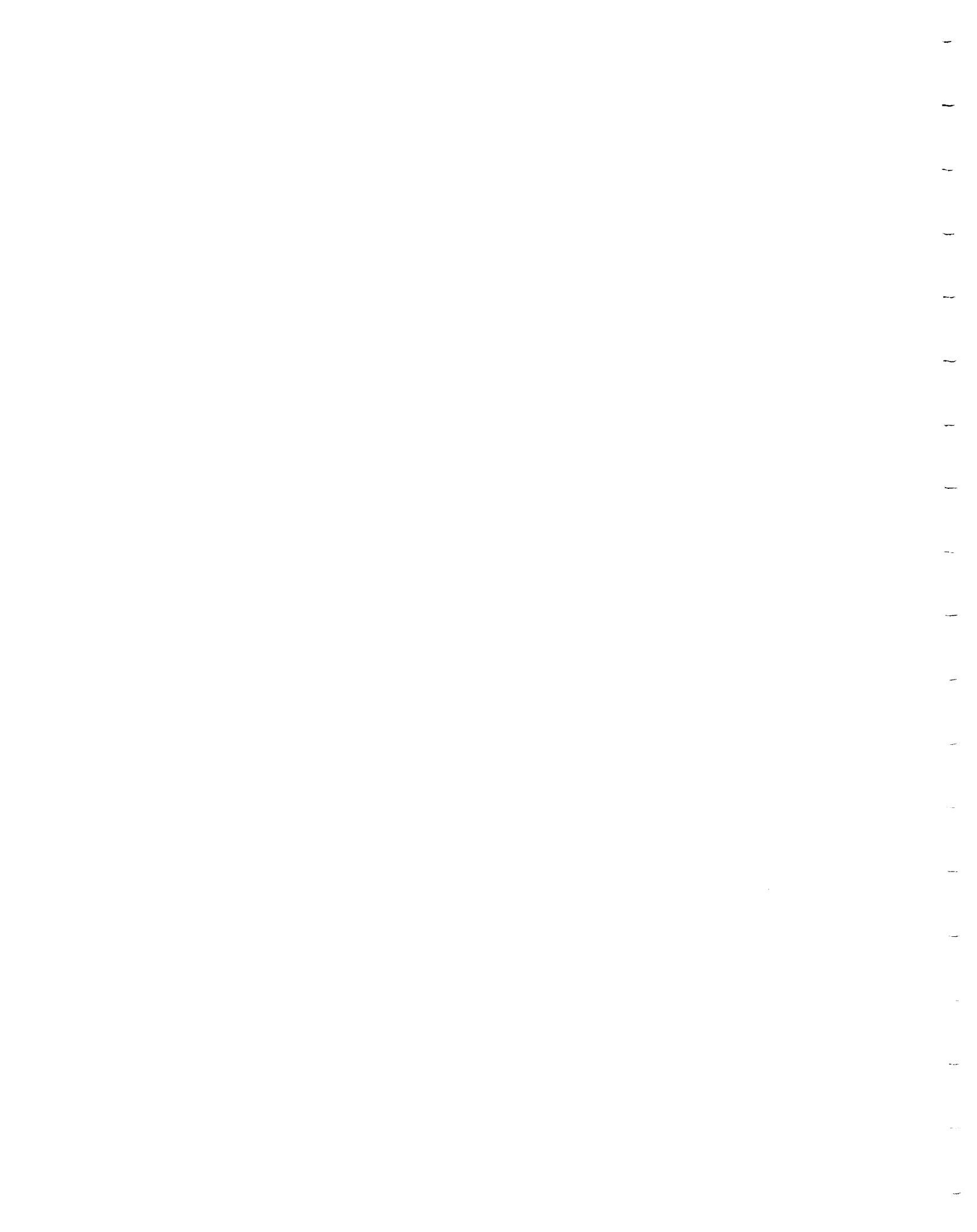


Figure 49b Looking up into the back; a series of relatively thin (~10-20 cm)  $A_3$  "albitite" dykes cutting a large, strongly silicified pink-brown, Au mineralised  $A_1$  "albitite" dyke; 3850 ft level. The  $A_1$  dyke has the bulk of main stage Au mineralisation superimposed on it, whereas the  $A_3$  dykes are hydrothermally altered but not significantly mineralised; hence the bulk of main stage mineralisation is bracketed in time by  $A_1$  and  $A_3$  dykes (see Figure 32). The exact location of this photograph (P2) is given on the map of the 3815-79 stope (Figure 46b). For scale, the rock bolt plate is 10.5 cm square; the margins of the  $A_3$  dykes have been emphasised by black lines (on the rock surface).

Figure 49c Looking up into the back. Unusual triple junction contact between  $A_1$ ,  $A_2$  and  $A_3$  "albitite" dykes; 3850 ft level. The oldest  $A_1$  dyke, in the lower part of the photograph, is characterised by significant quartz veining, strong silicification and dispersed pyritic Au mineralisation. It is cut by a centrally located wedge-shaped  $A_2$  dyke with no quartz veining and weak hydrothermal alteration (only weak silicification). The youngest  $A_3$  dyke in the upper part of the photograph shows a network of fine planar veinlets with marginal, paler hydrothermal alteration selvages between which are dark grey weakly altered areas of mafic "albitite" dyke. *Clearly the bulk of main stage Au mineralisation in this location (P3; 3815-79 stope, 3850 ft level; Figure 46b) developed between the  $A_1$  and  $A_2$  dykes.* The visible part of the scale is ~26 cm.

Figure 49d Polished slab of the contact between a moderately altered, granular, grey  $A_3$  "albitite" dyke (upper part) and an intensely silicified quartz-carbonate veined pale pink-brown  $A_1$  "albitite" dyke; 3850 ft level. It may be seen clearly that (i) the  $A_3$  dyke does not show the same degree of silicification as the  $A_1$ , and (ii) the  $A_3$  dyke clearly truncates a significant quartz-carbonate vein in the  $A_1$  dyke. The location of the sample from which this photograph (P11) was obtained is shown in the map of the 3815-79 stope (Figure 46b). The width of the  $A_3$  "albitite" dyke part of the sample is 3.5 cm.

Figure 50 Zr/TiO<sub>2</sub> vs. Nb/Y plot (Winchester and Floyd, 1977) of relatively immobile trace element ratios towards classification of the Kerr Addison mafic "albitite" dykes (n = 56). Except for a few intensely silicified  $A_1$  "albitite" dykes, which tend towards higher Zr/TiO<sub>2</sub> ratios due to preferential loss of titanium on advanced hydrothermal alteration, the 56 samples define a coherent data set mostly in the andesite to andesite-basalt field.

212

213

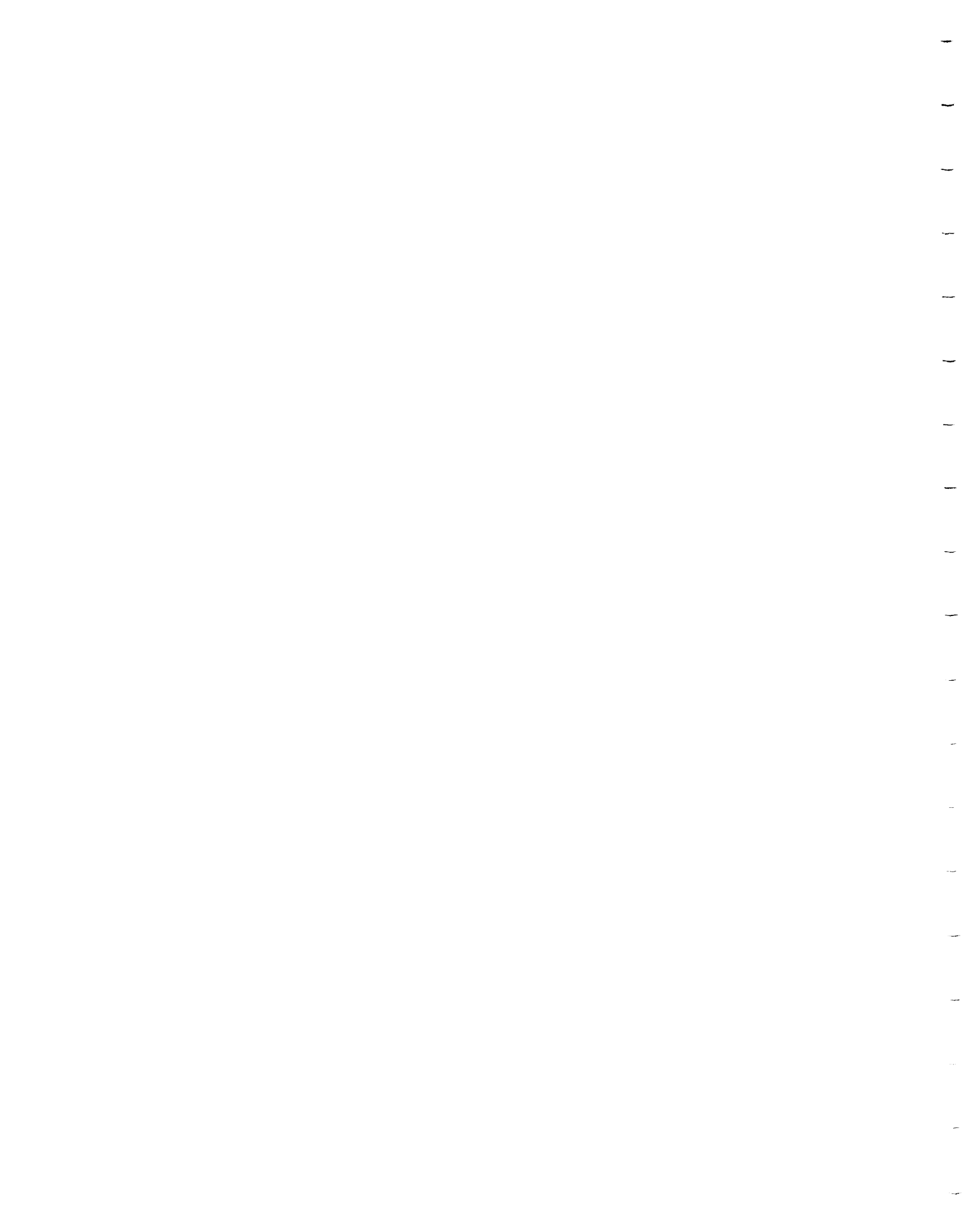


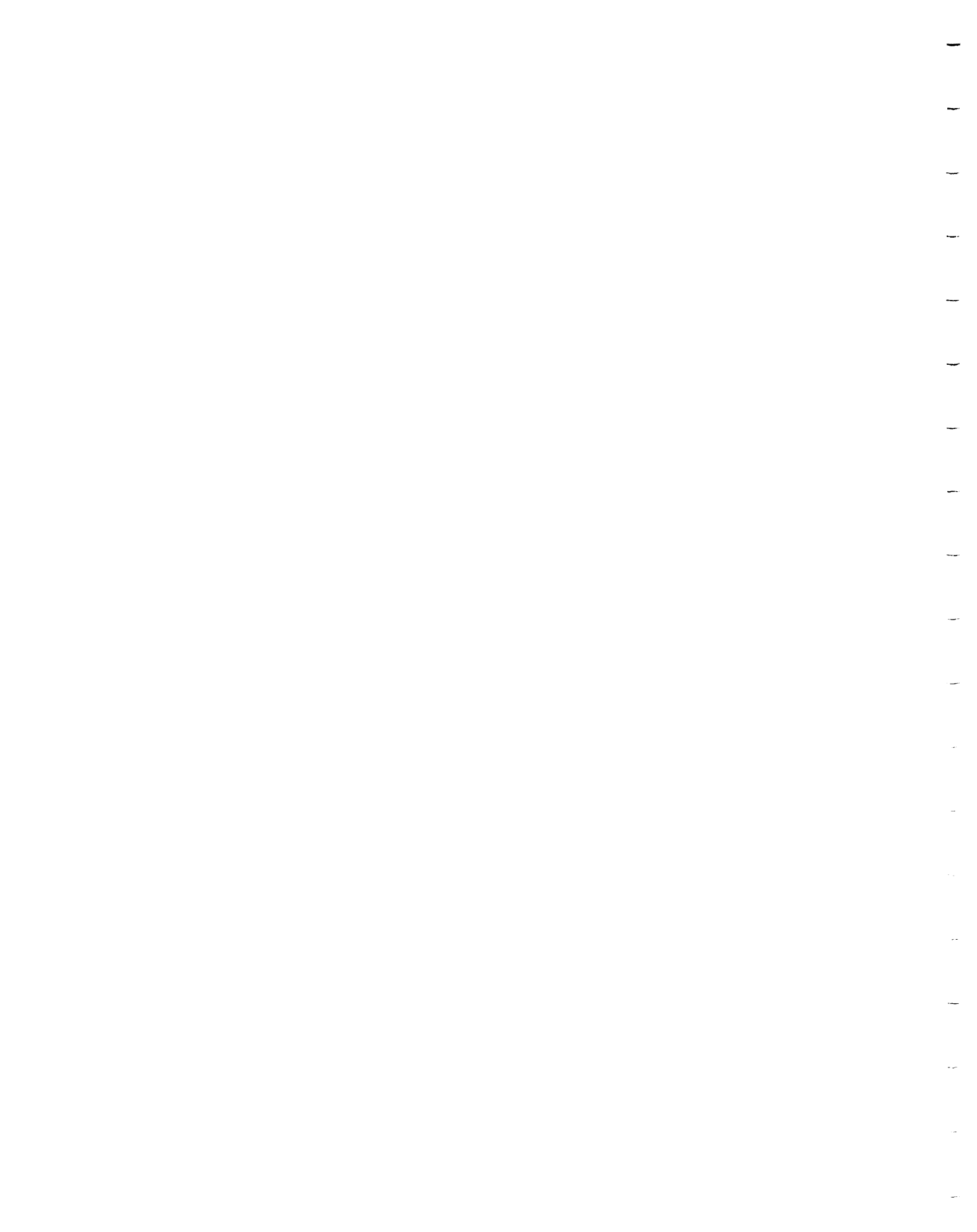
Figure 51 Longitudinal contour diagram of the Kerr Addison - Chesterville Au system showing total green carbonate alteration width (perpendicular to the plane of the diagram). Contours are in 50 ft intervals, and the data point density on which the diagram was based is also shown (a total of 910 data points). The boundary of the Au system is given by the edges of the green carbonate alteration envelope - a 0ft limiting contour. The diagram shows at depth a central wide green carbonate root zone (300 ft contour at the 4400 ft level), fed from below by a pipe-like feeder alteration zone, which splits upwards into an east and a west branch (as shown by dashed lines joining local maxima). Between these lies a zone in which only narrow green carbonate (<100 ft contour) is developed. Contours die off near the surface, especially in the east, showing that the system would just have penetrated above the present erosion surface (e.g. in the west).

214

Figure 52 Longitudinal contour diagram of the Kerr Addison - Chesterville Au system showing total quartz vein intersection width (perpendicular to the plane of the diagram). Contours are in 5 ft intervals, and the data point density on which the diagram was based is also shown (a total of 1,580 data points). The boundary of the Au system is given by the edges of the green carbonate alteration envelope, which can be considered a 0 ft limiting contour. The diagram shows that quartz vein distribution is approximately V-shaped in longitudinal profile (as defined by the outlined 5 ft contour line), expanding upwards from a root zone on the ~4800 ft level and feathering out upwards (as shown by closure of contours) as the system dies out, particularly in the east. Dashed lines which join up local maxima show that the main pathway for fluid flow and quartz vein (25-30 ft) development was up the mid- to western side of the system, emerging near surface at the present day #10 orebody glory holes (section 40E). A smaller quartz vein concentration occurs around section 60E. Some lateral feeding of ore fluids, as shown by quartz vein development, may have occurred between east and west.

215

Figure 53 Longitudinal contour diagram of the Kerr Addison - Chesterville Au system showing total quartz vein intersection width (perpendicular to the plane of the diagram) as a percentage of the width of total green carbonate alteration. Contours are in 5% intervals, and the data point density on which the diagram was based is also shown (a total of 1,580 data points). The boundary of the Au system is given by the edges of the green carbonate alteration envelope, which can be considered a 0% limiting contour. The diagram shows that the highest % quartz..





veining (of green carbonate alteration width) lies in an approximately centrally distributed zone within the Au system, decreasing both east and west. Closure of contours (e.g. 5% contour highlighted) clearly indicates that quartz veins die out (as a % of green carbonate) upwards, especially in the east, reflecting a decrease in the amount of hydraulic fracturing.

216

Figure 54 Longitudinal contour diagram of the Kerr Addison - Chesterville Au system showing total "albitite" intrusion intersection width (perpendicular to the plane of the diagram). Contours are in 10 ft intervals, and the data point density on which the diagram was based is also shown (a total of 1,580 data points).

The boundary of the Au system is given by the edges of the green carbonate alteration envelope, which can be considered a 0 ft limiting contour. The diagram shows a marked concentration (50-110 ft / 15-30 m) of "albitite" intrusions up the east side of the Au system, corresponding to the Chesterville plug and its deep extensions. A weaker concentration (40-80 ft) corresponds to a western branch of igneous intrusions. Dashed lines which join up local maxima show that high "albitite" footage values at two places (~1900 ft and ~4000 ft levels) in the centre of the system are probably part of a lateral intrusive feeder system between the eastern and western branches. Although irregular, closure of contours (e.g. 10 ft contour highlighted) clearly indicates that "albitite" intrusions die out upwards, especially in the east. A narrow pipe-like intrusive feeder zone is indicated below ~4400 ft (1340 m).

217

Figure 55 Longitudinal contour diagram of the Kerr Addison - Chesterville Au system showing "albitite" intrusion intersection width (perpendicular to the plane of the diagram) as a percentage of the width of the ultramafic host rock unit. Contours are in 5% intervals, and the data point density on which the diagram was based is also shown (a total of 1,580 data points). The boundary of the Au system is given by the edges of the green carbonate alteration envelope, which can be considered a 0% limiting contour. The diagram shows a marked concentration (15-30%) of "albitite" intrusions up the east side of the Au system, corresponding to the Chesterville plug and its deep extensions. A weaker concentration (10-15%) corresponds to a western branch of igneous intrusions. Dashed lines which join up local maxima show that high % "albitite" values at two places (~1900 ft and ~4000 ft levels) in the centre of the system are probably part of a lateral intrusive feeder system between the eastern and western branches. Although irregular, closure of contours clearly indicates that "albitite" intrusions die out upwards.

218

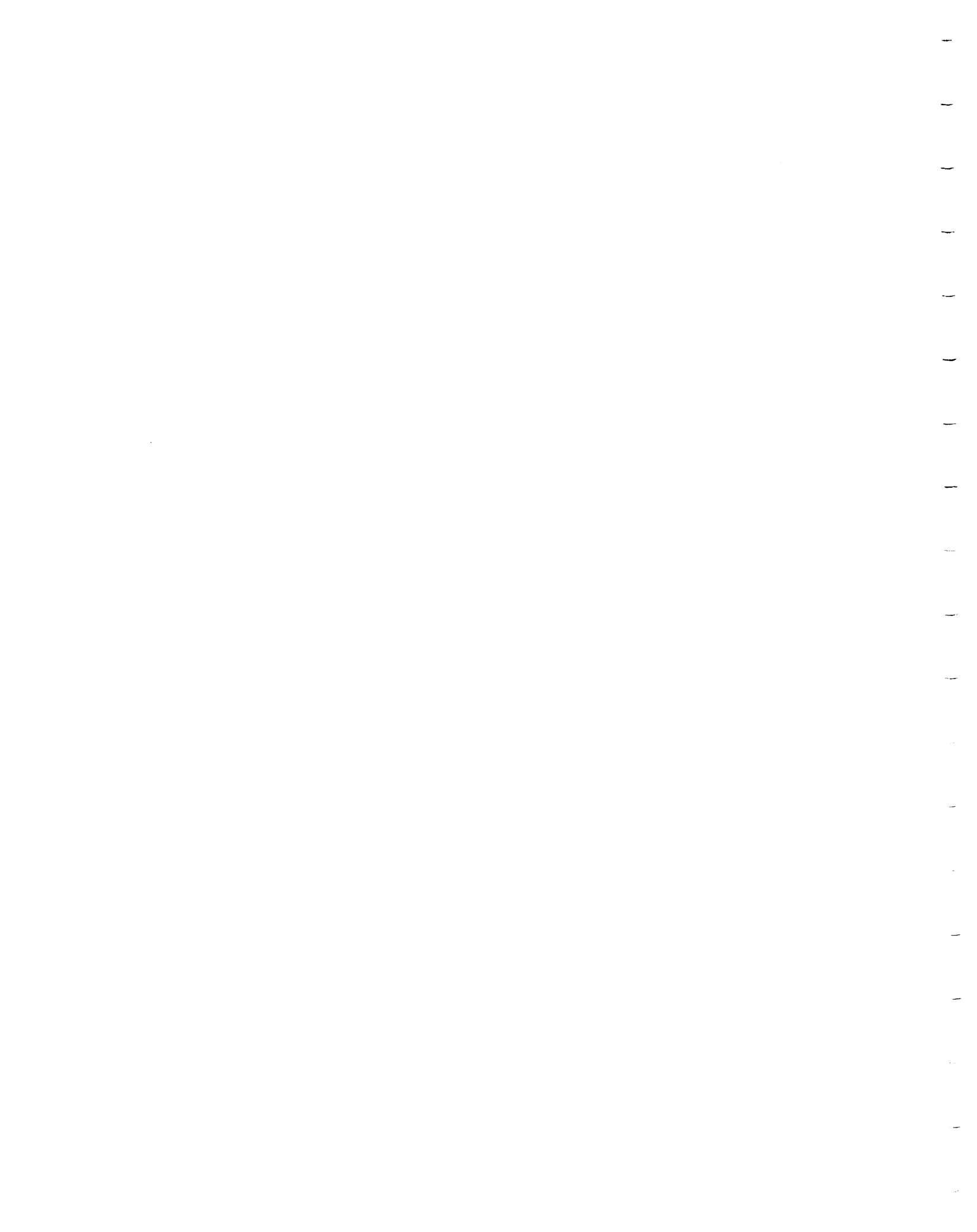


Figure 56 Graph showing the variation of green carbonate alteration area, its strike length and average width per level with depth, Kerr Addison - Chesterville Au system. Green carbonate alteration expands upwards ~5 times in area (~3 times in strike length and ~ 1.7 times in average width) from a root zone at ~4800 ft (1500 m) depth. The entire areal expansion takes place between the ~4800 ft (1500 m) and the ~2650 ft (800 m) levels; above this, between 2650 ft (800 m) and 500 ft (150 m) depths, green carbonate area remains relatively constant in area at x4-5 times that of the root zone, before dying off very rapidly near surface. Whereas strike length continues to expand upwards (exploiting the Break), average width reaches a broad maximum at around the 2650 ft (800 m) level and then declines upwards.

219

Figure 57 Graph showing the variation of quartz vein and "albitite" intrusion areas per level with depth, Kerr Addison - Chesterville Au system. Both quartz veins and "albitites" exhibit correlated areal expansions (x 6-7 times) from a root zone at ~4800 ft (1500 m) depth. Significantly, expansion did not occur between the 5600 ft (1700 m) and 4800 ft (1500 m) levels. Quartz vein areas appear to remain fairly constant in the mid to upper levels of the system between 2650 ft (800 m) and 850 ft (250 m); "albitites" show an initial maximum on the 3850 ft (1200 m) level where three major plugs are developed, then a trough at mine mid-levels and a second peak at the ~1300 ft level due to development of the Chesterville plug and an extensive dyke swarm. Both quartz vein and dyke areas then show a sharp correlated decrease in area between the ~1000 ft (300 m) level and the surface and can be projected to fade out completely just above the present erosion level.

220

Figure 58a A graph of ore tonnage per level against depth for flow ore, green carbonate ore and "albitite" ore, Kerr Addison. Flow ore shows a broad central tonnage peak in the mid levels (800-400 m depth) and a subsidiary peak at 1300-1050 m depth, and declines smoothly upwards in tonnage from ~450 m depth to surface. Green carbonate ore tonnage per level expands upwards gradually over 20 times, then declines very rapidly near surface as the ore system dies out.

221

Figure 58b A graph of ore tonnage per level against depth for individual flow ore bodies in the Kerr Addison mine, and variations of the overall flow ore tonnage total. Tonnage trends in the flow ore are dominated by the major #21 orebody, especially at depth, and are controlled mostly by the distribution and availability of favourable Fe-tholeiitic volcanic horizons within the ore system. Total flow ore tonnage shows



a broad peak at mid levels (800-400 m depth) and a subsidiary peak at 1300-1050 m depth, and declines smoothly upwards in tonnage from ~450 m depth to surface.

222

Figure 58c A graph of ore tonnage per level against depth for individual green carbonate ore bodies in the Kerr Addison mine, and variations of the overall green carbonate ore tonnage total. Individual ore bodies expand gradually in tonnage upwards from their base, reaching a maximum just before declining rapidly at their top. The larger green carbonate orebodies (#14, #10) appear to undergo two or three expansion/contraction cycles upwards. Smooth total green carbonate ore tonnage trends with depth emphasise the interconnectivity of the individual ore bodies within the ore system framework. Total tonnage per level expands upwards over 20 times, then declines very rapidly near surface as the ore system dies out.

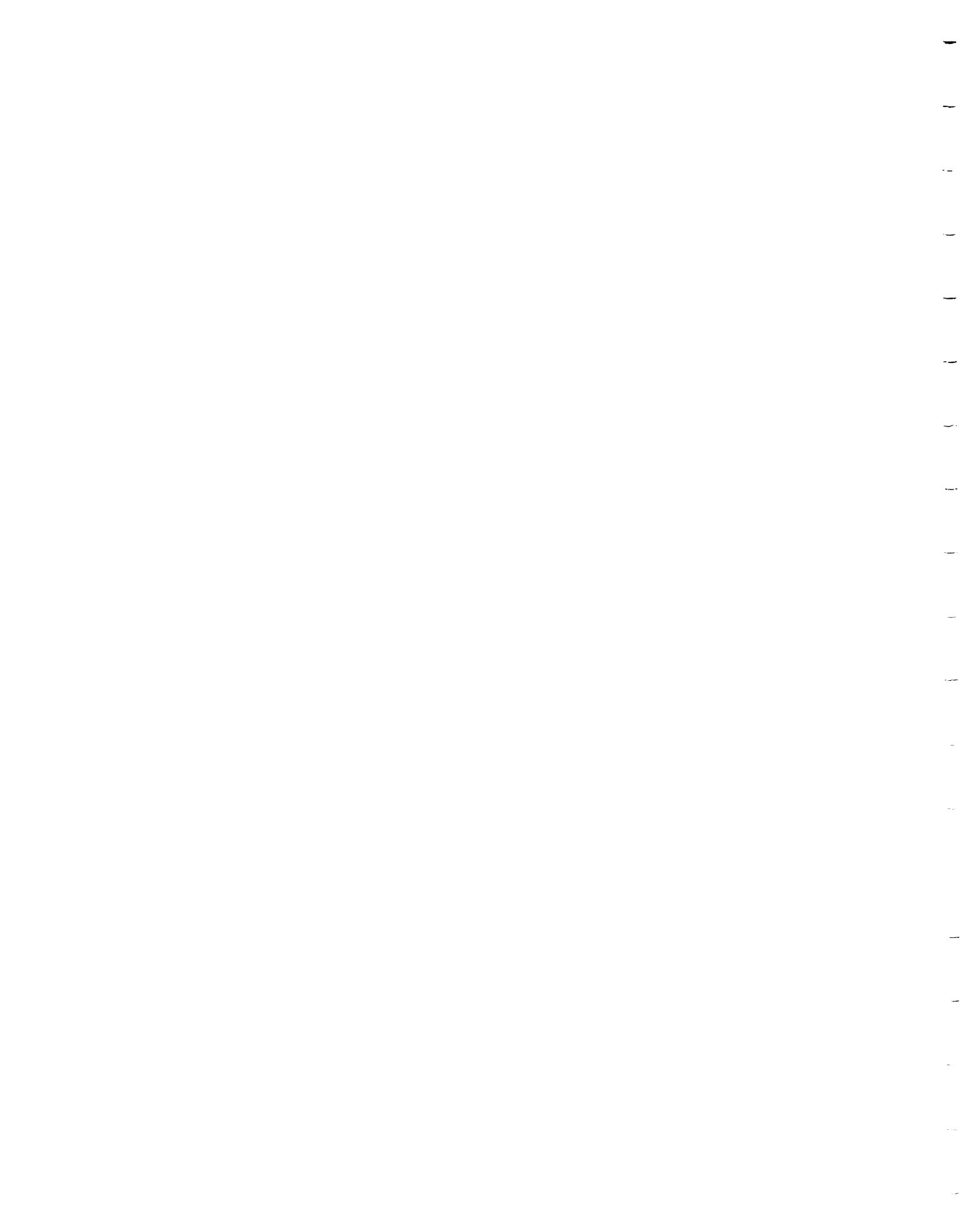
223

Figure 59a A graph of Au ore grade against depth for flow ore, green carbonate ore and "albitite" ore, Kerr Addison. Flow ore shows a narrow grade peak of ~20 g/t Au at ~1200 m depth, grade declining steadily to ~5 g/t Au at ~300 m depth before rising again to ~10 g/t Au near surface. This may be interpreted (see text) as due to intense initial sulphidation reactions precipitating Au at depth where hydrothermal fluids first encountered the Fe-tholeiite unit, followed by depletion of fluids in Au upwards, and finally fluid channelling near the top of the system and/or more selective mining raising Au grade near surface where the tonnage is minor. Green carbonate ore shows a broad grade peak of 9-11 g/t Au between 1000 and 500 m depth, climbing from a low of <5 g/t Au at 1300 m depth and declining upwards above 500 m to ~5 g/t Au near surface. In the green carbonate ore, Au grade is controlled by the abundance of Au-quartz veins which in turn is controlled by fluid-generated hydraulic fracturing due to H<sub>2</sub>O-CO<sub>2</sub> phase separation (see Channer and Spooner (1991) for fluid inclusion observations). Low grade at depth is due to a lithostatic pressure restriction on vein development; declining grade near surface is due to depletion of fluids in Au upwards (i.e. a closed system) and a decrease in the amount of hydraulic fractures near surface as the system dies off.

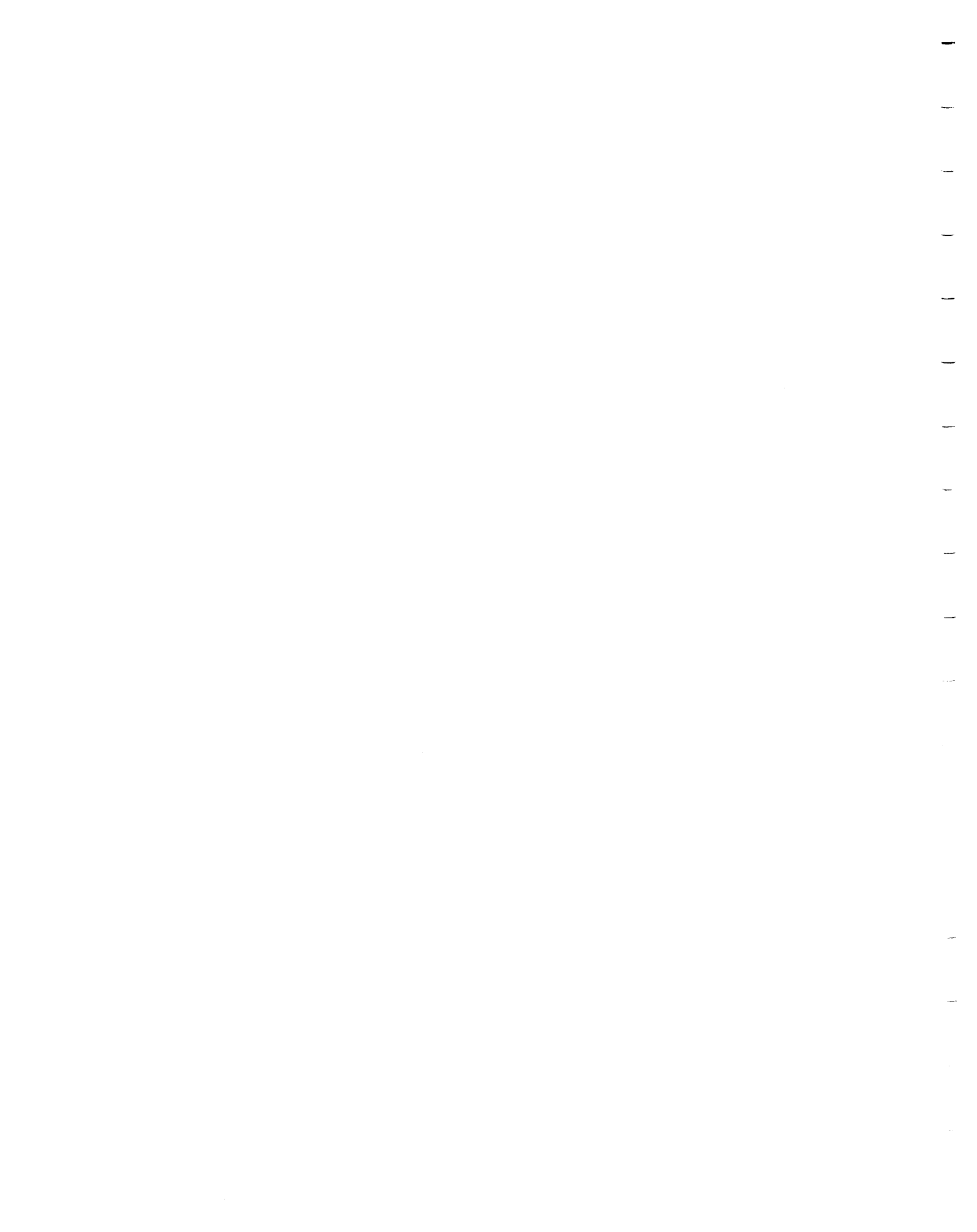
224

Figure 59b A graph of Au ore grade against depth for individual flow ore bodies in the Kerr Addison mine. Each orebody shows a wide range of grade values (between ~4 g/t Au and 15-20 g/t Au) and grade profiles with depth for each appear to follow a similar pattern: a rapid climb to a grade peak just above the base followed by a decline upwards to low grades, then a final grade increase near surface (see text for explanation).

225

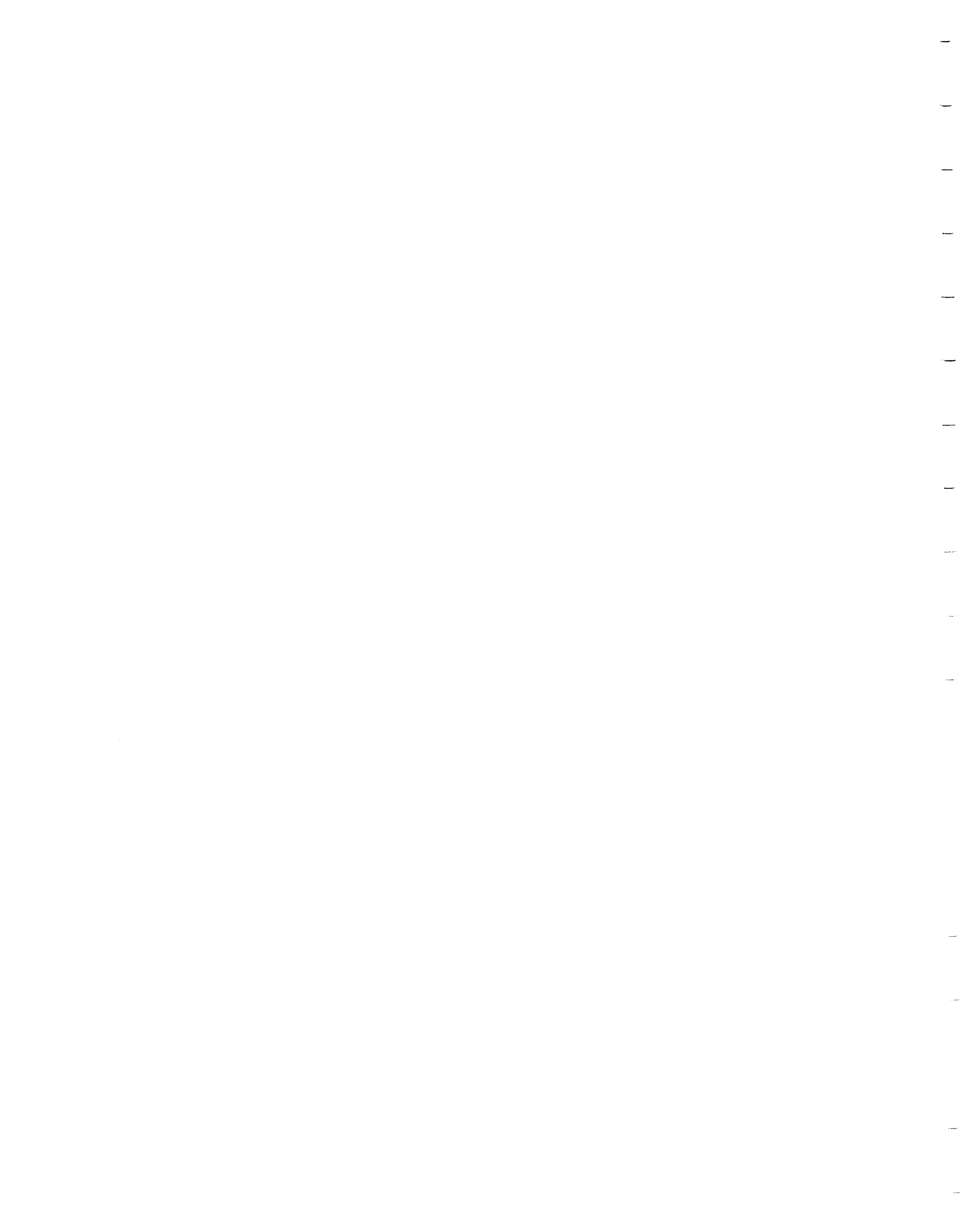


- Figure 59c A graph of Au ore grade against depth for individual green carbonate ore bodies in the Kerr Addison mine. Each orebody shows a wide range of grade values (between ~4 g/t Au and 10-16 g/t Au), and grade profiles with depth for each appear to follow a similar, fairly simple pattern: initially low grade at the base, rising to a grade peak at mid levels then grade declining upwards. The larger orebodies (#14, #10) show two or three repetitions of this cycle upwards. 226
- Figure 60a A graph of total Au produced per level against depth for the Kerr Addison mine, showing flow and green carbonate ore contributions. The approximately symmetrical rise and fall of total Au with depth shows that the Kerr Addison mine contains the complete productive vertical interval of an Archean Au system. Flow ore is the dominant ore type below ~600 m depth, and green carbonate most important in terms of total Au above 300 m depth, thus a change in ore emphasis takes place within the mine on passing upwards from the base. Green carbonate ore total Au rises steadily from near zero at the 1300 m level to a maximum near surface, before rapidly dying off (see text for reasons). Flow ore shows twin peaks in total Au abundance with depth, the first at ~1200 m is more grade driven, the second at ~700 m is more tonnage-driven. Flow ore starts to decline upwards in terms of total Au at the ~500 m level to zero at surface. 227
- Figure 60b A graph of total Au produced per level against depth for individual flow orebodies in the Kerr Addison mine and the overall flow ore total. There is an overall decline in total Au from about 18 tonnes Au per level at 1200 m depth to zero near surface, interrupted by a secondary peak in total Au at the 600-800 m levels. The major contributor at all levels, and particularly at depth, is the #21 orebody. Individual flow orebodies invariably show greatest total Au near their bases. 228
- Figure 60c A graph of total Au produced per level against depth for individual green carbonate orebodies and the overall green carbonate ore total. There is a rapid expansion in total green carbonate Au between 800 m and 500 m depth due to the major contribution of the #14 orebody. Higher up in the system the #10 orebody is the main contributor to green carbonate ore. Individual orebodies mimic the patterns of the overall system: they show an increase in total Au from a base to a peak at mid-levels, then like the system die off rapidly near their tops. 229



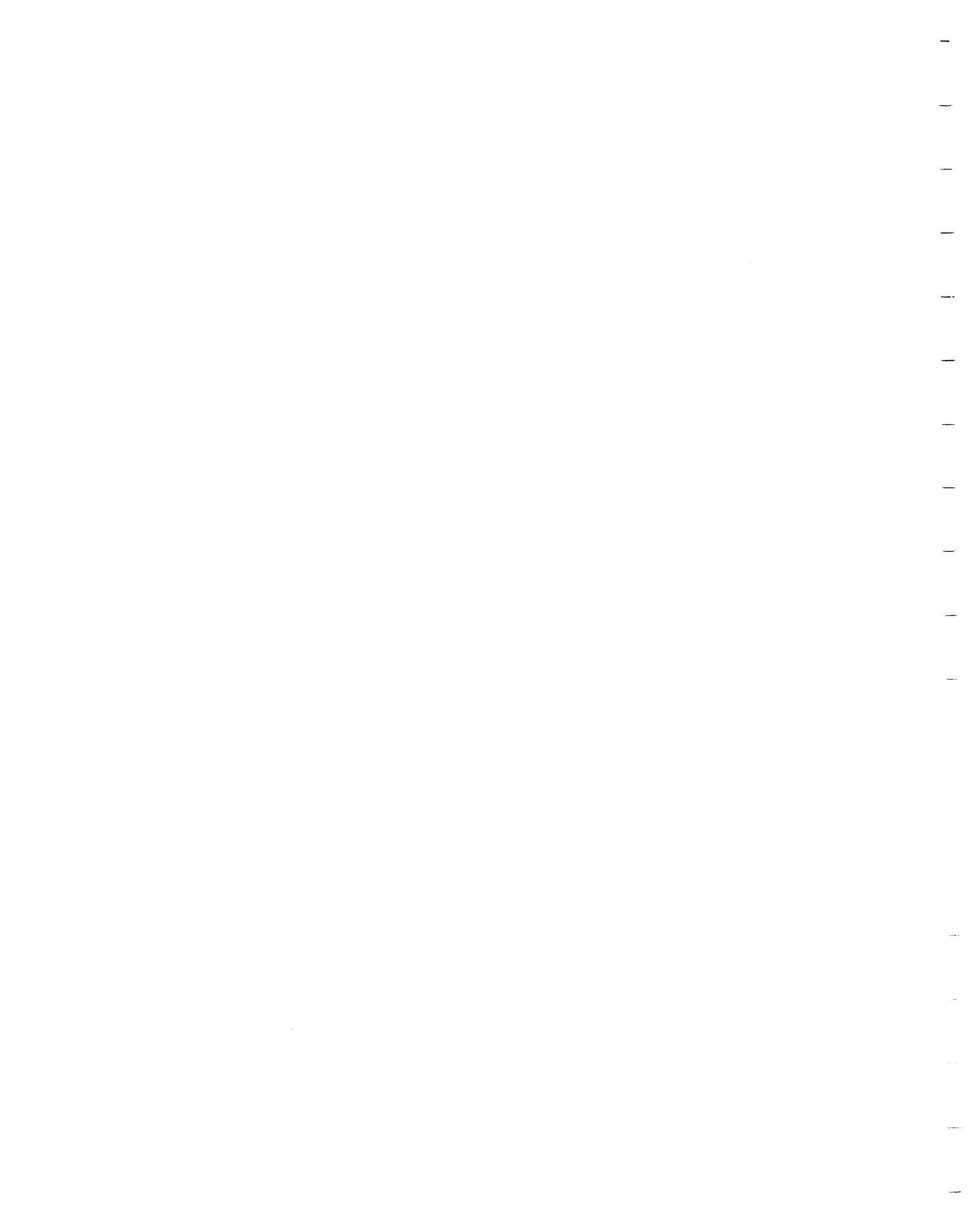


- Figure 61 A graph of annual Kerr Addison Au:Ag (kg) production ratio against year from 1938 to 1966. Because mining progressed downwards with time, this time axis also represents a moving average, mining depth axis. There is a clear inverse linear correlation ( $R^2 = -0.78$ ) between depth and Au:Ag ratio which changes smoothly from ~21:1 near surface to ~16:1 at the bottom of the mine (reached in 1965). See text for explanation. 230
- Figure 62 Major "siliceous break" quartz vein ~1.6 m wide containing typical wall rock green carbonate fragments; 30 ft above the 4000 ft level. *This "siliceous break" vein is not only a major guide structure for the 4014-631/2 stope (see Figure 35), but a major feeder channel or root zone for the bulk of the green carbonate ore stopes in the Kerr Addison mine (see longitudinal in Figure 28).* The exact location of this photograph (P1) is shown on the map of the 4014-631/2 stope in Figure 35. The fluid inclusion results described by Channer and Spooner (1991) were derived from quartz vein material from this locality. 231
- Figure 63 Composite cross-section of deep drill holes collared between mine sections 80-82E from the 5600 ft level (5603 E DR, 5605 E DR), looking east along the strike of the Break. Individual drill holes extend down to ~2000 m (6600 ft) depth, the deepest in the Kerr Addison mine. The section shows a ~50 m wide green carbonate altered zone in ultramafic host rocks north of the Kerr Fault; the green carbonate zone widens with depth and contains at ~1900-2000 m depth considerable widths of Au-mineralised (up to 7 g/t Au) mafic "albitite" intrusions up to ~10 m true width. The green carbonate alteration zone clearly focuses around the "albitite" intrusions at depth, and not the narrow, unmineralised Kerr Fault. The hydrothermal alteration-quartz veining/igneous "albitite" association at depth may reflect an association at source. 232
- Figure 64 Steeply dipping, graphitic Kerr Fault showing that is a typical fault produced by brittle failure and slip, and not a quartz feeder vein structure with associated hydrothermal alteration; 801 Main Crosscut, 850 ft level. In this photograph it is cutting altered and foliated mafic volcanic material. 233



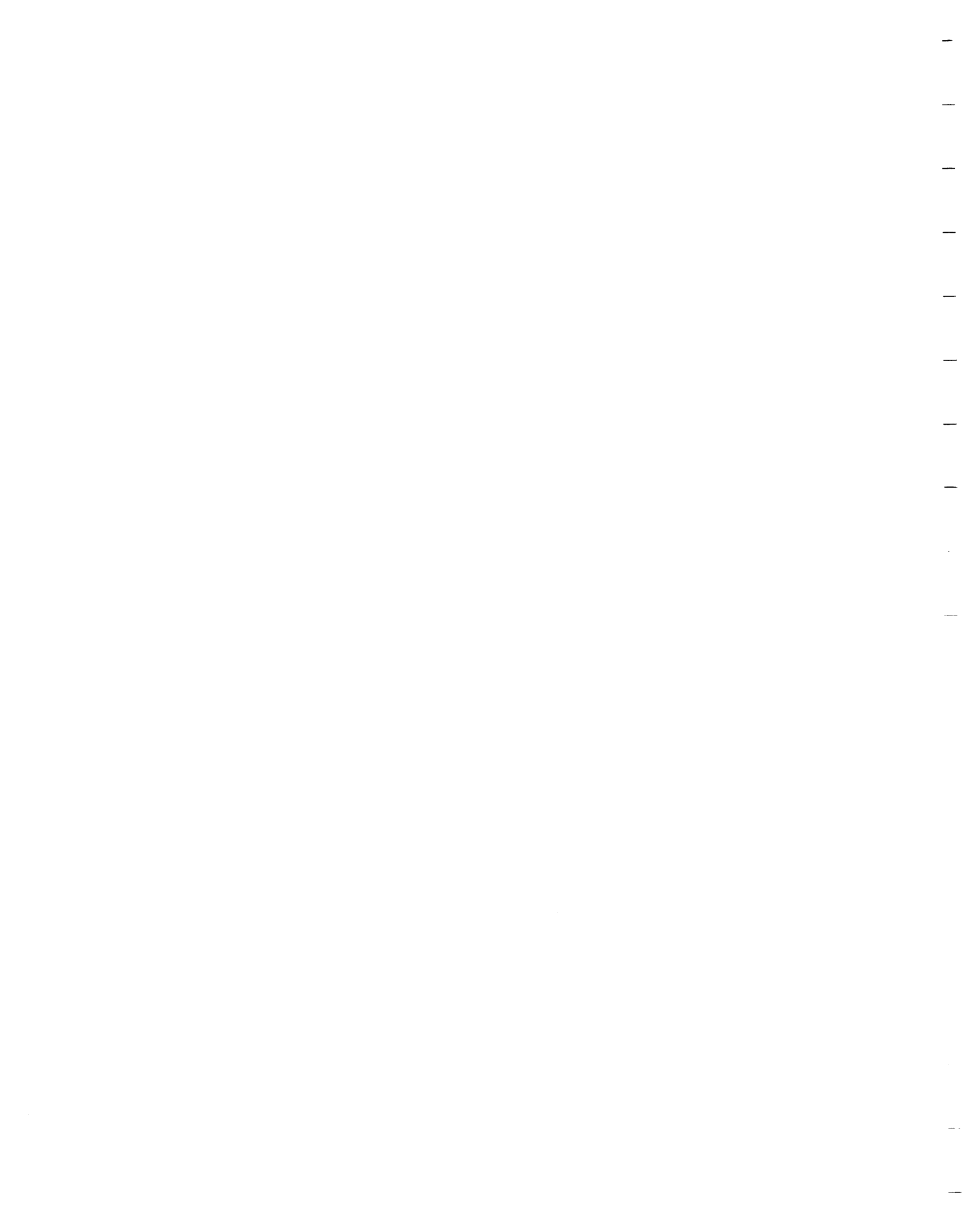
## List of Table Captions

- Table 1. Ranking of top 8 Superior Province Archean Au-quartz vein systems. The 8 systems all have historic production plus reserves of over 100 tonnes Au. **242**
- Table 2. Previous models for Au mineralisation in the Kerr Addison mine area and on the Larder Lake - Cadillac Break. Over 70 papers from the literature have been collated and tabulated according to their model for Au mineralisation under three broad categories: (i) structurally controlled/hydrothermal alteration and replacement; (ii) syn-sedimentary exhalative ( $\pm$  later remobilisation of Au); and (iii) models emphasising the role of specific lithologies. **243**
- Table 3A. Kerr Addison orebody production figures listed in order of decreasing Au produced. Figures based on over 2,500 compiled individual Kerr Addison stope data (F.R.P., 1990); sample grades and trammed tonnages not corrected for actual tonnages milled or bullion recovered in this case. **245**
- Table 3B. Chesterville (1939-1952) orebody production figures listed in order of decreasing Au produced. Data based on planimetry of Chesterville 1 inch: 40 ft scale sections at 50 ft spacing, and weighted average Au grades from drill hole intersections (F.R.P.), adjusted to tally with actual bullion production figures (see Section 2). **246**



## Appendices to the Thesis

Appendix I.	Conference abstracts (5; 1989-1991)	249
Appendix II.	Paper published in "Summary of Geoscience Research 1989-1990"; OGS Misc. Paper 150, p. 175-199	260
Appendix III.	Six drafted geological level plans not referred to in the main text	Back pocket
Appendix IV.	$\delta^{13}\text{C}$ - $\delta^{18}\text{O}$ /XRD vein carbonate analytical data with sample preparation and analytical techniques	262
Appendix V.	Igneous geochemical data with sample preparation and analytical techniques	270
Appendix VI.	Summary of numerical analysis data	303
Appendix VII.	List of ~55 underground areas studied as part of this thesis	308

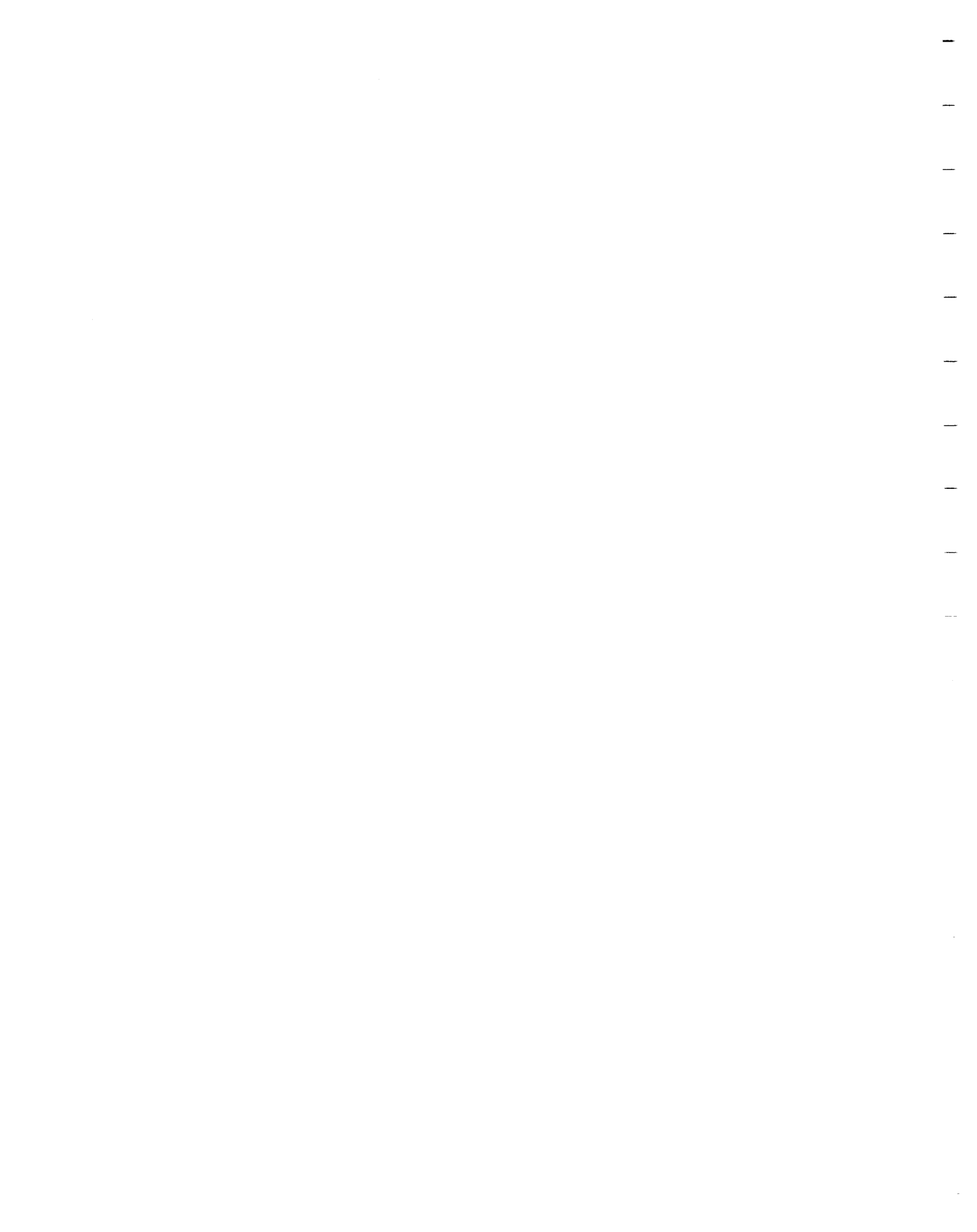


## Acknowledgements

This thesis would not have been possible without the help and support of many people. Particular thanks go to my supervisor, Prof. Ed Spooner, for his supportive financial backing and his ability to steer the research in useful and productive directions. Prof. Tony Naldrett and Dr. Mike Gorton are thanked for their scientific appraisal at committee meetings and for reading the thesis. I am especially grateful to co-authors Dave Broughton and Frank Ploeger for sharing their considerable expertise, and for their important scientific contributions to this study.

I would like to thank Golden Shield Resources (1987-1989) and GSR Mining/Deak Resources Ltd for their permission to publish this study, for their active help and co-operation throughout, and for employing me during the summers of 1988 and 1989. To mine managers Doug Douglass and Rod Doran, and Golden Shield staff Roger Milot, Dan McCormick, Mark Croteau, Jim Butler, Garry Kniereman and Kate Calberry go many thanks for advice and guidance, as well as to Jim Fortin, Margot Fortin and Ron Moran of GSR Mining/Deak Resources Ltd. The support and co-operation of Dave Toogood and Bill McGuinty of Queenston Mining Ltd., and Gary Grabowski and Gerhard Meyer of the Kirkland Lake Resident Geologist's Office, are gratefully acknowledged. Kerr Addison Mines Ltd. are thanked for their careful preservation of the mine geological records.

I am grateful to Jack Hamilton of Queen's University for permission to quote material from his M.Sc. thesis (1986) in the text and in Figure 9, and to Wayne Powell of Queen's University for permission to use his preliminary unpublished M.Sc. thesis map as part of Figure 1. I would like also to thank B.Sc. students Eira Thomas (University of Toronto) and Duncan Friend, Ruth Jones, Susan Middleton and Paul Thomas (University of Oxford) for their collaboration on project work. Samples of the Abitibi Batholith marginal diorites were kindly provided by Alan Smith, formerly of the Ontario Geological Survey.

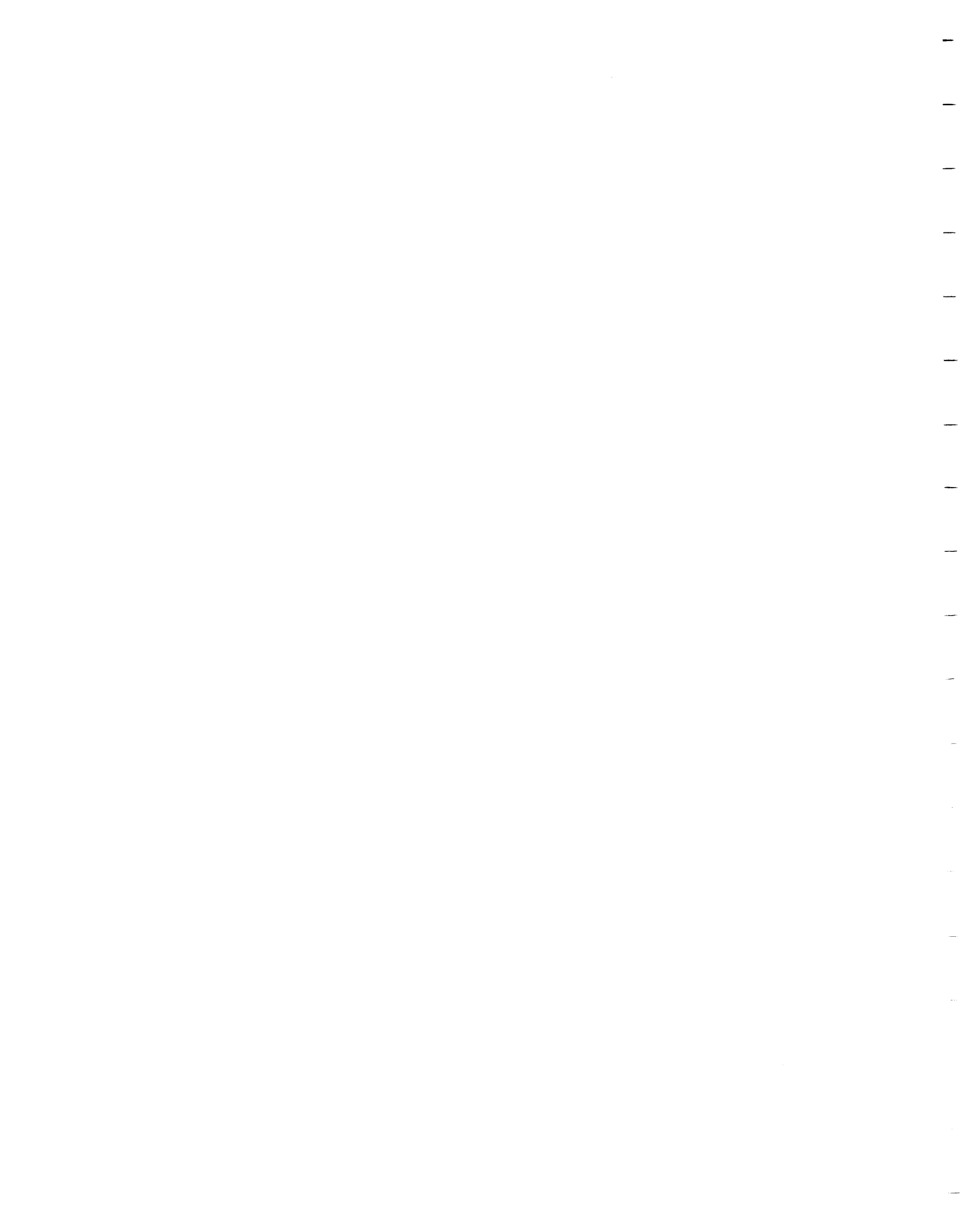




The technical production of this thesis would not have been possible without the significant input of several staff at the University of Toronto. I would particularly like to thank Master Draftsman Subhash Shanbhag for drafting and design of figures, Karyn Gorra for preparing the photographs, Jim Charters for computing advice, George Taylor and Shaun McConville for preparing thin sections, and Claudio Cermignani for instructing me in the use of the XRD apparatus. Department Administrator Roland Sharples, and office staff Brenda Laurent and Henny Wang are also thanked.

Financial assistance in the form of a University of Toronto Fellowship (1987-1989), a Differential Fee Waiver Scholarship (1987-1989), a research assistantship, and a teaching assistantship is gratefully acknowledged. Continued financial support by the Ontario Geoscience Research Grant Program (Grant #326) and NSERC Strategic Grant #G1862 (to Prof. E. T. C. Spooner) is similarly acknowledged.

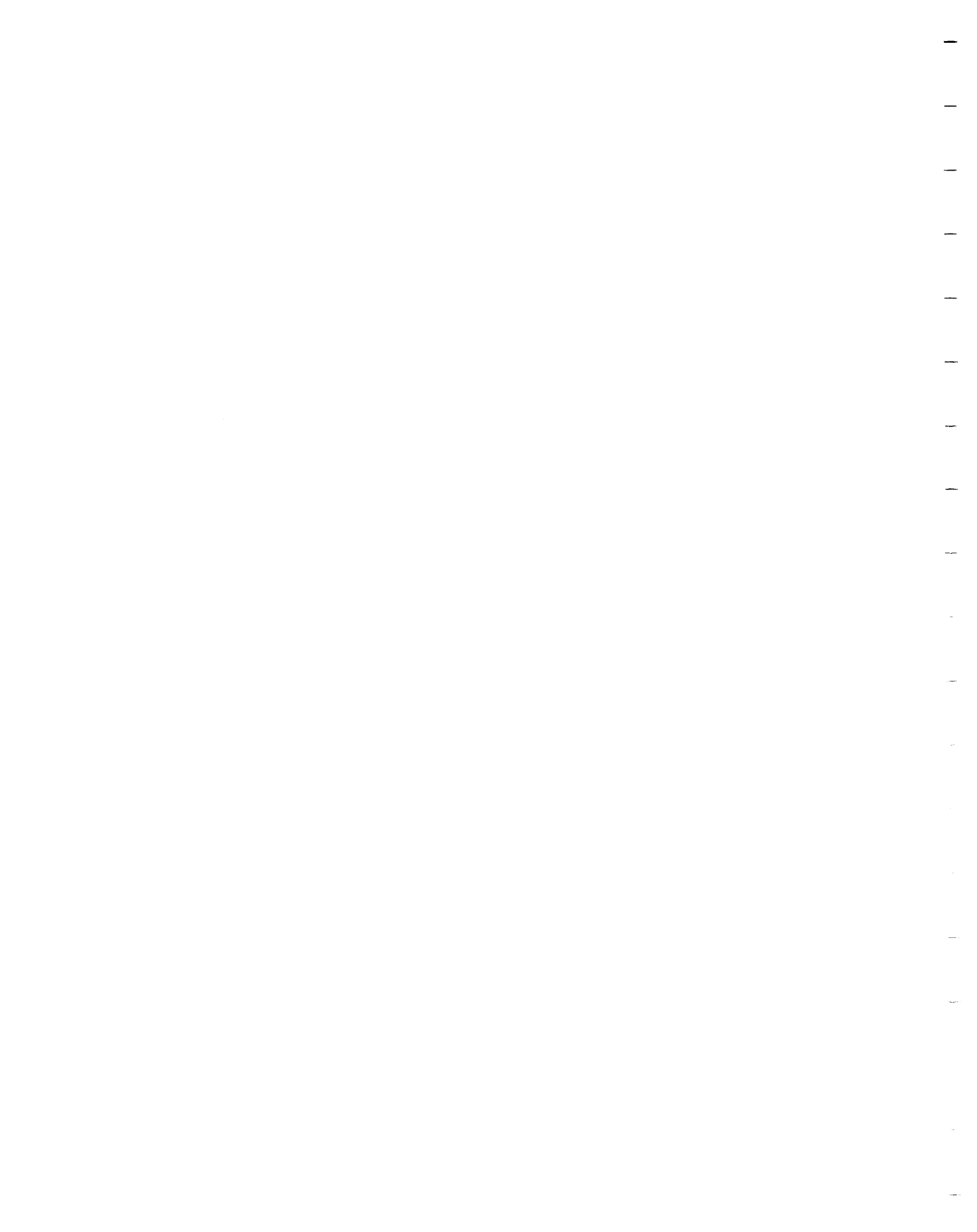
Finally I wish to thank geologist "Red" Parsons of Toronto, and my friends and colleagues at the University of Toronto, in particular Dominic Channer, Dick Jemielita, Cornel de Ronde, Dave Burrows, Andy Abraham and Colin Bray, for sharing their geological expertise and for their encouragement towards this one last deadline. And of course my family and Elizabeth for all their love and support.



## Abstract

The major Kerr Addison-Chesterville Archean Au-Ag-(W) epigenetic quartz vein/disseminated ore system (~335 t Au; #5 in the Superior Province) is, unusually, located within and is syndeformational with respect to the ~300 km long, first order, Larder Lake-Cadillac "Break" (~2,130 tonnes Au associated), which to the east defines the Pontiac-Abitibi subprovince boundary and to the west lies within the Abitibi greenstone belt. The ~150 m wide Break deformation zone at Kerr Addison is a flattened (~5:5:1), over-steepened, S-over-N thrust, characterised by intense foliation development and is localised by a thin ultramafic horizon; it is cross-cut by the brittle post-ore Kerr Fault. Inhomogeneous bulk shortening and dextral transpression, but not significant strike-slip movement, in the Break zone are possibly related to closure of a small Timiskaming intra-arc basin at ~2675-2670 Ma. Au was introduced by external hydrothermal fluids synkinematically relative to a late  $S_2$  flattening fabric and steep east-plunging lineation. Ore types comprise: "flow ore" in massive to pillowed Fe-tholeiites (20.9 mtonnes at 11.0 g/t Au; 230 tonnes Au), "green carbonate ore" in relict spinifex-textured komatiites with ~5-15 vol. % igneous "albitite" dykes (15.0 mtonnes at 7.8 g/t Au; 118 tonnes Au), "graphitic ore" which includes some graphitic Kerr Fault gouge (1.8 mtonnes at 7.9 g/t Au; 14 tonnes Au) and minor mafic intrusion-hosted "albitite ore" (0.8 mtonnes at 3.9 g/t Au; 3 tonnes Au). Mineralisation defined 20 (Kerr) and 9 (Chesterville) separate orebodies, the largest of which was the Kerr #21 flow orebody (13.7 mtonnes at 12.5 g/t Au; 172 tonnes Au). The composite hydrothermal/igneous Au system is partly contained ("green carbonate ore") in a flat funnel-shaped hydrothermal alteration envelope, plunging 70°E in the plane of the Break to a  $\geq 4$  km depth source, which contracts from ~900 x 60-75 m (surface) to ~300 x 20-50 m ( $\geq 5600$  ft level).

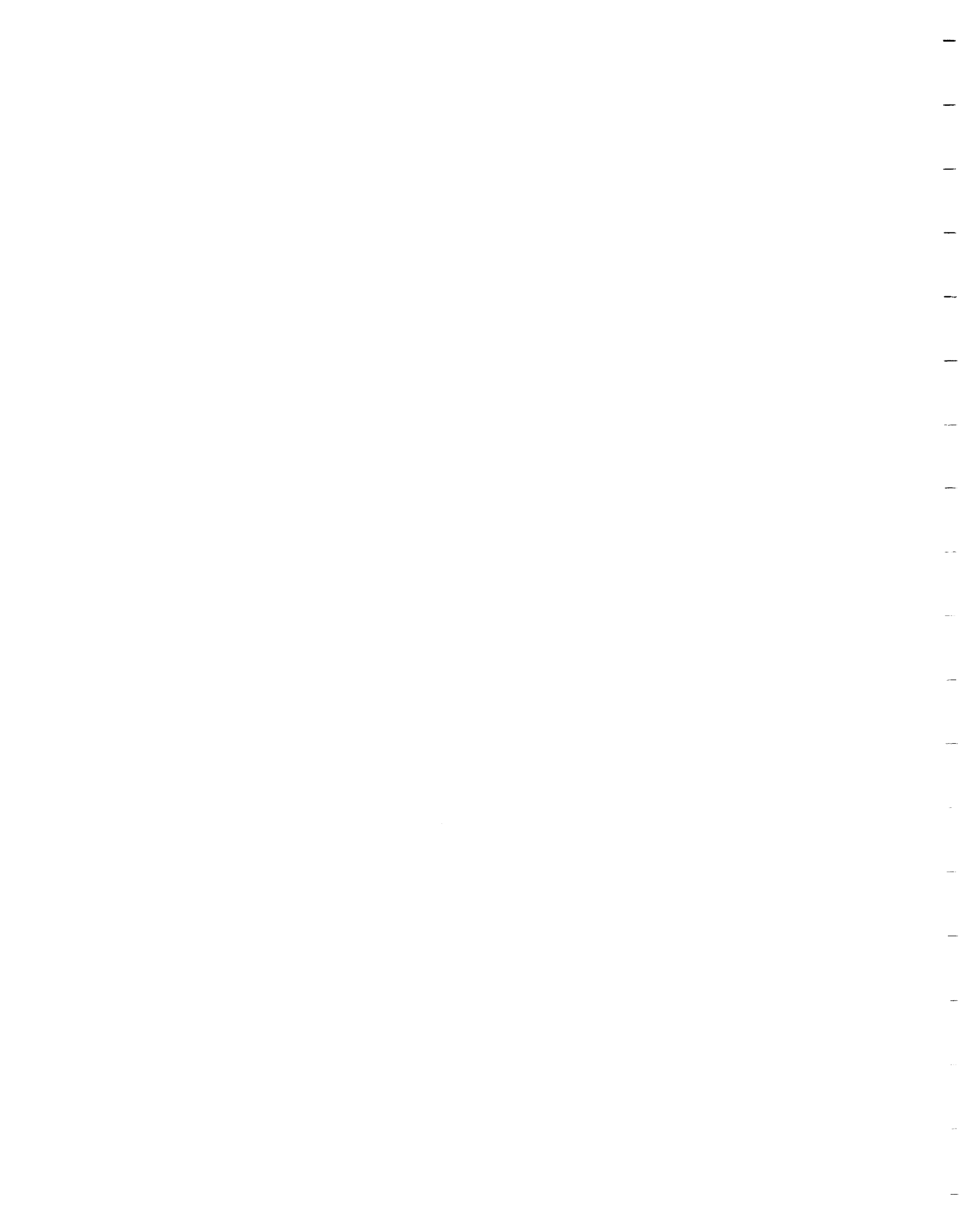
Multi-stage, vein related Au-Ag-(W) mineralisation and "albitite" dyke/plug intrusion are contained in time within the interval of Break ductile deformation, and Au mineralisation was approximately synchronous in the two major ore types; different mineralisation and alteration styles are host rock controlled. Barren pre/post-ore veining is also carbonate alteration-related. The Au-quartz vein system and associated hydrothermal alteration were developed co-spatially, co-structurally and co-temporally with respect to three mafic igneous plugs and a swarm of >5,000 mafic "albitite" dykes ( $A_1$ ;  $A_2$ ;  $A_3$ ); this association is present ~650 m *below* mined ore in a small (~300 x 50 m) feeder root zone at a depth of ~2,000 m below the current land surface, suggesting that it characterises the source region. Later dykes in the time sequence ( $A_2$ ;  $A_3$ ) clearly cross-cut earlier Au related veins and



earlier dykes (A<sub>1</sub>; A<sub>2</sub>), which contain more vein stages; the later dykes are also more altered, and mineralised to higher Au grades. A<sub>2</sub> dykes also contain xenoliths of earlier Au-pyrite mineralization. Hence, a significant amount of main stage Au mineralisation is clearly intra-"albitite" dyke intrusion in timing (e.g. A<sub>1</sub>/A<sub>2</sub>), and A<sub>2</sub> and A<sub>3</sub> "albitite" dykes are clearly intra-Au mineralisation in timing; the A<sub>1</sub>, A<sub>2</sub> and A<sub>3</sub> dykes also show no significant primary geochemical discontinuities.

Most Au is contained within a discrete ~1,130 m vertical interval, and Kerr Addison shows *both* the top and the bottom of an Archean Au ore system, including a sub-economic hydrothermal ore fluid feeder root zone (~300 x 20-50 m) which contains quartz veins with no Au; Au was in solution but did not precipitate. The Au system probably closed off ~150-300 m above the present erosion level, and developed internally in the Archean crust without connecting to the paleosurface as a major altered zone (c.f. Chesterville East zone). Green carbonate alteration, quartz veins and "albitite" intrusions show correlated expansion and contraction profiles with height above the same small root zone, and were temporally and physically linked in order to transmit and equalise hydraulic pressure. Correlated decreases in Au grades,  $\Sigma$ Au, Ag: Au ratio, "albitite" intrusion (>0.3m) thickness,  $\Sigma$ quartz vein (>0.3m) thickness and green carbonate alteration width in the top of the system can be used as approximate guides to vertical level in exploration/evaluation drilling.

Features of the Au system can be best explained by an hydraulic fracturing/fluid inflation model rather than a "fault valve" model. Sulphidation reactions (e.g. Phillips et al., 1984) controlled disseminated pyrite mineralisation in the "flow", "graphitic" and "albitite" ores, whereas fluid supply and native Au deposition in the "green carbonate ore" are interpreted to have been controlled by H<sub>2</sub>O-CO<sub>2</sub> phase separation (e.g. Spooner et al., 1987b; Bowers, 1991), fluid inclusion evidence for which has been described from the deepest "green carbonate ore" on the 4000 ft level by Channer and Spooner (1991). Dimensional constancy of the hydrothermal alteration feeder zone at  $\geq$  the 5600 ft level suggests that H<sub>2</sub>O-CO<sub>2</sub> phase separation started in the 4800-5600 ft level interval. Au:Ag ratios increase smoothly upwards from ~16:1 to ~22:1, due to partition of Ag into Au<sup>0</sup>. The weight of the geological evidence indicates that mafic "albitite" (?shoshonitic) intrusions and Au-bearing hydrothermal fluids in the Kerr Addison-Chesterville ore system were sufficiently correlated in space, structure and time, including the root zone at ~2 km present depth, to have been derived from a larger, common parent intrusive body at  $\geq$ 4 km depth below the present erosion level.



**ARCHEAN AU-AG-(W) QUARTZ VEIN / DISSEMINATED  
MINERALISATION WITHIN THE  
LARDER LAKE - CADILLAC BREAK,  
KERR ADDISON - CHESTERVILLE SYSTEM,  
NORTH-EAST ONTARIO, CANADA**

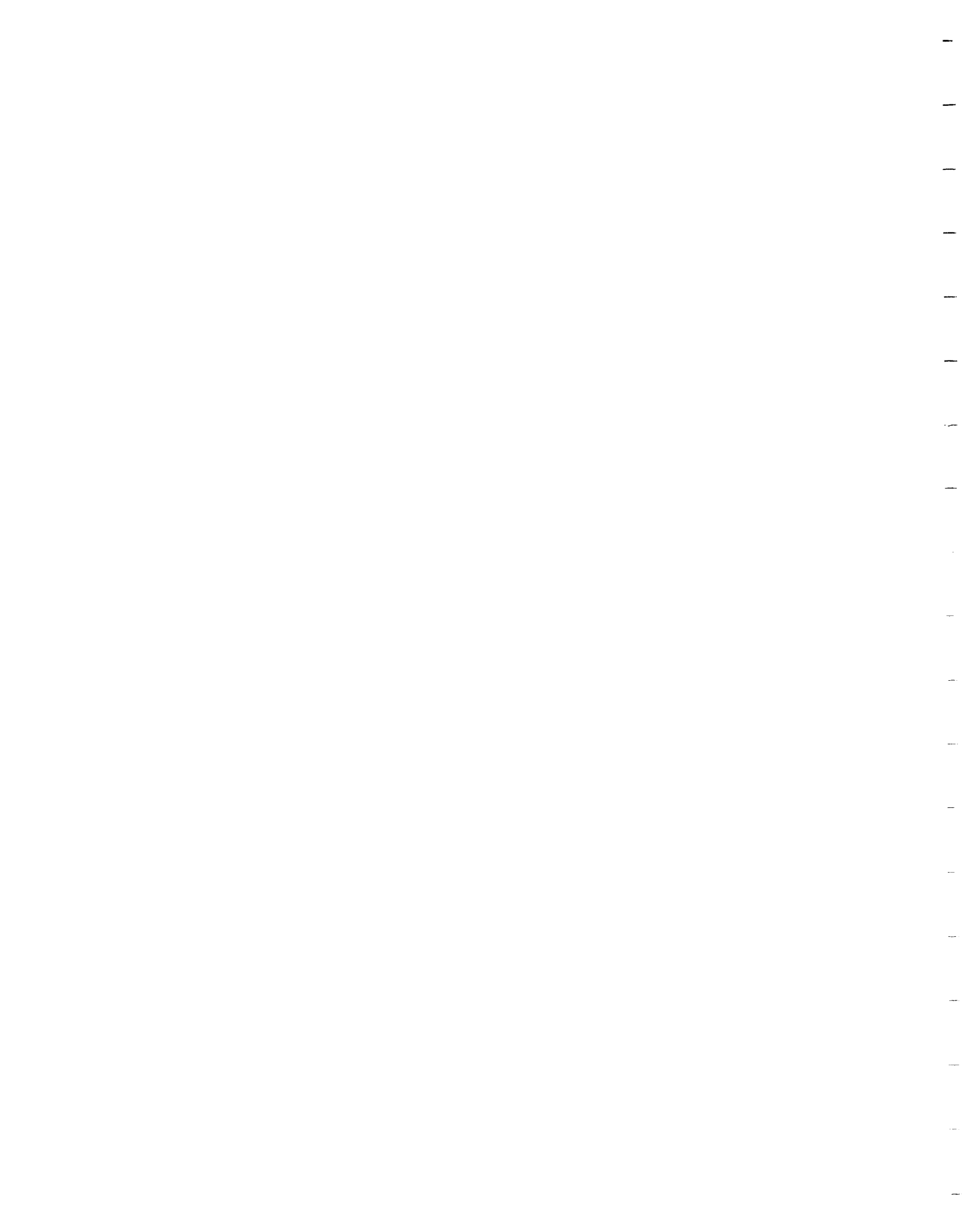
**STRUCTURAL SETTING, GEOLOGICAL CHARACTERISTICS, TIME  
SEQUENCE, MAFIC "ALBITITE" DYKE SWARM AND ORE CONTROLS**

**J.P. Smith, E.T.C. Spooner,**  
Department of Geology, Earth Sciences Centre, University of Toronto,  
22 Russell St., Toronto, Ontario, Canada M5S 3B1.

**D.W. Broughton\***  
1987-1989, Golden Shield Resources, Kerr Addison Mine, Virginiatown,  
Ontario, Canada P0K 1X0.

**and F.R. Ploeger**  
GSR Mining / Deak Resources Ltd., Kerr Addison Mine, Virginiatown,  
Ontario, Canada P0K 1X0.

\* current address: Noranda Exploration Co. Ltd., 60 Shirley St. S., Timmins, Ontario,  
Canada P4N 7J5.





## 1. Introduction

The Kerr Addison - Chesterville Archean Au-quartz vein / disseminated ore system, located at Virginiatown / Kearns ~500 km north of Toronto, 2 km west of the Quebec border, is significant because of its size (~332 tonnes Au) and unusual location *within* the Larder Lake - Cadillac Break, a major tectonic structure ~300 km long which, to the east of Kearns, defines the Pontiac-Abitibi sub-province boundary (e.g. Robert, 1989); to the west, the Break lies within the Abitibi greenstone belt (see Figure 1).

A narrow ~5-10 km wide structural corridor along the Break constitutes a very significant Au producing zone, with total production plus reserves of ~2130 tonnes Au from ~72 mines (see Figure 1; data from Bertoni, 1983 and other sources). However, most of the mines are located on subsidiary structures rather than in the Break itself (e.g. Colvine et al., 1988). To the north of the Break examples include the Kirkland Lake camp related to the Kirkland Lake Main Break which merges to the west with the Larder Lake - Cadillac Break in the Kenogami Lake area (G. Grabowski, Ontario Geological Survey Resident Geologist, pers. commun. 1989), the Upper Canada deposit (Toogood, 1989), the Francoeur/Arntfield/ Wasamac deposits related to the Francoeur-Wasa Shear Zone (Couture et al., 1991), the Doyon-Bousquet-Dumagami system (Tourigny et al., 1988), and the Lamaque-Sigma Au system (e.g. Robert et al., 1983). To the south of the Break examples include Anoki (near Dobie), the Raven River and Laguerre mines in Larder Lake, and the Malartic camp in Quebec. Thus, the large Kerr Addison - Chesterville system is unusual because of its location *within* the main Break structure, where it is syn-deformationally (see below) contained within a ~150 m wide zone of foliation intensification, and cross-cut by the later, brittle Kerr Fault which, in part, uses earlier structures. Other examples of ore systems located within the Break (see Figure 1) include the McBean, Omega, Cheminis, Fernland, Barber Larder and Armistice deposits to the west in Ontario, and the McWatters and Astoria mines (near Rouyn) and the Orenada deposit (south of Val d'Or; Robert, 1989) to the east in Quebec.

As the data in Table 1 show, the combined Kerr Addison (35,313,000 tonnes at 9.1 g/t Au) - Chesterville (2,957,820 tonnes at 3.77 g/t Au) mines comprise the fifth largest known (~332 tonnes Au) typical Archean Au-quartz vein / disseminated ore system in the Superior Province, after Hollinger - McIntyre (production plus reserves: ~995 tonnes Au), the seven Kirkland Lake mines which define a single system (~720 tonnes Au), the Campbell - Dickenson Au system, Red Lake (460 tonnes Au) and the Dome mine (~391 tonnes Au). In common with many other Archean Au-quartz vein ore systems (e.g. Hollinger-McIntyre; Kolar, India; Lamaque-Sigma) the Kerr Addison - Chesterville Au system is locally enriched in W in the form of scheelite (e.g. 1,533 tonnes at 0.5 - 0.7 % WO<sub>3</sub> produced in 1942; reserves defined at that time of 46,300 tonnes at 0.085 % WO<sub>3</sub>).

Despite its importance, previous factual documentation of the Kerr Addison - Chesterville system has been relatively limited and hypotheses of its origin have been diverse, as summarised in Table 2. Hence, the principal objective of this research has been to analyse the lithological and structural characteristics of the ore; the relative time sequence of all deformation, mineralisation, veining, hydrothermal alteration and igneous intrusive events; to determine the exact controls on the horizontal and vertical distribution of Au; and to place mineralisation in a local/regional geological context. In order to contribute to an understanding of Archean Au-quartz vein ore systems in general, a second objective has been to describe and interpret the Kerr Addison - Chesterville system in a comparable degree of detail to the best described Archean Au deposits to date e.g. Lamaque (Burrows, 1991) - Sigma (Robert et al., 1983; Robert and Brown, 1986a,b; Robert and Kelly, 1987), Hollinger - McIntyre (Burrows and Spooner, 1986; Mason and Melnik, 1986; Wood et al., 1986a,b; Burrows, 1991), Pamour #1 (Walsh et al., 1984), Renabie (Callan, 1988; Callan and Spooner, 1989), Bousquet (Tourigny et al., 1988), the Kambalda area, Western Australia (Roberts, 1988), the Golden Mile, Kalgoorlie (Phillips, 1986; Clout, 1988a,b), and the mines of the Barberton area, South Africa (de Ronde et al., 1988; 1991; de Ronde, 1991).

This research is based on ~21 person-months of fieldwork over 3 years, including ~18 person-months of underground mapping and observations in ~55 areas of the Kerr Addison mine covering 8 of the 9 largest orebodies, correlation of over 6,000 drillholes towards complete geological reconstruction of 27 of the 31 Kerr Addison mine levels (J.P.S.), addition of all available data on Chesterville, 12 person-weeks of surface mapping at a scale of 1:10,000 along the Break in the Virginiatown area (1989), and compilation of previous published and unpublished literature on the two mines.

As mentioned above, the Kerr Addison - Chesterville system is a relatively less common case of Archean Au-quartz vein mineralisation occurring within a major first order structure. Hence, particularly because of its size, its geological characteristics, especially trends in the upper part of the ore system, are directly relevant to continued exploration along the Larder Lake - Cadillac Break, the Destor - Porcupine Break and along major Archean structures elsewhere.

## 2. Discovery and Production History

The discovery and production history of the Kerr Addison - Chesterville system are interesting because of the size of the Au deposit, because the initial showings were some of the earliest found in N.E. Ontario/N.W. Quebec and because those showings were low grade at the top of the Au-quartz vein ore system. In 1906, three groups of claims, the Reddick, the Kerr-Addison and the Hummel-Kearns, were staked on surface showings of low grade "green carbonate" rock, containing minor Au-quartz veins, by parties who travelled by canoe up the north-east arm of Larder Lake (c.f. Miller, 1902). Mr. H.L. Kerr, a 1903 graduate of the University of Toronto, had previously carried out a week of geological mapping in this area as an assistant to Dr. W.A. Parks of the Geological Survey of Canada (see Parks, 1904). The Hummel-Kearns claims were incorporated in 1907 under the name of Chesterville-Larder Lake Gold Mining Company Ltd., Chesterville (near Ottawa, S.E. Ontario) being the group's home town. Funding did not, however, become available for a drill programme on the Chesterville property until 1936. From 1908 to 1909, Reddick Larder Lake Mines Incorporated sank a 27 m shaft at the east end of their property (No. 2 Shaft; see Figure 7 below) and carried out 305 m of lateral development in green carbonate ore on the 83 ft level. A 20-stamp mill was erected and gold from this mill was used to produce Canada's first minted \$5 gold coins in 1908 in the reign of Edward VII.

In 1917, Associated Goldfields Ltd. acquired the "Kerr, Addison and Reddick claims". From 1920 to 1921, the 91 m No.1 Shaft was sunk at the west end of the property (see Figure 7) and significant underground development carried out on the 175 ft and 300 ft levels. At this time, the north cross-cut on the 300 ft level passed *between* the subsequent #9 and #10 green carbonate orebodies missing both by only ~6 m. At least one surface drill hole (#8) intersected the #10 orebody. However, work was abandoned by 1923.

In 1937, the newly-formed Kerr Addison Gold Mines Ltd. purchased the claims and drove four adits (Figure 7) into a low (~25 m), elongate, erosionally resistant hill at the west end of the property with green carbonate alteration (Figure 7). These adits encountered only low gold values. A final drillhole, #8A, was drilled down from adit No.1, beside former Associated Goldfields hole #8 (see above). This #8A discovery hole intersected the #10 green carbonate orebody at the 300 ft level, returning a grade of 10.5 g/t Au over 33 m. Further drilling and lateral development on the 175 ft and 300 ft levels quickly resulted in the delineation of 907,000 tonnes of green carbonate ore grading 10.5 g/t Au to 150 m depth. The No. 3 Shaft and a 450 tonne-per-day (t.p.d.) mill were constructed at a cost of \$1.75 million at that time, and milling started on 2nd May 1938; the first gold bar at Kerr Addison was poured on 11th June, 1938 (Figure 2). Significant tonnages of "flow" ore were not discovered until reaching the 1000 ft level of the Kerr Addison mine in 1940. In early 1937, a drilling programme on the Chesterville property successfully intersected a large body of ore on the first hole, and a 450 t.p.d. mill was built in 1938. The first gold bar at the Chesterville Mine was poured on 29th July, 1939.

At Kerr Addison, mill capacity was raised to 1090 t.p.d. in 1939 and 1725 t.p.d. in 1941, but production diminished during World War II to 1000 t.p.d. at which time exploration was also carried out for scheelite and a small quantity (1,533 tonnes at 0.2 - 0.7 %WO<sub>3</sub>) produced. From 1948 to 1961, production was expanded to over 3,630 t.p.d. with peak production between 1952 and 1960 of approximately 4,080 t.p.d. The best single year for Kerr Addison was in 1960, with production of 18,400 kg Au (see Figure 2) from 1,512,860 tonnes of ore milled, making it the top Au mine in North America for that year. Ore reserves reached a peak of 13,818,120 tonnes at 10.7 g/t Au in 1955.

In contrast, the Chesterville Mine was in operation for only 13 years (1939 - 1952) during which time it produced 2,957,820 tonnes of ore at the lower grade of 3.77 g/t Au (11,162 kg

Au; 603 kg Ag; Au: Ag = 18.51: 1). The Chesterville Shaft (Figure 7) reached a depth of 854 m and 18 mine levels were developed to a depth of 835 m. The Chesterville property was subsequently transferred to Kerr Addison Mines Ltd. in 1957 plus \$50,000 as settlement for a surface cave-in which took down part of the Kerr Addison timber yard.

The Kerr Addison No. 3 Shaft reached a depth of 1174 m in 1958, and deep drillholes to the 4200 ft level appeared to confirm the downward extension and high grade (~20 g/t) of the major #21 "flow" orebody. A decision was made in 1959 to construct the No. 4 Internal Shaft from the 3850 ft to the 6000 ft levels (1829 m depth), 823 m north-west of the No. 3 Shaft, with a conveyor way between the two shafts. Unfortunately, economic mineralisation (flow ore) was found to pinch out completely by the 4600 ft level, just beyond the reach of the original drilling, and after 1960 the ore reserves declined rapidly. A recommendation was made in 1963 to discontinue all further exploration and mine out the remaining ore as a salvage operation. Production declined to 970 t.p.d. in 1967 and 760 t.p.d. in 1970 (see Figure 2 for Au and Ag production). However, the rise of the deregulated Au price from \$35 per oz in 1971 to a high of over \$800 in 1980 resulted in a new lease of life for the Kerr Addison mine. In June 1987, the Kerr Addison - Chesterville property was purchased by a junior mining company, Golden Shield Resources Ltd., who initiated an aggressive exploration programme. However, with a sharp drop in the price of Au, Golden Shield was forced into bankruptcy and ceased operations on 28th June, 1989.

The assets of Golden Shield were acquired in 1989 by GSR Mining Corp., which is 77% owned by GSR Acquisition Corp. (itself 90% owned by Deak Resources Corp., Toronto) and 23% by the former creditors of Golden Shield. With GSR Mining as operator, both surface pit and underground mining were restarted in 1990 (The Northern Miner, 23rd July, 1990, p.21) and continue today (December 1991). Ongoing operations were aided by a C\$2.0 million grant from the Ontario Heritage Fund in April 1991.

Total production to date from the Kerr Addison Mine over its 53-year history (1938-1991) comprises 35.3 million tonnes at a grade of 9.1 g/t Au (321,055 kg Au; 17,690 kg Ag; Au: Ag = 18.2 :1), making it still Canada's historically fifth largest *individual* gold mine. Current ore reserves (all categories, July 1991) stand at ~2,500,000 tonnes at an average grade of 4.5 g/t Au.

### 3. The Structural Nature of the Larder Lake - Cadillac Break

Because of its regional geological importance (e.g. Card and Ciesielski, 1986; Daigneault and Archambault, 1990) and because of its local significance as the major structural control on the localisation of the Kerr Addison - Chesterville Au system, current understanding of the structural characteristics of the Larder Lake - Cadillac Break is summarised in this section. The Break (Figure 1) is a ~300 km strike length ductile/brittle shear zone, ~10-200m wide in outcrop, contained within a structural corridor up to ~5 km wide which is characterised by heterogeneous deformation in the form of strong foliation, tight folding and the development of splays and subsidiary shears (e.g. Gunning and Ambrose, 1927; Norman, 1948; Thomson, 1948; Wilson, 1948; Kalliokoski, 1968; Kutina and Fabbri, 1971; Hamilton, 1986; Tourigny et al, 1988; Robert, 1989).

The Break is localised at the contact between, to the north, a <5 km wide, sinuous belt of locally foliated, coarse to medium grained clastic sediments (Timiskaming and Cadillac Groups) which unconformably overlie tholeiitic to calc-alkaline volcanics (Kinojévis Group in the Larder Lake area) and, to the south (in the Kirkland Lake - Larder Lake area), tholeiitic to ultramafic (komatiitic) volcanics and sediments, and ( in the Cadillac - Malartic - Val d'Or area) mafic to ultramafic volcanics immediately north of the large Pontiac plutonic-sedimentary terrane. The Abitibi rocks are regionally metamorphosed from sub-greenschist to greenschist facies (Jolly, 1974, 1978) with local, narrow amphibolite grade contact metamorphic zones around the large granitoid batholiths. The Pontiac terrane contains kyanite-bearing, amphibolite grade metapelites (e.g. Goulet, 1978).

in addition to its strike extent, several lines of evidence indicate that the Larder Lake - Cadillac Break is a major structural discontinuity across which stratigraphy cannot be correlated, except by absolute age comparisons:



(i) Lithoprobe seismic data (Green et al., 1990; Jackson et al., 1990) confirm that the Break is a major, sub-vertical lithological and structural discontinuity traceable to >15 km depth.

(ii) Contrasting geochemistries of Timiskaming sediments with those south of the Break (Feng and Kerrich, 1990) indicate compositionally different source areas, and tectonic juxtaposition of their volcanic-sedimentary basins.

(iii) Geochronological studies (Frarey and Krogh, 1986; Mortensen, 1987a,b; Corfu et al., 1989) indicate similar ages and parallel development of the juxtaposed basal volcanic rock sequences.

### **Structural and Kinematic Observations; Kirkland Lake - Val d'Or**

In the Kirkland Lake - Larder Lake area, the Larder Lake - Cadillac Break is specifically localised at the contact between Timiskaming sediments to the north and a schistose ultramafic unit at the base of the south-facing Larder Lake Group. Strain is heterogeneously developed within and across the Break and continues into both footwall and hanging wall rocks with associated tight folding. In terms of its surface expression, the Break has an extremely variable dip and strike, being mostly south dipping west of Kerr Addison, steeply north dipping in the Kerr Addison - Chesterville area, and ~70° north dipping in Quebec. There are comparatively few previous descriptions of the ductile strain and kinematics on or near the Break, notably Robert (1989) in the Val d'Or area, Tourigny et al. (1988) in the Bousquet area, Goulet (1978) in the Rouyn area, Hamilton (1986), Hamilton and Hodgson (1983, 1984) and Jackson (1988) in the Larder Lake - Kearns area, and Hodgson and Hamilton (1989), Toogood and Hodgson (1985, 1986), and Toogood (1986a,b) in the Kirkland Lake-Larder Lake area. Their work is summarised in Figure 3.

Based on internal fabrics, Robert (1989) considers the Break in the Val d'Or area (dip ~80°N, strike ~100°) to be a zone of dextral transpression resulting from two increments of the same progressive deformation, evolving from a significant D<sub>1</sub> shortening event to more transcurrent (D<sub>2</sub>) shearing. The slight obliquity of sub-vertical S<sub>1</sub> fabrics to the Break, the orientations

of intrafolial folds and a sub-vertical to steep east dipping  $S_1$  stretching lineation require dextral and vertical components of  $D_1$  motion.  $D_2$  is characterised by asymmetric Z-folds, which resulted from strong dextral transcurrent shearing related to NE-SW compression.

Hamilton (1986) documented two distinct deformation events in the Larder Lake area:  $D_1$  related to a N-S to NNE-SSW compressional event, and  $D_2$  related to NNW-SSE compression.  $D_1$  is characterised by large scale WNW-ESE folding of the Kinojévis and Larder Lake Group volcanics and Timiskaming sediments, development of a regional axial planar  $S_1$  cleavage and initiation of the Break as a south-dipping, south over north reverse structure or sinistral transpression zone, depending on its relative strike orientation.

$D_2$  was considered by Hamilton (1986) to involve the selective development of an intense  $S_2$  fabric and tight asymmetric folding centred on the Break and conforming to its dip (~70-80°S) and strike (060-100°). The  $S_2$  fabric overprints any previous fabric within the Break, shows a strong flattening component, and shows sub-vertical to steep east-dipping elongation lineations. Asymmetric  $F_2$  folds correspond to south over north translation with a minor dextral component of motion. Jackson (1988) also observed flattened, elongated clasts in sediments south of and adjacent to the Break, defining a steeply east-plunging lineation within the steep east-west fabric.

Toogood and Hodgson (1985, 1986) and Toogood (1986a,b) reported two stages of deformation in the Gauthier Township area, where the Break strikes unusually at ~120°, and dips ~70° south. The earlier  $S_1$  fabrics were considered by them to comprise a shear zone-related, sub-vertical S-C foliation set, interpreted to result from dextral strike slip motion on the Break. The  $S_1$  fabric is overprinted by a pervasive, sub-vertical, north-east striking (030-070°)  $S_2$  cleavage, related to flattening, pressure solution and/or crenulation, rarely associated with folds. Toogood (1986a,b) tentatively interpreted this  $S_2$  regional fabric to result from continued dextral strike-slip movement and expansion of the Break deformation zone.

However, the occurrence of tight to isoclinal, NW-SE striking folds and overturned bedding in the adjacent Timiskaming sediments to the north of the Break in Gauthier Township (Thomson and Griffis, 1944; McLean, 1950; Friend, 1990) would appear to require also a N-S to NNE-SSW shortening component of the early  $S_1$  deformation, in agreement with Hamilton (1986). Toogood (1986a,b) also documented late stage, north side up narrow shear zones, associated with minor crenulation and open folding of the  $S_2$  fabric.

We suggest that the observations of all the above workers, as well as this study, may be mutually reconciled in terms of the overall Break kinematics shown in Figure 3. The *specific* kinematics at any one locality studied appear to be a function of the relative strike orientation of that particular Break segment to the principal  $D_1$  (N-S to NNE-SSW) and  $D_2$  (NNW-SSE to NW-SE) compression directions. Thus the Break may be interpreted in terms of two phases of bulk shortening and dextral transpression along an irregular boundary. However, structural studies and tectonic models disagree as to whether collision was north-over-south, related to northward-directed underplating of a southern terrane (especially the Quebec portion: Dimroth et al., 1982; 1983a,b; Ludden and Hubert, 1986; Ludden et al., 1986; Gauthier, 1988; Hodgson and Hamilton, 1989) or in fact south-over-north (especially Ontario portion: Hamilton, 1986; Jackson and Sutcliffe, 1990). This work indicates a *south over north*, flattened and over-steepened thrust origin for the Break (see below). Steeply plunging lineations in the Break are difficult to reconcile with some tectonic models (e.g. Hubert et al., 1984; 1991) which invoke large strike-slip wrench fault displacements.

Hodgson and Hamilton (1989) considered that the Larder Lake - Cadillac Break marked an initial collision zone with southward-directed overthrusting. Later movement involved backthrusts with significant uplift and erosion of the upper amphibolite grade Bellecombe (Pontiac) terrane. The major NNE-SSW shear zone inferred to occur underneath the north east arm of Larder Lake (Hamilton, 1986) and later reactivated as a graben containing Cobalt

sediments (Lovell and Caine, 1972) may also have played an important “triple junction” role in accommodating differential relative movement between the blocks south of the Break (Feng, 1991). Powell et al. (1989, 1990) showed that south-side-down brittle-ductile fault reactivation of the Break continued into the Proterozoic, induced deformation in the overlying Huronian sediments, and may have even offset Matachewan dyke swarm patterns (a related Hearst swarm mafic dyke was U-Pb zircon dated at  $2454 \pm 2$  Ma by Heaman, 1988).

The absolute ages of the various stratigraphic units, and the likely timing of deformation on the Larder Lake Break and introduction of Au mineralisation, based on this study, are shown schematically in Figure 4. Within the structural framework outlined above, we attempt to show in this paper that Au mineralisation in the Kerr Addison - Chesterville system was introduced syn-deformationally relative to the  $D_2$  structural event (see below), in agreement with timing observations by Robert (1989) on the Orenada deposit south of Val d’Or. In addition, previous workers (Thomson, 1941; Hodgson, 1986) noted a correlation in the Kirkland Lake - Larder Lake area between the occurrence of significant Au deposits and those portions of the Break and associated splays which are generally east-north-east trending i.e almost perpendicular to the inferred NNW-SSE direction of  $D_2$  compression. These segments were probably active as reverse shear zones and/or backthrusts during Au mineralisation (c.f. Hodgson and Hamilton, 1989).

Finally, underground observations on the 3850 ft level of the Kerr Addison mine (for further details see below) indicate that the Break in this locality is a ~150 m wide high strain zone, characterised by a very prominent but heterogeneously developed, lithologically controlled foliation showing local internal intensification in ~1-10 m wide high strain zones. Foliation is particularly strongly developed in spinifex-textured komatiitic ultramafics, <10 - 150 m wide, which have been traced through mapping semi-continuously along the Break from the Quebec border to Kenogami Lake, west of Kirkland Lake (see Figure 5 of Tihor and Crocket,

1978), and which may correlate with the Piché Group ultramafics in Quebec which are present as far east as Val d'Or (e.g. Fig. 3 of Robert, 1989; Orenada deposit). Even further west, in the vicinity of the Au mines of the Matachewan area, Sinclair (1982) and Lovell (1967b) reported observations of an ultramafic horizon associated with fluvial sediments, later interpreted as part of the western extension of the Break by Powell et al. (1989; 1990).

Evidence from detailed mapping in the Barber Pit area (see below) supports a south-over-north, flattened and steepened thrust origin for the Break near Larder Lake. Hence, the *fundamental original thrust discontinuity* is interpreted to be located at the north contact of the thin ultramafic unit which forms the base of a south-facing Larder Lake Group stratigraphic package. The locally transgressive nature of this structural contact accounts for the variation in width and occasional complete pinching out of the ultramafics (e.g. between Bear Lake and Barber Lake, McGarry Township) observed during mapping along the Break .

#### 4. Lithologies Associated with the Larder Lake - Cadillac Break

The stratigraphic units of the Kirkland Lake to Malartic area may be grouped and correlated as follows (see Figure 1; after MERQ/OGS, 1983; Jensen and Langford, 1985):

##### 4.1. North of the Larder Lake - Cadillac Break:

***Kinojévis Group - Rouyn-Noranda Tholeiitic Unit*** (~2702 Ma, Corfu et al., 1989). These groups consist mainly of Mg-rich and Fe-rich tholeiitic basalt flows with some tholeiitic dacite and rhyolite towards their tops. They form the immediate basement beneath the Timiskaming sediments in the Virginiatown area.

***Blake River Group*** (2701±2 Ma to 2698±1 Ma; Mortensen, 1987a,b). This group consists mainly of calc-alkaline basalt and andesite forming massive, pillowed and fragmental flows. Some Mg-rich tholeiites, calc-alkaline dacites, and rhyolite flow breccias and tuffs also occur.

***Timiskaming Group*** (~2686 Ma to ~2677 Ma, Corfu et al., 1991) - ***Cadillac Group***. The Timiskaming Group comprises polymict fluvial conglomerates, arkosic sandstones, turbiditic greywackes, quartz-rich siltstones (e.g. Hyde, 1980), and mafic to felsic trachyte flows, flow breccias and tuffs ranging from saturated to undersaturated in normative quartz (Cooke and Moorhouse, 1969). Sedimentary material is mostly derived locally, with occasional exotic clasts (e.g. ultramafic fragments; jasper pebbles). The Cadillac Group comprises distal conglomerates and greywackes.

The Kinojévis and Blake River Groups define the 50-60° east-plunging Blake River Synclinorium, unconformably overlain on its south limb by the Timiskaming Group (Pyke et al., 1973). The Timiskaming Group in Ontario forms a narrow (<5 km), elongate (>100 km) belt along the north side of the Larder Lake - Cadillac Break, defining an overall south-facing succession which may be locally folded and/or overturned. The Timiskaming

northern contact with the Kinojévis Group has been clearly shown to be a basal angular unconformity (Thomson, 1941, 1946; Thomson and Griffis, 1944; Hewitt, 1963; Hyde, 1978; Jensen, 1978b; Downes, 1979; Kimberly et al., 1985; Jackson, 1988) and a significant age difference between the Timiskaming and its basement has been confirmed by geochronological studies (see above). Equivalent lithologies (Cadillac Group) have been shown to occur on both sides of the Break south of Rouyn/Noranda, unconformably overlapping *both* the Kinojévis and Pontiac Groups (C. Hubert: p 118 in Transcriptions of Plenary Discussion Sessions, NUNA Research Conference, Val d'Or, May 1990).

Previous interpretations of the tectonic setting of the Timiskaming Group have involved its sedimentology (e.g. Hewitt, 1963; Hyde, 1978; 1980; Friend, 1990; Feng and Kerrich, 1990), its volcanic and intrusive geochemistry and petrography (Cooke, 1966; Cooke and Moorhouse, 1969; Capdevila et al., 1982; Kerrich and Watson, 1984; Ujike, 1985; Hattori and Hart, 1991), and its distribution, structural setting and spatial association with the Larder Lake - Cadillac Break (e.g. Colvine et al., 1984; Toogood and Hodgson, 1985; Wyman and Kerrich, 1988; Hodgson and Hamilton, 1989; Corfu et al., 1991). These interpretations are presented in the following paragraphs:

(i) Hyde (1980) showed that the Timiskaming sediments (*sensu strictu*, north of the Break) were mainly of fluvial origin, with facies typical of braided river and floodplain deposition. In Gauthier and McVittie Townships, the fluvial sediments grade abruptly (with *no* intervening shoreline or shallow shelf facies) into deep water proximal turbidites, interpreted to have formed in a submarine fan environment (Hyde, 1980).

(ii) Cooke and Moorhouse (1969) identified four episodes of alkaline volcanism within the Timiskaming stratigraphy, each episode showing evolution from early mafic trachyte flows to later, abundant, pseudoleucite-bearing trachyte flows, flow breccias and finally, alkaline pyroclastics. The stratigraphically lowest volcanic episode is the least differentiated and

comprises abundant calc-alkaline lavas (andesites and minor basalts). Cooke and Moorhouse (1969) showed that the petrography and major element compositions of the more evolved Timiskaming alkaline volcanics were similar to those of modern pseudoleucite-bearing lavas from the Roman province of western Italy, Central Java and the Wyoming-Montana region, and were thus characteristic of the late stages of island arc development. Jensen (1981b) redefined the volcanics as comprising mainly trachytes, trachyandesites and K-rich dacites. Using trace elements (Zr, Y, REE), Capdevila et al. (1982) confirmed the resemblance of the Timiskaming to modern high-K volcanic arc rocks and showed that the Timiskaming trachytes had highly fractionated REE patterns ( $La_N/Yb_N = 13$  to  $63$ ).

Based on their spatial association and mineralogical and geochemical similarities to the mafic and pseudoleucite trachytes respectively, intrusions of mafic and felsic syenite in the Kirkland Lake - Larder Lake area were considered by Cooke and Moorhouse (1969) to be co-magmatic with the Timiskaming volcanics, possibly defining former volcanic centres. Kerrich and Watson (1984) found that the mafic, felsic and porphyritic syenite intrusions hosting the Kirkland Lake Au-quartz vein system defined coherent steep REE patterns ( $La_N/Yb_N \sim 15$ ), suggesting their common magma parentage. They found, however, that these alkaline intrusions were compositionally distinct from typical syenites in terms of Ti/Zr, Nb/Y, REE patterns and other diagnostic trace element ratios, and were instead closely similar to the alkali basalt-gabbro series. Hattori and Hart (1991) showed that both the syenite intrusions and the Timiskaming alkaline volcanics of the Kirkland Lake camp possessed distinctive island arc signatures shown by Nb-Ta-Ti troughs and strong LILE enrichments on extended trace element diagrams. These authors redefined the Kirkland Lake alkaline rocks as being of *shoshonitic* affinity, a conclusion endorsed by Corfu et al. (1991).

(iii) Some authors (e.g. Colvine et al., 1984; Toogood and Hodgson, 1985; Wyman and Kerrich, 1988) have considered that the Timiskaming lithologies formed in strike slip pull-apart basins or transtensional grabens which developed along the major Larder Lake -



Cadillac Break structure, particularly where segments occurred oriented at an angle to the overall orientation of the Break.

(iv) Hodgson and Hamilton (1989) considered that the Timiskaming sediments formed as a syntectonic molasse assemblage of fault scarp-related conglomerates and mass flow deposits, related to the erosion of major thrust hanging wall blocks with deposition of debris in footwall troughs.

Of the interpretations proposed above, we do not support (iii) due to the lack of evidence for major strike slip movements, and we suggest that (iii) and (iv) are invalidated by the following evidence:

(a) timing:  $D_1$  and  $D_2$  deformations are both superimposed on, and therefore postdate, formation of the Timiskaming (Hamilton, 1986);

(b) Hyde (1980) explicitly states that for the Timiskaming conglomerates there is a “.. *lack of evidence for sub-aerial debris flow, sieve deposition or talus accumulations. Rounded clasts and abundant cross-stratification in both sandstones and conglomerates argue against mass flow processes.*”;

(c) An apparent spatial relationship between the Timiskaming Group and the Larder Lake - Cadillac Break, or the occurrence of unconformable Timiskaming sediments on either side of the Break, are *not* sufficient evidence to link the two genetically. In the case of the syntectonic, thrust-related sediments of the Moodies Group, Barberton greenstone belt, South Africa (de Wit et al., 1987), to which comparison of the Timiskaming Group was made by Hodgson and Hamilton (1989), far more stringent rules were applied, for example the occurrence in later conglomerates of *clasts of deformed earlier conglomerates*.

Based on the evidence outlined in (i) and (ii), the most likely tectonic setting for the Timiskaming lithologies is an intra-arc extensional basin or downwarp (e.g. Recent West

Pacific: Woodlark Basin; Manus Basin; Fiji area; ?Chile: Altiplano). The present linear configuration of the Timiskaming Group along the Larder Lake - Cadillac Break (Figure 1) appears to be a *relict geometry* after collisional tectonics, closure and elimination of a small intervening basin, and significant south-over-north thrust displacement on the Break which generally terminates Timiskaming outcrop on the latter's south side. The unconformable position and late timing of the Timiskaming and its related alkaline intrusions, and their inferred intra-arc/ collisional tectonic association, are both compatible with models for shoshonite formation (e.g. Morrison, 1980) as late stage island arc rocks.

The Kinojévis and Blake River Groups are intruded by ultramafic sills and syn-volcanic diorites and tonalites e.g. Flavrian Batholith (trondhjemite,  $2701 \pm 2$  Ma), Watabeag Batholith (early dioritic phase,  $2699 +3/-2$  Ma) and later, but pre-shear zone development, quartz porphyries (e.g. analogous to those at Hollinger and Dome mines, 2691 - 2688 Ma). The Kinojévis and Blake River volcanics, as well as the Timiskaming sediments and volcanics, are intruded by undersaturated felsic to basic syenites, feldspar syenite porphyries and monzonites in the interval from  $\sim 2685$  Ma to  $\sim 2675$  Ma (ages quoted in this paragraph and their sources are summarised in Corfu et al., 1989, 1991). These intrusions are generally pre-shear zone development and Au mineralisation. Examples include the Garrison Stock (monzonite-granodiorite,  $2678 \pm 2$  Ma), Watabeag Batholith (quartz monzonite,  $2681 \pm 2.5$  Ma to  $2676 \pm 2$  Ma), and Winnie Lake Stock (quartz monzonite,  $2677 \pm 2$  Ma; see Corfu et al., 1991). Wyman and Kerrich (1988) also published a titanite U-Pb age of  $2673 \pm 2$  Ma for a lamprophyre dyke from the Adams Mine area (Boston Township) which they interpreted to be synchronous with potassic hydrothermal alteration and Au mineralisation in this locality (cf. Ridler, 1976; potassic "tuffs").

#### 4.2. South of the Larder Lake - Cadillac Break; West of Kearns

*Larder Lake Group* (base  $2705 \pm 2$  Ma; Corfu et al., 1989). This group consists of ultramafic to basaltic komatiite lavas (e.g. Jensen, 1978a; Jensen and Pyke, 1982) and Mg-rich tholeiitic basalts, some Fe-rich tholeiitic basalts, fine grained, thinly-bedded distal turbiditic sediments, and interflow calc-alkaline cherty dacites and rhyolitic tuffs near the base. Between Virginiatown and Larder Lake townsite, and south of Larder Lake, turbiditic sediments are extremely prominently developed and comprise the majority of the Larder Lake Group. Rare chert-magnetite BIF, possibly correlated with the Boston Iron Formation to the south-west, also occurs within the sediments (e.g. on Highway 66 at Larder Lake townsite and south of the Cheminis Mine; and at the small waterfall south of Misema Bridge).

Fold relationships and timing of deformation for the Larder Lake Group are similar to those described for the Kinojévis and Blake River Groups (above). Corfu et al. (1989) highlighted an apparent age reversal between the Larder Lake Group ( $2705 \pm 2$  Ma) and the Skead Group ( $2701 + 3 / - 2$  Ma), inconsistent with the earlier stratigraphic subdivisions proposed by Jensen (1985a) and Jensen and Langford (1985) who favoured a continuous 35 km volcanic succession. Corfu et al. (1989) considered this age reversal to imply early southward-directed thrusting of the older Larder Lake Group over the Skead Group, a topic later discussed structurally by Jackson and Harrap (1989) and Jackson and Sutcliffe (1990).

The Larder Lake Group is intruded by syn-volcanic peridotite sills, and gabbroic and dioritic intrusions. Later intrusions are syn- to post-Timiskaming monzonites, syenites, feldspar syenite porphyries, and two generations of lamprophyres (Hamilton, 1986). From field relations (this work), these intrusions are post-regional folding and some are syn-deformational with respect to early fabric development in the Larder Lake - Cadillac Break zone. Examples include the Otto Stock (syenite;  $2680 \pm 1$  Ma) studied by Smith and Sutcliffe (1988), the Lebel Stock (undated), the McElroy Stock (undated) and the Murdoch Creek intrusion south

of Kirkland Lake (Rowins et al., 1989). Syn-deformational mafic "albitite" dykes occurring in the Break in the Kerr Addison - Chesterville Au system will be discussed separately below. *"Albitites" of identical chemistry and similar setting occur in the Hollinger - McIntyre Au system and have been dated at 2673 ± 6/-2 Ma (Corfu et al., 1989). If this date is applicable to the Kerr Addison "albitites", it provides an estimate of the time of ductile-brittle strain on the Larder Lake - Cadillac Break.*

The 40x45 km Round Lake Batholith to the south of the Break (Figure 1; phases at ~2703 Ma and ~2697 Ma; Mortensen, 1987a,b) is a large, composite tonalite-granodiorite intrusion (Lafleur and Hogarth, 1981; Lafleur, 1986), emplaced partly by solid-state diapirism, which has updomed the surrounding volcanics into an anticlinal, outward-younging succession (Jensen and Langford, 1985; Jackson and Harrap, 1989).

#### **4.3. South of the Larder Lake - Cadillac Break; East of Kearns**

*Pontiac Group* (exact age unknown). This assemblage comprises extensive, mature, quartz-rich turbidites (>90% quartz framework in the sandstone component; Lajoie and Ludden, 1984) with local interbeds of komatiitic basalt (MERQ-OGS, 1983; Lajoie and Ludden, 1984). Craton-derived rounded zircons of ages up to 2.9 Ga (Gariépy et al., 1984) and the REE chemical signatures (Ujike, 1984) of the sediments have been interpreted by Lajoie and Ludden (1984) to suggest a passive continental margin setting. Allochthonous units resulting from southward-directed thrusting have been suggested to occur in the Pontiac terrane by Jackson and Sutcliffe (1990) and Jackson et al. (1990), based on shallow-dipping seismic reflectors at depth. The Pontiac Group is intruded by increasingly voluminous granitoids south of the Break, and its metamorphic grade increases rapidly southwards from lower greenschist to upper amphibolite facies (Goulet, 1978).

## **5. Distribution of Ore Host Lithologies in the Kerr Addison - Chesterville Area**

Geological compilation maps of 3 x 8 km and 2 x 1 km areas in McGarry Township containing the Kerr Addison - Chesterville Au system are shown in Figures 6 and 7.

### **5.1. Ultramafic Horizon (Base of Larder Lake Group)**

Throughout McGarry Township along strike from the Kerr Addison - Chesterville Au system a thin (usually <30 m), laterally extensive horizon of altered ultramafic, komatiitic flows occurs within the Larder Lake - Cadillac Break high strain zone (see Figure 6; Downes, 1980, 1981; this work). The Kerr Addison - Chesterville Au system is characterised by a thick lens (~100-150 m) of these ultramafics which narrow, or pinch out, both to the west of Kerr Addison and to the east of Chesterville. The komatiites locally exhibit well-preserved pseudomorphed spinifex textures in all stages of deformation and alteration; the identification of these spinifex textures by Tihor and Crocket (1977) was one of the most significant findings in understanding the origin of these rocks. Ultramafic breccias are not seen along this horizon, which appears to consist of altered flows.

The ultramafics have been traced >1km east of Kearns by drilling underneath the unconformable Proterozoic Huronian sediments, and probably correlate further east with the Piché Group volcanics (~50-1000m thick) in Quebec. They are also traceable as a semi-continuous horizon for >50km to the west along the Break as far as Kenogami Lake (Figure 6; Tihor and Crocket, 1977) and appear also to be present in the Matachewan area (Lovell, 1967b; Sinclair, 1982; Powell et al., 1989, 1990). Hence, the ultramafics are traceable for most of the length of the Break high strain zone itself (~300 km) lending significant support to the interpretation presented here that the original fundamental structural discontinuity was that between the ultramafics at the base of the Larder Lake Group to the south and the Timiskaming sediments which rest unconformably on the Kinojévis Group volcanics to the north.

## **5.2. South of the Ultramafic Horizon (Larder Lake Group)**

In the vicinity of Kearns and Virginiatown the area immediately south of the ultramafic horizon (see Figure 6) comprises a south-facing (see below), ~400m thick mixed assemblage of predominantly Fe-tholeiitic massive to pillowed lavas, with lesser ultramafics, tuffs, volcanoclastic breccias and sediments of the Larder Lake Group. A further ~300 m wide zone of ultramafics, of unknown strike extent, occurs underneath the north-east arm of Larder Lake and outcrops on its north shore. South of this, surface drilling below the ice on Larder Lake has detected significant widths of Larder Lake Group greywackes extending south under the Proterozoic Huronian sediments.

Within the Kerr Addison - Chesterville Au system, an horizon (width = 20-50 m) of Fe tholeiite pillow lava is mineralised to form the "flow ore" type (e.g. #21 and #16 orebodies). However, the #21/#16 flow ore host rocks appear to be a stratigraphically isolated inclusion of mafic volcanics within ultramafic to transitional mafic-ultramafic flows, and cannot be correlated with complete confidence with mafic volcanics south of the Kerr Fault. Graphitic interflow sediments occur within the mafic volcanics and, together with previous structures, have localised post-ore faults (e.g. the Kerr Fault, which displaces part of the #21 orebody; graphitic faults south of the Barber Larder Pit and Omega deposits). Conglomerates and breccias with spinifex-bearing ultramafic fragments are exposed in a cliff SE of the Kerr Addison tailings pond (e.g. Figure 3e/f of Kishida and Kerrich, 1987); however, their precise stratigraphic relations are not yet clear.

Further to the west, a large area extending down to the shore of Larder Lake comprises fine grained, thinly-bedded distal turbidites. Near the Break, between these sediments and the ultramafics, lies a thin massive to pillowed mafic flow/hyaloclastite horizon, which is mineralised to form the ore in the Barber Pit and the Cheminis mine. Evidence from graded bedding in the steeply south-dipping Larder Lake Group sediments in the south wall of the

Barber Pit indicates that local facing is to the south (1989 observations, J.P.S. and E.T.C.S.; Figure 8). There is no evidence for major discontinuities (except perhaps for the graphite/mafic contact on the south side of the Barber Pit) in the above sequence. Hence the Larder Lake Group is interpreted as a south-facing succession of ultramafic and tholeiitic volcanics, volcanoclastic breccias and distal turbiditic sediments, north-dipping (i.e. overturned) in the vicinity of the Kerr Addison mine.

### **5.3. North of the Ultramafic Horizon (Timiskaming and Kinojévis Groups)**

In the northern part of McGarry Township (see Figure 6) occur a series of north-facing, alternating Mg- and Fe-tholeiitic basalt flows assigned to the Kinojévis Group. Scattered outcrops of fine-grained, massive or brecciated rhyolite also occur (Hamilton, 1986). The older volcanics are clearly overlain with angular unconformity (e.g. Thomson, 1946; Jackson, 1988) by opposite (south-) facing coarse basal conglomerates of the Timiskaming Group. The conglomerates are polymict, clast-supported, and interbedded with thick lenses of fluvial trough cross-bedded sandstones (Hyde, 1978). Stratigraphically above these, the sequence is dominated by feldspar-porphyrific, trachytic agglomerates and flow breccias, with narrow interbedded conglomerate horizons. The trachytes are cut on their south side, north of Virginiatown, by structural discordance 'A' of Downes (1980, 1981; see Figure 6).

South of the discordance occur thin-bedded, fine- to medium-grained proximal turbidites with background fine-grained black argillites (Hyde, 1978). These are again south-facing. Across a further discordance to the south occur thicker-bedded, coarser grained turbidites with increased sand contents (Hamilton, 1986). These become tightly folded at the nose of the Spectacle Lake Anticline, and a thin (<30 m) south limb of schistose fine-grained sediments continues adjacent to the Break, just north of the Kerr Addison mine, and connects and opens out westwards through to a thicker section of Timiskaming sediments north of the Armistice and Barber Larder deposits.

It has been considered (e.g. Ridler, 1970, 1976; Hyde, 1980) that the sediments south of the Larder Lake Break can be correlated with the Timiskaming succession, due to their general lithological similarities. However, it has been shown (e.g. Thomson, 1941; Jensen, 1985b; Hamilton, 1986; Toogood and Hodgson, 1986) that marked differences in clast contents exist between conglomerates of the two sediment types. For example, the Timiskaming contains abundant distinctive trachyte (locally derived from volcanics), jasper (unknown distal source) and only occasional ultramafic clasts; whereas the Larder Lake Group generally has no trachyte or jasper, and abundant locally-derived, intra-formational ultramafic/mafic and banded iron formation clasts. Recent precise U/Pb geochronology (Corfu et al., 1991) and trace element geochemistry of the two sedimentary types (Feng and Kerrich, 1990) show that they are of different ages (~2705 Ma versus ~2680 Ma), were derived from compositionally different source areas, and were tectonically juxtaposed across the Break.



## 6. Structural Development in the Virginiatown Area

### 6.1. The Nature of the Larder Lake - Cadillac Break

The Larder Lake Group ultramafic - Timiskaming sediment contact (see Figures 6 and 7) is interpreted originally to have been a S-over-N reverse structure for the following reasons:

(i) way-up determinations from normal grading and trough cross-bedding in sediments either side of the contact (Figure 8) indicate that both units are south-facing, although locally overturned and north-dipping;

(ii) south-over-north kinematics based on asymmetrically folded fabrics were described by Hamilton (1986);

(iii) a sub-vertical to steeply east-plunging lineation defined by elongation of clasts and varioles occurs within the plane of the foliation, indicating a steep plunging movement vector;

(iv) associated early  $F_1$  folds are upright to north-east verging;

(v) evidence exists for a possible southward-shallowing at depth, listric geometry to the Break, from underground development and drilling at the Cheminis, Omega and McBean/Anoki mines (Jenney, 1941; Thomson, 1941; Hamilton, 1986; Queenston Mining Ltd., Kirkland Lake, pers. comm., 1989);

(vi) U/Pb geochronology (Corfu et al., 1989; 1991) indicates that older Larder Lake units thus structurally overlie the younger Timiskaming units.

A thrust origin for the Break is in agreement with ideas suggested by Thomson (1941; 1948) and Hamilton (1986). A few N-S or NE-SW shear zone structures also approach the Break from the south at a high angle, notably at Misema River, Larder Lake (e.g. Raven River mine) and the north-east arm of Larder Lake, in each case corresponding to a change in Break dip and strike, and may be kinematically linked to deformation on the Break, as suggested by Hamilton (1986).

In McGarry Township (see Figures 6 and 7), the Break is characterised by intense foliation development over a width of ~50-150 m, within a wider zone (2-3 km; Hamilton, 1986) of moderate fabric development. Fabric intensity is closely related to lithology, especially in ultramafic host rocks, and proximity to the ultramafic - greywacke contact. Evidence for a strong component of flattening is derived from aspect ratios (e.g. ~5:5:1, J.P.S. measurements) of finite strain markers (e.g. pillows, varioles and polyhedral vein networks). Lineations are poorly-developed or absent in the ultramafics, possibly reflecting the extreme incompetence of these talcose rocks (for an anhydrite mechanical analogy, see Lloyd and Schwerdtner, 1990). In the pillowed mafic volcanics, deformed varioles are observed which are flattened perpendicular to the foliation, and locally, according to observations to date, define a steep easterly-plunging (~70°) lineation (see below) indicating a component of transpressional movement.

Based on detailed field mapping between Larder Lake and Kearns, Hamilton (1986) divided the Larder Lake - Virginiatown area into coherent lithostructural domains and sub-domains, separated by structural discontinuities. The Larder Lake - Cadillac Break and associated structures were considered to define a several km wide east-west deformation zone. Within this zone, strain is heterogeneously developed as small (tens of metres wide) high strain zones, sub-parallel to or splaying off the Break, and anastomosing around lozenge-shaped lower strain areas.

## **6.2. Sequence of Deformation (after Hamilton, 1986)**

In contrast to Jensen and Langford (1985), Hamilton (1986) demonstrated that fabrics are pervasively developed throughout the area, and that overprinting of fabrics of different orientations does occur. The sequence of deformation after Hamilton (1986; see Figures 9a to 9c for plotted stereograms) is as follows:

***D<sub>0</sub> early deformation (no associated fabric)***

This sub-division comprises syn-sedimentary folds and slumps, confined to certain horizons, as well as a  $D_0$  deformation event confined to the pre-Timiskaming volcanic basement, defined by Hodgson and Hamilton (1989). The latter comprises generally east-west folding and tilting (with no apparent foliation) and faults developed early in the compressional deformation and mostly pre-dating the deposition of the younger, unconformable sedimentary assemblage. This phase of folding and tilting may be due to the emplacement of major intrusions (c.f. Schwerdtner et al., 1979) such as the Round Lake Batholith (~2703 to 2697 Ma; Mortensen, 1987a,b).

***D<sub>1</sub> NNE-SSW compression; regional folding and axial planar cleavage; initiation of the Break***

$D_1$  is characterised by vertical to north-east verging, WNW-ESE trending regional  $F_1$  folds (see Figure 9a) with originally shallow-plunging axes. Examples in the map area include the Spectacle Lake Anticline and Beaver Lake Syncline. A sub-vertical  $S_1$  cleavage occurs axial planar to the  $F_1$  folds (Figure 9b), and parallel to the WNW-ESE regional strike of lithological units. The  $S_1$  fabric is defined by a pressure solution cleavage and segregational banding, particularly in the sediments. Relatively minor translation on cleavage surfaces and strained, oblate pebbles within the plane of  $S_1$  foliation indicate a strong  $D_1$  flattening component. In the vicinity of the Break,  $S_1$  cleavages show variable re-orientation due to folding by later  $D_2$  deformation (Figures 9b and 9c).

$D_1$  deformation initiated two sets of early, relatively wide ductile shear zones either parallel to lithological contacts or forming boundaries to structural domains. The shear zones comprise an earlier E-W trending set, the largest of which is the Larder Lake - Cadillac Break itself, cut with sinistral offset by a NE-SW trending set (e.g. along the north-east arm of Larder Lake). The Break *truncates* large folds such as the Spectacle Lake Anticline, developed during earlier stages of the progressive  $D_1$  deformation, since the contacts between the Timiskaming sediments and Kinojévis volcanics on either side of the anticline

were shown by Jackson (1988) to be folded unconformities, and *not* early  $D_1$  thrusts as suggested by Hamilton (1986). The axial trace of the Spectacle Lake Anticline in McGarry Township changes strike from  $110^\circ$  to  $070^\circ$  as the fold is rotated into the Break with a sinistral sense of movement. South of the Break, fold axes trend into the Break at approximately  $050^\circ$ . Drag folding, anti-clockwise rotation and truncation of units were interpreted by Hamilton (1986) to indicate oblique slip, south-over-north,  $D_1$  thrusting from the SSW, with a sinistral sense of horizontal movement.  $D_1$  fold and thrust events largely determined the subsequent distribution of lithologies.

***D<sub>2</sub> NNW-SSE compression; fabric overprint localised along Break as a reverse shear zone***

$D_2$  is characterised by the selective development of tight to isoclinal folding and a penetrative, overprinting  $S_2$  crenulation cleavage along pre-existing  $D_1$  structures such as the Break (Hamilton, 1986). The  $S_2$  fabric shows a strong flattening component, and asymmetric  $F_2$  folds correspond to south over north translation with a minor *dextral* component of motion. As the Break changes dip ( $\sim 70$ - $80^\circ$ S) and strike ( $060$ - $100^\circ$ ), the trend of  $S_2$  swings around sub-parallel in response.  $S_2$  cleavages strike at  $040^\circ$  to  $095^\circ$ , dip steeply north or south (Figure 9c), and are intensely developed in narrow anastomosing high strain zones which envelop lensoid pods of lower strain and/or  $F_2$  fold hinges axial planar to the  $S_2$  cleavage (Hamilton, 1986). Two E-W and NE-SW surfaces are observed to co-exist with dextral and sinistral lateral offsets respectively, consistent with conjugate shear.

$L_2$  clast elongation lineations within the plane of the  $S_2$  foliation plunge vertically to steeply east (Figure 9c; c.f. Jackson, 1988). North of the Break,  $F_2$  fold hinges and intersection lineations plunge east to north-east, whereas south of the Break fold hinges and lineations plunge south-west. This change in plunge across the Break was first observed by Thomson (1941), and later emphasised by Downes (1980) and Toogood and Hodgson (1986). Hamilton (1986) interprets the plunge difference as due to the superimposition of  $F_2$  folds on *oppositely* dipping limbs of  $F_1$  fold structures.  $D_2$  deformation produced relative dextral

movement on narrow, brittle-ductile WSW-ENE shear zones, sinistral movement on N-S shear zones, and compression (flattening) normal to 050-060°. Hamilton (1986) considered a large component of the D<sub>2</sub> deformation to be pure shear, involving flattening strains, consistent with bulk inhomogeneous shortening (e.g. Coward, 1976; Bell, 1981).

### ***Later fabrics***

Two sets of small scale open folds and crenulations cut the S<sub>2</sub> fabric and define shallow plunging intersection lineations, especially near the Break. Hamilton (1986) considered these to be due to oblique, near-vertical post-D<sub>2</sub> movement. A sub-vertical S<sub>3</sub> crenulation cleavage is developed in some areas at 030-065°, showing sinistral offset of S<sub>2</sub> (Figure 9c).

### ***Late brittle faults***

WSW-ENE trending, north-dipping, brittle faults occur along and parallel to the Break (e.g. graphitic Kerr Fault) and may pre-date deposition of the Huronian (see Figures 6 and 7). These faults show reverse, north-over-south offset, with a sinistral component of horizontal motion (in agreement with Powell et al., 1989; 1990). A set of sub-vertical, N-S to NE-SW normal cross-faults, probably linked to graben formation along the north-east arm of Larder Lake and *post-dating* the Huronian sediments (Lovell and Caine, 1972), cut and offset the steeply dipping stratigraphy, the Break and the sub-parallel late faults (see Figures 6 and 7; D. Bigelow, Armistice Project Geologist, pers. comm. 1989; D.W. B., unpubl. data, Barber Pit). *Importantly, west of Kerr Addison, these cross-faults downfault to the west, thus exposing higher structural / erosion levels and causing ore targets to lie potentially at greater depths.*

## **6.3. Strain of Host Lithologies in the Kerr Addison - Chesterville Au system**

After describing the nature of the original host lithologies in the Kerr Addison - Chesterville Au system, and before discussing the characteristics of the principal ore types developed from those lithologies, it is important to discuss briefly the strain characteristics of the host lithologies on a small scale *within* the ore system. This section connects with the previous sections on the structural nature of the Larder Lake - Cadillac Break.

The overturned lithologies in the ore zone, which strike at  $\sim 060^\circ$  and dip at  $\sim 78^\circ$  to the north-west (see mine geology level plans below), are characterised by intensification of a strong foliation (statistically identical with the  $S_2$  of Hamilton, 1986; Figure 9b) over a horizontal width of  $\sim 150$  m which defines the Break deformation zone and which strikes at  $\sim 057^\circ$  dipping  $78^\circ$  to the north-west (see Figures 10a and b). For example, on the 3850 ft level foliation intensity increases very sharply in a talcose unit over  $\sim 5$ - $10$  m *before* the main orebody is reached approaching from the south. The northern limit on the 3850 ft level is characterised by a wide zone ( $\sim 38$  m) of intense foliation development which coincides exactly with the ultramafic flows - Timiskaming sediment contact, interpreted as the critical original structural discontinuity. Approximately 12 m of the foliation intensification occurs to the south in talcose material (see Figure 11a), strain picking up over  $\sim 1$ - $2$  m; the exact contact is not definable within  $\sim 1$ - $2$  m because of extreme foliation development. Very strong foliation continues in fine-grained clastic sediments for  $\sim 26$  m (see Figure 11b) and then  $\sim 103$  m of still strongly foliated sediments occur before significantly less strained Kinojévis volcanics in the core of the Spectacle Lake Anticline. Hence, this high strain zone is a total of  $\sim 141$  m thick within which  $\sim 38$  m are particularly highly strained. Unfortunately, neither facing directions for the sediments can be observed nor the nature of the strain (flattening vs. stretching) because of the lack of passive strain markers in this locality.

Within the ore zone, foliation development is highly heterogeneous being characterised by  $\sim 1$ - $10$  m wide high strain zones, both in spinifex-textured ultramafics and in the mafic flows, separated by relatively unstrained zones within which original textures and early vein stages are preserved. Passive strain markers are uncommon in the host lithologies, consisting of pillow varioles, clasts and fragments in some lithologies (e.g. volcanic units, dykes), and polyhedral shapes defined by an early polygonal vein stage. Strain is certainly characterised by a strong  $\sim 5:5:1$  flattening and may also be characterised by a generally steep ( $\sim 70^\circ$ ) east-plunging elongation, suggesting dextral transpression, which has been observed in some localities (e.g. 1117-63 stope; 1021-52E drift; 1021-59 crosscut; see Figure 12). Asymmetric

folding of small-scale quartz veins gave conflicting kinematic results and was not found to be particularly useful.

Relative timing relationships between ductile strain in the Break deformation zone and vein stages are discussed in detail below. However, to summarise, observational evidence indicates that ductile strain started *within* an episode of pre-ore, barren, polygonal carbonate vein development, with which fuchsitic green carbonate alteration is *not* associated, and continued just after main stage Au mineralisation (late main stage Au-quartz veins at a high angle to foliation in *high strain zones* are tightly folded). Main stage Au-quartz vein mineralisation formed *during* ductile strain in the Break deformation zone. Since many main stage veins in both green carbonate ore and flow ore are essentially mesoscopically unstrained when crossing only moderately strained lithologies, it appears that the bulk of main stage Au mineralisation occurred in the later stages of ductile strain on the Break.

Previous workers (e.g. Thomson, 1941; Buffam and Allen, 1948) noted that lithological units within the top ~150 m of the Chesterville mine, usually dipping ~70°N and striking 045°, were strongly affected by an easterly-plunging, S-shaped cross-fold which altered their strike to a more northerly direction and caused the ore bodies to “roll over” to a shallow north-west dip near surface. This was interpreted as a drag fold due to late (?) movement within the Break. Although a synclinal axis strikes at ~050° into the Break a few hundred metres west of Kerr Addison (Thomson, 1941; Buffam and Allen, 1948; Downes, 1980; 1981), no evidence has yet been found to suggest that the Kerr Addison mine occurs on the thickened hinge of an anticlinal fold structure, as suggested by Downes (1980; 1981) and Charteris (1984). The Kerr Addison - Chesterville Au system, and the blind Chesterville East orebody (see below) both plunge at ~70° east within the plane of the Break deformation zone.

## 7. Geological Characteristics and Distribution of the Principal Ore Types

The main Kerr Addison - Chesterville Au system comprises four main ore types, in order of total Au produced: “flow ore”, “green carbonate / siliceous break ore”, “albitite dyke ore” and “graphitic ore”, distributed among 20 (Kerr Addison) and 9 (Chesterville) orebodies (“siliceous break” or “sil break” is a local mine term for major quartz-dominated, often Au mineralised vein structures with included wallrock fragments; these have widths of ~1-10 m, mapped strike lengths of <10 m to >100 m, and can be traced for vertical intervals of as much as ~300-700 m; see photograph in Figure 13). The definition, terminology and numbering of the orebodies is part geological, part historical. Flow ore bodies tend to occur within discrete Fe-tholeiite stratigraphic units, or else are bounded by precisely definable planar faults, and were often mined in their entirety. Green carbonate ore, however, represents high grade ore shoots corresponding to vein concentrations within a continuum of lower grade, sub-economic Au mineralisation - several green carbonate ore bodies join upwards or laterally with their neighbours within an overall mining framework, the boundaries of each orebody being fairly arbitrary.

Based on ~2,500 compiled individual stope data (F.R.P.), the total Au production, Au grades, total tonnes of ore, vertical extent and types of the Kerr Addison ore bodies are listed in Table 3A together with summated data for the principal ore types. Based on planimetry and drill intersection grades, similar orebody data (F.R.P.) are listed for the Chesterville mine in Table 3B. These data combined show that:

- (i) the total tonnage of ore trammed (raw data, uncorrected for exact mill tonnage processed) was 38.53 million tonnes at a car/head grade of 9.47 g/t,
- (ii) flow ore was the most important ore type in terms of tonnage (20.91 million tonnes) and grade (11.00 g/t) compared with green carbonate ore (15.03 million tonnes at 7.82 g/t), producing approximately twice as much total contained Au,



(iii) graphitic ore and separate "albitite" dyke ore were distinctly less significant (1.81 and 0.77 million tonnes respectively), although green carbonate ore actually contains ~5-15% "albitite" dyke ore on average,

(iv) the largest orebody, the #21 flow orebody, was impressive in tonnage (13.77 million tonnes), grade (12.47 g/t) and total contained Au (~172 tonnes; uncorrected data) making this type of orebody an excellent exploration target, and

(v) Kerr Addison contained seven >1.5 million tonne orebodies (four green carbonate, three flow) at head grades of 5.65 - 10.72 and 12.47 g/t Au.

The Kerr Addison - Chesterville ore zones were developed principally from strained and altered massive Fe-tholeiite volcanics (sometimes pillowed), ultramafic komatiites, mafic "albitite" intrusions (see photograph in Figure 14) and graphitic metasedimentary horizons over a ~900 m strike length near surface which shortens to ~500 m at the 3850 ft level, and over maximum widths of ~150-200 m. The characteristics of the principal ore types are as follows:

### 7.1. Green Carbonate / Siliceous Break Ore

The green carbonate/siliceous break ore host rocks are variably deformed ultramafic komatiite flows (Kishida and Kerrich, 1987) with discontinuous spinifex horizons (Figure 15a) showing their origin (Tihor and Crocket, 1977), which occur immediately south of the contact with Timiskaming sediments; no economic mineralisation, but ppb Au enrichment, is known north of this contact in the Kerr mine area. No interflow sediments have been identified within this horizon. The ultramafics were altered *before* Au-quartz vein mineralisation to a talc-chlorite-carbonate rock, and were, unsurprisingly, also a preferred location for the development of foliated high strain zones. The strained ultramafics were also a preferred locus for the development of thick (>0.3 m) quartz veins (Figure 13), and an intense swarm of mafic "albitite" dykes and plugs (Figures 14 and 15b) sub-parallel to

and utilising the strong foliation fabric. The bulk of the mineralisation occurs as native Au which was deposited in composite, milky quartz-carbonate "siliceous break" related veins and quartz stringers (Figures 15c and 15d); the latter were developed on a major scale, at impressive vein densities and with considerable variation in vein attitude from relatively consistently oriented to extremely variable (see below; see also map in Figure 16 of complex quartz veining in the Chesterville 9D1 green carbonate ore stope redrafted from Buffam and Allen, 1948). Mine terminology misleadingly describes such ore as "green carbonate breccia".

As will be discussed, main stage Au mineralisation developed during a short, brittle-ductile event which was late syn-deformational with respect to overall ductile deformation within the Break. Five vein generations contain Au, with only two (#3, #4; see Figure 32 below) hosting significant Au. Approximate contributions to total Au in the green carbonate ore are as follows: main stage milky quartz veins (#4) ~80%, "cherty siliceous break" quartz veins (#3) ~10%, and disseminated pyrite (+Au) in mineralised mafic "albitite" dykes and plugs ~10% (see below). Potassic green carbonate alteration caused by dispersed fuchsite (Cromuscovite) specifically occurs as selvages to Au-bearing veins and is contemporary with host vein formation; successive vein stages, each with green carbonate alteration, are observed to cross-cut each other. With increased density of veining, alteration selvages overlap to give the appearance of a uniform green carbonate rock. Essentially all Au values occur in the quartz veins and stringers; the green carbonate alteration itself does not host significant mineralisation and only contains low Au values, except in lithologies transitional to flow ore. *Au showed a relatively high nugget effect in the green carbonate ore such that only 20-25% of drill holes would give good ore intersections through subsequent stopes.*

A complete spectrum is observed from 100% vein-hosted "sil break" ore, which was separately stoped in places with sil break zones varying in width up to 15 m, to 100% green carbonate / quartz stringer-hosted ore. A complete gradation of alteration is also seen from

precursor, relict “horses” of barren talc rock to green carbonate ore zones. The limits of emerald green, fuchsitic alteration define a hydrothermal alteration envelope which contains all the individual green carbonate orebodies (see reconstructed level plans below). This prominent alteration envelope has a strike length of ~900 m on surface decreasing to ~300 m at the 5600 ft level, and a maximum width of ~120 m.

## 7.2. Flow Ore

The flow ore host rocks are mafic volcanics of Fe-tholeiite composition (Kishida & Kerrich, 1987) which are generally massive, but locally do show pillow structures with prominent variolitic rims (e.g. Figure 17a). They also contain minor flow breccia, hyaloclastite, tuff/agglomerate and graphitic interflow sediments, and occur south of the ultramafic horizon. Stope mapping (e.g. Figure 18) shows clear primary lithological variations within the flow ore which control Au mineralisation to an extent (see below). The bulk of Au mineralisation occurs in pyritic wallrock alteration selvages related to quartz-carbonate veins (Figure 19) and healed pyritic fractures; some coarse visible gold does occur in the veins (Figure 18). The pyrite-Au mineralisation is *not* syngenetic since dispersed pyrite occurs clearly in approximately symmetrical selvages related to cross-cutting quartz veins (e.g. four veinlets in Figure 17b; Figure 19). As Figure 17b also shows, the disseminated pyrite penetrates away from the veins using the foliation. With increased density of veining, pyrite selvages may overlap to give the appearance of a uniform, disseminated pyritic ore (Figure 19). Grade can be directly estimated from the abundance of disseminated *fine* (1-2 mm) pyrite (up to a maximum of 10-15% by weight).

Au in the flow ore was relatively homogeneously distributed such that drilling was a good guide to ore (almost 100% successful). Studies of the milling properties of these refractory ores (Hawkes, 1947) indicate that the Au is contained within the pyrite as tiny  $<10\mu\text{m}$  inclusions in size (mean diameter  $\sim 4\mu\text{m}$ ). A coarse (5-10 mm) variety of pyrite also occurs,

but appears to only carry low grade values (mine geologists, pers. commun., 1988). The ore material of the large (13.77 million tonnes), high grade (12.47 g/t) #21 orebody was distinctly more silicified and sulphide-mineralised than other flow ore material, producing a sulphide-rich, massive, pale grey lithology, particularly at depth. Strong silicification in the #21 orebody appears to be related to wide quartz veins at its north and south marginal contacts, reported from drill hole records and limited underground mapping. Mafic "albitite" dykes are essentially absent from the flow ore, probably due to its competency and foliation contrast with the green carbonate ore, and poor visual contrast between dykes and flows. Flow ore is cut and offset by post-ore graphitic faults (e.g. Kerr Fault), which partly utilise earlier structures, and includes some graphitic ore from their vicinity (e.g. #16 orebody; see below).

Detailed underground mapping has delineated the overall mechanism of Au mineralisation in the flow ore as well as six small scale lithological controls (see below). As mentioned above, the bulk of Au mineralisation occurs in bleached pyritic wallrock alteration selvages to quartz-carbonate veins and healed pyritic fractures; lesser coarse visible gold also occurs in the veins. Grade can be directly estimated from the abundance of disseminated fine pyrite (up to 10-15% by weight). The overall control is thus chemical reaction between the Fe-rich mafic flows (Fe as FeO = 17%; James et al., 1961) and mineralising fluids to form pyrite (with Au as <10µm inclusions). Local lithological controls on the distribution and grade of Au mineralisation represent either favourable or unfavourable structural-chemical sites and are listed below:

*tuff / sedimentary horizons:* Fine-grained, grey-green tuff / sedimentary units with occasional dark green chloritic fragments occur within the #21 and #16 flow ore host rock packages. These are typically 0.3 m to 1.2 m wide; one such unit has been traced via mapping for >110 m along strike in the #16 orebody on the 2050 ft level. The tuff horizons are invariably *less* mineralised than adjacent mafic flows, possibly due to their lower Fe-content

and less tendency to sustain brittle fractures. Discordant veins are observed to terminate at, or follow along, the tuff contacts. Such concordant, low grade horizons are also traceable from drillhole data within the #21 orebody.

***pillowed / variolitic horizons:*** These comprise distinct mappable units ~1.5 - 4 m wide, probably representing flow tops. Pillows are up to 1 m in size, contain multiple concentric rings of varioles, and massive coalesced cores. The dark chloritic interpillow flow/hyaloclastite material is *more* favourable for the development of veins and pyritic bleached selvages than the pillowed/variolitic units, which are almost unmineralised. Veins are observed to disappear into variolitic horizons or persist as narrow healed fractures with minimal pyritic alteration selvages. These observations are consistent with varioles representing spherulitic felsic crystallisation centres (less Fe-rich), due to undercooling of an Fe-tholeiitic magma (Fowler et al, 1987).

***early Au-related alteration:*** Early, low grade (~1.0-1.7 g/t Au) disseminated pyrite alteration occurs preferentially at pillow/variole margins and flow contacts and is characterised by mm-scale pyritic microveining. The accompanying silicification appears to increase the competency of the host tholeiitic flows locally, making them more favourable to subsequent overprinting by main stage Au brittle fractures; the latter occur in close proximity to areas of earlier disseminated low grade Au.

***intercalated graphitic lenses:*** Discontinuous, primary graphite-rich lenses have been mapped in the #16 and #6 orebodies. These are <30 cm thick, and contain 5-10% pyrite by weight with locally high grade Au values.

***proximity to graphitic Kerr Fault:*** Detailed mapping of the 2016-65 and 2016-67<sup>1</sup>/<sub>2</sub> sills shows a close correlation between ore and proximity to the graphitic Kerr Fault and its branches. Detailed examination indicates that a network of pyrite-mineralised fractures (+Au), containing mechanically remobilised graphite, occurs adjacent to the faults.

*diffusion of fluids along foliation:* Where vein stringers in the flow ore cross-cut a well-defined foliation, bleached pyritic alteration assemblages are observed to be preferentially elongated parallel to the foliation planes either side of the veins (e.g. Figure 17b). Detailed examination indicates that ore fluids preferentially diffuse along individual foliation planes, rather than across them. However, possible correlation between the occurrence of veining and/or higher grade flow ore, and zones of high strain was, for the most part, not rigorously examined.

### **7.3. Scheelite Mineralisation in Transitional Mafic / Ultramafic Host Rocks**

The scheelite in the Kerr Addison deposit (e.g. 46,300 tonnes at 0.085% WO<sub>3</sub> defined in 1942) occurs principally in transitional mafic-ultramafic host rocks to the north of the #21 orebody on the mid- to upper levels of the mine (Folinsbee, 1943). In 1990, we located a scheelite bearing section in transitional lithologies using a short wavelength UV lamp on the 850 ft level (814-61 sill; see stope map in Figure 19). Widespread scheelite grains ~2-10 mm in size fluoresced a bright mauve-blue, indicating a lack of Mo, and were pale creamy-white in visible light, showing approximately euhedral crystal faces in several cases. Detailed observations showed that the scheelite occurs in an *early*, significantly strained minor vein stage which predates both “cherty siliceous breaks” (vein stage #3; see Figure 32) and main stage Au-quartz veins (#4). On the 850 ft level scheelite was not present in typical flow ore (e.g. 866 south crosscut), but did occur as infrequent grains in quartz veins in the green carbonate ore.

### **7.4. “Albitite” Dyke Ore**

The host rocks for “albitite” dyke ore consist of three mafic plugs and an intense swarm of >5,000 mafic “albitite” dykes, which preferentially intruded the highly foliated ultramafic host rock forming ~10% of its volume (see Figures 14 and 15b; also reconstructed level plans Figures 20 to 27). Parts of the altered mafic plugs were individually stoped as ore (e.g. #15W and “J” orebodies). Dykes occur significantly more frequently in areas of green carbonate

alteration than outside, and are often preferentially mineralised relative to their host rocks. The dykes have irregular, tabular to boudinaged or podiform geometries. Intrusive contacts cross-cut weak fabric development but dykes can be highly deformed in high strain zones; hence the dykes intruded syn-deformationally. The bulk of Au mineralisation occurs in disseminated pyrite, related to cross-cutting vein generations (e.g. early network grey pyritic "crackle" veins; later main stage Au milky quartz veins) and associated hydrothermal alteration. Lesser native Au occurs in main stage Au quartz-carbonate veins. Hence, the principal reason for selective Au precipitation was probably sulphidation of an Fe-rich (~10-12% Fe as FeO) mafic dyke host rock. The major Chesterville plug is mineralised semi-continuously from surface to the deepest drill hole intersection obtained (~6.2 g/t Au over 9 m) at ~2200 m depth.

#### **7.5. Graphitic Ore**

This ore type is represented principally by the #16 orebody, where two types of graphitic ore have been identified. Host rocks for the first type comprise Fe-tholeiite flows identical to those of the flow ore, locally containing interflow graphitic metasedimentary horizons, occasionally with nodular pyrite, along which syn- and post-ore faults have developed. Graphite is mechanically remobilised along mineralised fractures adjacent to these faults. The second ore type comprises a graphitic fault gouge along the post-Au mineralisation Kerr Fault (e.g. 1916-67 stope) which incorporates fragments and lenses of mineralised flow material and broken quartz veins from the adjacent #21 and #16 flow orebodies. In both ore types spectacular visible gold may be locally found plated and smeared along thin graphitic slips. Graphitic ore creates special milling problems in the Kerr mill circuit, as described by McQuiston and Shoemaker (1975).

## 7.6. Ore Distribution Relative to Level Plan Geology

Nine representative reconstructed mine level plans (5600, 4800, 4400, 4200, 3850, 2650, 1750, 700, 175 ft levels) are given in Figures 20 to 27, and show the following features:

- (i) the north contact between the altered komatiites and the Timiskaming sediments which is interpreted to be the primary structural discontinuity, and which is a locus of marked strain intensification,
- (ii) the lens shape of the ultramafic host rocks, narrowing down or pinched out both to the west and to the east,
- (iii) the isolated sliver of mafic flows hosting the #21 and #6/#8 orebodies,
- (iv) a narrow zone of transitional mafic to ultramafic rocks between the komatiitic and tholeiitic lithologies,
- (v) a package of dominantly mafic flows and volcanoclastic breccias to the south, with lesser tuffs and sediments,
- (vi) repetition of units and ore bodies across the late, graphitic post-ore Kerr Fault,
- (vii) major intrusive mafic plugs, particularly in the east (Chesterville Plug) and west of the system at deeper levels, and an intense swarm of mafic "albitite" dykes (many of which derived from the east plug, in particular), confined mainly to the ultramafic unit and co-extensive with the limits of ore, green carbonate alteration and quartz veining,
- (viii) a swarm of major "siliceous break" main stage Au-quartz veins, especially in areas of green carbonate ore and therefore showing a co-occurrence with green carbonate alteration and also with igneous dykes/plugs, and
- (ix) barren "horses" of talc-chlorite-carbonate rocks representing relict, previously altered ultramafic precursors *not* overprinted by later Au-related alteration, which tend not to



contain quartz vein development or significant dyke concentrations, and which expand in the upper part of the mine above the 1750 ft level.

The ore bodies are contained largely within the mafic and ultramafic units, with the transitional volcanics being less favourable to Au mineralisation but containing local W (scheelite) enrichment (e.g. 814-61 sill). No economic mineralisation is known to occur north of the ultramafic - Timiskaming sediment contact in this area, but at least three mineralised zones occur *south* of the main Kerr Addison system, itself on the south side of the Break contact (see below).

The reconstructed Kerr Addison mine level plans were prepared (J.P.S.) by measuring off, projecting and connecting up data derived from one inch to 20 ft (1:240 scale) vertical fan drill holes on half-sections (spacing 11 m) perpendicular to the strike of the ore system onto one inch to 100 ft (1:1200 scale) mine level ventilation plans. To these were appended the geological plans (originals at one inch to 40 ft scale; 1:480) for the nearest equivalent Chesterville levels, redrawn at the same scale, based on flat fan drill holes and limited vertical section drilling. The horizontal positions of the Chesterville plans were adjusted slightly to take into account the differences in elevation of the Chesterville levels relative to the Kerr Addison levels which were used as the datum and the 78° north-west dip of the ore system. Good agreement was found between the lithological terminologies used in the two mines enabling full correlation of units to be made.

### **7.7. Ore Distribution Relative to Longitudinal Sections**

Figures 28 and 29 show vertical longitudinal projections of the Kerr Addison - Chesterville Au system onto a plane containing the strike of the Break, for the green carbonate and flow ores respectively. *These have been drawn from the reconstructed level plans (27 levels in total).* The main features shown are as follows:

- (i) the ultramafic-hosted ore is contained within a flat funnel-shaped green carbonate alteration envelope ~50-120 m wide which decreases in strike length from ~900 m near surface to ~300 m at ~1700 m depth, and which plunges ~70° east to a deep focal ore fluid source at ≥4 km depth,
- (ii) stoped green carbonate / “albitite” dyke orebodies within the overall envelope begin at three “root zone” localities on the 4000 ft level and expand considerably upwards,
- (iii) one major and two subsidiary mafic “albitite” plugs (c.f. 4800, 4400, 4200, 3850, 2650 and 1750 ft level geology plans, Figures 21 - 25) have been identified within the green carbonate ore system both of which die out before reaching surface: in the #15W and “J” orebodies, parts of the plugs were locally stoped as “albitite” ore,
- (iv) the spatial envelopes marking the limits of green carbonate alteration and “albitite” dyke occurrence are closely similar, proven by drilling outside the system (see below),
- (v) the stoped root zones of the Au system in both green carbonate and flow ores do not coincide with the geological, green carbonate alteration envelope root of the system,
- (vi) with depth the alteration system *converges* on the larger mafic plug to the east: deep drilling indicates that this plug is the *only* significantly mineralised unit below the limit of economic green carbonate ore at the 4000 ft level (~1250 m) to >2000 m depth,
- (vii) the Chesterville East Zone (c.f. 2650 ft level, Figure 24) is a separate, blind, green carbonate / “albitite” dyke potential ore target which plunges sub-parallel to the main Kerr Addison - Chesterville system; the Chesterville East Zone has no surface indication, the green carbonate alteration dying out upwards just above the ~1600 ft level,
- (viii) the flow ores coincide longitudinally with, but are asymmetrical to, the green carbonate envelope in the adjacent ultramafics,

(ix) stope flow ore extends down to the 4600 ft level, and pinches out downwards and to the east due to complete pinch-out of the host lithology,

(x) present flow ore distribution is partly due to later displacement by post-ore faults e.g. the graphitic Kerr Fault and its branches (see below),

(xi) green carbonate ore bodies tend to form eastern and western zones which fork at approximately the 2050 ft level leaving a barren zone between; in projection this barren zone is occupied by the #21 flow orebody suggesting it was the major locus for fluid flow in the central part of the ore system, and

(xii) mineralised zones (stopes) in both green carbonate and flow ores decrease markedly near surface between the 300 ft and 850 ft levels, suggesting that the current erosion level is near the top of the system (see below).

#### **7.8. Ore Distribution Relative to True Scale Vertical Cross Sections**

Figure 30 shows a true scale vertical cross section, compiled from one inch to 20 ft (1:240 scale) fan drill hole sections, of the Kerr Addison mine from surface to the 4800 ft level. This vertical cross section emphasises the following:

(i) the tabular nature of the orebody, confined within the Break deformation zone, and its extreme down dip continuity (~1400 m) relative to its width of ~50 to ~100 m,

(ii) the massive feeder quartz vein system within the green carbonate ore e.g. the major "siliceous break" quartz veins of the #14 orebody; these veins were stoped individually over widths of up to 15 m and vertical intervals of over 700 m,

(iii) the particular concentration of stoped ore on either side of the footwall contact of the ultramafic and mafic host rocks within the north-dipping Break deformation zone,

(iv) a wide (~100 m) zone of green carbonate alteration and quartz veining which occurs at the mid- to lower levels of the mine (e.g. 3100 - 2200 ft levels); this zone forks upwards at approximately the 2050 ft level into two narrower zones in the footwall (#14 orebody) and hanging wall (#24 and #18 orebodies) of the ultramafic unit, enclosing a central, vertically elongated (~500 m), ~30 m wide "horse" of barren talc-chlorite-carbonate altered ultramafic host rock, which tends not to contain quartz veins or significant dyke concentrations, and

(v) the V-shaped alteration "nick" point into the talcose ultramafic host rock below the deposit, due to the steep eastward plunge of the western margin of the alteration envelope out of the plane of the diagram.

Figure 31 shows a cross section of the upper levels of the Chesterville Mine (after Buffam and Allen, 1948), which illustrates:

(i) the close spatial association within the ultramafic unit of green carbonate alteration, orebodies (e.g. D, E, F, J) and mafic "albitite" igneous intrusions, including the composite Chesterville Plug,

(ii) some ore bodies (e.g. "J") were almost entirely hosted by "albitite" intrusions, and

(iii) the green carbonate ore system in this area largely dies off before reaching the surface, but scattered patches of flow ore (e.g. A, B, C orebodies) continue to surface in the mafic volcanics adjacent to the south.

## **7.9. Mineralised Zones Outside the Main Ore Zone**

Three potentially significant sub-parallel mineralised zones are known to occur south of the main Kerr Addison - Chesterville Au system, within the Larder Lake group package of mafic to ultramafic flows, volcanoclastic breccias, tuffs and graphitic sediments (Figure 7). Hence, these zones are also of general interest because they are in the less common location south of the Break (c.f. Anoki; Laguerre- Raven River; Malartic camp), rather than being located to the north (see Figure 1). They are termed the Town, Mill and Lake zones, and are located

~150 m, ~240 m and ~380 m south of the Kerr Addison #3 Shaft respectively (on the 1000 ft level). Information on these quartz vein stockwork zones with disseminated pyrite was compiled by Cunningham (1987), and their projections to surface are shown in Figure 7. The characteristics of these zones are described briefly below:

***Town Zone(?) Chesterville "G" Zone:*** The Town Zone comprises shear-hosted mineralisation in mafic volcanics over a strike length of ~600 m, and a true width of up to ~15 m at grades of ~1.4 to ~6.9 g/t Au. The Town Zone has been tested vertically from surface to the 1000 ft level and between the 3700 and 3850 ft levels, where it passes close to the bottom of the #3 Shaft. On surface the Town Zone is a weak green carbonate horizon parallel to the laneway behind Olive's Store, Virginiatown. Underground it projects to an area ~150 m south of the #3 Shaft on the 1000 ft level where a value of 8.3 g/t Au over 1.3 m was recorded in a weak green carbonate alteration zone within massive to pillowed mafic flows. Further drilling is needed to define whether the Town Zone connects downwards to a mineralised zone ("Diorite Zone"; ~2.1 g/t Au over >9 m width) ~100m south-west of the main orebody on the 5600 ft and 4800 ft levels (Figures 20 and 21), hosted within and adjacent to an elongate (>300m strike length), mineralised, dark grey feldspar porphyry intrusion (identification based on drill core examination). The Chesterville "G" Zone (see Figures 7 and 29), located near the Chesterville shaft, about 240 m south and parallel to the #21 orebody, may be equivalent to the Town Zone. The "G" zone, defined by drilling down to the Chesterville 9th level (1184 ft) and open at depth, occurs as silicified, pyritised flows within a sequence of pillowed and massive flows with interbedded tuffs and graphitic sediments. The zone is 2-14 m wide, averaging ~5 m; it dips steeply south but reverses dip towards surface.

***Mill Zone:*** This zone comprises shear-hosted mineralisation in mafic volcanics ~240 m south of the Kerr Addison #3 Shaft or 300 m south of the #21 orebody on the 1000 ft level. The Mill Zone has a strike length of ~480 m, and true widths of over 12 m at grades of ~1.7 to 7.5 g/t Au, with visible gold locally. It is, however, not a single well defined zone, but

rather an en echelon series of silicified pyritic horizons on or within ~15 m of the north dipping ultramafic-mafic volcanic flow contact on the 1000 ft level. There are a few quartz veins present as well as silicification and pyritisation of the host mafic-ultramafic rocks. Overall the Mill Zone is a weak mirror image of the main Kerr Addison - Chesterville system. It has been tested vertically from surface to the 1000 ft level by drilling and some visible gold was reported.

**Lake Zone:** This zone comprises shear zone-hosted minor quartz veining, but no Au values, in green carbonate-altered ultramafic host rocks over a strike length of ~480 m, exposed in the cliff on the north shore of Larder Lake and crossed there by an adit. The Lake Zone was tested by drilling from a long cross-cut ~420 m south of the Kerr Addison #3 shaft on the 1000 ft level, which intersected weak grey carbonate altered ultramafics but no Au values.

Two further Au mineralised exploration targets occur along the Break at depth to the east and the west of the main Kerr Addison - Chesterville Au system. These are the Chesterville East Zone and the Armistice deposit which are described below:

**Chesterville East Zone:** This is a Break/ultramafic-hosted, *blind* green/brown carbonate zone centred ~450 m east of the Chesterville workings, with an apex at about 500 m depth. Very limited drilling of the zone was carried out from two long easterly drifts on the Chesterville 12th (1635 ft) and 19th (2590 ft) levels. On the 12th level, the zone averaged 3.5 g/t Au over narrow widths along a 30-60 m strike length; on the 19th level, 7 of 17 holes through the zone returned economic intersections including 4 with visible gold. The strike extent on the 2590 ft level is ~360 m and the zone, which plunges steeply east, is open at depth and to the east. "Albitite" dykes similar to those of the main Au system were identified on the 2590 ft level but these were not present at the higher 1635 ft level.

**Armistice Property:** Along the Break from Kerr Addison, west of the "Armistice Cross Fault" (see Figures 6, 7, 28 and 29), an old shaft on the Armistice property was deepened

from the 1000 ft to the 2250 ft level and new ore zones defined (1990 reserves: 544,000 tonnes at ~5.2 g/t Au) between 1987 and 1990. Throw on the fault, the exposure of which is poorly defined at surface, is claimed by Armistice Resources Ltd. to be ~900 m down to the west, such that the upper levels of the Armistice ore body could represent high level continuations of the Kerr Addison - Chesterville system, which is itself asymmetrically concentrated at its west end in the upper levels. The Armistice ore zones occur in two geological horizons: (i) the more southerly Armistice Horizon (100N zone; figures refer to distance in ft north of a baseline which passes through the Armistice shaft bearing 245°), and (ii) the more northerly Sheldon horizon (185N, 260N and 325N zones). The Sheldon horizon is considered to be approximately stratigraphically equivalent to the Kerr Addison Mill Zone/Chesterville "G" Zone. The Armistice ore system appears to plunge ~65°W within the plane of the Break i.e. opposite to the main Kerr Addison - Chesterville system.

The Armistice 100N zone (2-5 m wide; 1600-2300 ft levels) is located at an ultramafic-mafic volcanic contact; the highest grade Sheldon 185N zone (2-4 m wide; 1600-2000 ft levels) is similar to Kerr flow ore; and the Sheldon 260N and 325N zones are in green-grey carbonate altered ultramafics (with weakly Au mineralised "albitite" dykes noted in drill core; J.P.S., D. Bigelow, Armistice Project Geologist, pers. obs., 1989). Deeper Armistice drill intersections at >1100 m depth do not appear to be a downfaulted Kerr orebody extension, and instead may represent a completely new blind ore system analogous to the Chesterville East Zone. GSR Mining Ltd., the operators of the Kerr Addison property, have an option to earn a 50% interest in the Armistice Property by carrying out \$5 million of exploration work over 5 years (1989-1994). However, exploration has been discontinued at the present time due to low Au prices (December, 1991).

## 8. Time Sequence of Deformation, Hydrothermal Alteration, Mineralisation and Igneous Intrusive Events

A relative time sequence of deformation in the Break zone which contains the Kerr Addison - Chesterville system, veining, alteration, mineralisation and mafic "albitite" dyke intrusion has been built up using mapped cross-cutting relationships in ~55 areas of the mine. The areas mapped between 1987 and 1990 are representative of 14 of the 20 Kerr Addison ore bodies and 24 of the 28 levels developed in ore, and range from depths of 90 m to 1250 m below surface. The results are summarised in Figure 32. The most important points shown by this diagram are as follows:

- (i) processes started with early, polygonal carbonate veining which appears to have overlapped the beginning of ductile deformation in timing,
- (ii) the interval of ductile deformation represented by the Break contains the period of Au-quartz vein mineralisation (e.g. main stage Au-quartz veining in green carbonate ore related to prominent "siliceous break" veins; main stage Au veins in flow ore),
- (iii) physical correlation, through mapping in three different localities, has been made between Au mineralisation in the green carbonate ore and that in the flow ore,
- (iv) mafic "albitite" dyke intrusion (3 generations, A<sub>1</sub> to A<sub>3</sub>; or a continuum) is *co-temporal* (see Section 9 below) with the main interval of Au mineralisation and was therefore also contained within the interval of ductile Break deformation,
- (v) the fact that there is significant intra-dyke intrusion Au mineralisation is definite, based on observed cross-cutting relationships (see below); there is also no significant change in dyke geochemistry (see Section 9), and
- (vi) green carbonate ore shows *ten* distinct stages (*five* of which are Au-related) of quartz-carbonate veining and associated alteration; these can be grouped approximately as follows:



(#1) early barren magnesite-dolomite veining and alteration; (#2-#5) Au-related quartz-ferroan dolomite veining with associated fuchsitic green carbonate alteration; and (#6-#10) later quartz-dolomite, dolomite and calcite veining, faulting and apparent Au remobilisation, which post-date ductile Break deformation.

The observational basis for these points is now discussed by going through each major ore type in detail, discussing cross-cutting relationships and characterising the nature, abundance and distribution of each distinct vein event, and its relationship to deformation and ore.

### 8.1. Kerr Addison Green Carbonate Ore Vein Stages

#### *Stage #1: polygonal carbonate veins*

These comprise early barren polygonal carbonate vein networks which occur throughout the ultramafic host rocks (including the talc areas) where they can form ~30% of their volume. Where observed in unstrained lithons, the veins define equant 3-dimensional polygons ~5-15 cm across (Figure 33a); individual veins are ~2-10 mm in width, and in some cases may have followed previous polysuture cooling fractures in the komatiitic ultramafics, which would account for the widespread similarity in polygon size. However, in most cases it appears that the veins occupy a newly-generated polygonal fracture network. In a few locations, the early polygonal vein segments can be observed to use a very early, weak foliation fabric, and to be significantly larger and longer (~20-60 cm) than normally found elsewhere (Figure 33b). This indicates that at least part of the #1 vein set is syndeformational. Hence, in the time sequence evolution diagram in Figure 32 this vein stage is shown overlapping the *beginning* of ductile Break fabric development. The veins are associated with coarse carbonate replacement and compositional alteration zoning of the ultramafic host rock inside the polygons. Veins consist of diffuse grey to white carbonate (~60/40 ratio magnesite/dolomite) which can be “lumpy” in appearance, and chlorite. No fuchsitic green carbonate alteration has been observed associated with this vein set. Geochemical analysis

indicates that the polygonal veins and associated early carbonate alteration are barren of Au (< 1ppb detection limit: n=4). Hence it appears that they pre-dated Au mineralisation. Within the Kerr Addison - Chesterville Au system, the polygonal carbonate veins are subsequent markers of ductile, flattening deformation, and generally occur as fabric-parallel background veins defining a local “schistosity”, yet still maintaining vein bridges with each other which may be distinctly folded (e.g. Figure 33b).

***Stage #2: local carbonate stockworks and pods***

These are early syn- ductile deformation carbonate stockworks and pods which locally cut and overprint earlier fabric defined by deformed polygonal #1 veins in pre-existing talc-chlorite-carbonate host rocks. They show patchy spatial preservation, appear to be restricted to higher strain zones, and are definitely locally cut by early A<sub>1</sub> dykes which pre-date main stage Au mineralisation (e.g. 3801-56 main crosscut, 3850 ft level; Figure 15b). The #2 veins consist of ~1-2 cm wide stockwork/polygonal to deformed “shredded” veins with grey-brown to weak green alteration at vein margins. Mineralogy consists of milky white carbonate (ferroan dolomite) and albite, with minor quartz and pyrite. Sampled veins show ppb Au enrichment (~9ppb Au: n=2); a grab sample of an early, folded carbonate-pyrite pod from the 1719-74 stope assayed 1.7 g/t Au (J.P.S., 1989). The presence of weak fuchsitic, potassic alteration and low grade Au shows that this vein stage is a precursor to Au mineralisation. The early scheelite-bearing vein stage may be part of this #2 set.

***Stage #3: cherty “siliceous break” veins***

These are syn-deformational, fine-grained SiO<sub>2</sub> “cherty” vein structures which cut and overprint fabric and deformed #1 and #2 veins (see Figure 33c). They range from quartz-replaced, narrow (~ 5-50 cm) shear zones to thin (~ 5-15 cm), subtle “weak” fractures with silicified grey-green fault gouge, defining an open-intersected, curvilinear branching framework within the green carbonate altered ultramafics. These “cherty siliceous break”

veins have steep N-S to NW/SE dips (Figure 34a), and mostly strike at low angles ( $\pm 30^\circ$ ) to the Break fabric. They crosscut from high to low strain areas (e.g. 3214-65 sill) and are not closely related to ductile deformation. Offset of lithological markers (e.g. spinifex horizons and some dykes) across the faults indicates a possible dextral, south-over-north sense of motion. The veins mostly contain cherty grey-green quartz (due to grain size reduction by local deformation and dynamic recrystallisation), with minor carbonate (ferroan dolomite/ankerite). They are surrounded by ~30-60 cm wide haloes of weak green carbonate alteration and silicification. Visible gold is occasionally well developed along the “cherty” veins, but overall they form a maximum of only ~10% of the green carbonate ore. Millimetre-scale, grey network quartz-pyrite “crackle” veins (+Au) internal to the A<sub>1</sub> “albitite” dykes (see below) appear to be related through branching to the “cherty siliceous break” vein generation outside the dykes. The “cherty siliceous break” faults formed channels for subsequent main stage Au fluids and acted as guides for vein dilatancy and green carbonate alteration (see below).

***Stage #4: main stage, milky Au-quartz veins and massive siliceous break veins***

The “cherty siliceous break” veins are cross-cut and dilated by main stage Au-quartz veins which occupy pinch and swell zones of dilatancy along, and branching between, the guiding cherty siliceous break structures (e.g. Figure 35). The main stage Au-quartz veins in green carbonate ore (e.g. Figures 15c and 15d) are contemporary through branching relationships with the major siliceous break veins (e.g. Figures 13 and 33d) which are *the major fluid supply structures in the green carbonate ore* since the latter can be traced for tens to hundreds of metres both laterally and vertically on level plans and vertical sections (e.g. Figures 20 - 27; Figure 30). The Au-quartz veins are brittle fractures syn-kinematic with respect to overall ductile deformation since they cross-cut some fabric but may be strongly folded, especially where crossing local high strain zones at a high angle (e.g. Figures 36a and 36b). Up to four different preferred vein orientations occur, ranging from steep to shallow in dip

(Figure 34a), although the majority are steep dipping. Main stage Au-quartz vein style and geometry are characterised by branching, steep mutually open-intersected vein systems (e.g. Figure 15c) with high pressure fluid “spurs”. Hydraulic brecciation and intense “breakout” stockwork veining (e.g. Figure 15d) often occur on one side (e.g. hanging wall) of planar “siliceous break” structures or at their intersections. Individual veins and vein zones range from <0.3 m to >15 m in width (Figure 37); siliceous breaks are typically 1-2m in width.

Vein mineralogy comprises massive, milky white quartz, zoned with fringes of delicate wedge-shaped carbonate (ferroan dolomite / ankerite) crystals, pyrite, coarse visible native Au particularly in the quartz, occasional vein albite, and occasional tetrahedrite usually where cutting “albitite” dykes. The Au is clearly depositional within the quartz veins and contemporary with vein formation. Where narrow quartz stringers at a high angle to fabric have been folded, Au is observed to be locally remobilised into axial planar fractures (D. McCormick, Kerr Addison Mine Geological Staff, pers. comm., 1989). Minor pyrite, chalcopyrite, galena, sphalerite, arsenopyrite, enargite, scheelite and millerite (NiS) have also been reported from the ore (e.g. Thomson, E., 1941; Buffam and Allen, 1948; Baker et al., 1957). The veins are surrounded by intense emerald green fuchsite-bearing (Cr-mica) carbonate alteration selvages, with little or no pyrite.

Compressed “stylolitic” inclusions of green carbonate wallrock, indicating repeated vein opening, and fragments of wall rock and even “albitite” dyke are found in the larger veins (e.g. Figure 33d); the latter relationship shows that siliceous break/main stage veining postdates A<sub>1</sub> “albitite” dykes. The #4 main stage Au-quartz veins host the bulk (~70%) of total Au mineralisation in green carbonate ore and are ubiquitous in all the green carbonate ore zones (e.g. Figure 16). Main stage Au-quartz veins which cut A<sub>1</sub> “albitite” dykes produce disseminated pyrite mineralisation in the dyke wallrocks; such dyke-hosted veins also locally contain visible gold.

***Stage #5: late minor quartz stringers; 020° galena-sphalerite bearing vein set***

These comprise late syn-deformational, volumetrically minor vein stringers which postdate deformed main stage Au-quartz veins and have also been observed to cross-cut the A<sub>3</sub> dyke set (see below). An unusual 020° galena-sphalerite bearing vein set, which can locally host most of the ore in the #10 orebody (e.g. 1910-26, 1710-26 and 1610-26 stopes) and which visibly cross-cuts main stage siliceous break-related Au-quartz veins (Figure 38), may belong to this set. Stage #5 veins are steeply dipping (Figure 34c), <30 cm in width, extremely planar, and most recognisable when cutting at a high angle across the fabric and earlier, more deformed, milky main stage Au-quartz veins. Vein mineralogy comprises milky to lime green quartz, zoned with carbonate (ferroan dolomite) crystals at vein margins, and locally abundant galena, pyrite and sphalerite in the areas of ore outlined above. Green carbonate alteration at the vein margins occurs in the ultramafics; the veins also have bleached carbonate-pyrite alteration haloes where cutting the later, less altered mafic “albitite” dykes (A<sub>2</sub> to A<sub>3</sub>).

***Stage #6: vein fragmentation / silicified fault breccias / “mylonitic” zones***

These comprise steep, post- ductile deformation fault structures, characterised by vein fragmentation zones and silicified fault breccias. The brittle faults cut across previously developed ductile fabrics and offset the green carbonate ore zones. Fault zones vary from <0.3 m up to 4 m in width; the largest are traceable vertically for several levels (e.g. 2015-64 sill, 1915-69 exploration drift, 1715-66 exploration drift). They usually form north-dipping sets, parallel to the Break, and rarely cross-cut fabric at higher angles (Figure 34c). Where adjacent to previous siliceous break / Au-quartz vein zones, the faults incorporate fragments of earlier veins (e.g. Figure 36c). Sinistral, north-over-south motion is indicated by the sense of drag of lithological units into the faults, and sigmoidal, en echelon shallow south-dipping extension veins (see below, #8). Alteration associated with this event consists of intense grey fault gouge silicification and disseminated pyrite mineralisation, due to

abundant cm-scale irregular grey-green/black cherty quartz “jigsaw” vein breccias. Intense yellow alteration of green carbonate and disseminated pyrite mineralisation in dykes (one grab sample from the 1915-69 exploration drift assayed 4.8 g/t Au) also occur adjacent to such veins. Close examination reveals that the fragmentation appears to be mostly *in situ* vein brecciation, without significant tectonic movement. Visible gold occurs locally in cherty, recrystallised “mylonitic” quartz veins (e.g. 1014-52 exploration drift) and may have been remobilised. In places (e.g. the 1715-66 exploration drift at the east end of Kerr Addison; 1750 ft level) these fault gouges contain 3-5% disseminated pyrite and form potential mineralised targets, or were even stoped as ore (e.g. part of Chesterville “F1” orebody, 1750 ft level; Figure 25).

***Stage #7: local irregular steep veins cutting silicified fault breccias***

These local steep irregular veins were observed in two localities (1014-52 exploration drift; 2015-64 sill) cross-cutting a silicified fault breccia containing fragmented quartz veins. In the 2015-64 sill two open intersected orientations of the steep veins, forming a conjugate set, were themselves cut by shallow “flats” (stage #8). The #7 vein set is slightly irregular and deformed across the fault structure; veins have maximum dimensions of ~3 m in length and ~10 cm in width, and comprise quartz and carbonate (dolomite). No Au values or significant alteration are associated with these veins.

***Stage #8: sigmoidal, en echelon shallow-dipping “flat” veins***

A set of en echelon, shallow-dipping “flat” veins is widespread, occurring throughout the mine particularly localised by competent structures such as silicified fault gouges, major “siliceous” quartz veins (e.g. Figure 33d) and silicified dykes (Figure 15b). The flat veins are not observed to be folded, and sharply cross-cut even the most intense high strain zones (e.g. 1014-52 exploration drift). They define a set of shallow, en echelon gash vein fractures and hydraulic fracture “spurs”, locally intersecting with steep quartz veins in a ladder

fashion. The flat veins can reach maximum widths of ~30 cm (e.g. 1715-66 exploration drift), and may extend >5 m away either side of the generating structure. Their mineralogy ranges from milky white quartz-carbonate to coarse, brown-white carbonate (dolomite); patches of grey tetrahedrite (and minor chalcopyrite) are reasonably common within the flat veins, but they are *barren* of Au and do not have visible alteration halos. Similar late flat veins have been observed in the Barber-Larder open pit (see Figure 8).

***Stage #9: late chloritic faults and slips***

A variety of orientations of late chloritic faults and slips cut all units in the green carbonate ore; clean white carbonate (dolomite) veins up to ~5-10 cm wide are occasionally developed along these slips. These slips may be related to some part of the movement on the Kerr Fault, but very few have been traced across back into this structure. Late N-S, shallow-dipping graphitic faults occur in the flow ore with up to 1.5 m offset, e.g. 2215-64 stope (D.W.B.).

***Stage #10: late calcite-hematite fissures***

These comprise narrow NW-SE fissures, normal to the Break, across which there has been no significant offset (e.g. 1719-74 sill). The fissures are coated by specular hematite at their margins and infilled by translucent, coarse vuggy calcite.

**8.2. Kerr Addison Flow Ore Vein Stages**

***Early low grade, disseminated pyrite mineralisation***

Mapping in several flow ore stopes (e.g. 1117-63 stope) has defined early, low grade (~1.0-1.7 g/t Au) disseminated pyrite mineralisation, rarely observed outside areas of subsequent ore. This early, grey-brown alteration occurs preferentially at pillow/varirole margins, flow contacts and within tuffaceous units and is characterised by mm-scale pyritic micro-veining. The accompanying silicification appears to increase locally the competency of the host tholeiitic flows, making them more favourable to subsequent overprinting by main stage Au

brittle fractures. Main stage ore veins occur in close proximity to areas of earlier disseminated low grade Au.

***Main stage Au-quartz veins, stringers and healed pyritic fractures***

These are quartz-filled brittle fractures developed within the mafic Fe-tholeiitic host rocks; timing is late relative to Break strain since many veins are relatively undeformed (e.g. Figures 17b and 36d). Fractures are filled by gash-type, single opening veins, ranging from ~30-60 cm in maximum width and ~12-15 m in maximum strike length (e.g. 817-61 sill; Figure 19) down to <2-5 cm wide veins, and healed fractures with pyritic alteration haloes. Irregular stockwork-type veining also occurs locally. Some main stage Au-quartz veins are strongly folded where they cross-cut fabric at a high angle (e.g. Figures 36b and 36d). Four to five different preferred vein orientations occur ranging from steep to shallow dip (Figure 34b), although the majority are steep. Veins are observed to be mutually open intersected.

Mineralogy in the larger veins consists of massive black/smoky quartz, especially if near graphitic horizons or where compressed and folded at a high angle to the fabric. Stringer veins consist of zoned glassy grey to milky white quartz, with margins of delicate wedge-shaped carbonate (ankerite) crystals. Occasional coarse visible native gold is deposited within the quartz, and rarely vein albite. Minor chalcopyrite, sphalerite, arsenopyrite, galena, marcasite, gersdorffite and scheelite have also been reported from the ore (e.g. Thomson, E., 1941; Buffam and Allen, 1948; Baker et al., 1957). The veins are surrounded by beige-purple, bleached pyrite (fine-grained, 1-2 mm)-carbonate-albite-quartz alteration selvages up to 5 or 6 times greater than the vein widths (e.g. Figure 17b). Disseminated pyrite in wallrock associated with this vein set hosts >95% of the Au mineralisation in flow ore (e.g. Figure 18).



### ***Barren post-ore steep / flat veins related to late faults***

These occur as late steep, occasionally flat, open intersected ladder veins and breccias within or adjacent to post-ore graphitic faults. The late veins cut across main stage Au-quartz veins and also occur as tension fractures across the larger smoky quartz veins, perpendicular to their contacts. The veins are volumetrically minor, usually less than 10 cm in width, and are developed over maximum lengths of 4-5 m. They may be oriented perpendicular, or even parallel to, the flow ore zones, and have in places been observed to re-open previous Au-quartz vein fractures. The late veins are infilled by granular, milky carbonate  $\pm$  quartz, do *not* have bleached pyritic alteration haloes and are barren of Au.

### **8.3. Kerr Addison Graphitic Ore Timing Relations**

#### ***Syn-ore, dextral movement in graphitic zones:***

The graphitic ore (1.81 million tonnes at 7.9 g/t Au) is a special case of flow ore, due to the complicating presence of interflow graphitic metasedimentary horizons along which syn- and post-ore movement has occurred. Detailed mapping of the 2016-65 and 2016-67<sup>1/2</sup> sills (D.W.B.) shows a close correlation between ore and proximity to the graphitic Kerr Fault and its branches. Detailed examination indicates that a network of pyrite-mineralised fractures, containing mechanically remobilised graphite, occurs adjacent to the faults. The sense of swing of foliation into the graphitic faults is interpreted to reflect a *syn-ore, dextral* component of motion.

#### ***Post-ore, sinistral, reverse north-over-south fault movement:***

The above sense of motion is in contrast with the more obvious *post-ore, sinistral, reverse* north-over-south motion on the Kerr Fault, which displaced the flow orebodies (Figure 39). Fragments and lenses of mineralised flow material and broken quartz veins from the adjacent #21 and #16 flow orebodies are incorporated into the graphitic fault gouge, which is locally stoped as ore (see above).

#### **8.4. Kerr Addison “Albitite” Ore Timing Relations**

Three episodes of mafic “albitite” dyke and plug intrusion occur within the green carbonate ore, based on mapped cross-cutting relationships confirmed throughout the mine (see Figure 32). Parts of the larger altered mafic plugs were individually stoped as ore (e.g. 15W and “J” orebodies). “Albitite” dykes are spatially coincident (e.g. dyke / siliceous break pairs), co-structural (similar dips/strikes; see below) and significantly overlapping in time with main stage Au “siliceous break” veining (Figures 20 to 27, 28, 30 and 32) and comprise ~5-15% by volume (~10% total Au) of the green carbonate ore. Detailed timing relationships of mafic “albitite” intrusive events relative to the above vein stages (e.g. Figure 32), and alteration in the green carbonate ore, are discussed in Section 9 below.

#### **8.5. Discussion of Timing Relationships; Correlation of Ore Types**

Physical correlation through mapping in three different localities (866 south crosscut; 1610-25½ sill; 3821-63 rib) has been made between main stage Au mineralisation in the green carbonate ore (vein stage #4) and that in the flow ore. For example, in the 866 south crosscut, which is located in a pillar separating stopes in the large #21 flow orebody, a transition from green carbonate to flow ore shows the following features:

- (i) typical main stage quartz-carbonate veins with fuchsitic green carbonate wall rock alteration selvages;
- (ii) a typical ~1 m wide siliceous break quartz vein with coarse crack-seal wall rock inclusions, located ~3.5 m from the flow ore contact (Figure 40a);
- (iii) veins traceable from the major siliceous break vein which *cross-cut* the contact with flow ore (Figure 40b);
- (iv) prominent pyrite mineralisation selvages to this same main stage siliceous break-related vein set in the flow ore, whereas veins in the green carbonate ore do not have pyritic selvages;

(v) curved and branching quartz-carbonate veins in flow ore (Figure 40c) similar in appearance to veins in Hollinger - McIntyre (e.g. Wood et al., 1986a,b) and, also being similar to Hollinger-McIntyre, particular concentrations of pyrite in wall rock related to sharp vein terminations (Figure 40d).

The correlation between flow and green carbonate ores is further reinforced by similar overall Au:Ag ratios of ~18 : 1 in both ore types (James et al., 1961). Structural measurements (Figures 10a and b, Figures 34a and b) also indicate that closely similar orientations of foliation and main stage Au-quartz veins occur in *both* the green carbonate and flow ore types. The veins exhibit comparable strain states and geometries in *both* ore types: thus there is no evidence to suggest that ductile deformation and development of a progressive flattening fabric were not approximately synchronous in both host rocks. There are, however, fewer vein stages recorded in the flow ore, possibly because of its higher competency.

It is suggested that the "cherty siliceous break" vein stage in the green carbonate ore and the early low grade Au disseminated pyrite event in the flow ore are similar in age. This correlation is based on the fact that they both pre-date main stage Au and contain some Au (Figure 32). The microvein-controlled early mineralisation in the flows is also similar in style and geometry to the grey network, quartz-pyrite "crackle" veins (+Au) internal to the A<sub>1</sub> "albitite" dykes, which may branch off the "cherty siliceous break" vein generation. However, the geometry of the microveins (flow ore) and crackle veins (dyke) were not documented in detail, and appeared quite random.

The post-ore silicified "mylonitic" fault gouges in the green carbonate ore and the graphitic faults in the flow ore appear to share similarities in relative timing, orientation and north-over-south (sinistral) kinematics, and may be correlated. However, both ductile strain and brittle faulting appear to have continued for longer (beginning earlier and ending later), and with greater magnitude, along the incompetent graphitic horizons (see above).

## 9. Mafic "Albitite" Dyke Swarm / Intrusive Plug Igneous System

A significant finding of this study is that the Kerr Addison - Chesterville ore system is characterised by three major plugs and an intense swarm of >5,000 mafic "albitite" dykes (see level plans in Figures 20 to 27; photographs in Figures 14 and 15b). These intruded preferentially (>97% of total intrusions by volume) into the least competent, highly foliated ultramafic host rock and comprise ~10% of its volume. A small part (<3% of total intrusions by volume) of the dyke swarm also occurs within the transitional mafic/ultramafic lithology north and south of the #21 orebody. However, no dykes have been clearly identified in the flow ores, possibly due to the latter's greater relative competency, or to poor visual contrast. The petrography and preliminary geochemistry of the intrusions (Smith and Spooner, in prep.) indicate that they were originally mafic, alkaline, and possibly shoshonitic in composition, before variable sodic alteration ( $\pm$  strong carbonate alteration; silicification) to "albitites" consisting of secondary albite-quartz-carbonate-pyrite(+Au)-mica and rutile.

The intrusive plug/dyke swarm system shows the following principal geometric features relative to the green carbonate ore (see Figures 20 to 27, 28, 30 and 31):

(i) it is spatially co-extensive with the same green carbonate hydrothermal alteration envelope that contains the individual green carbonate orebodies.

(ii) major and subsidiary plugs are located as follows (see Figure 28):

(a) the Chesterville Plug occurs near the east edge of the green carbonate alteration envelope and extends upwards from below the deepest drilled depth of ~2000 m to ~180 m below the land surface. *The alteration root of the Kerr Addison - Chesterville system converges on this plug at depth.* Towards the present erosion surface, the Chesterville plug first of all thins down and then feathers out upwards into a series of dykes which in turn decline markedly in abundance upwards by the 500 ft level (see

comparison of parts of the 1150, 1000, 850 and 500 ft levels in Figure 41); this trend clearly indicates a decline in amount of igneous intrusive material in the upper part of the Au system;

(b) a second, subsidiary plug occurs near the west edge of the alteration envelope between the 4800 ft and 2650 ft levels which has been mined between the 4000 ft and 3250 ft levels (#15W orebody);

(c) a smaller plug occurs central to the Au system from below the 4000 ft level to the 3700 ft level.

Dykes are observed to coalesce and thicken laterally towards these and other smaller plugs.

(iii) The dyke swarm has an overall strike length near surface of ~900 m and an average width of ~50-60 m, decreasing to a ~300 m strike length and a width of ~25 m at the 5600 ft level. The swarm is made up of mappable dyke segments of ~12-25 m average measurable strike length.

(iv) Dyke/plug intersection widths (measured perpendicular to the strike of the orebody) range from <0.3 m to 40 m. The width distribution (Figure 42) is strongly positively skewed with a mode of 0.3 m and an arithmetic mean of 2.0 m (data truncated at minimum value of 0.3 m due to the resolution limit of the original drill hole information). Underground mapping and drill core observations further indicate that the frequency of occurrence of narrow dykelets <0.3 m in width is comparable to that of measured dykes >0.3 m in width.

(v) Dyke distribution statistics (frequency, average width, volume) within the dyke swarm show the following trends with depth in the Au system:

(a) dyke frequency of occurrence is greatest in the mid- to upper levels of the mine (2050-1000 ft levels) corresponding to subdivision upwards of plugs into dykes, decreasing with depth and dying off near the surface (Figure 43);

(b) average intersection width (Figure 44) is greatest (~3.9 m) around the 3550-3700 ft levels, with a subsidiary peak (~2.9 m) at the 1600-850 ft level; the former corresponds to the deep level interval with well developed plugs and the latter to the upper part of the Chesterville plug. Pronounced minima in dyke widths (~1.3 m) are noted in the mid-levels of the mine (3100-1750 ft levels; Figure 44) corresponding to high frequencies of narrow dykes;

(c) volume % of dykes (% of ultramafic host rock) data show two volume peaks at ~14% each on the 3550 ft and 1150 ft levels, and strong decreases both at surface and below the 4000 ft level (Figure 45). Low dyke abundances at surface are confirmed from examination of the walls and remaining pillars of the #10 orebody glory holes and a surface pit in the #19 orebody (pers. obs., 1990) and suggest that the top of the igneous system has been reached (see below for detailed discussion).

(vi) Measured orientations of dyke contacts (n = 63) are shown in Figure 34d. Dykes mostly strike sub-parallel or at a low angle (<30°) to the mean foliation and exhibit steep north-west or south-east dips. Hence, they are sub-parallel to the major siliceous break fluid supply veins, as mentioned above, and both the latter are sub-parallel to the foliation.

### **9.1. Intrusive Time Sequence Relative to Deformation, Veining and Au Introduction**

After having recognised a spatial and structural association between main stage Au-quartz vein mineralisation and a mafic “albitite” dyke swarm/plug system, it is important to evaluate relative timing relationships. Based on mapped cross-cutting relationships, three distinct generations of mafic “albitite” dyke intrusion have been distinguished within the ultramafic-hosted green carbonate ore (see Figure 32). The nature, abundance and distribution of each intrusive episode is discussed below, and the observational evidence for its timing with respect to deformation, hydrothermal alteration, veining and mineralisation, based on cross-cutting relationships (see Figure 32), is presented:

***Stage A<sub>1</sub> : mineralised and silicified dykes cut by multiple Au-quartz-pyrite vein generations***

Based on mapping and drillhole data, these dykes comprise an estimated ~50% by volume of the mafic “albitite” intrusive material, including the parts of the three major plugs that were stoped as “albitite” ore (e.g. #15W and “J” orebodies). The A<sub>1</sub> dykes are early syn-deformational relative to ductile fabric development within the Break deformation zone. Their locally irregular intrusive contacts cut spinifex-textured ultramafics, fabric defined by deformed, flattened #1 polygonal carbonate veins (e.g. 3815-79 stope), and deformed #2 carbonate stockwork veins (e.g. 3801-56 main cross-cut, 3850 ft level). However, the dykes are commonly podiform and boudinaged. A<sub>1</sub> dykes are massive (silicified), pale grey/beige/pinkish in colour with abundant disseminated pyrite (~2-5 %), and are rarely xenolithic. They are cross-cut by multiple Au-quartz-pyrite vein generations (#3, #4, #5 etc.) and are the *only* intrusive phase to contain millimetre-scale, irregular networks of grey quartz-pyrite “crackle” veins with significant Au as inclusions in the pyrite. The A<sub>1</sub> dykes are also cut by irregular, main stage milky Au-quartz veins (#4), which have pyritic alteration selvages and locally contain visible gold. The A<sub>1</sub> dykes comprise the highest grade, most consistently mineralised “albitite” ore (up to 10.3 g/t Au; 3815-79 stope; see Figure 46a).

An important point is that the highly silicified A<sub>1</sub> dykes pre-date the bulk of main stage Au-quartz vein mineralisation, although they are also intra-mineralisation in age since they do cross-cut minor Au mineralisation in the green carbonate ore #2 vein stage (e.g. 3801-56 main cross-cut, 3850 ft level). The reasons for this conclusion are:

(i) where A<sub>1</sub> dykes occur in highly silicified and veined green carbonate ore they show a closely similar degree of strong silicification and veining to the host rock (Figure 47a; for exact location and locations of Figures 47 b-d see Figure 46b) with veins freely crossing the dyke/host rock contact (e.g. south side of pillar, 3815-79 stope, Figure 46a; also 1715-66 exploration drift / north crosscut);

(ii) in the 1915-69 exploration drift a dyke/siliceous break pair was observed in which the strong veining and silicification of the A<sub>1</sub> dyke was related directly to the adjacent main stage Au, siliceous break vein;

(iii) A<sub>1</sub> dykes are cross-cut by, and therefore pre-date, grey quartz-pyrite vein networks which may correlate with the #3 cherty siliceous break vein stage, the latter in turn pre-dating main stage (#4) Au-quartz veining and mineralisation (Figure 32).

***Stage A<sub>2</sub> : foliated dykes; mixed xenolith suite***

These dykes comprise an estimated ~35-40% by volume of the mafic "albitite" suite. The A<sub>2</sub> dykes are syn-deformational relative to ductile fabric development since:

(i) they observably cross-cut A<sub>1</sub> dykes which cross-cut early fabric,

(ii) they show irregular intrusive contacts which cross-cut fabric (Figure 47b), but

(iii) they are frequently foliated to some degree and, in local high strain zones, very highly foliated (Figure 47c) and boudinaged.

A<sub>2</sub> dykes are mustard-beige/yellow in colour with variable contents of disseminated pyrite, do not show the density of quartz veining and intensity of silicification shown by the A<sub>1</sub> dykes, and are locally characterised by abundant (3-5%) contained fuchsite flakes. These dykes usually form lower grade, sub-economic mineralisation (~2 - 4 g/t Au).

The most important timing aspect shown by these A<sub>2</sub> dykes is that they are late, *syn*-main stage Au mineralisation in relative age. Hence, a significant amount of main stage Au mineralisation in the Kerr Addison - Chesterville system is intra-"albitite" dyke in timing (A<sub>1</sub> / A<sub>2</sub>), and, conversely, all dykes (A<sub>1</sub>; A<sub>2</sub>; A<sub>3</sub>; see below) are intra-Au mineralisation in age (Figure 32). The reasons for deducing this relative timing relationship for the A<sub>2</sub> dykes are as follows:



(i) in several locations (e.g. 1715-66 exploration drift/north cross-cut; 1915-69 exploration drift; 3815-79 stope, see geological map in Figure 46a) A<sub>2</sub> dykes with relatively much less alteration (silicification) and mineralisation observably cross-cut contrastingly highly silicified/veined A<sub>1</sub> dykes showing that the metasomatic silicification process had been fully active in that precise location, but had not fully affected the A<sub>2</sub> dykes (see Figures 48a-d; for exact locations of Figures 48a and 48b see Figure 46b);

(ii) A<sub>2</sub> dyke contacts are clearly observed to truncate main stage Au-quartz veins cutting A<sub>1</sub> dykes (see close-ups, Figures 48b and 48d); but

(iii) A<sub>2</sub> dykes are themselves cross-cut to a moderate extent by later main stage Au-quartz vein stringers (Figure 47d), and are altered and weakly mineralised;

(iv) A<sub>2</sub> dykes (e.g. 1715-66 exploration drift) are further characterised by a mixed xenolith suite, including

(a) yellow/green and black altered (?) ultramafic fragments,

(b) talc-chlorite-carbonate schist fragments and, most importantly,

(c) mineralised quartz-pyrite and carbonate-pyrite vein fragments,

(d) mineralised A<sub>1</sub> dyke fragments (Figure 49a; for exact location and locations of Figures 49b-d, see Figure 46b), and

(e) schistose green carbonate with deformed carbonate veins and fuchsite flakes (disaggregated green carbonate wallrock).

Mineralised xenolith type (c) was sampled and assayed up to 2.8 g/t Au (J.P.S., 1989). The latter Au-mineralised xenoliths clearly indicate that A<sub>2</sub> dykes post-date some Au mineralisation, a relationship which is verified by mapped cross-cutting relationships in, for example, the 3815-79 stope area (see above).

***Stage A<sub>3</sub>: mafic, granular, simple xenolithic dykes***

These dykes form an estimated ~10-15% by volume of the mafic “albitite” suite. They have a mafic, crystalline granular “salt-and-pepper” texture with pinker matrix patches. Individual dykes are often zoned from pale beige, well-altered margins to mafic, dark grey/green less-altered centres. The A<sub>3</sub> dykes are syndeformational relative to ductile fabric development since they show irregular intrusive contacts which cross-cut fabric but may also contain a well-developed foliation. They are crosscut by minor late Au-quartz vein stringers, contain dispersed pyrite, but are only geochemically anomalous in Au. At locations where A<sub>3</sub> dykes were determined to crosscut the texturally similar A<sub>2</sub> “albitite” dyke suite, the A<sub>3</sub> dykes were observed to contain a simpler xenolith suite of predominantly mafic/ultramafic fragments, and were visibly less foliated than the A<sub>2</sub> dykes. Mapping in the 3815-79 stope area (Figure 46a) verified the following cross-cutting relationships:

- (i) A<sub>3</sub> dykes clearly cross-cut both A<sub>1</sub> and A<sub>2</sub> dykes (e.g. Figures 49b and 49c) with sharp intrusive contacts;
- (ii) most importantly, where A<sub>3</sub> dykes cut highly silicified, metasomatised and quartz-veined A<sub>1</sub> dykes, A<sub>3</sub> dykes are, contrastingly, very significantly less altered (Figure 49c);
- (iii) as the photograph of an A<sub>3</sub> / A<sub>1</sub> dyke contact in a polished slab shows in Figure 49d, A<sub>3</sub> dykes actually cut main stage (#4) Au-quartz veins.

Hence A<sub>3</sub> dykes post-date the bulk of main stage Au-quartz vein mineralisation in this locality, confirming that main stage Au mineralisation is significantly intra-dyke in relative timing. However, A<sub>3</sub> dykes are cross-cut by minor Au-quartz veins and are slightly enriched in pyrite and Au (mean 450 ppb Au or 0.45 g/t Au; n=12; Smith, 1991) due to weak alteration, showing that they were intruded in the waning stages of main stage Au mineralisation (see Figure 32).

## 9.2. Discussion of Mafic "Albitite" Dyke Relationships

The relationships discussed above indicate that the mafic "albitite" plug/dyke swarm in Kerr Addison - Chesterville is closely associated in space, structure and relative timing (intra-dyke intrusion Au mineralisation; intra-main stage Au-quartz vein dyke intrusion) with main stage Au-quartz vein mineralisation in the system. For example, on each mining level of the Kerr Addison - Chesterville Au system (Figures 20 to 27), the mafic "albitite" dyke swarm is approximately co-extensive with the limits of main stage Au-related alteration, characterised particularly by the green carbonate alteration of the ultramafic host rocks. In longitudinal projection (Figure 28), the limits of dyke occurrence are closely similar to the flat funnel-shaped green carbonate alteration envelope. *Extensive drilling over a >2.5 km strike length of the Break, and at all depths down to >5600 ft level, has demonstrated that these dykes do not occur outside the main Kerr Addison - Chesterville and Chesterville East Zone ore systems.* The area of the dyke swarm expands upwards in an identical manner to the rapid areal expansion of both the green carbonate alteration and its contained quartz vein system (see below).

Furthermore, within the boundaries of the green carbonate hydrothermal alteration envelope, intrusions are not homogeneously distributed but are an order of magnitude more abundant (~11% dykes per unit area) in areas of Au-related metasomatism than in the barren "horses" of relict talc-carbonate ultramafic host rocks (~1% dykes per unit area). The latter observation suggests a close connection between intrusions and Au-related hydrothermal alteration, and a possible cryptic (early) metasomatic control on host rock competency and subsequent localisation of dyke intrusion. Structural data (Figures 34a and 34d) show that dyke orientations are closely similar to the orientations of major "siliceous" quartz veins, indicating that the two are approximately co-structural.

As discussed above, cross-cutting relationships indicate that mafic "albitite" dyke intrusion significantly overlapped main stage (#4) Au-quartz vein mineralisation (Figure 32). An

important point is that immobile element geochemical data (see Appendix V) indicate that the mafic "albitite" dykes are mostly very similar in composition regardless of timing (e.g. Figure 50). Hence, there was no discontinuity in dyke composition during Au mineralisation and A<sub>1</sub> - A<sub>3</sub> form a coherent, evolving suite (probably co-magmatic). The greater abundance of xenoliths in A<sub>2</sub> and A<sub>3</sub> compared to A<sub>1</sub> may indicate a trend towards greater volatile contents and more explosive emplacement over time.

A final point is that more detailed observations, were they possible, might show that dyke characteristics and relationships are actually a continuum, and that subdivision into stages is a statistical consequence of mapping detailed cross-cutting relationships in a small number of locations. Indications of such a continuum were obtained from observations in the area of the 1715-66 exploration drift and north crosscut.

## 10. Characteristics, Distribution and Timing of Hydrothermal Alteration

The entire Kerr Addison - Chesterville igneous/hydrothermal system, which has been described above, is contained within a flat, funnel-shaped alteration envelope, defined by green carbonate alteration in the ultramafics and carbonate/pyrite alteration and silicification in the mafic volcanics (e.g. Figures 20 to 29). A geochemical traverse across the ore zone on the 3850 ft level of the Kerr Addison mine (internal mine data, Kerr Addison Mines Ltd., ca. 1970; Kishida and Kerrich, 1987) shows that the Au system is part of a larger alteration halo of elements such as Hg, Au and Ag which extends to a distance of ~200 m away from the deposit. In addition, Kerrich (1983) and Kishida and Kerrich (1987) showed that both ore types are geochemically enriched in SiO<sub>2</sub>, CO<sub>2</sub>, Sr, Ca, Au, Ag, As, Sb, B and W, the green carbonate ore in K<sub>2</sub>O, Ba and Rb, and the flow ore in S and Na<sub>2</sub>O, compared to unaltered, equivalent lithologies elsewhere. Thomson (1980) showed that hand-held gamma ray mapping (of <sup>40</sup>K) was an effective method for locating main stage Au-related potassic alteration in the ultramafic komatiites in both the broad deposit sense, and for the individual green carbonate orebodies.

On a smaller scale, mine geology level plans (Figures 20 to 27) and cross sections (Figure 30) indicate that there is a precise correlation between the distribution of fuchsite, green carbonate alteration in the ultramafics and the major Au-quartz vein networks. This is in agreement with observations from stope scale mapping which indicate that green carbonate alteration occurs as wide haloes (2-3 m) around the larger composite "siliceous break" Au-quartz vein packages, individual Au-quartz veins and stringers having emerald green fuchsite-carbonate (Cr-mica) wallrock alteration selvages. Green carbonate alteration is contemporary with host vein formation (successive vein stages, each with green carbonate alteration, cross-cut each other; see above). With increased density of veining, alteration selvages overlap to give the appearance of a uniform green carbonate altered rock.

Within the hydrothermal Au-quartz vein system, alteration type depends on (i) host lithology and (ii) stage of alteration. The same hydrothermal fluids which cause *potassic* green carbonate alteration of the ultramafics also cause *sodic* alteration (+ pyritisation, silicification and carbonate alteration) of the contained mafic "albitite" dykes. An identical relationship is seen across green carbonate ore/flow ore contacts. For example in the 3821-63 rib, a sheeted, sub-parallel quartz vein system with green carbonate alteration selvages carries visible gold (vein assays up to ~22 g/t Au) in the ultramafic host rock, passing into quartz veins with strong, bleached pyrite-carbonate-albite alteration halos in the adjacent flow ores (wall rock assays up to ~15 g/t Au).

#### **10.1. Stages of Alteration; Ultramafic Host Rock**

The progressive stages of hydrothermal alteration of the komatiitic ultramafic host rock in the Kerr Addison - Chesterville system have been described by Buffam and Allen (1948), Baker et al. (1957) and James et al. (1961). Observations from underground mapping in this study indicate the following:

(i) early alteration of the ultramafics is shown by widespread areas of dark blue-grey, talc-chlorite-carbonate rocks containing polygonal carbonate veins (set #1), which define barren "horses" of the host rock. Pervasive carbonate (magnesite-dolomite) replacement of the primary minerals is evident without any noticeable metasomatic or colour zonation around the veins (see Figures 33a and 33b);

(ii) occurring near areas of subsequent ore, and/or at the margins of the areas of talcose rocks in (i), are areas of dark olive-green, chlorite-carbonate alteration (without talc) grading into light grey-brown *quartz*-chlorite-carbonate alteration. Both these alteration types contain a polygonal carbonate vein network which is similar in style to that in the talcose rocks in (i), and can be physically correlated with the latter (e.g. 1014-52 exploration drift). This vein network consists of chlorite and diffuse grey to white carbonate (magnesite/dolomite) which

has an unusual "lumpy" appearance (Figure 33a). Compositional alteration zoning of the ultramafic host rock inside these polygons is observed from brown polygon centres to grey margins adjacent to the veins. Hence, the areas of chlorite-carbonate and quartz-chlorite-carbonate alteration appear to represent a more advanced form of early (pre-Au mineralisation) alteration contemporary with the (#1) polygonal veins in the talc-chlorite-carbonate areas. Similar early co-existing assemblages have been reported from altered ultramafic rocks of the Kidd Creek area, Timmins by Schandl (1989). The close spatial relationship between brown-grey, quartz-chlorite-carbonate alteration and subsequent Au-related fuchsite green carbonate alteration, Au-quartz veining and dyke intrusion (see above) may demonstrate an early metasomatic control on host rock competency. Localisation of brittle-ductile "cherty siliceous break" fault structures might occur in the more competent quartz-chlorite-carbonate rocks in preference to the softer talc rocks;

(iii) main stage Au-quartz vein-related, fuchsite (Cr-muscovite) green carbonate alteration and silicification completely overprints the earlier alteration types, the intensity of the alteration being directly related to the abundance of quartz-carbonate veins, in turn related to the proximity of major siliceous break composite vein structures. Previous workers (see above) divided the Au-related alteration into "weak green carbonate" (<5% quartz veins), "medium green carbonate" (5-15% quartz veins) and "strong emerald green carbonate" (>15% quartz veins). An interesting empirical observation, noted by Buffam and Allen (1948; see Figure 16) and during this study, has been that where green carbonate ore zones come into contact with chlorite-carbonate-talc rocks, the Au-quartz veins die out rapidly into the latter as predominantly carbonate veins, with considerable amounts of visible gold being deposited at the transition.

## 10.2. Types of Carbonate Alteration and Their Relevance to Au Exploration

This study illustrates the importance of determining the timing and distribution of Au-related alteration where multiple vein stages are involved. Carbonate alteration of the ultramafics can be non Au-related due to both pre- and post-ore veining and hydrothermal alteration (potentially confusing for exploration). Particularly important in this regard is the early (#1 vein stage; see Figures 32 and 33a-b), pre-deformational polygonal carbonate veining (barren of Au) and pervasive carbonate replacement noted to occur only in the ultramafics. Studies by Greenwood (1967), Johannes (1969) and Schandl (1989) have shown that ultramafic komatiites are *extremely* susceptible to Mg-Ca carbonate alteration by fluids with as little as 0.85 volume % CO<sub>2</sub>. Field mapping (this work) indicates that such rusty-weathering carbonate veins and alteration are common in the ultramafic komatiitic rocks along the Break e.g. at the McBean open pit, the Highway 66 road cut at Misema Bridge, and the Bear Lake/Cheminis mine area. This lithology was formerly known as “carbonate rock” (e.g. Ridler, 1970, 1976). Such early carbonate alteration may be distinguished here from the later Au-related, *green carbonate alteration (+quartz veining)* using e.g.  $\delta^{13}\text{C}$ - $\delta^{18}\text{O}$  isotopic analyses (see data in Appendix IV).

Mapping shows that green carbonate alteration with quartz veins and probable anomalous Au is specifically localised at discrete intervals along the Break-associated ultramafic horizon between Kirkland Lake and Larder Lake, corresponds to Au mines or showings, and overprints the previous talc-chlorite-carbonate (magnesite/dolomite) altered host rocks. The principal visual distinguishing points are (i) strong emerald green colour due to fuchsite (Cr-muscovite) development especially along cleavage planes, (ii) relative absence of dark blue-grey talc, magnesite or chlorite, (iii) presence of distinctive bright yellow microscopic specks of leucoxene (TiO<sub>2</sub>) and (iv) paler overall hue (pink to orange-brown weathering) with quartz-carbonate veins/stringers and Au values, but usually sparse disseminated pyrite.



## 11. Longitudinal Contour Diagrams (Green Carbonate Ore)

### 11.1. Methodology

In order to describe fully the geometry of the green carbonate alteration envelope, and vertical and lateral trends in the distribution of mafic "albitite" intrusions and major "siliceous break" Au-quartz veins *within* the alteration envelope, five longitudinal contour diagrams have been prepared (see Figures 51 to 55). The relatively flat, funnel-shaped geometry of the alteration envelope, with its extremely long strike and down-dip continuities relative to its width, lends itself particularly well to this kind of numerical analysis. Primary data, in terms of summated intersection widths of particular variables (e.g. green carbonate alteration (minus contained intrusive material, but including quartz veins); total quartz vein footage; total dyke footage) normal to the strike of the principal ultramafic unit, were measured from 27 (reconstructed) and 4 (original, based on flat drill holes only) Kerr Addison level plans at either ~11 m or ~22 m horizontal intervals. Since the main ultramafic unit contains all the green carbonate alteration, ~97 volume % of the "albitite" dyke / plug intrusive material and ~87 volume % of the measured quartz veins (data from Smith, 1992), then the data obtained are representative of the whole Au system. Data from the closest equivalent Chesterville levels were also added.

The data were plotted in longitudinal projection on a vertical plane parallel to the strike of the Break where they form a grid of piercing-point values spaced horizontally ~11 m (Figures 52 to 55) or ~22 m (Figure 51) apart on each ~45-61 m vertically spaced level. Hence, a total of ~1,580 (Figures 52 to 55) or ~910 (Figure 51) data points per diagram were contoured using the programme MacGridzo™ (Rockware Inc., Denver, Colorado) run on a Macintosh SE/30™ personal computer. A simple inverse square weighting allocation for four nearest neighbours and a grid cell size of 45 x45 m were used, and control values were forced onto the grid. The contours were superimposed on the outline of the green carbonate alteration envelope from Figure 28 which was used as a reference, and for most variables

plotted was a zero contour line; contours were truncated at the envelope. The principal features shown by Figures 51 to 55 are listed below.

## **11.2. Green Carbonate Alteration (Minus Contained Intrusion Widths)**

Figure 51 shows the following principal features:

- (i) A clear root zone which occurs approximately centrally located in the overall green carbonate alteration envelope on the 5600 ft and 4800 ft levels, with dimensions of ~15-30 m (50-100 ft) in width and ~210 m (~700 ft) in strike length .
- (ii) The strike length of >15 m (~50 ft) thickness green carbonate increases upwards markedly from ~210 m to ~640 m between the 4800 ft and 3700 ft levels.
- (iii) The thickness of the green carbonate is >91 m (~300 ft) at the 4400 ft level in the west part of the system, which corresponds exactly to an intrusive sub-centre (see Figure 28).
- (iv) From this point, the thickest part of the green carbonate splits into western and eastern branches. The western branch corresponds with the western intrusive sub-centre and an inclined zone of stopes which extends all the way up to the present surface as the #10 orebody (and glory holes). The eastern branch corresponds to the Chesterville Plug-related intrusive centre and a second zone of stopes which extend almost to the present land surface. In projection, the central inclined gap in the thickness of green carbonate alteration corresponds to a talc zone (see level plans, Figures 20 to 27; true scale cross section, Figure 30).
- (v) At surface, the green carbonate alteration closes off to the east, as shown by the 50 ft (~15 m) contour. Both principal green carbonate branches extend up to the current erosion level and are separated by a <15 m (~50 ft) thick zone; the western branch is stronger, reaching the surface at 45-60 m (~150-200 ft) thick, compared with the eastern branch at <30 m (~100 ft) thick. The western branch was the location of the original discovery intersection at a depth of ~90 m in 1937; the surface showings were sub-ore grade.

Hence, the contoured green carbonate alteration diagram gives a clear image of a root zone, two prominent branches within a widening, flattened funnel, and a marked reduction, particularly in the eastern part, near surface. By comparison with the Chesterville East Zone, and trends discussed below, it seems relatively certain that the Kerr Addison - Chesterville system closed off a short distance above the present erosion surface (~150-300 m for 15 m (50 ft) thickness contour), never connected to surface originally as a major altered zone, and therefore developed internally in the Archean crust.

### 11.3. Quartz Veins (>0.3 m width)

Figure 52 shows the bottom and top of this major Archean Au-quartz vein system very clearly; only major feeder veins >0.3 m (~1 ft) have been considered, and not thinner veins:

(i) The bottom of the quartz vein system is well defined by the 5 ft (~1.5 m) contour line which corresponds very well with the green carbonate alteration contours (Figure 51). Again, the system is shown to intensify in terms of an increase in the strike length of >1.5 m (~5 ft) cumulative quartz vein thickness upwards between the 4800 ft and 3700 ft levels from ~220 m to ~480 m.

(ii) The main ore system is characterised by 3-6 m (~10-20 ft) cumulative quartz vein thicknesses with high values of up to 10-15 m (~30-45 ft).

(iii) Prominent is a continuous western branch of >0.3 m thick quartz veins which corresponds with:

(a) the western green carbonate alteration branch,

(b) the western intrusive sub-centre, and

(c) the mining root of the system which converges on the small central intrusive plug and is slightly west of centre relative to the overall alteration envelope. This branch is defined by a "ridge" in cumulative quartz vein thickness of 6-12 m (~20-40 ft) between the 4400 ft and 1150 ft levels.

(iv) High quartz vein density zones extend to the east on the 4400 - 4200 ft, ~3250 ft and ~2350 ft levels suggesting the possibility that quartz veins penetrated laterally eastwards. An eastern branch is well defined in the upper 2500 - 850 ft levels.

(v) The decrease in significant cumulative quartz vein thickness corresponds well with the western green carbonate limit; data are unavailable for the eastern side (Chesterville).

(vi) The top of the system is very clearly defined by the cumulative quartz vein 5 ft (~1.5 m) contour which is deeper in the east (~1150 ft level) compared with the west (175-700 ft level), corresponding with the green carbonate alteration pattern (Figure 51).

These data clearly show that the top of the green carbonate ore system was controlled by a decrease in hydraulic fractures represented by quartz veins (also see below).

#### **11.4. Percent Quartz Veins (>0.3 m width) in Green Carbonate Alteration**

Figure 53 shows three zones of contrasting behaviour:

(i) At depth there is a root zone with a fairly fixed quartz vein (>0.3 m) % thickness of green carbonate alteration at ~5-15 % corresponding to previously defined root zones (see above).

(ii) In the central part, typically 10-20% quartz veins (>0.3 m) occur, with values of up to 30% at the 1150-1300 ft level; contours are irregular. Along the western margin of the system, the only margin, for which there are available data, the % of quartz veins (>0.3 m) in green carbonate alteration, *decreases*. Thus green carbonate alteration persists further laterally to the west than significant quartz veining (>0.3 m), as also shown by mine geology level plans (see Figures 23 to 25).

(iii) Exactly the same pattern is shown at the top of the system by the 10% and 5% contours. Hence, the frequency of >0.3 m quartz veins actually decreases at the top of the Kerr Addison - Chesterville system showing that upwards, green carbonate alteration and quartz veins/veinlets

(<0.3 m width) persist significantly further than the major guide veins. These points have been verified by observations (J.P.S., E.T.C.S., 1989) in the walls and remaining pillars of the #10 orebody glory holes, and the #19 orebody open pit, which show markedly low >0.3 m quartz vein densities in general.

#### **11.5. Total and Percent Mafic "Albitite" Dyke/Plug Thickness (>0.3 m width)**

Figures 54 and 55 show the following principal features:

(i) A well defined intrusive root zone at 3-5 m (10-15 ft) cumulative width (or ~5-10% of total ultramafic unit thickness) which corresponds spatially to the eastern part of the green carbonate alteration root zone.

(ii) A sinuous western concentration of dykes (~5-20%) corresponding approximately to the western intrusive sub-centre (#15W "albitite" orebody) at depth, and with the western green carbonate alteration / quartz vein branches, but not precisely. Some concentrations of "albitite" dykes persist to surface locally. Cumulative dyke (>0.3 m) thickness typically varies from ~6 m (20 ft) to highs of ~15-25 m (50-80 ft).

(iii) An eastern branch corresponding to the Chesterville Plug which shows prominent thickening at the ~4000 ft and ~1750 ft levels (~30% maximum of total ultramafic unit thickness); cumulative dyke (>0.3 m) thicknesses are >6 m (20 ft) and up to ~30 m (100 ft).

(iv) On both the ~3850 ft and ~1900 ft levels there are central dyke thickness maxima of ~3-12 m (10-40 ft) and ~6-25 m (20-80 ft) respectively, above low cumulative dyke thicknesses, suggesting *lateral* injection from the east, supported by level plan patterns showing dyke extensions from the eastern (Chesterville) plug system. Lateral dyke injection is now a well documented phenomenon (e.g. Krafla, Iceland).

(v) Sharp lateral decreases correspond to the limits of the green carbonate alteration envelope; truncation of contours at the green carbonate envelope is a consequence of

machine contouring of a sharp contact. It is well known from drilling that "albitite" dykes do *not* occur significantly outside the ore system to the east and to the west.

(vi) Marked decreases occur at the top of the system particularly in the east, as previous patterns have also shown. The top is defined by the ~3 m (10 ft) contour (~5% of total ultramafic unit thickness). As previous diagrams have shown, the western branch did extend above the present land surface, but probably not by a large distance.

#### **11.6. General Points from The Longitudinal Contour Diagrams**

(i) The root zone of the system is characterised by a ~15-30 m (50-100 ft) width of green carbonate alteration, containing 5-10% quartz veins (>0.3 m) and ~5-10% dykes (>0.3 m).

(ii) There is a good correspondence between the distributions of green carbonate, quartz veins and to some extent "albitite" dykes both laterally, at the bottom of the system and at the top; two main branches are seen.

(iii) The bulk of Au mineralisation is contained within ~1,130 vertical metres between the ~4000 ft and ~300 ft levels, and is characterised by ~5-20%, >0.3 m to ~11 m thick quartz veins and 5-25%, >0.3 m to ~35 m thick "albitite" intrusions.

(iv) The top of the system is characterised by closure of the contours, particularly in the east. Hence, the east branch dies out upwards below the west branch.

(v) In general terms, the diagrams show green carbonate alteration with quartz veins/veinlets (<0.3 m width) persisting upwards further than major quartz veins (>0.3 m) which themselves persist upwards to about the same extent as, or possibly a little further than, the "albitite" dykes (>0.3 m); the decrease in "albitite" dyke cumulative thickness is more irregular.

(vi) The closure of contours particularly in the east and the completely blind nature of the Chesterville East Zone strongly suggest that the system closed off and did not penetrate to the Archean paleosurface, except possibly as minor leakage veins and hydrothermal alteration zones. In the west, the contours suggest that significant green carbonate alteration (>15 m thickness) probably did not extend more than ~150-300 m above the present land surface (Spooner et al., 1991). Thinner localised widths of green carbonate and primary geochemical dispersion would have penetrated upwards further and may be used in exploration (cf. Noranda/Freewest Resources' Lightning Zone on the Porcupine-Destor Break, near Matheson, N. Ontario).

## **12. Vertical Trends in Green Carbonate Alteration and Quartz Vein / Dyke Areas per Level**

### **12.1. Methodology**

In order to isolate vertical trends in *areas* of green carbonate alteration, major quartz veins (>0.3 m width) and "albitite" dykes (>0.3 m) per fully drilled level of the Kerr Addison - Chesterville Au system, data used in the longitudinal contour diagrams (see above) were integrated on each level using a trapezium method. The method of area calculation was as follows: the total intersected footage of a particular unit on each level was divided by the number of equally spaced lines of information measured across the system normal to its strike direction, giving a mean intersection width per line of information; this value was then multiplied by the total strike length at that level to give the area of the unit in question (e.g. green carbonate, quartz veins, "albitite" dykes). The data are plotted in Figures 56 and 57. The figures were ratioed to their equivalent values on the 5600 ft level, so that changes in areas upwards could be more easily compared. In many ways these diagrams are a summation and simplification of the contour diagrams discussed above. The geological details of the trends discussed below may be seen by examination of mine level plans (Figures 20 to 27).

### **12.2. Green Carbonate Alteration**

Figure 56 shows the changes in strike length, average intersection width and total area (the product of length and width multiplied) of the green carbonate altered rocks relative to values on the 5600 ft level. The following important points are evident:

(i) Green carbonate alteration expands upwards *5 times* in total area between the 5600 ft and 2800 ft levels (a vertical interval of ~850 m), the most rapid expansion (from 1.4 to 3.6 times the area on the 5600 ft level) being between the 4800 ft and 3850 ft levels (a vertical interval of ~290 m). This expansion can be seen very clearly by examining the plans for the 5600,



4800, 4400, 4200 and 3850 ft mine levels (Figures 20 to 23). The deep dimensions (>4800 ft level), however, show much less change suggesting that these are approaching the dimensions of a relatively small (~20-50 m x ~300 m) low-grade root feeder zone through which the total volumes of hydrothermal fluid and magma which produced the main ore system had to pass (see below for further discussion).

(ii) Area remains approximately constant (~4.5 to 5.0 times the value on the 5600 ft level) in the mid- and upper levels of the mine between the 2800 ft and 1150 ft levels (a vertical interval of ~500 m), before dropping slightly (to ~4 times the area on the 5600 ft level) in the 1000 ft to 500 ft level interval.

(iii) A *sharp* fall-off in the area of green carbonate is evident between the 500 ft and 83 ft levels, confirming that the Au system contracts markedly towards the present land surface (see also geological details in the plans for the 700 and 175 ft mine levels; Figures 26, 27).

(iv) Green carbonate shows a greater relative increase in length (up to 3.0 times the value on the 5600 ft level) than it does in width (up to 2.0 times) as it expands upwards. This is probably due to the hydrothermal ore fluids exploiting "cherty siliceous break" fault structures which are at a low angle to the Break and would allow more rapid fluid movement laterally than transverse to the Break; these in turn probably reflect the foliation fabric in the Break zone.

(v) Maximum width and maximum length of the green carbonate do not coincide: maximum widths (~2.0 times value on 5600 ft) occur between the 2800 ft and 1900 ft levels; upwards from the 1900 ft level the average width decreases (to ~1.5 times value on 5600 ft) while the length continues to increase to a maximum (of ~3.0 times the value on 5600 ft) between the 1450 ft and 1000 ft levels, before decreasing towards surface; the system becomes thinner and more elongated before contracting sharply.

### 12.3. Quartz Vein Area

Figure 57 shows the changes in total area (calculated as described above) occupied by major (>0.3 m width) quartz veins relative to the area value on the 5600 ft level. The diagram shows the following:

(i) No change in the total area of quartz veining occurs between the 5600 ft and 4800 ft levels, indicating that expansion of the vein system upwards had not yet begun at these levels and suggesting that these may be the characteristics of the feeder zone.

(ii) Quartz veining expands upwards *~6 times* in total area between the 4800 ft and 2800 ft levels (a vertical interval of *~600 m*); this inflation corresponds closely with the expansion of green carbonate alteration (see Figure 56), and correlates satisfactorily with the onset of economic Au mineralisation in the root zone of the green carbonate ore (#14 orebody) on the 4000 ft level (see longitudinal, Figure 28); by this level, the areal expansion of quartz veining has reached *~3 times* the value on the 4800 ft and 5600 ft levels.

(iii) The area of quartz veining remains approximately constant (*~6-8 times* the value on the 5600 ft level) in the mid- and upper levels of the mine between the 2800 ft and 850 ft levels (a vertical interval of *~590 m*), showing local peaks on the 2200 ft, 1750 ft and 1450 ft levels. This observation reflects a fairly constant degree of hydraulic inflation upwards.

(iv) Major (>0.3 m) quartz veins decrease *sharply* in area upwards between the 850 ft and 175 ft levels (from *~7.0 to 1.5 times* the area on the 5600 ft level) confirming that the ore system dies out towards the surface. The quartz vein area starts to decrease *below* that of green carbonate alteration; hence green carbonate alteration persists upwards higher than >0.3 m quartz veins.

#### 12.4. "Albitite" Intrusion (Dyke/Plug) Area

Figure 57 also shows the changes in total area (calculated as described above) occupied by major (>0.3 m width) "albitite" dykes relative to their area value on the 5600 ft level, and compared on the same diagram to changes in the area occupied by quartz veins (see above).

This diagram shows the following features:

- (i) No change in the total area of "albitite" dykes occurs from the 5600 ft to the 4800 ft level, suggesting that the absolute area values are characteristic of the root zone.
- (ii) "Albitite" dyke / plug material expands upwards *~6 times* in total area between the 4800 ft and 3850 ft levels (a vertical interval of *~290 m*), far more rapidly than the equivalent expansion of quartz veining over the same vertical interval; this is particularly due to the occurrence of three major plugs starting on the *~3850 ft* level. The relative amounts of quartz vein and "albitite" dyke expansion are very similar.
- (iii) The total area of "albitite" dykes decreases upwards from the 3850 ft level to the mid-levels (*~2800 ft to 2350 ft*) of the system (*~3.5 times* the area on the 5600 ft level; see also contoured longitudinals and mine level plans).
- (iv) A steady expansion occurs upwards from the 2350 ft level to a second peak in dyke total area (*~7 times* the area on the 5600 ft level) on the 1450 ft - 1150 ft levels.
- (v) Above the 1000 ft level, the total area of dykes (as a ratio to values on the 5600 ft level) falls off in a *very similar* fashion to that of the quartz veins as the Au system dies out near surface.

## **12.5. General Points: Green Carbonate/Quartz Vein/"Albitite" Dyke Areal Expansions**

(i) the green carbonate / quartz vein / dyke data (Figures 56 and 57) *all* show very similar expansion profiles from small root zones to relatively constant areas (~5 to 8 times their respective areas on the 5600 ft/4800 ft levels).

(ii) Importantly for exploration, quartz vein and dyke areas start to decrease from the 1000 ft level upwards in a coupled fashion, whereas the area of green carbonate alteration continues further upwards before decreasing sharply above the 500 ft level.

Both (i) and (ii) suggest that the emplacement of mafic "albitite" intrusions and hydrothermal fluids produced real hydraulic dilation and were temporally and physically linked.

(iii) Veins are still present below the base of economic green carbonate ore at the 4000 ft level, but areal expansion has not taken place and the veins do not carry significant Au values (see below).

### 13. Vertical Trends in Ore Tonnage / Grade / Total Au and Au:Ag Ratio per Level

Based on ~2,500 compiled individual stope data (F.R.P.), it has been possible, since the deposit has been well defined through mining, to break down the ore tonnage, Au grade and total Au production at Kerr Addison by mine level, ore type and individual orebody number to a high degree of precision. The results are shown in Figures 58 to 60, and will be discussed in turn below (see also Tables 3A, 3B for orebody totals).

#### 13.1. Ore Tonnage Vertical Trends

Figure 58a shows the variation in total tonnage with depth of the three principal ore types (flow ore, green carbonate ore and "albitite" ore; graphitic ore has been included with the flow ore) per ~46 m level interval (~61 m where stated) of the Kerr Addison mine. The main points shown by this diagram are as follows:

(i) Total tonnage figures start at the 4600 ft level with an initial rapid increase upwards to ~1.2 mt (million tonnes) per level at the 3850 ft to 3400 ft levels. A trough occurs (~0.8 mt per level) between the 3250 ft and 2800 ft levels followed by a steady climb to a tonnage peak (~2.2 mt per level) at the 1450/1600 ft levels. A decrease then follows to ~1.4 - 1.6 mt per level at the 300/500 ft levels before a *sharp* drop-off near the present surface. Hence, the complete Au productive vertical interval of the system is preserved.

(ii) Total tonnage figures are dominated by flow ore below the 1450 ft level, and green carbonate ore above the 1450 ft level. In comparison to these the "albitite" ore (#15W orebody, ~0.5 mt) contributes a very small tonnage. The combination shows a relatively smooth increase, a relatively smooth decline and then a sudden sharp decline near the present surface.

(iii) Flow ore tonnage increases steadily upwards from its mining root zone on the 4600 ft level to ~1.0 mt per level between the 3850 ft and 3400 ft levels, corresponding to a rapid initial increase in the strike length and thickness (partly due to folding) of the major #21

orebody (see Figure 29 for strike length). A broad maximum in flow ore tonnage of ~1.2 - 1.4 mt per level occurs between the 2650 ft and 1450 ft levels, followed by a steady decline upwards to near zero at surface.

(iv) In contrast, green carbonate ore shows an almost continuous expansion upwards in tonnage from its mining root zone at the ~4000 ft level to near surface. The most rapid expansion, however, occurs between the 2800 ft and 1300 ft levels (from ~0.2 mt per level to ~1.2 mt per level), *above* the principal expansion of green carbonate alteration. Maximum green carbonate ore tonnage was reached high in the system at the 300 ft level (~1.4 mt per level) above which it declines sharply to near zero at the 175 ft level (and surface), corresponding to the independently known low grade of the surface showings (the discovery intersection was approximately at the 300 ft level; section 2 above). The reason for the sharp drop in green carbonate ore tonnage is that grade finally dropped below cut-off (~5 g/t Au) at the 300 ft level (see below) after a steady decline from the 3050 ft level, although tonnage was increasing; when grade dropped below cut-off, mineable tonnage dropped to zero.

Figures 58b and 58c (respectively) show the contributions made to the total flow ore and green carbonate ore tonnages by the major individual orebodies. Points arising from these diagrams are as follows:

(i) Flow ore tonnage trends (Figure 58b) are dominated by the major #21 orebody (13.77 million tonnes). The #21 reaches its maximum tonnage (>0.8 mt per level) between the 4000 ft and 3400 ft levels with a subsidiary peak between the 1900 ft and 1450 ft levels at ~0.7 mt per level.

(ii) Significant flow ore tonnage also occurs in the #16 and #6 orebodies between the 2650 ft and 1150 ft levels (Figure 58b) contributing to the broad central flow ore total tonnage peak.

(iii) Green carbonate ore tonnage trends (Figure 58c) are dominated by the #14 orebody below the 1450 ft level, and by the #10 and #9 orebodies above the 1300 ft level; a number

of smaller orebodies also occur between the 2650 ft and 1000 ft levels which significantly contribute to the rapid increase in total tonnage over this vertical interval.

(iv) Individual green carbonate orebodies (e.g. #10, #9, #14) show tonnage trends in Figure 58c which mimic on a smaller scale those of the total green carbonate ore i.e. an expansion in tonnage upwards followed by a sharp decline at the top where the individual orebody dies out. This may indicate a degree of self-similar behaviour in these ore sub-systems compared to the total green carbonate ore system.

### 13.2. Ore Grade Vertical Trends

Figure 59a shows the variation in grade with depth of the three principal ore types (as above) per level interval of the Kerr Addison mine. The main points shown are as follows:

(i) Flow ore grade increases upwards steeply from ~9 g/t at the 4600 ft level to a grade peak of ~21 g/t at the 3850 ft level probably corresponding to intense sulphidation reactions, followed by a sharp decline to ~11 g/t at the 3250ft level. Overall, flow ore grade declines upwards (with some reversals) from the peak of ~21 g/t on the 3850 ft level to ~5 g/t at the 850 ft level. A reversal in the trend then occurs to ~10 g/t near surface, which appears to reflect a genuine increase in grade and not just more selective stoping methods.

(ii) Green carbonate ore grade increases rapidly upwards from ~4-6 g/t in the root zone of the system (4000 ft to 3700 ft levels) to a grade peak of ~12 g/t at the 3100 ft level; a slight trough in the grade profile of ~8 g/t at the 2200 ft level is then followed upwards by a second grade peak between the 2050 ft and 1450 ft levels of ~10 g/t. Green carbonate ore grade then decreases upwards steadily from ~10 g/t at the 1450 ft level to ~4-5 g/t near surface; upwards grade decline starts *before* the decline in quartz vein area per level. Two important points are that (a) thick quartz veins exist below the 4000 ft level but are very low grade (see below); hence the Au was in solution but did not precipitate, and (b) that grade increase correlates quite well with quartz vein area per level increase i.e. grade correlates with volumetric fluid inflation.

(iii) "Albitite" ore (from the #15W orebody in the western intrusive plug) is of lower grade (~3-5.5 g/t) than both the flow and green carbonate ores at the same level. In a similar fashion to the other ore types it shows an initial increase in grade (from ~3 to ~5.5 g/t) between the 3850 ft and 3400 ft levels, followed by a decrease upwards.

Figures 59b and 59c (respectively) show the contributions made to the total flow ore and green carbonate ore grades by the major individual orebodies. Points arising from these diagrams are as follows:

(i) Below the 1450 ft level the #21 orebody generally contains the highest grade flow ore (Figure 59b) on each level. The #6 orebody shows an almost identical grade-depth profile to the #21 orebody, which supports the suggestion (see above) that the #21 and #6-8 orebodies were formerly connected prior to offset on the post-ore Kerr Fault. The #16 orebody is generally of lower grade than the #21 and #6 orebodies at the same level, which supports the suggestion (see above; Figure 39) that the #16 represents a down-faulted, lower grade upper part of the #21 and #6-8 mineralised unit. In fact, by matching grade peaks of ~15-16 g/t in the #16 orebody (~2950 ft level) and #21 orebody (~2050 ft level), and subsequent steep declines in grade upwards in both orebodies, the amount of vertical Kerr Fault displacement may be estimated at ~270-300 m (south side down) which agrees well with other estimates (see above).

(ii) The major flow orebodies (#21, #16, #6-#8) all show mutually similar depth-grade profiles (Figure 59b) suggesting similar mechanisms of mineralisation i.e. a steep increase to maximum grade just above their base, followed by first a rapid decline then relative constancy or a slower decline in grade upwards; a reversal then occurs near the top of each individual orebody with a significant increase in grade upwards. These high level grade increases correspond to continued tonnage decreases and may therefore result from higher water/rock ratios and more locally intense sulphidation reactions associated with restricted quartz vein channelling of fluids.



(iii) Figure 59c shows that some individual green carbonate ore bodies reached considerably higher than average grades e.g. #24 orebody (up to 16 g/t), #14 and #15 orebodies (up to ~14 g/t). Vertical grade profiles for the green carbonate orebodies are more erratic than for the flow orebodies, but again show mutually similar depth-grade profiles (Figure 59c) suggesting similar mechanisms of mineralisation i.e. a fairly rapid increase to maximum grade at their mid-levels from a low grade initial root zone, followed upwards by a steep decline in grade. The more vertically extensive green carbonate orebodies (e.g. #14, #15, #10) even show two or three grade peaks with depth, separated by sharp troughs, suggesting a possible vertical periodicity to Au mineralisation in these orebodies.

### 13.3. Total Au Vertical Trends

Figure 60a shows the variation with depth of total Au in the three principal ore types i.e. the net effect produced by multiplication of the two previous sets of tonnage and grade figures (Figures 58a and 59a) per level. The main points shown by this diagram are as follows:

(i) Total Au figures are dominated by flow ore below the 2000 ft level, and green carbonate ore above the 1000 ft level. In comparison to these the "albitite" ore (#15W orebody) is insignificant.

(ii) Total Au increases rapidly upwards from the mining root zone (flow ore) on the 4600 ft level to a peak of ~20 tonnes Au per level on the 3850 ft and 3700 ft levels, then declines steeply upwards to a trough of ~8 tonnes Au per level on the 3250 ft level. A broad maximum in total Au of ~15-18 tonnes Au per level then occurs between the 2650 ft and 1450 ft levels, followed by a steady decline upwards in total Au to ~10 tonnes Au per level on the 300 ft level and a sharp drop off in total Au to near zero at the 83 ft level. *The approximately symmetrical rise and fall of total Au produced with depth shows very clearly that Kerr Addison - Chesterville preserves the complete productive interval of an Archean Au-quartz vein ore system.*

(iii) Flow ore total Au is concentrated in the lower part of the system, showing a sharp peak of ~17.5 tonnes Au per level on the 3850 ft - 3700 ft levels, and a lesser but broader peak of ~13-15 tonnes Au per level between the 2650 ft and 1750 ft levels, separated by an intervening trough of ~6 tonnes Au per level on the 3250 ft level. Flow ore total Au then declines steadily from ~10 tonnes Au per level on the 1450 ft level to almost zero near surface. Hence flow ore total Au production was principally grade-driven apart from a small tonnage of high grade ore above the 300 ft level.

(iv) In contrast, green carbonate ore total Au increases fairly steadily upwards from the root zone on the 4000 ft level to a maximum of ~9 tonnes Au per level on the 300 ft level, before sharply dropping off near surface. The total Au profile for green carbonate is therefore largely tonnage-driven (see Figure 58a) and total Au is concentrated in the top of the system. The most rapid increase in green carbonate total Au is between the 2350 ft and 1450 ft levels (from ~2 to ~9 tonnes Au per level) corresponding to an increase in the number of green carbonate ore bodies.

Figures 60b and 60c (respectively) show the contributions made to the flow ore total Au and green carbonate ore total Au by the major individual orebodies. Points arising from these diagrams are as follows:

(i) Flow ore total Au trends (Figure 60b) are dominated by the major #21 orebody (~172 tonnes Au). The #21 orebody total Au increases rapidly to reach its maximum (~18 tonnes Au per level) at the 3850 ft -3700 ft levels, then decreases steeply upwards to reach approximately constant values of ~6-8 tonnes Au per level between the 3200 ft and 1600 ft levels.

(ii) Significant flow ore total Au also occurs in the #16 and #6 orebodies between the 2800 ft and 1300 ft levels (Figure 60b) contributing to the broad central flow ore total Au peak.

(iii) Green carbonate ore total Au trends (Figure 60c) are dominated by the #14 orebody below the 1150 ft level, and by the #10 and #9 orebodies above the 1000 ft level; a number

of smaller orebodies also occur between the 2800 ft and 1300 ft levels which significantly contribute to the rapid increase in green carbonate total Au over the latter vertical interval.

(iv) Individual green carbonate orebodies (e.g. #10, #9, #14) show total Au trends which mimic on a smaller scale those of the total green carbonate ore i.e. a gradual increase to a maximum total Au upwards from a low total Au root zone, followed by a sharp decline in total Au as the orebody dies out upwards.

#### 13.4. Au:Ag Ratio Vertical Trends

Figure 61 shows the yearly Au:Ag production ratio from the Kerr Addison mine plotted against year. A reasonable assumption is that since the mining sequence progressed downwards with time, and at any particular time was concentrated in a relatively short vertical interval, then the x-axis (production year) can be interpreted as an approximate, moving-average *depth* axis from the top of the mine (started in 1938) to the bottom (4600 ft; reached in 1966). As expected, post-1966, when ore began to be stoped from a wide vertical spread of levels in the mine, the Au:Ag production ratio returned to approximately the overall mine average of ~18:1. Figure 61 therefore shows an approximately linear co-variation of the Au:Ag ratio with depth, from a value of ~21 at surface to ~16 at the bottom of the system; the correlation coefficient for these data of -0.78 is considerably above the critical correlation coefficient test for significance at the 95% confidence level for 27 samples (-0.38). Hence a significant vertical zonation in Au:Ag ratio exists, the total variation in Au:Ag ratio (~16 to ~22) being ~28% of the Kerr Addison mine average of 18.1.

This trend is a rare example of coherent vertical element zoning in an Archean Au-quartz vein system. The higher Au:Ag ratio of the Chesterville mine (18.5) is also consistent with the relatively shallow depth of its workings (to ~830 m), the bulk of the Chesterville ore being in fact located approximately in its top 400 m. An important point shown by the smooth trend is that *the green carbonate and flow ores were clearly linked as part of the same*

*hydrothermal fluid flow system since the upward increase in Au:Ag ratio is shown by both ore types; the reason being that total Au produced changed from flow ore dominated in the lower part to green carbonate ore dominated in the upper part. A reasonable explanation of the increase in Au:Ag ratio upwards is that the mineralising process, particularly in the flow ore, depleted the hydrothermal fluids more rapidly in Ag due to its efficient partition into Au<sup>0</sup> than it did Au, thus the Au:Ag ratio of the fluids increased smoothly as they moved upwards through the system, and was maintained through time. In conclusion, the steady change in Au:Ag ratio indicates a smooth precipitation gradient.*

## **14. The Nature of the Bottom and the Top of the Kerr Addison - Chesterville Ore System**

A unusual opportunity exists at the Kerr Addison mine to study both the bottom and the top of a major Archean Au-quartz vein ore system. The two principal reasons are as follows:

(i) an engineering misjudgement (see history, Section 2 above) caused an extra shaft (#4 Internal Shaft, 4000 - 6000 ft depth) and six extra mine levels (between the 4000 - 5600 ft levels) to be installed which provide geological information on the system *to ~600 m below the bottom of mined ore;*

(ii) as described in detail above, numerical analysis of the geometry and distribution of green carbonate alteration, quartz vein and "albitite" dyke total areas (e.g. longitudinal contour diagrams, Figures 51 to 55; areal expansion diagrams, Figures 56 and 57), and ore tonnage, grade and total Au figures (Figures 58 to 60) all indicate that the ore system dies out in the upper part of the mine and only just reached the present erosion surface.

### **14.1. The Bottom**

#### ***(i) Central Green Carbonate Ore Root Zone (~4000 ft level)***

As shown by the longitudinal diagram in Figure 28, the green carbonate / "albitite" dyke orebodies originate at depth as three separate narrow root zones positioned at the west and east ends (3850 ft level) and centrally (4000 ft level), within the overall green carbonate alteration envelope. The west and east root zones comprise disseminated pyrite ore zones completely hosted by silicified mafic "albitite" plugs (e.g. 3815-79 stope, Figure 46) without major quartz veins being present. However, the central green carbonate ore root zone mapped on the 4000 ft level, although spatially coincident with a minor "albitite" plug, is controlled by a single, anastamosing, major siliceous break quartz vein structure up to ~3 m wide and ~50 m long (e.g. 4014-63 1/2 stope and 4014-64 drift; see Figures 35 and 62) *which forms one of the main feeders for hydrothermal ore fluids to higher levels of the green*

*carbonate ore system.* This feeder vein locally contains fine visible gold and hydrothermal breccia fragments of green carbonate wallrock (Figure 62) and has been traced downwards by drilling below the 4000 ft level, where it does *not* contain economic Au mineralisation.

***(ii) Flow Ore Folding and Pinch Out (~4600 ft level)***

Below the 3200 ft level, the #21 orebody is the single remaining flow orebody, comprising highly sulphidised and silicified Fe-tholeiites which were high grade (~15-21 g/t) and entirely stoped. The Fe-tholeiites of the #21 orebody at these lower levels of the Kerr Addison mine are completely surrounded by the ultramafic unit (e.g. 3850 ft level, see Figure 23), and are thus physically isolated and possibly distinct stratigraphically from the mafic volcanics south of the Kerr Fault. From a strike length of ~450 m on the 3200 ft level, and a simple arcuate geometry (convex to the north west), the #21 flow orebody shortens with depth to ~310 m on the 4000 ft level and its geometry becomes extremely irregular. On the 3400 ft - 3700 ft levels the #21 orebody develops flexures and a folded, high grade ore (~20-25 g/t) "hook" at its west end.

On the 3700 ft and 3850 ft levels the #21 flows are greatly thickened (e.g. see tonnage figures for flow ore bodies with depth, Figure 58b) apparently due to isoclinal folding; and, a separate, detached flow orebody occurs to the south (#21 "S"; see Figures 23 and 29). The #21 "S" orebody reconnects to the main #21 flow orebody on the 4000 ft level. Below the 4000 ft level, the #21 flow orebody splits into a thinner east zone which pinches out downwards at the 4200 ft level, and a thicker west zone (~25 m width, ~130 m strike length) which plunges steeply east and shrinks to terminate in a *lithologically* defined root zone just above the 4600 ft level. This "mining root" (Kerr Addison flow ore, 4600 ft level) does not therefore correspond to the "geological root" of the system; the source of the hydrothermal ore fluids still lies at depth to the east as shown by the downward continuance of the green carbonate alteration envelope. As also noted by James et al. (1961, 1964), the west limit of

the alteration envelope, marked by the contact with the talcose ultramafics at the west end of the orebody, changes plunge from steep easterly above the 2500 ft level to shallower easterly below the 2500 ft level as the #21 flow orebody pinches out into root-like zones (Figure 29). Significant major quartz veins also occur directly underneath or in contact with the east end of the #21 orebody on the 4200 ft and 4400 ft levels (Figure 22). Thus it appears that the rising ore fluids used the structural anisotropy around the margins of the flow ore root zone to flow laterally to the west and mineralise the entire strike length of the Fe-tholeiite unit at higher levels.

*(iii) Deep (4800 ft / 5600 ft) Levels and Drilling Below the System to ~2000 m Depth*

Between 1960 and 1963 a deep exploration programme was carried out on the Kerr Addison and Chesterville properties to investigate whether further ore occurred at depth. The results were summarised in James et al. (1964). The programme consisted of lateral drifting on the 4800 ft and 5600 ft levels to both the west and east limits of the property (a total strike length of ~2.3 km along the Break). Widely spaced (every ~90 m) flat drilling was then carried out normal to the strike of the units. Drill holes across the main green carbonate alteration envelope were more closely spaced (~22 m). Figures 21 and 20 show the reconstructed geological plans for the 4800 ft and 5600 ft levels respectively, based on the flat drill hole data and some drift mapping. The footages and Au grades of quartz veins and dykes intersected by drilling on and below the 4800 ft and 5600 ft levels are listed in total in an Appendix to this paper; the data are summarised in the following sections.

**4800 ft level:** On the 4800 ft level (Figure 21), the overall green carbonate alteration envelope within the ultramafic unit has dimensions of ~450 m strike length and ~20 m average width, and is split into two parts separated by an irregular protruding "nose" of Timiskaming sediments and a screen of talcose ultramafics.

The ultramafic unit at this depth is itself quite narrow (~30-60 m) compared to its width at higher levels in the mine (up to ~150 m). In the western part of the system, despite pervasive and continuous green carbonate alteration across widths of up to ~50 m, the overall density of major (>0.3 m) quartz veins and dykes is extremely low, compared to higher levels of the system. In the east, a silicified "albitite" plug (~90 m strike length, ~10 m width; probably part of the Chesterville Plug) is intersected by a drift which contains low grade values of up to ~2.7 g/t Au.

As shown by the data in the Appendix, on the 4800 ft level there is a greater correlation between Au values and "albitite" dykes than there is with major quartz veins, probably reflecting sulphidation reactions of these higher Fe content rocks:

(i) Of a total of 14 major (~0.15 - 1.5 m) quartz vein intersections within the green carbonate envelope on the 4800 ft level, 10 assayed only trace values (<0.3 g/t Au) and the remaining 4 intersections assayed only 0.3 - 1.2 g/t Au across their widths. Three further vein intersections, outside the green carbonate envelope in a low grade mineralised zone ~100 m to the south west ("Diorite Zone", see below), also assayed <0.3 g/t Au.

(ii) A total of 48 dyke intersections were drilled by 27 holes on the 4800 ft level, comprising 24 intersections inside the green carbonate envelope, 12 in the "Diorite Zone" (mine sections 45 - 56E) which contains weak green alteration (see below) and 12 outside, but in the vicinity of, both these zones. Of the dyke intersections inside the green carbonate envelope, 22 were assayed of which 16 were mineralised at 0.3 - 2.9 g/t Au. Of the dyke intersections outside the green carbonate envelope, 18 were assayed of which 9 (including the "Diorite Zone") were mineralised between 0.3 - 4.2 g/t Au.

The "Diorite Zone" is a low grade mineralised zone (~2.1 g/t Au over >9 m width) ~100 m south-west of the main orebody on the 4800 ft and 5600 ft levels (see zone marked on 5600 ft level plan; Figure 20) and drilled to ~300 m below the 5600 ft level, hosted within and



adjacent to an elongate (>300 m strike length), mineralised, dark grey feldspar porphyry intrusion (identification based on drill core examination). Further drilling is needed to define whether the "Diorite Zone" connects upwards to a mineralised zone between the 3700 and 3850 ft levels near the bottom of the #3 shaft. All 12 of the dyke intersections in the "Diorite Zone" on the 4800 ft level (mine sections 45 - 56E) were associated with low grade Au values in the adjacent host rock, the development of massive quartz veining (up to 2.5 m wide), local green carbonate alteration of the mafic volcanic host rocks, brecciation, silicification and disseminated pyrite mineralisation.

*5600 ft level and deep drilling below the 5600 ft level:* On the 5600 ft level (Figure 20), the green carbonate alteration envelope within the ultramafic unit has shrunk longitudinally to a strike length of only ~300 m (from ~450 m), with a ~24 m average width. The ultramafic unit at this depth is again narrow (~30-50 m) and the overall density of major (>0.3 m) quartz veins and dykes within the green carbonate envelope is extremely low. There is again a greater correlation between Au values and dykes on and below the 5600 ft level than there is with major quartz veins:

(i) Of a total of 14 major (~0.15 - 1.5 m) quartz vein intersections within the green carbonate envelope on and below the 5600 ft level, 9 assayed only trace values (<0.3 g/t Au) and the remaining 5 intersections assayed only 0.3 - 1.5 g/t Au across their widths. Nine further vein intersections in the "Diorite Zone" assayed <0.3 - 0.9 g/t Au.

(ii) A total of 63 dyke intersections were drilled by 24 holes on and below the 5600 ft level, comprising 42 intersections inside the green carbonate envelope, 14 in the "Diorite Zone" (mine sections 40-48E, 60-65E, ~76E and ~88E) which contains weak green alteration (see above) and 7 outside, but in the vicinity of, both these zones. Of dyke intersections inside the green carbonate envelope, 28 were assayed of which 18 were mineralised at 0.3 - 4.3 g/t Au. Of dyke intersections outside the green carbonate envelope, 14 were assayed of which 11 (including the "Diorite Zone") showed mineralised intersections at 0.3 - 6.7 g/t Au.

In 1963, at the end of the Kerr Addison deep exploration programme, a fence of 10 deep holes was drilled below the 5600 ft level to test the nature of the main ultramafic horizon north of the Kerr Fault and the "Diorite Zone" south of the fault. These holes were angled at  $-60^{\circ}$  to  $-75^{\circ}$ , reached lengths of up to  $\sim 450$  m, and tested vertical depths of up to  $\sim 1980$  m below surface. The continuing steep eastward plunge of the green carbonate alteration envelope was confirmed, with a similar strike length ( $\sim 300$  m) at  $\sim 1900$  m depth (mine sections 71-85E) to that encountered on the 5600 ft level (mine sections 69-83E) but a greater width ( $\sim 50$  m; c.f. 24m); hence, the characteristics reconstructed for the 5600 ft level (Figure 20) appear to represent the true feeder zone for the Kerr Addison - Chesterville igneous/hydrothermal system. The most significant Au intersections ( $\sim 9$  m at 3.7 g/t Au;  $\sim 7.5$  m at 4.3 g/t Au) were at  $\sim 1920$ - $1970$  m depth at mine sections 80-82E.

Figure 63 shows a composite cross section below the 5600 ft level at mine sections 80-82E based on three deep drill holes (56-84, 56-85, 56-86). This diagram shows a  $\sim 50$  m wide green carbonate alteration zone within the ultramafic host rock which contains a silicified and Au mineralised "albitite" plug and dyke swarm; additional data show a  $\sim 300$  m strike length (see above). Significant Au values only occur in the intrusions, and not in rare quartz veins at this depth, again probably reflecting sulphidation reactions. Figure 63 also shows that there is no spatial association between hydrothermal alteration and Au values in the deep part of the system and the Kerr Fault (see below). Based on the other deep drilling data, there appear to be very few "albitite" dykes on and below the 5600 ft level on the west side of the system (e.g. mine sections 65-76E). The deep cross section at 80-82E (Figure 63), on the east side of the hydrothermal alteration envelope, thus represents the *only* part of the deep system below the 5600 ft level which has a high density of intrusions, and may in fact represent the *intrusive root zone/feeder system for the whole major eastern Chesterville Plug and the intense swarm of "albitite" dykes in the higher levels of the mine.*

## 14.2. Genetic Aspects of Deep Level Studies

Significant genetic and exploration aspects arising from the deep level studies are as follows:

(i) the entire volume of hydrothermal ore fluid which caused the quartz veining and green carbonate alteration at higher levels in the system (maximum dimensions of ~900 m length by ~45 m average width; ~1300 ft level), and the mafic "albitite" dyke swarm/intrusive plug system, must have passed upwards through the relatively small feeder zone defined by areas of green carbonate alteration containing quartz veins and "albitite" dykes on the 5600 ft level (300 m x ~25-50 m);

(ii) the concentration of "albitite" dykes and plugs in an intrusive root zone at mine sections 80-82E supports the suggestion (see above) that the source of the "albitite" intrusions at depth lies at the east side of the green carbonate alteration envelope, and that lateral feeding of intrusive material occurs from east to west at the higher levels of the system;

(iii) extremely low densities and total areas of quartz veins within still quite wide (~20-50m) zones of green carbonate alteration indicate that significant precipitation of silica (c.f. Walther and Helgeson, 1977) did not occur in vein fractures until higher levels of the Au system were reached (Figure 57);

(iv) some wide feeder quartz veins *do* occur on the 4800 ft and 5600 ft levels, but contain zero or very minor amounts of Au. In fact, quartz veins/veinlets associated with green carbonate alteration do not contain ore grade Au below the 4000 ft level (see Figure 28). This depth corresponds to the major expansion in quartz veins and "albitite" dykes (Figure 57) which starts at approximately the 4800 ft level. H<sub>2</sub>O-CO<sub>2</sub> phase separation could be an explanation for the observed phenomena of both dilation and Au precipitation (e.g. Spooner et al., 1987; Bowers, 1991), evidence for which has been found in excellent primary fluid inclusions in zoned quartz from the 4014-63½ stope (Figures 35 and 62; Channer and Spooner, 1991). *Hence, these data would suggest that H<sub>2</sub>O-CO<sub>2</sub> phase separation started*

*between the 4800 ft and 5600 ft levels since below the 5600 ft level there is no significant dimensional change.*

(v) the occurrence of Au values in "albitite" dykes rather than quartz veins at depth, both inside and outside the green carbonate envelope, indicates a strong spatial relationship between intrusions and Au-bearing hydrothermal fluids; the mafic nature of the dykes rendered them more susceptible to sulphidation reactions than the ultramafic host rock;

(vi) the occurrence of an elongate intrusion with low grade Au mineralisation at depth ("Diorite Zone"), possibly connecting upwards to a zone of higher grade mineralisation, may be genetically significant. The geochemical affinity of this intrusion to the mafic "albitite" dyke swarm has not been determined;

(vii) systematic drilling along a ~2.3 km strike length of the Break on the 4800 ft and 5600 ft levels and also further east higher up in the vicinity of the Chesterville East Zone (e.g. 2650 ft level: Figure 24) has shown that mafic "albitite" intrusions are specifically associated with zones of hydrothermal alteration and Au mineralisation along the Break and do *not* occur outside the Au systems. "Albitite" dykes have also been observed in drill core from green carbonate-altered rocks of the Armistice deposit to the west (D. Bigelow, Armistice Project Geologist; J.P.S.; pers. observations, 1990).

### **14.3. The Top**

#### ***(i) Green Carbonate Ore***

Based on data in Figures 51 to 60, and on surface observations (1989; e.g. #10 orebody glory holes), the Kerr Addison - Chesterville Au system dies out near the present land surface. Trends which show this decline are particularly clear for total quartz vein footage intersected (5 ft/1.6 m contour) and, above all, total Au produced per level which goes to zero at the 175 ft level. A vertical zonation, useful for exploration, occurs near the top of the system in the amounts present of ultramafic-hosted green carbonate alteration, quartz veins and "albitite"

dykes. On surface the distinctive green carbonate altered rocks outcrop as a series of disconnected patches (see Figure 7); the strongest patch in the west coincides with the #10 orebody glory holes. Figures 51 to 55 show that the top of the system is characterised by the closure, at different levels, of green carbonate (e.g. 100 ft/30 m), quartz vein (e.g. 5 ft/1.6m) and dyke (e.g. 10 ft/3 m) contours such that the vertical zonation is as follows:

- (i) weak green carbonate alteration, barren of significant Au and with only minor quartz veins and stringers (<0.3 m), occurs furthest vertically and distally away from the Au system; this overprints non Au-related, early talc-chlorite-carbonate alteration of the ultramafic host rock;
- (ii) medium green carbonate alteration with minor quartz veins/veinlets (less than 0.3 m width), and
- (iii) strong emerald green carbonate alteration containing major siliceous break quartz veins (>0.3 m); major quartz veins (>0.3 m) persist upwards to about the same extent as "albitite" dykes (>0.3 m), which die out more irregularly.

Both the major quartz veins and dykes become thicker and longer with increasing depth within well-defined zones of strong emerald green carbonate alteration, and the Au grade of the green carbonate ore increases downwards in the upper parts of the system.

The data show that green carbonate alteration >15 m (~50 ft) thick plus <0.3 m thick quartz veins/veinlets probably did not extend more than ~150-300 m above the present land surface at the west end of Kerr Addison. Comparison with the completely blind nature of the Chesterville East Zone green carbonate/dyke orebody strongly suggests that the system closed off and did not penetrate to the Archean paleosurface. The above findings are consistent with the early exploration history of the property (see above) in which it was quite easy to locate areas of characteristic green carbonate alteration and low grade erratic Au mineralisation, but difficult to hit consistent high grade ore and wide, major Au-quartz veins near surface (cf. discovery hole of 10.5 g/t Au over 33 m *at the 300 ft level*).

Hence, the surface green carbonate ore outcrops of the Kerr Addison discovery were characterised by (a) emerald green fuchsite-carbonate alteration with minor >0.3 m quartz veins, veinlets and stringers superimposed on earlier and non Au mineralisation-related, strained polygonal carbonate veining, (b) low grade (<5 g/t Au) and patchy Au mineralisation in channel samples, and (c) very minor "albitite" dykes; in fact, no clear "albitite" dykes were visible in the walls of the #10 orebody glory hole, although some have been recorded on the 83 ft level.

*(ii) Flow Ore*

The major #21 flow orebody appears to thin down, shorten and pinch out upwards between the 700 ft and 500 ft levels of the Kerr Addison mine (Figures 26 and 29). The #21 orebody is also cut by a south-dipping branch of the Kerr Fault on its south side (see cross section, Figure 30). Near the top of the #21 orebody (e.g. 850 ft level), the Fe-tholeiites are distinctly *less* altered than their highly silicified and pyritised equivalents at depth and the ore is distinctly lower in grade (~5 g/t Au). Discrete, irregularly curved "Hollinger-McIntyre type" milky quartz veins also appear to be characteristic of the upper parts of the #21 orebody. Small patches of flow ore (e.g. #6/#8 and #11 orebodies), located at the contact between mafic and ultramafic rocks, continue to surface just south of the #10 orebody glory holes, and were locally of quite high grade (up to ~11 g/t, see Figure 59b). South of the Kerr Fault, the #16 and Chesterville "A", "B" and "C" flow orebodies also continue to near surface.

## 15. Discussion; Exploration, Ore Controls & Genetic Aspects

### 15.1. Principal Geological / Geochemical Exploration Guides

#### *Shear Zone-Hosted*

The Kerr Addison - Chesterville Au-Ag-(W)-quartz vein/disseminated Au ore system is a prime example of a major (~332 tonnes Au) Archean Au-quartz vein deposit hosted within, and syn-deformational with respect to, a major first order ductile shear zone structure (the Larder Lake - Cadillac Break, which is ~50-150 m wide in this area), contained within a 2-3 km wide moderate to high-strain corridor. Elsewhere along the Break corridor (e.g. see Figure 1) smaller, second order shear zones and splays host many other Au systems, both large and small. It thus appears that the size of the hosting shear zone is not of particular genetic significance, except that it must be deep and large enough to tap a source of hydrothermal fluid at depth. Similarly, location of a Au deposit within the Break, to its north or to its south, does not appear to have any particular genetic significance since both large and small Au systems occur in all three categories, although mineralisation to the north is more prevalent and extends further away from the Break.

#### *Specific Orientation, Nature and Timing of Shear Zone Deformation*

Mineralisation in the Kerr Addison - Chesterville Au system was introduced syn-deformationally with respect to intense ductile fabric development in the Break deformation zone (~150 m width; strike 060°, dip 78°N). This foliation shows a strong component of flattening and a steeply east-plunging extension lineation, and is inferred to be a D<sub>2</sub> foliation, developed approximately normal to a NNW-SSE compressional event (Hamilton, 1986); no ductile fabrics post-dating D<sub>2</sub> were seen in the mine. According to Hamilton (1986), and empirical observations by other workers (e.g. Thomson, 1941; James et al., 1961; Hodgson, 1986), *D<sub>2</sub> shear zone structures, particularly where oriented E-W or ENE-WSW, are the most favourable hosts for Au mineralisation in this area, but not further east in Quebec.* D<sub>2</sub> structures developed relatively late in the structural evolution, post-dating the Timiskaming

sediments and volcanics (>2677 Ma) and late syenite intrusions in the Timiskaming (~2677 Ma). Syn-deformational "albitite" dykes at Kerr Addison are of similar geochemistry and structural setting to "albitite" dykes from the Hollinger-McIntyre mine (Timmins), dated at 2673+5/-2 Ma (Corfu et al., 1989), and may therefore place the timing of D<sub>2</sub> deformation and Au mineralisation at ~2675-2670 Ma (see Figure 4).

### ***Fe-Tholeiite Host Rocks***

~66% of the total Au at Kerr Addison (see Table 3) occurred in disseminated pyrite mineralisation ("flow ore") hosted by deformed, massive to pillowed / variolitic Fe-tholeiite flows of the Larder Lake Group. Due to its high Fe content (~17% Fe; James et al., 1961), this lithology was chemically reactive to sulphidation and readily formed pyrite (+Au). Due to its relative competence, the Fe-tholeiite host rock also fractured brittly allowing access to hydrothermal ore fluids. Of particular importance was the large #21 flow orebody, which was impressive in tonnage (13.77 million tonnes), grade (12.47 g/t Au) and total contained Au (~172 tonnes) making this type of orebody an excellent exploration target, and confirming Fe-tholeiites as a good target lithology.

### ***Green Carbonate Alteration***

Green carbonate alteration in the ultramafic host rocks has been shown to be a sensitive guide to Au mineralisation since:

- (i) underground observations show that green carbonate alteration selvages and zones are specifically related to main stage Au-quartz veins and not, for example, early barren polygonal carbonate veining, and
- (ii) the entire ore system is enclosed in a green carbonate alteration envelope.

As described above, green carbonate alteration persists further upwards and laterally than major feeder quartz veins >0.3 m in width.



### ***Major Quartz Veins***

The green carbonate ore zone is characterised by ~5-30% (see Figure 53) major quartz veins >0.3 m to ~15 m in width (Figure 37); stoped veins are typically 1-2 m wide. The green carbonate is further characterised by a high abundance of <0.3 m quartz vein networks which die out over ~2-6 m away from the major feeder vein structures into patchy green carbonate altered rock with only minor quartz stringers.

### ***Native Au and Disseminated Pyrite Mineralisation***

The bulk of main stage Au mineralisation at Kerr Addison comprises native Au in quartz-ferroan dolomite veins in the green carbonate ore and fine-grained Au in disseminated pyrite in the flow ore. A primary hydrothermal dispersion halo has also been documented up to a distance of ~200 metres away from the deposit for elements such as Hg, Au and Ag (internal mine report, Kerr Addison Mines Ltd., ca.1970; Kishida and Kerrich, 1987). Hence, anomalous Au is a good exploration guide.

### ***Ferroan dolomite***

The carbonate associated with Au mineralisation in the green carbonate ore is ferroan dolomite which can be stained blue in the standard carbonate mineralogical test, whereas the carbonate in pre-ore polygonal veins in ultramafic host rocks is magnesite/dolomite (60:40).

### ***Mafic "Albitite" Dykes***

A high frequency of pre- to syn-Au mineralisation "albitite" dykes must be regarded as very favourable since in the main Kerr Addison - Chesterville system, the Chesterville East Zone and the Armistice deposit they are closely spatially related to Au mineralisation. The main ore zone is characterised by ~5-15%, and locally up to 35% (by volume), "albitite" dykes (>0.3 m thick) averaging ~2 m and reaching up to 40 m thick in the mafic plugs. That dykes did die out upwards within the system is confirmed by observations in the walls and pillars of the #10 orebody glory hole, and in the #19 orebody open pit, which show no dykes.

***Vertical and Lateral Zonation of Quartz Veins, Dykes and Green Carbonate Alteration***

A final important exploration observation is that the Kerr Addison - Chesterville Au-quartz vein system dies off near the present erosion surface, and shows vertical and lateral zonation away from the deposit in the abundances and widths of Au-quartz veins, "albitite" dykes and alteration, particularly in the green carbonate ore (see above for precise details; Spooner et al., 1991). At Kerr Addison major Au-quartz veins ("siliceous breaks") and "albitite" dykes >0.3 m in width die out laterally and towards the surface, and pass upwards and distally into green carbonate alteration with minor quartz stringers and scattered Au values. Patchy, barren (possibly ppb Au enriched) green carbonate alteration without veins, silicification or dykes occurs further away from the deposit. At the Barber Larder Pit, such barren green carbonate alteration lies adjacent to mafic volcanic-hosted, disseminated pyrite replacement-type ores (up to 30g/t Au locally in high grade lenses; D.W.B.).

By using *in reverse* the observed statistical zonation of alteration, quartz veins and dykes, related to the known distribution and vertical interval of Au mineralisation at Kerr Addison (see Figures 78 to 80), these variables could be used as tracers when exploring along major breaks for the blind apices of Au-quartz vein systems or evaluating the depth potential of known Au-quartz vein / dyke / alteration showings (e.g. the Kakagi Lake property, near Kenora; B. Perry, Department of Geology, University of Toronto, pers. commun., 1990). *Certainly, surface showings of green carbonate alteration with quartz veins and anomalous Au values and "albitite" dykes already known in the Larder Lake area (e.g. Misema Bridge; Fernland property) should be tested at depth, using the above analogies with the Kerr Addison - Chesterville system to trace the down-plunge source of hydrothermal ore fluids.*

## 15.2. The Kerr Fault: A Late Post-Ore, Not a Major Hydrothermal Feeder Structure

The possibility of the Kerr Fault (and associated structures) acting as a major, Au-related hydrothermal feeder structure was first suggested by Baker (1944) and Baker et al. (1951, 1957) but this was not rigorously tested by relative timing observations. This theme was later repeated by Kishida and Kerrich (1984, 1987) without underground observation but based on an erroneous interpretation of symmetrical hydrothermal alteration patterns about the fault as being primary alteration-related, rather than simply *fault repetition of previously altered and mineralised rocks* (as shown below). However, observations in this study indicate that the Kerr Fault cannot be a major hydrothermal feeder structure for the following reasons:

(i) It is a 0.1 - 3 m wide fault zone with cataclasis (e.g. Figure 64) and local carbonate veinlets, which cuts and fragments previously mineralised lithologies e.g. quartz veins (as was recognised by Baker, 1944; Baker et al., 1951, 1957) and disseminated pyrite-mineralised flow ore. The fault may *in part* use previous structures (see above);

(ii) The Kerr Fault is *not* defined by a major high temperature quartz vein structure (e.g. Figure 64) with mineralisation and related alteration, as are the "siliceous breaks" in the green carbonate ore. The fault only very locally contains mineable material where it cuts and entrains previously mineralised rocks; this relationship is particularly well shown in the deep level studies (4800 ft and 5600 ft levels; see Section 14 above) where the Kerr Fault lies well to the south and is not correlated at all with the hydrothermal feeder quartz vein/green carbonate root zone to the Au ore system; and

(iii) The Kerr Fault cuts and significantly displaces part of the #21 flow orebody (see Figure 39). Based on restoration of the geometries of the #21, #6-8 and #16 orebodies, movement on the fault appears to have been sinistral, reverse (north-side-up) with a vertical component of displacement of ~270 m and a ~45°E plunging slip-vector. Possible anti-clockwise

rotation on the Kerr Fault about a hinge further to the west has been inferred by some authors (e.g. James et al., 1961; Downes, 1980, 1981) based on the easterly rake of the down-faulted #16 orebody which contrasts with the near-vertical rake of the #21 orebody.

Hence, the Kerr Fault is clearly a post-ore structure which partly uses earlier structures and in which there has been minor fluid flow as shown by carbonate veinlets. Some solution/redeposition of primary main stage Au mineralisation is evident from visible gold plated on thin graphitic slips. Instead, as geological observations readily show, the major hydrothermal fluid flow structures were the locally stoped siliceous break veins with which large scale green carbonate alteration is associated. These structures are impressive because of their vertical (up to ~700 m; see Figure 30) and lateral dimensions (10's to 100's of metres; see Figures 23 to 27), their locally high grade Au and, particularly, their widths which average ~0.62 m (for veins >0.3 m wide). ~10,500 quartz vein intersections >0.3 m wide have been measured from mine drill core data in this study; many are in the 2-11 m width range.

### **15.3. Principal Macroscopic Ore Controls**

#### ***Controls on the General Location and Geometry of the Au System***

The Kerr Addison - Chesterville Au-quartz vein system is confined entirely within the ~150 m wide high strain core of the Larder Lake - Cadillac Break zone, and has extremely long down-plunge continuity and strike length relative to its width. The Break is localised along a laterally extensive horizon of altered ultramafic komatiite flows and fine-grained sediments to the north, in which ductile flattening foliation is particularly strongly developed. The strike orientation of the Break at Kerr Addison is perpendicular to the inferred NNW-SSE compression direction of D<sub>2</sub> deformation syn-kinematic to the Au mineralisation event (Hamilton, 1986). The ore system is localised within and adjacent to an exceptionally thick (up to ~150 m wide) lens of these ultramafic rocks, narrowing or pinched out both west of Kerr Addison and east of the Chesterville mine. This incompetent ultramafic lens was a

particularly favourable site for access of mafic "albitite" intrusions and hydrothermal fluids from depth. A geochemically anomalous alteration halo, but as yet no significant mineralisation, occurs north of the contact between ultramafic and Timiskaming sediments at Kerr Addison.

Longitudinal sections (Figure 28) show that the ultramafic-hosted part of the Au system, bounded by the green carbonate alteration envelope, plunges on average  $\sim 70^\circ\text{E}$  to a deep ( $\geq 4$  km) focal fluid source. This plunge is sub-parallel to a steep east-plunging S-shaped fold hinge on the Chesterville property, and an  $S_2$  elongation lineation noted to occur in the vicinity of the Break (Buffam and Allen, 1948; Hamilton, 1986; Jackson, 1988), though no direct link with these structures has been established. The flow ores (after restoration of displacement across the Kerr Fault) coincide longitudinally with the green carbonate alteration envelope, though are slightly asymmetric to its west (Figure 29).

As described above, most of the ore occurs on the south side of the deposit, close to the present footwall of the north-dipping ultramafic unit and within the adjacent Fe-tholeiitic flows (Figure 30). Elsewhere along the Break to the west (e.g. the Cheminis and Omega mines; Thomson, 1941; Jenney, 1941; Clark and Bonnar, 1987), ore is also concentrated on the south side of the Break, but in its hanging wall due to its south dip. At Kerr Addison, the structural anisotropy of the #21 flow ore unit may have acted to localise strain and create dilatancy and veining in the adjacent green carbonate ore. This may explain the similar longitudinal distribution profiles of both ore types, particularly near their bases (e.g. 4000 ft to 3250 ft levels; Figures 28 and 29). The Chesterville East Zone is a separate (see 2650 ft level plan; Figure 24), blind, green carbonate/"albitite" dyke orebody within the main Break ultramafic unit, which appears to plunge sub-parallel to the main Kerr Addison - Chesterville system, as constrained by available drill data (Figure 28).

### ***Controls on Green Carbonate Ore***

The green carbonate alteration envelope exhibits a flat, funnel-shaped geometry, expanding upwards in average width (x2), strike length (x3) and total area (x6) relative to its dimensions on the 5600 ft level (Figure 56). The distribution of green carbonate ore within the ultramafic unit is controlled primarily by development of a mineralised, anastomosing fault/quartz vein framework which connects upwards through the entire ore deposit, but does not extend into the barren talc "horses". The faults are marked by extremely subtle, ductilely-deformed, <30 cm wide "cherty siliceous breaks" (vein stage #3, Figures 32 and 33c) which host minor visible gold, but are of subsidiary importance to the main stage Au vein event. The fault structures acted as stress guides to main stage Au-quartz vein dilatancy and formed feeders which controlled the supply of ore fluids from depth. The "cherty siliceous breaks" are cross-cut and massively dilated by main stage milky Au-quartz-carbonate veins which occupy pinch and swell zones of dilatancy along, and branching between, the fault structures.

Stoped green carbonate ore corresponds to the greatest density of "siliceous" Au-quartz veins (e.g. Figures 16 and 35) and abundant "albitite" dykes, both of which have 70-90° N or S dips, generally strike at a low angle ( $\pm 30^\circ$ ) to the Break and are co-structural with each other. There is occasionally a spatial association between high strain zones and green carbonate ore development; however, major vein structures generally cut across heterogeneously deformed host rocks, although minor veins exhibit more systematically controlled orientations in foliated rocks (e.g. 3214-65 sill). Barren talc "horses" may contain extremely deformed and schistose rocks, yet they have a noted absence of quartz veins, and very few dykes.

Main stage Au mineralisation in the green carbonate ore is interpreted to represent a relatively short, fluid-generated hydraulic fracturing event within the overall longer time-span of ductile deformation on the Larder Lake - Cadillac Break (Figures 4 and 32). The distribution of relatively more competent, early (grey/brown) chlorite-quartz-carbonate metasomatism in the ultramafics, compared with the softer talc-chlorite-carbonate assem-

blage, may have been a major primary control on the subsequent localisation of Au mineralisation.

***Green Carbonate "Root Zone" and Below the Deposit:***

The entire stoped green carbonate/"albitite" dyke ore system shrinks down to three narrow "root zones" on the 4000 ft level within an overall green carbonate alteration envelope which itself expands upwards six times in area from the 5600 ft level (~1750 m). Two of the root zones occur in major plugs near the west and east boundaries of the alteration envelope. The principal, central root zone (dimensions of ~10x50 m; see above) is controlled by major "siliceous break" vein structures and is "V"-shaped in longitudinal section (see Figure 28). The initiation of Au mineralisation in the root zone of the green carbonate ore was shown (see above) to coincide with a rapid expansion in the area of quartz veining over the same short vertical interval, since feeder quartz veins are still present at depth but become less frequent, narrower and carry increasingly low to zero gold values. It thus appears that depth, equivalent to a lithostatic pressure "threshold" value, is an important factor controlling the development and maintenance of an open vein fracture system in which hydrothermal ore fluids can flow, expand and precipitate Au (originally suggested by James et al., 1961).

The Kerr Addison - Chesterville hydrothermal Au-quartz vein system converges with depth on the major Chesterville Plug, which occurs at the east boundary of the alteration envelope and extends from ~180 m depth to well below the deposit (e.g. 4800 ft level, Figure 21; 1920-1980 m below surface, Figure 63). Significantly, this plug is the *only* unit to be ore-grade mineralised (e.g. ~6.2 g/t Au over 9 m at ~1950 m depth) below the limit of stoped green carbonate ore at the 4000 ft level (~1250 m). The green carbonate alteration package is continuous at depth where it is wide relative to the extent of remaining quartz veins.

### ***Lateral Controls on Green Carbonate Ore***

The more rapid increase (x3) upwards in the strike length of the green carbonate alteration envelope compared to its average width (x2; Figure 56) is probably due to the preferential expansion and flow of rising hydrothermal fluids along cherty "siliceous" fault structures which are sub-parallel or at a low angle ( $\pm 30^\circ$ ) to the Break foliation. Fluids are also observed to penetrate the ultramafic host rock locally along foliation planes. In the higher levels (e.g. 1750 ft level; see Figure 25) of the Kerr mine, the western downward decrease in green carbonate alteration is directly related to the narrowing and even pinching out of the host ultramafic unit. Lower down in the west, and along the whole east margin of the system (e.g. 2650 ft levels and below; see Figures 20 to 24), the green carbonate alteration *dies out naturally and is surrounded by unaltered talcose host rocks within a still wide zone of the ultramafic rocks.*

### ***Top of the Green Carbonate***

As described above, the Kerr Addison - Chesterville igneous / hydrothermal system starts to die out naturally near the present erosion surface, without any loss of the ultramafic horizon which in fact is thicker than average. The most significant decrease in the occurrence of green carbonate alteration, Au mineralisation, quartz veins and "albitite" dykes occurs at the east end of the system, where these become extremely patchily distributed and barely reach the surface. An extensive "cap" of unaltered, barren precursor talc-carbonate rocks overlies the upper reaches of green carbonate ore at the east end (e.g. 175 ft level; Figure 27). However, widespread green carbonate alteration and quartz veining ( $\pm$  dykes) are observed to occur at the west end of the deposit, which was mined through to surface as the #10 orebody glory holes. These observations indicate a markedly asymmetric concentration of fluid throughflow towards the west end near surface. The decrease in grade near surface of the green carbonate ore must indicate a progressive upwards depletion in Au of the hydrothermal ore fluids (due to Au precipitation in veins lower down in the system). In conclusion, the principal control on the top of the system is the upward extent of hydraulic fracturing.



### *Controls on Flow Ore*

Flow ore is best exemplified by the major tonnage, high grade #21 orebody (13.77 million tonnes at 12.47 g/t Au), hosted by a single mafic volcanic unit which was almost entirely stoped. Particularly at depth, the #21 flows form a physically isolated inclusion of mafic volcanics within ultramafic to transitional flows, and their precise stratigraphic correlation with the mafic volcanics south of the Kerr Fault is not certain. The distribution of flow ore is thus largely controlled by the geometry of the host mafic volcanics which form a tabular unit, V-shaped in longitudinal section and tapering to a root, with maximum strike length at its higher levels. The #21 orebody was formerly continuous with the #6, #8 and #16 orebodies, prior to displacement across the post-ore, graphitic Kerr Fault (Figure 39). The #21 flow ore unit pinches and swells in width, shows open flexures, and is occasionally necked down along strike and detached into boudins. This may be due to either ductile deformation or primary interdigitation with the surrounding lithologies.

Stoped flow ore corresponds to the greatest intensity of vein fractures with associated intense disseminated pyrite (+Au) mineralisation, silification and carbonate alteration. Some more extensive, discrete Au-quartz veins were also stoped individually (e.g. part of 1117-63 stope). Several local lithological controls on the development of Au mineralisation in the flow ore have been delineated (see above) e.g. the presence of tuffs/sedimentary layers, pillowed/variolitic horizons, early Au-related alteration and competency change, intercalated graphitic lenses, proximity to the Kerr Fault, and diffusion of fluids along an existing foliation. A spatial association may exist between high strain zones and flow ore development within the Fe-tholeiite host rocks, but access has not been sufficient to test this relationship more rigorously. Main stage Au-mineralisation in the flow ore was introduced syn-deformationally relative to ductile fabric development.

Available evidence indicates that the #21 Fe-tholeiite flows may have acted as a more competent structural unit within the softer ultramafic and transitional host rocks. Wide quartz veins and intense silification occur at the north and south margins of the #21 orebody, connected to quartz veining in the interior. The controls on flow ore distribution are thus : (i) proximity to fluid supply within the green carbonate alteration envelope in the adjacent ultramafic rocks; (ii) primary lithological, due to the geometry of the host Fe-tholeiite unit (possibly that of an original pillowed volcanic pile) modified by a structural overprint (boudinage, folding, flexures); (iii) structural: competency contrast during ductile deformation which resulted in increased dilatancy, veining and fluid flow particularly at the margins of the #21 orebody.

***Flow Ore at Depth: Isoclinal Folding and "Root Zone" Pinch Out***

With increasing depth below the 3250 ft level, the #21 flow lithology recedes and shortens from both ends, and develops a prominent, curved "hook" at its west end. Between the 3700 ft and 4000 ft levels, the #21 flow lithology is isoclinally folded and thickened, and a separate #21 "S" orebody appears to the south. Below this, the favourable flow lithology tapers down into two zones which pinch out completely just above the 4600 ft level. Thus the "mining root" (Kerr Addison flow ore; ~4600 ft) does not correspond to the "geological root" of the system; the source of the hydrothermal ore fluids still lies at depth to the east within the green carbonate alteration envelope. Flow ore grade is highest (~20 g/t Au) at the ~3850 ft level, due to intense wallrock sulphidation and initial precipitation of Au from hydrothermal solutions where the fluids first hit and interacted with the Fe-rich flow lithology. That this point of highest grade flow ore is some ~700 ft above its pinch out at the 4600 ft level may indicate that the fluids did not come up the Fe-tholeiite root exactly, but instead entered the flow ore lithologies laterally from the east at some point *above* the Fe-tholeiite root. This suggestion is in agreement with the observational evidence cited above.

### ***Lateral Controls on Flow Ore***

To the east and downwards the flow ore pinches out stratigraphically or structurally with a relatively blunt termination. To the west, on the lower levels below the 2650 ft level, it also pinches out in a similar fashion, but above the 2650 ft level the flow ore (#6 orebody) dies out laterally into barren mafic flows (Figure 29). This decline is due to increasing distance laterally away from the main focus of fluid flow in the adjacent green carbonate alteration envelope, itself apparently limited by the extent and thickness of the favourable ultramafic horizon. Between the 2650 ft and 1750 ft levels, a large gap or "hole" in flow ore longitudinal distribution between the #21 and #6 orebodies (Figure 29) is due to a complete absence of the mafic #21-#6 horizon, caused either by boudinage or a primary lithology (flow) distribution. Above the 1750 ft level, an even larger "hole" is due to offset of the intervening portion, downthrown as the #16 orebody by the Kerr Fault (Figure 39).

### ***Top of the Flow Ore***

At its west end, the #21 flow orebody is cut and terminated at its top by a south-dipping branch off the Kerr Fault. At its east end, the #21 orebody appears to thin and pinch out stratigraphically upwards in a similar fashion to its lateral termination, before being cut on its south side by the fault. The #8 orebody continues to near surface, south of the glory holes, as a small mineralised zone at the mafic/ultramafic contact. The #8 orebody is cut at its west end near surface by the Armistice Cross Fault (Figure 29). Grades in the #21 and #16 orebodies generally decrease upwards, probably reflecting a depletion of the hydrothermal fluids in Au (due to its precipitation) upwards. However, both the #8 and #16 orebodies show a near surface reversal in this trend, with grade actually *increasing* upwards. This may have been due to quartz vein-controlled fluid channelling or more selective mining.

## 15.4. Evidence for Au Precipitation Mechanisms

### *Flow Ore*

Observational and geochemical evidence suggests that Au mineralisation in the flow ore is controlled by a sulphidation reaction mechanism (e.g. Phillips et al., 1984) between hydrothermal ore fluids and the Fe-tholeiite wallrock. This interpretation is based on:

(i) the principal line of evidence is that the bulk (>95%) of Au mineralisation is associated with dispersed pyrite in the wallrock, and not commonly as native Au in quartz veins as observed in the green carbonate ore. Flow ore grade can be visually estimated from the amount of fine disseminated pyrite present - the Au occurs as small (~4 m) inclusions in the pyrite;

(ii) very high grades occur at depth where the hydrothermal ore fluids initially reacted with the Fe-tholeiite volcanics, followed by a steady upward decrease in grade, probably due to upward depletion of the fluids in Au due to its precipitation; although tonnages of flow ore increase upwards towards the mid levels, total contained Au *decreases* since it is more strongly controlled by the grade decrease;

(iii) geochemical studies (e.g. Kishida and Kerrich, 1987) have demonstrated strong flow ore enrichments in S, Na, SiO<sub>2</sub> and CO<sub>2</sub> (pyrite-albite-quartz-carbonate).

The sulphidation mechanism works (e.g. Phillips et al., 1984) by interaction of hydrothermal fluids with wallrock minerals (e.g. magnetite, chlorite, biotite) resulting in dissolution of Fe. The sulphur species in the fluid then react with the Fe such that the solubility of FeS<sub>2</sub> is exceeded and pyrite is precipitated. The removal of sulphur from solution results in the destabilisation of the Au(HS)<sub>2</sub><sup>-</sup> ligand species suggested to be the predominant carrier of Au under the conditions of P, T, fO<sub>2</sub>, fS<sub>2</sub> and pH inferred from studied Au deposits (e.g. Seward, 1973; Renders and Seward, 1989; Shenberger and Barnes, 1989), and co-precipitation of Au within the pyrite. Another reason for the increase in grade of the flow ore with depth may be the narrowing of the #21 flow ore unit with depth and a thinning of the transitional mafic/

ultramafic unit. This, together with more focused fluid flow, would result in exposure of the host Fe-tholeiite flows to greater integrated fluid/rock ratios, thus explaining their more advanced silification and abundant disseminated pyrite-hosted Au mineralisation.

### ***"Albitite" Ore***

The occurrence of vein/alteration-related, dispersed pyrite Au mineralisation within altered mafic "albitite" dykes and plugs suggests a mechanism of sulphidation similar to that inferred for the flow ore (see above). Thin section examination (J.P.S.) has confirmed that Au occurs as small inclusions both in the cores and rims of pyrite crystals. The pyrite overgrows foliation surfaces but itself may be slightly deformed and wrapped by the foliation; Au mineralisation is thus late syn-deformational relative to fabric development in the "albitite" dykes. Like the flow ore, the highest grades of "albitite" ore also appear to occur at depth. In fact, "albitite" ore stopes occurred on and above the 3850 ft level, associated with pervasive silicification within mafic "albitite" plugs, but with relatively minor quartz veining.

### ***Green Carbonate Ore***

Main stage Au-quartz vein style and geometry in green carbonate ore is characterised by mutually open-intersected irregular vein orientations. Hydraulic brecciation and intense stockwork veining often occur preferentially on one side (e.g. hanging wall) of "siliceous break" structures or at their intersections. These features may be a consequence of high fluid pressure and volumetric fluid inflation of the host rock. Several lines of evidence suggest that fluid supply and native Au deposition in the green carbonate ore may have been controlled by H<sub>2</sub>O-CO<sub>2</sub> phase separation (Drummond and Ohmoto, 1985; Spooner et al., 1987a; Bowers, 1991) as a mechanism:

(i) Zonally distributed, primary fluid inclusions from the main feeder quartz vein structure on the 4000 ft level indicate H<sub>2</sub>O-CO<sub>2</sub> phase separation (Channer and Spooner, 1991) above the inferred depth of initiation of H<sub>2</sub>O-CO<sub>2</sub> phase separation (4800 - 5600 ft levels; see above).

(ii) Green carbonate alteration expands dramatically in area upwards (x5 between the 4800 ft and 2950 ft levels) coinciding with the onset of economic Au mineralisation at the 4000 ft level; stoped ore in the #14 orebody also expands upwards from a narrow (50x10 m) root zone on the 4000 ft level, controlled by major "siliceous break" vein structures.

(iii) Individual quartz veins are zoned with initial precipitation of carbonate at vein margins (see Spooner et al., 1987a).

(iv) Green carbonate ore only contains trace amounts of pyrite in veins and wallrock alteration assemblages; thus sulphidation was not an important mechanism of Au precipitation in this ore type.

(v) Quartz veins are most abundant and grades are highest (~10.3 g/t Au) at mid-levels (between ~1750-2650 ft levels), decreasing both downwards and upwards.

(vi) Tonnage and total Au per mine level in the green carbonate ore steadily increase upwards from the base (Figures 58a and 58c, 60a and 60c).

The expansion that H<sub>2</sub>O-CO<sub>2</sub> phase separation generates could also explain the high fluid pressure structures, volumetric fluid inflation and geometric features noted above (e.g. Spooner et al., 1987a,b). The main control on ore is thus interpreted to be synkinematic H<sub>2</sub>O-CO<sub>2</sub> phase separation which produced volumetric inflation and subsequent Au deposition. The Au grade profiles and quartz vein area variations with depth may thus be due to:

(a) a threshold confining pressure requirement for initiation of phase separation between the ~4800 ft and 5600 ft levels and economic Au deposition above the ~4000 ft level, and

(b) depletion of fluids in dissolved Au (due to efficient Au precipitation) as they pass upwards through the system (e.g. Brown, 1986).

*Hence, Kerr Addison shows an excellent contrast between a chemically active (Fe tholeiite) and a chemically inactive (ultramafic komatiite) host rock to Au mineralisation. It is evident that the most important single factor to form a large Au deposit of this type is the adequate, focused supply of Au-bearing hydrothermal fluid; almost, but not quite a truism. The structures and lithologies present simply control the styles and grades of Au mineralisation, and not whether there are orebodies present or not; it is likely that they are secondary manifestations. If large amounts of Au-bearing hydrothermal fluids are produced, it is likely that an ore deposit will be formed somehow, unless the mineralisation is too dispersed in space or time.*

#### **15.5. Discussion of the "Fault Valve" Model**

A theory has been put forward (e.g. Sibson et al., 1988; Sibson, 1991) which attempts to explain some of the features of Archean Au-quartz vein systems, namely:

- (i) many Au deposits are localised along high angle reverse shear zones;
- (ii) Au deposits exhibit mixed brittle-ductile styles of deformation (e.g. ductile deformation zones; brittle vein fractures);
- (iii) Au deposits have considerable (>2 km) down-plunge vertical extents;
- (iv) steep fault-parallel and flat veins sometimes occur (e.g. Sigma Mine, Val d'Or, Quebec) with incremental, cyclic depositional textures.

The basis of the model is as follows:

- (i) reverse faults are unfavourably oriented structures which must have developed by reactivation of existing structures (e.g. steepened, initially thrust-sense shear zones);
- (ii) slip conditions dictate that reactivation of reverse faults in a compressive stress regime can only occur where fluid pressure exceeds the lithostatic load;

(iii) modern earthquake ruptures along large through-going faults (e.g. San Andreas Fault) nucleate at the base of the seismogenic zone (~10-15 km depth) and propagate up-dip. Some ruptures may also penetrate downwards. Discharges of meteoric water have been observed from fault zones following earthquakes;

(iv) pre-failure, the relative impermeability of the seismogenic zone allows metamorphic fluid pressure to build up with the incremental opening of flat veins;

(v) seismogenic fault failure creates fracture permeability within the rupture zone allowing sudden draining of the geo-pressurised fluid reservoir at depth; the fault thus acts as a *valve*;

(vi) hydrothermal deposition and self sealing leads to a re-accumulation of fluid pressure and repetition of the cycle.

*The model thus predicts large cyclic fluctuations in fluid pressure (of several hundred bars) between lithostatic and hydrostatic, and the common occurrence of flat veins particularly near the bottoms of Au systems.*

Several lines of evidence argue *against* the applicability of the fault valve model (e.g. Sibson et al., 1988, Sibson 1990) to the genesis of the Kerr Addison - Chesterville Archean Au system, however. These are as follows:

(i) There was no major, through-going controlling "fault". The controlling structures in the green carbonate ore are the relatively small "cherty siliceous breaks" which branch laterally to form a framework and die out, the main stage "siliceous break"/Au-quartz vein system, and the ductile Break deformation characterised principally by ~5:5:1 flattening, not relative displacement.

(ii) By analogy with the blind Chesterville East Zone, and based on the longitudinal contour diagrams (Figures 51 to 55) which show that the Au system starts to close off near surface,



it appears that the Kerr Addison - Chesterville orebody could *not* have been significantly connected to a near surface hydrostatic pressure regime.

(iii) Abundant evidence exists in the mine for volumetric fluid inflation of the host rock in the form of steep hydraulic vein fractures terminating in wedge-like spurs (e.g. Figures 40c and d; c.f. Beach, 1980; Wood et al., 1986). There are no significant flat veins at the base of (or even below) the Kerr Addison-Chesterville Au system, the root zone of which is so well exposed. Fluid overpressuring (supra-lithostatic) is also evident from hydrothermal vein breccias, open stockworks, and vein "breakout" structures (Figures 15c and 15d).

Also, very importantly, the "fault valve" model implies seismogenic fault rupture, but at Kerr Addison:

(i) Host rock deformation (which is largely flattening) is ductile, not brittle involving successive failure increments;

(ii) The controlling "cherty siliceous break" structures show only minor fault offsets, and main stage Au-quartz veins appear to be simple fluid dilational openings. Thus there is *no evidence* for control by a single major fault involving systematic displacement - only brittle/ductile shears within a wider zone of ductile deformation. This observation is supported by other observations at Lamaque, Hollinger-McIntyre and Renabie (Wood et al., 1986a,b; Spooner et al., 1987a,b; Callan, 1988; Callan and Spooner, 1989; Burrows and Spooner, 1989; Burrows 1991).

Hence, the evidence at Kerr Addison shows that a fault valve model is in fact *not* applicable and that the features can be much more easily explained by a simple fluid inflation model (Spooner et al., 1987a,b). In such a model, a deep fluid hydraulically fractures its way up from a narrow root zone, aided by H<sub>2</sub>O-CO<sub>2</sub> phase separation. Thus fluids may have played a much more active role in generating fractures than has usually been appreciated. The

brittle appearance of the dilational veins may thus be a function of high fluid pressure and not superimposed tectonic stresses.

The generation of high fluid pressure at Kerr Addison, suggested by the expansion of its entire green carbonate ore system from a single root zone vein structure, may be explained by:

- (i) irreversible fluid release from a crystallising deep parent magmatic source (see below);
- (ii) H<sub>2</sub>O-CO<sub>2</sub> phase separation (Channer and Spooner, 1991) and expansion;
- (iii) pressure communication with the swarm of "albitite" dykes which were intruded concurrently with multi-stage Au mineralisation; dykes die off in an identical fashion to the Au-quartz veins near surface (see below; Figure 57).

The multi-stage nature of Au mineralisation at Kerr Addison (four vein stages host primary Au; see Figure 32) may be linked to repeated episodes of "albitite" dyke and hydrothermal ore fluid release from a deep parent magma, and may not be due to "fault valving". The two rival hypotheses may be tested using fluid inclusion pressure estimate data. The fluid inflation model of Spooner et al. (1987 a,b) predicts that due to vein fracture crack-tip oscillation, pressure fluctuations in typical Au veins will be  $\leq \pm 70$  bars, compared to fluctuations of *several hundred bars* predicted in Sibson et al. (1988) and Sibson's (1990) "fault valve model".

#### **15.6. Discussion: Relevance of "Young" U-Pb Rutile Ages**

With respect to "young" (~2580-2630 Ma) U-Pb rutile dates recently obtained from Archean Au deposits in the Superior Province by Jemielita et al. (1990 a,b) and Wong et al. (1989, 1991), the argument here is as follows: Geological observations (listed above) indicate that Au mineralisation at Kerr Addison is significantly intra-dyke emplacement in relative timing (Figure 32). "Albitite" dykes are also co-spatial and co-structural with main stage

Au-quartz veins in the green carbonate ore, and both veins and dykes show similar initial areal expansions upwards from root zones, approximately constant areas at mid-levels, and areal decreases towards surface (Figure 57). Other workers (see summaries by Corfu et al., 1989, 1991; Colvine et al., 1988) have shown that Au mineralisation is one of the latest events in the Archean geochronological time sequence. The youngest Archean U-Pb zircon/monazite date in the Abitibi so far, apart from dates on the Preissac-Lacorne batholith, was obtained from a Hollinger-McIntyre "albitite" dyke of very similar geochemistry to the Kerr Addison "albitites" (Smith and Spooner, in prep) at  $2673 \pm 5/2$  Ma (Corfu et al., 1989). According to the data presented in this paper, Au mineralisation is related to a mafic "albitite" dyke/plug intrusion system and highly *unlikely* to be younger than ~2675-2670 Ma in age (see Figure 4). A Kerr Addison hydrothermal U-Pb rutile date of ~2580 Ma (~90 Ma younger than the "albitite" dyke age at Hollinger-McIntyre) obtained by Jemielita et al. (1990 a,b) is therefore highly unlikely to be related to primary Au mineralisation, but may instead represent a cooling/closure age or a later fluid overprint (these hypotheses can be tested). In fact such an overprint is seen at Kerr Addison (#6 to #8 vein stages; some Au remobilisation).

Hence other "young" U-Pb rutile dates are of no proven relevance to Archean Au-quartz vein mineralisation, in agreement with Spooner (1991a,b) citing other reasons. Two further arguments in Jemielita et al. (1990 a,b) are also invalid for the following reasons:

(i) the argument that agreement among different isotopic systems (U-Pb rutile;<sup>40</sup>Ar-<sup>39</sup>Ar mica; Sm-Nd scheelite) at the Sigma mine, Val d'Or indicates the age of Au mineralisation. This is invalid since by definition <sup>40</sup>Ar-<sup>39</sup>Ar ages record *closure* of the K-Ar isotopic system, thus the similar range of ages obtained by U-Pb rutile (~2580-2630 Ma) and <sup>40</sup>Ar-<sup>39</sup>Ar mica (e.g.  $2579 \pm 3$  Ma; Wong et al., 1989) dating methods could be used to argue the opposite - that the U-Pb rutile dates are *also* closure ages. In fact, Mezger et al. (1989) have shown experimentally that fine-grained rutile has comparable U-Pb retention characteristics to those for Ar in micas and that a similar range of closure ages would be expected.

(ii) Arguments involving difference from older metamorphic rutile. These assume that metamorphic and hydrothermal alteration rutile have the same U-Pb retention characteristics and thermal/fluid histories, assumptions which are not necessarily true and have not been proven. In summary, the U-Pb rutile dates have not been shown to be other than *minima* (cf. Spooner, 1991a,b).

### **15.7. Comparison with Archean Au-Quartz Vein Systems in the Timmins - Val d'Or Area** ***Similarities***

The Kerr Addison - Chesterville Au-quartz vein system shows many similarities to other Archean Au-quartz vein systems in the Timmins - Val d'Or area, for example:

(i) Shear zone-hosted, syn-deformational; it is confined within a high strain zone, Au-quartz veins being formed syn-deformationally with respect to ductile fabric development;

(ii) Relatively late structural timing; in the Kerr Addison area, post- regional folding of lithological units, including the Timiskaming, post-  $D_1$  thrusting, syn-  $D_2$  localised shear zone deformation (predominantly flattening; Hamilton, 1986);

(iii) Ore types; the Kerr flow ore is very similar in style, for example, to Hollinger-McIntyre and other smaller disseminated pyritic/vein Au deposits hosted by Fe-tholeiite volcanics. The graphitic ore is directly analogous to Au mineralisation in the Owl Creek and Hoyle Pond deposits in the Timmins area (e.g. Wilson & Rucklidge, 1986, 1987a,b). "Albitite" ore was stoped at depth in the McIntyre mine, Timmins (c.f. Wood et al., 1986a,b);

(iv) Mineral association; at Kerr: quartz-ferroan dolomite-pyrite-scheelite-tetrahedrite-galena-sphalerite-arsenopyrite (e.g. Thomson, E., 1941). Kerr Addison is, however, quite low in base metal sulphides, tellurides and tourmaline (observed in only one location), and has an unusually high average Au:Ag ratio of ~18:1; these may be characteristics of this particular local area;

(v) Dilatory quartz vein systems, with hydraulic spurs, coarse crack-seal textures and hydraulic breccias (cf. Renabie, Hollinger-McIntyre, Lamaque), and major Au-quartz vein guide structures (cf. Sigma);

(vi) Occurrence of mafic "albitite" dykes of very similar geochemistry to those seen in another large Archean Au system, Hollinger-McIntyre (~995 tonnes Au), spatially related to the ore system in both deposits; intrusions similar in appearance and spatially related to Au mineralisation have also been reported from the Astoria and Francoeur deposits near Rouyn, Quebec (e.g. Couture et al., 1990);

(vii) The Au-quartz vein system narrows down to a thin root zone controlled by relatively few, but large, veins as is also seen at Hollinger-McIntyre, Lamaque and Renabie; in fact, the Kerr Addison root zone is the *best* example seen to date;

(viii) Economic Au mineralisation extends over a significant vertical interval of ~1,400 m; other major Archean Au-quartz vein systems also show deep vertical continuities (Spooner et al., 1987b) e.g. Kolar, India (~3,300 m), Kirkland Lake, N. Ontario (~2,500 m) and Hollinger-McIntyre (~2,400 m);

(ix) Alteration assemblage, ore geochemistry and stable isotope ratios; studies by Kerrich (1983) and Kishida & Kerrich (1987) have confirmed that Au mineralisation at Kerr Addison shows similar elemental enrichments and inferred hydrothermal fluid properties (H<sub>2</sub>O-CO<sub>2</sub> fluids) as other Archean Au deposits.  $\delta^{18}\text{O}$  values for co-existing mineral pairs indicate temperatures of ore formation of ~300-350 °C (Kishida and Kerrich, 1987);

(x) hydrothermal ore fluids; a preliminary study by Channer and Spooner (1991) revealed typical Archean Au dilute NaCl, CO<sub>2</sub>-rich primary fluid inclusions, with a pure CO<sub>2</sub> component, undergoing H<sub>2</sub>O-CO<sub>2</sub> phase separation at temperatures up to ~330°C.

### ***Distinctive Aspects***

The Kerr Addison - Chesterville Au-quartz vein system shows the following distinctive aspects compared to most other Archean Au deposits:

- (i) Size (332 tones Au, Canada's fifth largest Archean Au-quartz vein system).
- (ii) Hosted by a major first order ductile structure, the Larder Lake - Cadillac Break (>300 km strike length, up to ~500 m wide), in common with a number of smaller deposits in a ~70 km segment of the Break from McBean (near Dobie, N.E. Ontario) to Astoria (south of Rouyn, N.W. Quebec), including the McBean, Omega, Cheminis, Fernland, Barber Larder, Armistice, McWatters and Astoria deposits. However, some Au mineralisation does occur on sub-parallel structures up to ~400 m south of Kerr Addison in the Larder Lake Group.
- (iii) Ultramafic-hosted "green carbonate ore"; the green carbonate ore at Kerr Addison (15.0 mtonnes at 7.8 g/tAu) is probably the finest known example of *ultramafic*-hosted Au-quartz vein mineralisation. Other, smaller examples of green carbonate ore include the Omega, Cheminis and Armistice deposits on the Larder Lake - Cadillac Break, and the St. Andrews Goldfields Ltd. Stock Township project on the Destor-Porcupine Break; green carbonate ore also occurs in the Barberton greenstone belt, South Africa (e.g. de Ronde, 1991);
- (iv) The intensity of the mafic "albitite" dyke swarm/plug system, and particularly the fact that dykes are closely spatially related to Au mineralisation right up through the mine; the latter relationship is very distinctive of the Kerr Addison - Chesterville system which is one of the finest known examples of this relationship;
- (v) Mafic "albitite" dyke/Au mineralisation cross-cutting relationships; although mafic "albitite" intrusions have been reported spatially related to Au mineralisation in other mines (e.g. Hollinger-McIntyre), dyke/dyke/Au mineralisation cross-cutting relationships at Kerr Addison are the first of their kind to be reported in the Abitibi greenstone belt, and thus significantly increase the genetic significance of these "albitite" dykes in other mines.

## 15.8. Overall Genetic Aspects & Significance of the Kerr Addison "Albitites"

### (i) *Confirmation of General Genetic Model*

Near the beginning of this paper, previous genetic models suggested for the Kerr Addison - Chesterville Au system were summarised in Table 2. Based on the previous discussions, Kerr Addison - Chesterville is considered to be a shear zone-controlled (Larder Lake - Cadillac Break), epigenetic Au-quartz vein/disseminated hydrothermal ore system, which formed relatively late in the development of the Abitibi greenstone belt. The principal evidence for this conclusion is that:

- (a) Cross-cutting/relative timing relationships indicate that Au-quartz vein/disseminated mineralisation developed synchronously with deformation in the Larder Lake - Cadillac Break, which is demonstrably a late ductile  $D_2$  structure in this area of the Abitibi greenstone belt;
- (b) Disseminated pyrite (+Au) mineralisation is partially superimposed on fabric, and is *epigenetic quartz vein-related in the flow ore*; free Au mineralisation is contained within cross-cutting quartz veins (e.g. 1 - 11 m width "siliceous break" veins) in green carbonate ore;
- (c) There is *definitely no evidence* for prior Au enrichment (e.g. syn-sedimentary) in areas free from hydrothermal alteration, even within the mine itself (e.g. talc "horses");
- (d) Green carbonate ore contains spinifex textures indicating its komatiitic flow origin;
- (e) Geochemistry shows that the "albitite" dykes and plugs are igneous intrusions and not intercalated sediments as proposed by many authors (see Table 2).

### (ii) *Mafic "Albitite" (?Shoshonite) Magmatic Hypothesis*

Based on the close space-structure-time relationships between main stage Au mineralisation and the mafic "albitite" plug/dyke swarm presented in this paper, the hydrothermal ore fluid is considered most likely to be *magmatically* derived. The weight of the geological evidence indicates that both mafic "albitite" intrusions and Au-bearing hydrothermal fluids in the Kerr

Addison-Chesterville Au-quartz vein system were derived from a larger, evolving, common parent magma system at depth, down plunge from the deposit. One of the clearest genetically important hydrothermal/igneous associations in Kerr Addison is in the small ~300 m x ~25-50 m feeder zone which has been drilled below the 5600 ft level (Figure 63) up through which all the hydrothermal fluid and magma must have flowed. The fact that hydrothermal alteration/quartz veins and "albitite" dykes are preferentially associated at this depth (~1980 m; Figure 63) is strong evidence that they were likewise associated at source.

Important supporting evidence is that the "albitite" dykes and Au-quartz veins are vertically and laterally co-extensive and show correlated areal expansions and contractions with height in the system. Thus the dykes and hydrothermal ore fluids must have been in physical contact in order to transmit and equalise hydraulic pressure, probably from their source at  $\geq 4$  km depth. These findings are significant since the large (~332 tonnes Au; Canada's #5) Kerr Addison - Chesterville system, except for some differences highlighted above, satisfies the criteria typical of the class of Archean, shear-zone-hosted lode gold deposits. These have produced to date almost 50% of the world's total Au (~51,000 tonnes Au; Witwatersrand included as having been derived via erosion of an Archean shield terrain; Woodall, 1988).

Petrography and geochemistry (Smith and Spooner, in prep.) indicate that the Kerr Addison mafic "albitite" intrusions form a coherent set of intrusions, thus the mafic "albitite" parent magma could have produced a hydrothermal fluid phase into which Au from the magma could have been partitioned (e.g. Spooner, 1991c). Mass balance arguments indicate that the measured volume of "albitite" intrusions in the Kerr Addison-Chesterville Au system (~0.01 km<sup>3</sup>), although significant, is too small to have supplied the amount of Au observed (~335 tonnes produced to date) at reasonable magmatic Au concentrations (e.g. 7 ppb mean Au content, Lamaque quartz monzonite plugs, Burrows & Spooner, 1989; 8-35 ppb Au content, Tabar-Feni Group alkali basalts, MacInnes, 1990). Assuming an equal (50% efficient) partition of Au between the parent magma and a generated hydrothermal fluid, and



the subsequent 100% efficient precipitation of Au, a parent intrusion supplying the amount of Au seen at Kerr Addison would have to range from ~6.5 km<sup>3</sup> (at 35 ppb Au) to ~32.4 km<sup>3</sup> (at 7ppb Au) in volume (assuming a density of ~3000 kg/m<sup>3</sup>) i.e. a moderately sized mafic stock (e.g. 1 km width x 4 km strike length x 8 km depth for 32 km<sup>3</sup>). Such a mafic stock might be elongated vertically and parallel to the Larder Lake - Cadillac Break's general ENE-WSW lithological/structural grain, at a depth of ≥4 km below the present surface, and might be detected using deep penetrating geophysical methods.

## Principal Conclusions

1. The Kerr Addison - Chesterville Au-Ag-(W) deposit (~335 tonnes Au) is a structurally controlled, quartz-carbonate vein and disseminated related Archean Au system with distinct similarities to other examples of the same type (e.g. Colvine et al., 1988). It is *not* syngenetic since time sequence analysis shows that Au was not introduced by externally-derived hydrothermal fluids until late in the history of ductile deformation and development of a flattening fabric. The carbonate-rich host lithologies to the green carbonate ore (15.0 mtonnes at 7.8 g/t Au; 118 tonnes Au) have been shown to be metasomatised, spinifex-textured komatiitic flows (Tihor and Crocket, 1977, 1978; Werniuk, 1979; Kishida and Kerrich, 1987); the higher tonnage/grade flow ore (20.9 mtonnes at 11.0 g/t Au; 230 tonnes Au) is hosted by massive to pillowed Fe-tholeiites. Minor additional ore types are "albitite" ore (0.8 mtonnes at 3.9 g/t Au; 3.0 tonnes Au) and graphitic ore (1.8 mtonnes at 7.9 g/t Au; 14.3 tonnes Au). In addition, green carbonate ore typically contains ~5-15 vol.% "albitite" dykes.

2. The deposit is located *within* the Larder Lake - Cadillac Break, a major 150 m wide ductile high strain zone in this area, which to the east defines the Abitibi - Pontiac subprovince boundary (e.g. Robert, 1989) and with which is associated ~2,130 tonnes Au production/reserves. This mode of occurrence in a major first order structure rather than in subsidiary structures is relatively uncommon along the ~300 km strike length of the Break, but is also shown by the McBean, Omega, Cheminis, Fernland and Barber Larder deposits immediately to the west of Kerr Addison, and the McWatters and Astoria deposits to the east in Quebec (a ~75 km strike length segment). Hence mineralisation is shear zone related, but occurs in a zone characterised predominantly by pure shear (flattening; ~5:5:1) on this particular 060° striking segment of the Break (perpendicular to NNW-SSE D<sub>2</sub> compression; Hamilton, 1986). There is no evidence for significant strike slip movement at this location. There is also *no evidence* for structures at a high angle to the Break at Kerr Addison having a causal relationship with the location of Au mineralisation (c.f. Hodgson, 1986).

3. The Larder Lake - Cadillac Break in this area is interpreted to be a flattened and oversteepened thrust localised in a thin, incompetent, laterally extensive ultramafic horizon. The locally south-facing, older Larder Lake Group ultramafic komatiite - pillowed Fe tholeiite - greywacke sequence was originally thrust over the younger Timiskaming sediments to the north. The Kerr Addison - Chesterville Au-quartz vein system is localised by a thick (~150m wide) lens of the ultramafic komatiites adjacent to this major discontinuity. Au mineralisation was introduced syn-kinematically relative to ductile deformation, mainly flattening, in the Break, and is hence post-Timiskaming (~2680 Ma) but significantly syn-"albitite" intrusion in age (~2670-75 Ma). This constraint is in agreement with the observed late timing of Au elsewhere in the southwestern Abitibi greenstone belt, e.g. post-dating intrusion of the Hollinger-McIntyre "albitite" dykes at 2673+6/-2 Ma (Corfu et al., 1989).

4. Inhomogeneous bulk shortening and dextral transpression on the Break are possibly related to closure (at ~2675-2670 Ma) of a small Timiskaming intra-arc basin. The main evidence for this is in the linear positioning of unconformable, pre-collisional tectonic Timiskaming sediments along one or both sides of the Break (MERQ-OGS, 1983; Figure 1), flattening fabrics and evidence for thrusting in the Break structure (e.g. Hamilton, 1986; this study), and modern convergent arc-type geochemical signatures of Timiskaming volcanics and "syenite" plutons (Hattori and Hart, 1991; Corfu et al., 1991), and Kerr Addison syndeformational mafic "albitite" intrusions (?shoshonites; this study).

5. A flat funnel-shaped hydrothermal alteration envelope, with dimensions of ~900 m (strike length) x 60-75 m near surface shrinking to ~300 m (strike length) x 20-50 m at the 5600 ft level and below defines the limits of the composite hydrothermal/igneous system. This green carbonate alteration envelope plunges ~70°E within the plane of the deformation zone to a deep (≥4 km) focal fluid source. A hydrothermal/igneous association is present at the maximum drilled depth of ~2,000 m and may, therefore, be a characteristic of the source.

Five smaller satellite Au exploration targets near the main Kerr Addison - Chesterville ore system along the Break and to its south form a cluster which share similar geological properties and probably a common hydrothermal origin.

6. The Kerr Addison - Chesterville Au-quartz vein/disseminated system and associated hydrothermal alteration were developed co-structurally, co-spatially and significantly overlapping in time with a mafic "albitite" dyke swarm/igneous intrusive plug system. The latter finding is based on observational evidence in the form of clear vein/dyke cross-cutting relations and xenoliths of mineralisation/quartz veins in dykes. Later dykes in the relative time sequence contain fewer Au-quartz vein stages and have been less altered and mineralised than earlier, higher-grade dykes which they crosscut. Such dyke-dyke-Au mineralisation cross-cutting relationships are the first of their kind to be reported in the Abitibi greenstone belt.

7. The spinifex-textured komatiites are chemically susceptible to widespread barren pre-ore (and minor post-ore) carbonate alteration (e.g. Schandl, 1989) which has caused them in the past to be termed "carbonate rock" (Ridler, 1970, 1976). Such alteration can cause confusion in regional exploration for Au. However, Kerr Addison and other Au-related green carbonate alteration along the Break is clearly distinct from the above, and is specifically localised within the small, discrete hydrothermal alteration pipes which contain the Au deposits themselves. Thus, hydrothermal processes leading to Archean Au mineralisation are probably *not* a regional CO<sub>2</sub> and LILE-rich "outgassing" phenomenon along the major Breaks as suggested by Kerrich et al. (1987) and Kerrich and Fryer (1988), but significantly more focused.

8. The bulk of Au mineralisation at Kerr Addison - Chesterville is contained within a discrete 1,130 m vertical interval principally between the 4000 ft and 175 ft levels; the approximately symmetrical rise and fall of total Au produced with depth shows very clearly that Kerr

Addison - Chesterville preserves the complete productive interval of an Archean Au-quartz vein ore system. In fact, the Au deposit *demonstrates very clearly the features of the top and bottom of an Archean Au ore system*, with a geological root zone at depth (>4800 ft level), two prominent branches of the system within a widening, flattened funnel, and a marked reduction in intensity (especially in the east) near surface.

9. Green carbonate/quartz vein/"albitite" intrusion areas per level show *correlated vertical expansion profiles* from a root zone on the 5600 ft level, with similar dimensions to the root zone at greater depth, as shown by drilling below the 5600 ft level, to relatively constant areas (x5 to x8 times those in the root zone) at mid-levels of the system. Quartz vein and "albitite" dyke areas then show a *marked, correlated decrease* from the 1000 ft level upwards, and *die out together quite sharply near the present erosion surface*. Thus the emplacement of both mafic "albitite" intrusions and hydrothermal ore fluids produced real hydraulic dilation, and were probably temporally and physically linked in order to transmit and equalise hydraulic pressure. The coherence of the patterns argues for a relatively short-lived fluid injection and Au mineralisation process, despite the multi-stage nature of the Au-quartz vein mineralisation. Distribution patterns of "albitite" intrusions confirm upward and lateral dyke injection (particularly from east to west) away from the major plugs.

10. The bottom of Kerr Addison is characterised by rapid expansion of the green carbonate ore system (e.g. quartz veins) upwards between the ~4800 ft and 3000 ft levels correlating with the onset of Au mineralisation. The V-shaped green carbonate ore "mining root zone" is defined by a width (~3 m) and grade (~5 g/t Au) cut-off at the 4000 ft level, below which, for the first time, the *sub-economic hydrothermal ore fluid feeder zone beneath a major Archean Au system* has been mapped and documented down to ~650 m below the level of economic ore. The small (~300 x 20-50 m) hydrothermal alteration "geological root zone" contracts around a Au-mineralised "albitite" intrusion in the east part of the deep system (e.g. 4800 ft level; drilling below 5600 ft level) which connects with the eastern Chesterville Plug

at higher levels. The hydrothermal root zone is characterised by a few large quartz veins but with very low Au grades; Au was in solution, but not precipitating. A key point is that the total volumes of hydrothermal fluid and magma which produced the green carbonate alteration, quartz veins and "albitite" intrusions *must* have passed up through this small, low grade feeder zone (see 4800 ft and 5600 ft level plans; drilling below 5600 ft level). The Fe-tholeiite horizon hosting the flow ore pinches out stratigraphically/structurally at the 4600 ft level.

11. The top of the system is characterised by marked *correlated* decreases in the abundances and intensities of green carbonate alteration (smooth trend), quartz veins (smooth) and "albitite" dykes (irregular), which form a zonation in the upper part of and above the deposit which can be used in reverse in exploration to estimate approximate vertical level. Au grades and total contained Au values per level start to decrease upwards *before* other parameters, at ~500 m depth, indicating upward depletion of the hydrothermal fluid in Au. Longitudinal contour diagrams confirm that the Kerr Addison - Chesterville Au system probably closed off 150-300 m above the present erosion surface, and developed internally in the Archean crust without connecting to the paleosurface as a major altered zone. The original surface showings and present day open pits are of sub-ore grade (~4-5 g/t Au). Thinner localised widths of green carbonate alteration without significant quartz veins may have penetrated upwards further.

12. Flow ore (20.9 mtonnes at 11.0 g/t; 230 tonnes Au) distribution is controlled by: (i) proximity and intensity of fluid supply, (ii) primary shape, modified by a structural overprint (boudinage, folding, flexures), and (iii) structure, due to competency contrast during ductile deformation. Sulphidation reactions (e.g. Phillips et al., 1984) between hydrothermal ore fluids and Fe-tholeiite wallrock controlled the bulk (>95%) of disseminated pyrite (+Au) mineralisation in the flow ore. Very high grades (~20 g/t Au) occur at depth, decreasing steadily upwards to ~6 g/t Au due to upward depletion of the ore fluids in Au. A similar sulphidation mechanism is observed in the vein/disseminated pyritic "albitite" and "graphitic" ores.

13. Green carbonate ore (15.0 mtonnes at 7.8 g/t; 118 tonnes Au) was controlled by a mineralised, anastomosing "cherty break" fault/quartz vein framework which acted as a guide to main stage milky Au-quartz vein ("siliceous break") dilatancy and formed feeders which controlled the supply of hydrothermal ore fluids from depth. Heterogenous pre-ore quartz-carbonate alteration may have also set up more competent zones in which the faults could form more readily. Fluid supply and native Au deposition in the green carbonate ore were probably controlled by H<sub>2</sub>O-CO<sub>2</sub> phase separation (Drummond and Ohmoto, 1985; Spooner et al., 1987b; Burrows, 1991) fluid inclusion evidence for which has been described by Channer and Spooner (1991) at Kerr Addison. Dimensional constancy of green carbonate alteration below the 5600 ft level compared with its increase above the 4800 ft level suggests that H<sub>2</sub>O-CO<sub>2</sub> phase separation may have started in the 4800 - 5600 ft level interval. Tonnage and total Au in the green carbonate ore increase upwards steadily from the base, but die off sharply near surface. Individual green carbonate orebodies appear similar in geometry and grade-depth profile to the overall ore system itself. Maximum grade (~10.3 g/t Au) occurs in the mid-levels, decreasing both downwards (due to a lithostatic pressure restriction on expansion and veining) and upwards to <5 g/t Au (due to depletion of fluids in Au and a lower incidence of hydraulic fractures).

14. Kerr Addison - Chesterville as a whole shows a rare example of vertical element zoning in an Archean Au-quartz vein system: the Au:Ag ratio increases smoothly upwards from ~16:1 to ~22:1, probably due to efficient partition of Ag into Au<sup>0</sup> during fluid flow.

15. The "fault valve" model of Sibson et al. (1988) and Sibson (1991) can be shown not to apply here, and features of the Kerr Addison - Chesterville Au system can be best explained by a *fluid inflation model* (Spooner et al., 1987a,b) in which a deep primary fluid hydraulically fractured its way up from a narrow root zone (5600 ft level and below), aided by H<sub>2</sub>O-CO<sub>2</sub> phase separation. Maximum expansion of the Au-quartz vein system between the 4800 ft and 2800 ft levels correlates with the onset of Au mineralisation. High fluid

pressures generating brittle fractures may be explained by irreversible fluid release from a crystallising deep parent magmatic source, H<sub>2</sub>O-CO<sub>2</sub> phase separation and expansion which is interpreted to have started between the 4800 ft and 5600 ft levels, and pressure communication with the "albitite" dyke swarm.

16. The Kerr Fault is a narrow, graphitic post-ore feature and *not* a major Au-related hydrothermal feeder structure as suggested by Kishida and Kerrich (1984, 1987) and others.

17. The weight of the geological evidence indicates that mafic "albitite" (?shoshonitic) intrusions and Au-bearing hydrothermal fluids in the Kerr Addison - Chesterville ore system were *sufficiently correlated in space, structure and time to have been derived from a larger, common parent body at ≥4 km depth*. In addition, the mafic "albitites" formed a coherent set of intrusions sampling the composition of a deep magma. These geological relationships are compatible with previous evidence for a magmatic origin for Archean Au deposits (e.g Burrows et al, 1986; Burrows and Spooner, 1987, 1989; Spooner, 1991a,b), and remain valid irrespective of the absolute age of Archean Au mineralisation at Kerr Addison. In fact, a U-Pb rutile date of ~2580 Ma (~90 Ma younger than the inferred "albitite" intrusion age of ~2675-2670 Ma) at Kerr Addison (Jemielita et al., 1990a,b) is highly *unlikely* to be related to primary Au mineralisation. Such U-Pb rutile dates have *not been shown to be other than minima*, and may instead represent cooling/closure ages (Mezger et al., 1989).

18. Mass balance arguments indicate that the measured volume of mafic "albitite" intrusions in the Kerr Addison - Chesterville Au system (~0.01 km<sup>3</sup>), although significant, is too small to have supplied the amount of Au observed at reasonable magmatic Au contents. Estimates for the size of the parent intrusion range from ~6.5 km<sup>3</sup> (at 35 ppb Au content) to ~32.4 km<sup>3</sup> (at 7 ppb Au content) in volume i.e. a moderately sized mafic stock. Such a mafic stock might be detected at depth using deep penetrating geophysical methods. Thus, the intrusive activity documented at Kerr Addison probably represents the *fortuitously exposed high level*



*expression of deeper magmatic processes, with physical separation between magma and hydrothermal fluid taking place at considerable depth ( $\geq 4$  km below current land surface). Given this scenario, it is not surprising that relatively few Archean Au systems show significant direct evidence of syn-Au mineralisation intrusive activity.*

**19.** The relatively mafic, "andesitic" (Figure 50) or (?) shoshonitic (Smith and Spooner, in prep.) original composition of the Kerr "albitite" dykes is consistent with the recent suggestion that Au fluids with significant magmatic components may have derived their characteristic element enrichments by high temperature fluid/vapour dissolution of magmatic sulphide liquid droplets/solids enriched in Au and associated chalcophile elements (Spooner, 1991c).

**20.** Significantly for continuing exploration for Archean Au in the Canadian Shield, the Kerr Addison - Chesterville mafic "albitite" dyke swarm - massive feeder Au-quartz vein system *passes upwards and distally into barren green carbonate alteration without quartz veins, silicification or dykes.* The rapidity with which the Au grade dies off near its top, analogous to the apex of the blind Chesterville East Zone (see Figure 28), is both a caution and an encouragement to future deep exploration for Au in the Abitibi and other Archean greenstone belts.

### **Dedication to James W. Baker**

This paper is dedicated to the memory of James W. Baker who was Chief Geologist of Kerr Addison Mine during its heyday, from its opening in 1937 until his untimely death in January, 1960. Prior to joining Kerr Addison he had been employed at the Lakeshore Mine, Kirkland Lake (along with W.S. Row, Mine Manager), and had been educated in the USA. Jim Baker is recognised here for his early contributions to the understanding of the principal ore types, identification of igneous "albitite" dykes, and his careful documentation, through underground mapping, of the structural controls on hydrothermal Au mineralisation in the Kerr Addison deposit (Baker, 1944; Baker et al., 1951, 1957).

## Acknowledgements

The authors wish to thank Golden Shield Resources (now GSR Mining/Deak Resources Ltd) for their permission to publish this study, for their active help and co-operation throughout, and for employing J.P.S. during the summers of 1988 and 1989. Mine managers Doug Douglass and Rod Doran, Golden Shield staff Roger Milot, Dan McCormick, Mark Croteau, Jim Butler, Garry Kniereman and Kate Calberry, and GSR Mining/Deak Resources Ltd. officers Jim Fortin, Margot Fortin and Ron Moran are thanked in particular. The support and co-operation of Dave Toogood and Bill McGuinty of Queenston Mining Ltd., and Gary Grabowski and Gerhard Meyer of the Kirkland Lake Resident Geologist's Office, are gratefully acknowledged. Kerr Addison Mines Ltd. are thanked for their careful preservation of the original mine geological records.

We are very grateful to Jack Hamilton of Queen's University for permission to quote material from his MSc. thesis (1986) in the text and in Figure 9, and to Wayne Powell of Queen's University for permission to use his preliminary unpublished M.Sc. thesis map as part of Figure 1. We would also like to thank B.Sc. students Eira Thomas (University of Toronto) and Duncan Friend, Ruth Jones, Susan Middleton and Paul Thomas (University of Oxford) for their collaboration on joint project work. The significant input of several staff at the University of Toronto is recognised. We particularly thank Master Draftsman Subhash Shanbhag for drawing the figures, Karyn Gorra for preparing the photographs, Jim Charters for computing advice, and Shaun McConville for the polished slab in Figure 49d.

Financial assistance in the form of a University of Toronto Fellowship (J.P.S., 1987-1989) and a Differential Fee Waiver Scholarship (J.P.S., 1987-1989) is gratefully acknowledged. Continued financial support by the Ontario Geoscience Research Grant Program (Grant #326) and NSERC Strategic Grant #G1862 (to E.T.C. Spooner) is similarly acknowledged.

## References

Baker, J.W., 1944. The effect of structure in relation to the formation and control of the orebodies at the Kerr Addison Mine. Paper submitted with talk at Prospectors and Developers Association Branch Meeting, January 29, 1944, Park Lane Hotel, Kirkland Lake, 13 pp.

Baker, J.W. and Geological Staff, 1951. Mine Geology. In: Kerr Addison Mine Special Issue, Canadian Mining Journal, 72, no.4, April 1951, pp 68-75 and 109-117.

Baker, J.W. and Geological Staff, 1957. Kerr Addison Mine. In: G. Gilbert (Editor), Structural Geology of Canadian Ore Deposits, Volume II. 6th Commonwealth Mining and Metallurgical Congress, Canada: pp 392-402.

Beach, A., 1980. Numerical models of hydraulic fracturing and the interpretation of syntectonic veins. Journ. Struct. Geol., 2: 425-438.

Bell, T.H., 1981. Foliation development - the contribution, geometry and significance of progressive, bulk, inhomogeneous shortening. Tectonophysics, 75: 273-296.

Bertoni, C.H., 1983. Gold production in the Superior Province of the Canadian Shield. CIM Bulletin, 76, no. 857: 62-69.

Bowen, N.L., 1908. Larder Lake Region. Ontario Bureau of Mines (now Ontario Department of Mines) Statistical Review, XVII: 10-11.

Bowers, T.S., 1991. The deposition of gold and other metals: pressure-induced fluid immiscibility and associated stable isotope signatures. Geochim. Cosmochim. Acta, 55: 2417-2434.

3

Brock, R.W., 1907. The Larder Lake District. Ontario Bureau of Mines (now Ontario Department of Mines) XVI, Part I: 202-218.

Brown, K.L., 1986. Gold deposition from geothermal discharges in New Zealand, *Economic Geology*, 81: 979-983.

Buffam, S.W. and Allen, R.B., 1948. Chesterville Mine. In: *Structural Geology of Canadian Ore Deposits. Canadian Institute of Mining and Metallurgy Jubilee Symposium Volume*, pp 662-671.

Burrows, D.R., 1991. Relationships between Archean lode gold-quartz vein deposits and igneous intrusions in the Timmins and Val d'Or areas, Abitibi sub-province, Canada. Unpubl. PhD. Thesis, University of Toronto, Toronto, Ontario, 217 pp.

Burrows, D.R. and Spooner, E.T.C., 1986. The McIntyre Cu-Au deposit, Timmins, Ontario, Canada. In: A.J. MacDonald (Editor), *Proceedings of Gold '86 Symposium*, Konsult Internat. Inc., Toronto, Willowdale, Ontario, pp. 23-39.

Burrows, D.R. and Spooner, E.T.C., 1987. Generation of a magmatic H<sub>2</sub>O - CO<sub>2</sub> fluid enriched in Mo, Au and W within an Archean sodic granodiorite stock, Mink Lake, northwestern Ontario. *Economic Geology*, 82: 1931-1957.

Burrows, D.R. and Spooner, E.T.C., 1989. Relationships between Archean gold quartz vein - shear zone mineralisation and igneous intrusions in the Val d'Or and Timmins areas, Abitibi subprovince, Canada. In: R.R. Keays et al. (Editors), *The Geology of Gold Deposits: The Perspective in 1988. Economic Geology Monograph 6*: 424-444.

Burrows, D.R., Wood, P.C. and Spooner, E.T.C., 1986. Carbon isotope evidence for a magmatic origin for Archean gold-quartz vein ore deposits. *Nature*, 321: 851-854.

Callan, N.J., 1988. Syn-deformational shear zone hosted Au-quartz vein mineralisation in TTG host rocks, Renabie mine area, North Ontario: structural analysis, microstructural characteristics and vein paragenesis. Unpubl. M.Sc. Thesis, University of Toronto, Toronto, Ontario, 233 pp.

Callan, N.J. and Spooner, E.T.C., 1989. Archean Au-quartz vein mineralisation hosted in a tonalite-trondhjemite terrane, Renabie mine area, Wawa, North Ontario. In: R.R. Keays et al. (Editors), *The Geology of Gold Deposits: The Perspective in 1988*. *Economic Geology Monograph* 6: 9-18.

Capdevila, R., Goodwin, A.M., Ujike, O. and Gorton, M.P., 1982. Trace element geochemistry of Archean volcanic rocks and crustal growth in SW Abitibi belt, Canada. *Geology*, 10: 418-422.

Card, K.D. and Ciesielski, A., 1986. Subdivisions of the Superior Province of the Canadian Shield. *Geoscience Canada*, 13: 5-13.

Channer, D.M. deR. and Spooner, E.T.C., 1991. Multiple fluid inclusion generations in variably deformed quartz: Hollinger-McIntyre and Kerr Addison - Chesterville Archean Au-quartz vein systems, Northern Ontario. *Ont. Geol. Surv. Misc. Paper*, 156: 47-64.

Charteris, S.N., 1984. Evaluation of the ore potential of the Kerr Addison Mine, Virginiatown, Ontario. Internal consultant's report, Kerr Addison Mines Ltd., 12 pp.

Clark, R.J. McH. and Bonnar, R., 1987. Gold mineralisation associated with Archean stratabound sulphides in the Cheminis deposit near Larder Lake, Ontario. *CIM Bulletin*, June 1987, 80, no. 902: 45-50.

Clout, J.M.F., 1988a. The tectonic setting and plumbing system of the Golden Mile, Kalgoorlie, Western Australia. Geol. Soc. Australia Abstr. Ser. 23, Gold '88, Melbourne, Australia, May 16-20, 1988, pp 65-67 (ext. abstr.).

Clout, J.M.F., 1988b. Geology of Kalgoorlie Mining Associated Leases, Kalgoorlie. In: J.H. Cleghorn and R.D. Watt (Editors), Bicentennial Gold '88, Excursion No. 6 Guide, Part 3, Norseman-Wiluna Belt, Australia, pp 70-77.

Colvine, A.C., 1989. An empirical model for the formation of Archean gold deposits: products of final cratonization of the Superior Province, Canada. In: R.R. Keays et al. (Editors), The Geology of Gold Deposits: The Perspective in 1988. Economic Geology Monograph 6: 37-53.

Colvine, A.C., Andrews, A.J., Cherry, M.E., Durocher, M.E., Fyon, A.J., Lavigne, M.J., Jr., Macdonald, A.J., Marmont, S., Poulsen, H.K., Springer, J.S. and Troop, D.G., 1984. An integrated model for the origin of Archean lode gold deposits. Ontario Geological Survey Open File Report 5524, 98 pp.

Colvine, A.C., Fyon, J.A., Heather, K.B., Marmont, S., Smith, P.M., and Troop, D.G., 1988. Archean lode gold deposits in Ontario. Ontario Geological Survey Miscellaneous Paper 139, 136 pp.

Cooke, H.C., 1966. The Timiskaming volcanics and associated sediments of the Kirkland Lake area, Ontario, Canada. Unpubl. PhD. Thesis, University of Toronto, Toronto, Ontario, 147 pp.

Cooke, D.L. and Moorhouse, W.W., 1969. Timiskaming volcanism in the Kirkland Lake area, Ontario, Canada. Canadian Journal of Earth Sciences 6, no. 2: 117-132.

Cooke, H.C., 1922. Kenogami, Round and Larder Lake areas. Geological Survey of Canada Memoir 131, no. 112, Geological Series: 17-61.

Cooke, H.C., 1923a. Recent gold discoveries at Larder Lake, Timiskaming district, Ontario. Geological Survey of Canada Summary Report, Part C1: 61-73.

Cooke, H.C., 1923b. Further developments at Larder Lake, Ontario. Geological Survey of Canada Summary Report, Part C: 17-19.

Corfu, F., Jackson, S.L. and Sutcliffe, R.H., 1991. U-Pb ages and tectonic significance of late Archean alkaline magmatism and nonmarine sedimentation: Timiskaming Group, southern Abitibi belt, Ontario. Can. Jour. Earth Sci., 28: 489-503.

Corfu, F., Krogh, T.E., Kwok, Y.Y., Marmont, S. and Jensen, L.S., 1989. U-Pb geochronology in the southwestern Abitibi greenstone belt, Superior Province. Canadian Journal of Earth Sciences, 26: 1747-1763.

Couture, J.F., Pilote, P. and Vachon, A., 1991. The Francoeur gold deposit: a shear zone hosted disseminated type Archean gold deposit. In: F. Robert et al. (Editors), Greenstone Gold and Crustal Evolution, Geol. Assoc. Canada NUNA Conference Volume, Val d'Or, Quebec, p 148.

Coward, M.P., 1976. Strain within ductile shear zones. Tectonophysics, 34: 181-197.

Crombie, G.P., 1939. The carbonated rocks of the Larder Lake area and their relation to the occurrence of gold. Unpubl. M.A. Thesis, University of Toronto, Toronto, Ontario, 34 pp.

Cunningham, L.J., 1987. Report on the ore potential of the Kerr Addison Mine, McGarry Township, Ontario. Internal consultant's report, Golden Shield Resources Ltd., 11 pp.

Daignault, R. and Archambault, G., 1990. Les grands couloirs de déformation de la sous-province de l'Abitibi. In: Rive et al. (Editors), The Northwest Quebec Polymetallic Belt, Can. Inst. Mining Metall. Special Volume 1, pp 43-64.



de Ronde, C.E.J., 1991. Structural and geochronological relationships and fluid-rock interaction in the central part of the ~3.2-3.5 Ga Barberton Greenstone Belt, South Africa. Unpubl. PhD. Thesis, University of Toronto, Toronto, Ontario.

de Ronde, C.E.J., de Wit, M.J. and Spooner, E.T.C., 1988. Characteristics of early Archean (>3.0 Ga) Au-quartz lode deposits from thrust zones in the mafic/ultramafic rocks of the Barberton Greenstone Belt, South Africa. Geol. Soc. Australia Abstr. Ser. 23, Gold '88, Melbourne, Australia, May 16-20, 1988, pp 7-12 (ext. abstr.).

de Ronde, C.E.J., Spooner, E.T.C., Bray, C.J. and de Wit, M.J., 1991. Mafic-ultramafic hosted, shear zone related, Au-quartz vein deposits in the Barberton greenstone belt, South Africa: structural style, fluid properties and light stable isotope geochemistry. In: E.A. Ladeira (Editor), The Economics, Geology, Geochemistry and Genesis of Gold Deposits, Proceedings of the Symposium Brazil Gold '91, Belo Horizonte, pp 279-286.

de Wit, M.J., Armstrong, R., Hart, R.J. and Wison, A.H., 1987. Felsic igneous rocks within the 3.3- to 3.5 Ga Barberton greenstone belt: High crustal level equivalents of the surrounding tonalite-trondhjemite terrain, emplaced during thrusting. Tectonics, 6: 529-549.

Dimroth, E., Imreh, L., Rocheleau, M. and Goulet, N., 1982. Evolution of the south-central part of the Archean Abitibi Belt, Quebec, Part I: Stratigraphy and paleogeographic model. Can. Jour. Earth Sci., 19: 1729-1758.

Dimroth, E., Imreh, L., Goulet, N. and Rocheleau, M., 1983a. Evolution of the south-central segment of the Archean Abitibi Belt, Quebec, Part II: Tectonic evolution and geomechanical model. Can. Jour. Earth Sci., 20: 1355-1373.

- Dimroth, E., Imreh, L., Goulet, N. and Rocheleau, M., 1983b. Evolution of the south-central segment of the Archean Abitibi Belt, Quebec, Part III: Plutonic and metamorphic evolution and geotectonic model. *Can. Jour. Earth Sci.*, 20: 1374-1388.
- Downes, M.J., 1979. Kirkland Lake area, stratigraphic mapping, district of Timiskaming. In: V.G. Milne et al. (Editors), *Summary of Fieldwork, 1979*. Ontario Geological Survey Miscellaneous Paper 90: 121-125.
- Downes, M.J., 1980. Structural and stratigraphic aspects of gold mineralisation in the Larder Lake area, Ontario. In: R.G. Roberts (Editor), *Genesis of Archean, Volcanic-hosted Gold Deposits*. Ontario Geological Survey Open File Report 5293: 92-103.
- Downes, M.J., 1981. Structural and stratigraphic aspects of gold mineralisation in the Larder Lake area, Ontario. In: E.G. Pye and R.G. Roberts (Editors), *Genesis of Archean, Volcanic-hosted Gold Deposits* (symposium held at University of Waterloo). Ontario Geological Survey Miscellaneous Paper 97, 66-70.
- Drummond, S.E. and Ohmoto, H., 1985. Chemical evolution and mineral deposition in boiling hydrothermal systems. *Economic Geology*, 80: 126-147.
- Feng, R., 1991. Geobarometry, differential block movements and crustal structure of the southwestern Abitibi greenstone belt: implications for mesothermal Au. In: F. Robert et al. (Editors), *Greenstone Gold and Crustal Evolution*, Geol. Assoc. Canada NUNA Conference Volume, Val d'Or, Quebec, pp 158-159.
- Feng, R., and Kerrich, R., 1990. Geochemistry of fine-grained clastic sediments in the Archean Abitibi greenstone belt, Canada: implications for provenance and tectonic setting. *Geochimica et Cosmochimica Acta*, 54: 1061-1081.
- Folinsbee, R.E., 1943. Scheelite at Kerr Addison Gold Mines Limited. Geological Survey of Canada internal report, 3 pp.

Fowler, A.D., Jensen, L.S. and Peloquin, S.A., 1987. Varioles in Archean basalts - products of spherulitic crystallisation. *Canadian Mineralogist*, 25: 275-289.

Frarey, M.J. and Krogh, T.E., 1986. U-Pb zircon ages of late internal plutons of the Abitibi and eastern Wawa subprovinces, Ontario and Quebec. *Canada Geol. Survey Paper 86-1A*: 43-48.

Friend, D., 1990. The geology of part of Gauthier Township, Dobie, Ontario. Unpubl. BSc. Thesis, Oxford University, England; also internal report, Queenston Mines Ltd., Kirkland Lake, Ontario, ca. 30 pp.

Fyon, J.A., Troop, D.G., Marmont, S. and Macdonald, A.J., 1989. Introduction of gold into Archean crust, Superior Province, Ontario - coupling between mantle-initiated magmatism and lower crustal thermal maturation. In: R.R. Keays et al. (Editors), *The Geology of Gold Deposits: The Perspective in 1988*. *Economic Geology Monograph 6*: 479-490.

Gariépy, C., Allegre, C.J. and Lajoie, J., 1984. U-Pb systematics in single zircons from the Pontiac sediments, Abitibi greenstone belt. *Can. Jour. Earth Sci.*, 21: 1296-1304.

Gauthier, N., Rocheleau, M. and St-Julien, P., 1988. The Cadillac - Larder Lake Fault Zone, Abitibi Belt, Canada: an example of an Archean accretionary prism hosting gold deposits. *Geol. Soc. Australia Abstr. Ser. 23*, Gold '88, Melbourne, Australia, May 16-20, 1988, pp 13-15 (ext. abstr.).

Goodwin, A.M., 1962. Volcanic complexes and mineralisation in N.E. Ontario. *Canadian Mining Geology*, April 1962: pp 62-66.

Goodwin, A.M., 1965. Mineralised volcanic complexes in the Porcupine - Kirkland Lake - Noranda Region, Canada. *Economic Geology*, 60: 955-971.

Goodwin, A.M., 1984. Archean greenstone belts and gold mineralisation, Superior Province, Canada. In: R.P. Foster (Editor), Gold '82, A.A. Balkema Publs., Rotterdam, pp 165-181.

Goulet, N., 1978. Stratigraphy and structural relationships across the Cadillac - Larder Lake fault, Rouyn - Beauchastel area, Quebec. Unpubl. Ph.D. Thesis, Queen's University, Kingston, Ontario, 141 pp.

Green, A.G., Milkereit, B., Mayrand, L.J., Ludden, J.N., Hubert, C., Jackson, S.L., Sutcliffe, R.H., West, G.F., Verpaelst, P. and Simard, A., 1990. Deep structure of an Archean greenstone terrane. *Nature*, 344: 327-330.

Greenwood, H.J., 1967. Mineral equilibria in the system MgO-SiO<sub>2</sub>-H<sub>2</sub>O-CO<sub>2</sub>. In: P.H. Abelson (Editor), *Researches in Geochemistry*, John Wiley and Sons, New York-London-Sydney, pp 542-567.

Gunning, H.C. and Ambrose, J.W., 1927. Cadillac - Malartic area, Québec. *Canadian Institute of Mining and Metallurgy Transactions*, 40: 341-362.

Hamilton, J.V., 1986. The structural and stratigraphic setting of gold mineralisation in the vicinity of Larder Lake, south-central Abitibi Greenstone Belt, Northeastern Ontario. Unpubl. M.Sc. Thesis, Queen's University, Kingston, Ontario, 156 pp.

Hamilton, J.V. and Hodgson, C.J., 1983. Geological study of the area of the Kirkland Lake - Larder Lake Break in central McGarry Township. *Ontario Geological Survey Miscellaneous Paper 116*: 179-184.

Hamilton, J.V. and Hodgson, C.J., 1984. Structural geology and gold mineralisation in the Kirkland Lake - Larder Lake Deformation Zone. In: J. Wood et al. (Editors), *Summary of Fieldwork, 1984*. *Ontario Geological Survey Miscellaneous Paper 119*: 220-225.

Hattori, K. and Hart, S.R., 1991. Late Archean magmatism in the Kirkland Lake gold camp: isotopic and geochemical constraints. In: F. Robert et al. (Editors), Greenstone Gold and Crustal Evolution, Geol. Assoc. Canada NUNA Conference Volume, Val d'Or, Quebec, pp 163-165.

Hawkes, G.J., 1947. A history of our refractory ores, Kerr Addison Gold Mines Ltd., 1938 - 1947. Internal report, Kerr Addison Mines Ltd., 16 pp.

Heaman, L.M., 1988. A precise U-Pb zircon age for a Hearst dyke. Geol. Assoc. Canada - Mineral. Assoc. Canada Ann. Meeting, St. John's, Newfoundland, Program with Abstracts, p.A53.

Hewitt, D.F., 1963. The Timiskaming Series of the Kirkland Lake area. Canadian Mineralogist, 7, no. 3: 497-523.

Hinse, G.J., 1978. An early Precambrian basal sedimentary group in the Virginiatown area, district of Cochrane, Ontario. Internal report, Kerr Addison Mines Ltd., 6 pp.

Hinse, G.J., Hogg, G.M. and Robertson, D.S., 1986. On the origin of Archean vein-type gold deposits with reference to the Larder Lake "Break" of Ontario and Quebec. Mineralium Deposita 21: 216-227.

Hodgson, C.J., 1986. Place of gold ore formation in the geological development of the Abitibi greenstone belt, Ontario, Canada. Transactions of the Institution of Mining and Metallurgy (Section B: Applied Earth Sciences) 95: 183-194.

Hodgson, C.J. and Hamilton, J.V., 1989. Gold mineralisation in the Abitibi greenstone belt: end stage result of Archean collisional tectonics?. In: R.R. Keays et al. (Editors), The Geology of Gold Deposits: The Perspective in 1988. Economic Geology Monograph 6: 86-100.

Hodgson, C.J., Hamilton, J.V. and Hanes, J.A., 1989. The late emplacement of gold in the Archean Abitibi greenstone belt: a consequence of thermal equilibration following collisional orogeny. GAC/MAC Program with Abstracts, 14: p A45.

Hopkins, P.E., 1919. Larder Lake gold area. Ontario Bureau of Mines (now Ontario Department of Mines), XXVIII, Part 2: 71-77.

Hopkins, P.E., 1923. Kirkland - Larder area; Ontario Bureau of Mines (now Ontario Department of Mines), XXXII, Part 4; + Map No. 32e.

Hopkins, P.E., 1924. Larder Lake gold area. Ontario Bureau of Mines (now Ontario Department of Mines), XXXIII, Part 3, 1-26.

Hubert, C., Ludden, J. and Brown, A., 1991. Tectonic framework of the southern Abitibi belt: lozenge-shaped domains and nature of their marginal tectonic zones. In: F. Robert et al. (Editors), Greenstone Gold and Crustal Evolution, Geol. Assoc. Canada NUNA Conference Volume, Val d'Or, Quebec, pp 172-173.

Hubert, C., Trudel, P. and Gelinas, L., 1984. Archean wrench fault tectonics and structural evolution of the Blake River Group, Abitibi belt, Quebec. Can. Jour. Earth Sci., 12: 1024-1032.

Hutchinson, R.W., Ridler, R.H. and Suffel, G.G., 1971. Metallogenic relationships in the Abitibi belt, Canada: a model for Archean metallogeny. CIM Bulletin, April 1971: 106-115.

Hyde, R.S., 1975. Depositional environment of Archean exhalites, Kirkland Lake - Larder Lake area, Ontario. Abstract with Programs, Joint GSA/GAC/MAC Annual Meeting, 7: 789.

Hyde, R.S., 1978. Sedimentology, volcanology, stratigraphy and tectonic setting of the Archean Timiskaming Group, Abitibi Greenstone Belt, N.E. Ontario, Canada. Unpubl. Ph.D. Thesis, McMaster University, Hamilton, Ontario, 422 pp.

Hyde, R.S., 1980. Sedimentary facies in the Archean Timiskaming Group, and their tectonic implications, Abitibi greenstone belt, northeastern Ontario, Canada. *Precambrian Research*, 12: 161-195.

Jackson, S.L., 1988. The Abitibi greenstone belt near Larder Lake: structural and stratigraphic studies. In A.C. Colvine et al. (Editors), *Summary of Field Work and Other Activities, 1988*. Ontario Geological Survey Miscellaneous Paper 141: 206-211.

Jackson, S.L. and Harrap, R.M., 1989. Geology of parts of Pacaud, Catherine and southernmost Boston and McElroy Townships. In: A.C. Colvine et al. (Editors), *Summary of Fieldwork and Other Activities 1989*, Ontario Geological Survey Miscell. Paper 146: 125-131.

Jackson, S.L. and Sutcliffe, R.H., 1990. Central Superior Province geology: evidence for an allochthonous, ensimatic southern Abitibi greenstone belt. *Can. J. Earth Sci.*, 27: 582-589.

Jackson, S.L., Sutcliffe, R.H., Ludden, J.N., Hubert, C., Green, A.G., Milkereit, B., Mayrand, L., West, G.F. and Verpaelst, P., 1990. Southern Abitibi greenstone belt: Archean crustal structure from seismic-reflection profiles. *Geology*, 18: 1086-1090.

James, W.F., Buffam, B.S.W., and Cooper, M.A., 1961. Report on geology and future exploration of Kerr Addison Gold Mines Ltd., McGarry Township, Ontario. Internal consultants' report, Kerr Addison Mines Ltd., 37 pp.

James, W.F., Buffam, B.S.W. & Cooper, M.A., 1964. Report on development and exploration, Kerr Addison Mine (1960-1964). Internal consultants' report, Kerr Addison Mines Ltd., 13 pp + tables.

Jemielita, R.A., Davis, D.W. and Krogh, T.E., 1990a. U-Pb evidence for Abitibi gold mineralisation postdating greenstone magmatism and metamorphism. *Nature*, 346: 831-834.

Jemielita, R.A., Wong, L., Davis, D.W. and Krogh, T.E., 1990b. The greenstone-gold relationship in the southern Superior Province: constraints from U-Pb dating of hydrothermal minerals. In: F. Robert et al. (Editors), *Greenstone Gold and Crustal Evolution*, Geol. Assoc. Canada NUNA Research Conference Volume, Val d'Or, Quebec, p 181.

Jenney, C.P., 1941. Geology of the Omega mine, Larder Lake, Ontario. *Economic Geology*, 36: 424-447.

Jensen, L.S., 1976. Regional stratigraphy and structure of the Timmins - Kirkland Lake area, District of Cochrane and Timiskaming, and Kirkland Lake area, District of Timiskaming. In: V.G. Milne et al. (Editors), *Summary of Fieldwork, 1976*. Ontario Division of Mines, Misc. Paper 67: 87-95.

Jensen, L.S., 1977. Regional stratigraphy and structure of the Timmins - Larder Lake area, and Kirkland Lake - Larder Lake areas. In: V.G. Milne et al. (Editors), *Summary of Fieldwork, 1977*. Ontario Geological Survey Misc. Paper 75: 98-101.

Jensen, L.S., 1978a. Archean komatiitic, tholeiitic, calc-alkalic and alkalic volcanic sequences in the Kirkland Lake area. In: A.L. Currie and W.O. Mackasey (Editors), *Toronto '78 Field Trip Guidebook*, Geological Association of Canada, pp 237-259.



Jensen, L.S., 1978b. Regional stratigraphy and structure of the Timmins - Kirkland Lake area, District of Cochrane and Timiskaming, and the Kirkland Lake - Larder Lake area, District of Timiskaming. In: V.G. Milne et al. (Editors), Summary of Fieldwork, 1978, Ontario Division of Mines, Misc. Paper 82: 67-72.

Jensen, L.S., 1979. Larder Lake synoptic mapping project, districts of Cochrane and Timiskaming. In: V.G. Milne et al. (Editors), Summary of Fieldwork, 1979. Ont. Geol. Survey Miscellaneous Paper 90: 64-69.

Jensen, L.S., 1980. Kirkland Lake - Larder Lake synoptic mapping projects. In: V.G. Milne et al. (Editors), Summary of Fieldwork, 1980. Ontario Geological Survey Miscellaneous Paper 96: 55-60.

Jensen, L.S., 1981a. Archean gold mineralisation in the Kirkland Lake - Larder Lake area. In: R.G. Roberts (Editor), Genesis of Archean Volcanic-hosted Gold Deposits. Ontario Geological Survey Open File Report 5293: 290-302.

Jensen, L.S., 1981b. Gold mineralisation in the Kirkland Lake - Larder Lake area. In: E.G. Pye and R.G. Roberts (Editors), Genesis of Archean, Volcanic-hosted Gold Deposits (symposium held at University of Waterloo). Ontario Geological Survey Miscellaneous Paper 97: 59-65.

Jensen, L.S., 1985a. Stratigraphy and petrogenesis of Archean metavolcanic sequences, south-western Abitibi subprovince, Ontario. In: L.D. Ayres et al. (Editors), Evolution of Archean Supracrustal Sequences, Geological Association of Canada Special Paper 28: 65-87.

Jensen, L.S., 1985b. Synoptic mapping of the Kirkland Lake - Larder Lake areas, District of Timiskaming. In: J. Wood et al. (Editors), Summary of Fieldwork and Other Activities, 1985, Ontario Geological Survey Miscell. Paper 126: 112-120.

Jensen, L.S. and Hinse, G.J., 1979. Geological environment of gold deposition in the Kerr Addison mine and vicinity. In: Gold Exploration and Outlook, McGill Adams Club Special Symposium, Department of Geological Sciences, McGill University, Montreal, pp 19-21.

Jensen, L.S. and Langford, F.F., 1985. Geology and petrogenesis of the Archean Abitibi belt in the Kirkland Lake area. Ontario Geological Survey Miscell. Paper 123, 130 pp.; Preliminary Maps P-2433 and P-2434.

Jensen, L.S. and Pyke, D.R., 1982. Komatiites in the Ontario portion of the Abitibi belt. In N.T. Arndt and E.G. Nisbet (Editors), Komatiites, George Allen and Unwin Ltd., London, pp 147-157.

Johannes, W., 1969. An experimental investigation of the system  $MgO-SiO_2-H_2O-CO_2$ . Amer. Journ. Sci., 267: 1083-1104.

Jolly, W.T., 1974. Regional metamorphic zonation as an aid in the study of Archean terrains, Abitibi region, Ontario. Canadian Mineralogist, 12: 499-508.

Jolly, W.T., 1978. Metamorphic history of the Archean Abitibi belt. In: Metamorphism in the Canadian Shield, Geol. Surv. Canada Paper 78-10: 63-78.

Kalliokoski, J., 1968. Structural features and some metallogenic patterns in the southern part of the Superior Province, Canada. Canadian Journal of Earth Sciences, 5, no. 5: 1199-1208.

Kerr Addison Geological Staff, 1967. Kerr Addison Mines Ltd. In: CIMM Centennial Field Excursion, N.W. Quebec - N. Ontario, October 1967, pp 96-100.

Kerrich, R., 1983. Geochemistry of gold deposits in the Abitibi greenstone belt. CIMM Publications, Special Volume 27, 75 pp.

- Kerrick, R. and Fryer, B.J., 1988. Lithophile-element systematics of Archean greenstone belt Au-Ag deposits: implications for source processes. *Can. Journ. Earth Sci.* 25: 945-953.
- Kerrick, R., Fryer, B.J., King, R.W., Willmore, L.M. and van Hees, E., 1987. Crustal outgassing and LILE enrichment in major lithosphere structures, Archean Abitibi greenstone belt: evidence on the source reservoir from strontium and carbon isotope tracers. *Contribs. Min. Pet.*, 97: 156-168.
- Kerrick, R. and Watson, G.P., 1984. The Macassa mine Archean lode gold deposit, Kirkland Lake, Ontario: geology, patterns of alteration and hydrothermal regimes. *Economic Geology*, 79: 1104-1130.
- Kimberly, M.M., Jensen, L., Grandstaff, D.E. and Foster, R.F., 1985. Archean palaeosol: weathered Kinojévis basalt beneath fluvial Timiskaming sandstone. *Geological Society of America Annual Meeting, Orlando, Florida, Program with Abstracts*, p 629.
- Kishida, A. and Kerrich, R., 1984.  $^{18}\text{O}/^{16}\text{O}$  evidence on hydrothermal regimes at the Kerr Addison Archean Au deposit. *GAC-MAC Ann. Meeting, London, Ontario, Program with Abstracts, 1984*, p 78.
- Kishida, A. and Kerrich, R., 1987. Hydrothermal alteration zoning and gold concentration at the Kerr Addison Archean lode gold deposit, Kirkland Lake, Ontario. *Economic Geology*, 82: 649-690.
- Kutina, J. and Fabbri, A.G., 1971. Relationship of structural lineaments and mineral occurrence in the Abitibi area of the Canadian Shield. *Geol. Survey of Canada Paper 71-9*: 1-36.
- Lafleur, P.J., 1986. The Archean Round Lake Batholith, Abitibi greenstone belt: a synthesis. Unpubl. M.Sc. Thesis, University of Ottawa, Ottawa, Ontario. 245 pp.

Lafleur, P.J. and Hogarth, D.D., 1981. Geology of the Round Lake Batholith, Kirkland Lake area, Ontario. In: Progress report on regional geological synthesis, central Superior Province, Geol. Survey of Canada Paper 81-1A: 77-93.

Lajoie, J. and Ludden, J., 1984. Petrology of the Archean Pontiac and Kewagama sediments and implications for the stratigraphy of the southern Abitibi belt. Can. Journ. Earth Sci., 21, 1305-1314.

Lloyd, M.J. and Schwerdtner, W.M., 1990. Fault-induced flow of Carboniferous evaporites in northwestern Ellesmere Island, Canadian Arctic Archipelago: anhydrite as a tectonic lubricant. Geological Society of America, 1990 Annual Meeting, Dallas, Program with Abstracts, 41: A105.

Lovell, H.L., 1967a. Geology and mineral deposits of the Kirkland Lake - Larder Lake mining area of N.E. Ontario; In: CIMM Centennial Field Excursion, N.W. Quebec - N. Ontario, October 1967, pp 72-77.

Lovell, H.L., 1967b. Geology of the Matachewan area, District of Timiskaming. Ontario Department of Mines, Geological Report 51, 61 pp.

Lovell, H.L., 1972. The Kirkland Lake area. In: Precambrian geology and mineral deposits of the Temagami, Cobalt, Kirkland Lake and Timmins region, Ontario, 24th International Geological Conference Field Excursion Guidebook A39, B39, C39: 27-56.

Lovell, H.L., 1980. Kirkland Lake - Larder Lake area gold deposits, regional setting and prospecting methods. In: Geological Division, CIMM Gold Symposium Guidebook, September 1980, pp 75-76.

Lovell, H.L. and Caine, T.W., 1972. Lake Timiskaming rift valley. Ontario Department of Mines Miscell. Paper 39: 1-16.

Lovell, H.L. and Grabowski, G.P.B., 1981. Report of the Kirkland Lake Regional Geologist. In: C.R. Kustra (Editor), Ontario Geological Survey Miscellaneous Paper 95: 86-107.

Lovell, H.L., Grabowski, G.P.B. and Guindon, D., 1985. Kirkland Lake resident geologist area, northern region, Ontario. Ontario Geological Survey Miscellaneous Paper 122: 162-196.

Lowrie, D.A. and Wilton, C.K., 1986. Geology of the Kerr Addison Mine - a review. Preprint for Annual General Meeting of C.I.M., Toronto, April 20-24, 1980, 9pp.

Ludden, J. and Hubert, C., 1986. A model for the geological evolution of the late Archean Abitibi greenstone belt of Canada. *Geology*, 14: 707-711.

Ludden, J., Hubert, C. and Gariepy, C., 1986. The tectonic evolution of the Abitibi greenstone belt of Canada. *Geol. Magazine*, 123: 153-166.

MacInnes, B., 1990. Relation of alkaline magmatic rocks to gold, Simberi island, Papua New Guinea. Central Canada Geological Conference CCGC'90, Ottawa-Carleton Geoscience Centre, Abstracts with Program, p 38.

Mason, R. and Melnik, N., 1986. The anatomy of an Archean gold system - the McIntyre-Hollinger complex at Timmins, Ontario, Canada. In: A.J. MacDonald (Editor), Proceedings of Gold '86 Symposium, Konsult Internat. Inc., Toronto, Willowdale, Ontario, pp 40-55.

McLean, A., 1950. Geology of Lebel Township. Ontario Department of Mines, Bulletin 150.

McQuiston, F.W. Jr. and Shoemaker, R.S., 1975. Kerr Addison Mines Ltd. In: Gold and Silver Cyanidation Plant Practice, American Institute of Mining, Metallurgical and Petroleum Engineers, Monograph, 1: 103-107.

MERQ-OGS: Ministère de l'Énergie et des Ressources de Québec - Ontario Geological Survey, 1983. Lithostratigraphic map of the Abitibi subprovince. Map 2484 in Ontario, Map D.V. 83-16 in Quebec; scale 1: 500,000.

Mezger, K., Hanson, G.N. and Bohlen, S.R., 1989. High precision U-Pb ages of metamorphic rutiles: application to the cooling history of high-grade terranes. *Earth Planet. Sci. Lett.* 96: 106-118.

Miller, W.G., 1902. Lake Timiskaming to the height of land. *Ontario Bureau of Mines Report*, 11: 214-230.

Morrison, G.W., 1980. Characteristics and tectonic setting of the shoshonitic rock association. *Lithos*, 13: 97-108.

Mortensen, J.K., 1987a. U-Pb chronostratigraphy of the Abitibi greenstone belt. *Geol. Assoc. Canada - Mineralog. Soc. Canada Program with Abstracts*, 12: 75.

Mortensen, J.K., 1987b. Preliminary U-Pb zircon ages for volcanic and plutonic rocks of the Noranda - Lac Abitibi area, Abitibi Subprovince, Quebec. In: *Current Research, part A, Geol. Survey of Canada Paper 87-1A*: 581-590.

Norman, G.W.H., 1948. Major faults, Abitibi region. In: *Structural Geology of Canadian Ore Deposits, CIMM Jubilee Symposium Volume*, pp 822-839.

Parks, W.A., 1904. The geology of a district from Lake Timiskaming northward. *Geological Survey of Canada Summary Report for 1904*, XVI, 198-225.

Phillips, G.N., 1986. Geology and alteration in the Golden Mile, Kalgoorlie. *Economic Geology*, 81: 779-808.

- Phillips, G.N., Groves, D.I. and Martyn, J.E., 1984. An epigenetic origin for Archean banded iron formation-hosted gold deposits. *Economic Geology*, 79: 162-171.
- Powell, W.G., Hodgson, C.J. and Hanes, J.A., 1989. The expression of the Larder Lake Break in the Matachewan area. In: V.G. Milne (Editor), Geoscience Research Grant Program, Summary of Research 1988-89, Ontario Geological Survey Miscell. Paper 143: 125-132.
- Powell, W.G., Hodgson, C.J. and Carmichael, D.M., 1990. Tectono-metamorphic character of the Matachewan area, northeast Ontario. In: V.G. Milne (Editor), Geoscience Research Grant Program, Summary of Research 1989-90, Ontario Geological Survey Miscell. Paper 150: 56-65.
- Pyke, D.R., 1975. On the relationship of gold mineralisation and ultramafic volcanic rocks in the Timmins area. Ontario Division of Mines, Miscell. Paper 62, 23 pp.
- Pyke, D.R., Ayres, L.D. and Innes, D.G., 1973. Timmins - Kirkland Lake Sheet, Cochrane, Sudbury and Timiskaming districts. Ontario Division of Mines, Geological Compilation Series, Map 2205; scale 1 inch to 4 miles.
- Renders, P.J. and Seward, T.M., 1989. The stability of hydrosulphido- and sulphido-complexes of Au (I) and Ag (I) at 25°C. *Geochim. Cosmochim. Acta*, 53: 249-253.
- Ridler, R.H., 1968. Archean stratigraphy and mineralisation in the Kirkland Lake area of north-eastern Ontario. Geological Survey of Canada Paper 68-1, Part A: 146-149.
- Ridler, R.H., 1969. The relationship of mineralisation to volcanic stratigraphy in the Kirkland Lake area, Northern Ontario, Canada. Unpubl. Ph.D. Thesis, University of Wisconsin, USA, 140 pp.

- Ridler, R.H., 1970. Relationship of mineralisation to volcanic stratigraphy in the Kirkland Lake - Larder Lake area, Ontario. *Geol. Assoc. Canada Proceedings*, 21: 33-42.
- Ridler, R.H., 1972. Volcanic stratigraphy of the Kirkland Lake area. In: A.M. Goodwin et al. (Editors), *Precambrian Volcanism of the Noranda - Kirkland Lake - Timmins, Michipicoten and Mamainse Point areas, Quebec and Ontario*, *Internat. Geol. Congress Guidebook*, A40-C40: 33-52.
- Ridler, R.H., 1975. Regional metallogeny and volcanic stratigraphy of the Superior Province. In: *Report of Activities, Part A, Geological Survey of Canada Paper 75-1A*: 353-358.
- Ridler, R.H., 1976. Stratigraphic keys to the gold mineralisation of the Abitibi belt. *Canadian Mining Journal*, 97, no. 6: 81-90.
- Robert, F., 1989. Internal structure of the Cadillac tectonic zone southeast of Val d'Or, Abitibi greenstone belt, Quebec. *Canadian Journal of Earth Sciences*, 26: 2661-2675.
- Robert, F. and Brown, A.C., 1986a. Archean gold-bearing quartz veins at the Sigma mine, Abitibi greenstone belt, Quebec; Part I. Geologic relations and formation of the vein systems. *Economic Geology*, 81: 578-592.
- Robert, F. and Brown, A.C., 1986b. Archean gold-bearing quartz veins at the Sigma mine, Abitibi greenstone belt, Quebec; Part II. Vein paragenesis and hydrothermal alteration. *Economic Geology*, 81: 593-616.
- Robert, F., Brown, A.C. and Audet, A.J., 1983. Structural control of gold mineralisation at the Sigma mine, Val d'Or, Quebec. *Canadian Institute of Mining and Metallurgy Bulletin*, 76, no. 850: 72-80.
- Robert, F. and Kelly, W.C., 1987. Ore-forming fluids in Archean gold-bearing quartz veins at the Sigma mine, Abitibi greenstone belt, Quebec, Canada. *Economic Geology*, 82: 1464-1482.



Roberts, D.E., 1988. Geology of Kambalda Gold Deposit, Western Mining Corporation Ltd. document, 60pp.

Rowins, S.M., Lalonde, A.E. and Cameron, E.M., 1989. Geology of the Archean Murdoch Creek intrusion, Kirkland Lake, Ontario. In: Current Research, part C, Geol. Survey of Canada Paper 89-1C: 313-323.

Schandl, E.S., 1989. Talc-carbonate alteration of ultramafic rocks in the Kidd Volcanic Complex, the Slade Forbes, and Munro asbestos deposits in the Abitibi greenstone belt, Timmins, Ontario. Unpubl. PhD. Thesis, University of Toronto, Toronto, Ontario, 255 pp.

Schwerdtner, W.M., Stone, D., Osadetz, K., Morgan, J. and Stott, G.M., 1979. Granitoid complexes and the Archean tectonic record in the southern part of northwestern Ontario. *Can. Journ. Earth Sci.*, 16: 1965-1977.

Seward, T.M., 1973. Thiocomplexes of gold and the transport of gold in hydrothermal ore solutions. *Geochim. Cosmochim. Acta*, 37: 379-399.

Shenberger, D.M. and Barnes, H.L., 1989. Solubility of gold in aqueous sulphide solutions from 150 to 350°C. *Geochim. Cosmochim. Acta*, 53: 269-278.

Sibson, R.H., 1991. Fault structure and mechanics in relation to greenstone gold deposits. In: F. Robert et al. (Editors), *Greenstone Gold and Crustal Evolution*, Geol. Assoc. Canada NUNA Conference Volume, Val d'Or, Quebec, pp 54-60.

Sibson, R.H., Robert, F. and Poulsen, K.H., 1988. High angle reverse faults, fluid pressure cycling and mesothermal gold-quartz deposits. *Geology* 16: 551-555.

Sinclair, W.D., 1982. Gold deposits of the Matachewan area, Ontario. In: R.W. Hodder and W. Petruk (Editors), *Geology of Canadian Gold Deposits*, Canadian Institute of Mining and Metallurgy, Montreal, Spec. Vol. 24: 83-93.

Smith, A.R. and Sutcliffe, R.H., 1988. Project Number 88-08. Plutonic rocks of the Abitibi Subprovince. In: A.C. Colvine et al. (Editors), Summary of Fieldwork and Other Activities 1988, Ontario Geological Survey Miscell. Paper 141: 188-196.

Smith, J.P. and Spooner, E.T.C., 1992 (in prep.). A preliminary examination of the igneous geochemistry of hydrothermally altered mafic "albitite" intrusions associated with multi-stage Archean Au-quartz vein mineralisation, Kerr Addison mine, N.E. Ontario.

Spooner, E.T.C., 1991a. Archean intrusion-hosted, stockwork Au-quartz vein mineralisation, Lamaque mine, Val d'Or, Quebec; Part II. Light stable isotope (H,O,C and S) characteristics and enriched calc-alkaline / shoshonitic igneous geochemistry. In: F. Robert et al. (Editors), Greenstone Gold and Crustal Evolution, Geol. Assoc. Canada NUNA Conference Volume, Val d'Or, Quebec, pp 205-210.

Spooner, E.T.C., 1991b. The magmatic model for the origin of Archean Au-quartz vein ore systems: an assessment of the evidence. In: E.A. Ladeira (Editor), The Economics, Geology, Geochemistry and Genesis of Gold Deposits, Proceedings of the Symposium Brazil Gold '91, Belo Horizonte, pp 313-318.

Spooner, E.T.C., 1991c. Magmatic sulphide/volatile interaction as a mechanism for producing chalcophile element enriched, Archean Au-quartz vein, epithermal Au-Ag and Au skarn hydrothermal ore fluids. Geol. Soc. Amer., Abstracts with Programs, 23: A230.

Spooner, E.T.C., Burrows, D.R., Callan, N.J., de Ronde, C.E.J. and Wood, P.C., 1987a. High hydrothermal fluid pressures, hydraulic fracturing, and fluid pressure dilation of shear zones in Archean Au-quartz vein systems. Geol. Assoc. Canada, Summer Field Meeting, Yellowknife, Program with Abstracts, p 24.

Spooner, E.T.C., Bray, C.J., Wood, P.C., Burrows, D.R. and Callan, N.J., 1987b. Au-quartz vein and Cu-Au-Ag-Mo-anhydrite mineralisation, Hollinger-McIntyre mines, Timmins, Ontario;  $\delta^{13}\text{C}$  values (McIntyre), fluid inclusion gas chemistry, pressure (depth) estimation and  $\text{H}_2\text{O}-\text{CO}_2$  phase separation as a precipitation and dilation mechanism. In: V.G. Milne (Editor), Geoscience Research Grant Program, Summary of Research 1986-87, Ont. Geol. Surv. Misc. Paper, 136: 35-56.

Spooner, E.T.C., Smith, J.P. and Ploeger, F.R., 1991. The Kerr Addison/Chesterville Archean Au-quartz vein system, Virginiatown, N. Ontario, II; the upper part. GAC-MAC-SEG Joint Meeting, Toronto, May 1991, Abstracts with Programs, p A117.

Springer, J.S., 1983. Invisible gold. In: A.C. Colvine (Editor), The Geology of Gold in Ontario, Ontario Geological Survey Miscell. Paper 110: 240-250.

Springer, J.S., 1985. Carbon in Archean rocks of the Abitibi belt (Ontario-Quebec) and its relation to gold distribution. Can. Journ. Earth Sci., 22: 1945-1951.

Springer, J.S., 1986. Gold in carbon-rich rocks. Canadian Inst. Mining and Metallurgy Special Volume 38: 104-112.

Stadelman, D.K., 1939. Carbonatization in the Barber Larder Lake area. Unpubl. M.A. Thesis, University of Toronto, Toronto, Ontario, 35 pp.

Stricker, S.J., 1978. The Kirkland - Larder Lake stratiform carbonatite. Mineralium Deposita, 13, 355-367.

Thomson, E., 1941. The mineralogy of the Kerr Addison ore, Larder Lake, Ontario. In: Contributions to Canadian Mineralogy 1941, University of Toronto Geological Series no. 46: 141-147.

Thomson, I., 1980. Gamma ray mapping of alteration zones associated with gold-bearing horizons : orientation studies at the Kerr Addison Mine, Virginiatown, district of Timiskaming. In: Summary of Fieldwork, 1980, Ontario Geological Survey Miscell. Paper 96: 145-149.

Thomson, J.E., 1941. Geology of McGarry and McVittie Townships, Larder Lake area. Ontario Department of Mines Annual Reports, 50, Part 7: 1-99; Maps 50a (1 inch to 1000 ft) McGarry Township; 50b (1 inch to 1000 ft) McVittie Township; 50d (1 inch to 400 ft) Kerr Addison and Chesterville mines.

Thomson, J.E., 1946. The Keewatin - Timiskaming unconformity in the Kirkland Lake district. Transactions of the Royal Society of Canada, Section IV, Series 3, 40: 113-122.

Thomson, J.E., 1948. Regional structure of the Kirkland Lake - Larder Lake area. In: Structural Geology of Canadian Ore Deposits, Canadian Inst. Mining and Metallurgy Jubilee Symposium Vol., pp 627-632.

Thomson, J.E. and Griffis, A.T., 1944. Geology of Gauthier Township, East Kirkland Lake area. Ontario Department of Mines, Annual Report, 50, Part 8, pp 1-29.

Tihor, L.A. and Crocket, J.H., 1976. Origin and distribution of gold-bearing carbonate zones of the Kirkland Lake - Larder Lake area, Ontario. In: Report of Activities, Part A, Geol. Survey of Canada Paper 1976-1A: 407-408.

Tihor, L.A. and Crocket, J.H., 1977. Gold distribution in the Kirkland Lake - Larder Lake area, with emphasis on Kerr Addison-type ore deposits - a progress report. In: Report of Activities, Part A, Geol. Survey of Canada Paper 77-1A: 363-369.

Tihor, L.A. and Crocket, J.H., 1978. Lithogeochemical guides to ore at the Kerr Addison gold mine, Ontario. In: J.R. Watterson and P.K. Theobald (Editors), Proceedings of the Seventh International Geochemical Exploration Symposium, Golden, Colorado, 1978, pp 269-275.

Tihor, S. L., 1978. The mineralogical composition of the carbonate rocks of the Kirkland Lake - Larder Lake Gold Camp. Unpubl. M.Sc. Thesis, McMaster University, Hamilton, Ontario, 93 pp.

Toogood, D.J., 1986a. Regional geology of the Abitibi belt in the vicinity of the Kirkland Lake - Larder Lake gold camps. In: Abitibi Belt - Timmins to Larder Lake, Gold '86 Excursion Guidebook, Toronto, pp 46-47.

Toogood, D.J., 1986b. McBean Mine and Kirkland Lake - Larder Lake Break. In: Abitibi Belt - Timmins to Larder Lake, Gold '86 Excursion Guidebook, Toronto, pp 48-49.

Toogood, D.J., 1989. The relationship between structure and Au mineralisation at the Upper Canada Mine, Dobie, N. Ontario; internal report, Queenston Mines Ltd., Kirkland Lake, Ontario.

Toogood, D.J. and Hodgson, C.J., 1985. A structural investigation between the Kirkland Lake and Larder Lake gold camps. In: J. Wood et al. (Editors), Ontario Geoscience Research Grant Program, Summary of Research 1984-85, Ontario Geological Survey Miscell. Paper 119: 200-204.

Toogood, D.J., and Hodgson, C.J., 1986. Relationship between gold deposits and the tectonic framework of the Abitibi greenstone belt in the Kirkland Lake - Larder Lake area. In: V.G. Milne (Editor), Ontario Geoscience Research Grant Program, Summary of Research 1985-86, Ontario Geological Survey Miscell. Paper 130: 79-86.

Tourigny, G., Hubert, C., Brown, A.C. and Crépeau, R., 1988. Structural geology of the Blake River Group at the Bousquet mine, Abitibi, Quebec. *Can. Journ. Earth Sci.*, 25: 581-592.

Trowell, N.F., 1980. Kirkland Lake area, stratigraphic mapping, district of Timiskaming. In: V.G. Milne et al. (Editors), Summary of Fieldwork 1980, Ontario Geological Survey Miscell. Paper 96: 99-100.

Ujike, O., 1984. Chemical composition of Archean Pontiac metasediments, southwestern Abitibi belt, Superior Province. *Can. Journ. Earth Sci.*, 21: 727-730.

Ujike, O., 1985. Geochemistry of Archean alkalic volcanic rocks from the Crystal Lake area, east of Kirkland Lake, Ontario, Canada. *Earth Planet. Sci. Lett.*, 73: 333-344.

Walsh, J.F., Cloke, P.L. and Kesler, S.E., 1984. Fluid (H<sub>2</sub>O - CO<sub>2</sub>) immiscibility and fO<sub>2</sub> as factors in gold deposition: Pamour No.1 mine, Timmins, Ontario. *Geol. Soc. of America Program with Abstracts*, 16: p 686.

Walther, J.V. and Helgeson, H.C., 1977. Calculation of the thermodynamic properties of aqueous silica and the solubility of quartz and its polymorphs at high pressures and temperatures. *Am. J. Sci.* 277: 1315-1351.

Warwick, M., 1981. Gold mineralisation of the flow ores at Kerr Addison Mine. Unpubl. B.Sc. Thesis, University of Western Ontario, Waterloo, Ontario, 101 pp.

Werniuk, G.M., 1979. The protolith of the carbonate rich rocks of the Larder Lake Break. Unpubl. B.Sc. Thesis, McMaster University, Hamilton, Ontario, 58 pp.

Wilson, G.C. and Rucklidge, J.C., 1986. Lithological features and economic significance of reduced carbonaceous rocks in gold deposits. In: V.G. Milne (Editor), Geoscience Research Grant Program, Summary of Research 1985-86, Ontario Geological Survey Miscell. Paper 130: 177-189.

Wilson, G.C. and Rucklidge, J.C., 1987a. Geology, geochemistry and economic significance of carbonaceous host rocks in gold deposits of the Timmins area. In: V.G. Milne (Editor), Geoscience Research Grant Program, Summary of Research 1986-87, Ontario Geological Survey Miscell. Paper 136: 66-76.

Wilson, G.C. and Rucklidge, J.C., 1987b. Mineralogy and microstructure of carbonaceous gold ores. *Mineralogy and Petrology*, 36: 219-239.

Wilson, M.E., 1910. Larder Lake and eastward. Geological Survey of Canada Summary Report 1909, pp 173-179; Maps 32A "Larder Lake and Opatatika Lake, economic geology" and 31A "Larder Lake".

Wilson, M.E., 1912. Geology and economic resources of the Larder Lake district. Geological Survey of Canada Memoir 17-E, pp1-57.

Wilson, M.E., 1948. Structural features of the Noranda-Rouyn area. In: Structural Geology of Canadian Ore Deposits, CIMM Jubilee Symposium Volume, pp. 672-683.

Wong, L., Davis, D.W., Hanes, J.A., Archibald, D.A., Hodgson, C.J. and Robert, F., 1989. An integrated U-Pb and Ar-Ar geochronological study of the Archean Sigma gold deposit, Val d'Or, Quebec. Geol. Assoc. Canada - Mineral. Assoc. Canada, Program with Abstracts, 14: 45.

Wong, L., Davis, D.W., Krogh, T.E. and Robert, F., 1991. U-Pb zircon and rutile chronology of Archean greenstone formation and gold mineralisation in the Val d'Or region, Quebec. Earth Planet. Sci. Lett., 104: 325-336.

Wood, P.C., Burrows, D.R., Thomas, A.V. and Spooner, E.T.C., 1986a. The Hollinger-McIntyre Au-quartz vein system, Timmins, Ontario, Canada; geologic characteristics, fluid properties and light stable isotope geochemistry. In: A.J. MacDonald (Editor), Proceedings of Gold '86 Symposium, Konsult Internat. Inc., Toronto, Willowdale, Ontario, pp 56-80.

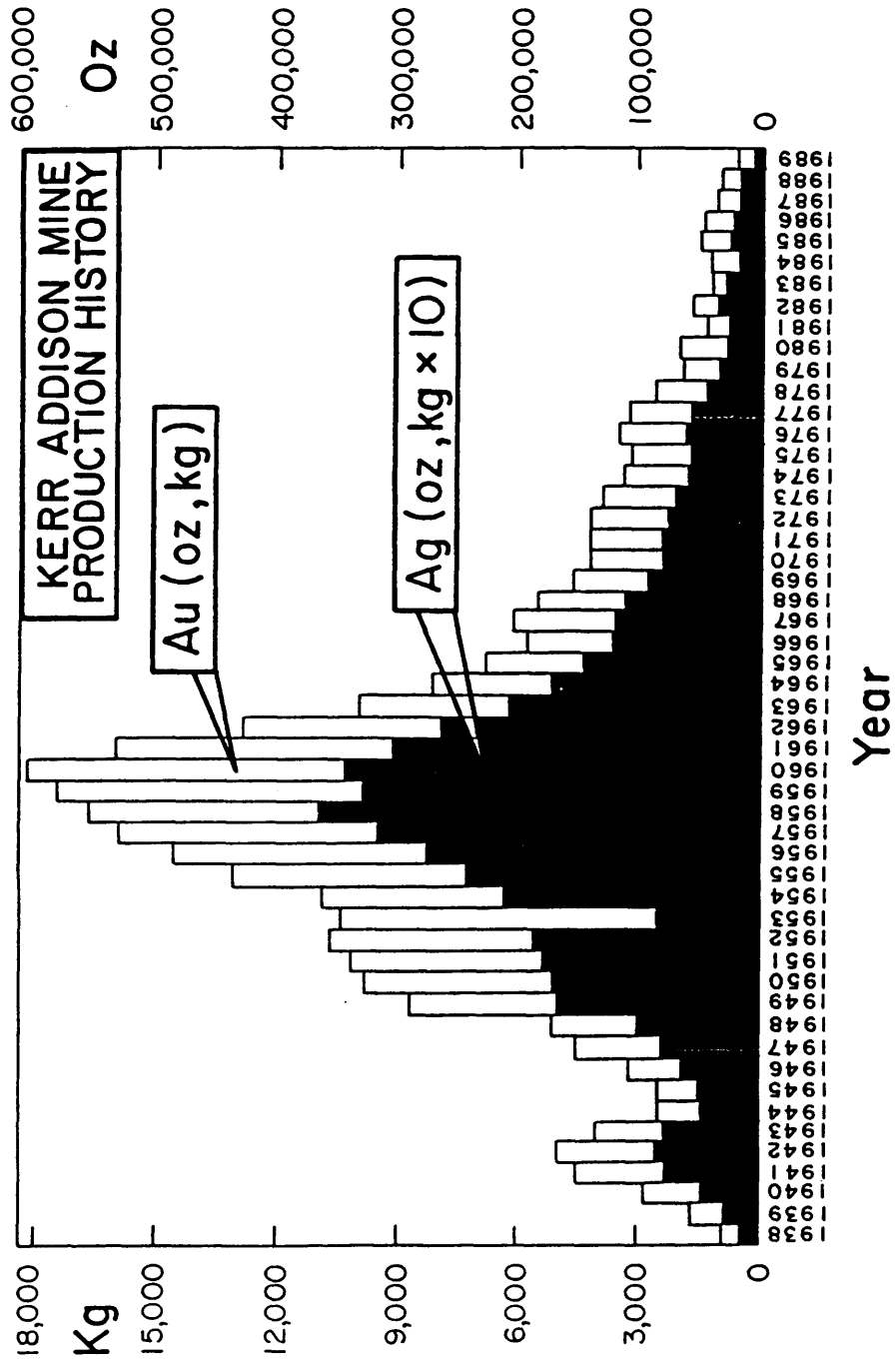
Wood, P.C., Burrows, D.R. and Spooner, E.T.C., 1986b. Au-quartz vein and intrusion-hosted Cu-Au-Ag-Mo mineralisation, Hollinger-McIntyre mines, Timmins, Ontario: geological characteristics, structural examination, igneous and hydrothermal alteration geochemistry, and light stable isotope (hydrogen and oxygen) geochemistry. In: V.G. Milne (Editor), Geoscience Research Grant Program, Summary of Research 1985-86, Ontario Geological Survey Miscell. Paper, 130: 115-137.

Woodall, R., 1988. Gold in 1988. In: Extended Abstracts Oral Programme, Bicentennial Gold '88, Melbourne, Australia, Geological Society of Australia Inc. Abstracts No. 22: 1-12.

Wyman, D. and Kerrich, R., 1988. Alkaline magmatism, major structures and gold deposits: implications for greenstone belt metallogeny. Economic Geology, 83: 454-461.

Wyman, D. and Kerrich, R., 1989. Archean lamprophyre dykes of the Superior Province, Canada: distribution, petrology, and geochemical characteristics. Journal of Geophysical Research 94, no. B4: 4667-4696.

Figure 2



1989  
1988  
1987  
1986  
1985  
1984  
1983  
1982  
1981  
1980  
1979  
1978  
1977  
1976  
1975  
1974  
1973  
1972  
1971  
1970  
1969  
1968  
1967  
1966  
1965  
1964  
1963  
1962  
1961  
1960  
1959  
1958  
1957  
1956  
1955  
1954  
1953  
1952  
1951  
1950  
1949  
1948  
1947  
1946  
1945  
1944  
1943  
1942  
1941  
1940  
1939  
1938



Figure 3

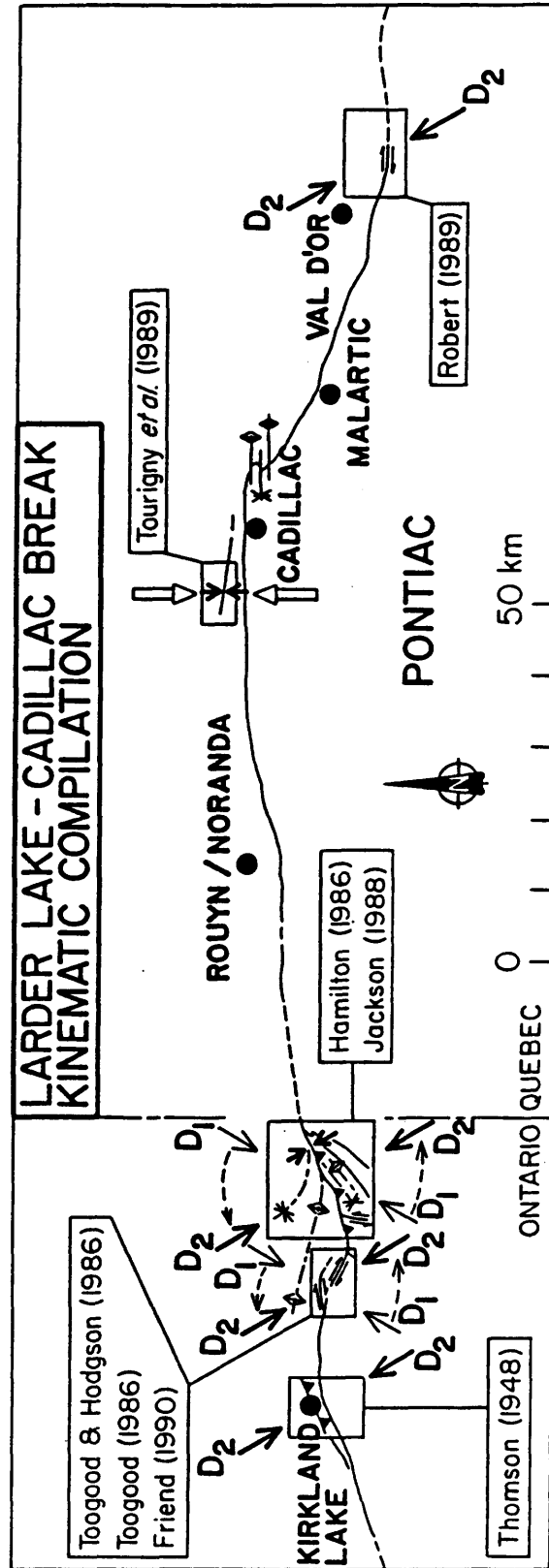




Figure 5

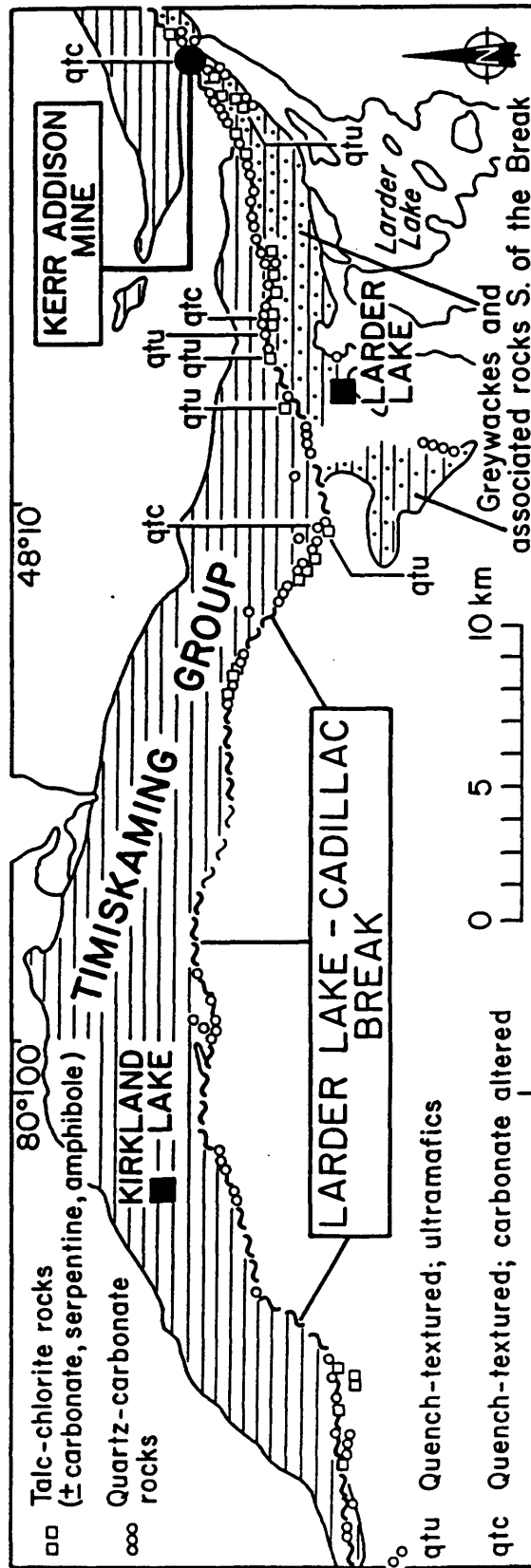


Figure 6

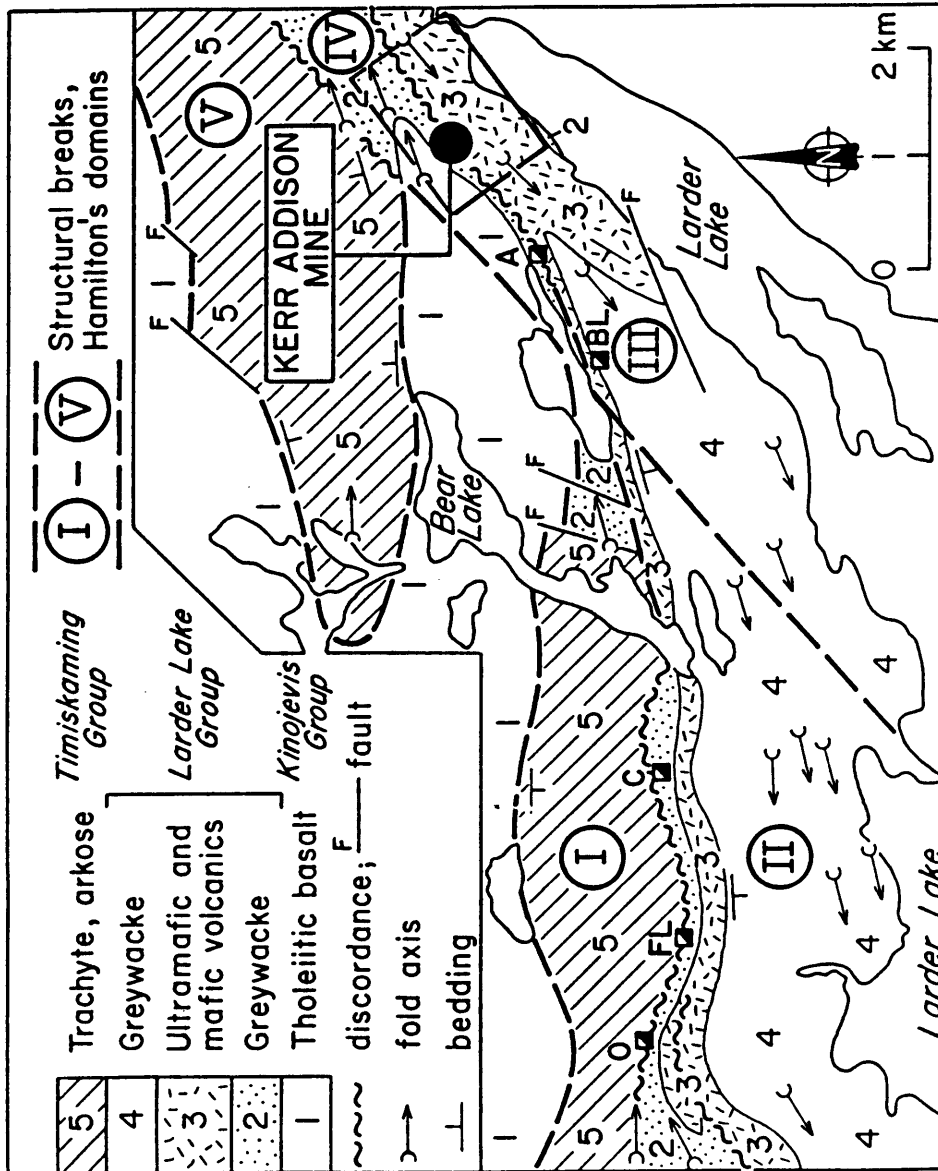


Figure 8

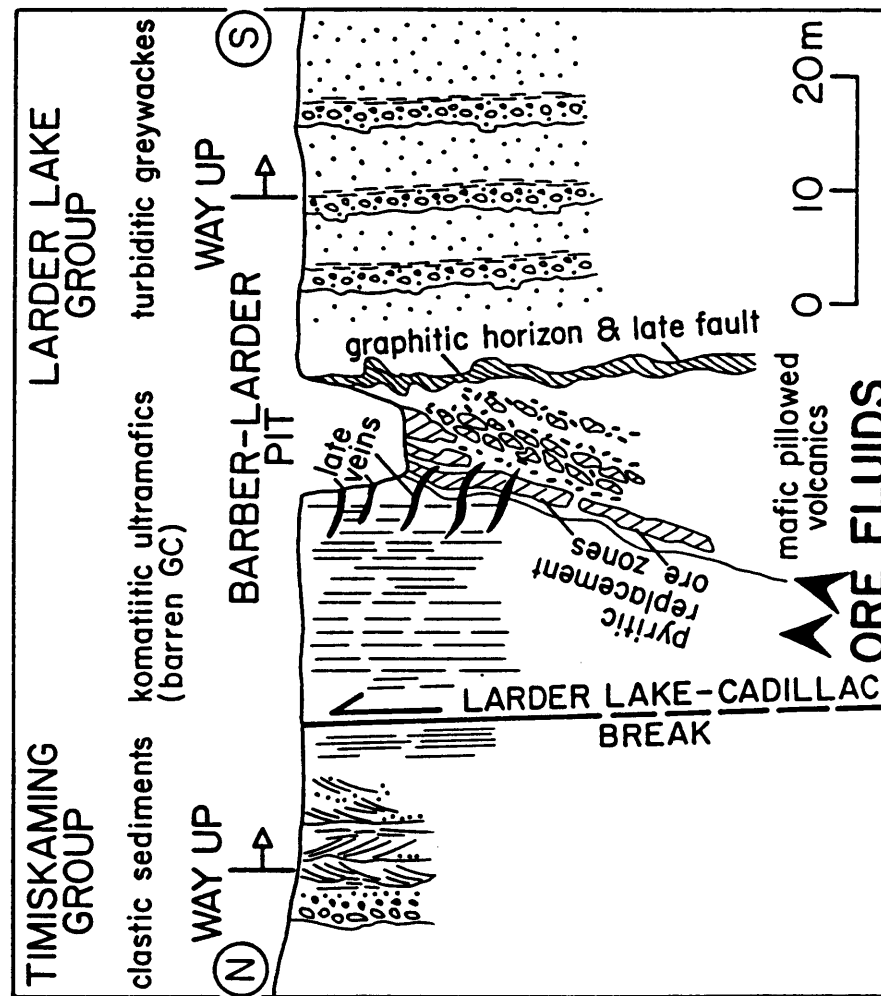


Figure 9

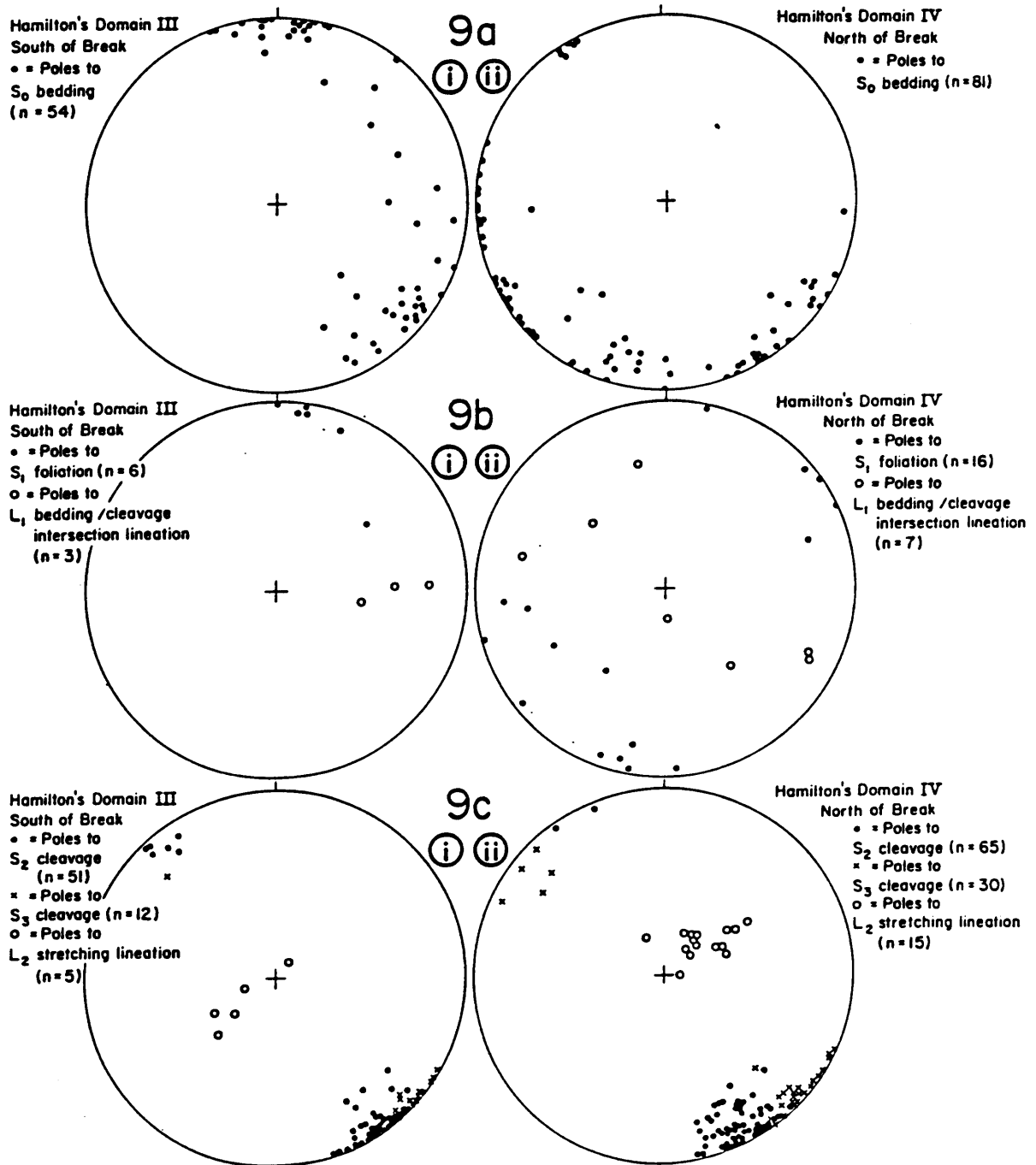


Figure 10 A

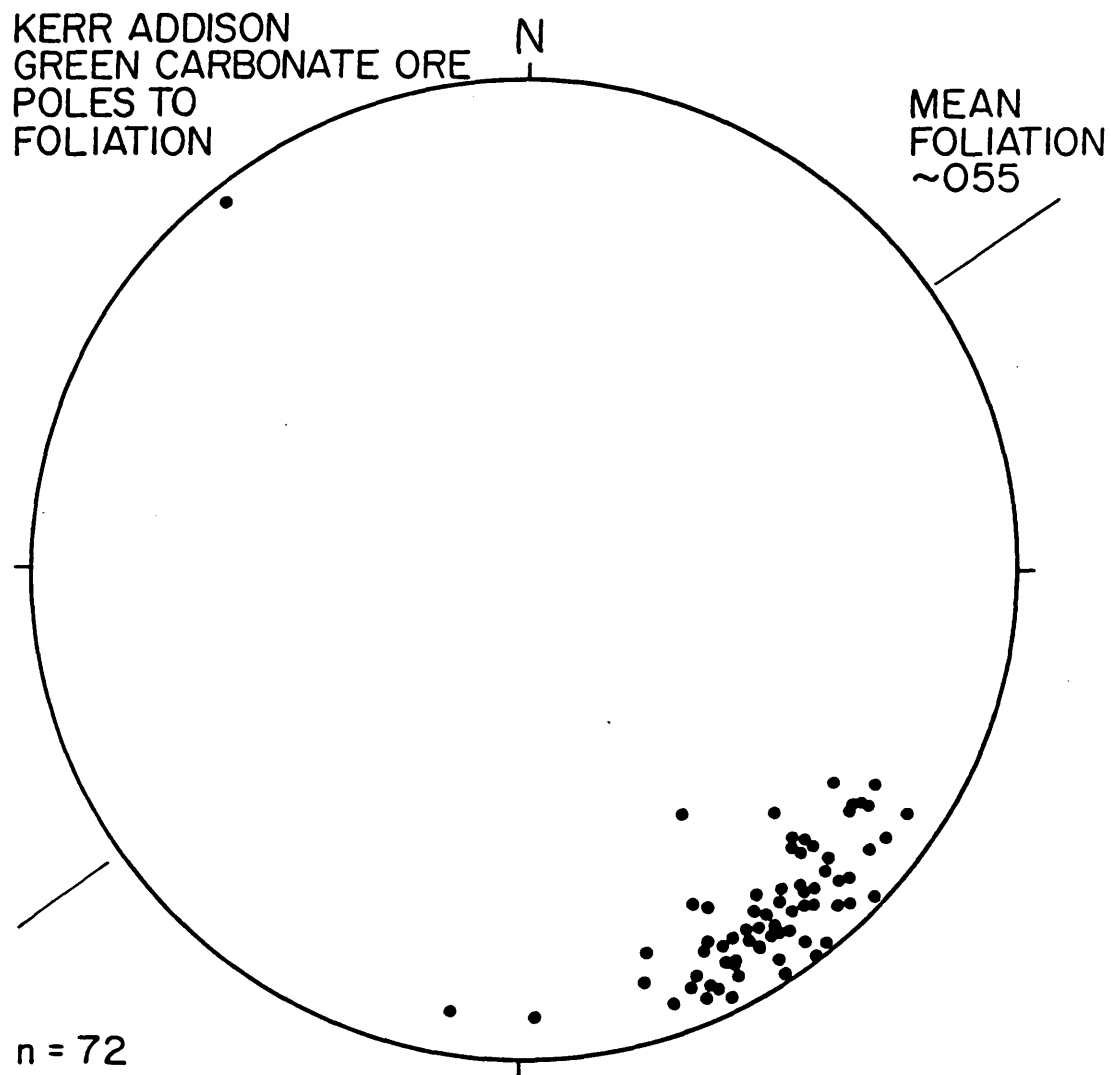


Figure 10 B

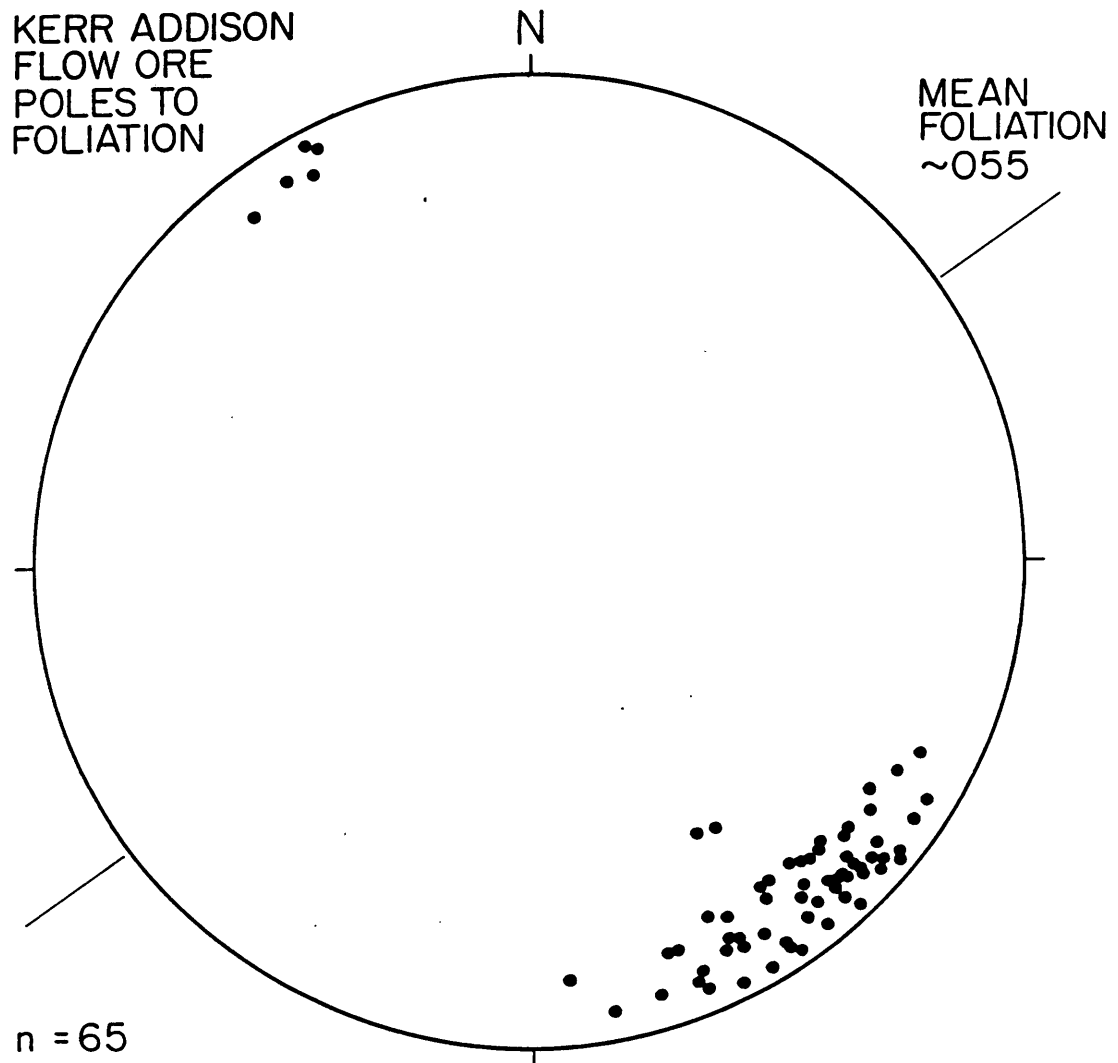




Figure 11

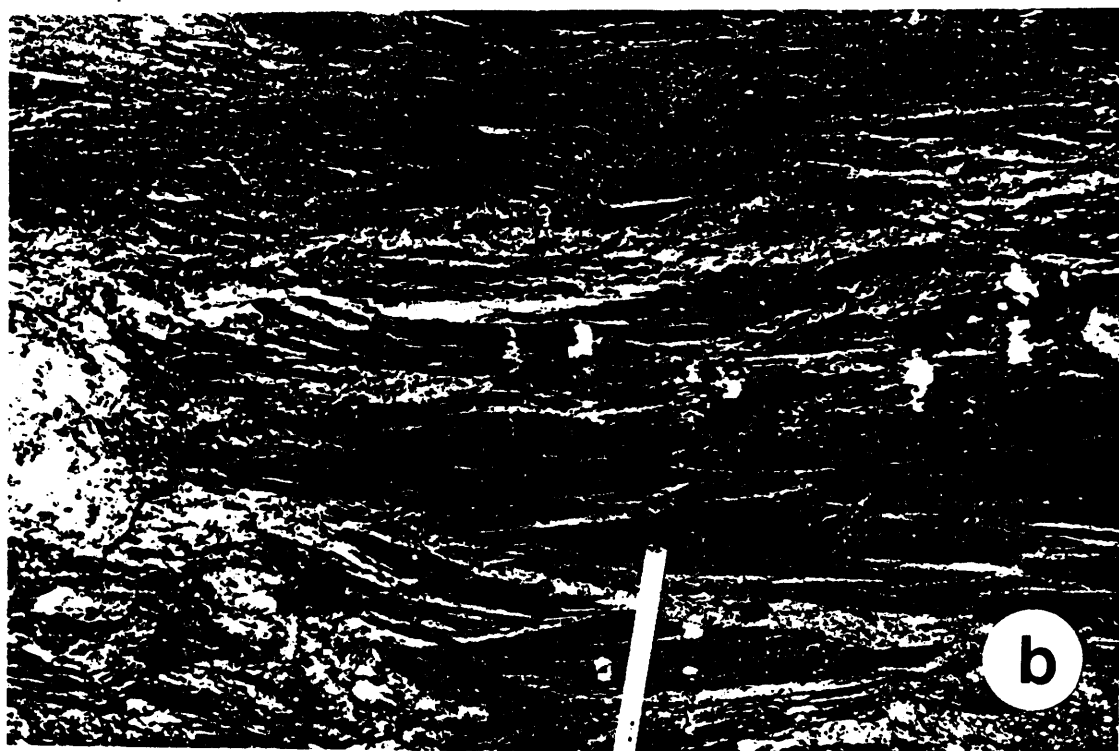
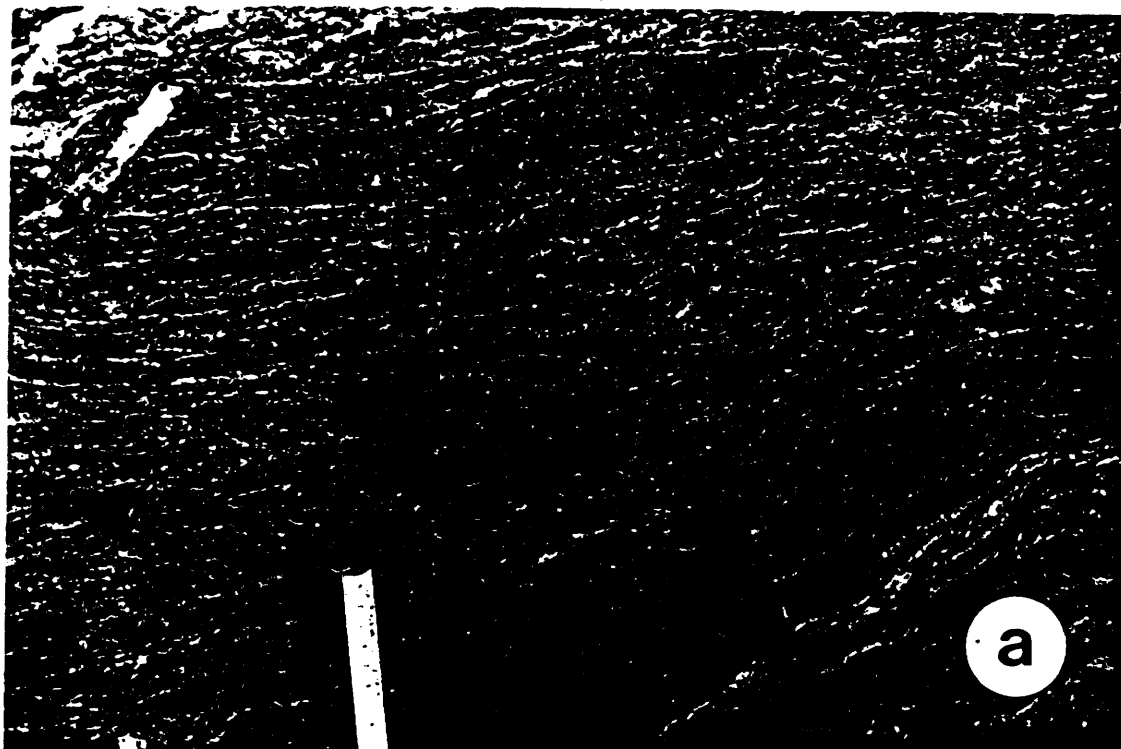


Figure 12



Figure 13



Figure 14



180

Figure 15

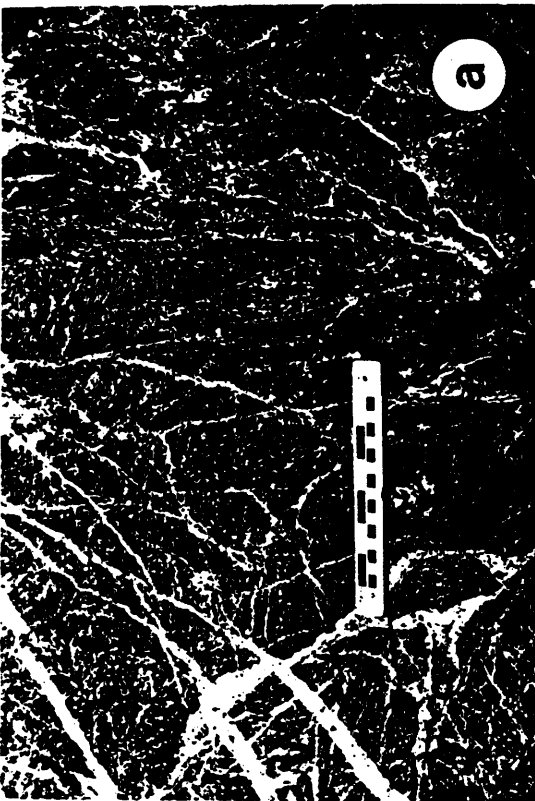
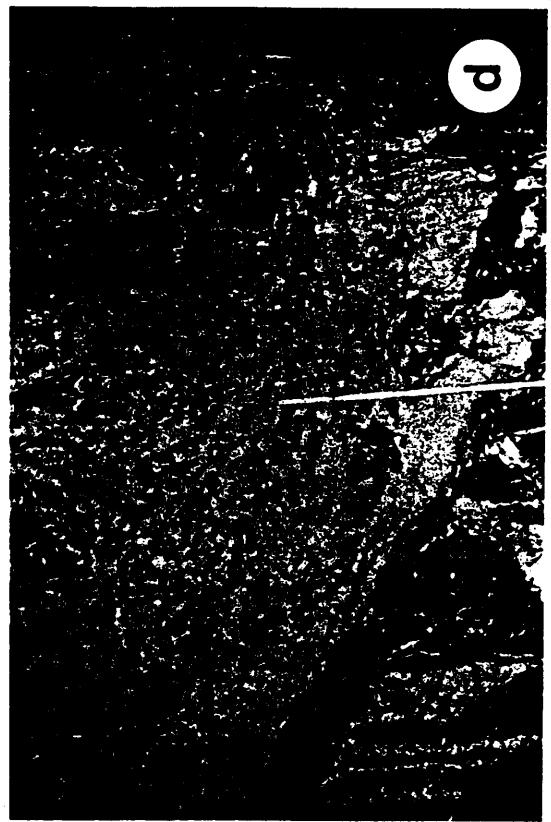
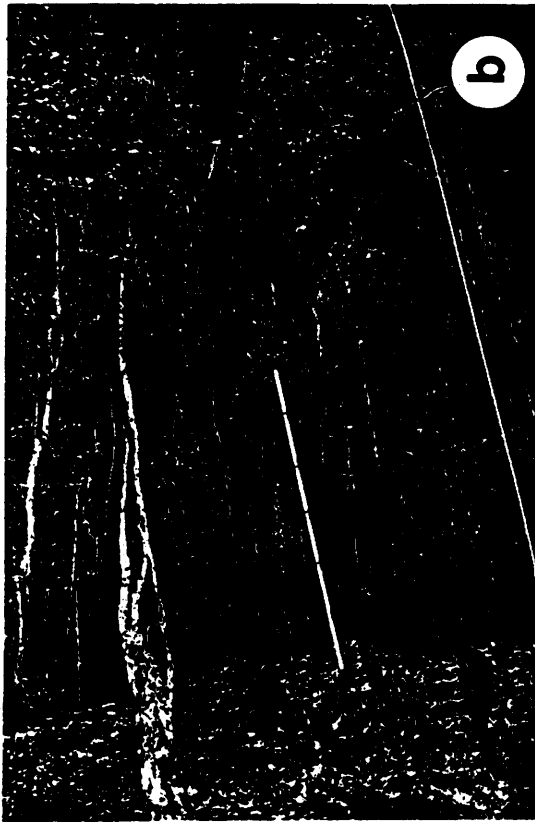


Figure 16

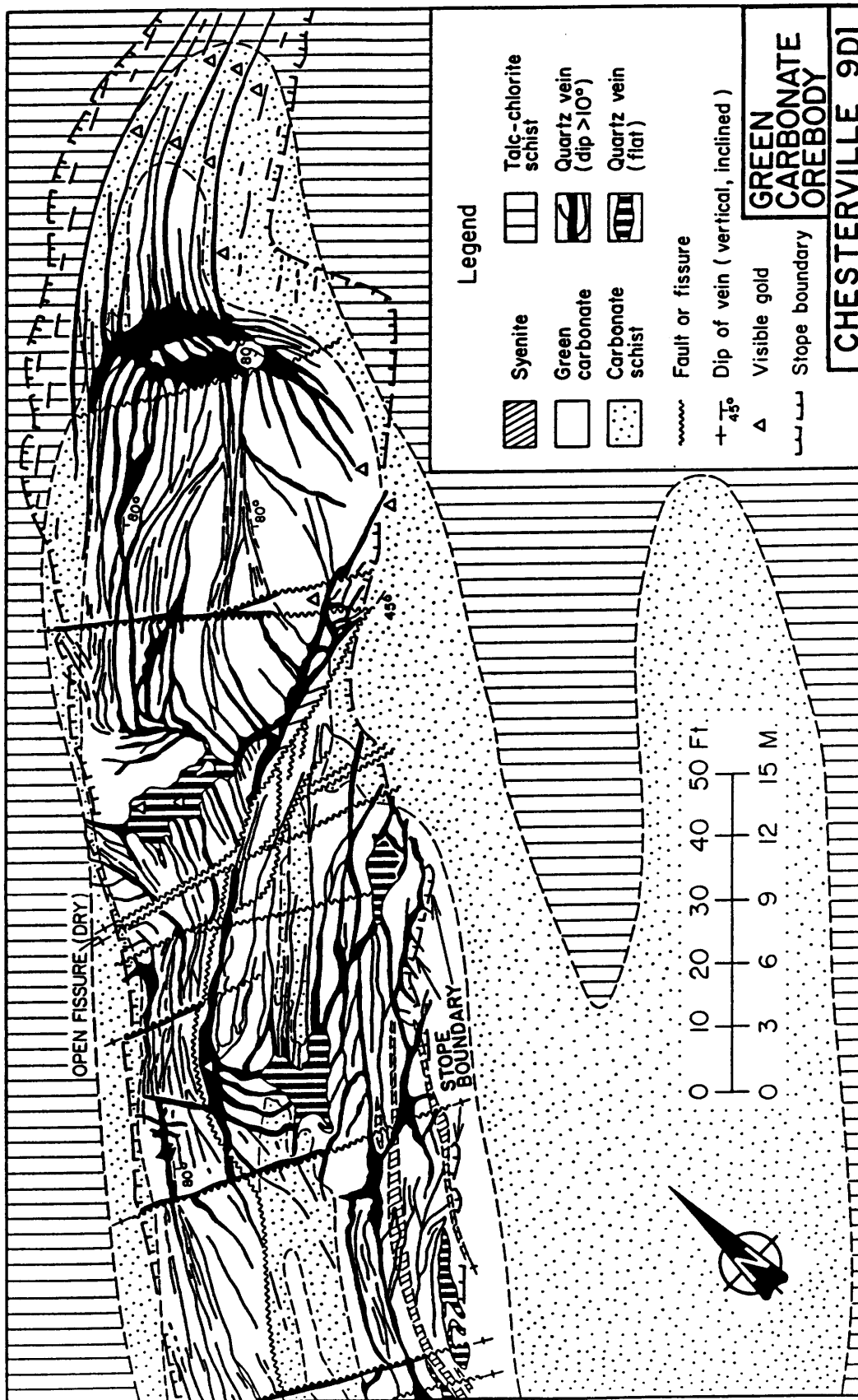


Figure 17

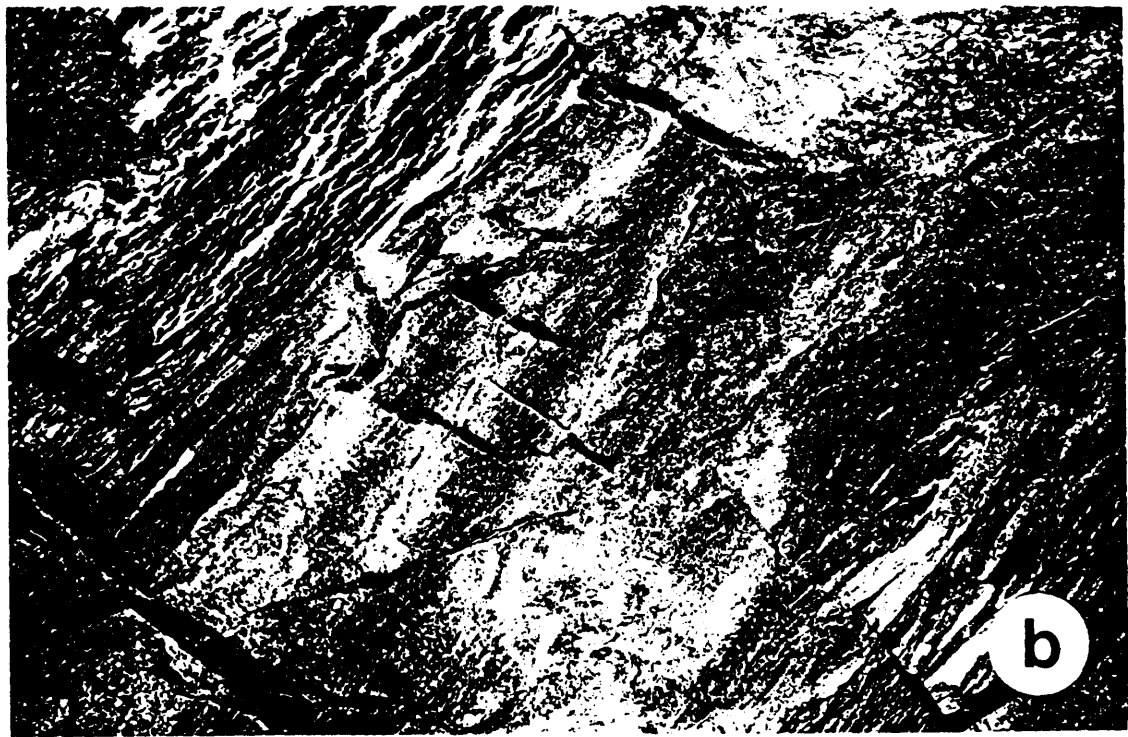
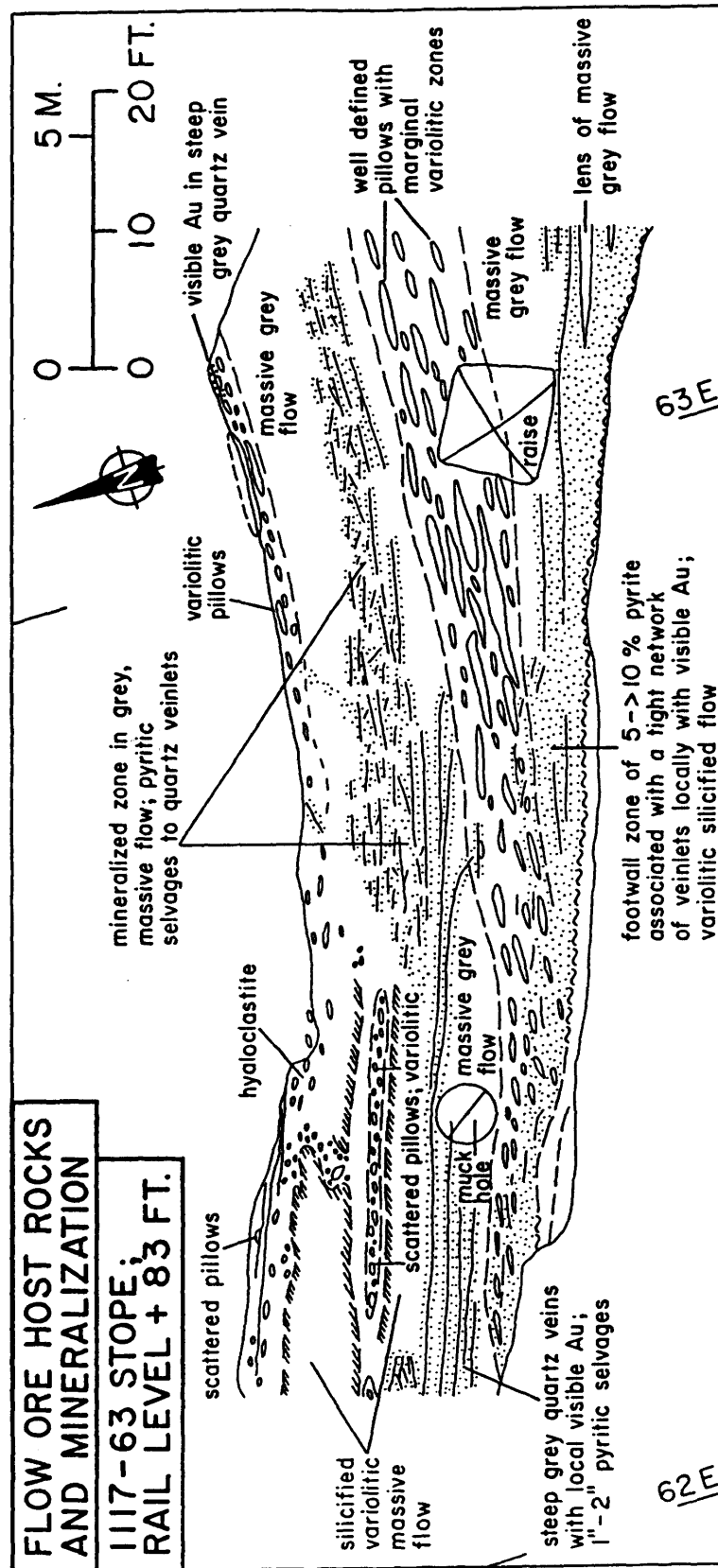


Figure 18







# KEY TO MAPS

## LEGEND






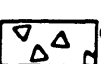
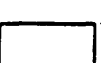
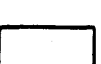



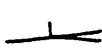

- |   |   |   |                     |
|---|---|---|---------------------|
|    | 1 | SEDIMENTS   | ] TIMISKAMING GROUP |
|    | 2 | MAFIC FLOWS, TUFFS & AGGLOMERATES                                   |                     |
|    | 3 | TRANSITIONAL MAFIC TO ULTRAMAFIC FLOWS                              | ] LARDER LAKE GROUP |
|    | 4 | ULTRAMAFIC FLOWS  |                     |
|    | 5 | SPHERULITIC BASALT MARKER HORIZON (CHESTERVILLE)                    |                     |
|   | 6 | MAFIC FLOWS WITH IN SITU GRAPHITIC MICROBRECCIATION (CHESTERVILLE)  |                     |
|  | 7 | GRAPHITIC INTERFLOW SEDIMENTS                                       |                     |
|  | 8 | BARREN TALC ROCK "HORSES" (PART OF 4)                               |                     |
|  |   | GREEN CARBONATE-ALTERED ULTRAMAFICS (PART OF 4)                     |                     |
|  |   | MAFIC "ALBITITE" DYKES & PLUGS                                      |                     |
|  |   | "SILICEOUS BREAKS" (MAJOR ZONES OF QUARTZ VEINING & SILICIFICATION) |                     |
|  |   | POST-ORE GRAPHITIC/CHLORITIC FAULTS                                 |                     |
|  |   | OLD STOPES (MINED OUT AREAS)  |                     |

Figure 22

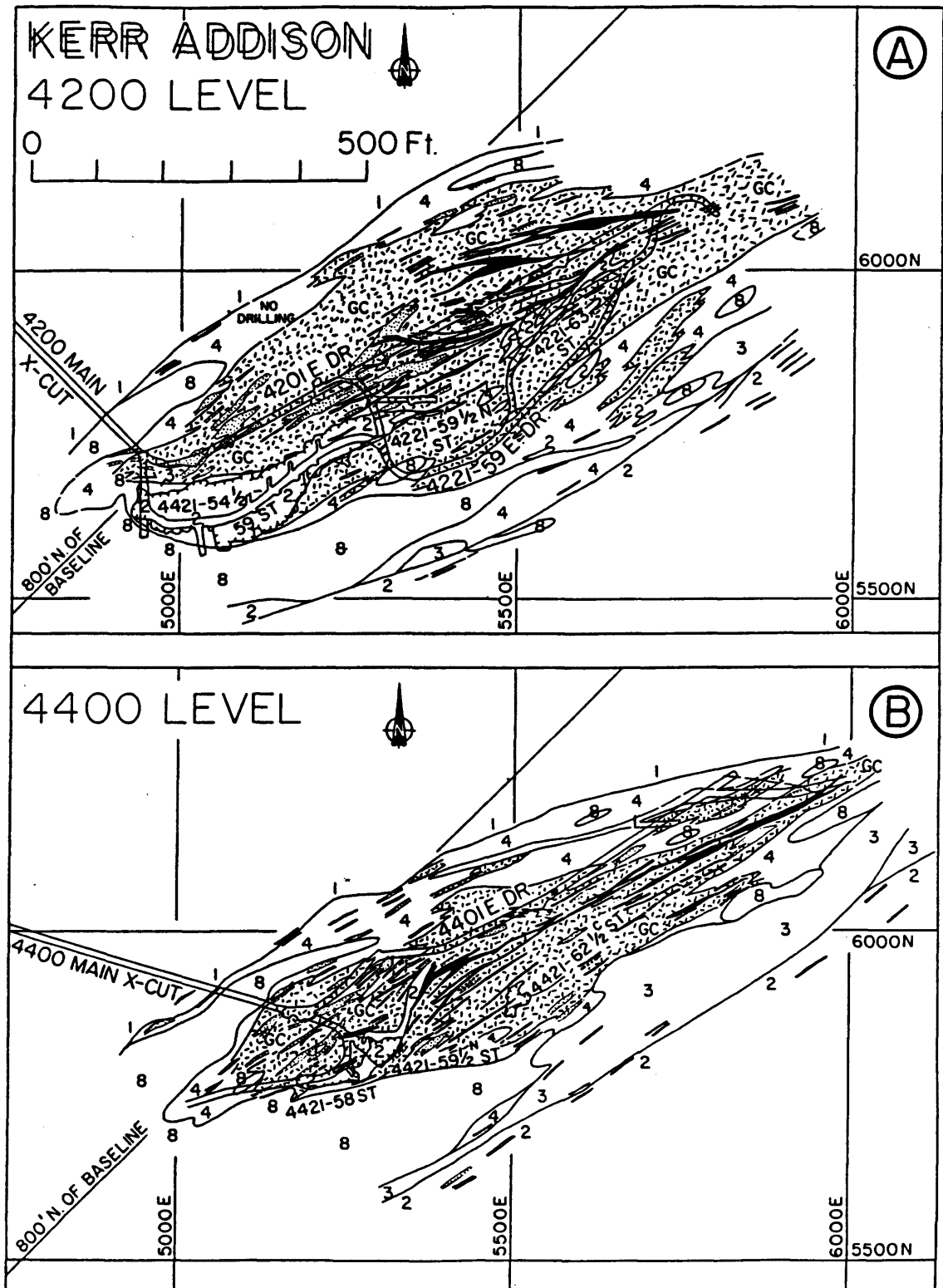


Figure 28

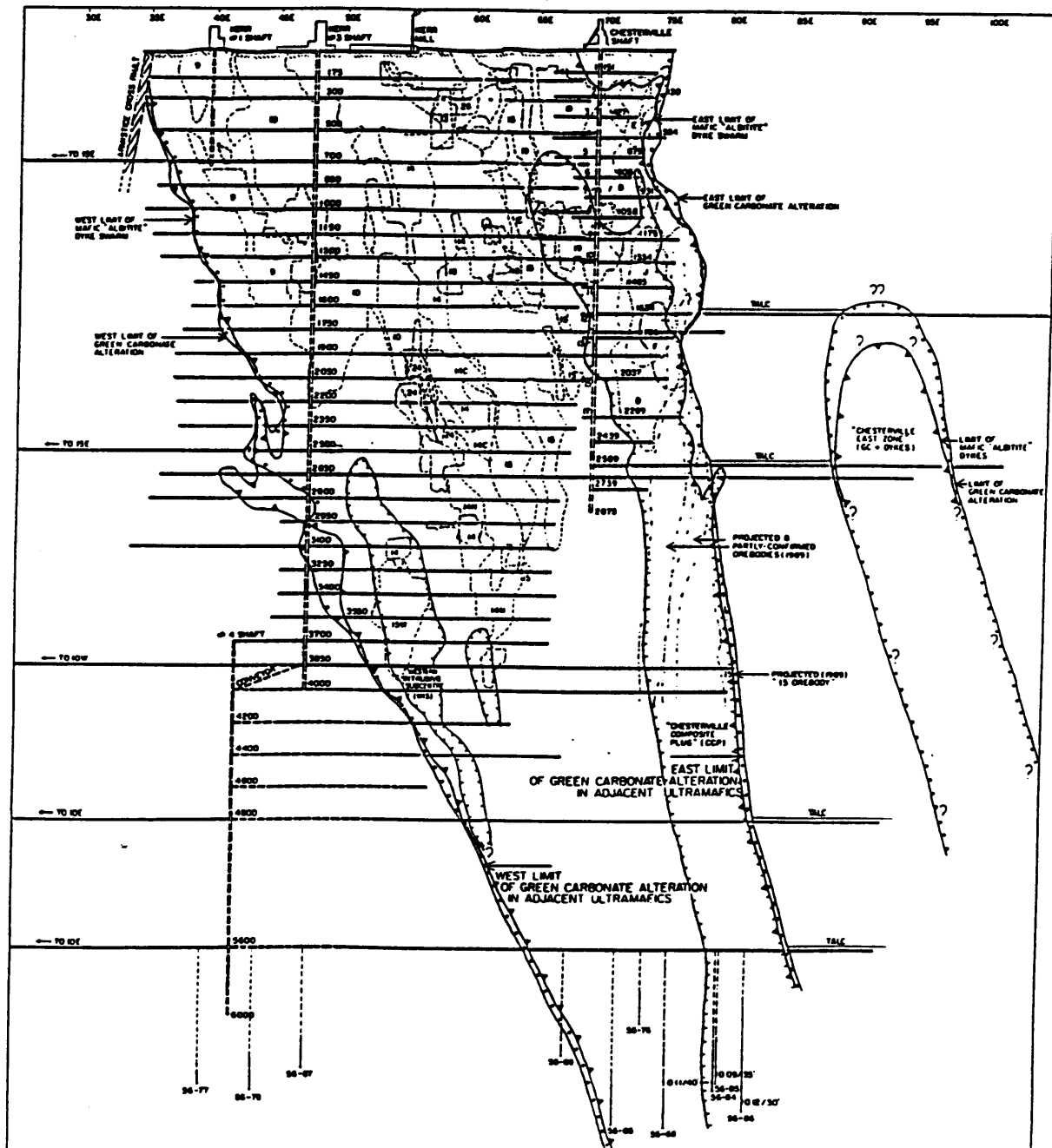


Figure 29

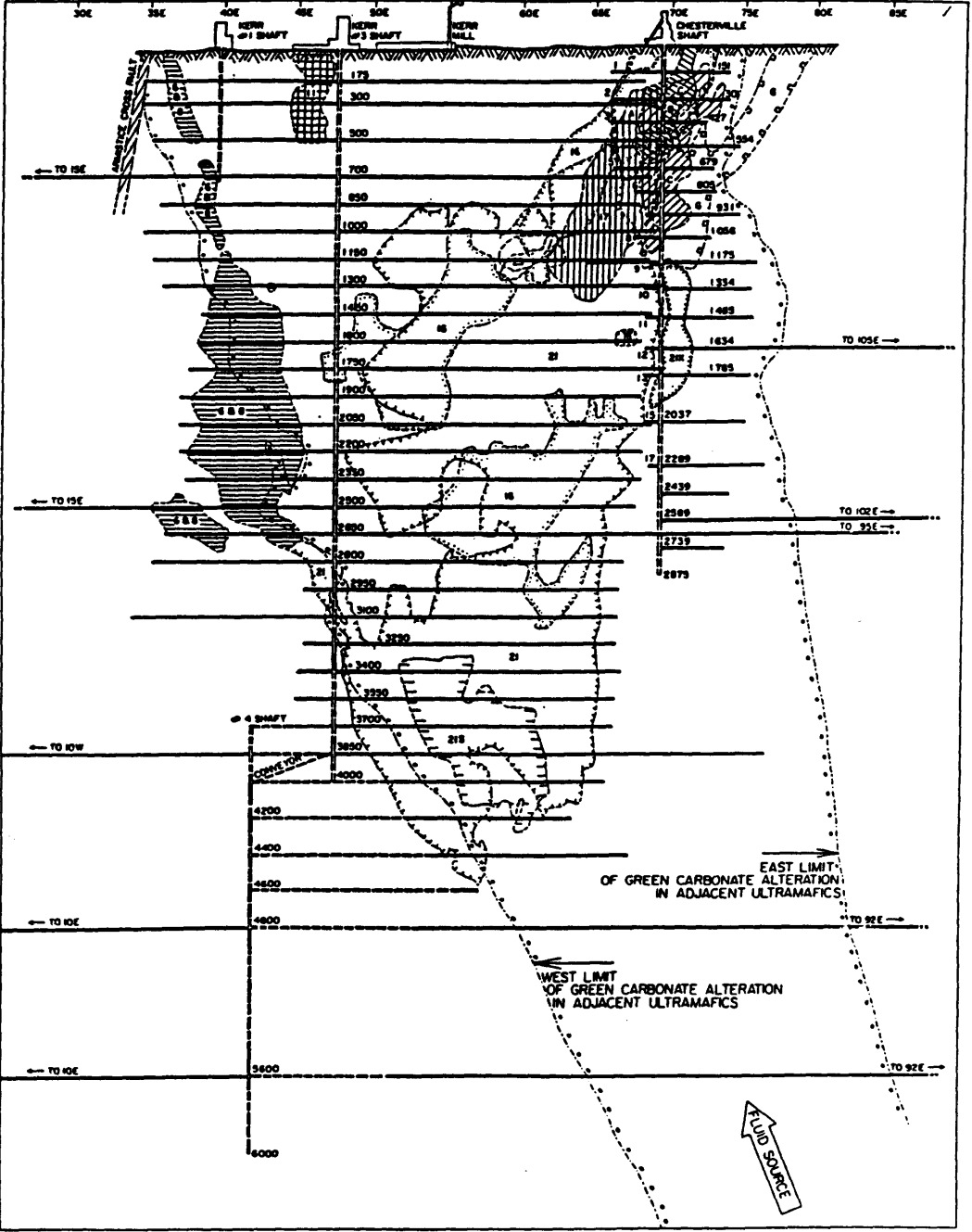
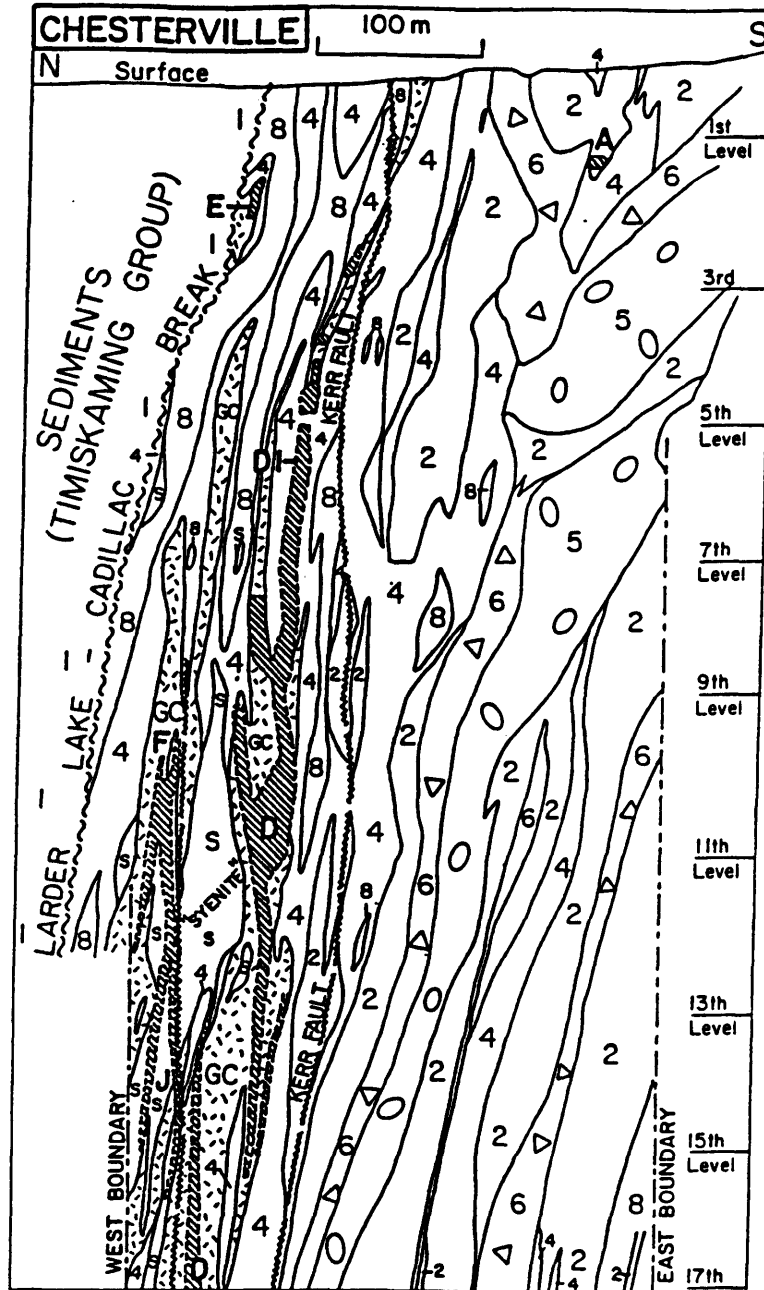


Figure 31



LEGEND


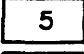
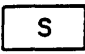
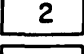
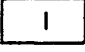
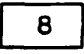
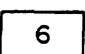
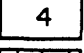
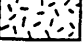
- |   |  |  |                                     |
|---|--|--|-------------------------------------|
|  | ORE BODY AND DESIGNATION               |  | " SPHERULITIC BASALT "              |
|  | INTRUSIVE MATERIAL; "SYENITE"          |  | MAFIC VOLCANICS                     |
|  | SEDIMENTS                              |  | TALC-CHLORITE SCHIST                |
|  | " AGGLOMERATE AND CARBONACEOUS SHALE " |  | " SCHIST "                          |
|   |  |  | GREEN CARBONATE ALTERED ULTRAMAFICS |

Figure 32

# TIME SEQUENCE KERR ADDISON GOLD MINE

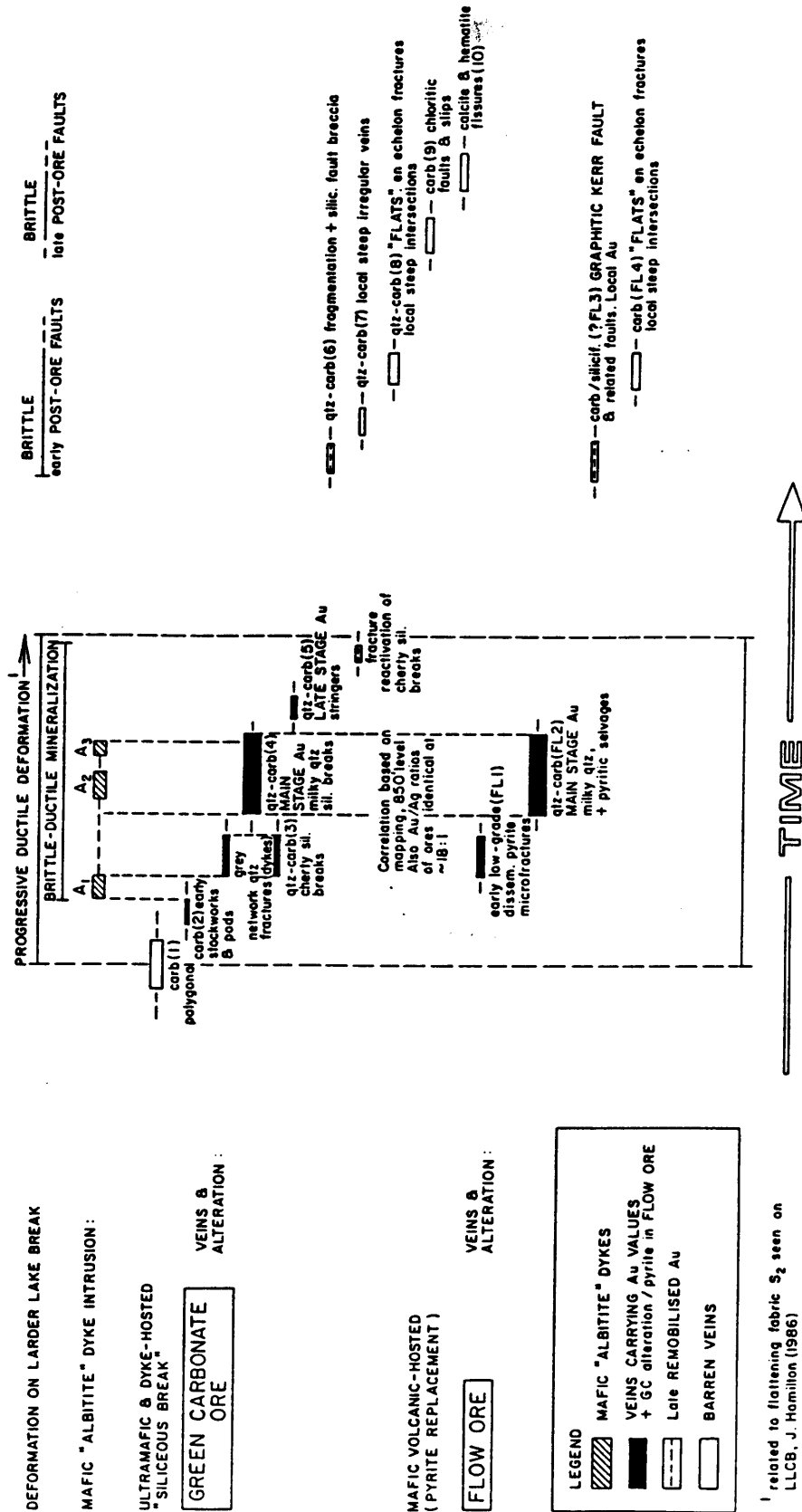


Figure 3 3

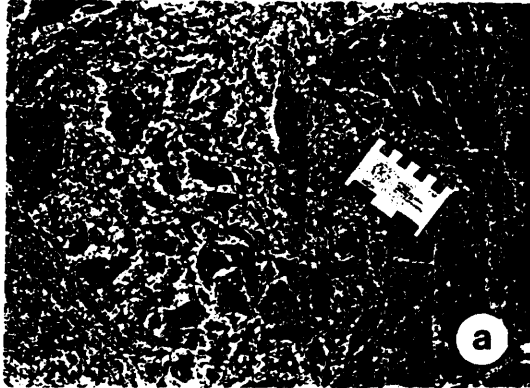




Figure 34A

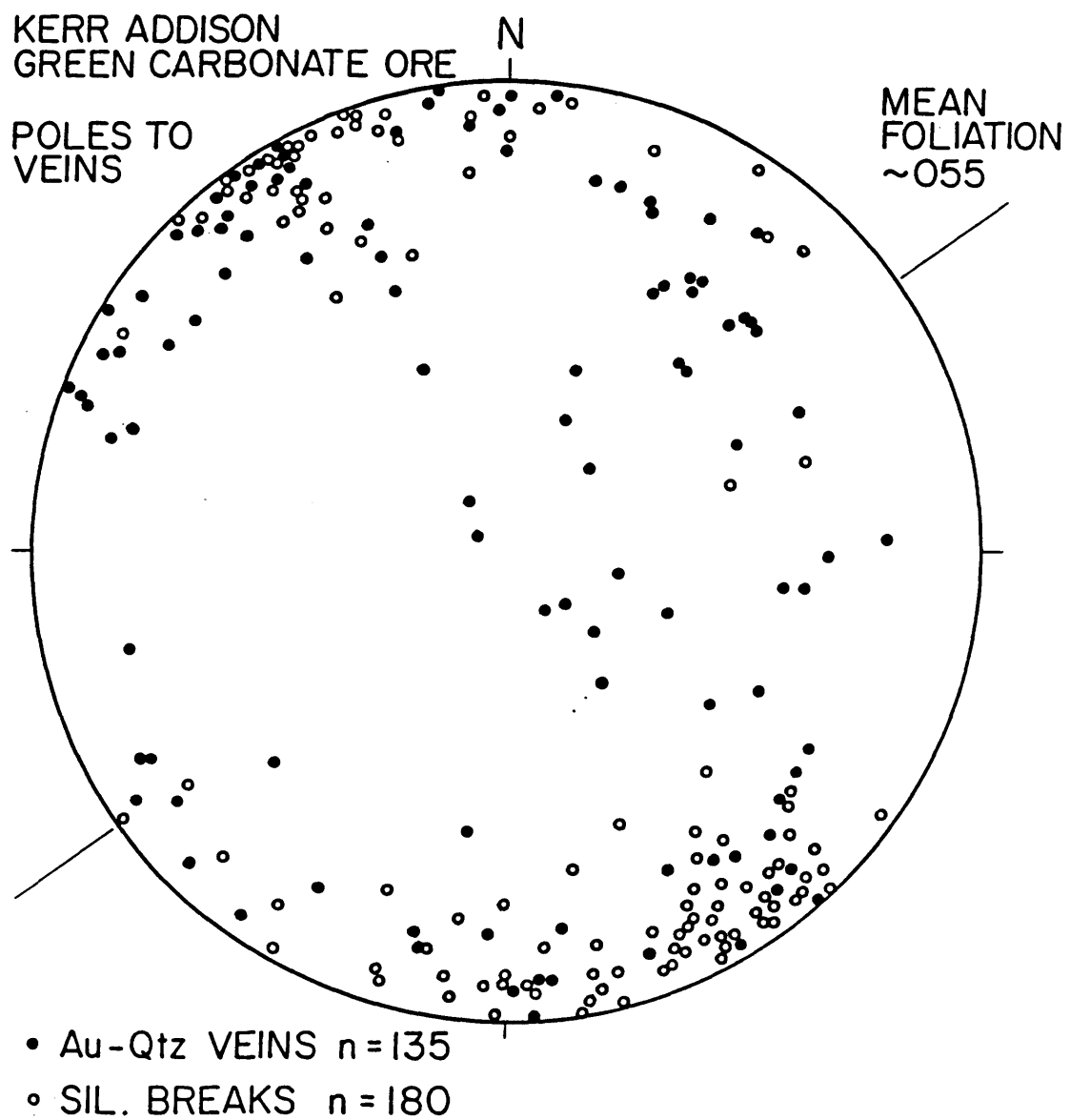


Figure 34B

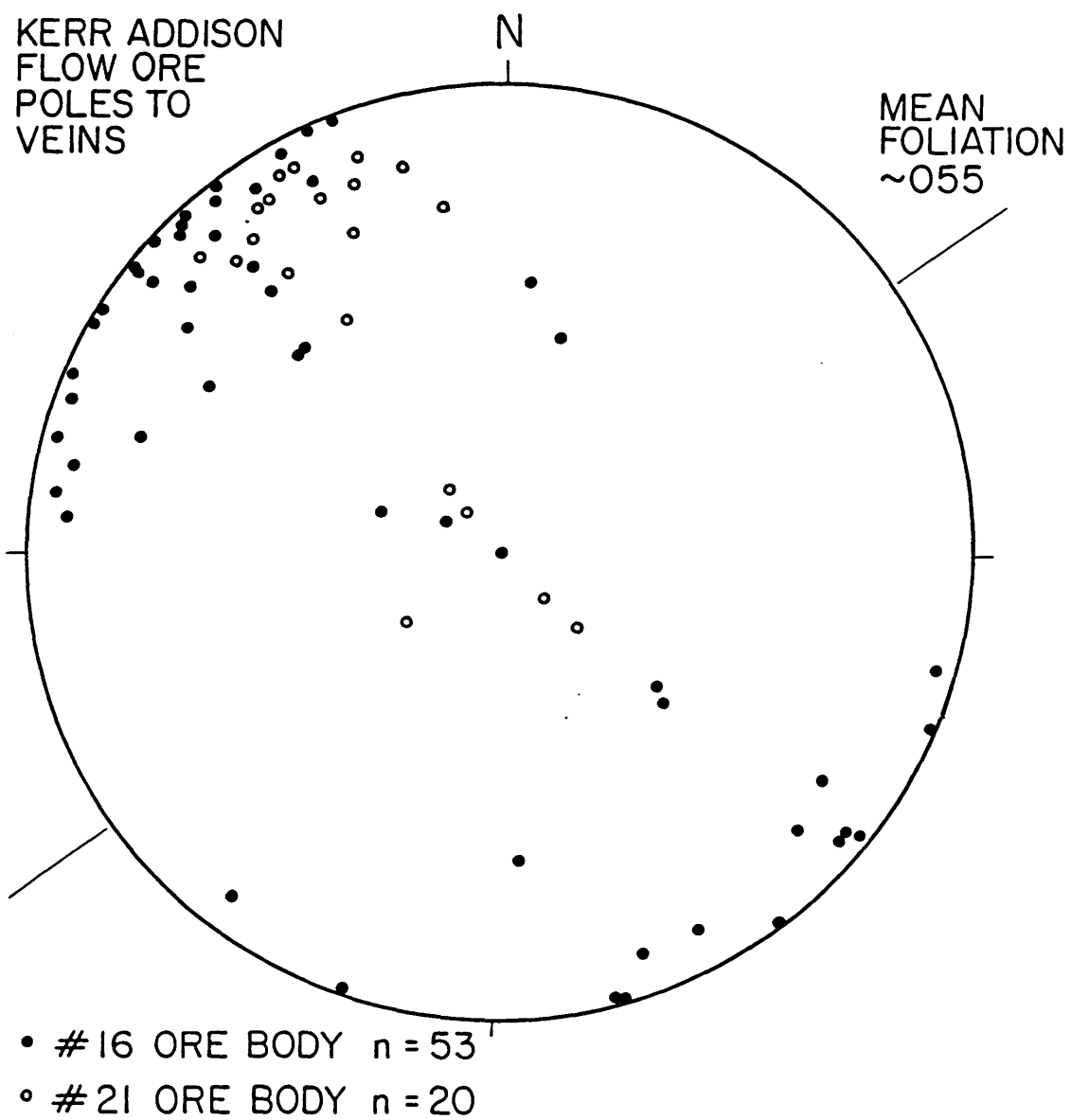


Figure 34C

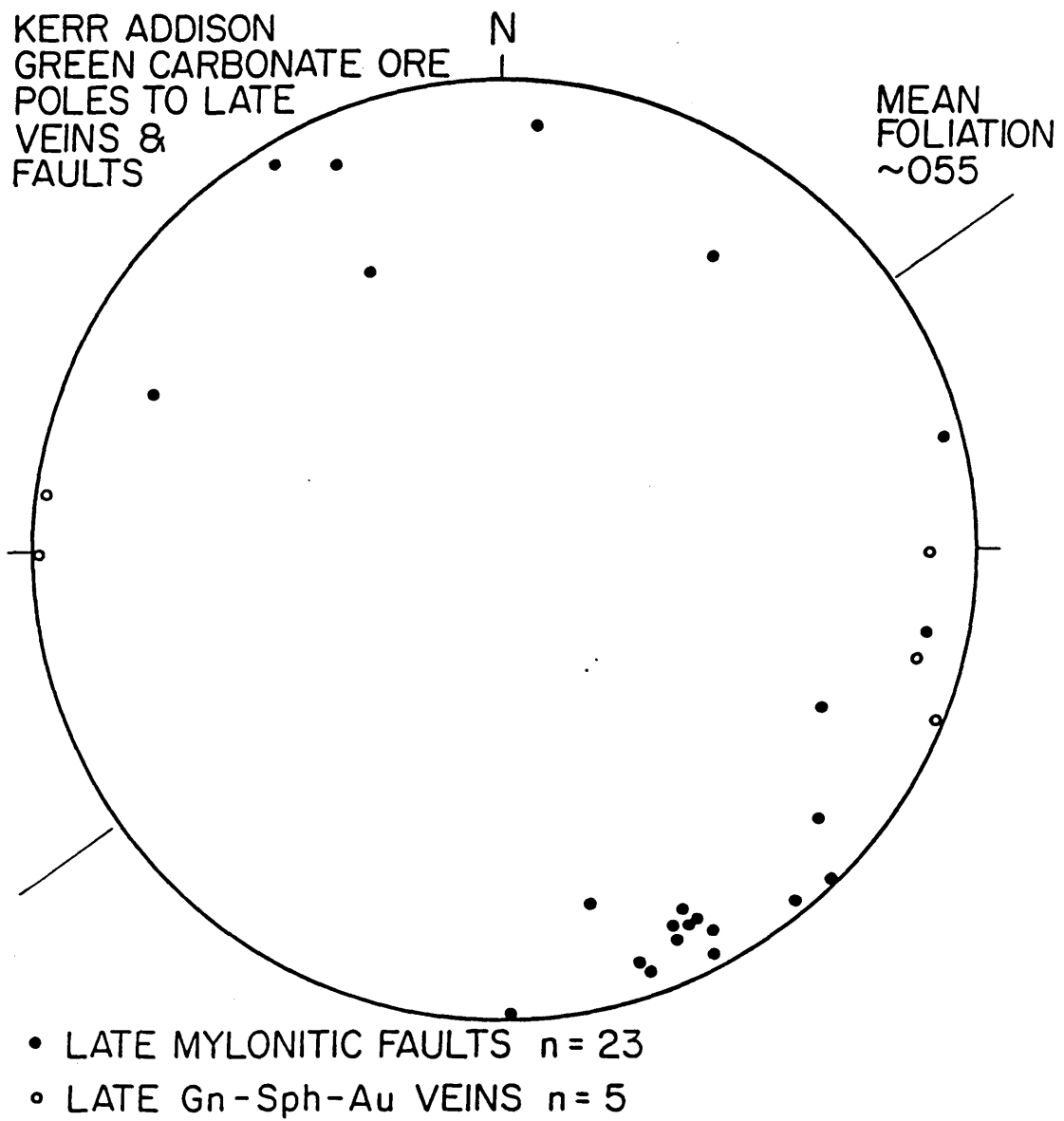


Figure 34 D

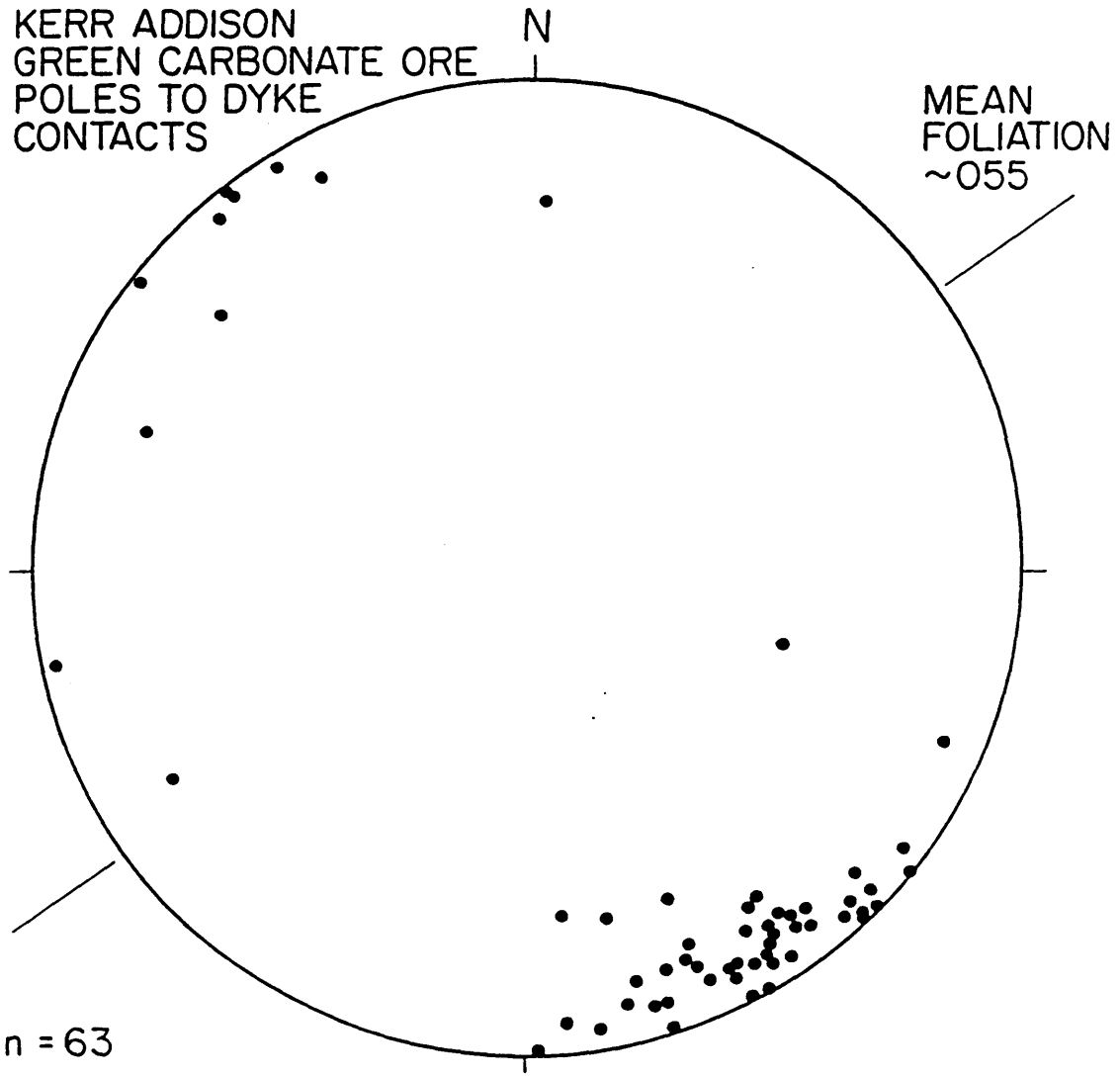


Figure 35

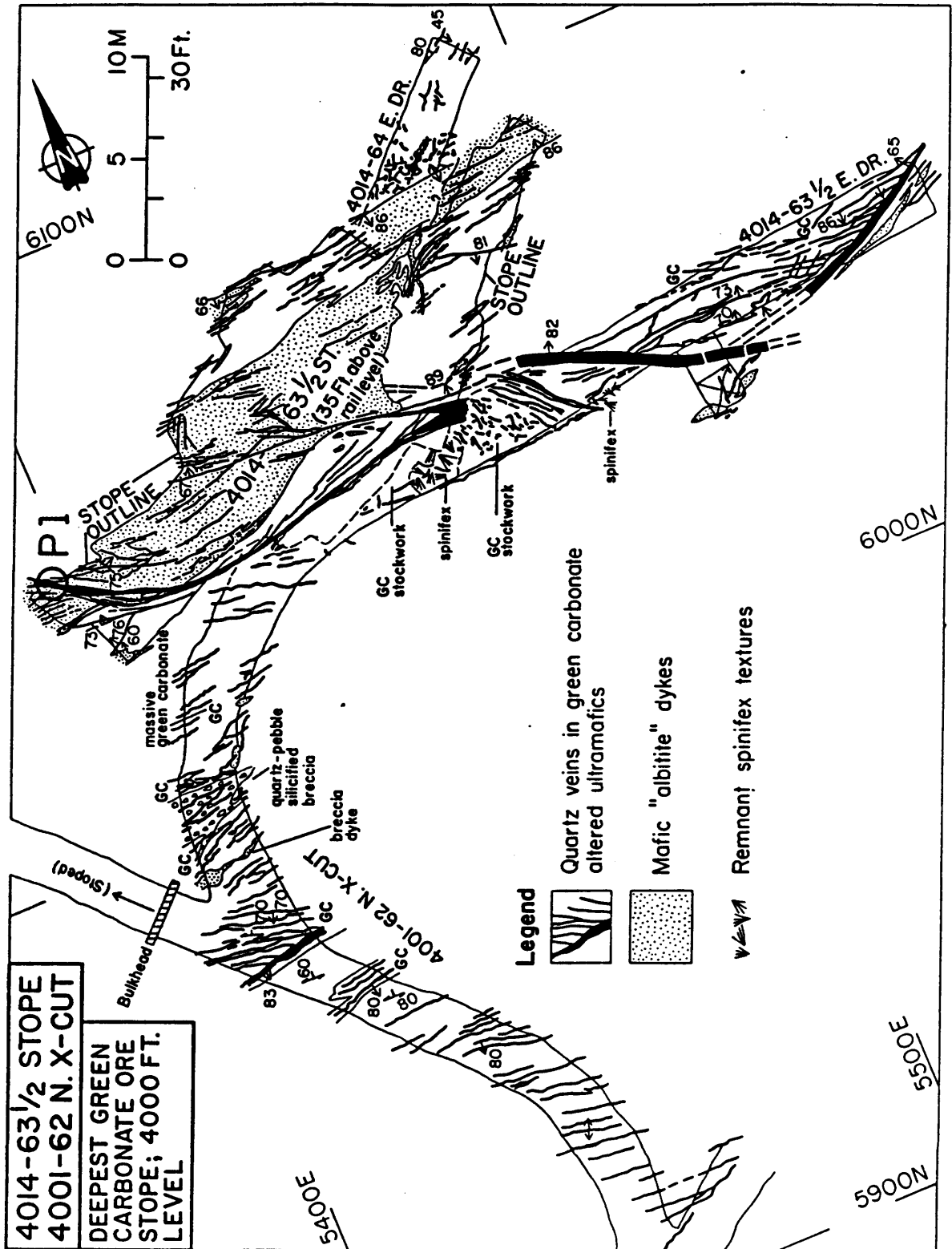


Figure 36

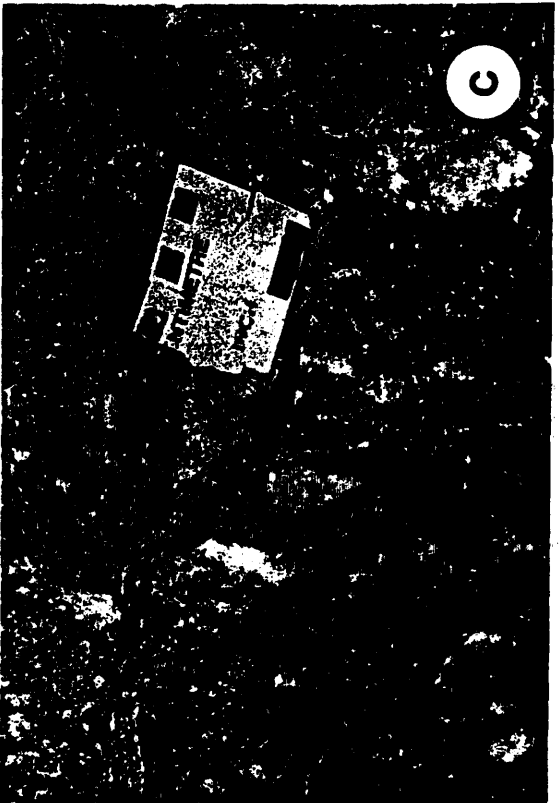
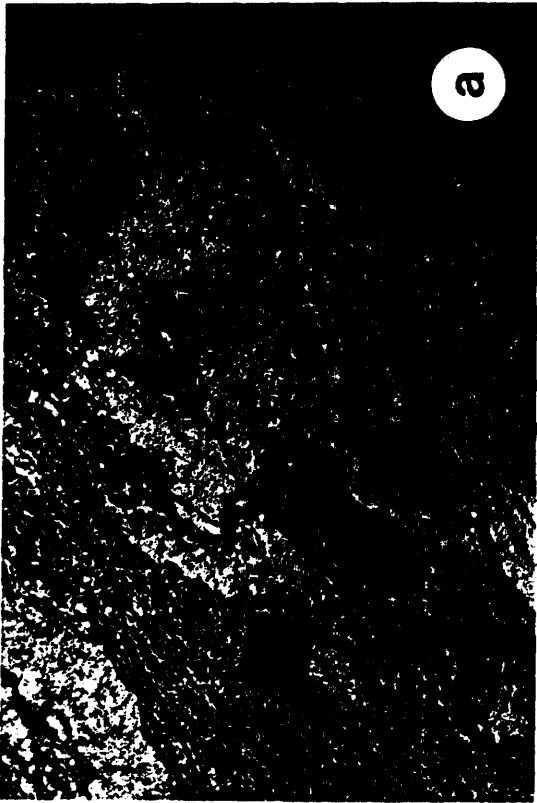


Figure 37

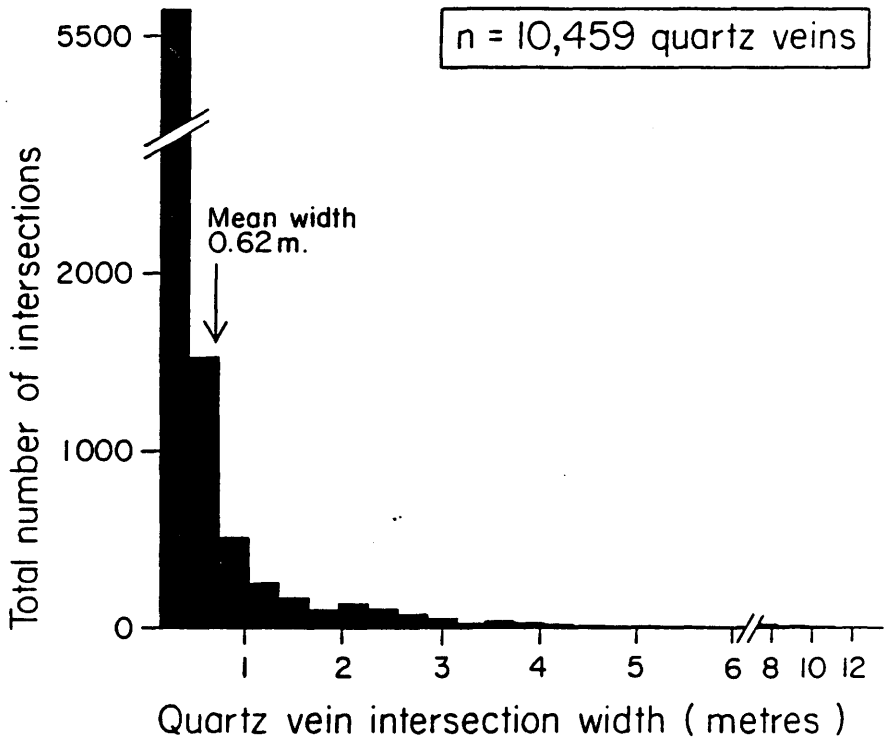


Figure 38

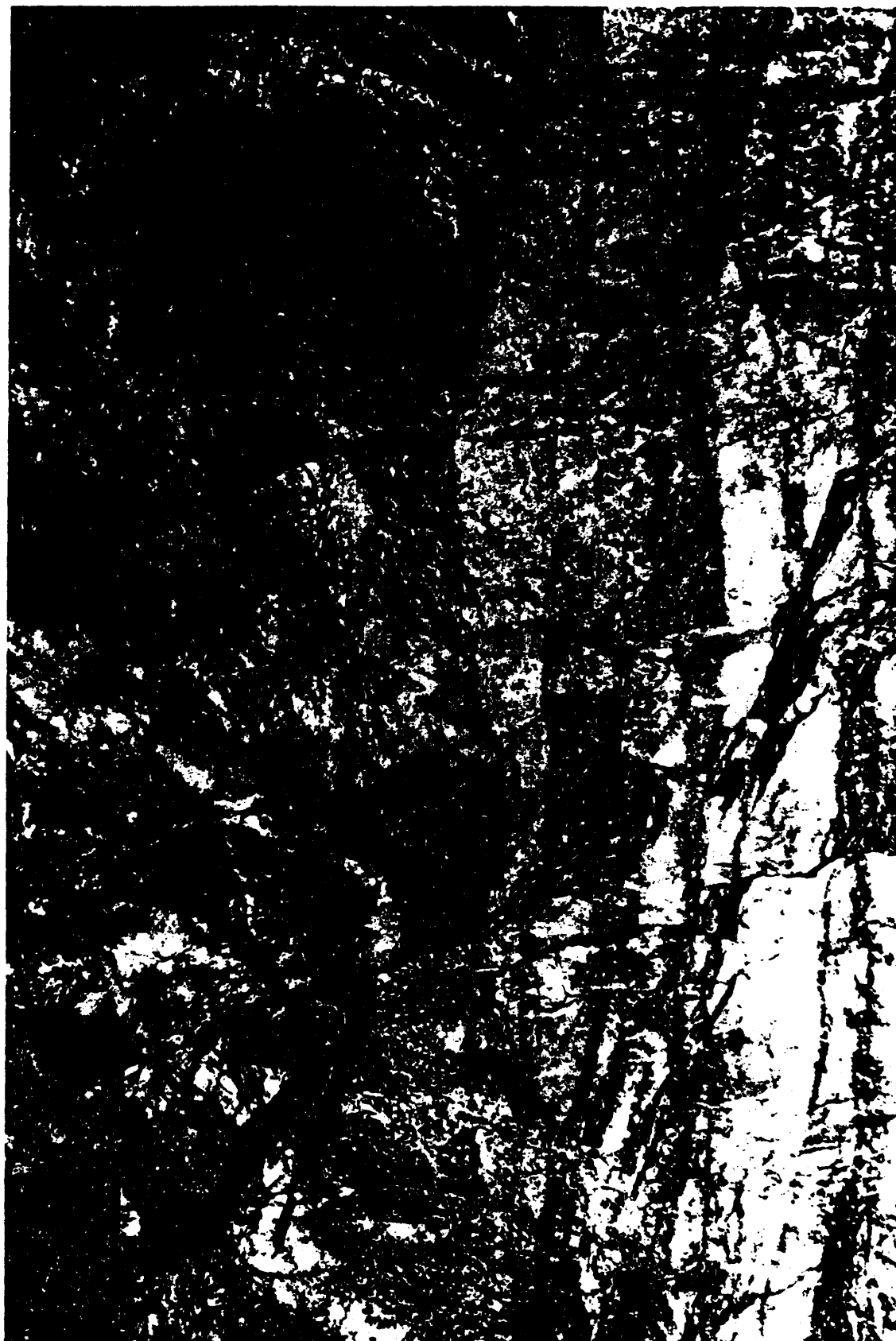






Figure 40



Figure 41

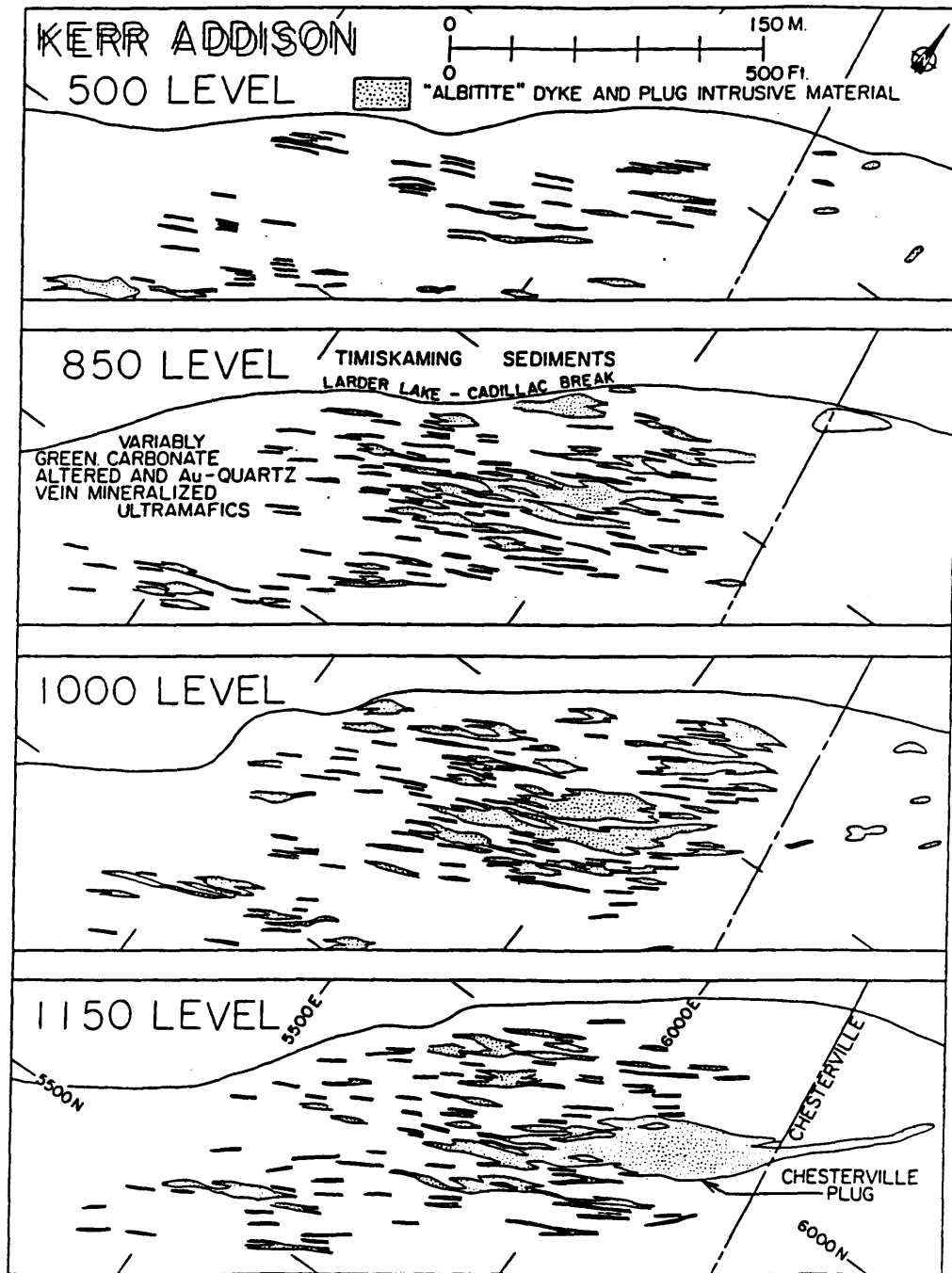


Figure 4 2

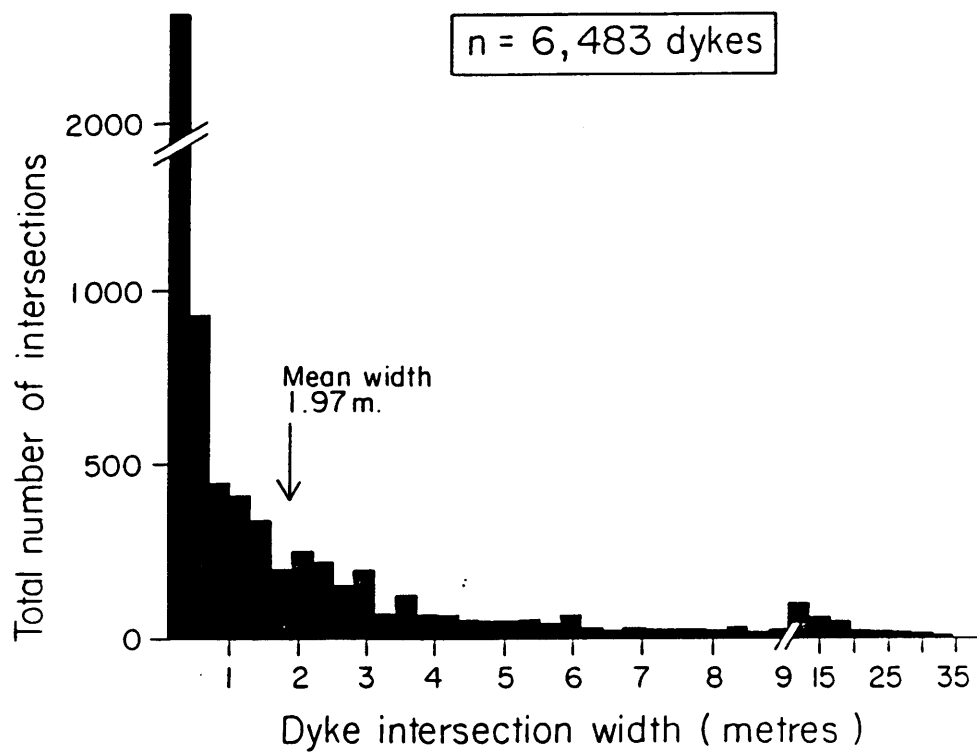


Figure 4 3

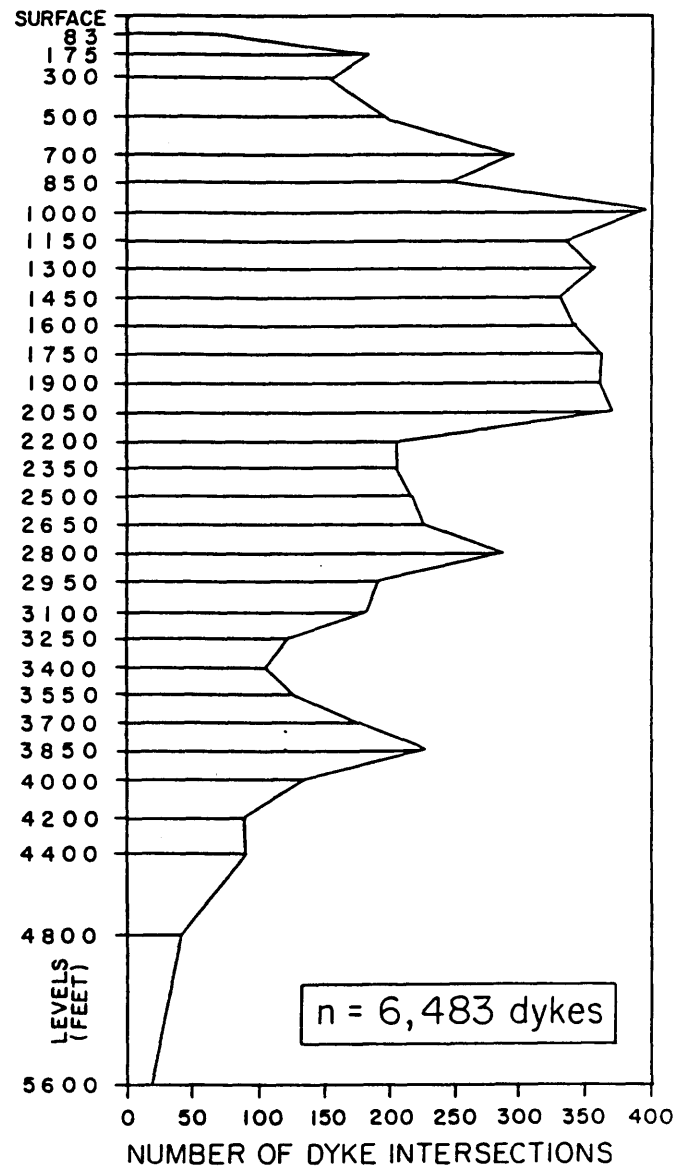


Figure 44

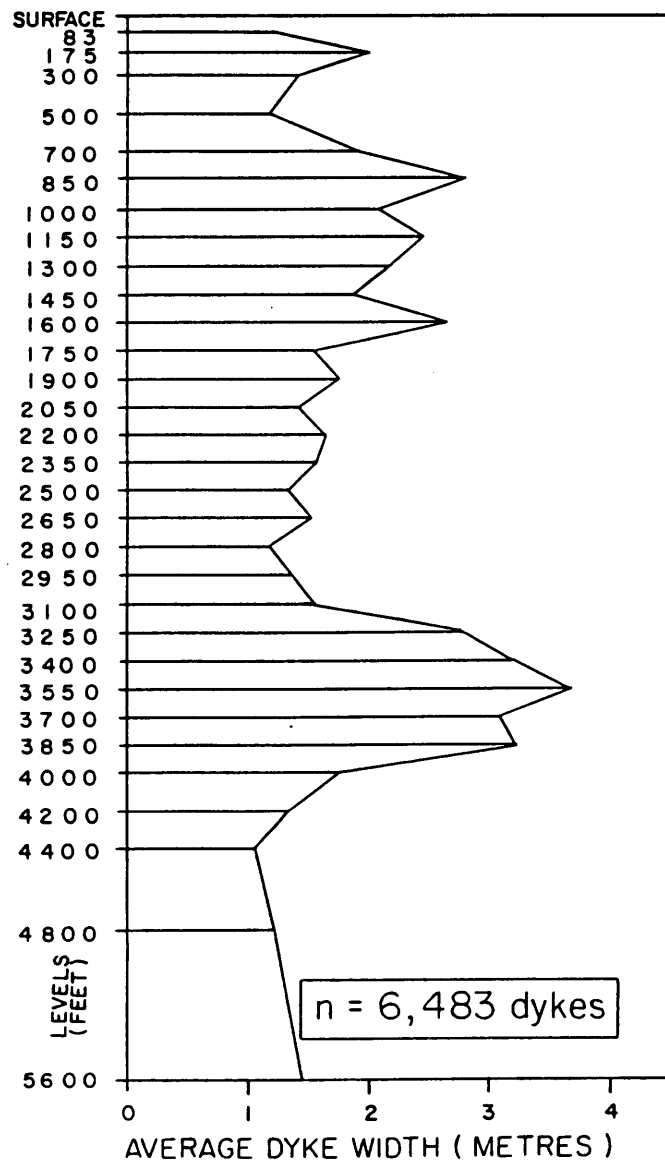


Figure 45

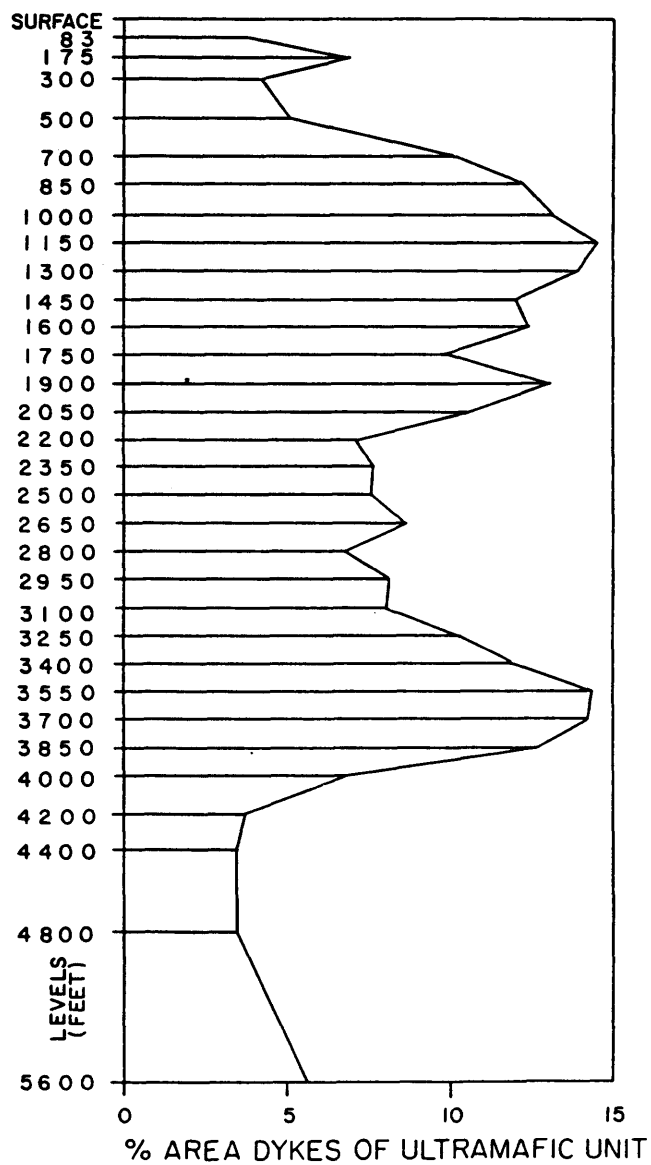


Figure 46A

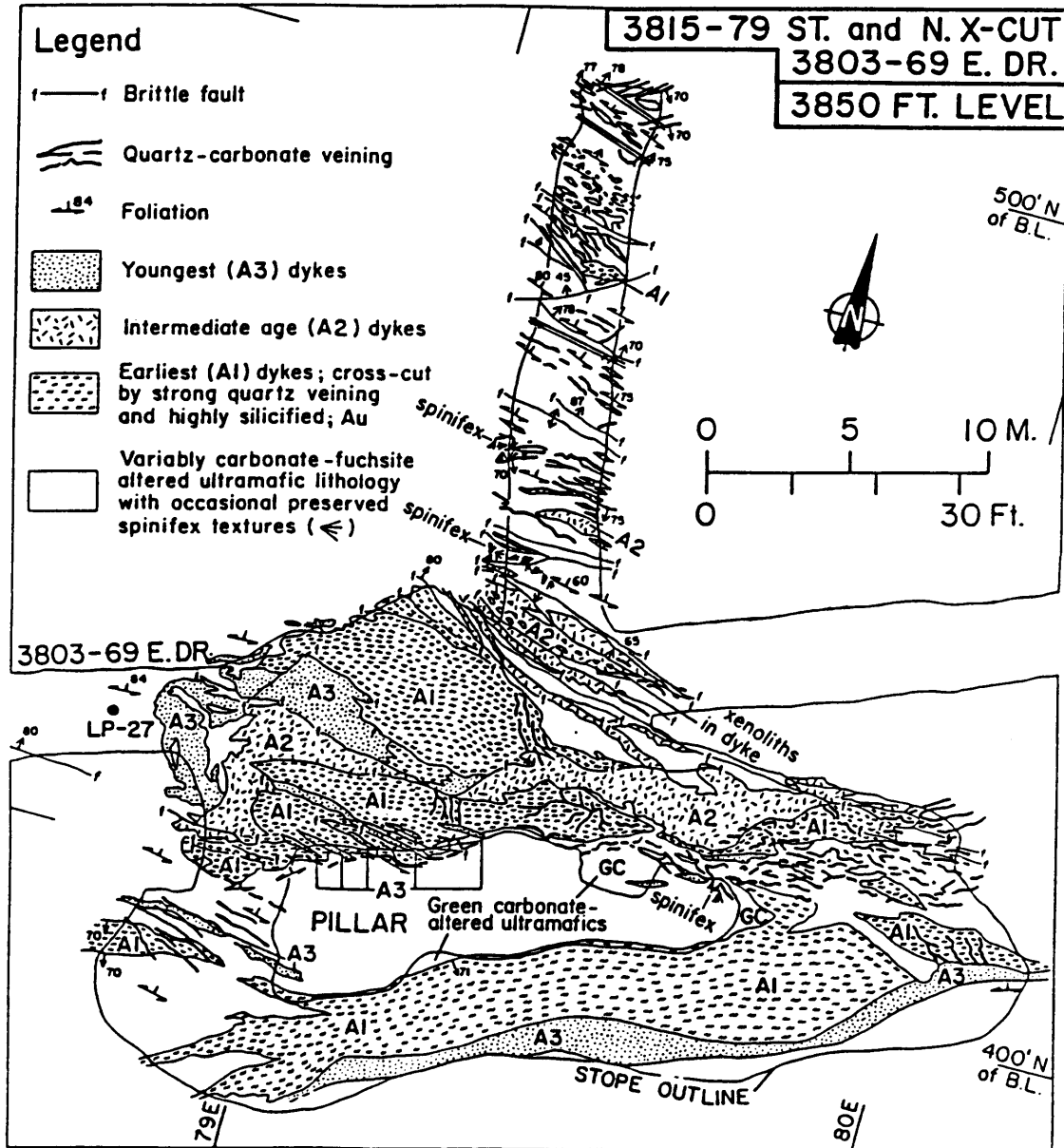




Figure 46 B

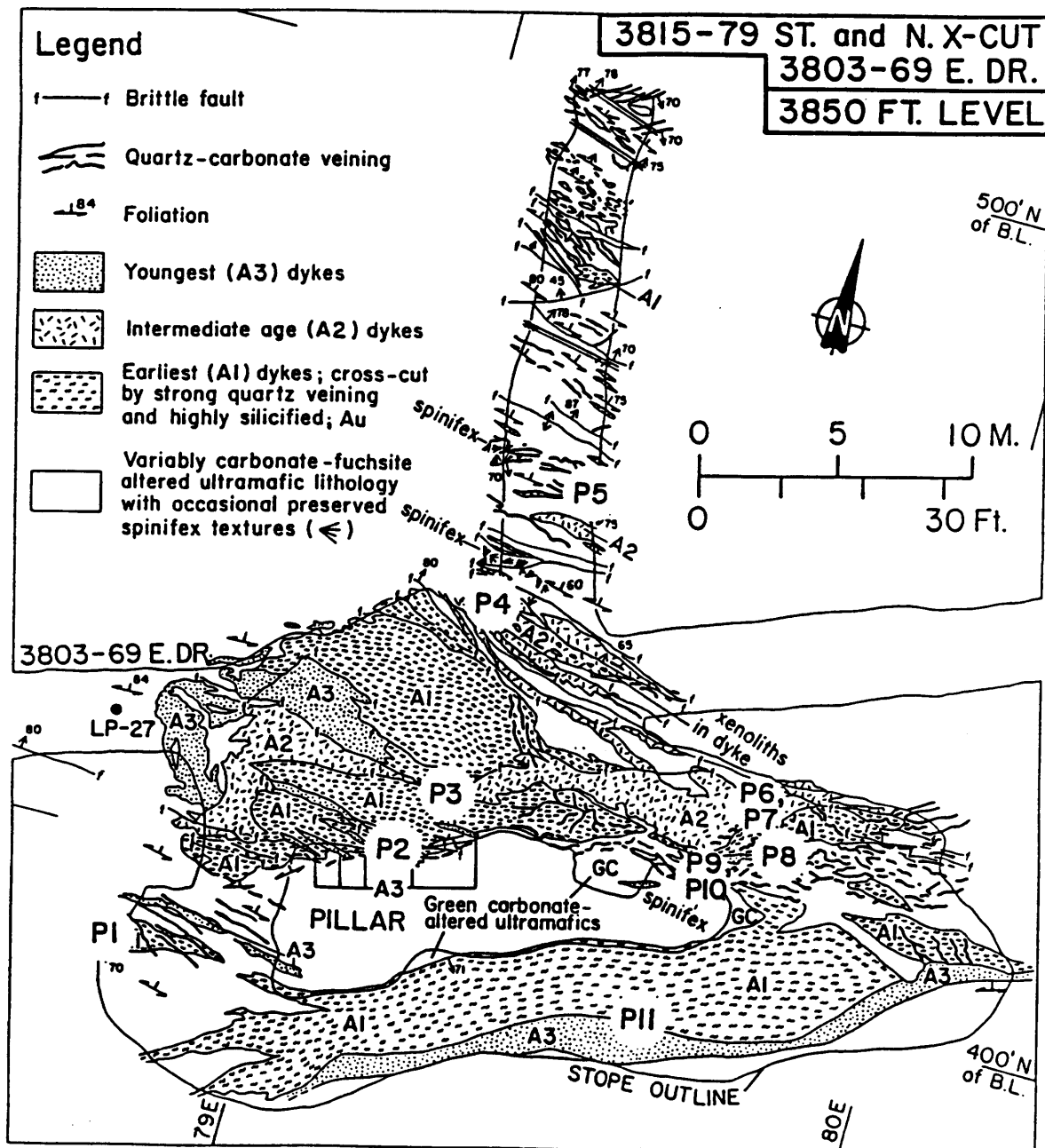


Figure 47



Figure 48

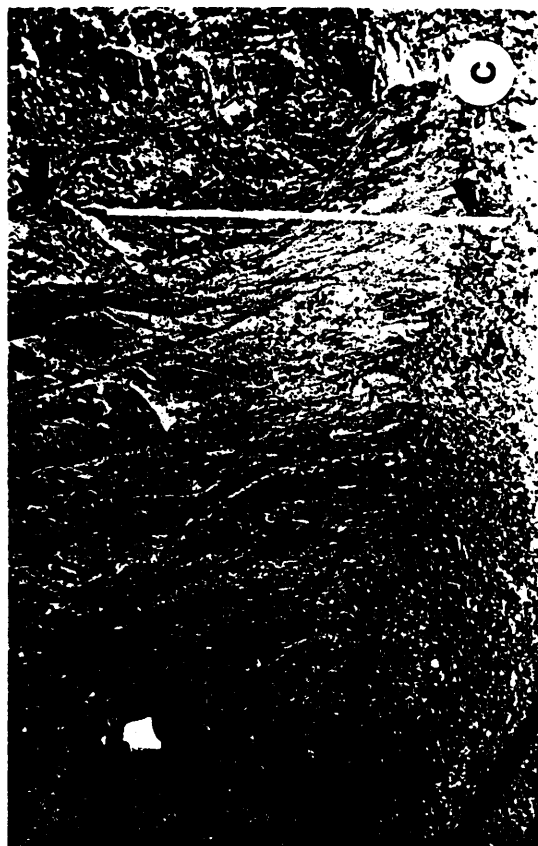


Figure 49

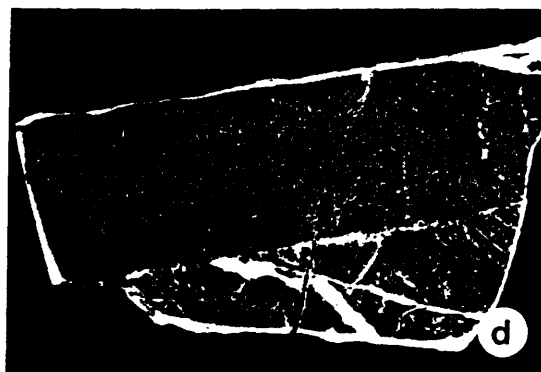
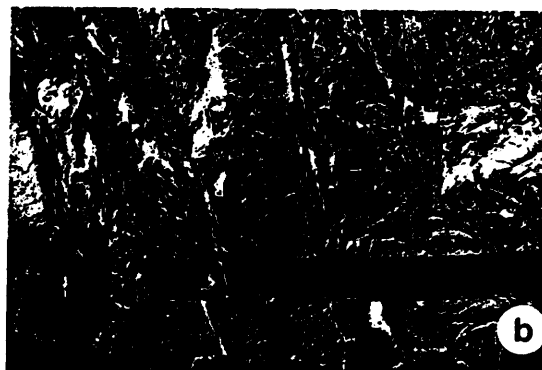


Figure 50

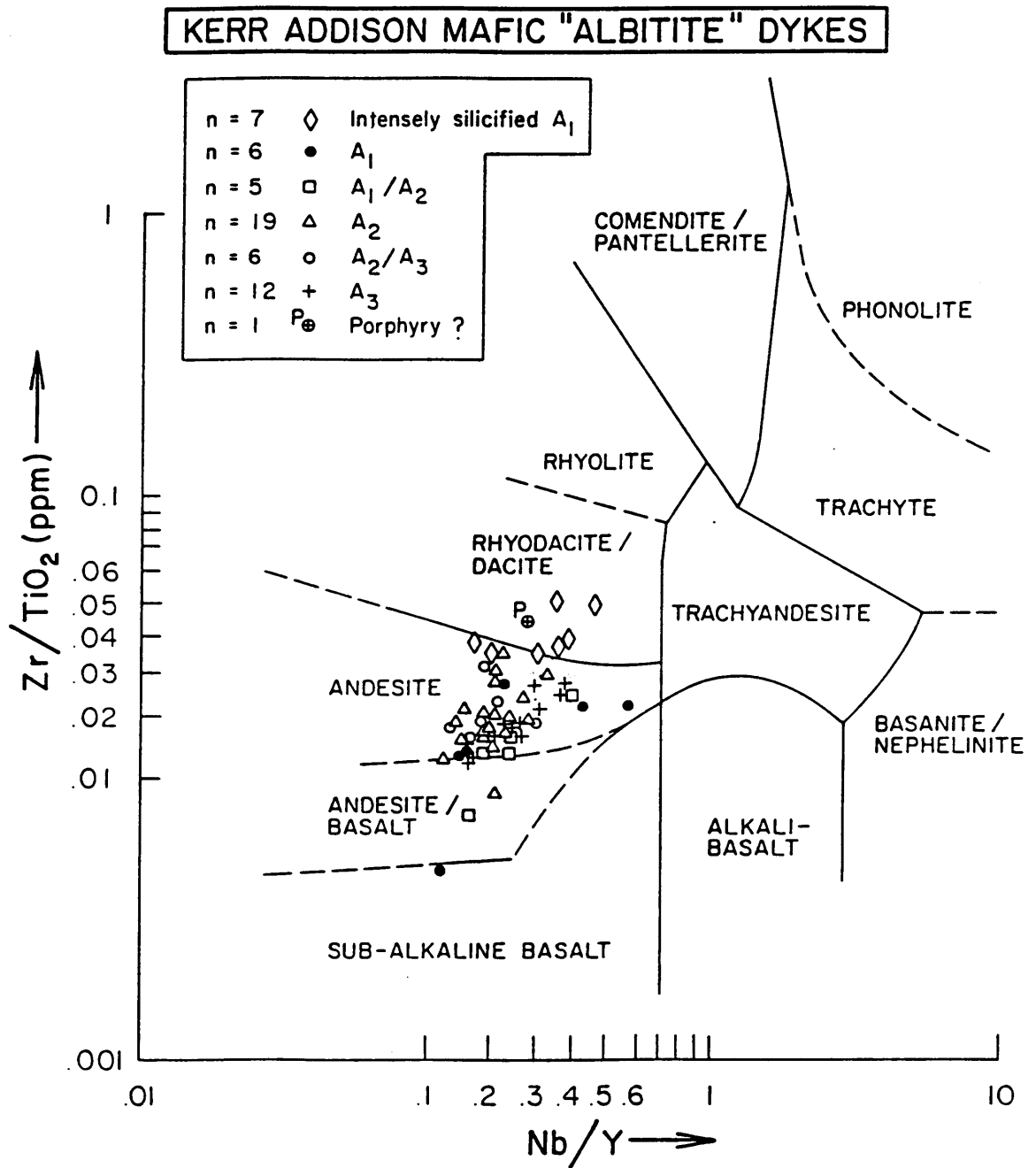


Figure 51

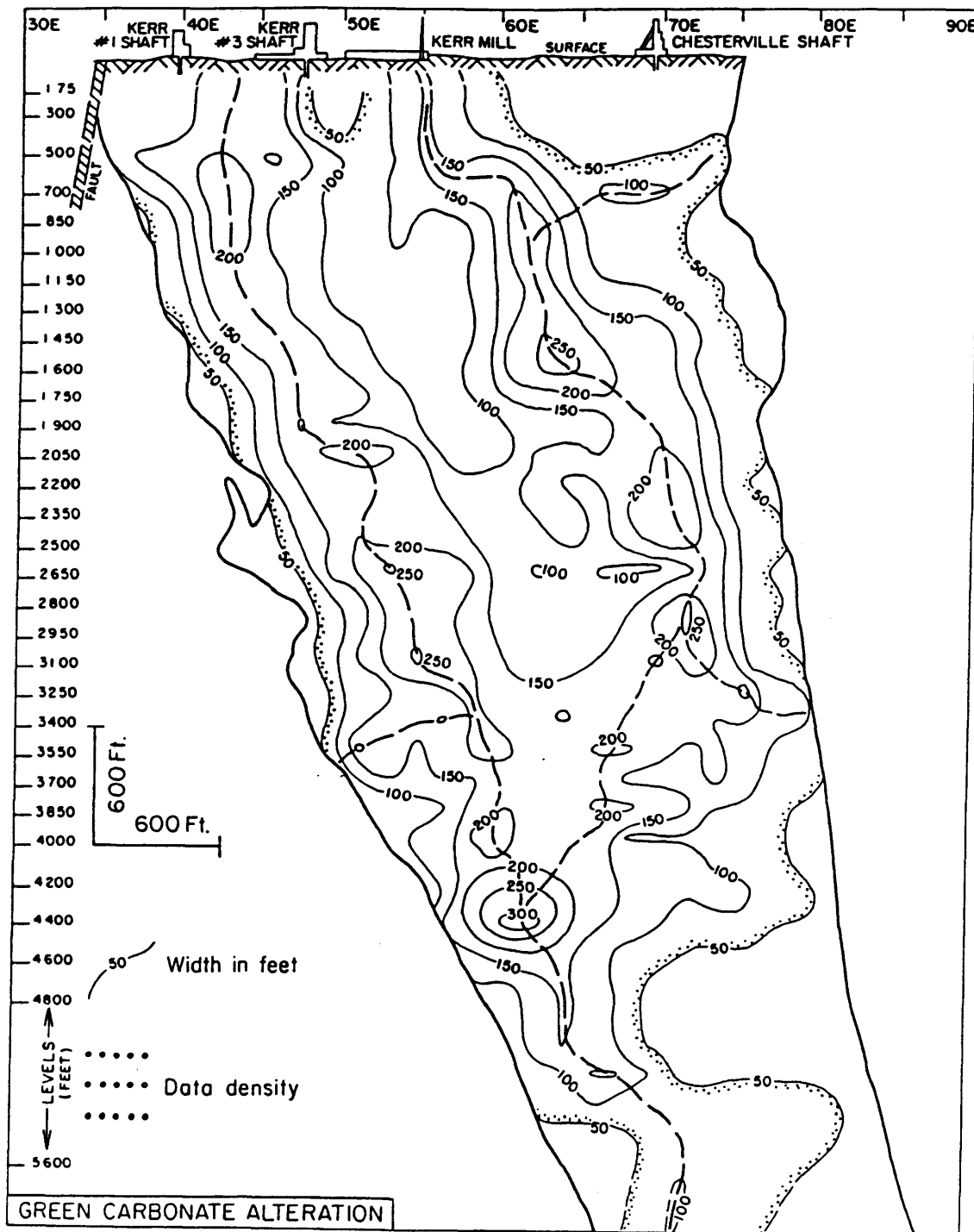


Figure 52

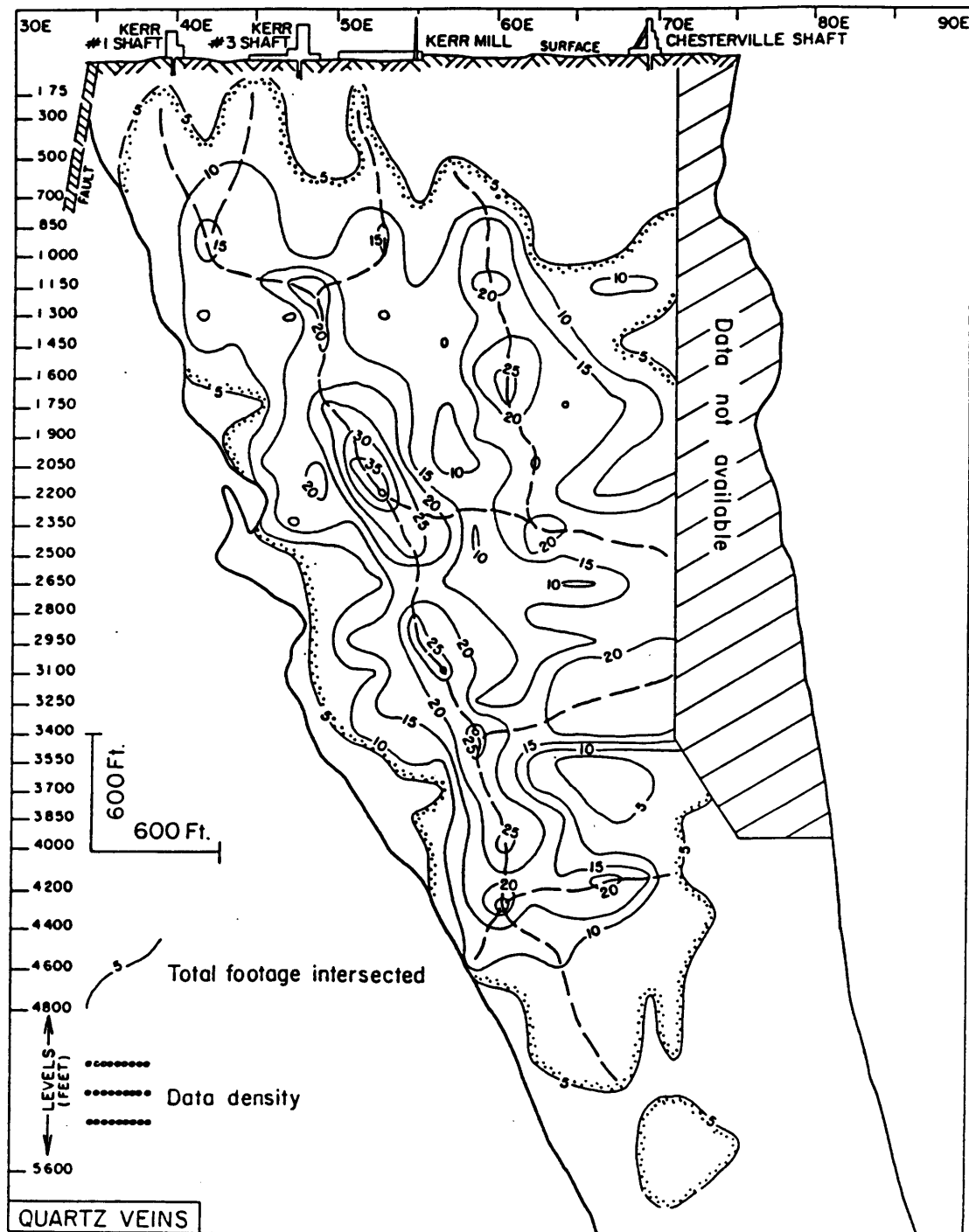


Figure 53

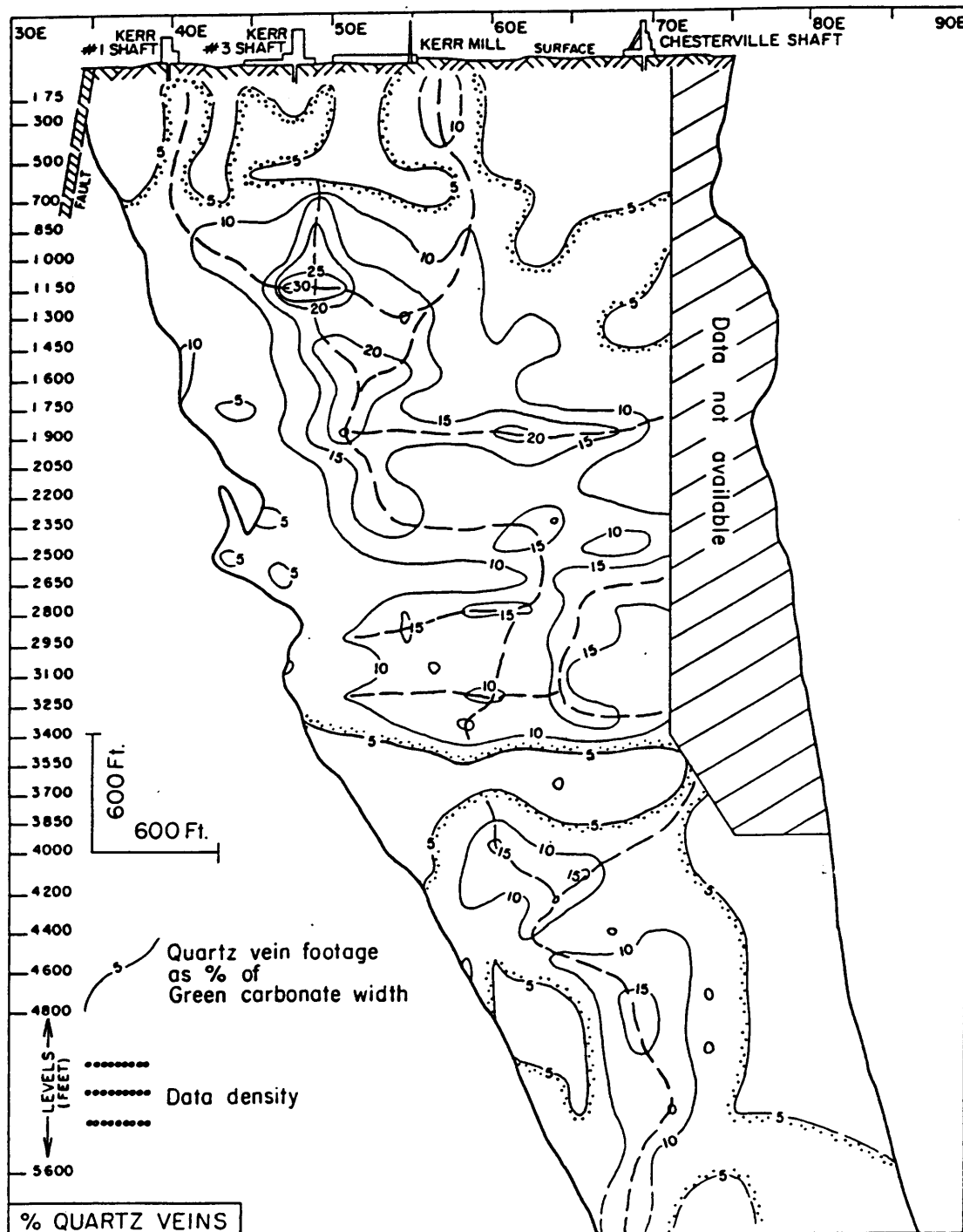




Figure 54

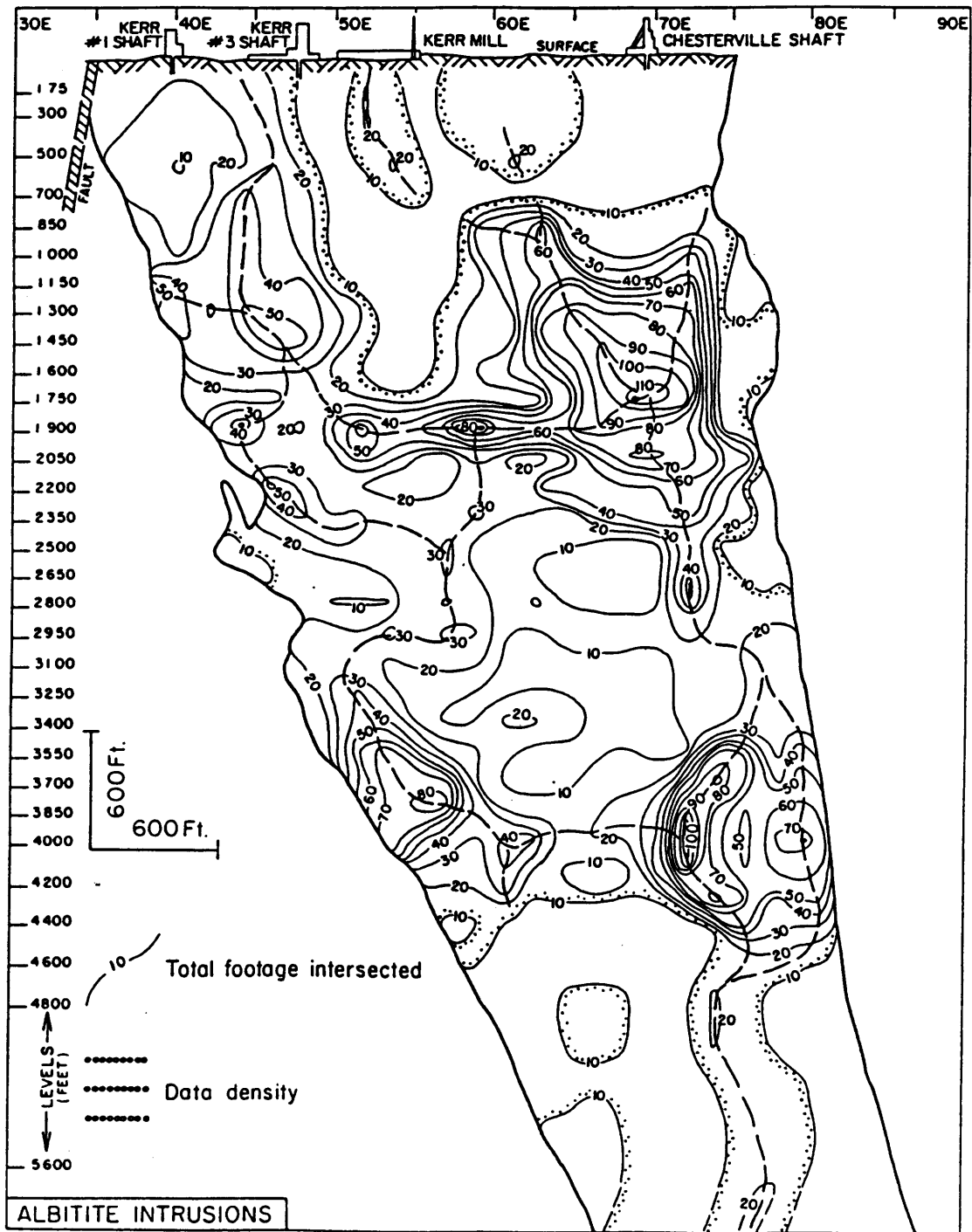


Figure 55

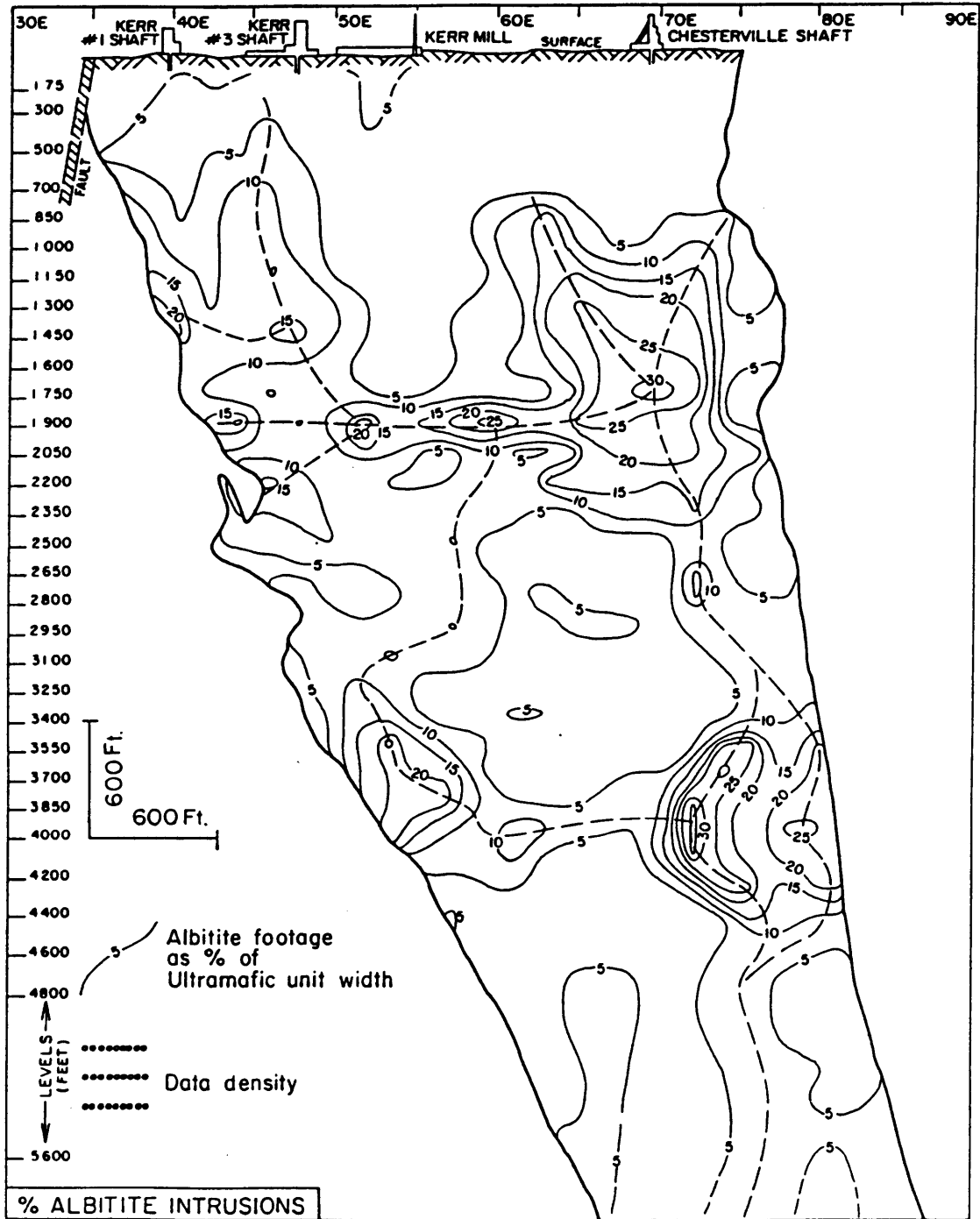


Figure 56

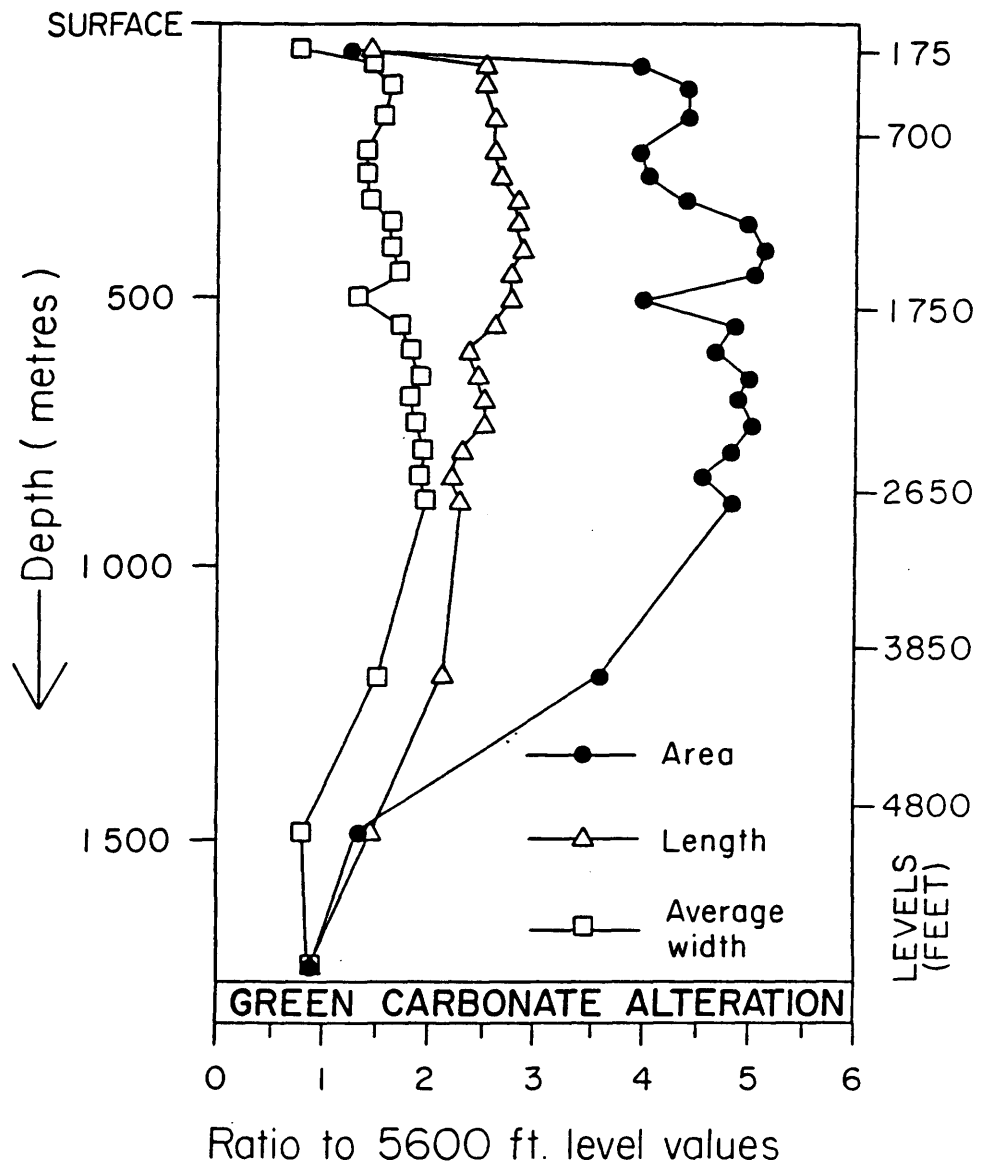


Figure 57

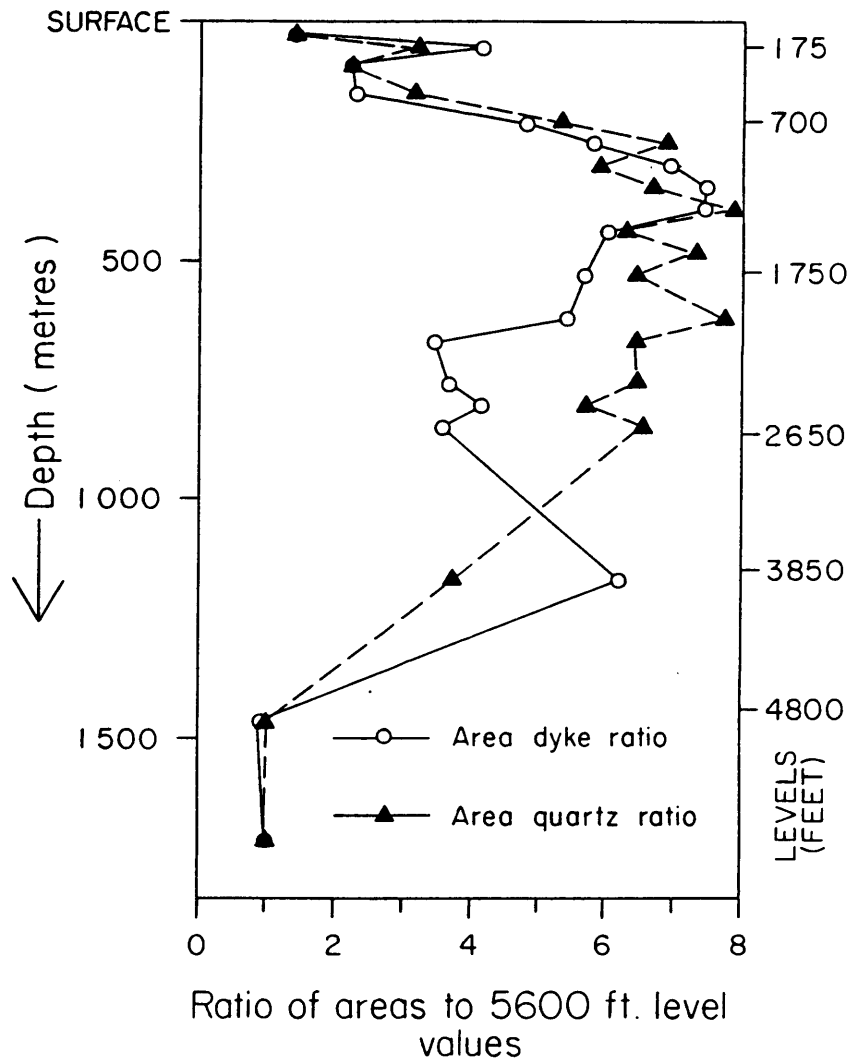


Figure 5 8 A

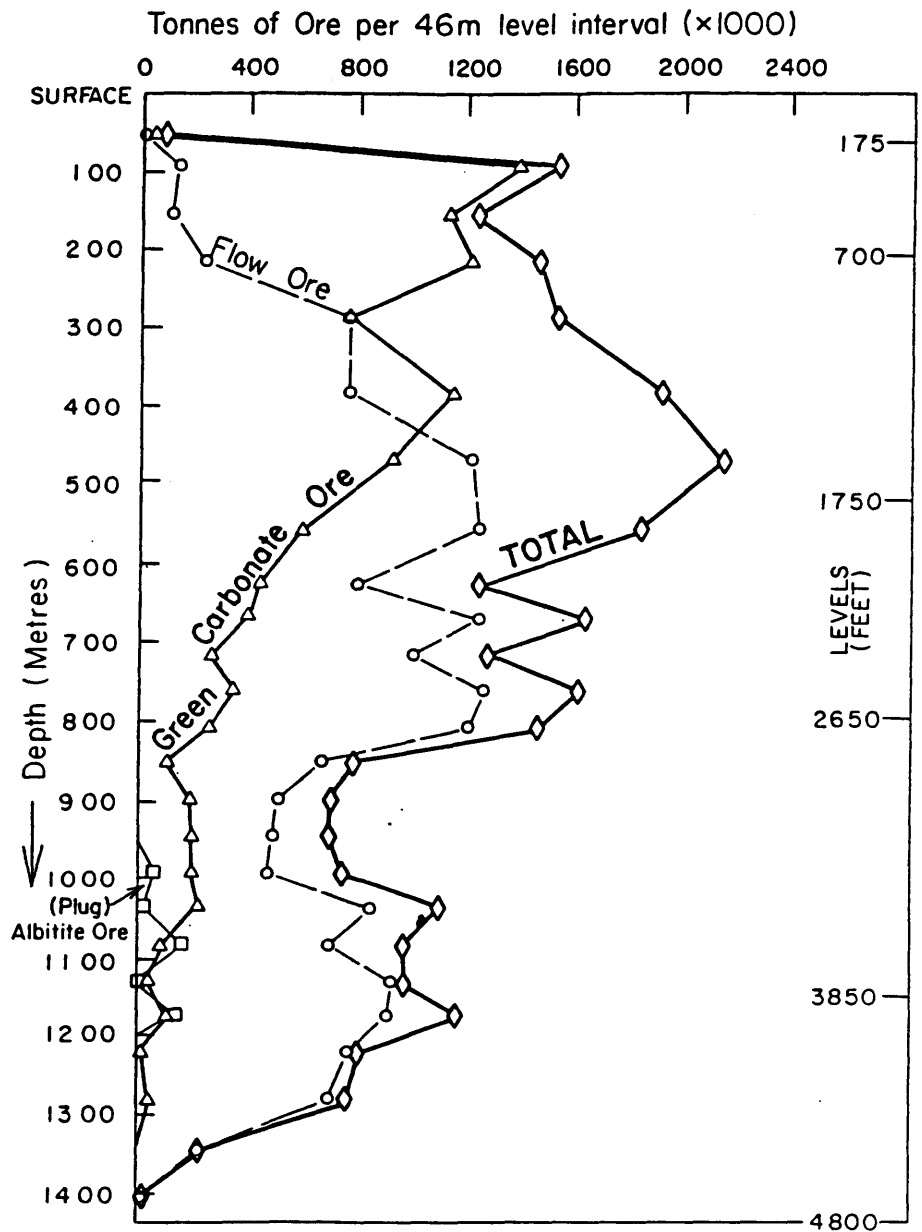


Figure 58B

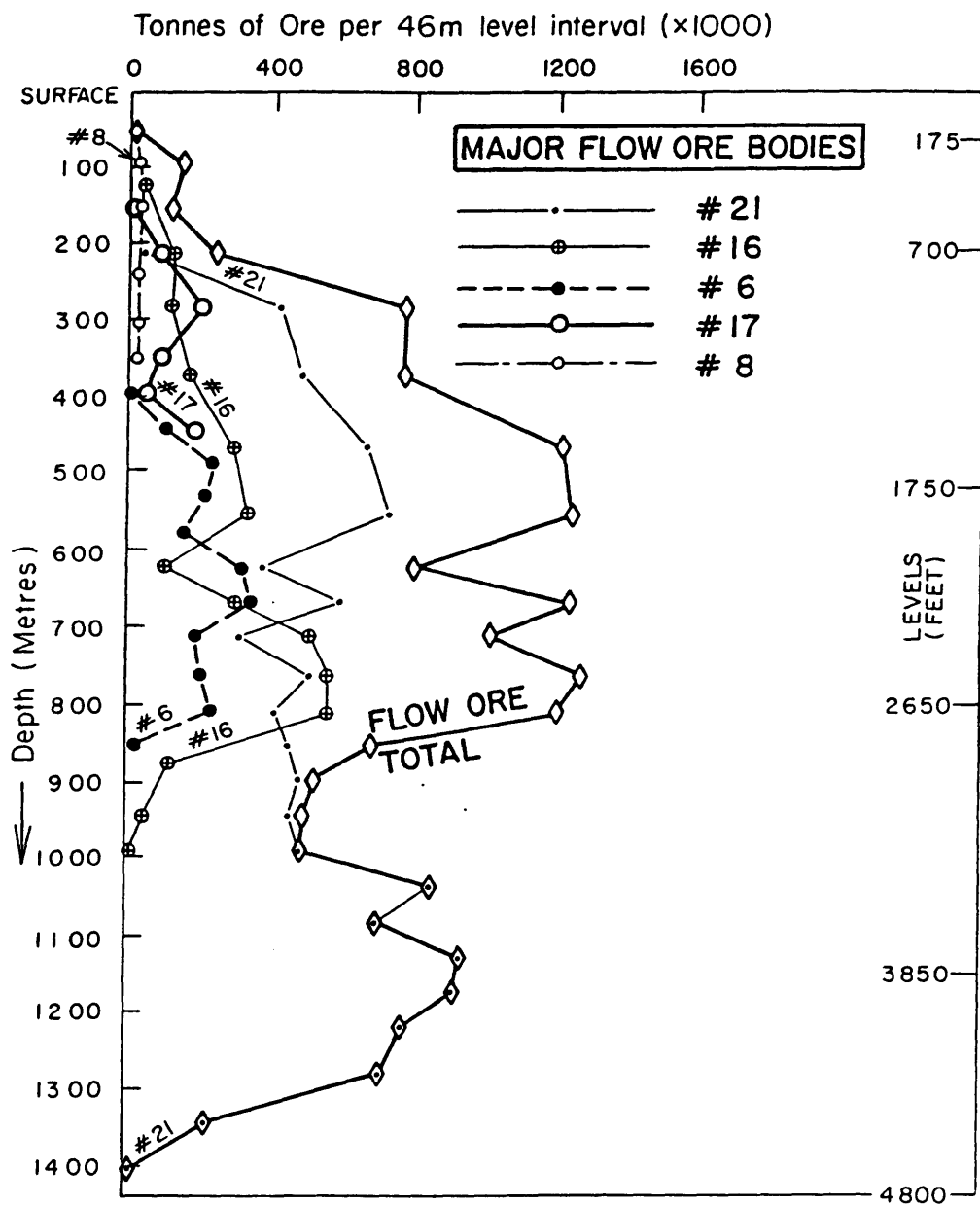


Figure 58C

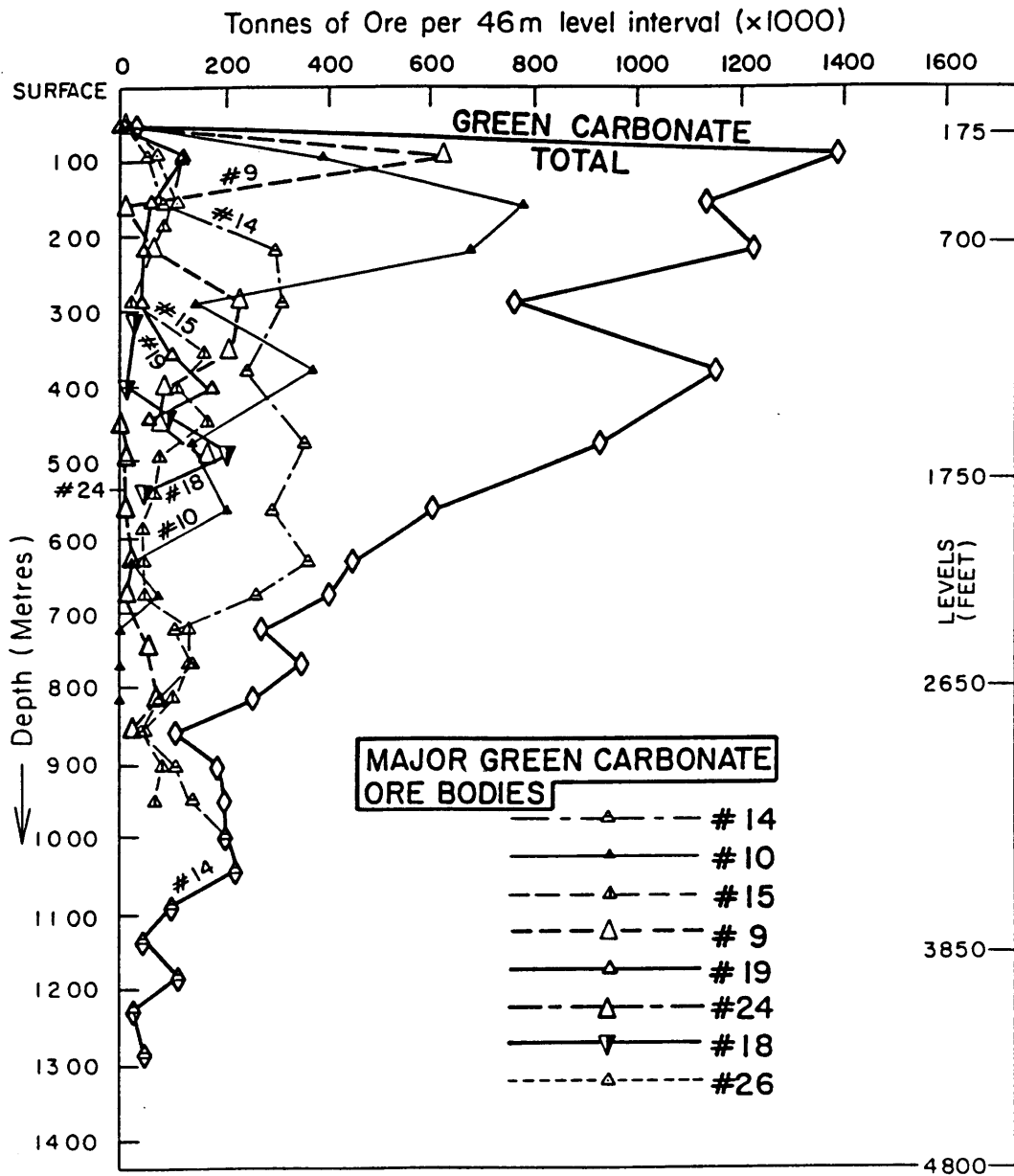


Figure 59A

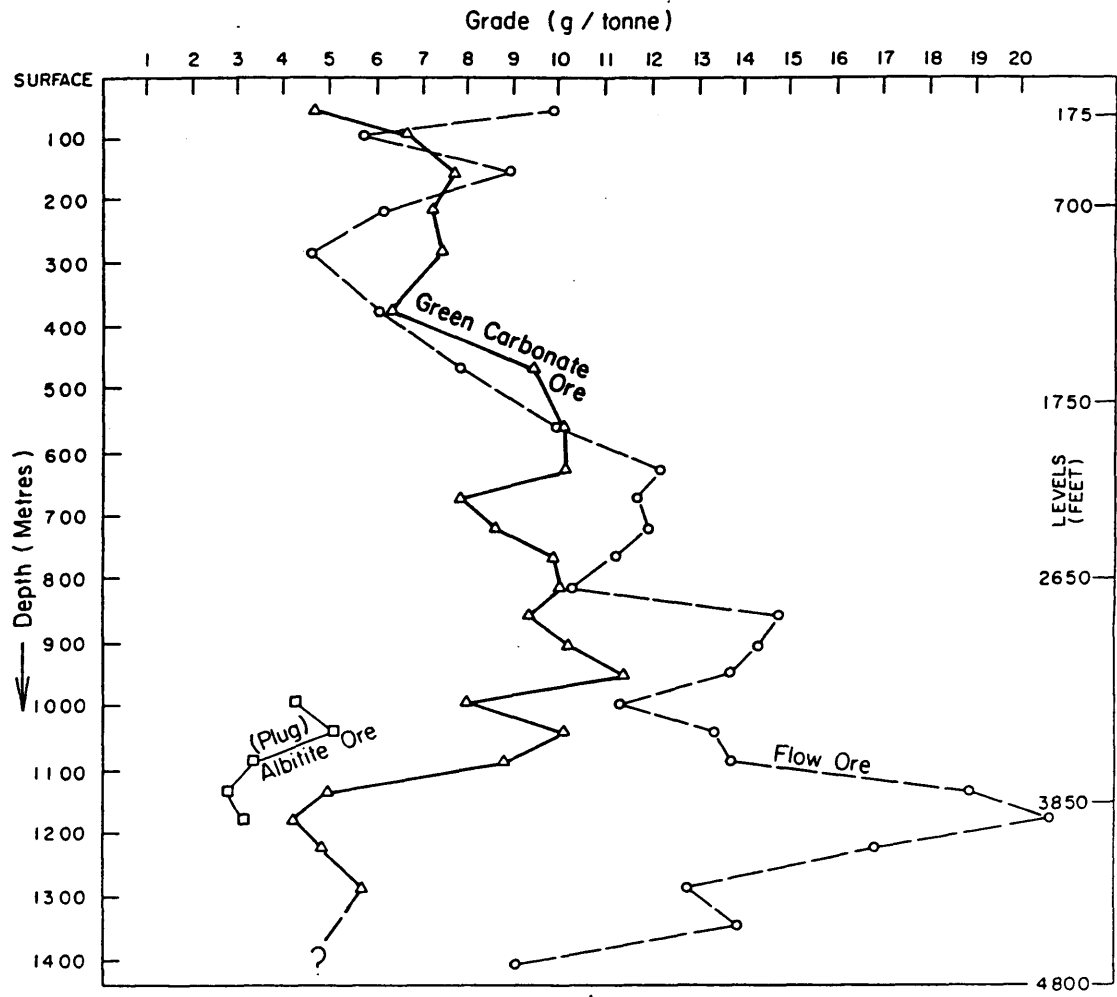




Figure 59B

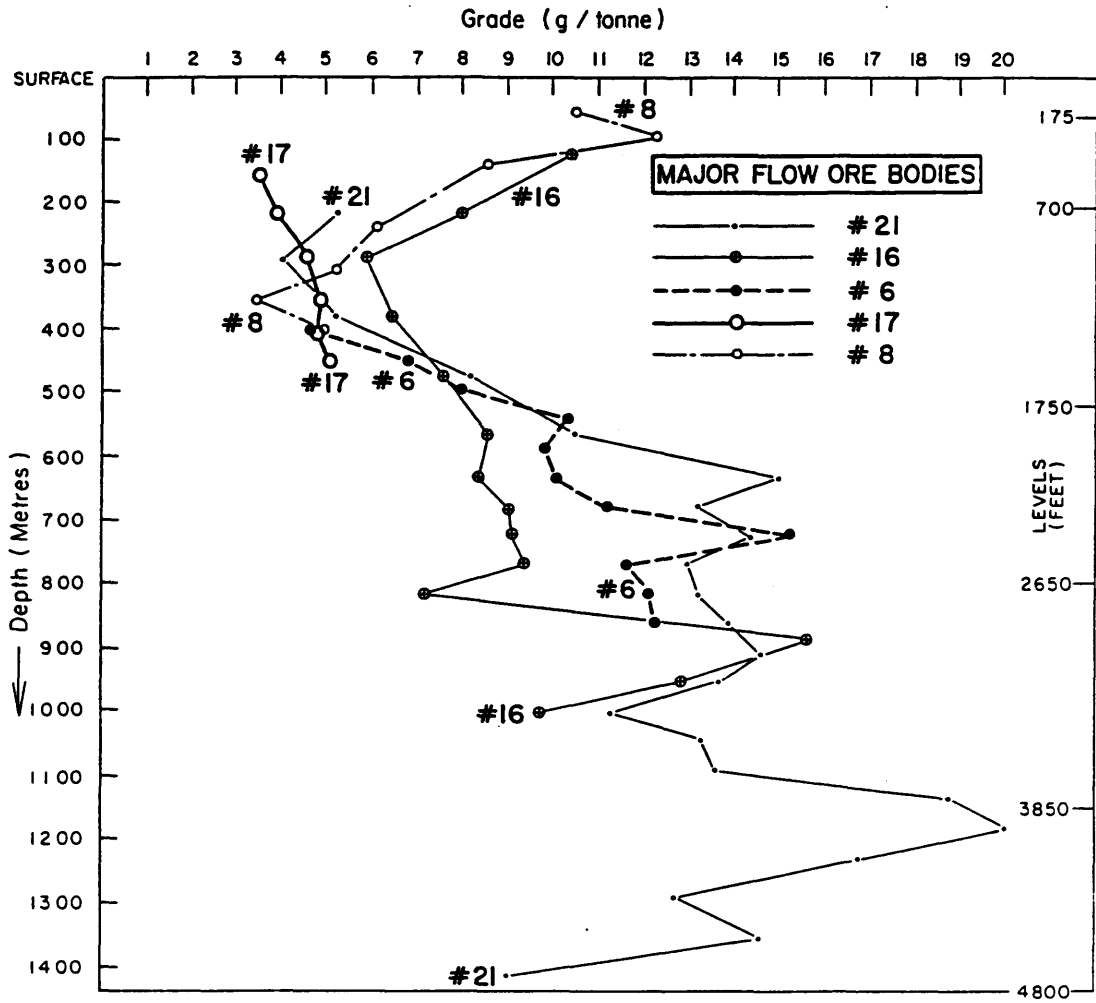


Figure 59c

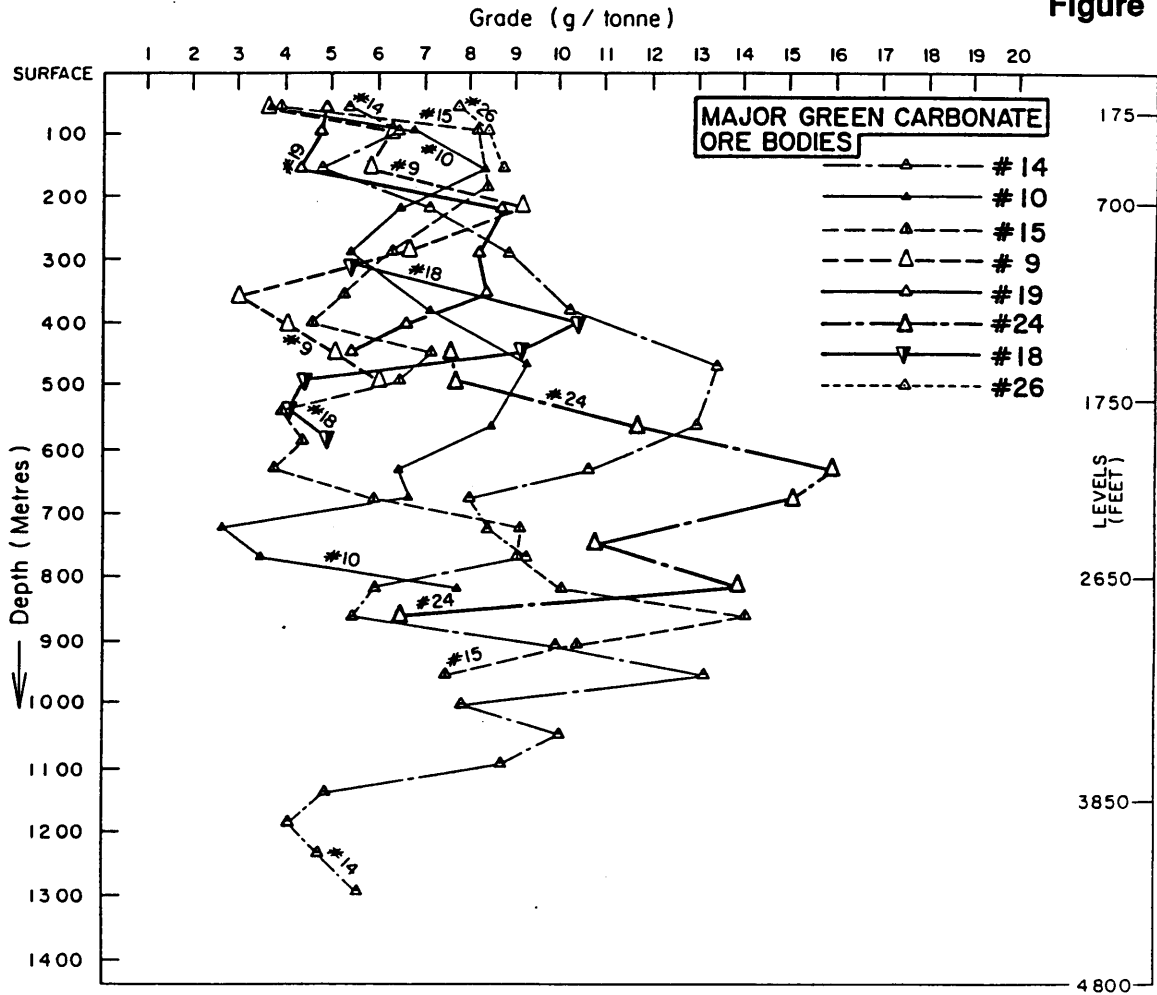


Figure 6 0 A

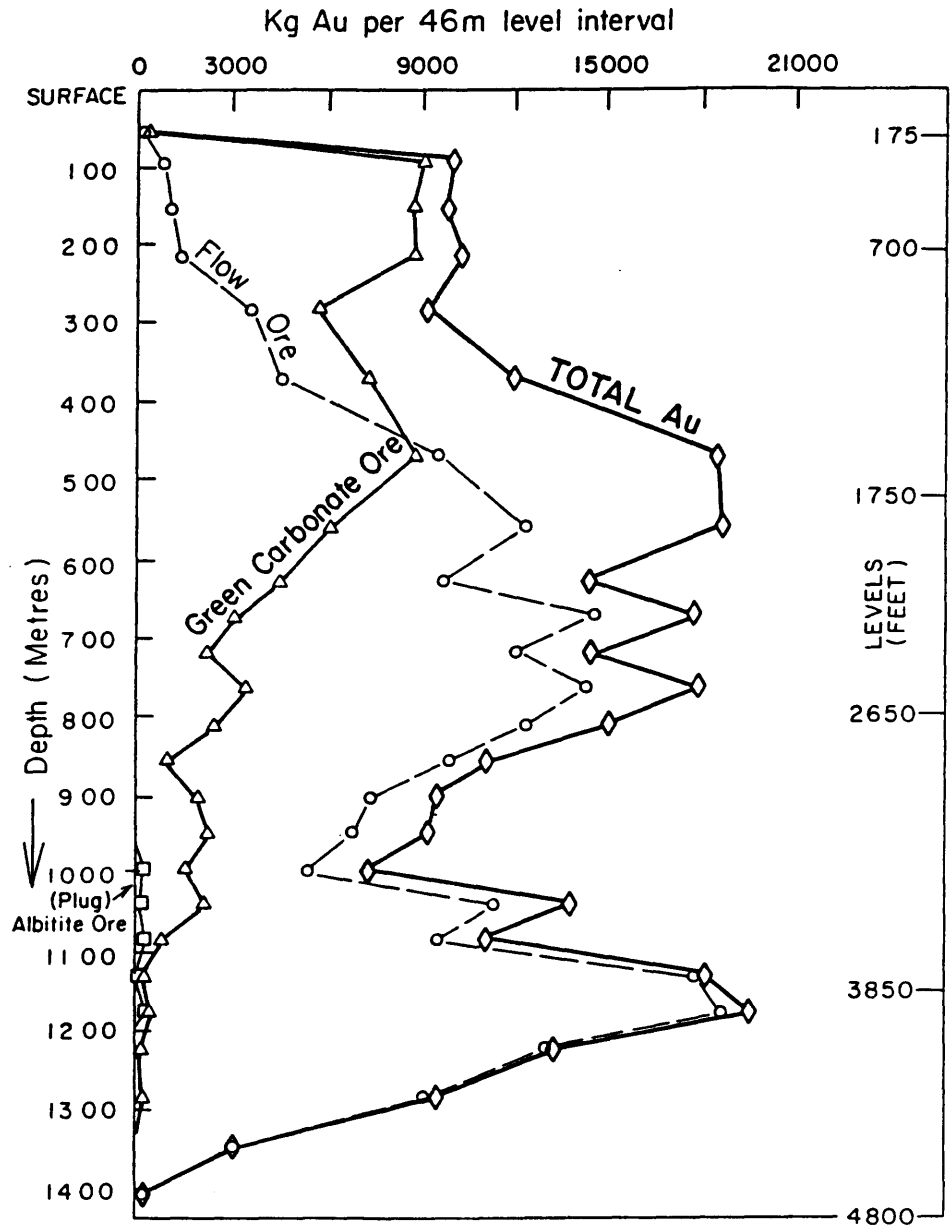


Figure 60B

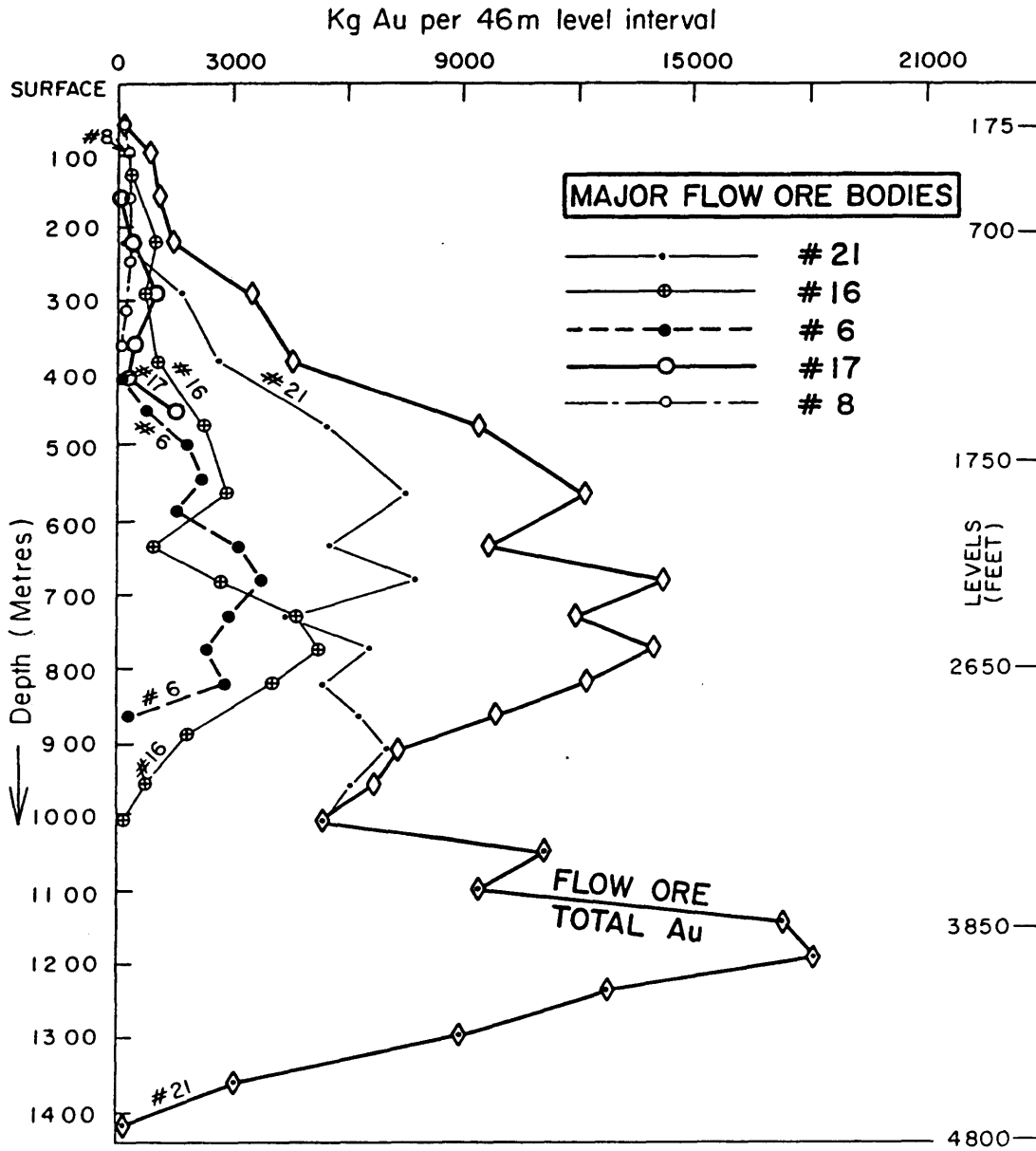


Figure 60C

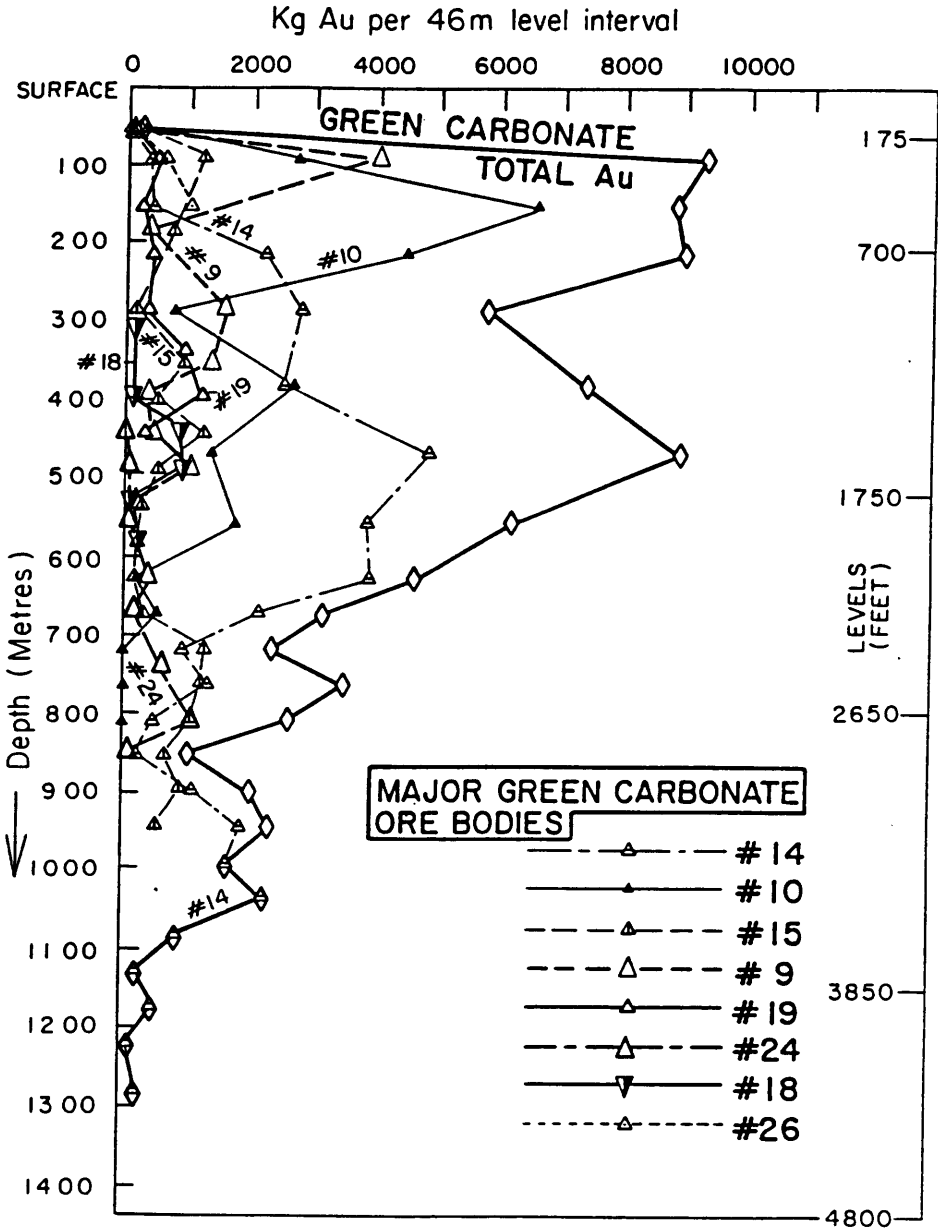


Figure 61

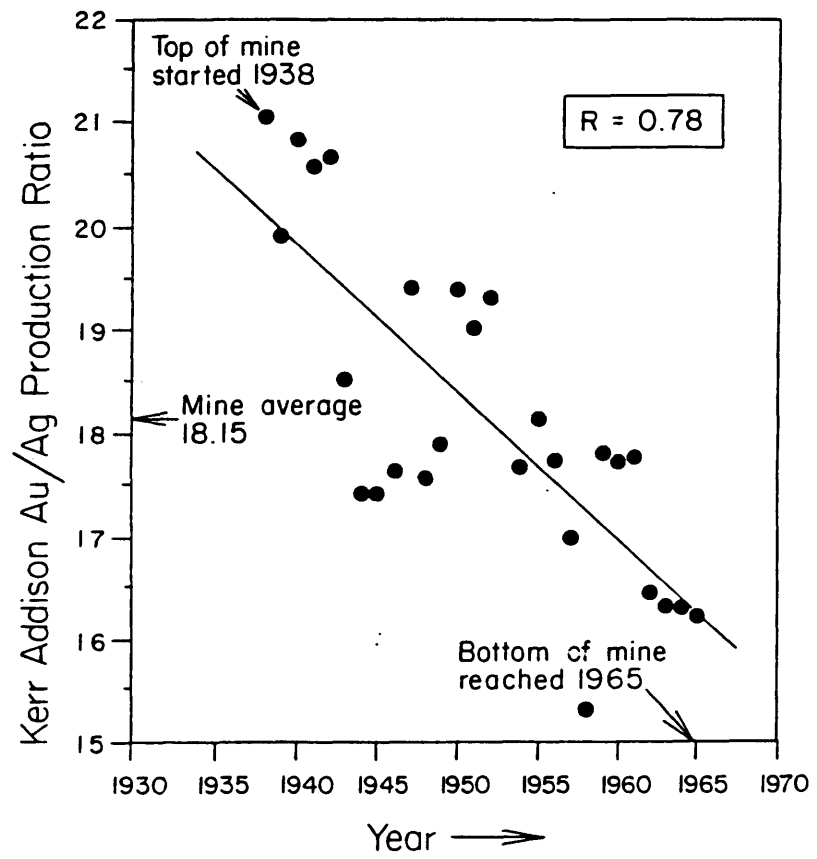




Figure 63

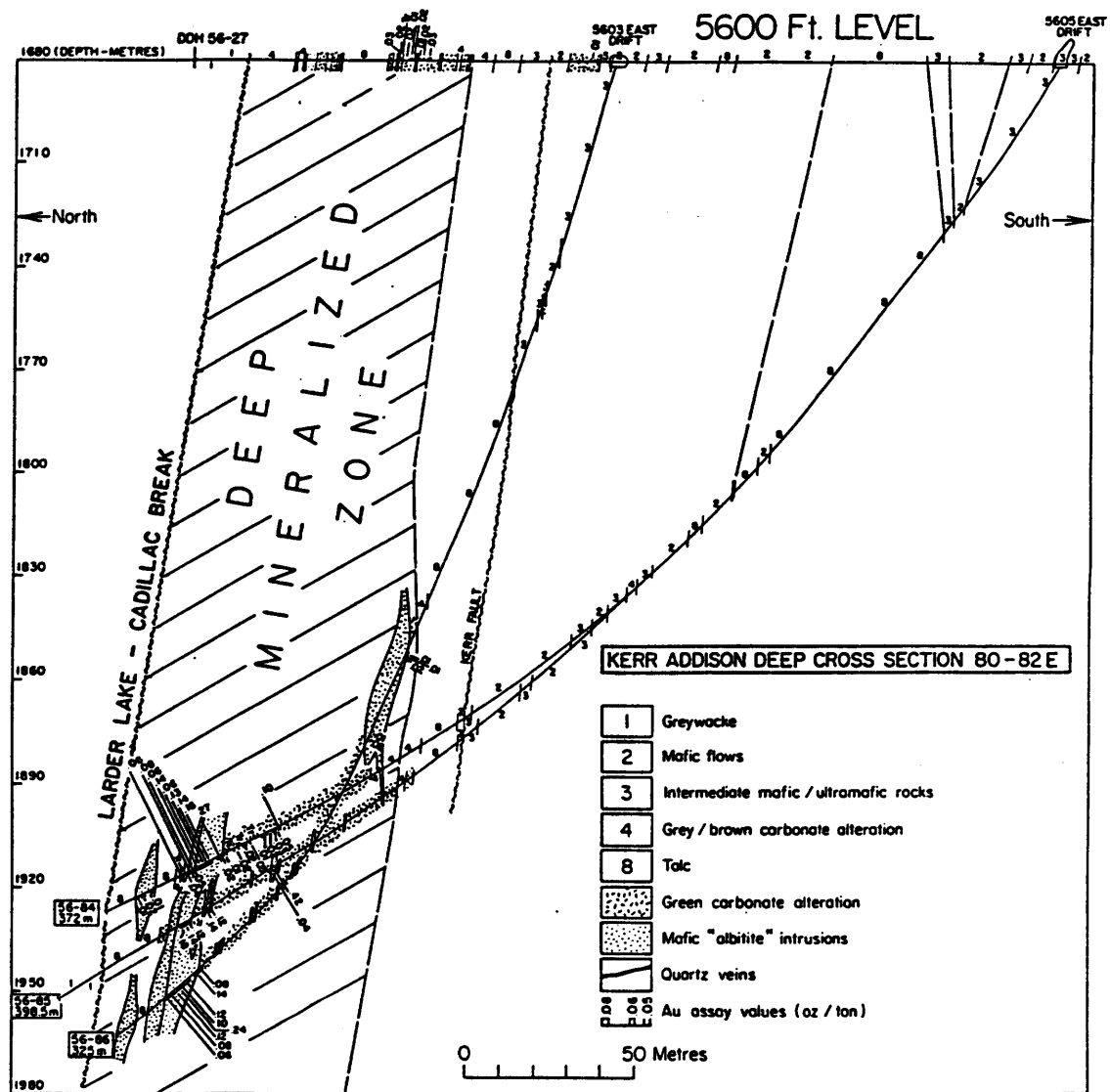




Figure 64



**APPENDIX: DIAMOND DRILL HOLE INTERSECTIONS ON THE 4800 FT  
AND 5600 FT LEVELS AND BELOW THE 5600 FT LEVEL**

**1.1 4800 FT LEVEL; DYKE INTERSECTIONS**

mine section	hole no.	location drilled from	direction drilled (N/S)	footage dyke (ft)	grade (oz/t Au)	within main Green carbonate envelope ? (√=yes; x=no)
---	48-2	4801 E DR	S	233 - 243 353.5 - 366 794 - 805	trace .07 (350-353 ft) .01 (361-366 ft)	√ x x
---	48-4	4801 E DR	S	299 - 300.5 395 - 398.5 403 - 406 409.5 - 412	.01 .01 .01 .01	x √ √ √
---	48-5	----	S	241 - 245.5 416 - 420.5 481.5 - 488	trace .02 zero	x √ x
---	48-6	4801 E DR	S	311.5 - 315.5 476 - 481 482 - 483	trace .01 .02	x √ √
67E	48-10	4801 E DR	S	234 - 237 240 - 251 286.5 - 291.5	n.d. n.d. .01 (280-285 ft)	√ √ √
69E	48-11	4801 E DR	S	455 - 468	up to .02	x
63E	48-22	4803 W DR	N	121 - 124.5	trace	√
62E	48-23	4803 W DR	N	96 - 106	trace - .01	√
52E	48-28	4803 W DR	N	63 - 68	zero	x
48E	48-32	----	N	145.5 - 153	n.d.	x

1.2 CHESTERVILLE PLUG (SECTIONS 75 - 80E):

76E	48-13	4801-74 E DR	N	13 - 16	.03 (16-20 ft)		x
76E	48-14	4801-74 E DR	S	48.5 - 50	trace	√	
76.5 E	48-15	4803-74 E DR	S	11.5 - 30	.02 - .09 (across width)	√	
77.5 E	48-16	4803-74 E DR	N	0 - 9	.05	√	
				9 - 11	.02	√	
				11 - 25	.02 - .03	√	
78E	48-17	4803-74 E DR	N	1 - 9	.01	√	
				15 - 27	.02	√	
80E	48-18	4801-74 E DR	N	0 - 10	.01	√	
80E	48-19	4803-76 E DR	S	0 - 4.5	.04		x
				14 - 16	trace		x
				18 - 18.5	trace		x
				20 - 21	trace		x
75E	48-63	4805-74 E DR	S	23.5 - 25.			
79E	48-64	4803-74 E DR	N	10.5 - 17.5	trace	√	

**1.3 NEW "DIORITE ZONE" OUTSIDE GC ENVELOPE  
(32E; 44-56E; strike length ~900 ft)**

COMMENTS

56E	48-21	4803 W DR	S	80.5 - 100	trace - .01	2.5 ft, 7.5 ft qtz + GC adj. to contacts
52E	48-29	4803 W DR	S	146 - 160.5 168.5 - 173	.14 (145-150 ft) trace (150-160 ft) .01	8.5 ft qtz + GC adjacent to contacts
48E	48-33	4803 W DR	S	141.5 - 173	n.d.	GC alteration adjacent
45.3 E	48-37	4803 W DR	S	18.5 - 58.3 93 - 97	trace trace	GC alteration adjacent breccia GC flows + silicif adj.
45.25 E	48-54	4803 W DR	S	17 - 55.5 89.5 - 99.5	n.d. n.d.	local GC + qtz local GC + qtz
45.25 E	48-55	4803 W DR	S	18 - 54.5 58 - 58.5	n.d. n.d.	local GC local GC
44E qtz	48-38	4803 W DR	N	8 - 46.5	trace .03 (46-48 ft)	breccia contacts + qtz contact zone
32E	48-46	4803 W DR	N	86 - 93	trace	weak GC alteration

### 1.4 QUARTZ VEIN INTERSECTIONS

mine section	hole no.	footage quartz (ft)	quartz intersection width (ft)	grade (oz/t Au)
<b>INSIDE GREEN CARBONATE ENVELOPE:</b>				
62E	48-23	179.5 - 182	2.5	trace - .01
		213 - 218.5	5.5	trace
		197 - 198.5	1.5	trace
67E	48-6	481 - 485	4	.01 - .02
		488 - 490	2	trace - .01
		579.5 - 584	4.5	trace
74E	48-12	122.5 - 125	2.5	trace
76E	48-14	22 - 23	1	trace
		52 - 53.5	1.5	trace
		130.5 - 131	0.5	trace
		133 - 133.5	0.5	trace
79E	48-64	4 - 5	1	trace
80E	48-18	10 - 13	3	.04
		26 - 27.5	1.5	trace
<b>OUTSIDE GREEN CARBONATE ENVELOPE:</b>				
56E	48-21	78 - 80.5	2.5 (grey quartz)	trace - .01
		100 - 107	7 (75% grey quartz)	trace
52E	48-29	160.5 - 168.5	8 (90% quartz)	.01

## 2.1 5600 FT LEVEL AND BELOW DYKE INTERSECTIONS

mine section	hole no.	location drilled from	direction drilled (N/S)	footage dyke (ft)	grade (oz/t Au)	within main GC envelope? (√=yes; x=no)
65E	56-5	5601 E DR	S	218 - 225.5 245 - 256	zero zero	√ x
69E	56-6	5601 E DR	S	233.5 - 237.5 358 - 362.5	n.d. .02	√ x
72E	56-8	5603 E DR	N	213.5 - 214	n.d.	√
76E	56-23	5603 E DR	N	282 - 287.5 290 - 292 293 - 293.5	.01 .02 .02	√ √ √
80E	56-27	5603 E DR	N	145 - 147.5 202 - 208 210 - 213 268 - 271 275 - 278 281.5 - 291 303 - 304.5	trace .02 - .03 trace trace trace trace n.d.	√ √ √ √ √ √ √
84E	56-31	5603 E DR	N	110 - 122	n.d.	x
52E	56-32	5603 W DR	N	124 - 125	.02 - .03 + qtz locally	x
74E	56-43	5603 E DR	N	250 - 251.5	trace / .02 adj.	√

**2.2 NEW "DIORITE ZONES" OUTSIDE GREEN CARBONATE ENVELOPE  
(40-48E; 60-65; ~76E; ~88E; all Au mineralised)**

COMMENTS

61E	56-4	5601 E DR	S	726 - 753.5 807 - 808.5	trace - .01 zero - .01	+ qtz adjacent
65E	56-21	5603 W DR	S	29 - 50	.01 - .05 (across width)	local GC alteration + pyrite + qtz
60E	56-25	5603 W DR	S	78.5 - 99	.04 (79.5-80 ft)	+ qtz locally
88E	56-34	5603 E DR	N	15 - 30.5 172 - 188	n.d. n.d.	local GC alteration + qtz
44E	56-39	5603 W DR	N	76 - 120	.12 (62-65.5 ft) (in GC flow)	local GC alteration
44E	56-44	5603 W DR	N	75.5 - 92	n.d.	local GC alteration
44E	56-45	5603 W DR	N	101-116	n.d.	local GC breccia

**2.3 NEW "DIORITE ZONES" - DEEP HOLES BELOW 5600 FT LEVEL (40-48E; ~76E)**

76E	56-68	5605 E DR	N -67°	878 - 892 1082 - 1098 1496 - 1499 1518.5 - 1522	n.d. trace - .04 trace trace	local GC + pyrite local GC + pyrite √ √
40E	56-77	5603-40 S X-C	N -60°	660.5 - 694	trace	local GC alteration
44E	56-78	5603-44 S X-C	N -60°	626.5 - 636.5 679 - 753 (74 ft)	trace trace - .01	local GC + qtz local GC alteration + pyrite + qtz
48E	56-82	5603-48 S X-C	N -60°	569 - 634 (65 ft) 637 - 643.5 682-769 (87 ft)	.01 - .02 .01 - .02 .02 (729-731 ft) .22 (731-735 ft)	local GC/qtz/pyrite local GC/qtz/pyrite

2.4 OTHER DEEP HOLES (BELOW 5600 FT LEVEL); CHESTERVILLE PLUG

74E	56-76	5605 E DR	N -40°	985.5 - 988	n.d.	√	
72E	56-65	5603-72 X-C	N -60°	1112 - 1115 1133 - 1136.5 1148 - 1154	n.d. n.d. n.d.	√ √ √	
80E	56-84	5605 E DR	N -60°	912 - 913.5 1033 - 1041 1130 - 1157 1157 - 1165 1168 - 1170 1200.5 - 1220	n.d. n.d. .14 (over 24 ft) .06 - .08 .06 trace - .02	√ √ √ √ √ √	x
80E	56-85	5605 E DR	N -60°	928 - 935 960 - 961.5 1004 - 1006 1085 - 1091 1083 - 1083.5 1156 - 1158 1163 - 1166 1169.5 - 1173.5 1177 - 1191 1191 - 1201.5	n.d. n.d. trace .02 - .45 trace .12 .14 .04 .12 - .18 n.d.	√ √ √ √ √ √ √ √ √ √	
82E	56-86	5603 E DR	N -75°	589 - 700 801 - 805 968.5 - 1011.5 1011.5 - 1013 1013 - 1032.5 1055 - 1075	.01 - .02 n.d. .12 (over 30 ft) n.d. .01 - .02 n.d.	√ √ √ √ √ √	



## 2.5 QUARTZ VEIN INTERSECTIONS

mine section Au)	hole no.	footage quartz (ft)	quartz intersection width (ft)	grade (2.5oz/t)
---------------------	----------	------------------------	-----------------------------------	--------------------

### INSIDE GREEN CARBONATE ENVELOPE: 5600 ft level flat holes

----	56-8	238.5 - 241 253 - 263	2.5 10 (sil break zone)	.02 trace
----	56-43	232 - 233 234 - 236.5 245 - 248 257 - 258 330 - 335	1 2.5 3 1 5	trace trace .02 trace trace
----	56-27	177 - 181 198.5 - 200.5 215.5 - 216	4 (sil. GC brecc./75%qtz) 2 0.5	trace - .03 .02 trace

### Deep holes below the 5600 ft level

----	56-86 N-75°N	894.5 - 896.5 898.5 - 900 920 - 925 935 - 947	2 (90% qtz) 1.5 5 (35% qtz) 12 (90% qtz)	trace trace trace trace - .05
------	--------------	--	---	--

### OUTSIDE GREEN CARBONATE ENVELOPE: New Diorite Zone; Deep holes below the 5600 ft level

----	56-65 (N-60°)	1031 - 1036 1045 - 1049.5	5 4.5	trace .02
----	56-68 (N-67°)	926 - 928	2 (80% qtz)	.02
----	56-76 (N-40°)	777.5 - 781 859.5 - 861	3.5 (qtz brecc. fault zone) 1.5 (sil. fault breccia)	.01 .01
----	56-78 (N-60°)	659 - 662	3	trace
----	56-82 (N-60°)	634 - 637 643.5 - 647	3 (qtz breccia) 3.5 (90% grey qtz)	trace trace - .01

**Table 1. Ranking of Top 8 Superior Province Archean Au-Quartz Vein Systems**

<b>RANKING</b>	<b>AU-QUARTZ VEIN SYSTEM</b>	<b>TONNES Au*</b>
1	Hollinger - McIntyre	995
2	Kirkland Lake (7 mines)	720
3	Campbell-Dickenson (Red Lake)	460
4	Dome	391
5	Kerr Addison - Chesterville	332
6	Lamaque - Sigma	254
7	Doyon - Bousquet - Dumagami	246
8	Pamour #1 (Timmins)	101

\* Production + Reserves

**Table 2. Previous Models for Au Mineralisation in the Kerr Addison Mine Area and on the Larder Lake - Cadillac Break**

1. Structurally Controlled / Hydrothermal Alteration and Replacement		INFERRED NATURE OF "BREAK"	INFERRED ORIGIN OF Au	INFERRED NATURE OF GREEN CARBONATE (GC) ORE AND "ALBITITE" DYKES	INFERRED NATURE OF FLOW ORE
<b>AUTHORS</b>					
<b>(a) Carbonate alteration by "magmatic" fluids</b>					
Bowen (1908)	Wilson (1912)	Hopkins (1919)	Major regional structure: strong, wide carbonate altered shear zone with S side upthrust relative to N.	Au localized by late faults within or close to the Break (e.g. Kerr Fault) due to fracturing of competent lithologies.	Mineralised and silicified volcanic flows; dissemin. pyrite related to the same vein event as seen in the adjacent GC ore.
Cooke (1922, 1923)	Stadelman (1939)			Carbonate-replaced volcanics due to quartz vein stockworks; "syenite" and "diorite" dykes predominate Au but cause carbonate alteration.	
Crombie (1939)	Jenney (1941)	Thomson (1941)			
Buffam and Allen (1948)	Baker et al. (1957)	James et al. (1961)	Cunningham (1987)		
<b>(b) Hydrothermal alteration (unspecified fluids)</b>					
KA Geol Staff (1967)	Downes (1980, 1981)	Thomson (1980)	Trowell (1980)	Late vein qtz-carb-K-metasomatism of ultramafic breccias / conglomerates. Au remobilised from syngenetic flow ore. "Albitites" postdate metasomatism.	Primary exhalative pyritic silicified tuffs with interbedded pillowed mafic volcanic flows.
Chartanis (1984)	Lowrie and Wilson (1986)			Altered spinifex-textured komatiites. GC alteration related to quartz-carbonate veins; "syenite" intrusions predominate Au.	Fe-tholeiite pillowed flows. Au in pyritic hydrothermal replacement zones.
Hamilton and Hodgson (1983, 1984)	Hamilton (1986)			Schistose high strain rocks at sediment - mafic/ultramafic volcanic contact; host rocks show extensive hydrothermal alteration and replacement.	
Toogood and Hodgson (1985)	Toogood and Hodgson (1986)	Toogood (1986, 1989)			
<b>(c) "Metamorphic fluids"</b>					
<b>(i) Accretionary prism dewatering</b>					
Gauthier et al. (1988)					
<b>(ii) Greenschist / amphibolite facies (upper crust)</b>					
Kerrich (1983)	Kerrich et al. (1987)	Kishida and Kerrich (1987)	Kerrich and Fryer (1988)	Stockwork hydrothermally brecciated fuchsite ultramafic protolith; "felsic" dykes may host ore veins.	Disseminated hydrothermal pyrite (± Au) in Fe-rich tholeiitic volcanics.
<b>(iii) Amphibolite / granulite facies (lower crust)</b>					
Hodgson and Hamilton (1989)	Hodgson et al. (1989)			Altered spinifex-textured komatiite flows and breccias.	Altered low-Mg tholeiites with interflow graphitic sediments.
				Komatiite - tholeiite volcanic assemblage formed at accreting oceanic margin.	
				Au derived from thickening-induced granulitisation in presence of mantle CO <sub>2</sub> fluid; felsic melts and hydrothermal fluids channelled Au up active end-D2 backthrusts.	

Author(s)	Key Findings / Geological Context	Rock Type	Notes
Colvine et al. (1988) Colvine (1989) Fyon et al. (1989)	Late prominent linear fault within large scale transcurrent / oblique slip deformation zone.	Basalt.	
Jemielita et al. (1990)	Major structural break	Komatite.	
	Au in late dilatational structures; Au fluids from lower crustal granulites via magma underplating, cratonisation.		
	"Young" (~2630-2580 Ma) fluids derived from lower crustal granulites.		

## 2. Syn-Sedimentary Exhalative (+/- Later Remobilisation of Au)

### (a) Carbonate facies iron formation

Brock (1907)

"Rusty, stratified ferrous dolomite".

Ridler (1968 to 1976)

No Break offset or change in m/n grade; Timiskaming correlated with auriferous Boston BIF to S and interbedded "K-rich tufts".

Folded, recrystallised auriferous carbonate facies BIF "remobilised" as "felsic" intrusions.

Hutchinson et al. (1971)

Goodwin (1962, 1965, 1984)

Syngenetic Au exhalite B.I.F. with alkaline pyroclastics derived from mineralized felsic syenite volcanic centres.

Tuffaceous lean sulphide facies BIF (17.2% Fe) with coarse decite breccia (cf. Noranda massive sulphides).

### (b) Chemical sediments: lagoonal / shallow shelf or playa-type evaporites

Hyde (1975)

Growth fault; accommodates basin subsidence between Kinopjavis and Larder L. volcanic piles; sediments incompetent i.e. folded and faulted.

Chemical sediments (carbonate from oxidation of organic carbon); Au remobilised into quartz veins by dehydrating; "albitite" dykes = "sandstones" talc-chlorite schists = ultramafic volcanics.

Jensen (1978)

Jensen and Hinze (1979)

Lovell (1967 to 1980)

Lovell and Grabowski (1981)

Lovell et al. (1985)

Hinze et al. (1986)

C- rich Au "proton" sediments at basin edge remobilised by hot intercalated volcanic flows; m/n brines and felsic magmas leach and carry Au to surface.

Cherty feldspathic carbonaceous pyritic chemical sediment; Au remobilised into carbonate-altered lava flows.

(c) Flow ore = syngenetic massive sulphide-type exhalite; green carbonate ore = remobilised Au hosted by ultramafics

Tabor, L. and Crockett (1976 to 1978)

Tabor, S. (1978)

Warwick (1981)

Zone of deformation; two foliations observed; intense regional carbonate alteration focused along the Break stratigraphic horizon.

Komatites with spinifex and flow textures; GC alteration grades into talcose ultramafics; "albitite/syenite" dykes = post-ore Na-rich melts which assimilate Au.

Syngenetic exhalative / stock work pyrite (+ Au) in low Mg tholeiites, tufts and pyroclastic breccias.

## 3. Emphasising the Role of Specific Lithologies

### (a) Ultramafic komatites

Pyke (1975)

Jensen (1977)

Ultramafic rocks are intimately associated with many major fault structures and Au deposits; Au is derived by leaching and lateral secretion from "source bed" komatites during metamorphism and carbonate alteration.

### (b) Graphitic / organic carbon

Springer (1983 to 1986)

Wilson and Rucklidge (1986, 1987)

Graphitic rocks are intimately associated with some Au deposits e.g. Kerr Addison, Hollinger-McIntyre, Omega, Owl Creek and Hoyle Pond, and exert a combined chemical and structural influence on external fluids i.e. precipitation of Au via local reduction, destabilisation of metallic complexes / scavenging by activated carbon or "semigraphitic", and fluid focusing through incompetent carbonaceous units.

### (c) Stratiform kimberlitic igneous carbonate / exhalite

Stricker (1978)

Modern Fe-Mg carbonates and aluminates of the East African Rift have anomalous Au contents (~20 ppb). The laterally extensive "carbonate rocks" along the Break are interpreted as a Au-hosting exhalative kimberlitic carbonatic, interfingering with ultramafic igneous rocks, in a rift environment associated with Timiskaming alkaline felsic volcanics.

**Table 3A. Kerr Addison Ore Body Production Figures\* Listed in Order of Decreasing Au Produced**

ORE BODY NUMBER AND TYPE	Total Au kg <sup>1</sup>	Grade g/t Au <sup>1</sup>	Ore Tonnage tonnes <sup>2</sup>	Levels Developed (ft) <sup>3</sup>
# 11 flow ore	171,834.7	10.6	13,273,669	700-3600
# 14 green carbonate ore	48,561.8	9.93	4,890,873	175-4200
# 18 flow-graphitic ore	37,574.4	8.73	4,266,313	300-3250
# 10 green carbonate ore	27,276.2	7.40	3,679,550	175-2650
# 4 flow ore	21,447.2	10.72	2,038,202	1300-2800
# 15 green carbonate / "albitite" ore	13,895.1	6.64	2,084,122	175-3850
# 9 green carbonate ore	10,931.9	5.65	1,935,526	175-1600
# 19 green carbonate ore	4152.5	6.58	629,510	175-1450
# 17 flow ore	3737.3	6.73	804,589	500-1450
# 24 green carbonate ore	3301.6	11.92	276,722	1450-2800
# 18 green carbonate ore	2463.5	5.75	428,660	300; 1000-1900
# 26 green carbonate ore	1501.5	8.60	176,002	175-500
# 8 flow ore	1041.8	7.16	145,186	175-1300
# 11 flow ore	648.2	5.00	129,741	175-700; 1450
# 13 green carbonate ore	374.7	7.09	52,910	300-700
# 23 flow ore	342.1	4.89	58,143	1000-2350
# 12 flow ore	131.3	6.04	52,287	175-300
# 22 green carbonate ore	37.4	5.14	7,276	500-1000; 1900
# 20 green carbonate ore	2.3	1.20	1,882	300
# 7 green carbonate ore	1.7	1.78	973	300
Miscellaneous green carbonate ore (Reddick, development drifts etc)	301.1	5.48	54,784	175-5600
<b>TOTAL FLOW ORE<sup>4</sup></b>	<b>222,917.7</b>	<b>11.41</b>	<b>19,524,220</b>	
<b>TOTAL GREEN CARBONATE ORE<sup>5</sup></b>	<b>111,330.6</b>	<b>8.07</b>	<b>13,789,004</b>	
<b>TOTAL GRAPHITIC ORE<sup>4</sup></b>	<b>14,299.0</b>	<b>7.90</b>	<b>1,810,000</b>	
<b>TOTAL "ALBITITE" ORE<sup>5</sup></b>	<b>1,484.4</b>	<b>3.54</b>	<b>419,786</b>	
<b>KERR ADDISON TOTAL</b>	<b>350,031.7<sup>6</sup></b>	<b>9.85<sup>6</sup></b>	<b>35,543,016</b>	

**\*NOTES:**

1 Calculated from summated muck (car) sample averages, corrected monthly to agree with back-calculated head grade (allowing for ~ 5-10% losses in the milling process).

2 Based on tonnages trammed, corrected monthly to agree with surveyed slope dimensions and measured weight of ore passing through the mill.

3 Refers to the mine level immediately below where stoping took place i.e. that on which the ore was trammed to the ore pass.

4 Estimated total graphitic ore data from Wilton and Lowrie (1986), and listed here separately from the totals for flow ore.

5 The #15 orebody between the 3250 ft and 3850 ft levels consists entirely of plug-hosted "albitite" ore which is listed here separately from the totals for green carbonate ore. Green carbonate ore is further estimated (this study) to contain ~5-15% "albitite" dyke ore (by volume).

6 Sum total kg Au and grade derived from above totals, based on monthly averages corrected to agree with the back-calculated mill head grade. Actual bullion production = 320,473.9 kg Au (91.56% of above total).

**Table 3B. Chesterville (1939-52) Ore Body Production Figures\* Listed in Order of Decreasing Au Produced**

ORE BODY NUMBER AND TYPE	Total Au kg <sup>1</sup>	Grade g/t Au <sup>2</sup>	Ore Tonnage tonnes <sup>3</sup>	Levels Developed (number) <sup>4</sup>
D "albite" / green carb ore	5,781.3	5.14	1,123,756	2nd - 18th levels
A flow ore	3,376.4	4.38	784,756	surface - 5th level
C flow / brown carb ore	2,882.3	5.59	460,591	surface - 6th level
J "albite" ore	1,551.4	4.39	353,496	10th - 18th levels
21K flow ore	486.1	3.68	84,676	10th - 13th levels
F green carbonate ore	390.5	3.76	103,739	4th, 13th-17th levels
B flow ore	142.8	3.74	28,024	surface - 4th level
G flow ore	70.5	3.23	21,618	surface - 9th level
E green / chloritic carb ore	57.5	3.64	15,794	2nd - 3rd levels
<b>TOTAL FLOW ORE</b>	<b>7,028.3</b>	<b>4.86</b>	<b>1,389,866</b>	
<b>TOTAL GREEN CARBONATE ORE<sup>5</sup></b>	<b>6,229.3</b>	<b>5.01</b>	<b>1,243,289</b>	
<b>TOTAL "ALBITITE" ORE<sup>5</sup></b>	<b>1,551.4</b>	<b>4.39</b>	<b>353,496</b>	
<b>CHESTERVILLE TOTAL</b>	<b>14,809.0</b>	<b>4.96</b>	<b>2,986,651</b>	

\*NOTES:

- 1 Calculated by multiplying average grade (#2) by tonnage (#3), adjusted for total amount of Au recovered (known).
- 2 Grade for each ore body based on the weighted average of drill intersection data across it (FRP).
- 3 Tonnage based on section-by-section planimetry (FRP), adjusted for total tonnage of ore recovered (known).
- 4 Refers to the mine levels between which stoping took place (unlike that in Table 3A).
- 5 The "J" orebody consists entirely of plug-hosted "albite" ore which is listed here separately from the totals for green carbonate ore. Green carbonate ore is further estimated (this study) to contain ~5-15% "albite" dyke ore (by volume).

**Key to Au mine localities along the Larder Lake - Cadillac Break in Figure 1  
(tonnes Au production + reserves<sup>1</sup> shown in brackets):**




1	Stairs (<0.1)	45	DOYON - BOUSQUET #1/#2 - DUMAGAMI *(246.0)
2	Ashley (1.6)	46	Bouscadillac (<0.1)
3	Young-Davidson (18.2)	47	New Alger/Thompson Cadillac (0.5)
4	Matachewan Consolidated (11.8)	48	Darius/O'Brien *(22.0)
5	Crescent Kirkland (<0.1)	49	Kewagama (<0.1)
6	Golden Gate (1.0)	50	Consolidated Central Cadillac (2.8)
7	Lucky Cross (<0.1)	51	Wood-Cadillac (0.9)
8	KIRKLAND LAKE CAMP (720.1 TONNES Au):	52	Lapa Cadillac (1.5)
	Macassa (85.0)	53	Pandora *(10.1)
	Kirkland Gold (36.5)	54	West Malartic (1.1)
	TECK-HUGHES (114.7)	55	Canadian Malartic (37.2)
	LAKESHORE (264.4)	56	Sladen Malartic (5.3)
	WRIGHT-HARGREAVES (149.8)	57	East Malartic (88.7)
	Sylvanite (51.9)	58	Malartic Goldfields (53.0)
	Tobum (17.7)	59	Camflo/Malartic Hygrade (51.0)
	Kirkland Townsite (<0.1)	60	Barnat (38.7)
9	Pawnee (<0.1)	61	Aur/First Canadian (<0.1)
10	Bidgood (5.0)	62	Kiena *(33.0)
11	Moffat-Hall (0.2)	63	Siscoe (27.4)
12	Morris Kirkland (0.5)	64	Sullivan Consolidated (36.7)
13	Anoki *(2.8)	65	SIGMA (100.1)
14	McBean/Queenston (1.4)	66	LAMAQUE (153.4)
15	Upper Canada (43.5)	67	Orenada (<0.1)
16	Princeton/Ritoria (<0.1)	68	Braminco #4 (<0.1)
17	Misema R. (<0.1)	69	Sigma-2 (<0.1)
18	Laguette (0.3)	70	Courvan-Bussieres (1.2)
19	Raven River (<0.1)	71	Louvicourt Goldfields (1.0)
20	Omega (6.7)	72	Chimo (<0.1)
21	Femland *(0.2)		
22	Cheminis *(13.2)		
23	Barber-Larder (0.6)		
24	Armistice/Arjon *(2.3)		
25	KERR ADDISON / CHESTERVILLE (331.4)		
26	Francoeur #1/#2/#3 *(19.8)		
27	Arntfield (1.7)		
28	Wasamac #1/#2 *(10.8)		
29	Wakeko (<0.1)		
30	Bazooka (<0.1)		
31	Durban (<0.1)		
32	Cinderella (<0.1)		
33	Granada *(5.4)		
34	Astoria (6.8)		
35	Plexore (<0.1)		
36	McWatters *(8.8)		
37	Rouyn Merger (?)		
38	Heva Cadillac (<0.1)		
39	Hosco (<0.1)		
40	Odyo/Calder Bousquet (<0.1)		
41	Norgold (<0.1)		
42	Doreva (<0.1)		
43	Mic Mac (3.2)		
44	Mooshla (<0.1)		

TOTAL (accounted for; 72 deposits) = 2130.9 TONNES Au


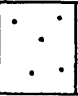

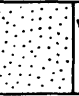


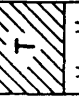
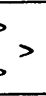
<sup>1</sup> Sources: Bertoni (1983); The Northern Miner (1988-1990); and other sources.

# LEGEND


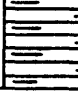
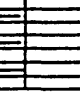


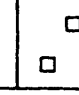

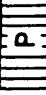
N	~ 2215 Ma <sup>1</sup>	NIPISSING DIABASE
H	~ 2400 Ma <sup>2</sup>	HURONIAN SEDIMENTS

	ULTRAMAFIC SILLS
	GRANITOIDS
	QUARTZ FELDSPAR PORPHYRY

## NORTH OF LARDER LAKE - CADILLAC BREAK:

	TIMISKAMING GROUP, CADILLAC GROUP
	UPPER BLAKE RIVER GROUP, GAUTHIER GROUP
	BLAKE RIVER GROUP
	KINOJEVIS GROUP, ROUYN THOLEIITE UNIT
	KEWAGAMA GROUP, CASTE GROUP
	MALARTIC GROUP, LA-MOTTE - VASSAN GROUP
	TISDALE GROUP
	HEVA FORMATION, VAL D'OR FORMATION

## SOUTH OF LARDER LAKE - CADILLAC BREAK:

	SKEAD GROUP, UPPER DELOORO UNIT
	LARDER LAKE GROUP (MAFIC / ULTRAMAFIC VOLCANICS) PICHE & VILLEBON GROUPS, HIGHWAY 11 BASALTS
	LARDER LAKE GROUP (SEDIMENTS), "PORCUPINE GROUP"
	CATHERINE GROUP
	WABEWAWA GROUP
	PACAUD TUFFS
	PONTIAC GROUP (SEDIMENTS)
	PONTIAC GROUP (ULTRAMAFICS)

<sup>1</sup> Corfu (1987), Noble (pers. comm. 1990)

<sup>2</sup> postdate Matachewan dyke swarm, 2452 ± 2/-3 Ma (Heaman, 1989)



## **Appendix I. Conference Abstracts (x5) Published during This Study**

- 1. Evidence for a mafic "albitite" intrusion/Archean Au association, Kerr Addison-Chesterville mines, N. Ontario.**  
SMITH, Justin P. and SPOONER, Edward T.C. (1990)  
Central Canada Geological Conference, Ottawa University, March 1990, Program with Abstracts.
- 2. Evidence for a mafic "albitite" intrusion/Archean Au structure-time association, Kerr Addison - Chesterville mines, northern Ontario.**  
J.P. Smith and E.T.C. Spooner (1990)  
In: F. Robert (Editor), NUNA Conference Volume: Greenstone Gold and Crustal Evolution, Val d'Or, Quebec, May 1990, GAC Mineral Deposits Division Special Publication, p 203-204a.
- 3. Evidence for a mafic "albitite" intrusion/Archean Au structure-time association, Kerr Addison - Chesterville mines, N. Ontario.**  
SMITH, Justin P. and SPOONER, Edward T.C. (1990)  
IAGOD Symposium, Ottawa-Carleton Geoscience Centre, August 1990, Program with Abstracts.
- 4. The Kerr Addison/Chesterville Archean Au-quartz vein system, Virginiatown, N. Ontario, I; The bottom and vertical trends.**  
Smith, J.P., Spooner, E.T.C. and Ploeger, F.R. (1991)  
GAC-MAC-SEG Joint Meeting, Toronto, May 1991, Abstracts with Programs, p A116.
- 5. The Kerr Addison/Chesterville Archean Au-quartz vein system, Virginiatown, N. Ontario, II; The upper part.**  
Spooner, E.T.C., Smith, J.P. and Ploeger, F.R. (1991)  
GAC-MAC-SEG Joint Meeting, Toronto, May 1991, Abstracts with Programs, p A117.

## **1. EVIDENCE FOR A MAFIC “ALBITITE” INTRUSION / ARCHEAN AU ASSO- CIATION, KERR ADDISON - CHESTERVILLE MINES, N. ONTARIO**

**SMITH, Justin P. and SPOONER, Edward T.C.**, Department of Geology, University of Toronto, 22 Russell St., Toronto, Ontario, M5S 3B1.

The combined Kerr Addison - Chesterville mines (340 tonnes Au) comprise Canada's #4-largest Archean Au-quartz vein / disseminated-type ore system, hosted within deformed spinifex-bearing komatiites and mafic pillow lavas of the Larder Lake Group, Abitibi Greenstone Belt. Gold mineralisation, bounded by a steep, funnel-shaped hydrothermal alteration envelope, is contained within the Kirkland - Larder Lake - Cadillac “Break”, a >300km strike length ductile/brittle shear zone interpreted as a flattened and steepened thrust (Hodgson et al, 1989; this work). Four main ore types are found, “flow ore”, “green carbonate / siliceous break ore”, “albitite dyke ore” and “graphitic ore”. In this study, underground mapping, structural and relative time sequence analysis have been combined with data from over 6000 drillholes to determine the detailed controls on the horizontal and vertical location of Au mineralisation. Work has mainly concentrated on the ultramafic-hosted “green carbonate / siliceous break ore” which shows nine stages (five Au-related) of quartz-carbonate veining and associated alteration, and four episodes of mafic “albitite” intrusion, based on mapped cross-cutting relationships confirmed throughout the mine. Main-stage Au mineralisation was introduced during ductile deformation, characterised by flattened aspect ratios (ca. 5:5:1) of finite strain markers. A significant finding of this study has been that the ore system is characterised by a major plug (Chesterville) and intense swarm of mafic “albitite” dykes (Kerr Addison, ca. 10% volume of the mine) exactly co-spatial, co-structural and significantly overlapping in time with main stage Au mineralisation. In view of this close igneous intrusion / Au association, it is possible that both mafic “albitite” intrusions and Au fluids were derived from a larger, evolving, parent magma system at depth.

## 2. EVIDENCE FOR A MAFIC “ALBITITE” INTRUSION / ARCHEAN AU STRUCTURE-TIME ASSOCIATION, KERR ADDISON - CHESTERVILLE MINES, NORTHERN ONTARIO

J.P. Smith and E.T.C. Spooner, Department of Geology, Earth Sciences Centre, University of Toronto, 22 Russell St., Toronto, Ontario M5S 3B1.

The combined Kerr Addison (34.93 million tonnes at 9.3 g/t Au) - Chesterville (2.96 mt at 3.8 g/t Au) mines comprise Canada's fourth largest (~335 tonnes Au) Archean Au-quartz vein / disseminated-type ore system. It is located **within the Larder Lake - Cadillac Break** at Virginiatown-Kearns, ~500 km north of Toronto, 2 km west of the Quebec border. The Break is a >300 km strike length ductile/ brittle shear zone interpreted from surface and underground mapping in the Larder Lake area as a flattened and steepened, south-over-north thrust (Hodgson and Hamilton, Economic Geology Monograph 6, p.86-100, 1989; this work). To the east, the Break defines the Pontiac-Abitibi sub-province boundary and is associated with the Piché Group ultramafics. The Kerr host rocks comprise deformed spinifex-textured komatiites and mafic Fe-tholeiite pillow lavas at the structural base of the Larder Lake Group, with a small percentage of interflow sediments. Units strike at 060° and dip 78° north-west, and appear to be overturned.

The ore system is contained within a funnel-shaped hydrothermal alteration envelope plunging 70°E in longitudinal section to a deep (≥4km) focal fluid source, and is lens-shaped in plan, elongated along the “Break”. The alteration envelope has a strike length of ~900 m on surface, decreasing to ~300 m at the deepest drilled depth of ~2000 m, and widths of up to 120 m in the ultramafic host rock and 50 m in the adjacent mafic volcanics to the south. The Au system consists of four main ore types: an intense feeder quartz vein system in altered ultramafics (“green carbonate / siliceous break ore”); more consistent-grade blocks

of vein /disseminated, pyritic “flow ore” developed in pillowed Fe-tholeiites; mafic dyke/ plug-hosted “albitite ore”; and interflow sediment-contaminated, flow-hosted “graphitic ore”. These are distributed among 19 (Kerr) and 8 orebodies (Chesterville). At Kerr Addison, historic production attributed to each ore type is as follows: flow ore - 21.08 mt at 11.2 g/t Au (including graphitic ore - 1.81 mt at 7.9 g/t Au) and green carbonate ore - 13.29 mt at 8.0 g/t Au (including ~15-20% “albitite” dyke ore).

In this study, underground mapping, and structural and relative time sequence analysis have been combined with data from over 6000 drillholes to determine the factors controlling the horizontal location, vertical interval and depth-grade trends of Au mineralisation. Work has mainly concentrated on the ultramafic-hosted “green carbonate / siliceous break ore” which shows nine stages (five Au-related) of quartz-carbonate veining and associated alteration, and four episodes of mafic “albitite” dyke / plug intrusion, based on mapped cross-cutting relationships confirmed throughout the mine. **Main-stage Au mineralisation was introduced during ductile deformation**, characterised by flattened aspect ratios (~ 5:5:1) of finite strain markers (e.g. pillows, varioles, polyhedral vein networks) and folding / boudinage of syn-kinematic Au-quartz veins and dykes. Potassic alteration of ultramafic host rocks to fuchsite (Cr-mica)-bearing “green carbonate” rock occurs only adjacent to main stage Au-quartz veins and is contemporary with vein formation. Carbonate alteration also occurs due to barren pre- and post-ore veining, which could cause potential confusion in regional exploration.

Stoped green carbonate ore corresponds to the greatest density of siliceous break quartz veins and abundant “albitite” dykes, both of which have 70-90° N or S dips and strike at low angles ( $\pm 30^\circ$ ) to the Break fabric. The ore is characterised by an anastomosing, early brittle-ductile fault framework which controlled subsequent Au-quartz vein dilatancy and the supply of ore fluids from depth. Vein systems expand upwards from a narrow root zone

controlled by major “sil. break” vein structures. A major plug (Chesterville) and intense swarm of >5000 mafic “albitite” dykes (Kerr Addison) occur preferentially in the least competent ultramafic host rock and form ~10% of its volume. **The dyke swarm is confined to the green carbonate alteration envelope, and is closely co-spatial, co-structural and significantly overlapping in time with main stage Au mineralisation.** Later dykes in the time sequence contain fewer vein stages and are less hydrothermally altered and mineralised than the earlier dykes which they observably cross-cut. Geochemistry and petrography of the intrusions indicate they were originally mafic, alkaline, and possibly of shoshonitic affinity, before variable sodic alteration to “albitites” consisting of secondary albite-quartz-carbonate-pyrite(+Au)-mica and rutile.

**The weight of the geological evidence suggests that both mafic “albitite” intrusions and Au fluids were derived from a larger, evolving, common parent magma system at depth, irrespective of the absolute age of mineralisation.** Significantly for exploration, the Kerr appears to pass upwards and distally into barren green carbonate alteration without quartz veins, silicification or dykes.

### 3. EVIDENCE FOR A MAFIC “ALBITITE” INTRUSION / ARCHEAN AU STRUCTURE-TIME ASSOCIATION, KERR ADDISON - CHESTERVILLE MINES, N. ONTARIO

SMITH, Justin P. and SPOONER, Edward T.C., Department of Geology, University of Toronto, 22 Russell St., Toronto, Ontario, M5S 3B1.

The combined Kerr Addison - Chesterville mines (~340 tonnes Au) comprise Canada's #4-largest Archean Au-quartz vein / disseminated-type ore system, located on the Kirkland Lake-Larder Lake-Cadillac “Break” at Virginiatown /Kearns, ca. 500 km north of Toronto, 2 km west of the Quebec border. The “Break” is a >300km strike length ductile/brittle shear zone interpreted in the Larder Lake area, from surface and underground mapping, as a flattened and steepened south side up thrust (Hodgson et al, 1989; this work). To the east, the “Break” defines the Pontiac sub-province boundary and lies within the ultramafics of the Piché Group.

The ore system is bounded by a funnel-shaped hydrothermal alteration envelope plunging 70°E in longitudinal section to a deep (> 4km) fluid source, and is lens-shaped in plan, elongated along the “Break”. It consists of an intense feeder quartz vein system (“green carbonate ore”) with more consistent-grade blocks of vein /disseminated-type pyritic “flow ore”. The host rocks comprise deformed spinifex-textured komatiites and mafic Fe-tholeiite pillow lavas at the structural base of the Larder Lake Group, with a small percentage of interflow sediments. Units strike at 060° and dip 78°N, and may be overturned. Four main ore types occur, these being “flow ore”, “green carbonate / siliceous break ore”, “albitite dyke ore” and “graphitic ore”, distributed among 19 orebodies (Kerr) and 8 orebodies (Chesterville). Main-stage Au mineralisation was introduced during ductile deformation, characterised by flattened aspect ratios (ca. 5:5:1) of finite strain markers (e.g. pillows,

varioles, polyhedral vein networks) and folding / boudinage of syn-kinematic Au-quartz veins and dykes. Potassic alteration of ultramafic host rocks to fuchsite (Cr-mica)-bearing “green carbonate” rock is a sensitive indicator of main stage Au-related veining.

In this study, underground mapping, and structural and relative time sequence analysis have been combined with data from over 6000 drillholes to determine the factors controlling the horizontal location and vertical interval of Au mineralisation. Work has mainly concentrated on the ultramafic-hosted “green carbonate / siliceous break ore” which shows nine stages (five Au-related) of quartz-carbonate veining and associated alteration, and four episodes of mafic “albitite” dyke / plug intrusion, based on mapped cross-cutting relationships confirmed throughout the mine. A significant finding of this study has been that the ore system is characterised by a major plug (Chesterville) and intense swarm of >5000 mafic “albitite” dykes (Kerr Addison), intruded preferentially into the least competent ultramafic host rock and forming ca. 10% of its volume. The dyke swarm is closely co-spatial, co-structural and significantly overlapping in time with main stage Au mineralisation as well as being syn-deformational relative to “Break” ductile strain. Stopped green carbonate ore corresponds to the greatest concentration of siliceous break quartz veins and “albitite” dykes, both of which have 70-90° N or S dips and strike at a low angle ( $\pm 30^\circ$ ) to the “Break” fabric. The densities of both dyke and vein occurrence fall off to zero at the margins of the green carbonate alteration envelope, and also decrease towards the surface.

In view of this close igneous intrusion / Au association, it is possible that both mafic “albitite” intrusions and Au fluids were derived from a larger, evolving, common parent magma system at depth.

#### 4. THE KERR ADDISON/CHESTERVILLE ARCHEAN AU-QUARTZ VEIN SYSTEM, VIRGINIATOWN, N. ONTARIO, I; THE BOTTOM AND VERTICAL TRENDS.

Smith, J.P., Spooner, E.T.C., Dept. of Geology, University of Toronto, 22 Russell St., Toronto, Ontario, M5S 3B1; and Ploeger, F.R., GSR/Deak Resources Ltd., Kerr Mine, Virginiatown, Ontario P0K 1X0.

The Kerr Addison/Chesterville Archean Au-quartz vein/disseminated ore system (~335t Au) developed syn-deformationally within the Larder Lake-Cadillac ductile deformation zone (width ~150 m ) and is characterized by a flat, funnel-shaped green (fuchsitic) carbonate alteration envelope plunging 70°E in the plane of the deformation zone; the latter shrinks from ~900 m (strike length)x 60-75 m near surface to ~300x 20-50 m (≥5600 ft level). The ore system expands and inflates ( e.g. quartz veins) upwards between the ~5000 and ~3000 ft levels showing correlated increases in length/width/area per level of green carbonate alteration (area ~x6), >0.3 m~11m thick quartz veins (max.~x8), >0.3 m~35m thick "albitite" intrusions (max.~x8), Au grade ( to~17 g/t for flow ore) and total contained Au (upward increase from 0 to ~18t Au/level between the 4600 and 3850 ft levels)

The hydrothermal alteration root zone is small (~300x 20-50 m; ≥5600 ft level) , characterized by major quartz veins (e.g. ~3x50 m; 4000 ft level) but with very low Au grades and Au mineralized "albitite" dykes. It contracts around an "albitite" intrusion/vein zone in the E. part of the deep system which connects with the eastern Chesterville plug within the hydrothermal alteration envelope at higher levels. The total volumes of hydrothermal fluid and magma which produced the green carbonate alteration, quartz veins and "albitite" dyke/plug swarm of the main system must have passed up tthrough this relatively narrow, low grade feeder zone. The bulk of the Au mineralization is contained within ~1130 vertical metres between the ~4000 and ~300 ft levels at ~9-18t Au/level, is characterized by 5-20%,



>0.3 m--11 m thick quartz veins and 5-25%, >0.3 m--35 m thick "albitite" intrusions and shows an upward increase in Au:Ag ratios from ~16 to ~21; the latter trend is a rare example of vertical zoning in an Archean Au-quartz vein system and must reflect Ag depletion in the fluid through partition into precipitated Au. Correlated volumetric inflation and Au deposition within quartz veins (green carbonate ore) can be interpreted to be a result of H<sub>2</sub>O - CO<sub>2</sub> phase separation.

## 5. THE KERR ADDISON/CHESTERVILLE ARCHEAN Au-QUARTZ VEIN SYSTEM, VIRGINIATOWN, N. ONTARIO, II; THE UPPER PART.

Spooner, E.T.C., Smith, J.P., Dept of Geology, University of Toronto, 22 Russell St., Toronto, Ontario M5S 3B1; and Ploeger, F.R., GSR/Deak Resources Ltd., Kerr Mine, Virginiatown, Ontario P0K 1X0.

The upper ~150-370 m of the Kerr Addison /Chesterville Archean Au-quartz vein/disseminated ore system (~335t; ~9g/t Au) show marked correlated decreases in the following (per level): green carbonate alteration, quartz veins (>0.3 m thick), % quartz veins (>0.3 m thick) and >0.3 m thick "albitite" intrusions; variations which can be used in exploration e.g. green carbonate alteration persists further than >0.3 m thick quartz veins and >0.3 m thick "albitite" intrusions, which decrease together, the decrease in "albitite" dykes being more irregular. Au grades and total contained Au values start to decrease upwards before other parameters, at depths of ~490-610 m, thus documenting depletion of the hydrothermal fluid in Au. These trends explain why green carbonate alteration + thin (>0.3 m) quartz veins are relatively low grade at the surface; the first ore intersected (1937) was at ~90 m. It is estimated that the height of green carbonate alteration (thickness >15m) above the present erosional level was only ~150-300 m and that therefore the Kerr Addison/Chesterville system did not penetrate to the Archean paleosurface c.f. blind Chesterville East zone. Thinner localized widths of green carbonate alteration would have penetrated upwards further. The fact that the top of the Kerr Addison/Chesterville system is close to the present erosion level is fortuitous. Hence, deep drilling of surface exposed hydrothermal alteration/low grade Au zones in the Timmins/Val d'Or area is justified (e.g. Norwanda/Freewest Resources Lightning zone) and trends in hydrothermal widths, >0.3 m quartz vein cumulative widths, >0.3 m "albitite" dyke (if present) cumulative widths, Au grade, Au:Ag ratio and possibly, fluid inclusion  $\text{CH}_4/(\text{CH}_4 + \text{CO}_2)$  ratio ( Spooner et al., 1987) can be used in

estimating vertical level. Kerr Addison/Chesterville shows an almost complete vertical interval for an Archean Au-quartz vein system containing in particular, very low grade quartz veins at both bottom and top; the latter feeders are low grade because the fluid was Au depleted. The correlated variations in quartz vein and "albitite" intrusion areas per level suggest that hydrothermal ore fluid and "albitite" magma were in physical contact in order to transmit and equalize hydraulic pressure.

**Appendix II: Grant 364 The Kerr Addison-Chesterville Archean  
Gold-Quartz Vein System, Virginiatown: Time Sequence  
and Associated Mafic "Albitite" Dyke Swarm.**

**J.P. Smith, E.T.C. Spooner, D.W. Broughton, and F.R. Ploeger , 1990**

**In: "Geoscience Research Program Summary of Research 1989-1990",  
Ontario Geological Survey, Miscellaneous Paper 150, pp 175-199.**

**Appendix III.**

**Reconstructed Kerr Addison - Chesterville Geological Level Plans**

**not included in main paper**

**Appendix IV. Vein Carbonate and Whole Rock  $\delta^{13}\text{C}$  and  $\delta^{18}\text{O}$  Analyses**

**Kerr Addison: Green Carbonate Ore Vein Stages  
Flow Ore  
"Albitite" Dyke Whole Rock**

**Barber-Larder Pit: Late Carbonate Flat Veins**

**Macassa Mine: Late Carbonate Veins**

**McBean Mine: "Albitite" Dyke Whole Rock**

## APPENDIX IV - $\delta^{13}\text{C}/\text{XRD}$ Vein Carbonate and Whole Rock Data

### Analytical Methods

Vein carbonate material used in this study was hand picked from a suite of samples from the Kerr Addison, Barber Larder Pit, Macassa and McBean mines (J.P.S., 1987-1989). These vein samples were mapped-in and their paragenetic position established from timing and cross-cutting relationships underground (e.g. see Figure 32). 36 vein samples were coarsely crushed and fragments free of wallrock (where applicable) were selected. These samples were then finely ground by tamping in a cylindrical steel mill. A further 10 "albitite" dyke whole rock powders, previously analysed for geochemistry (see Appendix V), were also sent for stable isotopic ( $\delta^{13}\text{C}_{\text{PDB}}$ ,  $\delta^{18}\text{O}_{\text{PDB}}$ ) analysis. The carbonate contents of the powders ranged from ~10-100%. Mass spectrometric analyses were carried out by Mary-Ellen Patton, Environmental Isotope Lab., Earth Sciences Department, University of Waterloo, Canada, to an accuracy  $\pm 0.05$  per mil. for  $\delta^{13}\text{C}_{\text{PDB}}$  and  $\pm 0.05$  per mil. for  $\delta^{18}\text{O}_{\text{PDB}}$ .

X-ray diffraction analyses were carried out by J. P. Smith at the University of Toronto. 46 vein and whole rock samples (see above) were ground to a fine powder using an agate mortar and pestle. The powder was then finely spread using ethanol on one side of a glass microscope slide which was mounted in the powder X-ray diffractometer.

Key: XRD abbreviations: mag = magnesite; dol = dolomite; qtz = quartz; chl = chlorite; ank = ankerite; cc = calcite; parag = paragonite; musc = muscovite

\* = average of two repeat samples

$\delta^{13}\text{C}$ ,  $\delta^{18}\text{O}_{\text{PDB}}$  analyses provided by:

Mary-Ellen Patton  
Environmental Isotope Lab.  
Earth Sciences Dept.  
University of Waterloo  
Waterloo, Ontario.  
Canada. N2L 3G1.

## Vein Carbonate/Whole Rock Sample Descriptions - Green Carbonate Ore

Sample No	Location	Description
<b>Vein Stage #1</b> <i>Barren polygonal carbonate veins, talcose ultramafic host rock</i>		
KA 87.26	3801 N X-C	stretched polygonal lumpy white ~6mm wide carbonate veins (~30%); coarse carbonate replacement of talcose ultramafic host rock
KA 87.48 KA 87.49	1014-52 EX DR	undeformed polygonal lumpy white ~6mm wide carbonate veins; grey/brown carbonate replacement of ultramafic host rock
KA 88.88	3801 N X-C	schistose ultramafic host rock with fabric-parallel carbonate veins
<b>Vein Stage #2</b> <i>Early carbonate stockwork, weak green carbonate alteration with trace Au</i>		
KA 87.25A	3801 N X-C	deformed, shredded white carbonate stockwork veins; local green carbonate alteration with trace (9 ppb) Au
KA 88.75	1903 E DR (69E)	polygonal green carbonate stockwork defining brown polygon cores with pyrite and minor Au
<b>Vein Stage #3</b> <i>Cherty "siliceous break" Au-quartz-carbonate veins, silicification</i>		
KA 88.59	4001-62 N X-C	1 ft wide green siliceous break
KA 89.54	1915-69 EX DR	6" mottled cherty siliceous break with inclusions of green carbonate wall rock
KA 89.65	3814-63 ST	6" cherty grey- green mottled vein; contains visible gold along strike
<b>Vein Stage #4</b> <i>Main stage milky Au-quartz-carbonate veins, intense green carbonate alteration</i>		
KA 87.53	1014-52 EX DR	2 ft milky quartz Au-bearing NW-SE siliceous break
KA 88.67	1014-52 EX DR	2 ft milky quartz siliceous break, mottled with green carbonate wallrock fragments
KA 89.01	"2321-58 N X-C"	visible gold-bearing steep/flat irregular and branching 2" vein
KA 89.11	4014-63 1/2 ST	major 2 ft siliceous break cutting through dyke, cut by minor flat veins
KA 89.16	4014-63 1/2 ST	major 2 ft siliceous break adjacent to dyke contact; greenish quartz with green carbonate wallrock inclusions
KA 89.34	1715-66 EX DR	2 ft milky white quartz siliceous break
KA 89.38	1715-66 EX DR	6"-1 ft milky white quartz siliceous break
KA 89.47	3414-62 ST	(3250 level) 6" cherty/milky quartz siliceous break containing VG
KA 89.67	3814-63 ST	shallow 2-3" zoned quartz-carbonate branch off major 1 ft sil break
KA 89.68	814-61 SILL	1-2" cross vein between 2 guiding cherty siliceous breaks



Sample No	Location	Description
<b>Vein Stage #6 Irregular grey-green or black cherty veins in green carbonate or dykes</b>		
KA 89.04	1719-74 SILL	2-3" irregular grey-green cherty vein/silicification cross-cuts shredded green carbonate
KA 89.43	1915-69 EX DR	network 1/2" irregular black cherty veins with pyritic selvages (+Au, remobilised)
KA 88.34	2015-64 POD	silicified fault breccia containing flecks of brown-yellow carbonate
KA 88.58	4001-62 N X-C	silicified fault breccia containing flecks of brown-yellow carbonate

**Vein Stage #8 Late flat quartz-carbonate veins; barren; contain tetrahedrite locally**

KA 87.24	3801 N X-C	1" wide late flat quartz-carbonate vein cutting 5 ft wide silicified dyke
KA 87.36	2514-57 1/2	3" wide flat quartz-coarse brown carbonate vein cutting Au-bearing siliceous break
KA 89.33	1715-66 EX DR	1-2" wide shallow dipping en echelon quartz-carbonate vein cutting a silicified fault breccia
KA 89.58	1915-69 N X-C	3-6" wide coarse brown carbonate-quartz shallow veins

**Vein Stage #9 Late chlorite-carbonate E-W slips**

KA 89.44	1915-69 EX DR	strong gougey 3" wide chloritic slip fault infilled by clean white interlocking coarse calcite
----------	---------------	--

**Vein Stage #10 very late N-S open fissure veins**

KA 89.09	1719-74 SILL	2" wide steep N-S vuggy fissure vein, with colourless crystalline calcite and hematite
----------	--------------	--

**Vein Carbonate/Whole Rock Sample Descriptions - Flow Ore**

Sample No	Location	Description
KA 87.43	1117-66ST	slightly smoky, deformed 3" wide quartz vein with a pyritic alteration selvage
KA 87.44	1117-66ST	1 ft wide smoky, folded and attenuated vein; minor pyrite selvage
KA 89.79 KA 89.82	866 SX-C	very irregular, deformed branching 5" wide milky quartz veins with pyritic alteration selvages

### BARBER-LARDER PIT

BP 89.01 at contact of ultramafic and mafic volcanics large ~1 ft wide shallow dipping en echelon late barren veins with coarse brown carbonate

### MACASSA MINE, KIRKLAND LAKE

MA 87.48 (Main Break 3000 ft level, #1 Shaft) deformed late pink calcite-quartz-chlorite veins in fault gouge cutting earlier mylonitised Au-quartz veins

MA 87.51 deformed white calcite-quartz-chlorite veins in fault gouge

### KERR ADDISON - WHOLE ROCK "ALBITITE" DYKE SAMPLES

Sample No	Location	Description
KA 87.02	3815-79 ST	10-20 ft wide pink-grey silicified A <sub>1</sub> dyke (grade up to 12 g/t Au)
KA 87.11	3801 N X-C	5 ft wide very pale silicified A <sub>1</sub> dyke (grade up to 6.9 g/t Au)
KA 88.47	1014-52 EX DR	10-15 ft wide brown silicified A <sub>1</sub> dyke (grade up to 4.1 g/t Au)
KA 87.17	3815-54 1/2 DR	~60 ft wide grey foliated A <sub>2</sub> dyke (trace Au grade)
KA 88.31	3815-79 ST	4 ft wide chloritic xenolithic A <sub>2</sub> dyke (trace Au grade)
KA 88.87	3815-79 ST	6 ft wide mustard-coloured, pyritic A <sub>2</sub> dyke (grade up to 2.1 g/t Au)
KA 88.32 KA 88.83	3815-79 ST	3 ft wide fresh crystalline mafic A <sub>3</sub> dyke (trace Au grade)

### McBEAN - WHOLE ROCK "ALBITITE" DYKE SAMPLES

Mc 87.01 Mc Bean open pit ore samples from surface stockpile.

Mc 87.02 Thin ~10 cm wide pink-brown "albitite" dykelets in green carbonate host rock

**$\delta^{13}\text{C}/\text{XRD}$  Vein Carbonate and Whole Rock Data**

Sample No	XRD major (minor) phases	$\delta^{13}\text{C}_{\text{PDB}}$	$\delta^{18}\text{O}_{\text{PDB}}$
<b>Green Carbonate Ore</b>			
<b>Stage #1 (see Figure 32)</b>			
KA 87.26	mag:dol (60:40), qtz, chl (?talcl)	-2.64*	-17.92*
KA 87.48	mag:dol (60:40), qtz, chl (?talcl)	-2.45	-17.15
KA 87.49	mag:dol (60:40), qtz, chl (?talcl)	-2.45	-17.25
KA 88.88	mag:dol (60:40), qtz, chl (?talcl)	-2.65	-18.44
<b>Stage #2</b>			
KA 87.25A	dol, mag, chl (?albite, ?qtz)	-3.28	-17.86
KA 88.75	mag, dol, qtz (?albite, chl)	-3.04*	-18.63*
<b>Stage #3</b>			
KA 88.59	mag, dol, qtz	-3.06	-18.20
KA 89.54	dol (mag) qtz	-2.55	-16.60
KA 89.65	dol (mag) qtz	-2.74	-17.65
<b>Stage #4</b>			
KA 87.53	dol (ank?) qtz	-2.80	-18.30
KA 88.67	dol (ank?) qtz	-2.88*	-18.05*
KA 89.01	dol (mag) qtz	-2.57	-18.08
KA 89.11	dol (ank?) qtz (?albite)	-2.85	-17.48
KA 89.16	dol (ank?) qtz (?albite)	-2.83	-17.91
KA 89.34	dol (mag) qtz	-3.73	-17.93
KA 89.38	dol (mag) qtz (?albite)	-3.63*	-17.89*
KA 89.47	dol (ank?) qtz (?albite)	-2.84	-18.50
KA 89.67	dol (ank?) qtz	-3.16	-18.53
KA 89.68	dol (ank?) qtz	-3.36	-17.72

Sample No	XRD major (minor) phases	$\delta^{13}\text{C}_{\text{PDB}}$	$\delta^{18}\text{O}_{\text{PDB}}$
<b>Stage #6 (see Figure 32)</b>			
KA 89.04	mag, dol, qtz (?albite)	-2.77	-15.67
KA 89.43	dol (cc ?) qtz, albite, py (?chl)	-3.26*	-19.38*
KA 88.58	mag, dol, qtz (?albite)	-2.60	-18.63
KA 88.34	mag, dol, qtz (?albite)	-3.02	-17.62
<b>Stage #8</b>			
KA 87.24	dol, (mag)	-2.88	-18.20
KA 87.36	mag, dol, qtz	-2.68	-17.92
KA 89.33	dol, mag, qtz	-3.60*	-18.36*
KA 89.58	dol, mag	-3.64	-17.83
<b>Stage #9</b>			
KA 89.44	dol (?qtz)	-2.33	-24.58
<b>Stage #10</b>			
KA 89.09	cc, (dol, (?ank), mag) (?qtz)	-3.60	-11.75
<b>Flow Ore</b>			
KA 87.43	dol/ank, qtz, albite, (?chl)	-3.12	-18.31
KA 87.44	dol/ank, qtz, albite	-3.14	-18.07
KA 89.79	dol/ank, qtz (?albite)	-3.57*	-18.83*
KA 89.82	dol/ank, qtz	-2.73	-18.03

Sample No	XRD major (minor) phases	$\delta^{13}\text{C}_{\text{PDB}}$	$\delta^{18}\text{O}_{\text{PDB}}$
<b>Barber-Larder Pit Late Flat veins</b>			
BP/89/01	dol	-3.24	-18.53
<b>Macassa Late Veins</b>			
Ma/87/48	dol, (cc), qtz	-3.35	-13.94
Ma/87/51	dol, (?ank), qtz	-3.09	-11.48
<b>Kerr Addison Dyke Whole Rock</b>			
KA 87.02	dol, (?ank), (mag), albite, qtz, py, ?anhydrite, ?chl)	-3.01	-18.19
KA 87.11	dol, albite, qtz, chl (?anhydrite)	-3.39	-18.30
KA 88.47	dol, mag, albite, qtz, anhydrite, (?chl)	-3.68	-19.86
KA 87.17A	dol, (mag), albite, qtz, chl, parag/musc	-2.61	-17.93
KA 88.31	dol (mag (cc?)), albite, qtz, chl	-2.47*	-18.55
KA 88.87	dol (mag (cc?)), albite, qtz, chl	-2.92	-17.92
KA 88.32	dol, ((cc?)), albite, chl, qtz	-2.57	-18.24
KA88.83	dol, ((cc?)), albite, qtz, chl, parag/musc	-2.48	-18.34
<b>McBean Dyke Whole Rock</b>			
Mc/87/01	dol, (mag), albite, qtz, parag/musc, py, (?anhydrite)	-3.98	-18.87
Mc/87/02	dol, (mag), albite, qtz, parag/musc, py, (?anhydrite)	-3.85*	-18.97*

## APPENDIX V

### **Igneous Geochemical Samples: Preparation and Analytical Methods**

Igneous intrusive material used in this study was hand picked from a suite of samples from the Kerr Addison, Macassa and McBean mines (J.P.S., 1987-1988). Samples of the Abitibi Batholith marginal diorites were kindly provided by A. R. Smith, formerly of the Ontario Geological Survey. The Kerr Addison fault gouges were sampled because underground mapping showed them to be planar structures (green carbonate ore vein stage #6) cutting main stage Au-quartz vein mineralisation. The gouges had a fine grained, brown matrix and it was therefore necessary to test whether this had an igneous (e.g. volatile-rich breccia dyke) geochemical component. (In fact this turned out not to be the case).

84 whole rock samples were crushed to a minus 300 mesh powder using an alumina ceramic puck and mill. Cross-contamination (particularly of Au) between samples was minimised by cleaning the mill with a run of silica sand between samples, and throwing away the first run of a new sample.

#### **Internal Analytical Work (J. P. Smith)**

X-ray fluorescence (XRF) spectroscopy trace element analyses (Ni, Cr, V, Ba, Rb, Sr, Zr, Y, Nb) were performed on pressed powder pellets using a Siemens SRS-100 (Department of Geology, University of Toronto). Accuracies achieved ( $\pm 1s$ ) were  $\sim 10\%$ .

Rare earth (La, Nd, Sm, Yb, Lu, Ce, Eu, Tb) and some trace element concentrations (U, Th, Co, Cs, Sc, Hf, Ta) were determined by instrumental neutron activation analysis (INAA) using a low flux (Slowpoke II) reactor. Sample preparation and analytical procedures were as described by Barnes and Gorton (1984). Accuracies achieved ( $\pm 1s$ ) were  $\sim 5\%$ . In all internal whole rock analyses, UTB1 (University of Toronto - Basalt) was used as the standard.

### **External Analytical Work (powders sent out to appropriate analytical companies)**

The following whole rock trace element concentrations were determined by Activation Laboratories Ltd of Brantford, Ontario (1988; analytical technique and quoted +/-1s detection limit shown in parentheses):

Au (fire assay neutron activation; 1 ppb)

As (0.5 ppm), Sb (0.1 ppm) and W (0.5 ppm; all by epithermal INAA)

The following major and trace element concentrations were determined by X-Ray Assay Laboratories Inc., Don Mills, Toronto (1988; analytical technique and quoted +/-1s detection limits shown in parentheses):

#### **MAJOR ELEMENTS**

SiO<sub>2</sub>, Al<sub>2</sub>O<sub>3</sub>, CaO, MgO, Na<sub>2</sub>O, K<sub>2</sub>O, Fe<sub>2</sub>O<sub>3</sub>, MnO, TiO<sub>2</sub>, P<sub>2</sub>O<sub>5</sub> (fused bead XRF; 0.01%)

H<sub>2</sub>O+, H<sub>2</sub>O- (wet chemistry; 0.1%), CO<sub>2</sub> (wet chemistry; 0.01%)

#### **TRACE ELEMENTS**

S (20 ppm), Cu (1 ppm), Zn (2 ppm; all by pressed powder pellet XRF)

Ag (10 ppb), Se (0.1 ppm; both by graphite furnace atomic absorption)

Pb (0.2 ppm), Mo (0.1 ppm), Bi (0.05 ppm; all by ICP/MS= inductively coupled plasma/mass spectrometry)

Li (1 ppm; atomic absorption)

#### **REFERENCE**

Barnes, S. J. and Gorton, M. P. (1984). Trace element analysis by neutron activation with a low flux reactor (Slowpoke II): results for international reference rocks. Geostandards Newsletter 8, 17-23.

**Appendix V. Major and Trace Element Geochemistry of Selected Intrusive Rocks from the Kerr Addison, Macassa and**

**272**

**McBean Mines, and the Abitibi Batholith.**

**Major elements in weight percent, trace elements in ppm except as noted**





**KERR ADDISON "ALBITTES"**

Sample no. type	KA.87.17A A <sub>2</sub>	KA.87.17B A <sub>2</sub>	KA.87.03 A <sub>3</sub>	KA.87.08 A <sub>2</sub>	KA.87.35 A <sub>1</sub> /A <sub>2</sub> ?	KA.87.15 A <sub>1</sub>	KA.87.58 A <sub>2</sub> /A <sub>1</sub> ?	KA.87.27 A <sub>1</sub> /A <sub>2</sub> ?	KA.87.02 A <sub>1</sub>	KA.87.22 A <sub>1</sub>
SiO <sub>2</sub>	42.0	43.0	45.3	41.5	46.6	41.7	42.0	45.4	55.3	59.8
TiO <sub>2</sub>	0.65	0.66	0.68	0.71	1.08	0.74	0.67	0.59	0.69	0.39
Al <sub>2</sub> O <sub>3</sub>	9.35	9.29	10.4	12.3	12.3	11.6	11.8	12.6	13.5	17.4
Fe <sub>2</sub> O <sub>3 total</sub>	8.22	8.34	8.20	7.49	7.62	8.31	9.36	6.63	6.29	2.29
MnO	0.15	0.15	0.16	0.13	0.14	0.14	0.18	0.13	0.12	0.05
MgO	9.07	9.18	8.41	7.04	6.17	7.87	6.27	6.26	3.29	2.17
CaO	7.97	7.90	7.17	6.41	5.59	5.58	6.41	6.06	3.13	2.12
Na <sub>2</sub> O	4.10	3.90	4.15	6.44	5.90	4.99	5.42	6.71	8.00	10.7
K <sub>2</sub> O	0.26	0.24	0.23	0.46	0.56	0.74	0.81	0.28	0.15	0.12
P <sub>2</sub> O <sub>5</sub>	0.31	0.31	0.72	0.62	0.12	0.05	0.37	0.37	0.50	0.02
H <sub>2</sub> O+	1.1	1.3	1.5	0.3	0.4	0.4	0.4	0.3	0.2	0.1
H <sub>2</sub> O-	0.1	0.1	0.1	<0.1	<0.1	<0.1	0.1	<0.1	<0.1	<0.1
LOI	15.5	14.0	13.6	11.9	10.4	12.5	14.2	13.3	6.31	3.47
Σ	97.9	97.3	99.2	95.1	96.6	94.3	97.6	98.4	97.4	98.6
*SiO <sub>2</sub>	51.17	51.83	53.03	49.94	54.14	51.03	50.43	53.39	60.79	62.91
*TiO <sub>2</sub>	0.79	0.80	0.80	0.85	1.25	0.91	0.80	0.69	0.76	0.41
*Al <sub>2</sub> O <sub>3</sub>	11.39	11.20	12.18	14.80	14.29	14.19	14.17	14.82	14.84	18.30
*Fe <sub>2</sub> O <sub>3 total</sub>	10.01	10.05	9.60	9.01	8.85	10.17	11.24	7.80	6.91	2.41
*MnO	0.18	0.18	0.19	0.16	0.16	0.17	0.22	0.15	0.13	0.05
*MgO	11.05	11.06	9.85	8.47	7.17	9.63	7.53	7.36	3.62	2.28
*CaO	9.71	9.52	8.39	7.71	6.49	6.83	7.70	7.13	3.44	2.23
*Na <sub>2</sub> O	5.00	4.70	4.86	7.75	6.85	6.11	6.51	7.89	8.79	11.26
*K <sub>2</sub> O	0.32	0.29	0.27	0.55	0.65	0.91	0.97	0.33	0.16	0.13
*P <sub>2</sub> O <sub>5</sub>	0.38	0.38	0.84	0.75	0.14	0.06	0.44	0.44	0.55	0.02
*Σ	100.00	100.01	100.01	99.99	99.99	100.01	100.01	100.00	99.99	100.00
CO <sub>2</sub>	15.8	14.9	13.4	14.7	13.0	15.6	13.6	13.9	6.80	4.53

Sample no. type	KA.87.17A A <sub>2</sub>	KA.87.17B A <sub>2</sub>	KA.87.03 A <sub>3</sub>	KA.87.08 A <sub>2</sub>	KA.87.35 A <sub>1</sub> /A <sub>2</sub> ?	KA.87.15 A <sub>1</sub>	KA.87.58 A <sub>2</sub> /A <sub>1</sub> ?	KA.87.27 A <sub>1</sub> /A <sub>2</sub> ?	KA.87.02 A <sub>1</sub>	KA.87.22 A <sub>1</sub>
La	44.04	43.56	86.85	96.77	26.27	22.87	28.76	51.32	39.56	32.67
Ce	90.25	88.35	181.27	198.17	52.91	49.40	55.81	116.89	83.82	63.04
Nd	43.61	44.75	88.72	98.69	26.28	26.08	30.30	52.48	41.58	28.41
Sm	7.48	7.41	12.59	14.88	4.98	6.12	5.90	8.62	8.39	3.99
Eu	1.662	1.583	3.460	2.967	1.121	1.393	1.294	1.877	1.778	0.735
Tb	0.561	0.474	1.090	0.763	0.494	0.633	0.574	0.684	0.693	0.188
Yb	1.265	1.375	1.962	2.141	1.650	1.772	1.718	1.715	1.783	0.574
Lu	0.235	0.191	0.313	0.347	0.261	0.308	0.303	0.278	0.344	0.107
La <sub>N</sub>	139.79	138.27	275.70	307.19	83.39	72.60	91.31	162.91	125.59	103.70
Ce <sub>N</sub>	111.01	108.67	222.40	243.75	65.08	60.77	68.64	143.77	103.10	77.54
Nd <sub>N</sub>	73.05	74.96	148.61	165.32	44.02	43.68	50.76	87.91	69.65	47.58
Sm <sub>N</sub>	38.93	38.60	65.59	77.47	25.94	31.87	30.71	44.91	43.68	20.80
Eu <sub>N</sub>	23.02	21.93	47.83	41.09	15.53	19.29	17.92	26.00	24.63	10.18
Tb <sub>N</sub>	11.45	9.67	22.14	15.57	10.08	12.92	11.71	13.96	14.14	3.84
Yb <sub>N</sub>	6.08	6.61	9.43	10.29	7.93	8.52	8.26	8.25	8.57	2.76
Lu <sub>N</sub>	7.28	5.91	9.69	10.74	8.08	9.54	9.38	8.61	10.65	3.31
La <sub>N</sub> /Y <sub>bN</sub>	22.99	20.92	29.23	29.85	10.51	8.52	11.06	19.76	14.65	37.59
Ce <sub>N</sub> /Y <sub>bN</sub>	18.26	16.44	23.58	23.68	8.20	7.13	8.31	17.44	12.03	28.10
S	3700	5640	2800	12,000	12,500	17,400	3200	2400	22,000	4000
Au (ppb)	16	12	45	620	6400	1310	240	12	9020	160
Ag	0.04	0.07	<0.01	0.02	0.06	0.23	<0.01	0.04	0.22	0.19
As	20	11	56	130	38	54	13	46	180	32
Sb	2.2	1.9	2.6	15	0.7	91	1.0	9.2	120	5.5
Bi	0.36	0.57	0.20	0.15	0.45	0.26	0.30	0.36	0.56	0.13
Se	0.4	1.0	0.1	0.4	0.6	0.4	0.1	0.2	1.1	0.4
Mo	0.3	0.4	0.3	0.5	0.5	0.2	0.4	0.6	1.0	0.5
Sc	24.33	24.26	25.45	21.57	23.33	29.99	29.20	20.12	12.96	4.59
V	n.d.	n.d.	n.d.	n.d.	n.d.	n.d.	n.d.	n.d.	n.d.	n.d.
Cr	n.d.	n.d.	n.d.	n.d.	n.d.	n.d.	n.d.	n.d.	n.d.	n.d.
Co	38.20	38.75	31.37	28.31	22.10	26.63	28.48	23.33	15.86	6.23
Ni	n.d.	n.d.	n.d.	n.d.	n.d.	n.d.	n.d.	n.d.	n.d.	n.d.
Cu	36	47	47	139	434	326	39	62	253	30
Zn	77	89	79	41	37	41	81	48	52	19

Sample no. type	KA.87.17A A <sub>2</sub>	KA.87.17B A <sub>2</sub>	KA.87.03 A <sub>3</sub>	KA.87.08 A <sub>2</sub>	KA.87.35 A <sub>1</sub> /A <sub>2</sub> ?	KA.87.15 A <sub>1</sub>	KA.87.58 A <sub>2</sub> /A <sub>1</sub> ?	KA.87.27 A <sub>1</sub> /A <sub>2</sub> ?	KA.87.02 A <sub>1</sub>	KA.87.22 A <sub>1</sub>
Li	25	20	32	4	6	4	3	3	2	1
Hf	1.83	2.00	3.83	3.01	1.73	2.29	1.95	3.18	4.18	2.95
Ta	0.23	0.21	0.35	0.25	0.17	0.20	0.18	0.36	0.50	0.17
W	7.5	<1.5	8.2	19	51	38	13	7.0	35	19
Pb	9.2	8.7	6.0	6.8	6.3	5.2	5.3	7.1	6.8	3.9
U	0.78	0.73	1.47	1.57	0.88	1.50	0.90	0.82	1.66	0.90
Th	5.13	4.92	9.13	10.27	4.22	5.22	4.51	6.26	7.34	5.77
Rb	n.d.	n.d.	n.d.	n.d.	n.d.	n.d.	n.d.	n.d.	n.d.	n.d.
Sr	888.55	895.82	456.35	288.10	219.59	163.22	275.49	360.20	336.13	215.83
Y	17.45	19.01	28.66	26.11	17.92	22.41	19.71	20.26	24.50	9.03
Zr	104.64	103.36	182.79	153.00	86.75	101.32	93.85	140.95	189.83	146.07
Nb	5.18	4.43	10.65	6.88	3.71	4.28	4.44	9.61	8.77	4.11
Ba	n.d.	n.d.	n.d.	n.d.	n.d.	n.d.	n.d.	n.d.	n.d.	n.d.
Th/Yb	4.06	3.58	4.65	4.79	2.56	2.95	2.63	3.65	4.11	10.05
Ce/Yb	71.34	64.25	92.16	92.56	32.07	27.88	32.48	68.16	47.01	109.82
Ta/Yb	0.184	0.152	0.178	0.118	0.105	0.111	0.106	0.209	0.281	0.303
Zr/Ti (ppm)	0.0161	0.0157	0.0269	0.0215	0.0080	0.0137	0.0141	0.0239	0.0275	0.0375
Nb/Y	0.240	0.180	0.302	0.187	0.151	0.146	0.175	0.376	0.236	0.344

Sample no. type	KA.88.01 A <sub>2</sub>	KA.88.02 A <sub>3</sub>	KA.88.03 A <sub>2</sub>	KA.88.04 A <sub>3</sub>	KA.88.05 A <sub>2</sub>	KA.88.06 A <sub>3</sub>	KA.88.07 A <sub>2</sub> /A <sub>3</sub> ?	KA.88.08 A <sub>3</sub>	KA.88.09 A <sub>2</sub>	KA.88.10 A <sub>3</sub>
SiO <sub>2</sub>	55.5	47.8	45.0	32.3	43.6	39.5	44.4	49.0	48.9	44.3
TiO <sub>2</sub>	0.46	0.66	0.72	0.62	0.99	0.81	0.93	0.59	0.62	0.61
Al <sub>2</sub> O <sub>3</sub>	13.2	11.7	13.1	7.55	14.3	12.6	13.0	10.4	10.7	10.5
Fe <sub>2</sub> O <sub>3 total</sub>	4.24	5.95	8.15	10.6	9.04	9.65	9.09	6.67	7.62	6.93
MnO	0.08	0.10	0.13	0.17	0.14	0.18	0.15	0.12	0.13	0.14
MgO	4.87	7.74	5.98	17.8	6.09	9.45	5.30	7.33	9.37	9.23
CaO	4.07	6.31	5.66	10.0	5.15	8.29	8.05	6.07	4.84	7.46
Na <sub>2</sub> O	7.71	6.31	4.94	1.52	6.14	5.02	6.79	4.92	4.56	4.69
K <sub>2</sub> O	0.27	0.06	1.36	0.09	0.86	0.08	0.40	0.63	0.06	0.06
P <sub>2</sub> O <sub>5</sub>	0.15	0.56	0.51	0.70	0.47	0.44	0.57	0.51	0.38	0.45
H <sub>2</sub> O+	0.4	1.1	0.8	4.0	0.5	2.7	0.5	0.4	1.8	1.4
H <sub>2</sub> O-	<0.1	<0.1	<0.1	<0.1	<0.1	<0.1	<0.1	<0.1	<0.1	<0.1
LOI	8.70	11.8	10.7	18.2	11.2	13.3	10.5	12.6	11.8	14.8
Σ	99.4	99.4	96.5	99.8	98.1	99.4	99.3	99.0	99.2	99.6
*SiO <sub>2</sub>	61.29	54.82	52.60	39.70	50.24	45.92	50.07	56.82	56.09	52.51
*TiO <sub>2</sub>	0.51	0.76	0.84	0.76	1.14	0.94	1.05	0.68	0.71	0.72
*Al <sub>2</sub> O <sub>3</sub>	14.58	13.42	15.31	9.28	16.48	14.65	14.66	12.06	12.27	12.45
*Fe <sub>2</sub> O <sub>3 total</sub>	4.68	6.82	9.53	13.03	10.42	11.22	10.25	7.73	8.74	8.21
*MnO	0.09	0.11	0.15	0.21	0.16	0.21	0.17	0.14	0.15	0.17
*MgO	5.38	8.88	6.99	21.88	7.02	10.99	5.98	8.50	10.75	10.94
*CaO	4.49	7.24	6.62	12.29	5.93	9.64	9.08	7.04	5.55	8.84
*Na <sub>2</sub> O	8.51	7.24	5.77	1.87	7.08	5.84	7.66	5.71	5.23	5.56
*K <sub>2</sub> O	0.30	0.07	1.59	0.11	0.99	0.09	0.45	0.73	0.07	0.07
*P <sub>2</sub> O <sub>5</sub>	0.17	0.64	0.60	0.86	0.54	0.51	0.64	0.59	0.44	0.53
*Σ	100.00	100.00	100.00	99.99	100.00	100.01	100.01	100.00	100.00	100.00
CO <sub>2</sub>	9.75	11.4	12.4	14.7	11.9	11.4	10.8	14.0	11.9	14.6

Sample no. type	KA.88.01 A <sub>2</sub>	KA.88.02 A <sub>3</sub>	KA.88.03 A <sub>2</sub>	KA.88.04 A <sub>3</sub>	KA.88.05 A <sub>2</sub>	KA.88.06 A <sub>3</sub>	KA.88.07 A <sub>2</sub> /A <sub>3</sub> ?	KA.88.08 A <sub>3</sub>	KA.88.09 A <sub>2</sub>	KA.88.10 A <sub>3</sub>
La	41.76	62.13	38.43	53.36	38.17	24.12	33.00	23.80	25.85	30.19
Ce	114.85	195.48	109.99	189.74	135.65	95.18	101.06	69.45	75.73	85.50
Nd	45.33	75.10	42.39	67.42	49.16	32.37	44.34	29.92	34.33	33.79
Sm	6.76	11.50	6.86	11.28	8.74	6.33	8.00	5.27	5.61	6.19
Eu	1.960	3.43	2.173	3.236	2.737	1.797	2.517	1.537	1.590	1.831
Tb	0.564	0.863	0.758	1.069	2.668	0.838	0.962	0.453	0.589	0.496
Yb	0.960	1.071	2.010	0.674	1.661	1.685	1.819	1.155	1.172	1.292
Lu	0.159	0.166	0.297	0.112	0.307	0.275	0.297	0.210	0.188	0.203
La <sub>N</sub>	132.56	197.24	122.00	169.39	121.17	76.58	104.74	75.55	82.06	95.84
Ce <sub>N</sub>	141.27	240.45	135.28	233.38	166.85	117.07	124.31	85.43	93.15	105.16
Nd <sub>N</sub>	75.93	125.79	71.00	112.93	82.35	54.22	74.27	50.11	57.50	56.60
Sm <sub>N</sub>	35.20	59.91	35.71	58.75	45.52	32.94	41.67	27.46	29.21	32.21
Eu <sub>N</sub>	27.15	47.49	30.10	44.82	37.91	24.89	34.86	21.29	22.02	25.36
Tb <sub>N</sub>	11.51	17.61	15.47	21.82	21.02	17.10	19.63	9.24	12.02	10.12
Yb <sub>N</sub>	4.62	5.15	9.66	3.24	7.99	8.10	8.75	5.55	5.63	6.21
Lu <sub>N</sub>	4.92	5.14	9.17	3.47	9.50	8.51	9.20	6.50	5.82	6.28
La <sub>N</sub> /Yb <sub>N</sub>	28.72	38.31	12.63	52.28	15.17	9.45	11.98	13.61	14.57	15.43
Ce <sub>N</sub> /Yb <sub>N</sub>	30.61	46.70	14.00	72.03	20.90	14.45	14.22	15.39	16.53	16.93
S	7200	940	23,000	120	30,000	180	2200	7000	10,000	1900
Au (ppb)	400	3	530	250	4740	6	15	2250	620	320
Ag	0.02	<0.01	0.17	0.19	0.16	0.01	0.01	0.59	0.04	<0.01
As	21	30	140	34	45	30	19	140	49	33
Sb	1.3	7.6	20	5.2	1.9	6.3	6.9	30	2.9	4.3
Bi	n.d.	n.d.	n.d.	n.d.	n.d.	n.d.	n.d.	n.d.	n.d.	n.d.
Se	0.1	0.2	0.3	0.1	0.7	<0.1	0.4	0.2	0.3	0.2
Mo	n.d.	n.d.	n.d.	n.d.	n.d.	n.d.	n.d.	n.d.	n.d.	n.d.
Sc	11.69	18.52	22.65	23.18	25.73	29.01	28.07	18.87	23.03	22.60
V	n.d.	n.d.	n.d.	n.d.	n.d.	n.d.	n.d.	n.d.	n.d.	n.d.
Cr	n.d.	n.d.	n.d.	n.d.	n.d.	n.d.	n.d.	n.d.	n.d.	n.d.
Co	17.10	32.16	32.40	65.85	31.08	43.20	32.11	30.87	38.33	35.52
Ni	n.d.	n.d.	n.d.	n.d.	n.d.	n.d.	n.d.	n.d.	n.d.	n.d.
Cu	216	<1	113	5	454	79	98	131	62	45
Zn	42	71	41	98	38	65	59	51	63	70

Sample no. type	KA.88.01 A <sub>2</sub>	KA.88.02 A <sub>3</sub>	KA.88.03 A <sub>2</sub>	KA.88.04 A <sub>3</sub>	KA.88.05 A <sub>2</sub>	KA.88.06 A <sub>3</sub>	KA.88.07 A <sub>2</sub> /A <sub>3</sub> ?	KA.88.08 A <sub>3</sub>	KA.88.09 A <sub>2</sub>	KA.88.10 A <sub>3</sub>
Li	<1	5	<1	51	<1	22	20	5	17	21
Hf	3.69	3.73	3.01	2.06	3.78	2.77	3.41	2.70	2.34	3.05
Ta	0.27	0.41	0.25	0.10	0.31	0.25	0.29	0.29	0.20	0.25
W	37	<0.5	15	4.6	44	3.9	2.3	22	13	4.4
Pb	n.d.	n.d.	n.d.	n.d.	n.d.	n.d.	n.d.	n.d.	n.d.	n.d.
U	1.74	1.12	1.04	0.58	0.96	0.95	0.87	1.45	0.86	1.06
Th	9.18	8.75	7.49	7.32	6.70	4.50	5.61	6.40	5.37	6.33
Rb	n.d.	n.d.	n.d.	n.d.	n.d.	n.d.	n.d.	n.d.	n.d.	n.d.
Sr	281.16	641.96	474.87	317.77	259.14	203.97	338.52	353.45	315.26	615.94
Y	13.79	17.95	21.30	19.59	26.07	22.29	23.87	15.27	14.59	14.98
Zr	167.83	174.42	133.69	77.16	165.21	118.79	144.74	115.00	98.60	134.31
Nb	2.08	5.63	2.06	2.27	4.46	1.54	3.05	1.92	2.67	4.64
Ba	n.d.	n.d.	n.d.	n.d.	n.d.	n.d.	n.d.	n.d.	n.d.	n.d.
Th/Yb	9.56	8.17	3.73	10.86	4.03	2.67	3.08	5.54	4.58	4.90
Ce/Yb	119.64	182.52	54.72	281.52	84.20	56.48	55.56	60.13	64.62	66.17
Ta/Yb	0.280	0.378	0.122	0.142	0.189	0.148	0.157	0.255	0.172	0.194
Zr/Ti (ppm)	0.0365	0.0264	0.0186	0.0124	0.0167	0.0147	0.0156	0.0195	0.0159	0.0220
Nb/Y	0.223	0.369	0.144	0.167	0.198	0.159	0.170	0.191	0.183	0.310

Sample no. type	KA.88.11 A <sub>2</sub>	KA.88.12 A <sub>3</sub>	KA.88.13 A <sub>3</sub>	KA.88.14 A <sub>1</sub>	KA.88.15 A <sub>3</sub>	KA.88.16 A <sub>1</sub> /A <sub>2</sub> ?	KA.88.18 A <sub>1</sub>	KA.88.19 porph?	KA.87.11 A <sub>1</sub>	KA.87.20 A <sub>2</sub> /A <sub>3</sub> ?
SiO <sub>2</sub>	37.9	46.1	45.8	68.1	48.2	41.0	69.4	69.1	67.3	50.1
TiO <sub>2</sub>	0.77	0.60	0.64	0.32	0.65	1.02	0.29	0.27	0.29	0.70
Al <sub>2</sub> O <sub>3</sub>	9.59	11.2	10.9	13.8	10.6	14.0	15.0	16.1	14.3	12.2
Fe <sub>2</sub> O <sub>3 total</sub>	10.6	7.27	5.88	1.72	7.64	9.27	1.90	1.12	1.60	7.25
MnO	0.18	0.13	0.11	0.02	0.13	0.14	0.02	0.01	0.03	0.11
MgO	9.30	8.45	8.10	1.17	8.54	6.14	1.15	2.62	1.60	7.04
CaO	6.43	6.07	7.50	1.45	6.83	7.00	0.56	0.44	2.37	6.50
Na <sub>2</sub> O	4.13	4.67	5.84	8.49	5.45	5.72	9.12	8.69	8.96	5.02
K <sub>2</sub> O	0.79	0.58	0.04	0.11	0.16	1.08	0.31	0.26	0.15	0.16
P <sub>2</sub> O <sub>5</sub>	0.31	0.37	0.55	0.09	0.63	0.63	0.10	0.10	0.14	0.35
H <sub>2</sub> O+	0.4	1.3	1.1	0.2	2.2	0.5	0.2	1.2	0.2	2.1
H <sub>2</sub> O-	<0.1	<0.1	<0.1	<0.1	0.2	0.1	<0.1	0.1	<0.1	0.1
LOI	16.1	13.8	13.8	4.62	8.62	11.0	2.54	1.39	3.70	9.62
Σ	96.3	99.5	99.4	100.0	97.6	97.1	100.5	100.2	100.6	99.3
*SiO <sub>2</sub>	47.38	53.96	53.66	71.48	54.26	47.67	70.92	70.00	69.57	56.02
*TiO <sub>2</sub>	0.96	0.70	0.75	0.34	0.73	1.19	0.30	0.27	0.30	0.78
*Al <sub>2</sub> O <sub>3</sub>	11.99	13.11	12.77	14.49	11.93	16.28	15.33	16.31	14.78	13.64
*Fe <sub>2</sub> O <sub>3 total</sub>	13.25	8.51	6.89	1.81	8.60	10.78	1.94	1.13	1.65	8.11
*MnO	0.23	0.15	0.13	0.02	0.15	0.16	0.02	0.01	0.03	0.12
*MgO	11.63	9.89	9.49	1.23	9.61	7.14	1.18	2.65	1.65	7.87
*CaO	8.04	7.10	8.79	1.52	7.69	8.14	0.57	0.45	2.45	7.27
*Na <sub>2</sub> O	5.16	5.47	6.84	8.91	6.14	6.65	9.32	8.80	9.26	5.61
*K <sub>2</sub> O	0.99	0.68	0.05	0.12	0.18	1.26	0.32	0.26	0.16	0.18
*P <sub>2</sub> O <sub>5</sub>	0.39	0.43	0.64	0.09	0.71	0.73	0.10	0.10	0.14	0.39
*Σ	100.02	100.00	100.01	100.01	100.00	100.00	100.00	99.98	99.99	99.99
CO <sub>2</sub>	19.0	14.0	14.1	2.39	8.89	13.2	1.90	<0.01	3.43	9.15

Sample no. type	KA.88.11 A <sub>2</sub>	KA.88.12 A <sub>3</sub>	KA.88.13 A <sub>3</sub>	KA.88.14 A <sub>1</sub>	KA.88.15 A <sub>3</sub>	KA.88.16 A <sub>1</sub> /A <sub>2</sub> ?	KA.88.18 A <sub>1</sub>	KA.88.19 porph?	KA.87.11 A <sub>1</sub>	KA.87.20 A <sub>2</sub> /A <sub>3</sub> ?
La	12.94	28.66	58.04	20.88	25.67	33.45	11.19	13.13	13.16	41.95
Ce	41.84	77.48	176.68	56.02	94.23	100.13	33.30	39.70	37.38	122.36
Nd	20.41	32.13	75.94	20.21	31.44	46.56	8.07	13.34	13.80	49.58
Sm	3.82	5.28	11.11	2.81	5.71	8.02	1.99	2.35	2.33	7.02
Eu	1.101	1.554	3.141	0.755	1.644	2.316	0.639	0.701	0.686	2.036
Tb	0.484	0.515	0.785	0.229	0.649	0.854	0.173	0.175	0.244	0.666
Yb	1.563	0.879	0.939	0.463	1.297	2.010	0.395	0.158	0.403	1.439
Lu	0.241	0.178	0.170	0.080	0.218	0.298	0.084	0.038	0.070	0.243
La <sub>N</sub>	41.09	90.97	184.27	66.27	81.50	106.19	35.53	41.67	41.78	133.17
Ce <sub>N</sub>	51.46	95.30	217.32	68.91	115.90	123.16	40.96	48.83	45.98	150.50
Nd <sub>N</sub>	34.18	53.83	127.20	33.86	52.66	77.99	13.52	22.34	23.11	83.05
Sm <sub>N</sub>	19.89	27.51	57.85	14.61	29.73	41.79	10.35	12.25	12.12	36.56
Eu <sub>N</sub>	15.25	21.52	43.50	10.46	22.77	32.08	8.85	9.71	9.50	28.20
Tb <sub>N</sub>	9.88	10.51	16.02	4.67	13.24	17.43	3.53	3.57	4.98	13.59
Yb <sub>N</sub>	7.51	4.23	4.51	2.23	6.24	9.66	1.90	0.76	1.94	6.92
Lu <sub>N</sub>	7.46	5.51	5.26	2.48	6.75	9.27	2.60	1.18	2.17	7.52
La <sub>N</sub> /Yb <sub>N</sub>	5.47	21.53	40.82	29.78	13.07	10.99	18.71	54.90	21.57	19.25
Ce <sub>N</sub> /Yb <sub>N</sub>	6.85	22.56	48.14	30.97	18.59	12.75	21.57	64.34	23.74	21.76
S	16,000	2600	1900	9000	9800	31,000	5000	520	5900	19,000
Au (ppb)	300	<1	12	60	520	3180	590	27	100	40
Ag	0.09	<0.01	<0.01	0.16	0.18	0.10	0.06	<0.01	0.10	0.07
As	49	12	27	6.4	68	120	25	4.5	31	21
Sb	3.9	3.9	7.9	2.9	3.4	3.2	21	1.8	33	1.2
Bi	n.d.	n.d.	n.d.	n.d.	n.d.	n.d.	n.d.	n.d.	n.d.	n.d.
Se	0.9	0.2	0.1	0.4	0.3	0.4	<0.1	<0.1	0.1	0.3
Mo	n.d.	n.d.	n.d.	n.d.	n.d.	n.d.	n.d.	n.d.	n.d.	n.d.
Sc	39.91	21.43	18.65	2.81	21.20	26.46	2.56	1.63	3.47	21.71
V	n.d.	n.d.	n.d.	n.d.	n.d.	n.d.	n.d.	n.d.	n.d.	n.d.
Cr	n.d.	n.d.	n.d.	n.d.	n.d.	n.d.	n.d.	n.d.	n.d.	n.d.
Co	44.23	37.23	30.86	7.36	48.26	29.31	5.14	8.34	5.93	28.96
Ni	n.d.	n.d.	n.d.	n.d.	n.d.	n.d.	n.d.	n.d.	n.d.	n.d.
Cu	102	55	<1	9	28	735	49	3	74	59
Zn	70	78	58	19	67	36	26	30	27	92



Sample no. type	KA.88.11 A <sub>2</sub>	KA.88.12 A <sub>3</sub>	KA.88.13 A <sub>3</sub>	KA.88.14 A <sub>1</sub>	KA.88.15 A <sub>3</sub>	KA.88.16 A <sub>1</sub> /A <sub>2</sub> ?	KA.88.18 A <sub>1</sub>	KA.88.19 porph?	KA.87.11 A <sub>1</sub>	KA.87.20 A <sub>2</sub> /A <sub>3</sub> ?
Li	4	29	8	<1	15	3	<1	18	<1	5
Hf	1.78	2.27	3.34	2.77	2.95	3.40	2.92	3.17	2.47	2.73
Ta	0.17	0.20	0.38	0.16	0.33	0.28	0.13	0.13	0.17	0.30
W	12	4.7	1.8	7.5	23	16	3.3	4.2	9.2	17
Pb	n.d.	n.d.	n.d.	n.d.	n.d.	n.d.	n.d.	n.d.	n.d.	n.d.
U	0.32	0.99	1.12	0.92	1.47	0.93	0.55	0.38	0.60	0.41
Th	2.02	6.28	8.11	5.53	6.48	5.79	3.55	2.37	3.49	6.29
Rb	n.d.	n.d.	n.d.	n.d.	n.d.	n.d.	n.d.	n.d.	n.d.	n.d.
Sr	341.95	559.85	356.27	235.61	492.04	300.88	239.59	529.71	481.66	730.68
Y	15.97	13.44	17.42	6.15	16.40	24.88	6.03	3.74	5.68	18.59
Zr	69.41	108.41	159.79	128.54	118.22	153.87	115.99	131.44	106.58	132.39
Nb	3.35	3.29	6.57	2.29	4.08	5.91	n.d.	n.d.	n.d.	4.26
Ba	n.d.	n.d.	n.d.	n.d.	n.d.	n.d.	n.d.	n.d.	n.d.	n.d.
Th/Yb	1.29	7.14	8.64	11.95	4.99	2.88	8.99	15.03	8.67	4.37
Ce/Yb	26.77	88.15	188.31	121.00	72.65	49.82	84.31	251.28	92.76	85.03
Ta/Yb	0.111	0.226	0.400	0.343	0.257	0.137	0.332	0.804	0.429	0.206
Zr/Ti (ppm)	0.0090	0.0181	0.0250	0.0402	0.0182	0.0151	0.0400	0.0487	0.0368	0.0189
Nb/Y	0.210	0.245	0.377	0.372	0.249	0.238	0.166	0.283	0.199	0.283

Sample no. type	KA.87.33 A <sub>1</sub>	KA.88.23 A <sub>1</sub>	KA.88.25 A <sub>1</sub>	KA.88.26 A <sub>2</sub>	KA.88.27 A <sub>2</sub>	KA.88.28 A <sub>2</sub>	KA.88.29 A <sub>2</sub> /A <sub>3</sub> ?	KA.88.30 A <sub>2</sub> /A <sub>3</sub> ?	KA.88.31 A <sub>2</sub>	KA.88.32 A <sub>3</sub>
SiO <sub>2</sub>	53.1	57.7	71.5	42.7	43.7	45.6	48.0	47.6	44.8	41.4
TiO <sub>2</sub>	0.49	0.42	0.17	0.71	0.72	0.57	0.66	0.92	0.57	0.88
Al <sub>2</sub> O <sub>3</sub>	11.3	16.7	12.9	12.3	12.7	10.9	11.1	15.8	10.8	11.5
Fe <sub>2</sub> O <sub>3</sub> total	5.79	2.38	0.97	6.83	6.66	6.86	6.59	6.92	6.41	9.05
MnO	0.07	0.06	0.02	0.12	0.11	0.13	0.13	0.03	0.10	0.18
MgO	5.34	2.41	1.20	7.05	7.99	8.56	8.05	10.4	10.4	7.90
CaO	6.21	4.32	1.96	7.20	5.59	5.31	5.20	2.82	8.41	8.59
Na <sub>2</sub> O	5.60	10.2	8.20	6.39	6.75	4.89	5.41	4.64	3.29	5.13
K <sub>2</sub> O	0.54	0.16	0.08	0.40	0.38	0.80	0.39	0.61	0.33	0.53
P <sub>2</sub> O <sub>5</sub>	0.16	0.02	0.06	0.66	0.32	0.34	0.46	0.48	0.37	0.56
H <sub>2</sub> O+	0.5	0.2	0.2	0.3	0.3	0.6	0.7	4.2	2.5	2.3
H <sub>2</sub> O-	0.1	<0.1	<0.1	<0.1	<0.1	0.1	0.1	0.2	0.1	0.3
LOI	8.39	5.23	3.08	12.8	13.2	15.1	13.2	6.85	14.5	11.8
Σ	97.1	99.7	100.2	97.3	98.2	99.2	99.3	97.3	100.2	97.7
*SiO <sub>2</sub>	59.93	61.14	73.67	50.62	51.46	54.31	55.82	52.76	52.41	48.30
*TiO <sub>2</sub>	0.55	0.45	0.18	0.84	0.85	0.68	0.77	1.02	0.67	1.03
*Al <sub>2</sub> O <sub>3</sub>	12.75	17.70	13.29	14.58	14.96	12.98	12.91	17.51	12.63	13.42
*Fe <sub>2</sub> O <sub>3</sub> total	6.53	2.52	1.00	8.10	7.84	8.17	7.66	7.67	7.50	10.56
*MnO	0.08	0.06	0.02	0.14	0.13	0.15	0.15	0.03	0.12	0.21
*MgO	6.03	2.55	1.24	8.36	9.41	10.20	9.36	11.53	12.17	9.22
*CaO	7.01	4.58	2.02	8.53	6.58	6.32	6.05	3.13	9.84	10.02
*Na <sub>2</sub> O	6.32	10.81	8.45	7.57	7.95	5.82	6.29	5.14	3.85	5.98
*K <sub>2</sub> O	0.61	0.17	0.08	0.47	0.45	0.95	0.45	0.68	0.39	0.62
*P <sub>2</sub> O <sub>5</sub>	0.18	0.02	0.06	0.78	0.38	0.40	0.53	0.53	0.43	0.65
*Σ	99.99	100.00	100.01	99.99	100.01	99.98	99.99	100.00	100.01	100.01
CO <sub>2</sub>	10.8	6.05	2.38	14.3	14.1	16.0	13.2	2.94	12.1	11.8

Sample no. type	KA.87.33 A <sub>1</sub>	KA.88.23 A <sub>1</sub>	KA.88.25 A <sub>1</sub>	KA.88.26 A <sub>2</sub>	KA.88.27 A <sub>2</sub>	KA.88.28 A <sub>2</sub>	KA.88.29 A <sub>2</sub> /A <sub>3</sub> ?	KA.88.30 A <sub>2</sub> /A <sub>3</sub> ?	KA.88.31 A <sub>2</sub>	KA.88.32 A <sub>3</sub>
La	22.28	24.73	8.57	66.72	35.62	27.49	52.51	49.50	25.56	34.15
Ce	64.98	66.53	24.88	192.85	105.40	80.75	153.75	143.56	71.96	104.51
Nd	29.67	24.47	10.38	78.76	47.02	33.50	58.70	61.19	31.39	48.24
Sm	4.36	3.15	1.90	10.41	7.27	5.57	8.24	9.31	4.92	7.33
Eu	1.363	0.854	0.514	3.013	2.188	1.633	2.402	2.749	1.514	2.216
Tb	0.517	0.307	0.240	0.724	0.823	0.678	0.647	0.831	0.549	0.615
Yb	1.163	0.822	0.366	1.886	1.236	0.977	1.256	1.456	0.966	1.530
Lu	0.200	0.102	0.064	0.291	0.232	0.219	0.265	0.300	0.187	0.246
La <sub>N</sub>	70.72	78.50	27.21	211.80	113.09	87.26	166.71	157.15	81.15	108.43
Ce <sub>N</sub>	79.93	81.83	30.61	237.20	129.64	99.32	189.11	176.58	88.51	128.55
Nd <sub>N</sub>	49.69	40.98	17.39	131.92	78.76	56.11	98.33	102.50	52.58	80.80
Sm <sub>N</sub>	22.69	16.42	9.91	54.21	37.84	28.99	42.93	48.49	25.64	38.15
Eu <sub>N</sub>	18.88	11.83	7.12	41.73	30.30	22.62	33.27	38.07	20.97	30.69
Tb <sub>N</sub>	10.55	6.27	4.90	14.78	16.80	13.84	13.20	16.96	11.20	12.55
Yb <sub>N</sub>	5.59	3.95	1.76	9.07	5.94	4.70	6.04	7.00	4.64	7.36
Lu <sub>N</sub>	6.19	3.16	1.98	9.01	7.18	6.78	8.20	9.29	5.79	7.62
La <sub>N</sub> /Y <sub>N</sub>	12.65	19.87	15.47	23.36	19.03	18.58	27.50	22.45	17.47	14.74
Ce <sub>N</sub> /Y <sub>N</sub>	14.30	20.71	17.40	26.16	21.82	21.15	31.32	25.23	19.06	17.48
S	4200	8200	4500	11,000	8300	3700	4100	9400	720	4500
Au (ppb)	11,200	1820	310	620	630	560	150	1250	25	1130
Ag	0.24	0.08	0.29	0.28	0.22	0.02	<0.01	<0.01	<0.01	0.08
As	26	36	28	83	170	190	13	64	5.7	100
Sb	0.7	1.4	17	26	26	5.3	8.3	9.5	5.7	2.9
Bi	n.d.	n.d.	n.d.	n.d.	n.d.	n.d.	n.d.	n.d.	n.d.	n.d.
Se	1.7	0.2	0.1	0.1	0.3	<0.1	0.1	0.3	0.1	0.2
Mo	n.d.	n.d.	n.d.	n.d.	n.d.	n.d.	n.d.	n.d.	n.d.	n.d.
Sc	13.06	6.78	2.09	21.84	17.00	21.29	21.15	24.67	21.21	28.34
V	n.d.	n.d.	n.d.	n.d.	n.d.	n.d.	n.d.	n.d.	n.d.	n.d.
Cr	n.d.	n.d.	n.d.	n.d.	n.d.	n.d.	n.d.	n.d.	n.d.	n.d.
Co	23.58	6.69	4.18	30.65	36.44	35.02	33.14	53.51	29.58	39.21
Ni	n.d.	n.d.	n.d.	n.d.	n.d.	n.d.	n.d.	n.d.	n.d.	n.d.
Cu	14	8	48	44	49	30	30	166	57	141
Zn	28	25	19	40	44	54	53	78	84	61

Sample no. type	KA.87.33 A <sub>1</sub>	KA.88.23 A <sub>1</sub>	KA.88.25 A <sub>1</sub>	KA.88.26 A <sub>2</sub>	KA.88.27 A <sub>2</sub>	KA.88.28 A <sub>2</sub>	KA.88.29 A <sub>2</sub> /A <sub>3</sub> ?	KA.88.30 A <sub>2</sub> /A <sub>3</sub> ?	KA.88.31 A <sub>2</sub>	KA.88.32 A <sub>3</sub>
Li	37	<1	<1	<1	<1	<1	9	70	46	16
Hf	2.32	2.98	2.21	2.76	3.89	2.31	2.73	4.20	2.36	3.12
Ta	0.32	0.20	0.24	0.28	0.34	0.23	0.19	0.27	0.20	0.27
W	25	31	6.6	15	13	13	7.1	18	4.7	16
Pb	n.d.	n.d.	n.d.	n.d.	n.d.	n.d.	n.d.	n.d.	n.d.	n.d.
U	0.35	0.54	0.78	0.36	0.62	0.59	0.44	0.61	0.65	0.54
Th	5.50	5.38	2.65	8.73	7.15	5.60	7.76	10.35	5.61	5.40
Rb	n.d.	n.d.	n.d.	n.d.	n.d.	n.d.	n.d.	n.d.	n.d.	n.d.
Sr	160.78	438.34	285.33	267.85	169.68	252.62	249.27	148.61	385.06	706.47
Y	13.38	8.01	5.55	23.40	20.29	15.55	18.44	21.76	13.38	21.02
Zr	110.00	147.84	89.37	139.99	201.14	111.30	128.90	213.06	104.00	154.51
Nb	6.58	1.40	2.52	4.81	5.59	2.63	5.49	5.79	4.76	5.97
Ba	n.d.	n.d.	n.d.	n.d.	n.d.	n.d.	n.d.	n.d.	n.d.	n.d.
Th/Yb	4.73	6.54	7.23	4.63	5.79	5.73	6.18	7.11	5.81	3.53
Ce/Yb	55.87	80.93	67.98	102.06	85.27	82.65	122.41	98.60	74.49	68.31
Ta/Yb	0.275	0.238	0.656	0.149	0.275	0.240	0.150	0.188	0.215	0.176
Zr/Ti (ppm)	0.0224	0.0352	0.0526	0.0197	0.0279	0.0195	0.0195	0.0232	0.0182	0.0176
Nb/Y	0.567	0.300	0.454	0.206	0.325	0.233	0.189	0.220	0.281	0.236

Sample no. type	KA.88.33 A <sub>1</sub>	KA.88.33 A <sub>2</sub>	KA.88.39 A <sub>2</sub>	KA.88.40 A <sub>1</sub>	KA.88.44 A <sub>2</sub>	KA.88.45 A <sub>2</sub>	KA.88.46 A <sub>2</sub>	KA.88.47 A <sub>1</sub>	KA.88.48 A <sub>2</sub>	KA.88.54 A <sub>1</sub>	KA.88.61 A <sub>1</sub> /A <sub>2</sub> ?
SiO <sub>2</sub>	63.4	38.7		36.2	24.3	42.7	43.2	43.4	20.0	46.9	26.5
TiO <sub>2</sub>	0.29	0.80		1.45	1.03	0.71	0.60	0.71	1.09	0.60	1.13
Al <sub>2</sub> O <sub>3</sub>	15.1	9.85		12.0	8.82	10.9	14.5	12.1	11.1	12.3	9.84
Fe <sub>2</sub> O <sub>3 total</sub>	2.43	9.82		13.7	8.36	7.48	6.21	9.65	13.7	7.06	12.3
MnO	0.05	0.18		0.23	0.18	0.14	0.13	0.18	0.25	0.15	0.20
MgO	1.53	8.68		6.97	9.35	8.90	6.72	6.25	14.5	5.78	16.2
CaO	3.06	9.14		6.88	17.2	6.22	7.01	6.18	6.93	5.94	3.65
Na <sub>2</sub> O	9.46	2.55		3.57	2.75	4.77	5.85	5.53	1.56	5.94	2.79
K <sub>2</sub> O	0.09	1.32		1.29	1.06	0.75	1.20	0.79	2.30	0.58	1.03
P <sub>2</sub> O <sub>5</sub>	0.25	0.47		0.12	1.08	0.13	0.29	0.39	0.73	0.31	0.48
H <sub>2</sub> O+	0.1	0.7		0.7	0.5	0.4	0.8	0.4	0.8	0.4	0.7
H <sub>2</sub> O-	<0.1	0.1		0.1	0.1	0.1	0.1	0.1	0.1	<0.1	0.1
LOI	3.85	18.6		18.1	21.4	16.5	13.3	13.9	23.9	12.3	25.6
Σ	99.7	100.3		100.6	95.6	99.4	99.1	99.2	96.2	98.0	99.9
*SiO <sub>2</sub>	66.28	47.48		43.93	32.78	51.63	50.40	50.95	27.72	54.82	35.75
*TiO <sub>2</sub>	0.30	0.98		1.76	1.39	0.86	0.70	0.83	1.51	0.70	1.52
*Al <sub>2</sub> O <sub>3</sub>	15.79	12.08		14.56	11.90	13.18	16.92	14.21	15.38	14.38	13.28
*Fe <sub>2</sub> O <sub>3 total</sub>	2.54	12.05		16.62	11.28	9.04	7.25	11.33	18.99	8.25	16.59
*MnO	0.05	0.22		0.28	0.24	0.17	0.15	0.21	0.35	0.18	0.27
*MgO	1.60	10.65		8.46	12.61	10.76	7.84	7.34	20.09	6.76	21.86
*CaO	3.20	11.21		8.35	23.20	7.52	8.18	7.26	9.60	6.94	4.92
*Na <sub>2</sub> O	9.89	3.13		4.33	3.71	5.77	6.83	6.49	2.16	6.94	3.76
*K <sub>2</sub> O	0.09	1.62		1.57	1.43	0.91	1.40	0.93	3.19	0.68	1.39
*P <sub>2</sub> O <sub>5</sub>	0.26	0.58		0.15	1.46	0.16	0.34	0.46	1.01	0.36	0.65
*Σ	100.00	100.00		100.01	100.00	100.00	100.01	100.01	100.00	100.01	99.99
CO <sub>2</sub>	4.07	20.3		19.3	25.4	17.8	14.5	15.6	27.0	8.05	26.8

NO  
CO  
CT

Sample no. type	KA.88.33 A <sub>1</sub>	KA.88.39 A <sub>2</sub>	KA.88.40 A <sub>1</sub>	KA.88.44 A <sub>2</sub>	KA.88.45 A <sub>2</sub>	KA.88.46 A <sub>2</sub>	KA.88.47 A <sub>1</sub>	KA.88.48 A <sub>2</sub>	KA.88.54 A <sub>1</sub>	KA.88.61 A <sub>1</sub> /A <sub>2</sub> ?
La	30.25	21.36	3.16	49.16	16.37	42.35	21.47	30.49	32.12	22.11
Ce	90.34	72.59	11.10	152.54	52.97	124.26	63.07	92.48	95.32	68.52
Nd	35.59	27.84	6.63	57.38	21.17	47.21	26.28	39.79	41.17	32.24
Sm	4.68	5.76	2.45	12.27	3.67	6.93	4.68	7.39	6.26	5.83
Eu	1.440	1.773	1.089	3.952	1.038	2.038	1.450	2.048	1.812	1.863
Tb	0.468	0.785	0.630	1.697	0.403	0.495	0.569	0.926	0.697	0.796
Yb	1.391	1.396	2.837	3.721	1.183	1.262	1.692	1.972	1.239	2.249
Lu	0.224	0.228	0.424	0.583	0.175	0.228	0.280	0.324	0.177	0.322
La <sub>N</sub>	96.04	67.82	10.02	156.06	51.95	134.44	68.16	96.78	101.96	70.17
Ce <sub>N</sub>	111.12	89.29	13.65	187.63	65.15	152.84	77.58	113.75	117.24	84.28
Nd <sub>N</sub>	59.61	46.64	11.11	96.12	35.47	79.08	44.02	66.66	68.95	54.00
Sm <sub>N</sub>	24.38	29.98	12.78	63.88	19.11	36.11	24.39	38.50	32.60	30.37
Eu <sub>N</sub>	19.94	24.56	15.08	54.74	14.38	28.23	20.14	28.37	25.10	25.80
Tb <sub>N</sub>	9.55	16.02	12.86	34.63	8.22	10.10	11.61	18.90	14.22	16.24
Yb <sub>N</sub>	6.69	6.71	13.64	17.89	5.69	6.07	8.13	9.48	5.96	10.81
Lu <sub>N</sub>	6.93	7.06	13.13	18.05	5.42	7.06	8.67	10.03	5.48	9.97
La <sub>N</sub> /Yb <sub>N</sub>	14.36	10.11	0.74	8.72	9.14	22.16	8.38	10.21	17.12	6.49
Ce <sub>N</sub> /Yb <sub>N</sub>	16.62	13.31	1.00	10.49	11.46	25.19	9.54	12.00	19.69	7.80
S	12,000	4400	4800	19,000	3900	7000	7300	9900	13,000	2000
Au (ppb)	104	23	70	3230	700	320	820	7400	175	17
Ag	<0.01	<0.01	0.02	1.17	0.07	0.02	0.07	0.66	0.40	0.56
As	7.1	83	81	110	210	83	31	120	110	36
Sb	4.4	2.1	2.3	25	4.4	3.4	1.6	13	58	0.8
Bi	n.d.	n.d.	n.d.	n.d.	n.d.	n.d.	n.d.	n.d.	n.d.	n.d.
Se	1.1	<0.1	<0.1	0.4	0.2	0.1	0.1	0.2	0.2	<0.1
Mo	n.d.	n.d.	n.d.	n.d.	n.d.	n.d.	n.d.	n.d.	n.d.	n.d.
Sc	1.43	27.68	45.61	33.64	23.37	21.61	32.18	45.58	19.37	32.13
V	n.d.	n.d.	n.d.	n.d.	n.d.	n.d.	n.d.	n.d.	n.d.	n.d.
Cr	n.d.	n.d.	n.d.	n.d.	n.d.	n.d.	n.d.	n.d.	n.d.	n.d.
Co	3.55	36.65	45.24	37.58	39.31	27.66	31.55	55.35	23.60	43.62
Ni	n.d.	n.d.	n.d.	n.d.	n.d.	n.d.	n.d.	n.d.	n.d.	n.d.
Cu	20	97	154	83	30	8	99	377	236	14
Zn	20	55	65	42	46	38	79	67	55	83

N  
O  
O

Sample no. type	KA.88.33 A <sub>1</sub>	KA.88.39 A <sub>2</sub>	KA.88.40 A <sub>1</sub>	KA.88.44 A <sub>2</sub>	KA.88.45 A <sub>2</sub>	KA.88.46 A <sub>2</sub>	KA.88.47 A <sub>1</sub>	KA.88.48 A <sub>2</sub>	KA.88.54 A <sub>1</sub>	KA.88.61 A <sub>1</sub> /A <sub>2</sub> ?
Li	<1	<1	<1	<1	2	4	7	2	<1	3
Hf	3.25	2.88	2.07	7.21	2.53	3.16	2.21	3.15	2.68	3.03
Ta	0.48	0.24	0.26	0.57	0.22	0.26	0.20	0.28	0.38	0.39
W	13	17	12	58	25	9.3	13	18	31	46
Pb	n.d.	n.d.	n.d.	n.d.	n.d.	n.d.	n.d.	n.d.	n.d.	n.d.
U	0.77	0.70	0.05	1.42	0.54	1.05	0.76	1.00	0.72	0.74
Th	6.95	3.78	0.38	10.52	3.34	7.15	4.60	5.85	5.80	4.24
Rb	n.d.	n.d.	n.d.	n.d.	n.d.	n.d.	n.d.	n.d.	n.d.	n.d.
Sr	270.62	177.83	167.86	265.89	151.00	207.01	266.43	120.46	427.27	105.71
Y	15.68	21.05	25.98	46.26	13.78	16.96	19.52	29.70	19.10	25.13
Zr	162.66	114.80	80.80	311.69	107.14	144.91	92.30	136.59	131.07	142.19
Nb	7.40	6.18	5.01	9.79	2.11	4.43	2.90	3.64	7.86	7.03
Ba	n.d.	n.d.	n.d.	n.d.	n.d.	n.d.	n.d.	n.d.	n.d.	n.d.
Th/Yb	4.99	2.71	0.134	2.83	2.83	5.66	2.72	2.97	4.68	1.88
Ce/Yb	64.94	52.00	3.912	40.99	44.77	98.46	37.28	46.90	76.93	30.47
Ta/Yb	0.346	0.168	0.092	0.153	0.189	0.206	0.118	0.140	0.308	0.173
Zr/Ti (ppm)	0.0561	0.0144	0.0056	0.0303	0.0151	0.0242	0.0130	0.0125	0.0218	0.0126
Nb/Y	0.344	0.199	0.116	0.212	0.153	0.261	0.149	0.123	0.412	0.240

Sample no. type	KA.88.63 A <sub>2</sub> /A <sub>3</sub> ?	KA.88.64 A <sub>2</sub> /A <sub>3</sub> ?	KA.88.72 A <sub>2</sub>	KA.88.82 A <sub>3</sub>	KA.88.83 A <sub>3</sub>	KA.88.87 A <sub>2</sub>
SiO <sub>2</sub>	44.4	44.5	36.0	43.9	44.4	45.1
TiO <sub>2</sub>	0.58	0.67	0.80	0.73	0.75	0.68
Al <sub>2</sub> O <sub>3</sub>	10.5	12.9	6.60	10.3	10.9	10.6
Fe <sub>2</sub> O <sub>3</sub> total	7.11	6.30	8.88	9.17	8.78	7.76
MnO	0.14	0.10	0.16	0.15	0.15	0.17
MgO	8.67	7.53	14.0	9.37	8.65	7.60
CaO	7.34	5.27	6.74	7.55	7.54	7.42
Na <sub>2</sub> O	3.56	6.12	1.29	3.48	4.04	5.04
K <sub>2</sub> O	0.73	0.73	1.30	0.56	0.61	0.31
P <sub>2</sub> O <sub>5</sub>	0.37	0.53	0.58	0.42	0.43	0.72
H <sub>2</sub> O+	1.5	0.4	0.6	2.7	2.5	0.7
H <sub>2</sub> O-	<0.1	<0.1	<0.1	<0.1	0.1	<0.1
LOI	15.5	12.9	23.1	11.8	11.3	13.7
Σ	99.1	97.7	99.7	97.7	97.8	99.3
*SiO <sub>2</sub>	53.24	52.57	47.15	51.27	51.48	52.81
*TiO <sub>2</sub>	0.70	0.79	1.05	0.85	0.87	0.80
*Al <sub>2</sub> O <sub>3</sub>	12.59	15.24	8.64	12.03	12.64	12.41
*Fe <sub>2</sub> O <sub>3</sub> total	8.53	7.44	11.63	10.71	10.18	9.09
*MnO	0.17	0.12	0.21	0.18	0.17	0.20
*MgO	10.40	8.90	18.34	10.94	10.03	8.90
*CaO	8.80	6.23	8.83	8.82	8.74	8.69
*Na <sub>2</sub> O	4.27	7.23	1.69	4.06	4.68	5.90
*K <sub>2</sub> O	0.88	0.86	1.70	0.65	0.71	0.36
*P <sub>2</sub> O <sub>5</sub>	0.44	0.63	0.76	0.49	0.50	0.84
*Σ	100.02	100.01	100.00	100.00	100.00	100.00
CO <sub>2</sub>	15.2	15.2	24.2	11.1	11.0	15.2



Sample no. type	KA.88.63 A <sub>2</sub> /A <sub>3</sub> ?	KA.88.64 A <sub>2</sub> /A <sub>3</sub> ?	KA.88.72 A <sub>2</sub>	KA.88.82 A <sub>3</sub>	KA.88.83 A <sub>3</sub>	KA.88.87 A <sub>2</sub>
La	25.57	45.90	48.63	26.48	27.17	59.62
Ce	76.68	138.90	145.60	81.53	85.97	182.16
Nd	33.16	50.20	55.47	34.54	36.27	67.63
Sm	5.51	9.48	9.69	6.44	6.62	12.12
Eu	1.654	2.922	3.182	1.839	1.911	3.520
Tb	0.604	0.922	0.951	0.663	0.606	1.148
Yb	1.160	1.532	1.507	1.477	1.548	1.719
Lu	0.188	0.209	0.320	0.255	0.232	0.294
La <sub>N</sub>	81.18	145.70	154.38	84.07	86.24	189.27
Ce <sub>N</sub>	94.32	170.85	179.08	100.28	105.75	224.05
Nd <sub>N</sub>	55.55	84.09	92.92	57.85	60.75	113.27
Sm <sub>N</sub>	28.71	49.40	50.45	33.53	34.47	63.10
Eu <sub>N</sub>	22.91	40.47	44.07	25.47	26.47	48.75
Tb <sub>N</sub>	12.33	18.82	19.41	13.53	12.37	23.43
Yb <sub>N</sub>	5.58	7.37	7.25	7.10	7.44	8.26
Lu <sub>N</sub>	5.82	6.47	9.91	7.89	7.18	9.10
La <sub>N</sub> /Yb <sub>N</sub>	14.56	19.78	21.31	11.84	11.59	21.95
Ce <sub>N</sub> /Yb <sub>N</sub>	16.92	23.20	24.72	14.12	14.21	25.98
S	1900	17,000	2200	5200	5600	9100
Au (ppb)	2	7100	30	360	490	420
Ag	0.01	0.34	0.65	0.04	0.03	0.01
As	10	270	450	130	120	76
Sb	3.3	34	69	2.5	2.7	4.2
Bi	n.d.	n.d.	n.d.	n.d.	n.d.	n.d.
Se	<0.1	0.4	<0.1	0.1	0.1	0.2
Mo	n.d.	n.d.	n.d.	n.d.	n.d.	n.d.
Sc	21.94	18.04	27.81	29.48	28.25	25.54
V	n.d.	n.d.	n.d.	n.d.	n.d.	n.d.
Cr	n.d.	n.d.	n.d.	n.d.	n.d.	n.d.
Co	37.24	33.55	52.74	44.95	45.33	30.73
Ni	n.d.	n.d.	n.d.	n.d.	n.d.	n.d.
Cu	70	219	110	116	70	75
Zn	73	45	65	88	83	66

Sample no. type	KA.88.63 A <sub>2</sub> /A <sub>3</sub> ?	KA.88.64 A <sub>2</sub> /A <sub>3</sub> ?	KA.88.72 A <sub>2</sub>	KA.88.82 A <sub>3</sub>	KA.88.83 A <sub>3</sub>	KA.88.87 A <sub>2</sub>
Li	34	3	5	38	36	11
Hf	2.50	4.51	4.21	2.63	2.70	3.89
Ta	0.20	0.40	0.37	0.22	0.25	0.40
W	2.3	58	34	13	13	18
Pb	n.d.	n.d.	n.d.	n.d.	n.d.	n.d.
U	0.90	0.76	1.01	0.38	0.42	0.56
Th	5.31	8.42	10.09	4.71	5.05	9.44
Rb	n.d.	n.d.	n.d.	n.d.	n.d.	n.d.
Sr	459.87	309.95	152.47	647.11	656.43	505.05
Y	15.07	24.88	23.76	19.09	20.27	29.01
Zr	105.56	209.07	173.31	113.72	122.58	190.13
Nb	2.97	5.99	4.56	5.05	7.31	8.42
Ba	n.d.	n.d.	n.d.	n.d.	n.d.	n.d.
Th/Yb	4.58	5.49	6.69	3.19	3.26	5.49
Ce/Yb	66.11	90.67	96.61	55.20	55.54	105.97
Ta/Yb	0.175	0.260	0.244	0.148	0.159	0.231
Zr/Ti (ppm)	0.0182	0.0312	0.0217	0.0156	0.0163	0.0280
Nb/Y	0.131	0.201	0.150	0.212	0.262	0.221

KERR ADDISON FAULT GOUGES

Sample no.	KA.88.24	KA.88.34	KA.88.51	KA.88.52	KA.88.56	KA.88.58	KA.88.76
SiO <sub>2</sub>	35.9	55.9	27.7	87.7	66.7	62.4	51.2
TiO <sub>2</sub>	0.29	0.17	0.32	0.04	0.14	0.15	0.19
Al <sub>2</sub> O <sub>3</sub>	5.27	4.45	5.24	1.24	5.67	7.15	5.74
Fe <sub>2</sub> O <sub>3 total</sub>	7.67	4.92	9.04	0.39	3.53	4.02	5.35
MnO	0.16	0.10	0.16	0.02	0.06	0.07	0.11
MgO	15.8	11.2	20.6	2.16	8.76	9.80	12.1
CaO	7.85	4.83	6.42	3.26	2.16	2.34	5.59
Na <sub>2</sub> O	0.92	0.25	0.31	0.09	0.36	0.41	0.33
K <sub>2</sub> O	0.04	0.03	0.02	0.03	0.04	0.03	0.04
P <sub>2</sub> O <sub>5</sub>	0.03	0.01	0.01	0.01	0.01	0.01	0.01
H <sub>2</sub> O+	0.3	0.4	0.4	0.2	0.3	0.4	0.4
H <sub>2</sub> O-	<0.1	<0.1	<0.1	<0.1	<0.1	<0.1	<0.1
LOI	24.9	17.1	29.5	5.00	11.7	13.0	18.5
Σ	99.1	99.2	99.6	100.0	99.3	99.5	99.4
*SiO <sub>2</sub>	48.56	68.29	39.67	92.37	76.29	72.24	63.48
*TiO <sub>2</sub>	0.39	0.21	0.46	0.04	0.16	0.17	0.24
*Al <sub>2</sub> O <sub>3</sub>	7.13	5.44	7.51	1.31	6.49	8.28	7.12
*Fe <sub>2</sub> O <sub>3 total</sub>	10.37	6.01	12.95	0.41	4.04	4.65	6.63
*MnO	0.22	0.12	0.23	0.02	0.07	0.08	0.14
*MgO	21.37	13.68	29.50	2.28	10.02	11.35	15.00
*CaO	10.62	5.90	9.20	3.43	2.47	2.71	6.93
*Na <sub>2</sub> O	1.24	0.31	0.44	0.09	0.41	0.47	0.41
*K <sub>2</sub> O	0.05	0.04	0.03	0.03	0.05	0.03	0.05
*P <sub>2</sub> O <sub>5</sub>	0.04	0.01	0.01	0.01	0.01	0.01	0.01
*Σ	99.99	100.01	100.00	99.99	100.01	99.99	100.01
CO <sub>2</sub>	24.2	16.9	30.3	4.75	11.9	26.8	19.1

Sample no.	KA.88.24	KA.88.34	KA.88.51	KA.88.52	KA.88.56	KA.88.58	KA.88.76
La	2.04	0.29	0.87	0.10	0.42	0.31	0.33
Ce	7.38	1.57	3.95	0.81	0	1.95	1.92
Nd	4.12	0	0.02	0	0	1.62	0.06
Sm	0.73	0.26	0.52	0.07	0.18	0.24	0.25
Eu	0.28	0.14	0.25	0.07	0.09	0.11	0.15
Tb	0.17	0.10	0.19	0	0.10	0.01	0.06
Yb	0.78	0.44	0.53	0	0.24	0.36	0.38
Lu	0.08	0.06	0.09	0.01	0.04	0.04	0.06
La <sub>N</sub>	6.49	0.92	2.77	0.32	1.33	0.99	1.05
Ce <sub>N</sub>	9.08	1.93	4.85	1.00	0	2.40	2.36
Nd <sub>N</sub>	6.90	0	0.04	0	0	2.72	0.11
Sm <sub>N</sub>	3.79	1.33	2.72	0.38	0.95	1.27	1.32
Eu <sub>N</sub>	3.88	1.93	3.49	0.97	1.27	1.50	2.02
Tb <sub>N</sub>	3.43	2.08	3.96	0	1.96	0.27	1.31
Yb <sub>N</sub>	3.74	2.12	2.52	0	1.16	1.71	1.82
Lu <sub>N</sub>	2.60	1.86	2.66	0.40	1.08	1.36	1.80
La <sub>N</sub> /Yb <sub>N</sub>	1.74	0.43	1.10	n.d.	1.15	0.58	0.58
Ce <sub>N</sub> /Yb <sub>N</sub>	2.43	0.91	1.92	n.d.	0	1.40	1.30
S	1400	400	760	340	220	200	660
Au (ppb)	49	26	22	14	<1	2	44
Ag	0.04	<0.01	0.17	0.01	<0.01	0.01	0.03
As	960	770	1100	76	330	340	740
Sb	22	8.1	15	5.4	3.1	3.1	8.1
Bi	n.d.	n.d.	n.d.	n.d.	n.d.	n.d.	n.d.
Se	0.1	<0.1	0.1	<0.1	<0.1	<0.1	<0.1
Mo	n.d.	n.d.	n.d.	n.d.	n.d.	n.d.	n.d.
Sc	16.78	10.49	18.77	1.29	7.35	8.83	10.78
V	n.d.	n.d.	n.d.	n.d.	n.d.	n.d.	n.d.
Cr	n.d.	n.d.	n.d.	n.d.	n.d.	n.d.	n.d.
Co	65.93	43.00	71.83	5.42	29.76	32.94	47.59
Ni	n.d.	n.d.	n.d.	n.d.	n.d.	n.d.	n.d.
Cu	22	<1	<1	5	<1	<1	<1
Zn	44	44	61	18	37	43	49

Sample no.	KA.88.24	KA.88.34	KA.88.51	KA.88.52	KA.88.56	KA.88.58	KA.88.76
Li	8	<1	<1	6	<1	<1	<1
Hf	0.57	0.26	0.39	0	0.34	0.34	0.34
Ta	0	0	0	0	0.04	0	0
W	12	9.8	25	1.6	5.3	6.4	12
Pb	n.d.	n.d.	n.d.	n.d.	n.d.	n.d.	n.d.
U	0	0	0.08	0	0	0	0
Th	0.39	0	0.17	0.00	0.16	0.14	0
Rb	n.d.	n.d.	n.d.	n.d.	n.d.	n.d.	n.d.
Sr	269.01	76.29	113.17	40.48	35.34	42.78	96.51
Y	7.08	3.72	7.22	1.66	2.18	3.09	4.68
Zr	20.36	7.43	13.32	n.d.	5.25	6.82	7.62
Nb	1.89	1.42	n.d.	n.d.	0.37	n.d.	0.53
Ba	n.d.	n.d.	n.d.	n.d.	n.d.	n.d.	n.d.
Th/Yb	0.495	0	0.044	n.d.	0.676	0.390	0
Ce/Yb	n.d.	n.d.	n.d.	n.d.	n.d.	n.d.	n.d.
Ta/Yb	0	0	0	n.d.	0.166	0	0
Zr/Ti (ppm)	0.0070	0.0044	0.0042	n.d.	0.0038	0.0045	0.0040
Nb/Y	0.267	0.382	n.d.	n.d.	0.170	n.d.	0.113

**MACASSA MINE, KIRKLAND LAKE**

Sample no.	basic syenites		felsic syenites		syenite porphyries		Macassa "Break Ore"		
	Ma.87.45	Ma.87.11	Ma.87.47	Ma.87.58	Ma.87.63	Ma.87.25	Ma.87.02	Ma.87.04	Ma.87.53
SiO <sub>2</sub>	49.6	48.6	56.6	56.7	64.9	62.8	44.7	55.6	50.0
TiO <sub>2</sub>	0.84	0.80	0.70	0.59	0.37	0.38	0.84	0.51	0.68
Al <sub>2</sub> O <sub>3</sub>	13.5	12.4	15.8	18.3	14.7	14.4	15.0	12.6	14.0
Fe <sub>2</sub> O <sub>3 total</sub>	8.57	8.55	4.11	3.51	3.14	3.57	7.88	4.65	6.50
MnO	0.12	0.11	0.08	0.06	0.05	0.07	0.12	0.10	0.10
MgO	5.45	6.74	1.22	1.06	1.46	2.03	3.91	2.94	3.17
CaO	5.89	6.73	4.54	2.07	2.66	3.11	5.63	5.19	5.47
Na <sub>2</sub> O	2.85	2.24	5.54	3.73	6.18	5.42	3.00	5.49	3.77
K <sub>2</sub> O	5.58	4.80	5.04	8.89	2.52	3.13	5.25	2.69	4.54
P <sub>2</sub> O <sub>5</sub>	0.58	0.56	0.30	0.27	0.16	0.21	0.43	0.32	0.37
H <sub>2</sub> O+	1.4	2.0	0.8	0.6	0.7	0.8	0.9	0.4	0.8
H <sub>2</sub> O-	0.1	0.1	0.1	0.1	0.1	0.1	0.1	0.1	0.1
LOI	6.08	7.16	3.23	3.77	2.54	4.00	9.08	7.77	7.77
Σ	99.5	99.2	97.5	99.2	99.2	99.7	96.1	98.1	96.6
*SiO <sub>2</sub>	53.34	53.10	60.26	59.57	67.51	66.02	51.52	61.72	56.43
*TiO <sub>2</sub>	0.90	0.87	0.75	0.62	0.38	0.40	0.97	0.57	0.77
*Al <sub>2</sub> O <sub>3</sub>	14.52	13.55	16.82	19.23	15.29	15.14	17.29	13.99	15.80
*Fe <sub>2</sub> O <sub>3 total</sub>	9.22	9.34	4.38	3.69	3.27	3.75	9.08	5.16	7.34
*MnO	0.13	0.12	0.09	0.06	0.05	0.07	0.14	0.11	0.11
*MgO	5.86	7.36	1.30	1.11	1.52	2.13	4.51	3.26	3.58
*CaO	6.33	7.35	4.83	2.17	2.77	3.27	6.49	5.76	6.17
*Na <sub>2</sub> O	3.07	2.45	5.90	3.92	6.43	5.70	3.46	6.09	4.26
*K <sub>2</sub> O	6.00	5.24	5.37	9.34	2.62	3.28	6.05	2.99	5.12
*P <sub>2</sub> O <sub>5</sub>	0.62	0.61	0.32	0.28	0.17	0.22	0.50	0.36	0.42
*Σ	99.99	99.99	100.02	99.99	100.01	99.99	100.01	100.01	100.00
CO <sub>2</sub>	4.06	4.85	3.39	3.24	1.43	2.91	9.62	8.63	8.47

Sample no.	basic syenites		felsic syenites		syenite porphyries		Macassa "Break Ore"		
	Ma.87.45	Ma.87.11	Ma.87.47	Ma.87.58	Ma.87.63	Ma.87.25	Ma.87.02	Ma.87.04	Ma.87.53
La	43.94	48.82	45.00	49.40	27.86	n.d.	51.02	38.56	45.21
Ce	97.80	93.62	89.00	98.55	58.69	87.25	109.76	82.82	94.84
Nd	45.08	45.36	30.83	36.05	25.67	n.d.	49.27	37.21	40.02
Sm	8.80	8.61	6.32	6.20	5.32	n.d.	9.08	6.64	7.46
Eu	2.116	2.022	1.480	1.488	1.354	1.636	2.161	1.540	1.885
Tb	0.780	0.707	0.578	0.505	0.449	0.449	0.798	0.590	0.577
Yb	1.900	1.719	1.772	1.848	1.440	n.d.	1.942	1.501	1.429
Lu	0.322	0.308	0.296	0.311	0.296	n.d.	0.357	0.270	0.296
La <sub>N</sub>	139.48	135.94	142.86	156.82	88.43	n.d.	161.96	122.42	143.53
Ce <sub>N</sub>	120.30	115.15	109.47	121.21	72.19	107.32	135.00	101.87	116.66
Nd <sub>N</sub>	75.50	75.97	51.64	60.39	42.99	n.d.	82.53	62.50	67.04
Sm <sub>N</sub>	45.85	44.86	32.92	32.31	27.71	n.d.	47.30	34.59	38.87
Eu <sub>N</sub>	29.31	28.01	20.48	20.61	18.25	22.66	29.93	21.29	26.11
Tb <sub>N</sub>	15.92	14.43	11.80	10.31	9.16	9.16	16.29	12.04	11.78
Yb <sub>N</sub>	9.13	8.26	8.52	8.88	6.92	n.d.	9.34	7.22	6.87
Lu <sub>N</sub>	9.97	9.54	9.16	9.63	9.16	n.d.	11.05	8.36	9.16
La <sub>N</sub> /Y <sub>N</sub>	15.27	16.45	16.77	17.65	12.77	n.d.	17.34	16.96	20.89
Ce <sub>N</sub> /Y <sub>N</sub>	13.17	13.93	12.85	13.64	10.43	n.d.	14.46	14.12	16.98
S	<20	<20	3440	3100	<20	1700	13,000	4000	13,900
Au (ppb)	3	5	11	74	3	3	10,600	430	3580
Ag	0.05	0.07	0.02	0.05	<0.01	0.04	1.10	0.08	1.00
As	3.6	3.4	2.7	4.3	2.3	4.1	n.d.	5.5	12
Sb	1.4	1.3	1.2	2.3	1.6	0.7	n.d.	4.4	5.1
Bi	0.27	0.74	0.64	0.19	0.15	0.44	0.45	0.28	0.19
Sc	0.3	0.4	0.5	0.3	<0.1	0.2	0.7	0.1	0.7
Mo	1.3	0.6	3.0	1.5	0.7	0.5	43.6	5.6	56.9
Sc	21.25	21.65	5.53	3.38	7.19	7.76	17.54	10.68	12.95
V	207.80	219.06	72.62	90.66	49.89	53.18	384.74	99.61	248.03
Cr	197.70	275.41	67.00	27.72	71.46	81.21	166.88	135.69	123.28
Co	29.43	31.77	16.19	9.43	7.18	9.75	30.87	16.32	29.72
Ni	53.94	103.96	14.66	3.06	25.39	38.12	38.13	28.55	28.18
Cu	61	28	<1	15	<1	7	5	3	12
Zn	89	96	28	35	44	71	68	45	54

Sample no.	basic syenites		felsic syenites		syenite porphyries		Macassa "Break Ore"		
	Ma.87.45	Ma.87.11	Ma.87.47	Ma.87.58	Ma.87.63	Ma.87.25	Ma.87.02	Ma.87.04	Ma.87.53
Li	46	39	12	19	29	28	52	8	28
Hf	3.52	3.55	4.43	4.75	4.16	4.48	4.33	3.92	3.83
Ta	0.28	0.42	0.50	0.64	0.46	0.47	0.47	0.43	0.45
W	0.7	2.4	0.7	5.6	<0.7	<0.7	n.d.	8.7	23
Pb	15.7	18.9	12.5	9.7	14.0	30.6	22.9	7.6	21.9
U	1.83	1.71	2.85	2.21	2.42	n.d.	2.44	2.29	2.23
Th	8.49	8.25	11.81	14.42	5.92	8.46	11.75	9.48	10.70
Rb	198.87	193.56	97.47	215.90	79.54	104.01	234.24	70.25	172.28
Sr	1197.18	1591.92	930.25	380.57	1581.31	1740.29	483.64	720.06	517.97
Y	22.78	21.62	16.00	19.30	18.36	18.10	25.29	18.96	21.24
Zr	132.37	127.08	164.84	215.85	132.53	140.48	191.97	165.66	170.16
Nb	n.d.	n.d.	n.d.	n.d.	n.d.	n.d.	n.d.	n.d.	n.d.
Ba	2162.51	2107.97	1571.66	1583.63	2172.13	2630.24	857.13	885.27	800.01
Th/Yb	4.47	4.80	6.66	7.80	4.11	n.d.	6.05	6.32	7.49
Ce/Yb	51.48	54.46	50.22	53.33	40.76	n.d.	56.52	55.18	66.37
Ta/Yb	0.149	0.242	0.282	0.346	0.317	n.d.	0.243	0.286	0.312
Zr/Ti (ppm)	0.0158	0.0159	0.0235	0.0366	0.0358	0.0370	0.0229	0.0325	0.0250
Nb/Y	n.d.	n.d.	n.d.	n.d.	n.d.	n.d.	n.d.	n.d.	n.d.



**McBEAN MINE, nr. DOBIE**

Sample no.      "albitites"      syenite porphyry  
                          Mc.87.01      Mc.87.02      Mc.87.06

SiO <sub>2</sub>	43.3	45.7	63.1
TiO <sub>2</sub>	0.70	0.70	0.39
Al <sub>2</sub> O <sub>3</sub>	15.0	14.7	16.6
Fe <sub>2</sub> O <sub>3</sub> total	8.83	8.96	3.87
MnO	0.14	0.12	0.08
MgO	5.01	5.60	1.87
CaO	6.00	5.37	3.56
Na <sub>2</sub> O	5.33	5.61	6.75
K <sub>2</sub> O	2.41	1.80	2.77
P <sub>2</sub> O <sub>5</sub>	0.45	0.38	0.14
H <sub>2</sub> O+	0.6	0.5	0.4
H <sub>2</sub> O-	0.1	<0.1	<0.1
LOI	8.00	8.31	0.93
Σ	95.3	97.4	100.5
*SiO <sub>2</sub>	49.67	51.38	63.65
*TiO <sub>2</sub>	0.80	0.79	0.39
*Al <sub>2</sub> O <sub>3</sub>	17.21	16.53	16.75
*Fe <sub>2</sub> O <sub>3</sub> total	10.13	10.07	3.90
*MnO	0.16	0.13	0.08
*MgO	5.75	6.30	1.89
*CaO	6.88	6.04	3.59
*Na <sub>2</sub> O	6.11	6.31	6.81
*K <sub>2</sub> O	2.76	2.02	2.79
*P <sub>2</sub> O <sub>5</sub>	0.52	0.43	0.14
*Σ	99.99	100.00	99.99
CO <sub>2</sub>	10.9	11.0	0.22

"albitites" | syenite porphyry

Sample no.	"albitites"		Mc.87.02	Mc.87.06
	Mc.87.01	Mc.87.02		
La	29.72	28.25	26.14	
Ce	63.51	59.48	52.12	
Nd	32.95	32.38	23.51	
Sm	6.32	6.03	4.33	
Eu	1.501	1.392	0.994	
Tb	0.505	0.501	0.293	
Yb	1.648	1.350	1.216	
Lu	0.283	0.272	0.194	
La <sub>N</sub>	94.35	89.69	82.98	
Ce <sub>N</sub>	78.12	73.16	64.10	
Nd <sub>N</sub>	55.20	54.24	39.38	
Sm <sub>N</sub>	32.94	31.41	22.55	
Eu <sub>N</sub>	20.79	19.28	13.77	
Tb <sub>N</sub>	10.31	10.22	5.98	
Yb <sub>N</sub>	7.92	6.49	5.85	
Lu <sub>N</sub>	8.76	8.42	6.01	
La <sub>N</sub> /Yb <sub>N</sub>	11.91	13.82	14.20	
Ce <sub>N</sub> /Yb <sub>N</sub>	9.86	11.27	10.97	
S	23,600	24,000	<20	
Au (ppb)	430	2400	2	
Ag	1.00	1.20	<0.01	
As	<0.9	1.7	2.2	
Sb	0.8	0.6	<0.1	
Bi	1.67	1.24	0.08	
Se	1.3	1.4	<0.1	
Mo	2.8	2.0	0.3	
Sc	19.60	19.47	7.59	
V	201.28	201.95	81.29	
Cr	45.01	50.79	34.54	
Co	29.77	31.75	10.18	
Ni	20.48	59.77	6.99	
Cu	158	166	4	
Zn	54	67	66	

Sample no.	"albitites"		syenite porphyry	
	Mc.87.01	Mc.87.02	Mc.87.06	Mc.87.06
Li	11	8	2	
Hf	2.11	2.16	3.05	
Ta	0.22	0.19	0.24	
W	18	17	<1.2	
Pb	10.6	11.1	14.8	
U	2.29	0.94	1.33	
Th	4.27	4.29	4.78	
Rb	48.80	38.77	39.23	
Sr	279.82	276.57	1275.95	
Y	18.34	16.03	10.11	
Zr	98.28	95.70	111.26	
Nb	n.d.	n.d.	n.d.	
Ba				
Th/Yb	2.59	3.17	3.93	
Ce/Yb	38.54	44.06	42.86	
Ta/Yb	0.133	0.139	0.197	
Zr/Ti (ppm)	0.0140	0.0137	0.0285	
Nb/Y	n.d.	n.d.	n.d.	

ABITIBI BATHOLITH MARGINAL DIORITES

Sample no.	88.ARS.10	88.ARS.12	88.ARS.13	88.ARS.37	88.ARS.48	88.ARS.1024	88.ARS.1025	88.ARS.1031	88.ARS.1037
SiO <sub>2</sub>	60.4	51.3	50.0	57.7	55.1	68.6	56.0	60.3	65.5
TiO <sub>2</sub>	0.55	1.67	0.71	0.73	0.98	0.41	0.76	0.52	0.50
Al <sub>2</sub> O <sub>3</sub>	15.4	16.6	21.0	15.4	17.7	15.9	21.0	17.1	17.0
Fe <sub>2</sub> O <sub>3 total</sub>	5.56	10.8	7.68	7.82	7.51	3.36	5.59	4.56	4.03
MnO	0.10	0.17	0.12	0.12	0.14	0.04	0.06	0.08	0.07
MgO	3.70	5.44	5.25	5.65	2.84	1.21	2.33	3.74	1.64
CaO	5.67	8.09	6.84	7.06	4.74	4.62	8.07	6.08	6.06
Na <sub>2</sub> O	4.56	3.67	4.18	3.19	3.42	4.41	5.17	4.61	4.33
K <sub>2</sub> O	2.14	0.46	1.44	0.85	2.43	0.90	0.58	1.59	0.59
P <sub>2</sub> O <sub>5</sub>	0.20	0.53	0.27	0.14	0.23	0.14	0.15	0.20	0.18
H <sub>2</sub> O+	1.1	1.3	2.4	1.7	2.8	0.5	0.7	1.2	0.5
H <sub>2</sub> O-	0.1	0.1	0.1	<0.1	0.1	<0.1	<0.1	0.1	<0.1
LOI	1.54	1.16	2.77	1.70	5.08	0.39	0.70	1.47	0.47
Σ	100.0	100.0	100.4	100.5	100.3	100.1	100.5	100.5	100.5
*SiO <sub>2</sub>	61.46	51.96	51.29	58.48	57.95	68.88	56.16	61.04	65.57
*TiO <sub>2</sub>	0.56	1.69	0.73	0.74	1.03	0.41	0.76	0.53	0.50
*Al <sub>2</sub> O <sub>3</sub>	15.67	16.81	21.54	15.61	18.61	15.97	21.06	17.31	17.02
*Fe <sub>2</sub> O <sub>3 total</sub>	5.66	10.94	7.88	7.93	7.90	3.37	5.61	4.62	4.03
*MnO	0.10	0.17	0.12	0.12	0.15	0.04	0.06	0.08	0.07
*MgO	3.76	5.51	5.39	5.73	2.99	1.21	2.34	3.79	1.64
*CaO	5.77	8.19	7.02	7.16	4.98	4.64	8.09	6.16	6.07
*Na <sub>2</sub> O	4.64	3.72	4.29	3.23	3.60	4.43	5.19	4.67	4.33
*K <sub>2</sub> O	2.18	0.47	1.48	0.86	2.56	0.90	0.58	1.61	0.59
*P <sub>2</sub> O <sub>5</sub>	0.20	0.54	0.28	0.14	0.24	0.14	0.15	0.20	0.18
*Σ	100.00	100.00	100.02	100.00	100.01	99.99	100.00	100.01	100.00
CO <sub>2</sub>	0.13	<0.01	<0.01	0.03	2.70	0.02	0.01	0.03	0.02

Sample no.	88.ARS.10	88.ARS.12	88.ARS.13	88.ARS.37	88.ARS.48	88.ARS.1024	88.ARS.1025	88.ARS.1031	88.ARS.1037
La	18.17	10.69	5.45	12.30	8.16	15.09	2.75	18.08	20.44
Ce	57.56	36.52	18.28	39.92	29.48	42.20	10.44	57.89	53.48
Nd	22.02	18.77	7.13	16.51	13.74	11.07	6.09	23.81	17.85
Sm	3.73	4.01	1.64	3.04	2.65	1.57	1.66	3.61	2.37
Eu	1.092	1.915	0.976	0.950	1.015	0.706	0.785	1.208	0.861
Tb	0.357	0.639	0.270	0.525	0.513	0.146	0.287	0.274	0.236
Yb	0.915	1.693	0.796	1.486	1.408	0.288	0.593	0.573	0.423
Lu	0.162	0.270	0.138	0.240	0.225	0.052	0.109	0.104	0.080
La <sub>N</sub>	57.70	33.92	17.31	39.05	25.92	47.90	8.71	57.39	64.90
Ce <sub>N</sub>	70.80	44.92	22.49	43.10	36.26	51.91	12.85	71.20	65.78
Nd <sub>N</sub>	36.88	31.44	11.94	27.65	23.02	18.55	10.19	39.87	29.90
Sm <sub>N</sub>	19.41	20.90	8.56	15.84	13.82	8.19	8.65	18.79	12.32
Eu <sub>N</sub>	15.12	26.52	13.52	13.14	14.06	9.78	10.87	16.73	11.93
Tb <sub>N</sub>	7.29	13.04	5.51	10.71	10.47	2.98	5.86	5.59	4.82
Yb <sub>N</sub>	4.40	8.14	3.83	7.14	6.77	1.38	2.85	2.75	2.03
Lu <sub>N</sub>	5.02	8.36	4.27	7.43	6.97	1.61	3.37	3.22	2.48
La <sub>N</sub> /Y <sub>bN</sub>	13.12	4.17	4.53	5.47	3.83	34.61	3.06	20.84	31.92
Ce <sub>N</sub> /Y <sub>bN</sub>	16.09	5.52	5.88	6.87	5.36	37.50	4.51	25.86	32.36
S	100	440	780	160	300	120	100	120	100
Au (ppb)	<1	<1	<1	<1	<1	<1	<1	<1	<1
Ag	0.03	0.04	0.04	0.02	0.02	0.03	0.02	<0.01	0.06
As	<0.5	0.7	<0.5	0.6	<0.5	<0.5	<0.5	<0.5	<0.5
Sb	<0.1	<0.1	<0.1	<0.1	<0.1	<0.1	<0.1	<0.1	<0.1
Bi	n.d.	n.d.	n.d.	n.d.	n.d.	n.d.	n.d.	n.d.	n.d.
Se	0.2	0.4	0.2	0.2	<0.1	0.3	0.6	0.4	0.3
Mo	n.d.	n.d.	n.d.	n.d.	n.d.	n.d.	n.d.	n.d.	n.d.
Sc	14.71	25.42	12.41	18.30	16.25	3.46	12.69	10.58	6.74
V	n.d.	n.d.	n.d.	n.d.	n.d.	n.d.	n.d.	n.d.	n.d.
Cr	n.d.	n.d.	n.d.	n.d.	n.d.	n.d.	n.d.	n.d.	n.d.
Co	20.51	35.97	33.83	32.47	19.96	8.98	17.93	19.66	11.16
Ni	n.d.	n.d.	n.d.	n.d.	n.d.	n.d.	n.d.	n.d.	n.d.
Cu	19	19	39	<1	2	<1	4	<1	7
Zn	73	122	88	82	114	72	72	84	70

Sample no. 88.ARS.10 88.ARS.12 88.ARS.13 88.ARS.37 88.ARS.48 88.ARS.1024 88.ARS.1025 88.ARS.1031 88.ARS.1037

Li	13	9	32	11	13	19	15	13	15
Hf	3.15	1.31	0.80	3.58	2.99	4.49	2.40	2.70	5.06
Ta	0.31	0.69	0.15	0.54	0.52	0.40	0.12	0.18	0.40
W	<0.5	<0.5	<0.7	<0.5	<0.5	<0.5	<0.5	<0.5	<0.5
Pb	n.d.	n.d.	n.d.	n.d.	n.d.	n.d.	n.d.	n.d.	n.d.
U	0.40	0.08	0	0.31	0.19	0.18	0.11	0.16	0.23
Th	3.79	0.56	0.30	3.17	1.60	3.05	0.59	1.74	2.93
Rb	n.d.	n.d.	n.d.	n.d.	n.d.	n.d.	n.d.	n.d.	n.d.
Sr	n.d.	n.d.	n.d.	n.d.	n.d.	n.d.	n.d.	n.d.	n.d.
Y	n.d.	n.d.	n.d.	n.d.	n.d.	n.d.	n.d.	n.d.	n.d.
Zr	n.d.	n.d.	n.d.	n.d.	n.d.	n.d.	n.d.	n.d.	n.d.
Nb	n.d.	n.d.	n.d.	n.d.	n.d.	n.d.	n.d.	n.d.	n.d.
Ba	n.d.	n.d.	n.d.	n.d.	n.d.	n.d.	n.d.	n.d.	n.d.
Th/Yb	4.14	0.33	0.37	2.13	1.13	10.58	1.00	3.03	6.92
Ce/Yb	62.90	21.57	22.97	26.86	20.94	146.52	17.61	101.03	126.43
Ta/Yb	0.336	0.409	0.182	0.361	0.366	1.389	0.201	0.305	0.943
Zr/Ti (ppm)	n.d.	n.d.	n.d.	n.d.	n.d.	n.d.	n.d.	n.d.	n.d.
Nb/Y	n.d.	n.d.	n.d.	n.d.	n.d.	n.d.	n.d.	n.d.	n.d.

**Appendix VI. Kerr Addison - Chesterville Numerical Analysis Data**

**based on measured intersection data from >6000 drillholes,**

**27 mine levels, Kerr Addison - Chesterville**

**1. MAFIC "ALBITTE" INTRUSIONS (>1 FT WIDTH)**

**Number:**

- a. total no. of drilled dyke intersections measured **7034**
- b. no. of dyke intersections inside main ultramafic unit **6483 = 92.17% of a.**
- c. no. of dyke intersections outside main ultramafic unit **551 = 7.83% of b.**
- d. no. of dyke intersections in talc rocks of main ultramafic unit **203 = 3.13% of b.**
- e. no. of dyke intersections hosted by Au-metasomatised ultramafics **6280 = 96.87% of b.**

**Footage:**

- f. total footage of dyke intersections measured **43,375 ft (13,222 m)**
- g. total footage of dyke intersections inside main ultramafic unit **41,820 ft (12,755 m) = 96.41% of f.**
- h. total footage of dyke intersections outside main ultramafic unit **1555 ft (474 m) = 3.59% of f.**
- i. footage of dyke intersections in talc rocks of main ultramafic unit **1062 ft (324 m) = 2.54% of g.**
- j. footage of dyke intersections hosted by Au-metasomatised ultramafics **40,758 ft (12,431 m) = 97.46% of g.**
- k. % volume of dykes in talc rocks of main ultramafic unit **1.35% of 3d.**
- l. % volume of dykes hosted by Au-metasomatised ultramafics **11.52% of (3b-3d).**



Mean Width:

- m. mean width of all dyke intersections measured 6.17 ft (1.88 m)
- n. mean width of dyke intersections inside main ultramafic unit 6.45 ft (1.97 m)
- o. mean width of dyke intersections outside main ultramafic unit 2.82 ft (0.86 m)
- p. mean width of dyke intersections in talc rocks of main ultramafic unit 5.23 ft (1.59 m)
- q. mean width of dyke intersections in Au-metasomatised ultramafics 6.49 ft (1.98 m)

Volume data:

- r. total volume of intrusions in main ultramafic unit (surface - 5600 ft level)  $9.01 \times 10^6 \text{ m}^3$  (~0.01 km<sup>3</sup>)
- s. total mass of intrusions in main ultramafic unit (surface - 5600 ft level) (density ~2800 kg/m<sup>3</sup>) ~25.5 million tonnes
- t. total footage of main ultramafic unit intersected during dyke footage measurements 433,168 ft (132,116 m)
- u. % volume of intrusions in main ultramafic unit (surface - 5600 ft level) 9.65%

2. MAJOR QUARTZ VEINS (> 1FT WIDTH)

Number:

- a total no. of drilled quartz vein intersections (>1 ft) measured 10,459
- b. no. of quartz vein intersections (>1 ft) inside main ultramafic unit 8668 = 82.88% of a.
- c. no. of quartz vein intersections (>1 ft) outside main ultramafic unit 1791 = 17.12% of a.

**Footage:**

- d. total footage of quartz vein intersections (>1 ft) measured 20,343 ft ( 6205 m)
- e. total footage of quartz vein intersections (>1 ft) inside main ultramafic unit 17,735 ft (5409 m) = 87.18% of d
- f. total footage of quartz vein intersections (>1 ft) outside main ultramafic unit 2608 ft (795.4 m) = 12.82% of d

**Mean Width:**

- g. mean width of all quartz vein intersections (>1 ft) measured 1.95 ft (0.59 m)
- h. mean width of quartz vein intersections (>1 ft) inside main ultramafic unit 2.05 ft (1.97 m)
- i. mean width of quartz vein intersections (>1 ft) outside main ultramafic unit 1.46 ft (0.455 m)

**Volume data:**

- j. total volume of quartz veins (>1 ft) in main ultramafic unit (surface - 5600 ft level)  $3.8 \times 10^6 \text{ m}^3$  (~0.0038 km<sup>3</sup>)
- k. total mass of quartz veins (>1 ft) in main ultramafic unit (surface - 5600 ft level; density ~2700 kg/m<sup>3</sup>) ~10.3 million tonnes
- l. total footage of main ultramafic unit intersected during quartz vein footage measurements 433,168 ft (132,116 m)
- m. % volume of quartz veins in main ultramafic unit (surface - 5600 ft level) 4.09%
- n. mean % volume of quartz veins in green carbonate altered rocks (surface - 5600 ft level; quartz veins assumed only to be in GC areas) 9.86%

### 3. ALTERATION TYPES (ULTRAMAFIC HOST ROCK)

- a. volume of mine enclosed within boundaries of green carbonate envelope ~0.1 km<sup>3</sup>
- b. total footage of main ultramafic unit drilled (on full sections) 292,691 ft (89,271 m)
- c. total footage of green carbonate drilled (on full sections) 121,419 ft (37,033 m) = 41.5% of b
- d. total footage of talc rocks drilled (on full sections) 53,721 ft (16,385 m) = 18.36% of b
- e. volume of green carbonate altered rocks in main ultramafic unit ~0.04 km<sup>3</sup>

Hence the main ultramafic unit within the boundaries of the green carbonate alteration envelope comprises:

- 41.5% green carbonate alteration + quartz;
- 30.5% intermediate (brown/grey) alteration;
- 18.35% talc rocks; and
- 9.65% mafic "albite" dykes.

**Appendix VII.**

**Underground Areas Studied during the Course of this Thesis**

**Kerr-Addison Mine**

**J.P.Smith, E.T.C. Spooner, D.W. Broughton, F.R.Ploeger (1987-90)**

## AREAS STUDIED (55)

### 1. J.P.S. : Maps/Notes/Samples (19 areas):

814-61	SILL†	"2321-58"	N X-CUT
861	S X-CUT*	3414-62	ST
864	S X-CUT*	3814-63	ST
866	S X-CUT*	38"25"-79	ST
1014-52	EX DR	3815-54 1/2	DR
1014-59/61	DR	3801-56	N X-CUT
1715-66	EX DR	4014-63 1/2	ST
1719-74	SILL	4014-64	E DR
1915-69	EX DR	4001-59	N X-CUT
2015-64	SILL		

### 2. J.P.S. : Sketch maps/Notes/Photos (6 areas):

1117-63	ST*
1117-66	ST*
1114-59	ST
1910-26	SILL
3815-73	POD
4001-69	EX DR

### 3. J.P.S./E.T.C.S. : Observations/Notes/Photos (24 areas + 4 levels):

219-59	ST SILL	2516-58	PILLAR*
1321-60	ST*	2614-57 1/2	ST
1906-18	"N" ST*	2615-67	SILL
1921-64	E DR	2616-53	ST*
1921-68	N X-CUT*	2616-57 1/2	PILLAR*
1915-62/64	E DR†	3521-61	PILLAR*
2016-65	SILL	3521-63	PILLAR*
2015/62/64	E DR	3721-62 3/4	PILLAR*
2015-71	ST SILL	3821-63	PILLAR*
2215-66	SHRINK ST†	3703	EX DR
2216-57 1/2	ST*	3814-59	ST
2216-60	ST*		
2216-62	ST*		

+ 850 ft, 3250 ft, 3850 ft, 4000 ft levels

### D.W.B./F.R.P. : Other areas (6):

1114-50/52	ST
1610-26	SILL
1710-26	SILL
1918-59	SILL
2010-24	ST
2321-58	ST*

† Transitional flow/ green carbonate ore

\* Flow ore

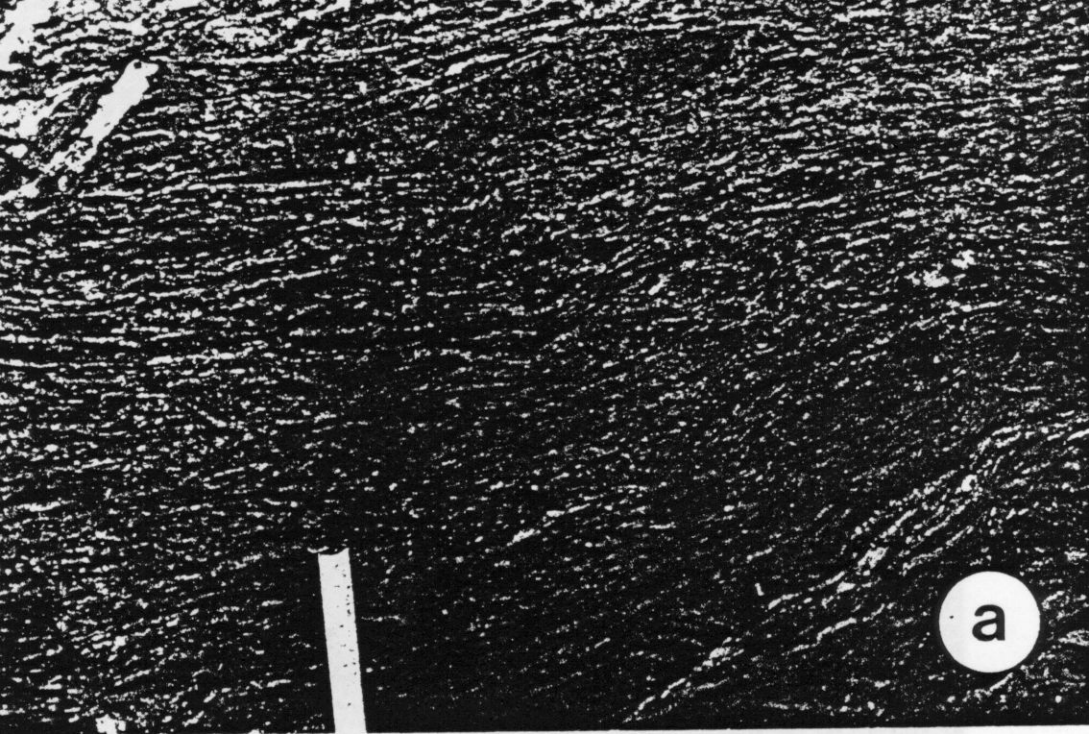
**CONVERSION FACTORS FOR MEASUREMENTS IN ONTARIO GEOLOGICAL SURVEY PUBLICATIONS**

Conversion from SI to Imperial			Conversion from Imperial to SI		
<i>SI Unit</i>	<i>Multiplied by</i>	<i>Gives</i>	<i>Imperial Unit</i>	<i>Multiplied by</i>	<i>Gives</i>
<b>LENGTH</b>					
1 mm	0.039 37	inches	1 inch	<b>25.4</b>	mm
1 cm	0.393 70	inches	1 inch	<b>2.54</b>	cm
1 m	3.280 84	feet	1 foot	<b>0.304 8</b>	m
1 m	0.049 709 7	chains	1 chain	20.116 8	m
1 km	0.621 371	miles (statute)	1 mile (statute)	<b>1.609 344</b>	km
<b>AREA</b>					
1 cm <sup>2</sup>	0.155 0	square inches	1 square inch	<b>6.451 6</b>	cm <sup>2</sup>
1 m <sup>2</sup>	10.763 9	square feet	1 square foot	<b>0.092 903 04</b>	m <sup>2</sup>
1 km <sup>2</sup>	0.386 10	square miles	1 square mile	2.589 988	km <sup>2</sup>
1 ha	2.471 054	acres	1 acre	0.404 685 6	ha
<b>VOLUME</b>					
1 cm <sup>3</sup>	0.061 02	cubic inches	1 cubic inch	<b>16.387 064</b>	cm <sup>3</sup>
1 m <sup>3</sup>	35.314 7	cubic feet	1 cubic foot	0.028 316 85	m <sup>3</sup>
1 m <sup>3</sup>	1.308 0	cubic yards	1 cubic yard	0.764 555	m <sup>3</sup>
<b>CAPACITY</b>					
1 L	1.759 755	pints	1 pint	0.568 261	L
1 L	0.879 877	quarts	1 quart	1.136 522	L
1 L	0.219 969	gallons	1 gallon	<b>4.546 090</b>	L
<b>MASS</b>					
1 g	0.035 273 96	ounces (avdp)	1 ounce (avdp)	28.349 523	g
1 g	0.032 150 75	ounces (troy)	1 ounce (troy)	<b>31.103 476 8</b>	g
1 kg	2.204 62	pounds (avdp)	1 pound (avdp)	<b>0.453 592 37</b>	kg
1 kg	0.001 102 3	tons (short)	1 ton (short)	907.184 74	kg
1 t	1.102 311	tons (short)	1 ton (short)	<b>0.907 184 74</b>	t
1 kg	0.000 984 21	tons (long)	1 ton (long)	1016.046 908 8	kg
1 t	0.984 206 5	tons (long)	1 ton (long)	<b>1.016 046 908 8</b>	t
<b>CONCENTRATION</b>					
1 g/t	0.029 166 6	ounce (troy)/ ton (short)	1 ounce (troy)/ ton (short)	34.285 714 2	g/t
1 g/t	0.583 333 33	pennyweights/ ton (short)	1 pennyweight/ ton (short)	1.714 285 7	g/t

**OTHER USEFUL CONVERSION FACTORS**

	<i>Multiplied by</i>	
1 ounce (troy) per ton (short)	20.0	pennyweights per ton (short)
1 pennyweight per ton (short)	0.05	ounces (troy) per ton (short)

*Note: Conversion factors which are in bold type are exact. The conversion factors have been taken from or have been derived from factors given in the Metric Practice Guide for the Canadian Mining and Metallurgical Industries, published by the Mining Association of Canada in co-operation with the Coal Association of Canada.*

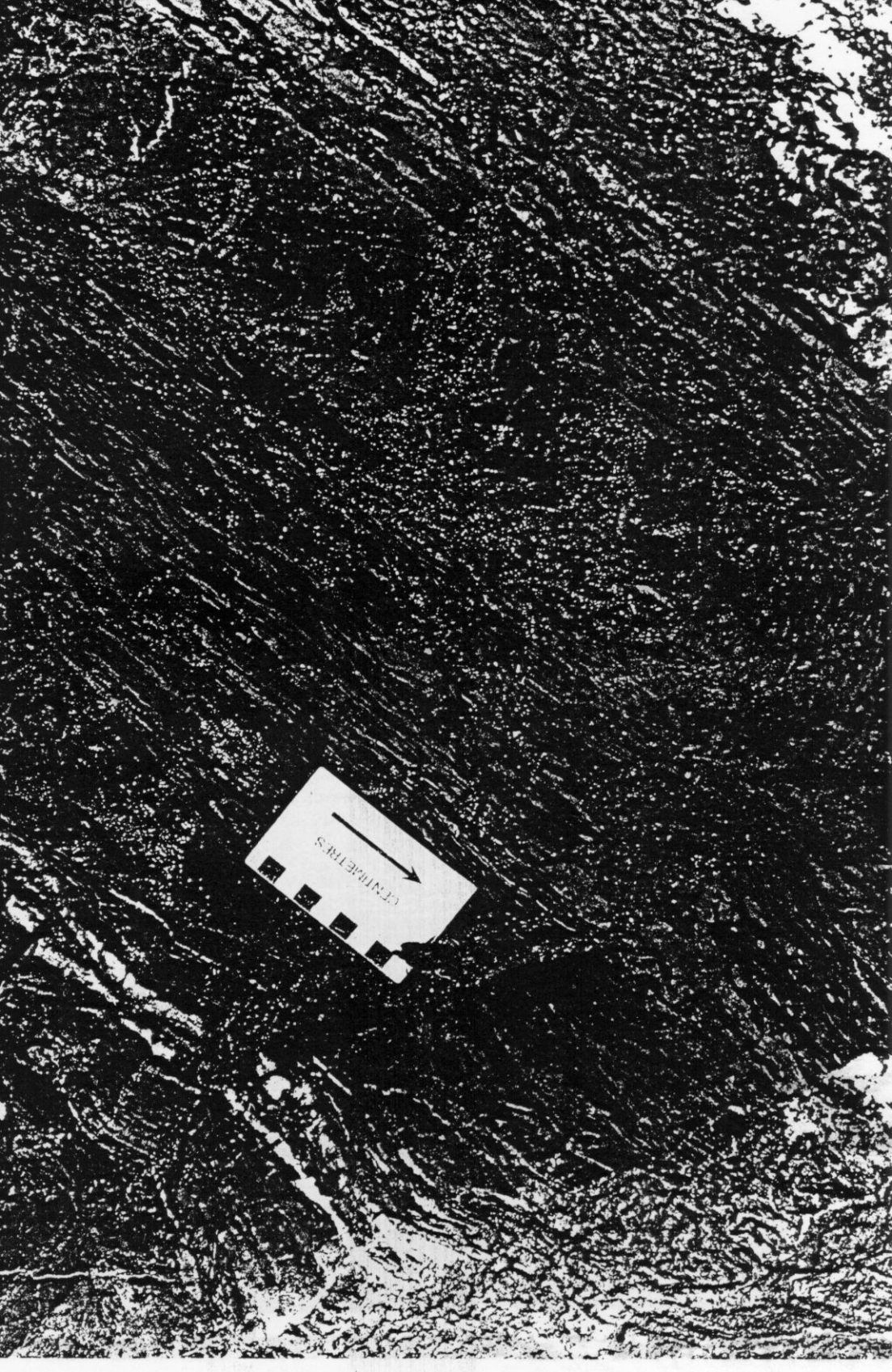


a



b





CENTIMETERS





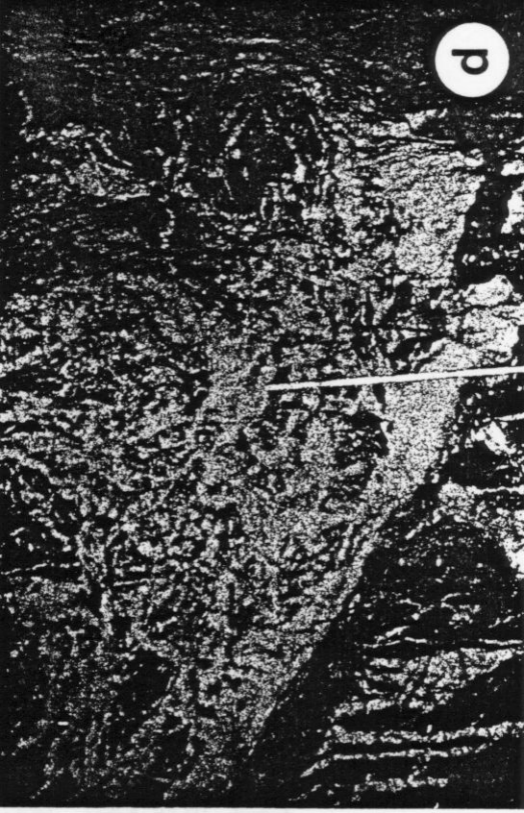




A high-contrast, black and white micrograph showing a dense, textured surface. The texture consists of numerous small, irregular, light-colored spots and fibers against a dark background. Several prominent, bright, vertical or near-vertical lines or ridges run through the field of view. In the upper right corner, there is a white circular label containing the lowercase letter 'b'. A thin, curved line extends from the label towards the center of the image.

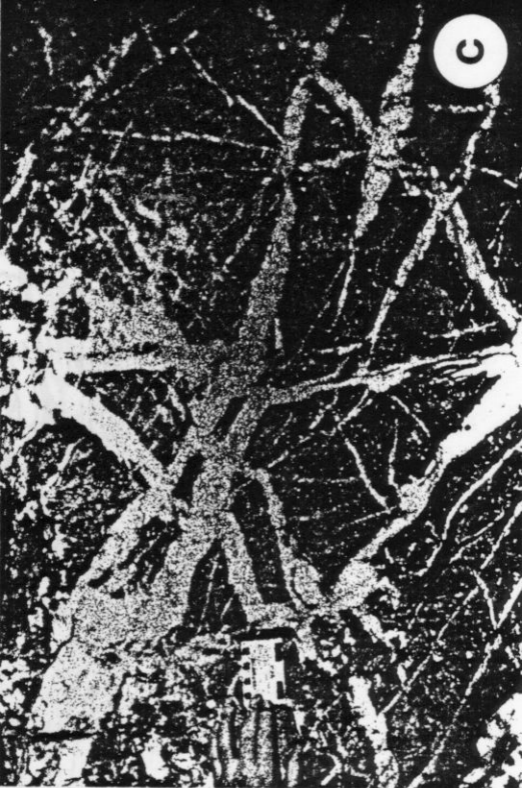
**b**

p



a

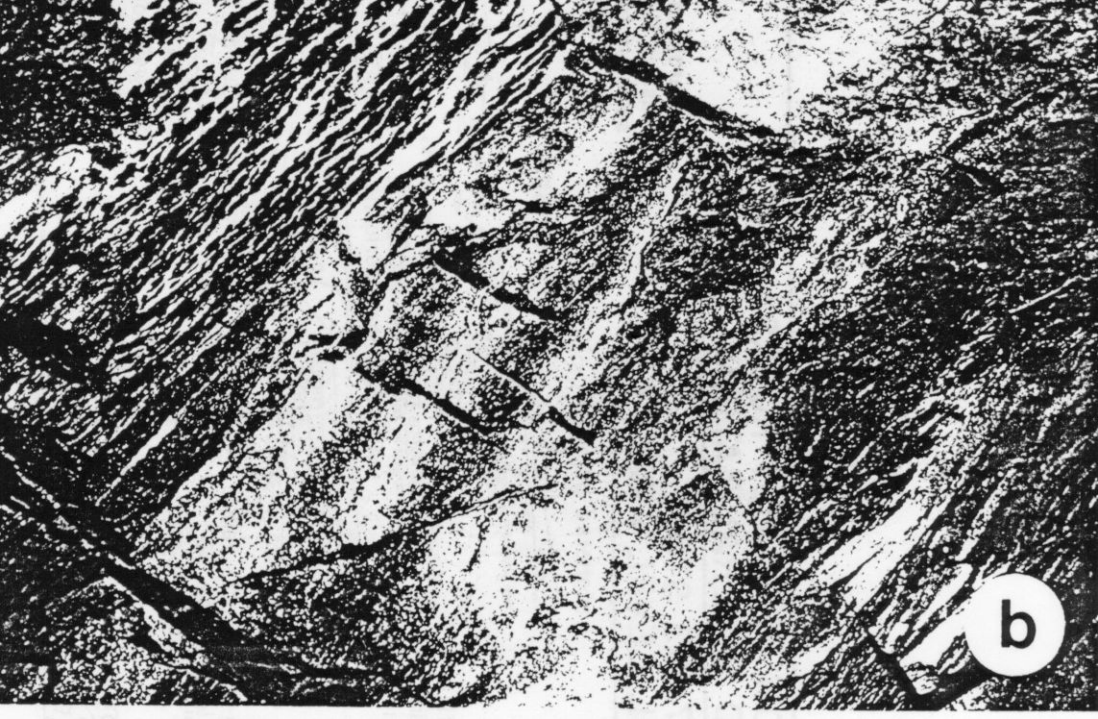






a





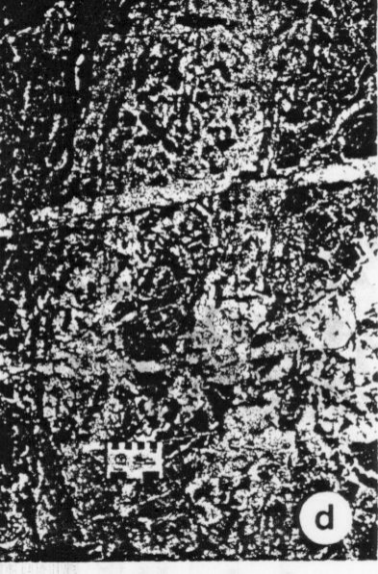


a



b

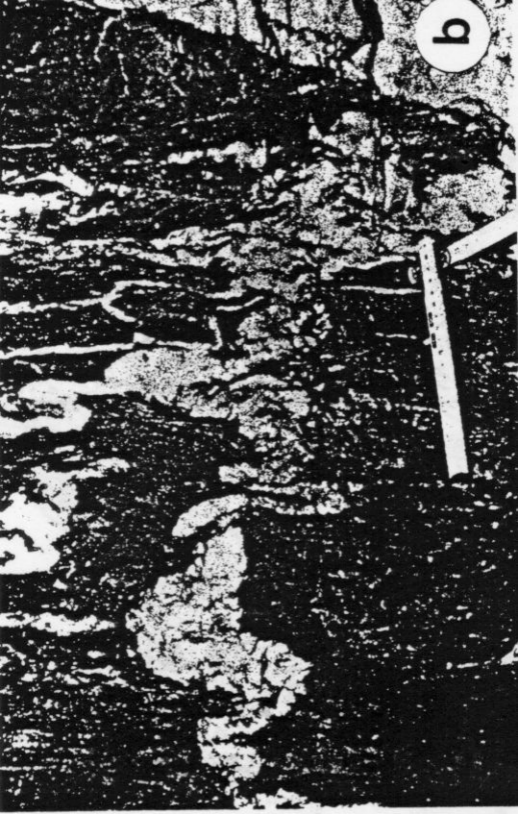




111

d

b



d





a



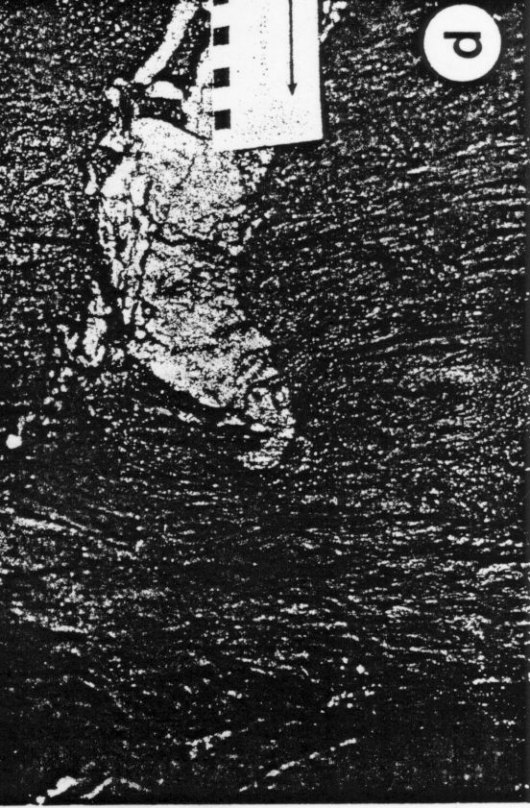




b



d





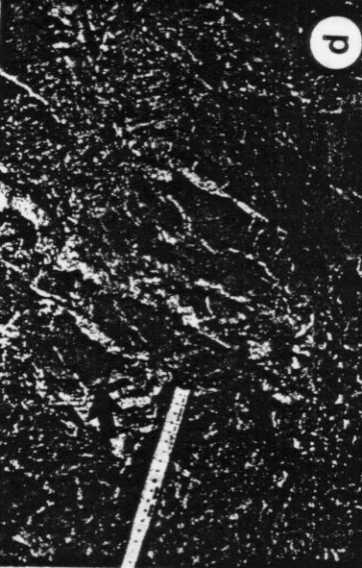
a



9



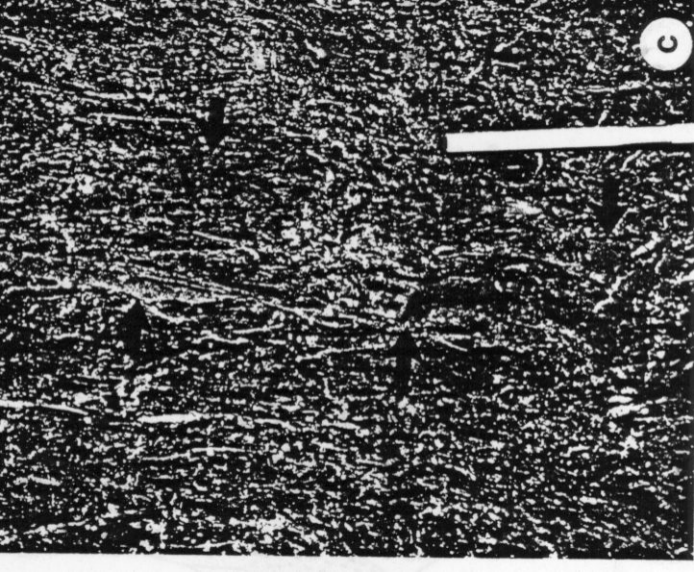
19





a







d

